Author:
Jackson, Laura

Title:
Aquaporins in pelvi-ureteric junction obstruction

Rodent and human studies of urinary tract aquaporin expression and excretion

Aquaporins in pelvi-ureteric junction obstruction: Rodent and human studies of urinary tract aquaporin expression and excretion

Laura Jackson

A dissertation submitted to the University of Bristol in accordance with the requirements of the degree of PhD in the Faculty of Health Sciences

School of Translational Health Sciences

January 2018

Word count: 79,772

Abstract

A major challenge in paediatric urology is determining which children with antenatally detected hydronephrosis and pelvi-ureteric junction obstruction (PUJO) need a pyeloplasty to relieve obstruction, and which do not. In part this is because the pathophysiology underpinning why children develop 'safe' or 'damaging' PUJO is not well understood. This research investigates whether aquaporins, as mediators of water-reabsorption from the renal tract, explain the mechanism behind these differing clinical outcomes. Furthermore, this research explores whether urinary aquaporin levels are good biomarkers to direct surgical management. A dual approach was employed involving interrogating an *in vivo* neonatal rat partial unilateral ureteric obstruction model, and implementing a complementary childhood PUJO study.

The rodent model demonstrated that kidneys with moderate hydronephrosis had normal renal architecture and raised intra-renal pelvis pressure, whereas severely hydronephrotic kidneys displayed obstructive nephropathy. While renal aquaporin isoform expression was maintained in moderate hydronephrosis, several, but not all, renal aquaporin isoforms were downregulated in severe hydronephrosis. Following characterisation of the aquaporin isoforms expressed by whole normal rodent and human renal pelvis, aquaporins 1 and 3 were localised to the vascular endothelium and the urothelium in both species respectively. The rat model established that aquaporins 1 and 3 were downregulated in obstructed renal pelvis. Downregulation was inversely related to hydronephrosis severity and, contrary to renal expression, was exhibited in both moderate and severe hydronephrosis. These findings may indicate that reduced urothelial aquaporin expression diminishes the urinary tract's ability to mitigate pressure rises, ultimately leading to severe hydronephrosis and renal damage. Rodent urinary aquaporin 1 excretion was unchanged between obstructed and sham rats, questioning the ability of this test as a non-invasive biomarker in the management of PUJO. A childhood PUJO study with full ethical approval is currently underway, having recruited 18 patients thus far. This study will investigate the same parameters as the rodent model, confirming whether results translate to the human scenario.

In conclusion, improving our understanding of the mechanism of renal injury through studies such as this will enable earlier diagnosis and better management of this important condition through the development of novel biomarkers and new therapies.

Acknowledgements

This work could not have been completed without the assistance and support of many people both within and outside the Bristol Renal Group. Many thanks particularly to my supervisors; Mr Mark Woodward for his work as the site investigator for the childhood study and his vital clinical and technical expertise with all surgical facets of this project. Professor Richard Coward for his exceptional guidance and patience through all aspects of this research, particularly in helping me to focus my ideas, my research direction and my writing. Finally, thanks to Dr Gavin Welsh for his invaluable insights into the laboratory aspects of the research and advice in preparing this thesis.

Secondly, many thanks to the funding bodies who have generously supported this research and without whom the last 3 years of valuable research experience would not have been possible; The Royal College of Surgeons of England, The British Association of Paediatric Surgeons and the David Telling Charitable Trust.

Thanks also to all former and current members of Bristol Renal who have helped me many times over the years. A special mention must be made to Jenny Hurcombe and Abi Lay who taught me everything I know in terms of laboratory techniques. Also to Fern Barrington who very generously gave her time to troubleshoot my difficulties with immunohistochemistry staining and went on to stain, image and assess my renal pelvis sections for aquaporin 3. Thank you to Hannah Rhodes for her invaluable advice regarding setting up clinical studies, Val Kuzmuk who very kindly counted glomeruli and assessed fibrosis in my rodent kidney sections and finally Pri Kutilake for his IT wizardry, and for keeping me topped up with copious volumes of confectionary and sweet treats. Thanks also to Dr Anne-Marie O'Carroll whose equipment I used to measure rodent intra-renal pelvis pressures and Dr Phil Griffiths who very kindly instructed me on how to use this equipment and the computer software.

Finally, I could not have completed this work without the incredible and unfailing support of my family and friends. Words cannot express my immense gratitude to my husband Dave, and my mum Janet, who have given so much of their time and energy to make this possible for me. Last, but not least, I must thank my daughter Isla, whose smile and laughter brightens our lives immeasurably.

Author's declaration

Some of the text in this thesis is taken directly from the paper "The molecular biology of pelvi-ureteric junction obstruction. Pediatr Nephrol. 2017 March 13. doi10.1007/s00467-017-3629-0" which I wrote, and which was edited by Mr Mark Woodward and Professor Richard Coward.

I declare that the work in this dissertation was carried out in accordance with the requirements of the University's Regulations and Code of Practice for Research Degree Programmes and that it has not been submitted for any other academic award. Except where indicated by specific reference in the text, the work is the candidate's own work. Work done in collaboration with, or with the assistance of, others, is indicated as such. Any views expressed in the dissertation are those of the author.

SIGNED: DATE:

Contents in brief

Table of contents

Table of figures

Table of tables

List of Abbreviations

ANH	Antenatal hydronephrosis
ANP	Atrial natriuretic peptide
APD	Anteroposterior diameter
AQP	Aquaporin
ATP	Adenosine triphosphate
BUO	Bilateral ureteric obstruction
COX-2	Cyclooxygenase 2
CTGF	Connective tissue growth factor
DMSA	Dimercaptosuccinic acid
DTPA	Diethylene-triamine-pentaacetate
ECM	Extracellular matrix
EGF	Epidermal growth factor
EMT	Epithelial-mesenchymal transition
eNOS	Endothelial nitric oxide synthase
ET-1	Endothelin 1
GFR	Glomerular filtration rate
HSP-70	Heat shock protein 70
ICAM-1	Intercellular adhesion molecule 1
IMCD	Inner medullary collecting ducts
IRAS	Integrated Research Application System
MAG 3	Mercapto acetyl tri glycine
MCP-1	Monocyte chemoattractant protein 1
MCUG	Micturating cystourethrogram
MIP-1α	Macrophage inflammatory protein 1α
MMP	Matrix metalloproteinase
NBC1	Electrogenic $Na^+/HCO3^-$ cotransporter
NBCn1	Electroneutral $Na^+/HCO3^-$ cotransporter
NF-κB	Nuclear factor kappa-light-chain-enhancer of activated B cells
NHE3	Type 3 Na^+/H^+ exchanger
NKCC2	Type 1 bumetanide sensitive Na^+-K^+ ($NH4^+$) -$2Cl^-$ cotransporter
nNOS	Neuronal nitric oxide synthase
NO	Nitric oxide
NOS	Nitric oxide synthase
PAI-1	Plasminogen activator inhibitor 1
PDGF	Platelet-derived growth factor
PGK1	Phosphoglycerate kinase 1
PUJ	Pelvi-ureteric junction
PUJO	Pelvi-ureteric junction obstruction
PUUO	Partial unilateral ureteric obstruction

R + D	Research and development
RANTES	Regulated on activation normal T-cell expressed and secreted
RBF	Renal blood flow
REC	Research ethics committee
ROS	Reactive oxygen species
RP	Renal pelvis
RT	Reverse transcriptase
RT-PCR	Reverse transcription-polymerase chain reaction
SEM	Standard error of the mean
TGF-β	Transforming growth factor-β
TIMP-1	Tissue inhibitor of metalloproteinases 1
TNF-α	Tumour necrosis factor-α
TonE	Tonicity-responsive element
TonEBP	Tonicity-responsive enhancer-binding protein
UUO	Unilateral ureteric obstruction
VCAM-1	Vascular cell adhesion molecule 1
VEGF	Vascular endothelial growth factor
VUR	Vesicoureteric reflux
α-SMA	α-smooth muscle actin

Chapter 1. Introduction

1.1 General Introduction

Antenatal hydronephrosis is a major clinical issue for paediatric urologists (incidence of 1 in 200), which has become more commonly recognised, and clinically problematic in infants since antenatal scanning became routine. Of these children approximately 1 in 7 will have pelviureteric junction obstruction (PUJO), a condition where narrowing of the junction between the renal pelvis and ureter obstructs urine drainage from the kidney. The major surgical issue is deciding which children require urgent surgery to relieve obstruction and limit kidney damage, and which do not. This is because some children with PUJO do not damage their kidneys, do not require surgery and ultimately grow out of the problem. Current management involves serial radiological imaging including invasive radioisotope scans to guide surgical decision making. The ability of these tests to adequately predict the need for surgery has been questioned for many years and unfortunately some children lose function in the affected kidney during the period of observation. Paediatric urologists need a reliable non-invasive test to distinguish between those children with high pressure damaging obstruction and those with safe non-renal damaging PUJO.

1.2 Antenatally detected hydronephrosis

1.2.1 Definition and grading of hydronephrosis

Hydronephrosis can be defined as renal collecting system dilatation [1]. It is not a diagnosis in itself but rather an indicator of potential urological abnormality. It is possible to detect hydronephrosis as early as 12-14 weeks gestation [2], however, in the UK it is usually noted on the anomaly scan performed routinely at 18-20 weeks gestation. The degree of hydronephrosis is graded ultrasonographically using the appearances or specific measurements of the renal parenchyma and collecting system. Various measurements of the renal collecting system have been used to identify hydronephrosis, however the maximum measurement of the anteroposterior diameter (APD) of the renal pelvis in the transverse plane is most popular and is the most widely used for antenatal assessment of hydronephrosis [3-5]. Debate continues regarding the threshold at which the antenatal APD is considered abnormal [6-8], particularly since measurements may be affected by other factors such as

the gestation of the fetus [9, 10] and maternal hydration [11, 12]. It is commonly accepted that antenatal hydronephrosis (ANH) diagnosed earlier in gestation [13] or of greater severity [3, 14] correlates with postnatal pathology of greater significance and greater likelihood of surgical intervention [15]. A large meta-analysis of the literature demonstrated the risk of postnatal nephrourological pathology to be 11.9% for mild ANH, 45.1% for moderate ANH and 88.3% for severe ANH [3]. It has also been shown that antenatal renal pelvic dilatation increases more rapidly as gestation progresses in those with obstructive pathology compared to those with non-obstructed kidneys [10]. Published data suggest an antenatal APD≥5 mm should instigate post-natal investigation. [6, 16].

Post-natally, the most commonly used methods to assess the degree of hydronephrosis are the maximum measurement of the renal anteroposterior diameter (APD) and the SFU (Society for Fetal Urology) grading system. The SFU grading system was first introduced in 1993 and concentrates on evaluating the appearance of the renal parenchyma and intrarenal collecting system with particular attention to the calyces [17].

SFU Grade	Pattern of Renal Sinus Splitting	Renal Parenchyma
0	No splitting	Preserved
1	Urine in pelvis barely splits sinus	Preserved
2	Urine fills intrarenal pelvis and extrarenal pelvis, major calyces dilated	Preserved
3	Grade 2 and minor calyces uniformly dilated	Preserved
4	Grade 2 and minor calyces uniformly dilated	Thin

Table 1.1 The Society for Fetal Urology Hydronephrosis Grading System [18]

1.2.2 Incidence of antenatal hydronephrosis

Antenatal detection of a renal abnormality by ultrasound scan was first reported in 1970 by Garrett *et al.* [19]. Over subsequent years, improvements in ultrasound technology and the introduction of routine antenatal scanning has resulted in increased detection of fetal

anomalies with greater accuracy [20]. Approximately 1-5% of fetuses have an anomaly detected on antenatal scanning [21-23] of which a significant proportion relate to the urinary tract, particularly hydronephrosis. The largest prospective data collection of non-selected pregnant women undergoing antenatal ultrasound at a mean gestation of 25 weeks demonstrated hydronephrosis (APD ≥5 mm) in 100/18766 fetuses (0.59%) [16]. More recent UK data, albeit with smaller study sizes of 11465 and 7000 fetuses, suggests the prevalence may be higher with hydronephrosis in 2.3% (APD ≥4 mm at a gestation of 18-23 weeks) [14] and 2% (APD ≥5 mm at a gestation of 20 weeks) [6] respectively.

1.2.3 Aetiology of antenatal hydronephrosis

The aetiology of ANH and thus the postnatal clinical significance in terms of treatment and prognosis is varied. Most causes of ANH can cause unilateral or bilateral hydronephrosis and they may be obstructive or non-obstructive in nature. Causes include; transient hydronephrosis, persistent non-obstructive hydronephrosis, vesicoureteric reflux, peli-ureteric junction obstruction, multicystic dysplastic kidney, megaureter, ureterocoele, ectopic ureter, posterior urethral valves and urethral atresia. The majority of patients (36-66%) [5, 14, 16] with ANH have transient hydronephrosis which is characterized by normal post-natal ultrasound scans and is of unclear origin. Immaturity of the urinary tract in relation to urine output, fetal ureteric folds and potentially vesicoureteric reflux have been suggested as potential causes of transient hydronephrosis [24]. A further 10-43% have persistent hydronephrosis with no obstruction [5, 14, 16, 24] and this hydronephrosis resolves spontaneously in 47-84% of children within 24 months [5, 14, 16].

Vesicoureteric reflux is demonstrated post-natally in 10.7-22% [5, 6, 16] of children with ANH, with the prevalence being affected by the institutions' policy regarding post-natal micturating cystourethrogram (MCUG). A micturating cystourethrogram is a test performed under x-day guidance which involves instilling radio-opaque contrast into the bladder via a urethral catheter followed by voiding of the contrast by the child. This test enables visualisation of the bladder and urethra during filling and voiding, and can identify the presence of reflux into the ureters. Those centres which favour performing an MCUG in all children with ANH, even in the presence of a normal post-natal scan, will undoubtedly discover more cases of low grade VUR which may be clinically asymptomatic [6].

Pelviureteric junction (PUJ) obstruction occurs in 3.8-12.6% [5, 6, 24] of children with ANH and is suspected when hydronephrosis is seen with a normal bladder and no ureteric dilatation on postnatal ultrasound scan. Further radiological investigation is required to support this diagnosis and much controversy remains, as will be discussed in section 1.3, regarding the timing and indication for surgical intervention.

Other less common causes of ANH include: megaureter (non-obstructed or obstructed), multicystic dysplastic kidney, ureterocoele, posterior urethral valves, ectopic ureter, prune belly syndrome, urethral atresia, extrinsic compression from intra-abdominal/pelvic masses and neurological abnormalities [24, 25].

1.2.4 Management of antenatally detected hydronephrosis

The vast majority of children with ANH do not require intervention at birth but go on to have regular radiological imaging, involving serial ultrasound scan, radioisotope scans and invasive micturating cystourethrograms. The major aim of postnatal management is to detect those at risk of deterioration in kidney function and prevent problems such as pain, urinary tract infection and stone formation while avoiding overzealous investigation of those with hydronephrosis that poses no future risk. There is however no agreed evidence-based consensus on post-natal investigation of these children [6, 24, 26, 27].

Unless there is an indication of bladder outlet obstruction or hydronephrosis in a single kidney, the first ultrasound scan is usually performed at around 7 days of life. It is important to ensure it is delayed beyond the first 48 hours as during this time the baby is usually relatively dehydrated and oliguric, which may underestimate hydronephrosis [24]. Ismaili *et al*. suggest a post-natal renal ultrasound scan should be performed at 5 days and 1 month. During their study of 213 infants they demonstrated that if one or both ultrasound scans are abnormal (APD≥7mm) then the sensitivity and specificity of finding a nephrourological pathology were 96% and 76% respectively with positive and negative predictive values of 72% and 97% respectively [5]. Dudley *et al*. define hydronephrosis as an APD≥5mm and suggest a further ultrasound scan at 12 months for all children who initially have two normal scans at 1 and 6 weeks of age [16]. A follow-up ultrasound at 1 year is supported by the most recent consensus statement from the Society for Fetal Urology (SFU) [18] as later re-presentation with previously resolved hydronephrosis has been documented [28, 29].

Hydronephrosis on post-natal ultrasound scan will prompt follow-up ultrasound scans and further investigation as detailed below.

An MCUG may be performed to assess for the presence of vesicoureteric reflux and other lower urinary tract pathologies such as posterior urethral valves. There is no consensus on which children should undergo this investigation, thus this test is variably implemented [27]. Some advocate an MCUG for all children who have had ANH even in the presence of normal post-natal ultrasound scans [6], while others perform an MCUG only when initial ultrasound scans have demonstrated hydronephrosis [16, 18]. Given the invasive nature of an MCUG and the fact that some of the VUR detected may be of doubtful significance it has been suggested MCUG may be safely reserved for children with higher grades of hydronephrosis [30].

When post-natal ultrasound scans demonstrate persistent hydronephrosis (SFU grade 3-4 or an APD >10 mm), particularly but not exclusively in the absence of VUR, diuretic renography is performed to assess for PUJO [2, 24]. The SFU consensus statement also recommends that children diagnosed with severe ANH (>10 mm in the second trimester, or >15 mm in the third trimester) should undergo diuretic renography regardless of the grade of post-natal hydronephrosis if their MCUG was negative [18].

Diuretic renography to determine differential function and drainage of the kidney may be achieved with both ^{99m}Tc-MAG 3 and ^{99m}Tc-DTPA radioisotopes. ^{99m}Tc-MAG 3 is preferred as it requires a smaller dose of radiation and has a much higher initial uptake within the kidney due to very high protein binding of the radioisotope, thus providing better parenchymal imaging and functional assessment [18, 20]. Diuretic renography should be performed around 6-8 weeks of age as renal immaturity may influence results obtained before this time [31].

1.3 The pelvi-ureteric junction

1.3.1 Embryology of the pelvi-ureteric junction

Understanding the normal embryology of PUJ formation is vital when considering where development may proceed incorrectly in congenital abnormalities such as PUJO. The kidney develops from metanephric mesoderm as far along the nephron as the distal tubules. The collecting duct onwards, including the major and minor calyces, renal pelvis, and ureter has a different embryological origin arising from the ureteric bud [32, 33]. Thus, the PUJ does

not represent an embryological fusion site, but is derived exclusively from the ureteric bud. The ureteric bud, consisting of a simple epithelial layer extending into loose mesenchyme, arises from the mesonephric duct during the fifth week of gestation in humans [34]. Epithelial cell proliferation and differentiation to form transitional epithelium leads to luminal obliteration, which at the end of the embryonic period is corrected by physiological recanalisation of the ureter. Epithelial paracrine and mesenchymal autocrine signalling stimulates the formation of smooth muscle cells from mesenchyme which begins at 12 weeks gestation in humans [34, 35]. Mouse models have implicated a number of signalling molecules in this process of proliferation, aggregation, differentiation and orientation of smooth muscle cells as they encircle the urothelial tube. In postnatal mice (equivalent to second trimester human) increased urine production matches the development of the renal pelvis. This is accompanied by a second phase of muscle differentiation, particularly affecting the renal pelvis and proximal ureter, regulated by calcineurin and angiotensin II signalling. [36, 37]. The important molecular pathways that form the ureter and PUJ are shown in Table 1.2 and Figure 1.1 [34, 38-40].

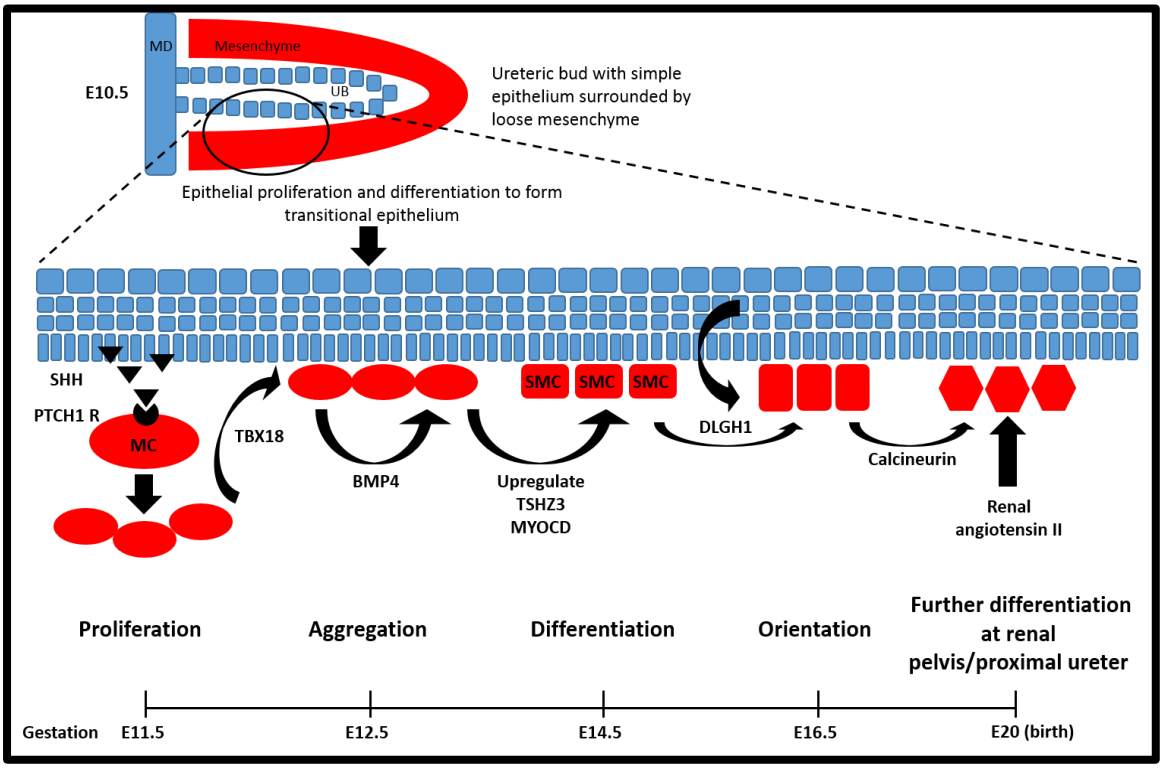

Figure 1.1 PUJ and ureteric embryological signalling pathways

The urothelium secretes SHH which activates the PTCH1 receptor on adjacent mesenchyme stimulating mesenchymal proliferation. Mesenchymal cells express TBX18 which enables their correct localisation and aggregation around the urothelium. The mesenchymal cells also express BMP4 which acts in an autocrine manner to upregulate TSHZ3 and MYOCD. MYOCD enables differentiation of smooth muscle cells by increasing the transcription of genes encoding smooth muscle contractile proteins. DLGH1, expressed by urothelium and smooth muscle cells, is responsible for the correct orientation of smooth muscle cells around

the urothelial tube. The timeline refers to days gestation in mouse models. MD – Mesonephric duct, UB – ureteric bud, MC – mesenchymal cells, SMC smooth muscle cells

Protein	Full protein name	Function	Ref
SHH	Sonic Hedgehog	Morphogen which stimulates peri-urothelial mesenchymal cell proliferation and regulates timing of smooth muscle cell differentiation	[41]
PTCH1 receptor	Protein patched homolog 1	Receptor for SHH, functions as tumour suppressor when unbound	[41]
BMP4	Bone morphogenetic protein 4	Growth factor, necessary for smooth muscle cell differentiation and ureter morphogenesis	[42]
TSHZ3	Teashirt zinc finger homeobox 3	Transcription factor-like protein necessary for myocardin expression and ureteric smooth muscle cell differentiation	[43]
MYOCD	Myocardin	Transcriptional co-activator, necessary for expression of contractile proteins	[43]
TBX18	T Box protein 18	Transcription factor necessary for correct localisation and aggregation of smooth muscle cells around ureteric urothelium	[44]
DLGH1	Disks large homolog 1	Scaffolding protein, regulates smooth muscle cell orientation	[45]

Table 1.2 Proteins/molecular pathways involved in ureteric and renal pelvis development

1.3.2 Anatomy and function of the pelvi-ureteric junction

The pelvi-ureteric junction is a region of gradual transition from the funnel-shaped renal pelvis to the proximal ureter [39] (Figure 1.2). It is a physiologic sphincter [46], characterised by prominent luminal folds with evidence of increased muscle thickness capable of creating a high-pressure zone to regulate urine flow. Similar to the adjacent renal pelvis and ureter, the PUJ comprises 3 main layers: inner urothelium, middle smooth muscle, and outer adventitia [39]. The muscle fibres of the ureter are primarily helical, however, their

final orientation is determined by the degree of vertical and transverse growth [47] with fibre arrangement changing with age from circular fibres in the neonate [48] to reach the mature mesh of spiral, longitudinal and transverse fibres.

The PUJ represents a region of transition from a broader helix proximally to a lengthened helix with more vertically orientated fibres distally [47]. Smooth muscle contraction propels urine from the renal pelvis to the bladder [49], coordinated by submucosal and intra-muscular nerve plexi [50] and modulated by autonomic innervation involving a range of neurotransmitters. These include; acetyl choline, noradrenaline, substance P, neurokinin A, calcitonin gene related peptide, neuropeptide Y, vasoactive intestinal peptide and nitric oxide [49]. Denervated ureters maintain peristaltic activity illustrating the ability of the upper urinary tract to independently initiate and control peristalsis [49]. Evidence suggests this is achieved by pacemaker cells within the muscle layers [49, 51-53], likely interstitial cells [39], which gradually reduce in number from the proximal to the distal ureter [54].

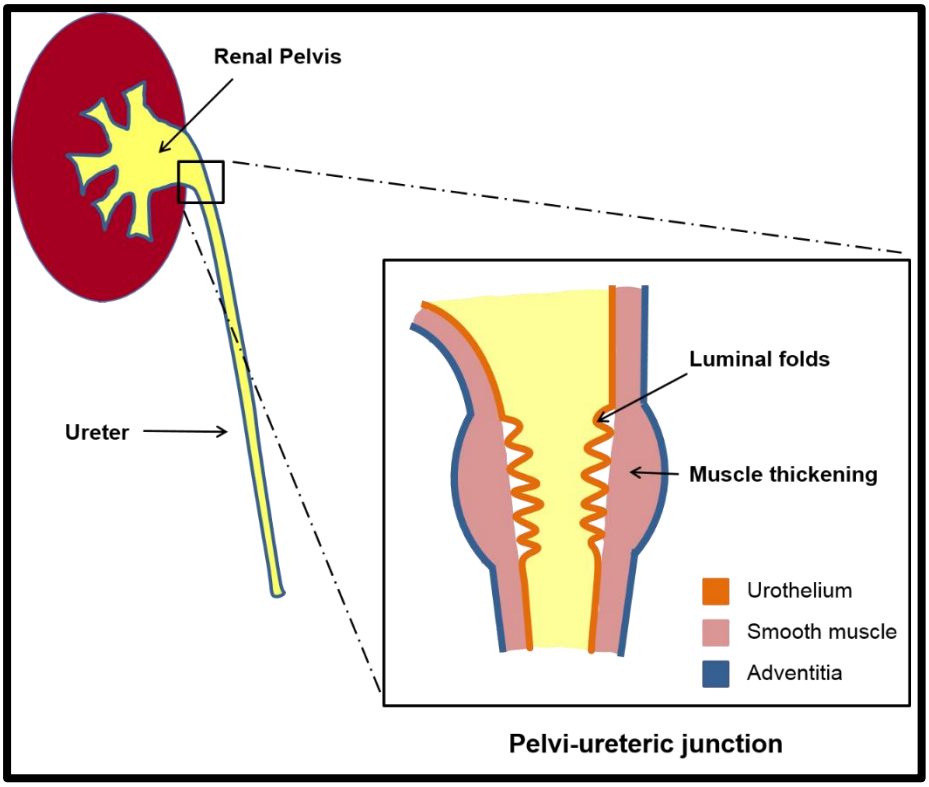

Figure 1.2 Diagrammatic representation of the pelvi-ureteric junction

The gradual transition from the renal pelvis to the proximal ureter is illustrated as well as increased mucosal folds and smooth muscle thickening in this region

1.4 Pelvi-ureteric junction obstruction

1.4.1 Definition and aetiology of pelvi-ureteric junction obstruction

In the context of neonatal hydronephrosis, obstruction has been defined by Peters as "a condition of impaired urinary drainage which, if uncorrected, will limit the ultimate functional potential of the developing kidney" [55]. PUJO results from a narrowing of the junction between the renal pelvis and the ureter. This impedes urine drainage from the collecting system into the proximal ureter, leading to dilation of the collecting system and potential renal damage. Intrinsic obstruction due to an adynamic stenotic segment at the PUJ is the most common aetiology (75% of cases) where failure of peristalsis produces an incomplete, functional obstruction [24]. A further 20% of cases are related to an accessory renal artery, this 'crossing vessel' causes extrinsic compression of the PUJ impeding urine drainage [24]. Other causes include peripelvic fibrosis, abnormal ureteric insertion, fibroepithelial polyps, and anatomical variants such as retrocaval ureter, duplex or horseshoe kidneys [24, 56-58].

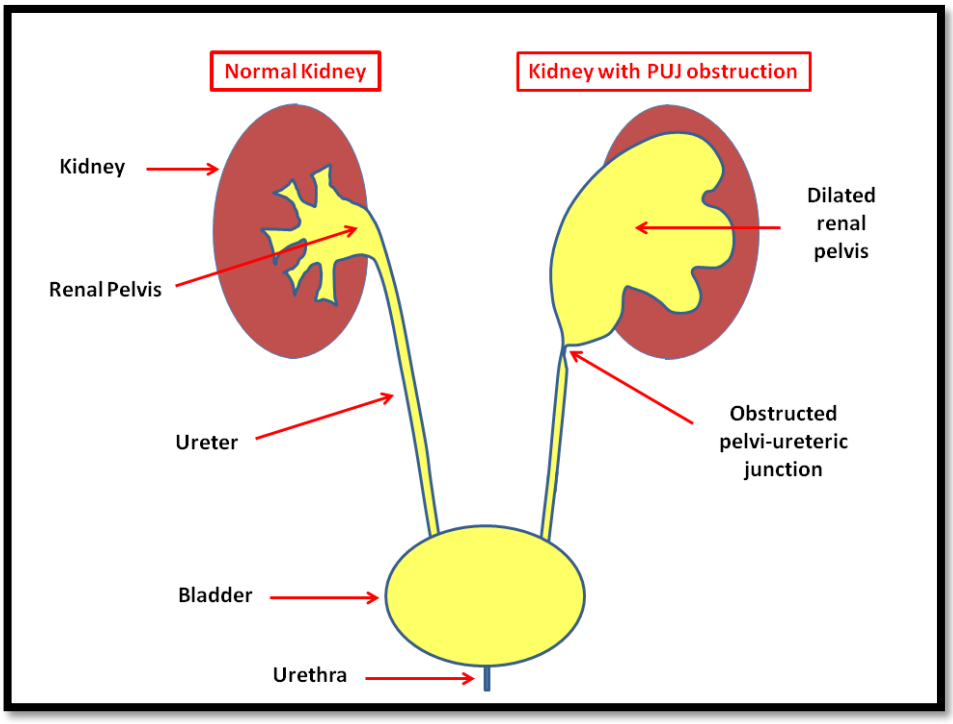

Figure 1.3 Diagrammatic representation of pelvi-ureteric junction obstruction

1.4.2 Demographics of pelvi-ureteric junction obstruction

PUJO has an incidence of 1 in 1000 – 1 in 2000 live births [6, 24, 58] and affects 3.8-12.6% of all children with antenatally detected hydronephrosis [5, 6, 24]. PUJO more commonly affects the left kidney (67%) [58] and is bilateral in 19-33% [16, 24, 59]. Males are affected three times more frequently than females [24]. The aetiology of this difference is currently unknown.

1.4.3 Diagnosis of pelvi-ureteric junction obstruction

Making the diagnosis of PUJO and deciding when to operate can be problematic, as the natural history of ANH is not fully understood. It is clear, however, that renal dilatation is not tantamount to obstruction. Prior to routine antenatal scanning most children with PUJO presented with symptoms or complications, namely; urinary tract infection (particularly in infants), loin/abdominal pain, frank haematuria, and nephrolithiasis. In the presence of supportive radiological investigations management was clear-cut, surgical intervention was indicated for these children.

As antenatal diagnosis of hydronephrosis became more common during the 1980's most infants underwent early surgery for PUJO to prevent the perceived potential deterioration in renal function. Disagreement with early surgery subsequently ensued as it was noted many infants with PUJO showed spontaneous resolution of hydronephrosis. Koff and Campbell reported their early experience with conservative treatment in the early 1990's [60, 61]. Koff went on to follow 104 children with severe (SFU grades 3 and 4), unilateral hydronephrosis of PUJ configuration over a period of 10 years. All children, regardless of initial degree of hydronephrosis or drainage/function on diuretic renogram, were initially managed non-operatively. Indications for surgery were increasing hydronephrosis on ultrasound scan and/or >10% deterioration of function. Pyeloplasty was subsequently performed in 23 children (22%) at a mean age of 4.8 months while eighty-one patients (78%) were managed conservatively. Of those managed conservatively hydronephrosis resolved completely in 69% and improved in 31%, with mean time to maximum improvement being 2.5 years. In terms of differential function on diuretic renogram, 78% of those managed conservatively had good initial differential function (>40%) with a final mean differential function of 48%. The remaining 22% of conservatively managed kidneys had initial reduced differential function with a mean of 25% however this improved spontaneously to achieve a final mean differential function of 48% (range 38-53%) for this group [62]. Crucially what this

demonstrates is that many children with ANH show spontaneous resolution of hydronephrosis, and in a smaller subset of children, while hydronephrosis does not resolve, there is no ongoing renal damage and in fact differential function seems to improve. Consequently, this research group advised that careful observation using radiological monitoring is safe and avoids unnecessary surgery in infants with PUJO. Due to the fact that all pyeloplasties were performed within the first 2 years they identified this period as being vitally important for monitoring which children require surgery, and suggested that the maximum interval between scans should be 3 months up to 2 years of age. Other groups have reported a similar phenomenon, whereby infants managed non-operatively show spontaneous resolution or improvement of hydronephrosis with only 36-52.2% of children with PUJO requiring surgery [26, 63].

There is little literature regarding the long-term outcome of children managed both operatively and non-operatively for PUJO. A recently published historical cohort study with a 30-year follow-up demonstrated that 0.8% (26/3198) of adolescents with normal renal function and a history of congenital anomalies of the kidney and urinary tract developed end-stage renal disease in adulthood. The risk of end-stage renal disease in these individuals was significantly increased (hazard ratio for ESRD, 5.19) compared to those with no history of renal disease [64].

Currently, approximately 80% of cases of PUJO are first noted on antenatal ultrasound scan generating a large pool of asymptomatic children with hydronephrosis. Unfortunately, the available diagnostic tests have changed little over the last 20 years and many have debated the ability of radiological investigations to adequately differentiate those children at risk of functional deterioration and determine the necessity of surgical intervention.

Diuretic renograms (^{99m}Tc-MAG 3 and ^{99m}Tc-DTPA) are performed to assess for the presence of obstruction and they generate three main pieces of data which should be analysed together; a drainage curve, the time taken for half of the radioisotope activity to clear ($t_{1/2}$) and differential kidney function expressed as a percentage. As previously stated ^{99m}Tc-MAG 3 is generally preferred due to the smaller amount of radiation involved and its superior ability to assess function [18, 20]. Furosemide is injected intravenously either at the same time (F0) or 20 minutes after (F+20) intravenous injection of the radioisotope. The creation of diuresis aims to aid identification of the truly obstructed system.

O'Reilly described four types of drainage curve based on children with equivocal upper urinary tract obstruction studied using the F+20 protocol. Type I curves show normal and prompt drainage. Type II curves show no drainage even in response to furosemide. Type III curves initially show no drainage but respond to furosemide with type IIIa showing a good response and Type IIIb showing a poor response. The interpretation of these curves was that type I shows no evidence of obstruction, type II and type IIIb were likely consistent with obstruction and type IIIa were unclear [65].

In addition to analyzing the shape of the drainage curve the $t_{1/2}$, the time taken for half of the radioisotope to clear from the renal pelvis, is calculated and provides a quantitative measure of drainage. A $t_{1/2}$ within 10-15 minutes is considered normal drainage, within 15-20 minutes is considered equivocal and a $t_{1/2}$ beyond 20 minutes suggests obstruction [24].

Despite the well-defined parameters described above it has been demonstrated that renography is an unreliable indicator of obstruction and predictor of renal damage. Gordon *et al*. reviewed data for 69 children with unilateral hydronephrosis of PUJ configuration who were monitored for up to 6 years with between 2 and 6 ^{99m}Tc-DTPA diuretic renograms. Obstructive renograms were observed in 32% of 78 renograms performed on 24 children who were managed non-operatively. None of these children developed a deterioration in function during the period of observation implying they did not have a true obstruction [66]. Similarly, Hafez *et al*. showed the drainage pattern on initial diuretic renogram has poor sensitivity and specificity (63% and 59% respectively) for diagnosing obstruction requiring pyeloplasty [26].

Differential kidney function and degree of hydronephrosis have been advocated as better predictors of those requiring a pyeloplasty [2]. Conversely others have demonstrated that differential function of <40% on initial diuretic renogram has poor sensitivity and specificity (56% and 66% respectively) for diagnosing obstruction. By logistic regression analysis they determined that both differential function and drainage pattern on initial diuretic renogram do not predict the subsequent need for pyeloplasty [26]. This is borne out by the observations by Ulman and Koff (described previously) that reduced function on initial diuretic renogram can improve spontaneously in children treated non-operatively [62]. Hafez *et al*. suggested progression of hydronephrosis on two consecutive renal ultrasound scans performed 4-6 weeks apart is an early sign of obstruction and should be an indicator for surgery [26], while others suggest that progression of hydronephrosis on serial ultrasounds should prompt further diuretic renography [20].

Due to the difficulty in predicting which children need surgery the management of those with antenatally detected PUJO is subjective [1]. Usually it takes the form of careful observation with repeat radiological tests however there remains debate regarding the parameters which indicate clinically significant obstruction requiring intervention. Generally, a pyeloplasty is performed for [56]:

- differential renal function deterioration (differential function <40% or falls by >10% on serial MAG 3 renograms)
- significant hydronephrosis with a renal pelvis anteroposterior diameter >3 cm on ultrasound scan
- increasing hydronephrosis with a rising anteroposterior diameter on serial ultrasound scan
- in symptomatic children

The drawback with the conservative approach is that despite careful observation there is a risk of loss of function in the affected kidney and this has been demonstrated to occur in up to 20% - 25% [67]. Although Ulman *et al*. reported functional improvement in all kidneys that required pyeloplasty for functional deterioration [62], others have shown that not all patients recover function [68], and that functional recovery is reduced in those who have a delayed pyeloplasty after conservative management compared to those who have an early pyeloplasty [69].

1.4.4 Surgical management of pelvi-ureteric junction obstruction

When required, a dismembered pyeloplasty is performed to relieve the obstruction and improve kidney drainage. This procedure involves excising the narrowed junction between the renal pelvis and proximal ureter, spatulating the ureter and performing a primary anastomosis (Fig.2). It may be performed as an open procedure at all ages or laparoscopically in the older child and has good results with minimal morbidity. The re-operation rate is approximately 3-5% [70]. Early complications of this procedure include: bleeding from the operative site, urine leakage via the anastomosis, urinary tract infection, clot retention and ileus. Late complications include recurrent PUJO [71].

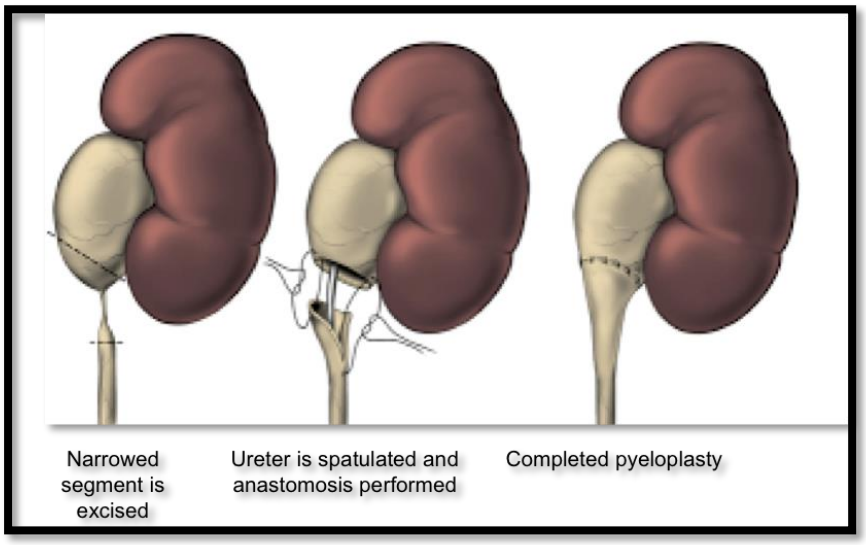

Figure 1.4 Diagram illustrating the major steps of a dismembered pyeloplasty

Adapted from **http://www.chennaiurology.com/robotics/Pyeloplasty.html**

1.4.5 Histopathological features of intrinsic pelvi-ureteric junction obstruction

The human PUJ in intrinsic obstruction demonstrates reduced luminal mucosal folds, inflammatory cell infiltration [72], varying degrees of fibrosis with excess collagen deposition [72-75], increased fibronectin and laminin expression [75] and abnormal muscle fibre arrangement [48]. Both muscular hypertrophy/hyperplasia [72, 74, 76] and atrophy/hypoplasia [48, 72] are reported alongside depletion of the interstitial cells [77, 78] and nerves to the muscular layer [73]. Conversely Koleda *et al.* reported increased interstitial cell density in the obstructed PUJ which decreased with the child's age. The authors suggested interstitial cell changes may be compensatory, subsequently failing over time rather than being causative of PUJO [79].

All of these pathological findings are noted when the PUJ is excised at pyeloplasty and therefore represent late features of PUJO (Figure 1.5). Although the time course of PUJ disease progression is unknown in humans, genetic mouse models of hydronephrosis show abnormalities of peri-urothelial mesenchymal organisation as early as E12.5 (equivalent to human 35 days gestation) [44] and smooth muscle cell differentiation at E15.5 (equivalent to human 12 weeks gestation) [43]. One week postnatally, mice with Id2 haploinsufficiency show smooth muscle irregularity and hypertrophy at the PUJ [80], features which are common to human PUJO. The possible molecular mechanisms underlying this PUJO are described in section 1.4.8.

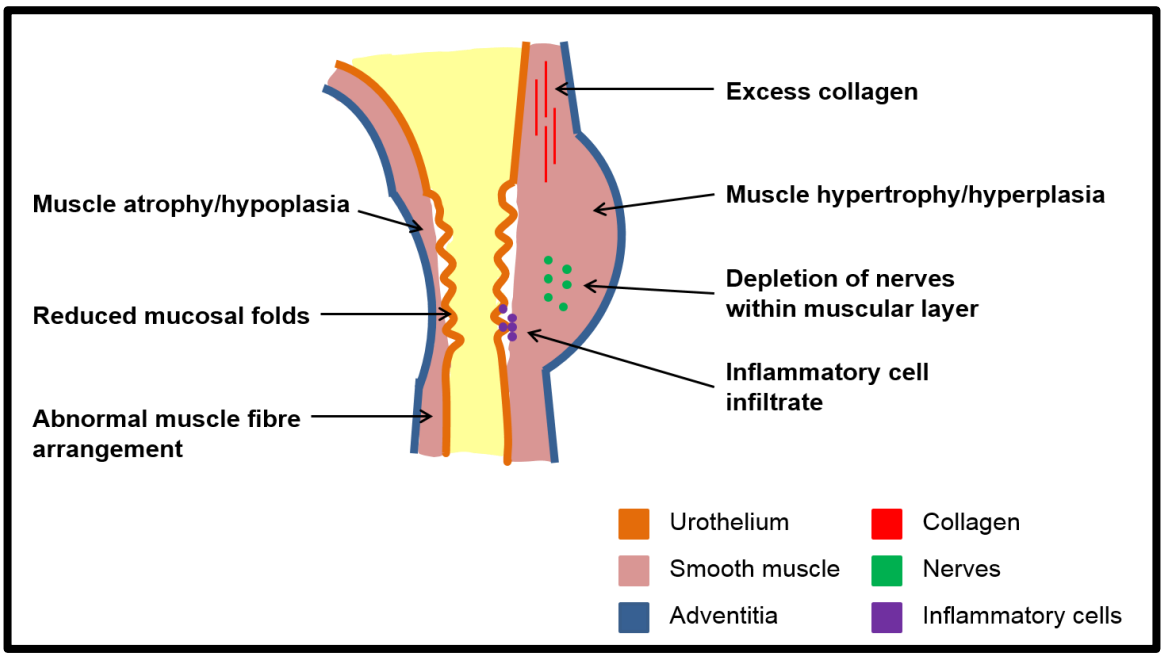

Figure 1.5 Pathological features of intrinsic PUJO

Reduced luminal mucosal folds, excess collagen deposition, depletion of nerves within the muscular layer, abnormal muscle fibre arrangement and both muscle hypertrophy/hyperplasia and muscle atrophy/hypoplasia are seen at the PUJ in human PUJO

1.4.6 Renal histopathological features of pelvi-ureteric junction obstruction

Biopsies from children undergoing pyeloplasty show a variety of histological findings similar to those seen in animal models of ureteric obstruction (discussed in section 1.4.7). The most common are glomerular changes such as glomerulosclerosis seen in 73% of biopsies. However; findings may be as subtle as increased glomerular density (reflecting decreased tubular mass) and decreased proximal/distal tubule ratio. Conversely, severe tubulointerstitial injury with inflammatory infiltrate, tubular atrophy, capsular thickening and interstitial fibrosis [81, 82] may be noted. Interstitial nephropathy is associated with earlier antenatal diagnosis, worse drainage on renogram and reduced differential function [83]. Overt interstitial fibrosis is seen in 26% of biopsies and is significantly more common in children over 1 year of age [82]. While Han *et al*. did not show an association between histological features of obstructive nephropathy and duration of obstruction [84], Valles *et al*. showed increased renal macrophage infiltration is associated with delay in pyeloplasty and decreased GFR [81]. Unlike animal models, renal tubular apoptosis [85] does not seem to be a significant occurrence in the nephron loss noted in PUJO [86].

1.4.7 Animal models of pelvi-ureteric junction obstruction

Adult and neonatal rodent models of complete and partial unilateral ureteric obstruction (UUO) have been used to investigate the molecular biology of congenital obstructive nephropathy. Neonatal models are particularly helpful because rodent nephrogenesis continues for 1 week postnatally and nephron maturation over the subsequent week. Thus, at birth and 1 week of age, rodent kidney development is equivalent to humans at the second trimester and birth respectively [87]. This gives a window in which surgery can be performed on the animals to mimic in utero obstruction in humans. A comprehensive review comparing neonatal models with human disease has affirmed their validity for investigating obstructive nephropathy [88].

Neonatal UUO in rodents causes renal pelvic dilatation, impedes nephron maturation, reduces glomerular tuft size and tubular cell proliferation, initiates tubular apoptosis and atrophy, and leads to progressive interstitial fibrosis [89-91]. However; the response to UUO is not uniform throughout the nephron with features of hypoxia and necrosis suggesting ischaemic injury secondary to vasoconstriction in the proximal tubule. In the more compliant distal nephron dilatation leads to stretch induced tubular cell apoptosis and peritubular fibrosis, both of which significantly correlate with the degree of dilatation [92]. Whether obstruction in the neonatal period is complete or partial there is nephron loss [89, 93], inhibition of ipsilateral renal growth [90] [94] and compensatory contralateral renal growth [87] with the definitive number of nephrons being inversely related to the period of obstruction [93].

Interestingly, adult rats subjected to 5 days of complete UUO followed by release do not show reduced nephron numbers. This underlines the susceptibility of the immature kidney to obstruction-induced injury during the period of nephrogenesis and renal maturation [93].

Relief of rat UUO in the neonatal period attenuates the renal injury although glomerular numbers remain reduced and there is evidence of hyperfiltration [90]. One year later ipsilateral renal growth is impaired, the number of glomeruli are further reduced and GFR has reduced to 20%. Histological features of tubular atrophy, interstitial fibrosis and glomerulosclerosis are increased and significantly these findings are also present in the contralateral unobstructed kidney [95]. When extrapolated to humans this data has implications for the timing of surgery and emphasizes the potential for renal function deterioration after pyeloplasty as a result of permanent damage to the immature kidney.

The renal pathological findings in neonatal and adult UUO models and the timescale of their development are presented in Figure 1.6 [90, 91, 94, 96-101].

1.4.8 Potential molecular mechanisms underpinning pelvi-ureteric junction obstruction

Below are highlighted some of the molecular steps that may lead to the development of intrinsic PUJO and subsequent obstructive nephropathy. Data has been obtained from both adult and neonatal models of complete and partial ureteric obstruction alongside evaluation of tissue obtained at pyeloplasty for human PUJO.

1.4.8.1 Abnormal innervation

Light microscopy reveals reduced innervation within the muscular layer of the PUJ in human specimens excised at pyeloplasty for PUJO [73]. This is associated with reduced expression of molecular markers including glial cell line-derived neurotrophic factor (GDNF – survival factor for neurons), protein gene product 9.5 (general neuronal marker), and nerve growth factor receptor protein in the muscle layers of the stenotic PUJ compared to controls.

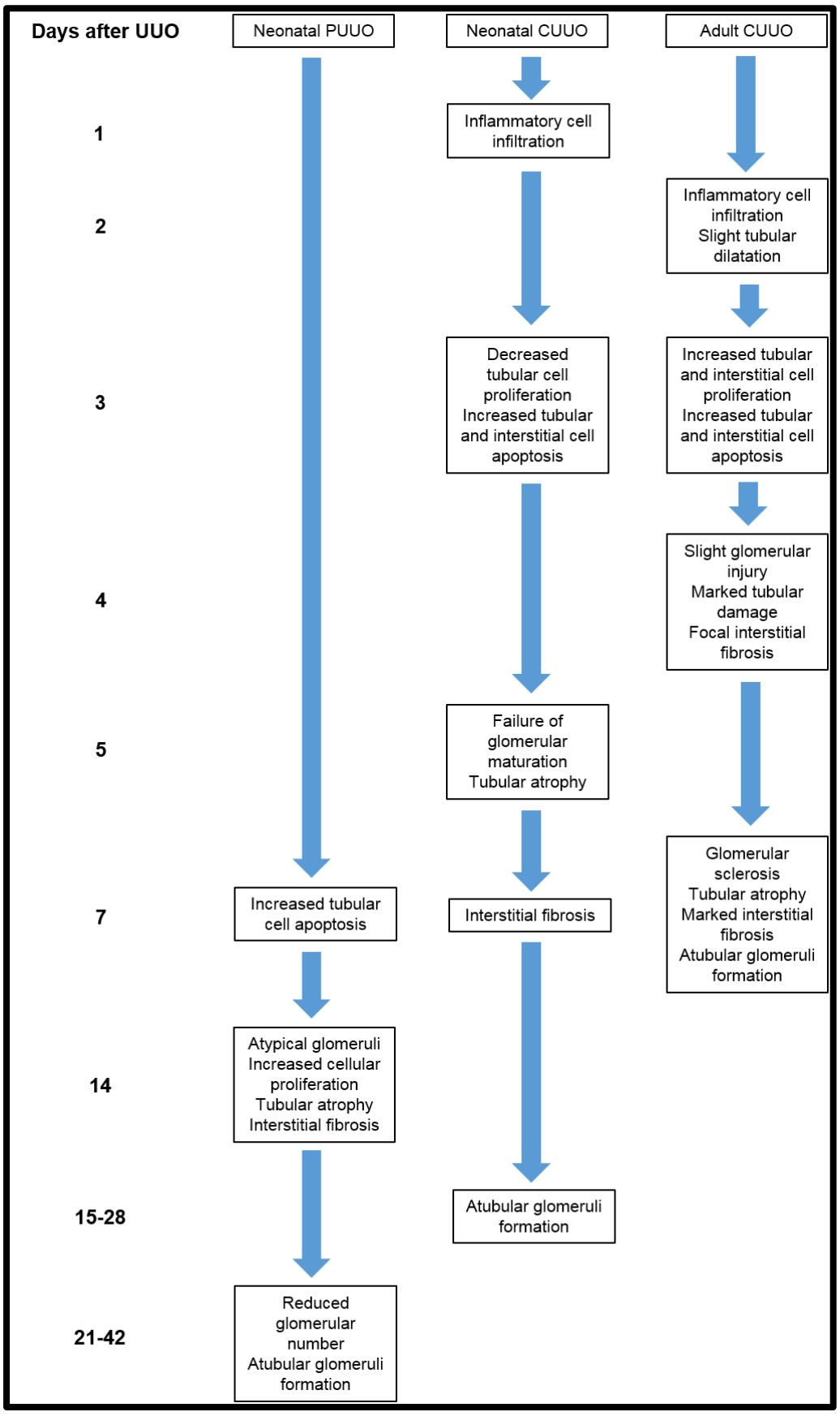

Figure 1.6 Pathological features of rodent models of UUO

Timeline of the development of renal pathogenic features in neonatal and adult models of UUO. CUUO – complete unilateral ureteric obstruction, PUUO – partial unilateral ureteric obstruction

Although it is speculated these neuronal changes may contribute to the pathogenesis of PUJO there is no evidence to confirm or refute this. Conflicting changes in synaptophysin (major synaptic vesicle protein p38) expression in both amount (increased and decreased) and distribution (localisation to the nucleus) are reported compared to control and are of uncertain significance. S-100 (Schwann cell marker) and neurofilament (neuronal protein) expression are unchanged demonstrating there is not a global reduction in neuronal components [74, 102].

1.4.8.2 Myogenic factors

Together with increased smooth muscle cell apoptosis [103], phenotypic and cytoskeletal smooth muscle cell changes are seen in the human PUJ excised at pyeloplasty for PUJO. The stenotic PUJ shows significantly increased expression of smooth muscle myosin heavy chain (MHC) isoforms 1 and 2 [76] as well as an altered ratio of integrin (transmembrane signalling receptors) isoform expression compared to control samples [103]. The preferential expression of immature integrins in the stenotic PUJ [103] may indicate developmental delay of the smooth muscle cells, potentially contributing to their altered function and increased apoptosis in PUJO.

Supporting a myogenic cause of PUJO, transgenic mouse models targeting smooth muscle differentiation generate a PUJ phenotype with hydronephrosis secondary to functional obstruction (Table 1.3).

Gene	Full gene name	Animal	Features and Mechanism	Human	Ref
Ace	Angiotensin converting enzyme	Ace-/- mice	Hydronephrosis, renal parenchymal atrophy		[104]
Adamts-1	A disintegrin-like and metallo - peptidase with thrombo-spondin type 1 motif, 1	Adamts-1-/- mice	PUJO, increased collagen at PUJ. Other urogenital anomalies.		[105]
Agt	Angiotensin	Agt-/- mice	Hydronephrosis, renal parenchymal atrophy,		[106]
Agtr 1a/b	Angiotensin II receptor type 1 (1a and 1b)	Agtr1-/- (1a and 1b) mice	Hydronephrosis in older mice, renal parenchymal atrophy, failure of renal pelvis development, ureteric smooth muscle hypoplasia and abnormal peristalsis		[37]
Aqp2	Aquaporin 2	Aqp2S256L/ S256L CPH mice	Mutation in CPH mice prevents Aqp2 phosphorylation and normal trafficking. Hydronephrosis secondary to polyuria		[107]
Calcineurin	Calcineurin. Also known as Protein phosphatase 3 (ppp3)	Pax3-CreT/+;Cnb1 flox/ flox mice	Calcineurin inactivation in metanephric and ureteral mesenchyme giving hydronephrosis, abnormal pyeloureteral peristalsis with defective renal		[36]

			pelvis and smooth muscle development		
Id2	Inhibitor of DNA binding 2	Id2-/- and Id2 +/- mice	Hydronephrosis and PUJ development		[80]
Nfia	Nuclear factor I/A	Nfia+/- and Nfia-/- mice	Hydrouretero - nephrosis, VUR, abnormal PUJ and VUJ development. CNS malformations.	Nfia+/- due to chromosomal translocation and deletion. VUR and CNS malformations	[108]
TBX18	T-box transcriptio n factor	Tbx18-/- mice	Hydrouretero-nephrosis, short ureters, ureteric smooth muscle defects due to abnormal smooth muscle cell differentiation and localisation	Hispanic family with autosomal dominant CAKUT predominantly PUJO. Heterozygous truncating mutation (c.1010delG) of Tbx18	[44, 109]
Tshz2 and 3	Teashirt zinc finger family member 2 and 3	Tshz3-/- mice	Hydronephrosis with PUJ configuration, abnormal smooth muscle differentiation proximal ureter	Tshz2/Tshz3 mutations not cause of PUJO in Albanian and Macedonian populations	[110, 111]

Table 1.3 Genes potentially involved in the pathogenesis of PUJ obstruction

Evidence derived from animal and human studies. Abbreviations: CNS – central nervous system, CPH – congenital progressive hydronephrosis, PUJO – pelvi-ureteric junction obstruction, VUJ – vescio-ureteric junction, VUR- vesico-ureteric reflux

1.4.8.3 Increased pressure, impeded blood supply and hypoxia

Obstructive hydronephrosis is associated with a doubling to trebling of renal pelvis pressure [46, 112-114]. The resultant increased intratubular hydrostatic pressure [115] stimulates the renopathogenic effects of obstruction via three proposed mechanisms: tubular ischaemia due to hypoperfusion, pressure induced mechanical stretch/compression of tubular cells and altered urinary shear stress. The latter two are likely the primary inducers of obstructive renal injury [88], causing dysregulation of many cytokines, growth factors, enzymes and

cytoskeletal proteins (Table 1.4), resulting in early renal haemodynamic changes followed by structural and functional alterations to the entire nephron. Figure 1.7 highlights the major mechanisms of renal injury in PUJO.

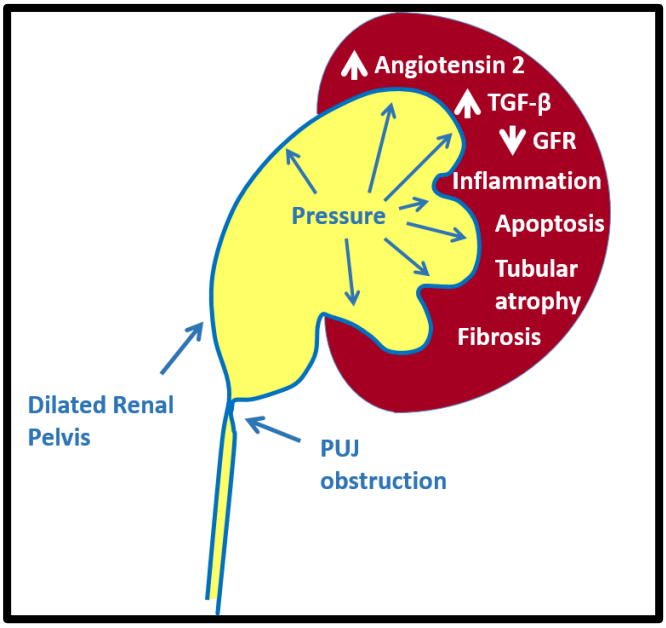

Figure 1.7 Major mechanisms of renal injury in PUJO

Following a short initial increase in renal blood flow related to local vasodilator production [88], the intra-renal renin-angiotensin-aldosterone system is activated causing pre and post glomerular vasoconstriction and a resultant fall in renal blood flow (RBF), medullary oxygen tension and glomerular filtration rate (GFR) [81, 87, 88, 116-119]. Proximal tubular hypoxia and necrosis in neonatal rats with UUO suggests vasoconstriction causes segment specific ischaemic injury [92]. Accordingly, AT1 receptor inhibition improves tubular function by increasing RBF and GFR [120].

Reduced urine production, continuing urine drainage by venous and lymphatic systems alongside tubular and renal pelvis dilatation results in a subsequent decline in renal pelvic pressure [88, 117, 121], which may be a compensatory mechanism to limit damaging increased intrarenal pressure [121].

Protein	Action	Change/timing	Species	Ref
Angiotensin II	Vasoregulatory, proinflammatory, proapoptotic, profibrotic	Increased 28 days Increased 1 week and 5 weeks Increased after mechanical stretch	Neonatal rat CUUO Adult rat CUUO In vitro podocytes	[122] [118] [123]
α-SMA	Increases myofibroblast contractility/EMT marker	Increased 5 days Increased 4 days	Neonatal rat CUUO Adult mouse CUUO	[90] [124]
Caspases	Proapoptotic	Increased 14 days Increased 1 day	Neonatal rat CUUO Adult rat CUUO	[125] [126]
Clusterin	Cytoprotective via pro-survival autophagy	Increased 5 days	Neonatal rat CUUO	[90]
COX-2	Polyuria and natriuresis, anti-apoptotic, antifibrotic	Increased 24 hours Increased 3 days (mRNA)	Adult rat CBUO Adult mouse CUUO	[127] [128]
CTGF	Profibrotic	Increased 2 days (mRNA)	Adult rat CUUO	[101]
EGF	Epithelial survival factor	Decreased 7 days (mRNA) (Undetectable expression in neonatal rat kidney before 4 days) Decreased 33 days Decreased at pyeloplasty (mean age 2yrs) (mRNA) Decreased at pyeloplasty (mean age 5yrs)	Neonatal rat CUUO Neonatal rat both CUUO and 5 day CUUO then release Human renal biopsy Human renal biopsy	[129] [90] [130] [131]
ET-1	Vasoconstrictor	Increased 2 days (mRNA)	Adult rat CUUO	[101]
Fas-L	Proapoptotic	Increased 1 day (mRNA)	Adult rat CUUO	[126]
HSP-70	Antiapoptotic	Decreased 14 days	Neonatal CUUO	[125]
ICAM-1	Proinflammatory	Increased 3 days	Adult mouse CUUO	[132]

Il-6	Proinflammatory	Increased 2 days (mRNA)	Adult rat CUUO	[101]
Integrin (β1)	Profibrotic	Increased 3 days Increased after mechanical stretch	Adult mouse CUUO In vitro proximal tubular cells	[133] [134]
MCP-1	Proinflammatory	Increased 12 days, no change 4 days Increased 2 days (mRNA) Increased at pyeloplasty (mean age 2yrs) (mRNA)	Neonatal rat CUUO Adult rat CUUO Human renal biopsy	[135] [101] [130]
MMP 2 and 9	ECM degradation	Decreased 3 days	Adult mouse CUUO	[132]
PAI-1	Profibrotic, inhibits ECM degradation	Increased 7 days	Adult mouse CUUO	[136]
PDGF	Profibrotic	Increased 4 days	Adult mouse CUUO	[124]
NF-κB	Regulatory transcription factor	Increased 2 days	Adult mouse CUUO	[101]
Nitric oxide	Vasodilator, anti-apoptotic, antifibrotic	Decreased 14 days	Neonatal rat CUUO	[125, 137]
Renin	Cleaves angiotensinogen upregulate renin angiotensin system	Increased 3 days (mRNA) Increased 5 days Increased 14 days (mRNA) Increased 4-5 weeks Increased 24 hours Increased after mechanical stretch	Neonatal rat CUUO Neonatal rat CUUO Neonatal rat CUUO Neonatal rat CUUO Adult rat CUUO In vitro proximal tubular cells	[129] [90] [122] [119] [138] [139]
TGF-β	Proinflammatory, proapoptotic, profibrotic, stimulates EMT	Increased 1 day (mRNA) Increased 33 days Increased 3 days (mRNA) Increased at pyeloplasty (mean age 5yrs)	Neonatal rat CUUO Neonatal rat both CUUO and 5 day CUUO then release Adult rat CUUO Human renal biopsy	[129] [90] [140] [131]

TIMP-1	Profibrotic, inhibits ECM degradation	Increased 5 days Increased 3 days	Adult rat CUUO Adult mouse CUUO	[141] [132]
TNF-α	Proapoptotic, proinflammatory	Increased 14 days (mRNA) Increased 1 day Increased 2 days (mRNA) Increased 1 day	Neonatal rat CUUO Adult rat CUUO Adult rat CUUO Adult rat CUUO	[142] [126] [101] [126]
VCAM-1	Proinflammatory	Increased 3 days (mRNA)	Adult mouse CUUO	[143]
VEGF (podocytes)	Endothelial survival factor	Increased 28 days Decreased 14 days	Neonatal PUUO Neonatal CUUO	[144] [144]
VEGF (tubules)	Endothelial survival factor	Variable expression Decreased 14 days	Neonatal PUUO Neonatal CUUO	[144] [144]
Vimentin	Intermediate filament protein/ EMT marker	Increased 5 days	Neonatal rat CUUO	[90]
WT-1	Transcriptional regulator, key role in renal development	Decreased 14 days	Neonatal rat CUUO	[142]

Table 1.4 The major cytokines, growth factors, chemokines, enzymes and cytoskeletal proteins demonstrating altered intrarenal regulation in obstructive nephropathy

The timing of changes and their mode of action is presented, and compared to sham animal or control human kidney. Change refers to protein expression unless otherwise state. Timing is days after creation of UUO. CUUO – complete unilateral ureteric obstruction, CBUO – complete bilateral ureteric obstruction, PUUO – partial unilateral ureteric obstruction, ECM – extracellular matrix

1.4.8.4 Initiation of proinflammatory cytokines

1.4.8.4.1 Cytokines in the stenotic PUJ

Increased transforming growth factor-β (TGF-β) expression is noted in the human stenotic PUJ compared to normal controls [145]. Furthermore, the smooth muscle regulators

endothelin-1 (smooth muscle constrictor) and adrenomedullin (smooth muscle relaxant) have been shown to be increased and decreased respectively in stenotic PUJ disease [146].

Analysis of paediatric renal pelvis tissue proximal to PUJO for cytokines that show altered renal expression in nephropathy demonstrates increased TGF-β and reduced macrophage inflammatory protein-1α (MIP-1α). In contrast epidermal growth factor, monocyte chemotactic peptide 1, Interferon-γ-inducible protein 10 and RANTES mRNA expression are unchanged suggesting that TGF-β and MIP-1α have important roles in the development of PUJO [116, 147].

1.4.8.4.2 Intrarenal cytokines

Increased intra-renal angiotensin II activates nuclear factor kappa B (NF-κB) and rho-associated coiled-coil forming protein kinase (ROCK) leading to cytokine release, interstitial macrophage infiltration and activation. Intra-renal selectins, integrins, intercellular-adhesion molecule 1, vascular cell adhesion molecule 1, interleukin 1, monocyte chemoattractant peptide 1, colony stimulating factor 1 and osteopontin expression are all involved in macrophage stimulation [87, 88, 116, 148]. Therefore, it appears that renal signals initiate and maintain the injurious inflammatory response to PUJO. Accordingly, both selectin and β2-integrin knockout mouse models show reduced macrophage infiltration into the obstructed kidney after UUO [99, 100].

1.4.8.5 Inflammatory infiltrates

Activated macrophages infiltrate the renal interstitium, sustaining the inflammatory response by releasing cytokines such as: TGF-β1, tumour necrosis factor-α (TNF-α), and platelet derived growth factor [87, 116].

1.4.8.6 Profibrotic processes

Tubulointerstitial fibrosis is the final common pathway for many chronic kidney disorders including obstructive uropathy and is instigated by altered cytokine expression (Table 1.5). Activated resident interstitial myofibroblasts [149], expressing α-smooth muscle actin (boosts cell contractility) [150], aggregate, proliferate and produce extracellular matrix. Extracellular matrix consisting of collagens I, III and IV, fibronectin, laminin and proteoglycans accumulates due to increased synthesis and reduced degradation [132, 151, 152]. Myofibroblasts amplify fibrosis by producing cytokines including TGF-β1 and TNF-

α [87]. Parenchymal damage and renal dysfunction results, such that in children with PUJO the extent of fibrosis significantly correlates with differential renal function [84].

Promote	Prevent
Angiotensin II	EGF
CTGF	MMP
ICAM-1	Nitric oxide
Integrins	VEGF
PAI-1	
PDGF	
TGF-β	
TIMP-1	

Table 1.5 Cytokines, growth factors, enzymes and adhesion molecules promoting or preventing tubulointerstitial fibrosis in ureteric obstruction

Angiotensin II upregulation is central to the pathogenesis of obstructive nephropathy (Figure 1.8, Figure 1.7) [87, 92, 97, 101, 118, 126, 140, 141, 153-162]. Angiotensinogen murine knockout studies show angiotensin II expression is responsible for at least 50% of renal fibrosis in chronic neonatal UUO [154]. Acting predominantly via the AT1 receptor [101, 155, 163] it regulates cytokine production and stimulates reactive oxygen species (ROS) generation, which propagate the proinflammatory, fibrogenic state [88, 154]. Additionally, ROS cause proximal tubular degeneration by apoptosis, autophagy and necrosis with destruction of the glomerulotubular junction forming atubular glomeruli [97, 159].

TGF-β1 is a profibrotic cytokine and fibroblast chemo-attractant which has a major role in fibrosis development via SMAD dependent and independent pathways (Figure 1.9) [132-134, 164-168]. Renal TGF-β expression is increased in experimental UUO [140, 153, 155, 157, 169-171] and children with PUJO, being positively correlated with the histopathologic grade, radioisotope drainage half-time ($t_{1/2}$) and post-void washout, and negatively correlated with pre-operative differential renal function [83, 131].

Nitric oxide (NO) is an endogenous vasodilator that protects against tubulointerstitial fibrosis and proximal tubular oxidant injury in obstructive nephropathy [137, 141, 172]. Animal models [161, 173, 174] and human studies of PUJO show altered endothelial nitric oxide synthase (eNOS) and inducible nitric oxide synthase (iNOS) expression/activity alongside reduced NO production. Lower eNOS expression/activity is associated with worse

creatinine clearance, reduced differential renal function [81, 175] and increased fibrosis [81, 175], oxidant injury and apoptosis [125, 137].

Urinary tract infection promotes progression of chronic kidney disease in patients with obstructive uropathy. Similarly, in animal studies, infected obstructed kidneys demonstrate interstitial nephritis and collagen deposition not detected in non-infected systems.

1.4.8.7 Antifibrotic processes

Renal cyclooxygenase 2 (COX-2) expression and prostaglandin production in experimental UUO is increased [127] and may be a protective response. COX-2 inhibition worsens obstructive nephropathy while prostacyclin analogue (ONO-1301) supplementation alleviates UUO induced fibrosis [176].

1.4.8.8 Cellular apoptosis

Apoptosis affects podocytes, endothelial and epithelial cells within the kidney leading to loss of glomeruli, peritubular capillaries and tubules [87]. Tubular cell mechanical stretch is a potent stimulator of apoptosis [92, 177] mediated via TGF-β1 and TNF-α [126, 160] released from tubular cells and infiltrating macrophages [116]. Other pro-apoptotic factors increased after UUO include Fas-L [101], p53, caspases and ceramide [87].

Downregulation of anti-apoptotic factors including epidermal growth factor, eNOS, NO, vascular endothelial growth factor, heat shock protein 70 and Wilms tumour-1 compounds the renal injury [87, 116, 125, 177, 178].

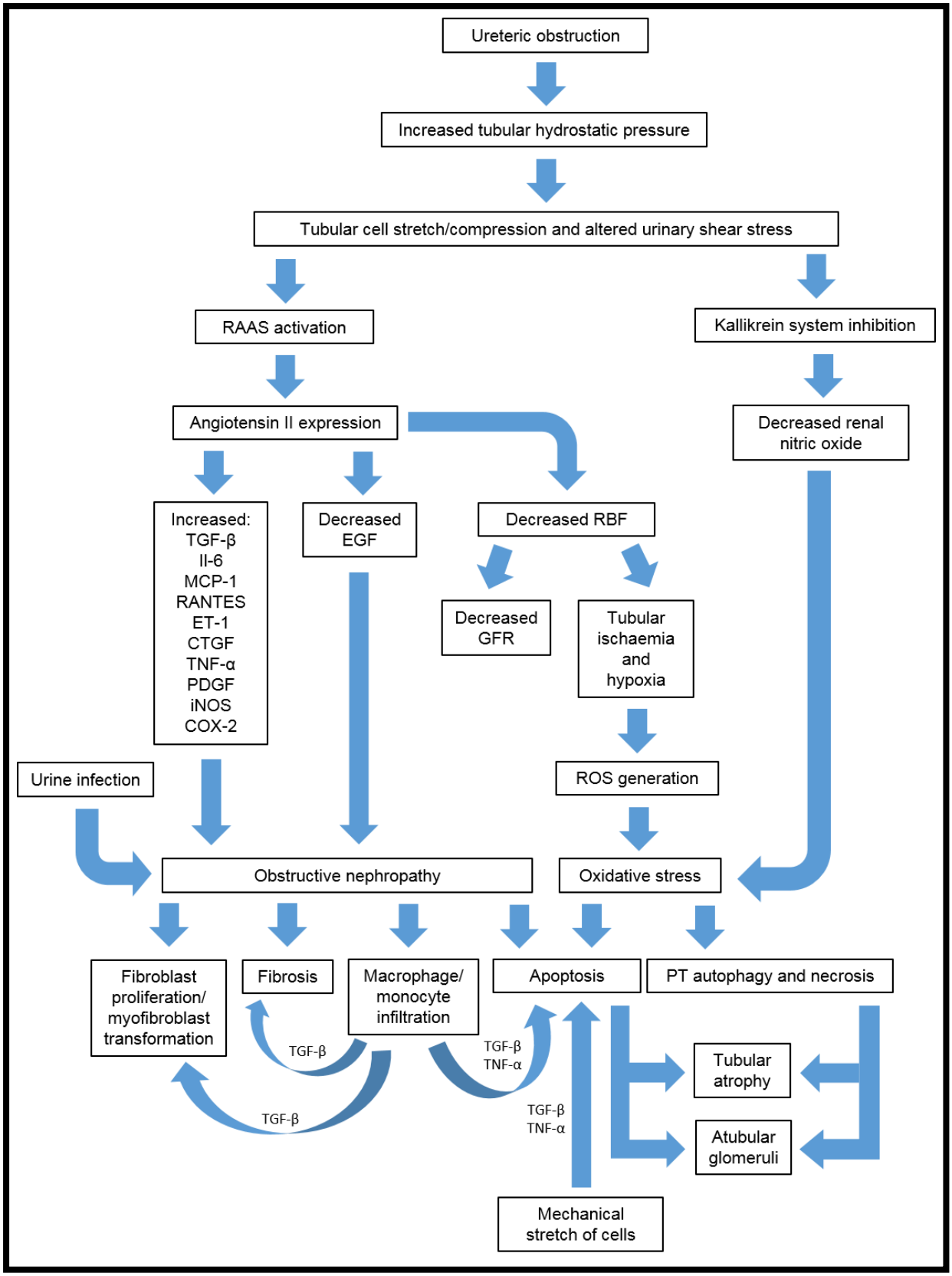

Figure 1.8 Major pathways involved in obstructive nephropathy development

Derived from animal and human studies. Urinary tract infection promotes progression of chronic kidney disease in patients with obstructive uropathy. Similarly in animal studies, infected obstructed kidneys demonstrate interstitial nephritis and increased collagen deposition compared to non-infected systems [179]. RAAS – renin angiotensin aldosterone system, ROS – reactive oxygen species, PT – proximal tubule.

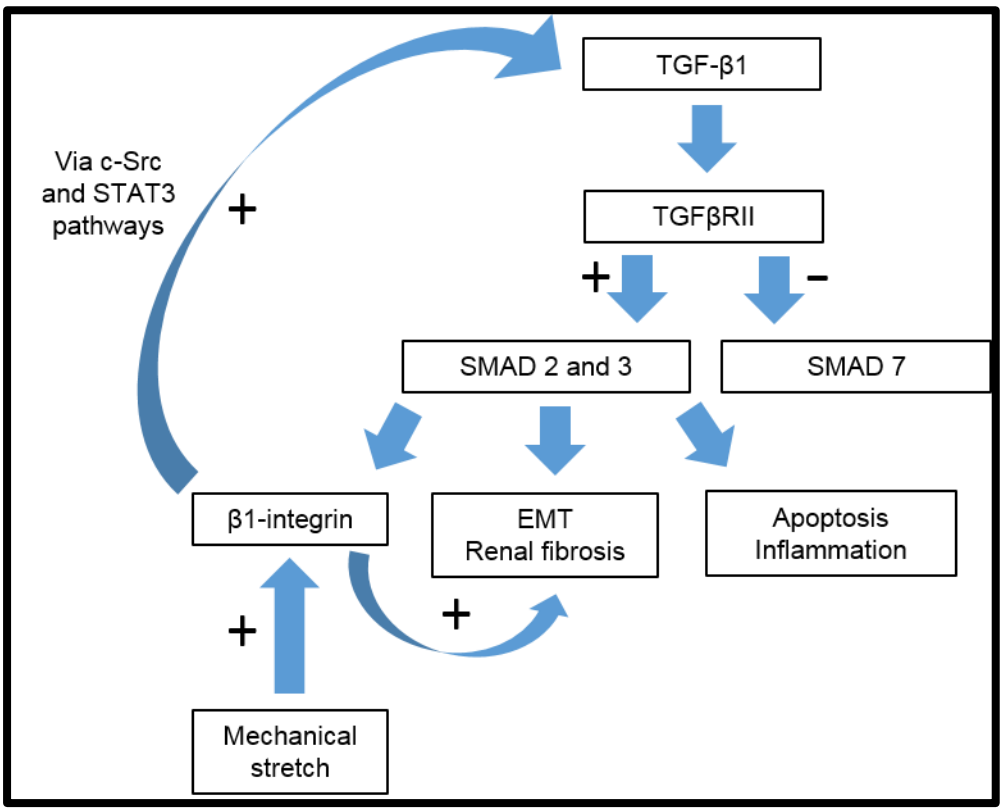

Figure 1.9 TGF-β1 signalling via SMAD dependent pathway

UUO induces increased TGF-β1 and transforming growth factor β receptor II (TGFβRII) expression, upregulating SMAD 2 and 3 and downregulating SMAD 7 (inhibitory for SMAD 2 and 3). β1-integrin is upregulated by both SMAD signaling and mechanical stretch, and contributes to a positive feedback loop regulating TGF-β1 expression via c-Src and STAT-3 pathways. EMT – epithelial mesenchymal transformation

1.4.8.9 Tubular function impairment

Ureteric obstruction leads to reduced renal expression of the V2 (vasopressin) receptor [180], renal sodium and urea transporters [181-183] and aquaporins [184-186]. Following relief of obstruction this is associated with natriuresis, polyuria and reduced urine concentrating ability [187-189]. Aquaporins are discussed in more detail in section 1.5.

1.4.9 Genetic mechanistic clues in pelvi-ureteric junction obstruction

Phenotypes similar to PUJO have been noted in numerous transgenic mouse models. Many genes involved in ureteric smooth muscle proliferation and differentiation are implicated supporting a primary myogenic aetiology. Importantly one of these genes has been implicated in human disease (Table 1.3).

TBX18 gene mutations are reported in association with congenital anomalies of the kidney and urinary tract (CAKUT). In particular, a heterozygous TBX18 truncating mutation (c.1010delG) showing autosomal dominant inheritance is described across four generations of a family with CAKUT and predominantly PUJO [109]. The transcription factor TBX18 is necessary for normal smooth muscle cell proliferation, differentiation and localisation around the developing urothelial stalk [44]. TBX18 also directs epithelial proliferation and when absent leads to an abnormally short ureteric bud [40]

In the majority of patients, however, PUJO is a polygenic disorder without an obviously inherited genetic component [87].

1.4.10 Therapeutic manipulation in rodent unilateral ureteric obstruction

Human and animal studies have highlighted a number of potential therapeutic targets that could be manipulated to alleviate the nephropathy sustained secondary to PUJO. Several drugs targeting these pathways have been assessed in rodent UUO models as described below, however, to our knowledge none of these therapies have been trialled in childhood human PUJO.

1.4.10.1 Angiotensin converting enzyme and angiotensin II receptor inhibitors

In adult rodent UUO models ACE inhibitors and AT1 receptor inhibitors given prophylactically (for the duration of obstruction) are beneficial in alleviating nephropathy. Specifically they reduce TGF-β [171, 190] and TNF-α [156] expression as well as macrophage infiltration and tubulointerstitial fibrosis [141, 155, 191]. Additionally, AT1 receptor inhibitors improve tubular function by improving RBF and GFR and attenuating the reduction in sodium transporter and aquaporin 2 expression thus reducing polyuria and natriuresis [120, 162].

ACE inhibitors reduce both AT1 and AT2 receptor stimulation [192] and indirectly increase NO levels via bradykinin generation [141]. This may explain why they confer additional benefits, particularly anti-inflammatory, compared to AT1 receptor inhibitors [148].

Unfortunately, inhibition of angiotensin during either the period of nephrogenesis (first 10 days after UUO) or renal maturation (second 10 days after UUO) in neonatal partial UUO

exacerbates renal injury in both the obstructed and contralateral kidney [193, 194]. These studies highlight the importance of these pathways in normal kidney development and maturation.

However, it is important to remember that ACE inhibitors and AT1 receptor inhibitors are frequently used in children with chronic kidney disease in whom they significantly reduce proteinuria [195], despite not significantly alleviating the natural decline in excretory function [196, 197]. They are largely well tolerated with no apparent effect on growth and development and a low incidence of side effects such as hyperkalaemia, hypotension and renal injury [195].

1.4.10.2 HMGCoA reductase inhibitors (Statins)

Statins ameliorate nephropathy when administered prophylactically in adult and neonatal rodent UUO models by reducing renal cytokine production (TGF-β, TNF-α), macrophage infiltration, oxidative stress, apoptosis and tubulointerstitial fibrosis [142, 198, 199]. These pleiotropic effects are achieved through decreased Ras/ERK/Akt signalling [200] and increased NO bioavailability [201]. Importantly statins remain beneficial in neonatal rodent UUO where an improvement in tubular dilatation and glomerular number and size are also seen [125, 137, 142]. Functionally, in UUO models, statins improve GFR and microalbuminuria [202], and increase urinary concentrating ability via boosting aquaporin 2 expression [203].

Statins are commonly used and usually well tolerated in adults. Side effects of treatment include: hepatic dysfunction, diabetes mellitus, benign proteinuria, peripheral neuropathy, myalgia and rhabdomyolysis [204]. Ten-year follow-up of children (≥8 years) treated with statins for familial hypercholesterolaemia demonstrated few discontinue therapy due to side effects and no serious adverse reactions. Additionally, growth, puberty and educational parameters were unaffected compared to controls [205].

1.4.10.3 TGF-β modulation

Prophylactic TGF-β receptor inhibition is renoprotective in adult rodent UUO models reducing apoptosis, macrophage infiltration, fibrosis, proximal tubular atrophy and atubular glomeruli formation [167, 206]. Similarly, anti-TGF-β antibody treatment increases NOS expression while reducing apoptosis and fibrosis [160]. Conversely prophylactic TGF-β receptor inhibition in neonatal mouse UUO causes widespread renal necrosis, exacerbating

the injury in the obstructed kidney and highlighting the differing responses to signalling cascades during renal development [167].

Anti- TGF-β antibody treatment (GC1008) has been trialled in human oncological disease and was generally well tolerated. However side effects included gingivitis, fatigue and skin rashes including keratoacanthoma and squamous cell carcinoma development (melanoma patients only). GC1008 treatment has not progressed beyond phase II clinical trials as drug development was discontinued by the manufacturer [207].

1.4.10.4 COX-2 inhibition

In adult rodent bilateral ureteric obstruction COX-2 inhibition alleviates aquaporin 2 and sodium transporter downregulation and improves post-obstructive polyuria, which would appear beneficial [127, 208]. However other studies have demonstrated that both genetic COX-2 knockout and prophylactic COX-2 inhibition in adult rodent UUO models increases tubular injury, apoptosis and fibrosis thereby negating its potential use in the clinical setting [128, 209].

Chronic celecoxib (COX-2 inhibitor) use in children demonstrates a similar frequency of adverse events as non-selective NSAIDS, which are most frequently gastrointestinal side effects [210].

1.4.11 Urinary biomarkers in pelvi-ureteric junction obstruction

Identifying early urinary biomarkers in PUJO may be beneficial for the diagnosis, management, and prognosis of this condition. Such biomarkers would enable timely detection of children with ‘damaging’ hydronephrosis who require surgery to protect renal function, while avoiding surgery in those with ‘safe’ hydronephrosis.

1.4.11.1 Urinary biomarkers in animal studies

There is little data from animal studies. Proteomics using a rat UUO model demonstrated increased urinary and renal levels of alpha-actinin-1 and moesin at 1 week which corresponded with histological evidence of tubular injury. Following 3 weeks of UUO urine and renal levels of vimentin, annexin A1 and clusterin were significantly elevated, corresponding with substantial renal interstitial fibrosis [211].

1.4.11.2 Urinary biomarkers in human studies

Many urinary cytokines, growth factors, chemokines, tubular enzymes and tubular transport proteins have been investigated from children undergoing pyeloplasty for PUJO. Studies with conservatively managed PUJO as a comparator are most useful to identify biomarkers able to aid selection of patients for surgery. Potential urinary biomarker proteins measured in bladder urine samples are presented in table 5.

Finding a suitable biomarker test with high sensitivity, specificity and predictive value is challenging [116], not least because these markers are excreted in health as well as disease, show significant intra and inter patient variation, and may be affected by patient age, the presence of urinary tract infection and other renal disorders [212, 213]. Furthermore, in PUJO, the transport of a urine biomarker from the affected kidney to the bladder is physically impeded, while dilution of proteins of interest in the bladder by urine from the normal contralateral kidney further reduces the likelihood of detecting a suitable voided biomarker.

A recent systematic review of urinary and serum biomarkers included 14 studies, reporting data on 380 surgically managed PUJO patients, 174 conservatively managed patients and 213 controls. This review reported a wide-range of sometimes conflicting results and was unable to draw any firm conclusions, attributing this to differences in study design with heterogeneous age groups, various or absent control groups and often short durations of follow-up [214].

More successfully, proteomics of neonatal urine identified a panel of 51 peptides which distinguish obstruction severity. When implemented in a prospective blinded study it had an accuracy of 94% to predict future need for surgery in newborns with PUJO [215]. However; beyond one year of age the sensitivity and specificity of this proteome profile diminished significantly [216].

Currently a single biomarker able to guide selection of patients for pyeloplasty has not been identified indicating a panel of biomarkers may be necessary to achieve this.

Urinary protein (corrected for creatinine)	Primary measured group	Compar-ator	Bladder urine protein level	Sensitivity (Se) Specificity (Sp) Accuracy (Ac)	Post-operative bladder urine (compared to pre-op)	Ref
ALP	Pyeloplasty	CMP	Increased pre-op	Se - 91.4% Sp - 100% Ac - 94%	Decreased 12 months post-op	[217]
Angiotens-inogen	Pyeloplasty	Healthy control CMP	Increased pre-op	Se - 93.3% # Sp - 60% #		[218]
B2-microglob-ulin	PUJO*	Healthy control	Increased		Decreased 42 months post-op	[219]
B2-microglob-ulin	Pyeloplasty	Healthy control	No change			[220]
Ca19-9	Pyeloplasty	Healthy control CMP	Increased pre-op	Se - 76% **$** Sp - 85% **$**	Decreased 3 months post-op	[221]
Ca19-9	Pyeloplasty	Healthy control Hydrocoe le/renal cyst	Increased pre-op	Se - 100% ^ Sp - 82.6% ^	Decreased 3 months post-op	[222]
CyC	Pyeloplasty	Healthy control	No change			[220]
EGF	PUJO*	Healthy control	Decreased (obstructed group only)		No change	[219]
EGF	Pyeloplasty	Healthy control	Decreased pre-op		Increased	[213]
EGF	Pyeloplasty	Healthy control	Increased pre-op	Se - 70.4% Sp - 69.2%	Decreased 3 months and 1 year post-op	[223]
EGF	Pyeloplasty	Healthy control	No change			[224]
ET-1	Pyeloplasty	Healthy control VUR Renal stones	Increased pre-op	Se - 74.3% Sp - 90% Ac - 81.5%	Decreased 12 months post-op	[225]
γGT	Pyeloplasty	CMP	Increased pre-op	Se - 62.9% Sp - 100% Ac - 74%	Decreased 12 months post-op	[217]
HO-1	Pyeloplasty	Healthy control CMP	Increased pre-op	Se - 72.2% # Sp - 78.1% #	Decreased 1 month post-op	[226]
IP-10	Pyeloplasty	Healthy control	No change			[223]
KIM-1	Pyeloplasty	Healthy control CMP	Increased pre-op	Se - 100% # Sp - 71.4% #		[227]

MCP-1	Pyeloplasty	Healthy control	Increased pre-op	Se - 77.8% Sp - 69.2%	Decreased 3 months and 1 year post-op	[223]
MCP-1	PUJO*	Healthy control	Increased		Decreased 42 months post-op	[219]
MCP-1	Pyeloplasty	Healthy control	Increased pre-op			[213]
MCP-1	Pyeloplasty	Healthy control CMP	Increased pre-op	Se - 100% # Sp - 0% #	Remains high 3 months post-op	[228]
MIP-1α	Pyeloplasty	Healthy control	Decreased pre-op		Increased 1 year post-op	[223]
NAG	Pyeloplasty	CMP	Increased pre-op	Se - 97.1% Sp - 80% Ac - 92%	Decreased 12 months post-op	[217]
NGAL	Pyeloplasty	Healthy control	No change			[220]
NGAL	Pyeloplasty	Healthy control	Increased pre-op			[229]
NGAL	Pyeloplasty	Healthy control CMP	Increased pre-op	Se - 100% # Sp - 28.6% #	Decreased 3 months post-op	[227]
OPN	Pyeloplasty	Healthy control	No change			[220]
OPN	Pyeloplasty	Healthy control CMP	Increased pre-op	Se - 98.5% # Sp - 10.5% #	Remains high 3 months post-op	[228]
RANTES	Pyeloplasty	Healthy control	No change			[223]
TGF-β	Pyeloplasty	Healthy control	Increased pre-op	Se -100% Sp - 80% Ac- 90.8%	Decreased 1 year post-op	[224]
TGF-β	Pyeloplasty	CMP	Increased pre-op	Se - 82% Sp - 86%		[230]

Table 1.6 Urinary proteins from studies in children with PUJO

Generally, the primary group measured is children undergoing pyeloplasty which are then compared to healthy control and/or conservatively managed PUJO (CMP). The exception is labelled PUJO* which includes conservatively managed PUJO split into 'functional' (t1/2 of renogram < 20 minutes) and 'obstructed' (t1/2 of renogram > 20 minutes). In these studies voided urine from children undergoing pyeloplasty was only obtained 42 months post-op. Where applicable sensitivity, specificity and accuracy of the test at best threshold value from ROC curve analysis is presented. NGAL – neutrophil gelatinase-associated lipocalin, CyC – cystatin-C, OPN – osteopontin, MIP-1α – macrophage inflammatory protein-1α, IP-10 – interferon-γ-inducible protein 10, HO-1 – Heme oxygenase-1, KIM-1 – kidney injury molecule-1, NAG – N-acetyl-beta-D-glucosaminidase, γGT – gamma-glutamyl transferase, ALP – alkaline phosphatase, Ca19-9 – carbohydrate antigen 19-9. # To detect DRF < 40% out of all hydronephrosis cases, $ To detect pyeloplasty cases out of all hydronephrosis cases, ^ To detect pyeloplasty cases out of all cases

1.5 Aquaporins

1.5.1 Aquaporin structure and function

Aquaporins (AQPs) are an ancient family of transmembrane proteins found in all organisms including eubacteria, yeasts, plants and mammals [231]. AQP1 (initially named CHIP 28) was the first to be described in 1988 by Agre *et al*. for which he subsequently received the Nobel prize for Chemistry [232]. This discovery finally revealed the mechanism by which water moves across the cell membrane along an osmotic gradient [233]. Subsequent studies have highlighted the vital role AQPs play in normal physiology alongside their involvement in both heritable and non-heritable diseases. There are 13 mammalian isoforms (AQP 0-12) [234] which are found in numerous body tissues in different cellular locations (Figure 1.10 and Table 1.7) [235].

These small, roughly 30kDa, hydrophobic proteins are classified into classical AQPs which are permeable only to water (AQP 0, 1, 2, 4, 5), aquaglyceroporins (AQP 3, 7, 9, 10) which transport water, glycerol and other small uncharged molecules and unorthodox AQPs (AQP 6, 8, 11, 12) made up of structurally and/or functionally distinct AQPs [231, 236-238]. Additionally, a number of AQPs have been shown to be permeable to other substances such as ammonia, hydrogen peroxide and carbon dioxide [239, 240].

Structural studies of a number of the AQPs show they have a similar basic structure comprising 2 tandem domains each consisting of 3 transmembrane α-helices and a hydrophobic loop with a highly conserved NPA (Asp-Pro-Ala) motif (Figure 1.11 and Figure 1.12) [235, 237, 241]. AQP1 assembles within the lipid bilayer as a homotetramer. Data suggests AQPs 2, 3 and 5 also exist as homotetramers however it is likely not all AQPs have this arrangement [241].

Aquaglyceroporins contain two extra peptide sequences compared to the classical AQPs [237] while AQPs 11 and 12 have limited homology with the other AQPs and have a unique NPA box [236]. Some AQP isoforms are N-glycosylated however this does not seem to be necessary for their function or transport to the membrane [242, 243].

AQP	Species	Extrarenal location	Function	Disease	Ref
0	Human	Lens of the eye	Water transport	Human - Missense mutations lead to autosomal dominant cataracts	[244]
1	Human, rat	Capillary endothelium external to brain (eg. lung, peritoneum, pancreas), lymphatic vessels, erythrocytes, choroid plexus, ciliary body, corneal endothelium, cholangiocytes, endothelia of dermis, intervertebral disc, cochlea	Water transport, ammonia transport (erythrocytes)	Human - AQP1 null – decreased pulmonary vascular permeability	[239, 245-248]
2	Human, rat, mouse	Uterus (oestrogen responsive), ureter and bladder urothelium, trigeminal ganglia	? Water transport	Rats - ? associated with detrusor overactivity Mice – AQP2 null, polyuria, failure to thrive and neonatal death Mice - ? associated with pain transmisison	[249-255]
3	Human, rat, mouse	Keratinocytes, subcutaneous and visceral adipocytes, oesphagus, stomach, ileum, colon, liver, intervertebral disc, urothelium of ureter/bladder	Water transport, glycerol transport (skin/fat/liver)	Mice - AQP3 null, impaired hydration of stratum corneum	[256-260]
4	Human, rat, mouse	Glial cells (brain and spinal cord), muscle fibres, retina, optic nerve, olfactory epithelium, cochlea, cardiomyocytes, stomach, small intestine, urothelium of ureter/bladder	Water transport	Mice - AQP4 null, impaired olfaction and retinal function, reduced brain/spinal cord oedema after injury Human - anti-AQP4 autoantibodies associated with neuromyelitis optica	[248, 256, 259, 261-268]
5	Human, rat, mouse	Salivary and lacrimal glands, lung, trachea, cochlea	Water transport ? osmosensor involved in regulating cell volume in concert with pendrin	Mice- AQP5 null produce reduced amounts of hypertonic saliva Human - Defective trafficking to the membrane in Sjogrens syndrome	[269-273]

6	Human, rat	Parotid gland, cochlea, retina	Anion transport		[248, 274, 275]
7	Human, rat	Subcutaneous and visceral adipocytes, testis (spermatids and spermatozoa), ovarian granulosa cells, liver, urothelium of ureter/bladder	Water transport, glycerol (important in adipose metabolism) transport	Mice – AQP7 null show obesity, heightened adipocyte triglyceride synthesis, increased adipose glycerol kinase activity	[258, 259, 276-279]
8	Human, rat	Exocrine pancreas acinar cells, liver, ovarian granulosa cells, trachea, bronchi, duodenum, jejunum, colon, epididymis, testis, salivary glands	Water transport	Mice – AQP8 null have a mild phenotype with increased testicular weight in males and multi-oocyte follicles in females	[276, 278, 280-284]
9	Human, rat	Subcutaneous and visceral adipocytes, liver, ovarian granulosa cells, peripheral leucocytes, spleen, lung, urothelium of ureter/bladder, brain	Water, glycerol (? role in metabolism), ammonia, urea + non-charged solutes (carbamide, polyol, purine, pyrimidine) transport	Mice- AQP9 null show increased plasma glycerol and triglycerides. Fasting in AQP9 null db/db mice causes reduced blood glucose compared to AQP9 +/- db/db mice (liver glycerol metabolism)	[259, 276, 278, 285-290]
10	Human (pseudogene in rat and mouse)	Adipocytes, duodenum, jejunum, ileum	Water, glycerol (important in adipose metabolism), urea transport		[260, 288, 291-293]
11	Rat	Testis, liver, brain, thymus	Water transport		[294-296]
12	Rat, mouse	Pancreas	Unknown	Mice – AQP12 null show more pancreatic damage in a pancreatitis model	[294, 297, 298]

Table 1.7 Extra-renal aquaporin expression

Details of the extra-renal location and function of renal aquaporin isoforms are presented. Human and murine diseases resulting from abnormalities/non-expression of these channels are indicated.

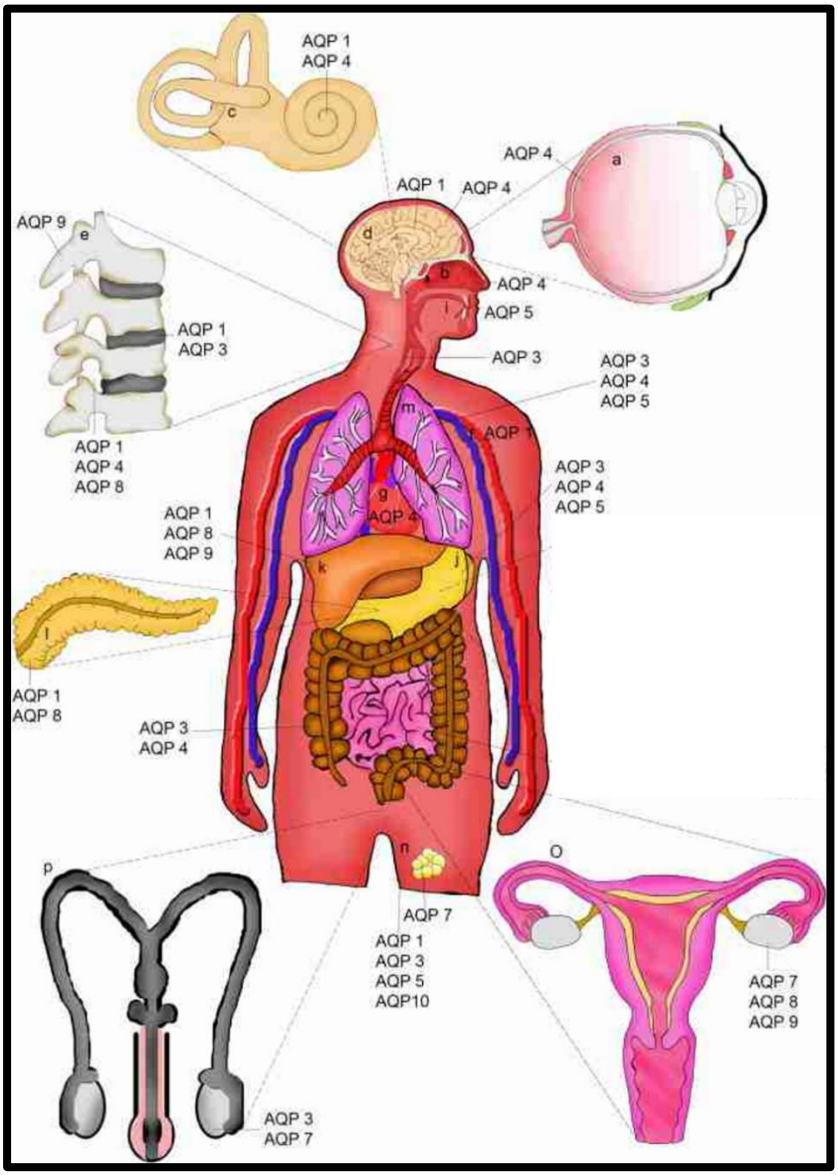

Figure 1.10 Human extra-renal aquaporin expression

Picture adapted from Day *et al*. 2014 [235]. This diagram highlights the extensive distribution of aquaporin isoforms throughout the human body

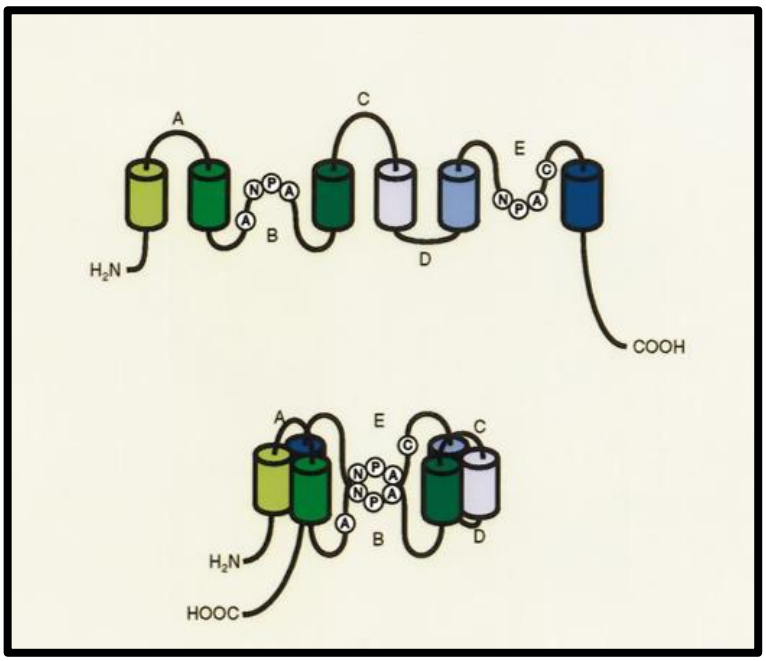

Figure 1.11 A diagrammatic representation of the structure of aquaporin 1

Picture taken from Nielsen *et al*., 2002 [241]. Each aquaporin monomer consists of 6 transmembrane domains connected by 3 extracellular loops and 2 intracellular loops. Both NH2 and COOH termini are intracellular. The aquaporin protein folds to bring the highly conserved B and E loops together forming an hourglass shaped aqueous channel. The hydrophobic NPA motif is vital for water permeability and proton exclusion

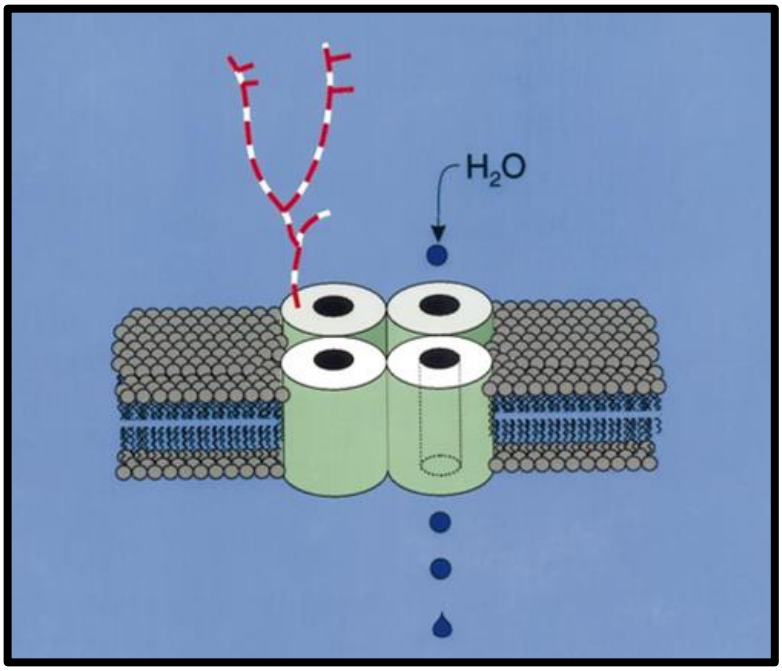

Figure 1.12 Assembly of aquaporin monomers

Picture taken from Nielsen *et al.*, 2002 [241]. Four aquaporin monomers assemble to form a homotetramer. Only one subunit carries a large glycan

1.5.2 Aquaporin expression in the kidney

The kidney is vital for physiological water, salt and acid-base balance alongside the excretion of waste products. AQPs are intrinsic to renal function and accordingly nine AQP isoforms are expressed (AQP1-8 and 11) at various sites along the nephron (Figure 1.13) [234, 299]. Within the kidney their primary role is water homeostasis and this is achieved predominantly by AQPs 1-4 which enable [255];

- near iso-osmolar reabsorption of water in the proximal tubule (AQP1)
- generation of medullary hypertonicity via participation in the counter-current exchange mechanism in the loop of Henle (AQP1)
- water re-absorption in the collecting duct regulated by circulating vasopressin (AQP2 in the apical membrane and AQPs 3 and 4 in the basolateral membrane)

The location of all renally expressed AQP isoforms alongside their potential functions and regulatory mechanisms are presented in Table 1.8.

Transgenic mice studies have eloquently demonstrated the renal role of AQP's as mice with deletions of AQP1-4 all show varying degrees of polyuria. Despite AQP4 knockout causing a four-fold reduction in the inner medullary collecting duct permeability it only leads to a mild polyuria as compared to the severe polyuria seen in the AQP3 knockout where membrane permeability is less significantly reduced. The likely explanation is that the majority of water reabsorption in the collecting duct is achieved in the connecting tubular and cortical collecting ducts and thus via AQP3 in the basolateral membrane (Table 1.9). Supporting the data from transgenic studies, mutations in AQP1 and 2 are described in humans leading to an inability to concentrate urine in response to water deprivation and nephrogenic diabetes insipidus respectively [236, 255].

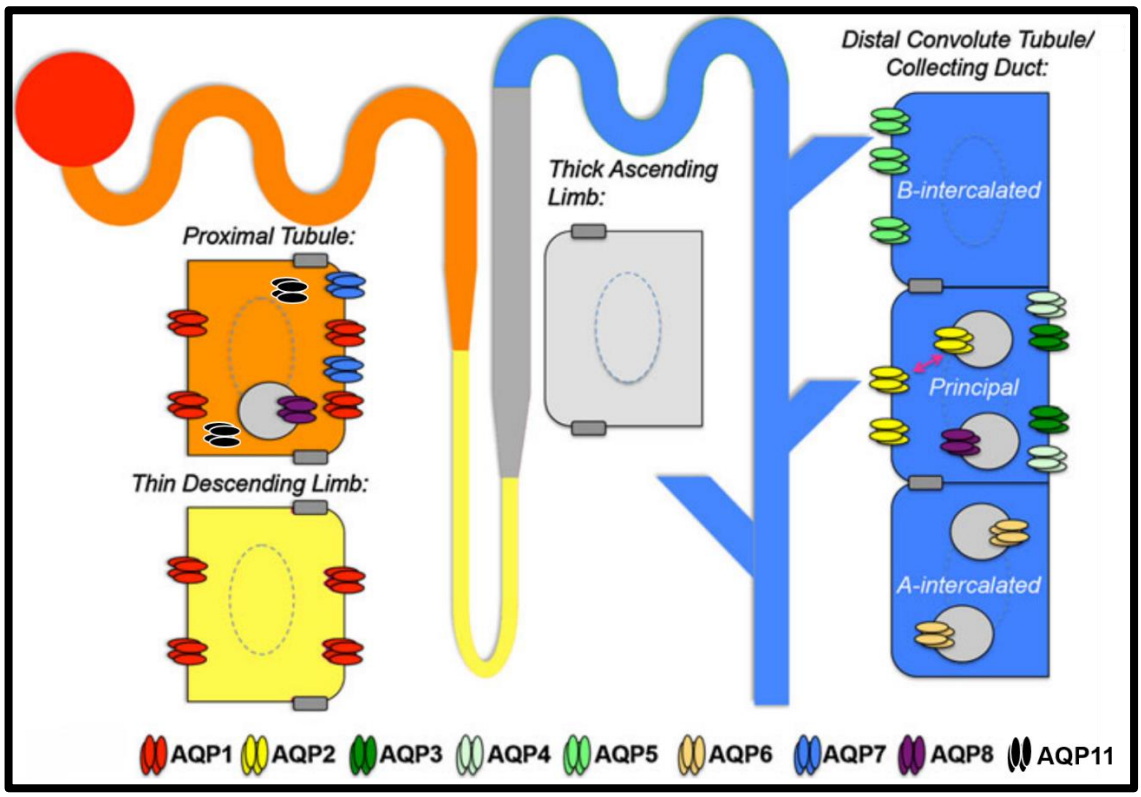

Figure 1.13 Distribution of aquaporin isoforms along the nephron

Picture adapted from Tamma *et al.* 2012 [236]. Up to 2/3 of glomerular filtrate is reabsorbed in the proximal tubule [300], the majority of which is achieved by transcellular water flow via apical and basolateral cell membrane AQP1 expression. AQP1 expression in the descending thin limb of the loop of Henle and the vasa recta also contributes significantly to the counter current exchange mechanism and the development of medullary hypertonicity. AQP2 expression in the collecting duct enables vasopressin regulated water reabsorption via the apical membrane which then exits the cell via AQPs 3 and 4 in the basolateral membrane. AQP3 is expressed in the cortical and inner/outer medullary collecting ducts while AQP4 is predominantly expressed in the inner medullary collecting ducts [255].

AQP	Species	Renal location	Subcellular location	Function	Disease (Human)	Regulation	Ref
0		Not present in kidney					
1	Human, rat, Human	Proximal tubule, descending thin limb of Henle, descending vasa recta Glomerular endothelial cells, peritubular capillaries, mesangial cells	Apical brush border, basolateral membrane Luminal and abluminal plasma membranes endothelial cells	Water transport - proximal tubule, vasa rectae, countercurrent multiplication process. Permeable to ammonia and CO_2	AQP1 null individuals have a urinary concentrating defect in response to water deprivation	Upregulated by hypertonicity (human proximal tubular cells and mouse IMCD-3 cells) via ERK, p38 kinase and JNK activation and hypertonicity responsive element (HRE) in AQP1 promoter (mouse IMCD cells). Upregulated by hypertonicity and angiotensin II (rat immortalized proximal tubule cells). Upregulated in kidney by angiotensin II (in vivo rat model)	[239, 241, 301-311]
2	Human, rat, LLC-PK1 cells, mpkCCD cells	Collecting duct principal cells, inner medullary collecting duct cells, connecting tubules	Intracellular vesicles in basal state, redistributes to apical membrane by exocytosis after vasopressin stimulation. Translocation is reversible on removal vasopressin	Regulated water reabsorption across apical membrane of connecting tubules and collecting duct	Autosomal recessive nephrogenic diabetes insipidus	Vasopressin is the major regulator of acute and chronic AQP2 expression Other regulating factors: Prostaglandin E_2, bradykinin, atrial natriuretic peptide, adenosine triphosphate, dopamine, nitric oxide, hyper/hypotonicity	[303, 312-321]

3	Human, rat	Connecting tubule cells Cortical, outer and inner medullary collecting duct cells (less at papillary tip)	Basolateral membrane	Water transport across basolateral border of collecting duct. Also glycerol, ammonia and urea transport ? role in kidney ? plays a role in acid secretion via NH_4^+		Long term but not short term upregulation by vasopressin in rats. Regulated by gating (See 1.5.3.3) Upregulated by hypertonicity (cultured human keratinocytes). Upregulated by insulin and leptin via PI3K/Akt/mTOR pathways (cultured human adipocytes and hepatocytes)	[238, 258, 288, 303, 322-325]
4	Human, rat	Collecting duct - principally inner medullary collecting duct	Basolateral membrane – predominantly basal membrane	Water transport across basolateral border of inner medullary collecting duct.		Long term regulation by vasopressin in rats. Upregulated by hyperosmolality in rat astrocytes via p38/MAPK pathway	[289, 303, 326, 327]
5	Human, rat and mouse	Connecting tubule and cortical collecting duct type-B intercalated cells	Apical membrane	Co-expressed with pendrin ? molecules co-operate as osmosensor Water and CO_2 permeable		Upregulated by hyperosmolality in rat astrocytes via ERK pathway Downregulated and moves to intracellular compartment in a murine potassium depletion model Downregulated by TNF-α associated with reduced acetylation of histone 4 (human salivary acinar cells)	[239, 289, 299, 328, 329]
6	Human, rat	Type A intercalated	Membrane of intracellular	Anions (particularly nitrate), urea,		Regulated by gating (see 1.5.3.3)	[239, 330-335]

		cells of cortical and medullary collecting duct, podocyte cell bodies and foot processes, segment 2 and 3 proximal tubule	vesicles which also contain H^+-ATPase and CIC-5 chloride channel	glycerol, ammonia, CO_2 transport, low water permeability at physiological pH ? involved in acid/base balance		Upregulated by chronic alkalosis and water loading	
7	Rat	S3 proximal tubule	Apical brush border	Predominantly glycerol transport. Also permeable to water, ammonia and urea ? involved in proximal tubular ammonia excretion/acid-base balance		Upregulated by insulin and downregulated by leptin via PI3K/Akt/mTOR pathways in cultured human adipocytes and hepatocytes	[238, 258, 336, 337]
8	Rat	Proximal tubular epithelial cells, weak expression collecting duct principal cells. Not detected in	Apical, central and basal cytoplasmic domains. Inner mitochondrial membrane	Ammonia (predominantly), water, H_2O_2 transport. ? involved in proximal tubular ammonia excretion/acid –base balance		Mitochondrial AQP8 upregulated by in vitro acidity/in vivo acidosis (HK-2 cells in acidic medium and rat studies after 7 days of oral $NH4^+Cl$ loading) Upregulated by hyperosmolality in rat astrocytes via ERK pathway	[281, 282, 288, 338-343]

		human kidney but expressed in HK2 cells.					
9	Human, rat	Not detected in kidney		Water, glycerol (? role in metabolism), ammonia, urea, CO_2, H_2O_2 + non charged solute (carbamide, polyol, purine, pyrimidine) transport		Upregulated by insulin and downregulated by leptin via PI3K/Akt/mTOR pathways in cultured human adipocytes and hepatocytes Upregulated after rodent cerebral ischaemia via p38/MAPK pathway Upregulated by hyperosmolality in rat astrocytes via p38/MAPK	[239, 240, 258, 286-289, 344, 345]
10	Human (pseudo gene in rat and mouse)	Not detected in kidney		Water, glycerol, urea transport			[238, 288, 291, 293]
11	Mouse	Proximal tubules	Endoplasmic reticulum membrane	Water transport ? renoprotective function			[294-296]
12	Rat	Not detected in kidney	Intracellular location when expressed in X. *Laevis* oocytes	Unknown			[238, 294, 297]

Table 1.8 Aquaporin isoform expression in kidney

Details of the renal location, subcellular location and function of renal aquaporins are presented. Human renal diseases resulting from abnormalities of these channels are indicated. Regulatory mechanisms of aquaporin isoform expression, investigated in renal and extra-renal tissues, are also presented.

Mouse AQP -/- knockout	Clinical features
1	Vasopressin resistant polyuria and polydipsia. Smaller then wild-type mice. Likely reduced intrauterine survival.
2	Failure to thrive and death within neonatal period with vasopressin insensitive polyuria. Inducible adult models show severe vasopressin resistant polyuria
3	Severe polyuria and polydipsia partially vasopressin sensitive, concomitant downregulation of AQP 2, hydronephrosis secondary to polyuria
4	Mild polyuria
5	No renal phenotype
7	Severe glyceroluria
8	No renal phenotype
11	Normal intrauterine survival but neonatal death due to renal failure resulting from large polycystic kidneys (cysts localized to renal cortex)

Table 1.9 Renal phenotype of murine AQP isoform congenital double knockout models [236, 255]

1.5.3 Aquaporin regulation

1.5.3.1 Regulation of renal aquaporin expression

The regulation of AQP expression in the kidney is complex and for many of the AQPs is not understood. AQP2 is the most studied as mutations of the AQP2 gene cause hereditary nephrogenic diabetes insipidus (NDI) [255]. Mutations causing both autosomal recessive (most common) and dominant NDI have been described where the mutant protein is usually retained intracellularly and thus rendered non-functional [346, 347]. X-linked nephrogenic NDI on the other hand results from mutations in the V_2 receptor for vasopressin [348]. More commonly NDI is acquired, with concomitant AQP2 downregulation. Causes include: drugs (lithium), electrolyte disturbances (hypokalaemia, hypercalcaemia) and urinary tract obstruction. [241, 347, 349].

AQP2 expression is upregulated by vasopressin secretion from the posterior pituitary gland in response to numerous stimuli including; increases in plasma osmolality, decreased circulating blood volume and angiotensin 2 acting via AT1 receptors [180]. Administration of an AT1 receptor blocker, for example, reduces vasopressin induced AQP2 expression in collecting ducts cells leading to an increased urine output [350].

In the basal state most AQP2 resides in intracellular vesicles. Acute changes in expression (seconds to minutes) occur by AQP2 trafficking from these vesicles to the apical plasma membrane of the collecting duct cells [241]. Phosphorylation of Ser-256 in the C-terminal cytoplasmic domain of AQP2 by protein kinase A (PKA) enables this vasopressin mediated transport.

Additionally, activated PKA phosphorylates, thus deactivating, the small GTPase Rho leading to the depolymerisation of F-actin allowing the intracellular vesicles access to the plasma membrane. Upon removal of vasopressin stimulation or following administration of a V2 receptor inhibitor, endocytosis of AQP2 from the membrane and back into intracellular vesicles quickly occurs [313, 315].

Long-term regulation (hours to days) of urinary concentration occurs via regulation of gene transcription and thus the total AQP2 protein levels [241]. Using the porcine kidney epithelial cell line LLC-PK1, Yasui *et al.* demonstrated that vasopressin acting via the V_2 receptor and the adenylyl cyclase/cAMP/PKA cascade, activates the transcription factors CREB (cAMP-response element binding protein) and c-Fos which bind to CRE and AP1 respectively in the AQP2 gene promoter to upregulate transcription [351].

Ultimately, vasopressin mediated AQP2 translocation to the apical membrane and upregulation of expression results in increased water reabsorption across the collecting duct and generation of a more concentrated urine [241, 313].

Although vasopressin acting via G-protein coupled V2 receptors is a major regulator of these short and long term changes it is not the sole contributor, as AQP2 expression can be altered independently of the action of vasopressin. The other factors involved in regulation are yet to be fully elucidated, however, studies suggest a role for prostaglandins by alteration of both trafficking to the cell membrane [241] and regulation of expression [352]. PGE_2 supplementation alone to rat renal inner medullary tissue does not alter AQP2 phosphorylation or its cellular distribution. Increased PGE_2 levels do, however, reduce vasopressin stimulated AQP2 translocation to the membrane [353]. Tamma *et al*. described

the mechanism behind this observation using primary rat inner medullary collecting duct cells (IMCD). PGE_2 via EP_3 receptors stimulates Rho (independent of increases in cAMP and calcium) leading to F-actin formation which physically hinders the translocation of AQP2 to the plasma membrane thus reducing apical membrane expression (Figure 1.14) [354].

In vitro studies have shown other molecules such as atrial natriuretic peptide (ANP), adenosine triphosphate (ATP), dopamine, nitric oxide and bradykinin counteract the vasopressin induced translocation of AQP2 to the apical membrane by various mechanisms. These include ubiquitination and internalisation of AQP2 from the apical membrane and lysosomal degradation (ATP and dopamine) [318], reduced gene transcription secondary to reduced cAMP levels (ATP and dopamine) [318], Rho activation via Gα/G13 protein receptors leading to F-actin polymerization (bradykinin) [319], and signalling via cGMP and protein kinase G (ANP and NO) [320]. Recent studies show further modulation of AQP2 trafficking to the membrane may be achieved by integrin signalling. AQP2 is the only AQP to contain the RGD integrin binding motif and has been shown to interact with integrin β1 by co-immunoprecipitation studies [355].

Furthermore, AQP2 is transcriptionally upregulated and downregulated by hypertonicity [356, 357] and hypotonicity respectively [321, 358]. This occurs via pathways independent of vasopressin, cAMP, PKA and CREB. Additionally, downregulation due to hypotonicity occurs independently of both prostaglandins and nitric oxide [321]. Although it has been suggested regulation by tonicity occurs via the known TonE in the AQP2 promoter alongside altered Ton EBP activity [357, 358], others have disputed this and propose that alternative transcription factors and promoter elements are involved [321].

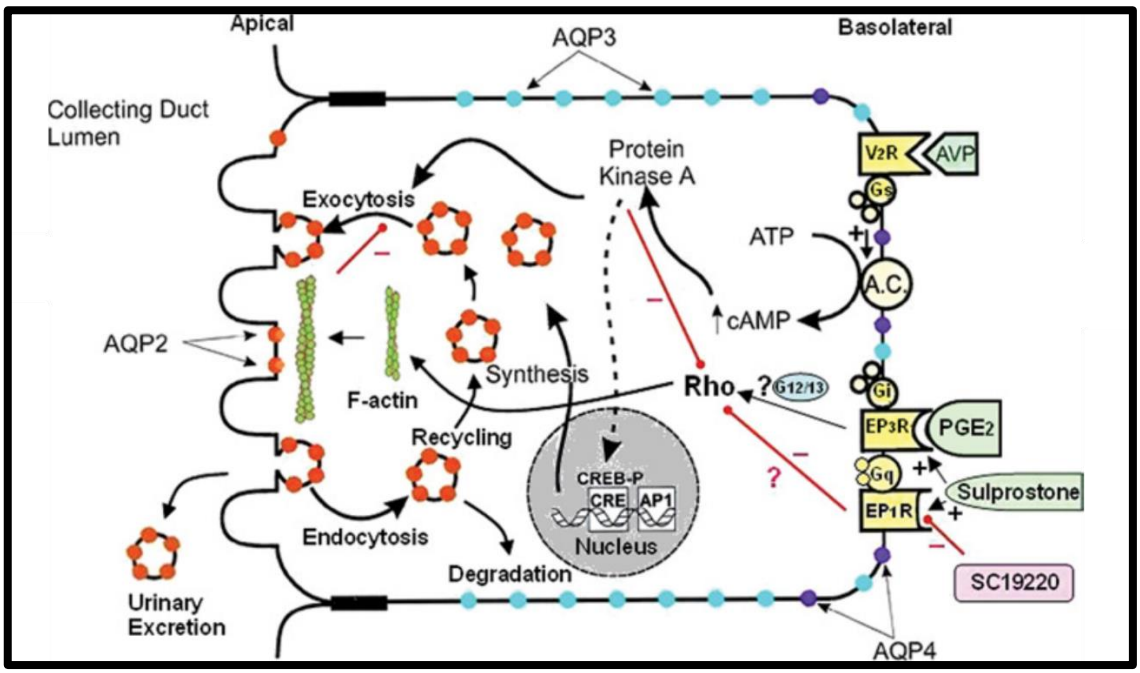

Figure 1.14 Regulation of AQP2 trafficking and synthesis in renal collecting duct cells

Picture taken from Chen *et al.* 2005 [234].Vasopressin binds to the Gs protein coupled V2 receptor which stimulates the adenylyl cyclase/cAMP/protein kinase A pathway. Subsequent phosphorylation of Ser 256 on the cytoplasmic c-terminal of AQP2 causes exocytosis of intracellular vesicles and insertion of AQP2 into the apical plasma membrane. Alongside this, PKA activation also phosphorylates, thus deactivating, Rho leading to the depolymerisation of F-actin allowing the intracellular vesicles access to the plasma membrane. Reduction in vasopressin binding to the V_2 receptor stimulates endocytosis of AQP2 back into intracellular vesicles. PGE_2 binds to the EP_3 receptor on the basolateral membrane of the collecting duct cell and via cAMP/calcium independent mechanisms activates Rho causing polymerization of F-actin which physically blocks the translocation of AQP2 to the apical membrane. EP_3 mediated inhibition of vasopressin stimulated AQP2 exocytosis is diminished by EP_1 receptor stimulation via an unknown mechanism. Vasopressin acting via the V_2 receptor also achieves long-term regulation of AQP2 expression by phosphorylating CREB which acts on the CRE promoter of the AQP2 gene thus upregulating transcription. Three to four percent of AQP2 from the apical membrane is shed within exosomes into the urine. Sulprostome is a PGE_2 analogue and EP1/EP3 agonist. SC19220 is an EP1 receptor antagonist. These compounds have been administered simultaneously during in vitro work to achieve selective EP_3 stimulation [234].

Trafficking of AQP2, to and from the apical membrane, is also affected by tonicity. Hypotonicity promotes internalisation of AQP2 from the membrane [359], while hypertonicity causes accumulation of AQP2 at the apical membrane [357].

Regulation of the other renal AQPs has been far less thoroughly investigated. In vitro and in vivo studies have demonstrated that AQP1 mRNA and protein expression is upregulated in rat proximal tubular cells by angiotensin II acting via the AT1 receptor. The response is biphasic with dose dependent increases in expression at lower concentrations of angiotensin II but suppression of AQP1 mRNA expression at higher strengths [308]. Vasopressin, however, does not directly regulate AQP1 expression [325].

In vitro studies using rat and human proximal tubular cells have demonstrated that AQP1 is also upregulated by extracellular hypertonicity [308, 309]. Using mouse IMCD-3 cells this has been demonstrated to occur via ERK, p38 kinase and JNK activation and the hypertonicity responsive element (HRE) in the AQP1 promoter [311].

AQP3 expression within the renal collecting duct shows long-term but not short-term regulation in response to vasopressin in rats [323, 325, 360]. Specifically, AQP3 is upregulated in the connecting tubules, cortical collecting ducts, inner stripe of the outer medullary collecting ducts and the initial inner medullary collecting ducts (IMCD). Interestingly, expression in the more distal IMCD is reduced in response to vasopressin [327]. Upregulation of AQP3 expression is also noted in response to hypertonicity, but this has only been demonstrated in cultured human keratinocytes [322]. Similarly, insulin and leptin have been shown to upregulate AQP3 expression via the PI3K/Akt/mTOR pathways, however this was undertaken in cultured human adipocytes and hepatocytes [258].

Using long-term vasopressin stimulation in brattleboro (vasopressin deficient) rats, Terris *et al*. demonstrated by immunoblotting that AQP4 protein expression was unchanged in the renal medulla and cortex versus control, suggesting AQP4 expression was not regulated by vasopressin [325]. Subsequently Poulsen *et al*. have challenged this view by demonstrating a varying response to vasopressin stimulation at different locations along the nephron by immunohistochemistry in this same model. In the connecting tubule and the cortical collecting duct where constitutional expression of AQP4 is low, the protein abundance of AQP4 increased following vasopressin stimulation. AQP4 expression was also increased in the inner stripe of the outer medullary collecting ducts and the initial IMCD. More distally along the IMCD however AQP4 was downregulated by vasopressin stimulation [327]. Furthermore, vasopressin stimulation has been demonstrated to affect the relative expression of various splice variants of AQP4 along the nephron [361].

Similar to the other 3 major renal AQPs, upregulation of AQP4 has been demonstrated in response to hyperosmolality in non-renal cells (rat astrocytes) via the p38/MAPK pathway [289].

Table 1.8 indicates regulatory factors identified for the other renal AQPs.

1.5.3.2 Inhibition of aquaporin isoform permeability

There are no specific inhibitors of individual aquaporin isoforms however many are inhibited by mecurials, the sensitivity to which is conferred by cysteine residues close to the conserved NPA motif for AQPs 1, 2 and 3 [237]. Notable exceptions are aquaporin 4 which is mercury insensitive being originally named mercurial insensitive water channel (MIWC) [362] and AQP 6 whose usually low water permeability is increased by mercurial treatment. Incidentally the permeability of AQP 6 for small anions is also increased by mercurial treatment signifying its potential role as an anion channel [335].

1.5.3.3 Gating of aquaporins

Studies of AQPs expressed in X. *laevis* oocytes demonstrate that external pH changes do not affect the water permeability of AQPs 0, 1, 2, 4 and 5 [363]. The water and anion permeability of AQP6, however, is promptly increased at pH<5.5. This phenomenon is reversed at physiological pH [335]. AQP3 is permeable to water and glycerol at physiological pH while at pH's around 6.1 it is predominantly permeable to glycerol as the water permeability of AQP3 is eradicated by acidic pH [363].

1.5.4 Aquaporin expression in urinary tract obstruction

AQP expression is of great interest in the context of PUJO as experimental rat models of ureteric obstruction show reduced renal expression of AQPs. Specifically, downregulation of AQPs 1, 2, 3 and 4 in the obstructed kidney and AQPs 1 and 2 in the contralateral kidney is noted following adult rat UUO suggesting both intrarenal and systemic factors are involved in their regulation [184, 186]. Bilateral ureteric obstruction followed by release is also associated with decreased renal AQP1, 2 and 3 expression, polyuria and reduced urinary concentrating ability [188, 189]. Reduction of AQP expression and significant polyuria persists at 30 days following release of bilateral ureteric obstruction and is associated with a significant urinary concentrating defect in response to thirst [189]. This suggests that reduced AQP expression is involved in the long-term concentrating defect seen after relief of urinary tract obstruction in a clinical setting. AQP expression may change with time in urinary tract obstruction as models mimicking congenital obstruction show an initial increase suggesting early compensation, followed by subsequent decrease in aquaporin expression possibly related to impairment of tubular function [364].

Dysregulation of AQP expression has also been demonstrated in humans. In children undergoing surgery for congenital hydronephrosis secondary to PUJO, renal expression of AQPs 1-4 is reduced at the mRNA and protein level compared to controls. The degree of reduction correlates with both the severity of hydronephrosis and the degree of functional impairment [187].

1.5.5 Regulation of renal aquaporin expression in the presence of urinary tract obstruction

In health, the administration of an AT1 blocker reduces vasopressin induced expression of AQP2 in collecting duct cells leading to an increased urine output [350]. In the context of ureteric obstruction however the administration of an AT1 receptor inhibitor attenuates the reduction in expression of AQP2 and improves the post-obstructive diuresis encountered following release of obstruction [162]. Similar to regulation of expression in the non-obstructed state, studies have shown that changes in expression of AQPs in obstruction may be regulated by other factors than angiotensin.

Renal levels of prostaglandin E2 and COX-2 are increased in animal models of ureteric obstruction alongside a reduction in expression of AQP2 and 3. This downregulation of AQP2 and 3 is not observed in COX-2 deficient mice with ureteric obstruction, suggesting upregulation of COX-2 and increased prostaglandin production is involved in reducing renal expression of AQPs in ureteric obstruction [352] This is supported by observations that selective COX-2 inhibition prevents AQP2 dysregulation and is associated with improvement of post-obstructive diuresis in a model of ureteric obstruction followed by release [127, 208].

Angiotensin-2 inhibition reduces COX-2 expression in ureteric obstruction and it is likely it is via this route which AT1 receptor blockers have their protective effect on AQP expression [162]. These effects are not confined to animal models, increased prostaglandin E2 excretion has been documented in children's urine alongside reduced urinary exosomal AQP2 levels in the post-operative period after pyeloplasty for PUJO [365].

Local renal production of metabolites (such as prostaglandins) resulting in reduced levels of AQPs would be consistent with the observation that in unilateral ureteric obstruction AQPs

are reduced to a far greater extent in the obstructed kidney as opposed to the unobstructed contralateral kidney [186].

1.5.6 Aquaporin expression in urothelium

The role of AQPs in the urinary tract is not confined to the kidney. Traditionally urothelium, the specialised barrier epithelium of the urinary tract, has been considered impervious to urine. However studies suggest it is able to mediate solute and water transport [366] and AQPs have been implicated in this process. Expression of AQPs 1, 2 and 3 have been demonstrated in rat bladder and ureter with expression of AQPs 2 and 3 being significantly increased in the presence of dehydration. Immunocytochemistry localises AQP2 and 3 to the urothelial cells while AQP1 is demonstrated in the vascular endothelial cells of the blood vessels [249, 367, 368].

Human urothelium expresses AQPs 3, 4, 7 and 9 at the mRNA and protein level. When cultured in vitro, human urothelial cells respond to changes in osmolality by regulating AQP3 and to a lesser extent AQP9 expression. Permeability of the urothelial cells to water and urea increases in response to an osmotic gradient, while non-selective blockade of AQP with mercuric chloride in the same model leads to reduced permeability. The authors suggest that urothelium responds to urine hypertonicity in order to regulate diffusion of water and urea [259, 369].

Alterations in AQP expression in response to urinary tract obstruction are not confined to renal tissue. In a rat model of partial bladder outlet obstruction AQP1 expression in the capillaries, arterioles and venules of bladder tissue was increased compared to controls [367] while AQP2 and 3 expression was increased in the bladder urothelial cells alongside the NOS isoforms eNOS and nNOS [368]. Currently there is no other reported work investigating changes in rodent or human urothelial AQP expression in response to urinary tract obstruction.

1.5.7 Urinary aquaporin excretion

Measuring proteins of interest in the urine is an exciting avenue of research, as it is non-invasive and offers the potential of developing biomarkers to aid in the diagnosis of disease, selection of patients for surgery and to inform clinicians and families about prognosis.

AQPs 1 and 2 are excreted in the urine of healthy humans, approximately 40-45% of which is membrane bound in extracellular vesicles [370, 371]. Conversely, in a rat model 97% of urinary AQP2 was membrane bound [372]. It is likely urinary excretion occurs via an apical pathway rather than whole cell shedding as minimal AQPs are found in urinary cellular debris and AQP3 (basolateral collecting duct expression) is absent in the urine [371, 372]. Excreted AQPs are associated with various sizes of membrane fragments, potentially representing shed plasma membrane, apoptotic bodies, microvesicles and multivesicular bodies, however, the major mode of membrane bound excretion is via exosomes [371-374]. Exosomes are nanovesicles (30-100 nm diameter) secreted by cells into the extracellular space or into body fluids such as urine. They are formed when a multivesicular body (MVB) fuses with the cell membrane and contain proteins indicating their cell of origin as well as mRNA and microRNA [375, 376]. This process is mediated by the endosomal sorting complex required for transport (ESCRT) machinery, although ESCRT independent generation of exosomes is also reported (Figure 1.15) [373].

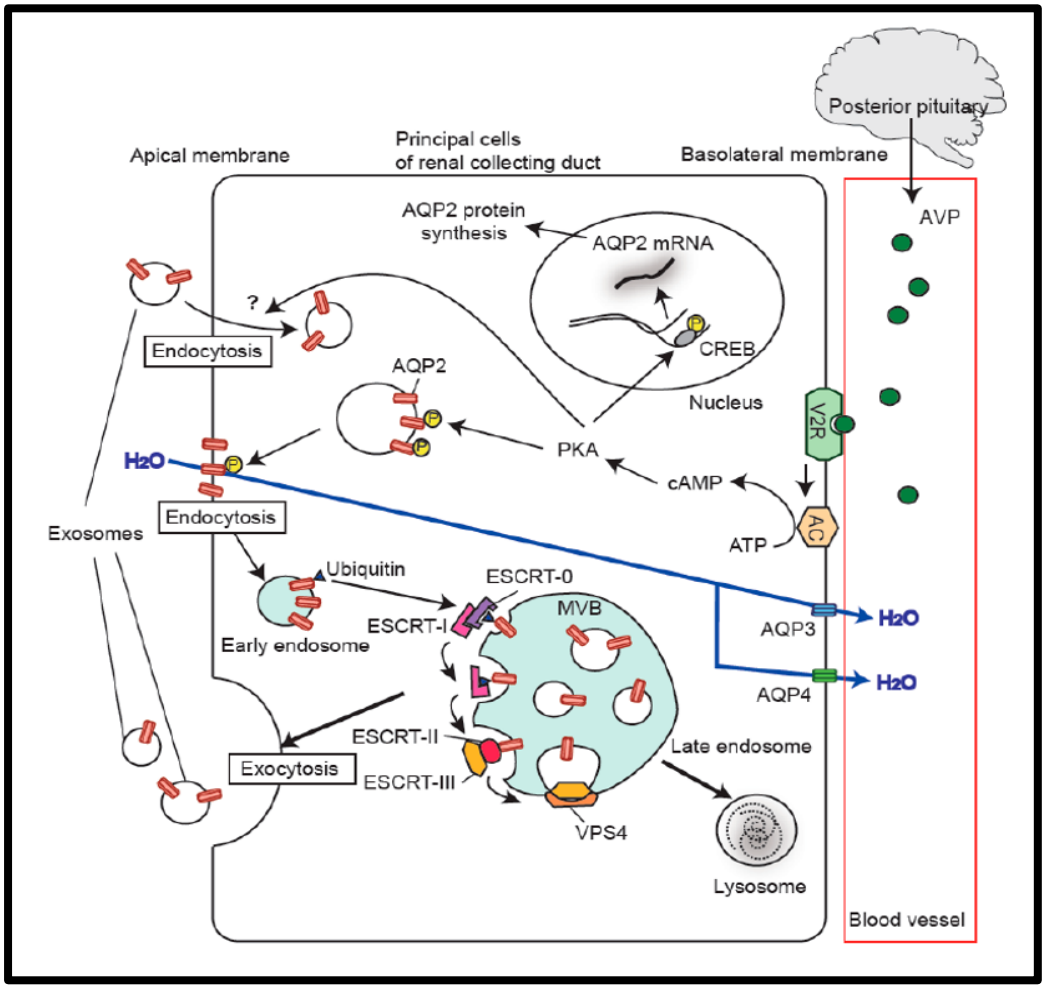

Figure 1.15 The mechanism of urinary exosomal AQP2 generation by renal collecting duct cells

Picture taken from Oshikawa *et al.*, 2016 [373] Vasopressin via V2 receptors and the cAMP/PKA pathway stimulates AQP2 trafficking to the membrane from intracellular vesicles, and upregulation of AQP2 gene transcription via the phosphorylation of CREB. Ubiquitination of apical AQP2 results in its endocytosis after which it is processed by the cytoplasmic ESCRT machinery. The ubiquitinated AQP2 is recognised and retained by ESCRT-0 (including HRS). ESCRT I (including TSG101), ESCRT II, and ESCRT III along with other proteins such as ALIX and VPS4 process the endosomes until the AQP2 is present in the membrane of intraluminal vesicles within the multivesicular body [373, 375]. The internalised AQP2 maintains the same orientation (cytoplasmic side inward) in the intraluminal vesicle membrane as it had on the cell plasma membrane. This is in contrast to endosomes where the orientation is inverted [374, 375]. Once within the multivesicular body the protein may be destined for the lysosomal pathway or exosomal release. The regulatory factors controlling this are not currently well known [375]. CREB – Cre binding protein, ESCRT – endosomal sorting complex required for transport, HRS – hepatocyte growth factor-regulated tyrosine kinase substrate, TSG101 – tumor susceptibility gene 101, ALIX – apoptosis-linked gene 2-interacting protein X, VPS4 – vacuolar protein sorting 4, MVB – multivesticular body

Exosomes have been detected from every cell type that contacts the urinary lumen along the nephron as well as urothelial cells from the lower urinary tract [374, 375]. Most urinary exosomal research has concentrated on biomarker discovery, however, exosomes have been implicated in both physiological and pathological roles including immune modulation and promoting cancer pathogenicity respectively [375, 377, 378]. The exact function of exosomal AQPs is unknown, although recent in vitro work highlights a role in intercellular signalling to the distal nephron and/or distal urinary tract. Street *el al*. demonstrated increased AQP2 expression and water permeability in unstimulated mCCDc11 (murine cortical collecting duct) cells incubated with exosomes containing AQP2. These results indicate the exosomal transfer of either signalling molecules upregulating endogenous AQP2 expression or functioning AQP2 channels to the recipient cells [379]. Subsequent in vitro and in vivo work confirmed vasopressin regulation of this process [380].

Broadly speaking the urinary excretion of both AQP1 and AQP2 parallel changes in renal expression. Total kidney AQP1 expression correlates with urinary excretion 96 hours following renal ischaemia/reperfusion in a rodent model [381]. Interestingly, acetazolamide treatment causes an increase in apical and a decrease in basolateral expression of AQP1 in proximal tubular cells which is associated with increased urinary exosomal AQP1 excretion [382].

Absolute excretion of AQP2 is the same for men and women and is unaffected by age in the adult population. AQP2/Creatinine ratios are, however, higher for women than men due to the generally lower amount of creatinine excreted in the urine [383]. Whether exogenous or endogenous (dehydration or hypertonic saline), increased levels of vasopressin result in increased urinary AQP2 excretion [371, 384, 385] mirroring the changes seen in whole kidney. On the contrary, water loading leads to reduced urinary AQP2 excretion [384, 385].

Additionally, data from rat studies suggests daily urinary excreted AQP2 represents approximately 3-4% of total kidney AQP2. However; while Rai *et al*. demonstrated this fraction was relatively unaffected by dehydration, Wen *et al.* showed that in response to changes in vasopressin urinary AQP2 levels closely follow those of AQP2 expression in the apical membrane rather than total kidney expression [372, 383]. Studies of patients with disorders of water homeostasis confirm the relationship between AQP2 excretion and vasopressin secretion whereby patients with congestive cardiac failure and cirrhosis have increased AQP2 excretion while patients with central diabetes insipidus have reduced urinary AQP2 levels [234].

Urinary excreted AQPs therefore show promise as non-invasive biomarkers of renal disease. Accordingly, post-operative urinary levels of urinary exosomal AQP1 [386] and AQP2 [365] are significantly reduced (64% and 54% respectively) in urine obtained from the obstructed kidney compared to the normal contralateral kidney in children who have had a pyeloplasty for PUJO. The reduction of AQP expression is noted for up to 4 days post-operatively, and is associated with a marked polyuria and significant decrease in urine osmolality from the obstructed kidney which persists for at least 4 days post-operatively [365]. Urinary TGF-β1 [386] and prostaglandin E2 [365] excretion is increased in urine from the obstructed kidney suggesting that changes in their production may be associated with the downregulation of aquaporins seen in urinary tract obstruction.

Proteomic studies have demonstrated the presence of exosomal AQPs 5 and 7, in addition to AQPs 1 and 2, in the urine of healthy humans [387] however this has not been confirmed by immunoblotting or ELISA.

We currently do not know what normal urinary AQP levels are in children. Additionally, there are no reports documenting urinary aquaporin levels in children being monitored for hydronephrosis with a PUJ configuration or pre-operatively in children undergoing pyeloplasty for PUJO.

1.6 Hypothesis and aims

1.6.1 Hypothesis

The central hypothesis for this project is that:

Urinary tract aquaporin expression and excretion predicts the severity of disease in human and rodent models of PUJO.

1.6.2 Aims

The specific aims of this project are to:

- ❖ Measure the distribution and quantity of AQPs in the kidney and lower urinary tract in rodent and human models of neonatal PUJO and compare this with non-obstructed kidneys. AQP expression will be correlated with renal pelvis pressure measurements and markers of kidney function.
    - **Clinical application** - Future manipulation of AQP expression in the kidney and lower urinary tract may lead to the development of new therapeutic approaches for PUJO and other obstructive uropathies.
- ❖ Establish the urinary AQP profile in high pressure (damaging) and low pressure (non-damaging) PUJO in rodents and humans
    - **Clinical application** - Defining AQP levels in the urine may lead to the development of novel operative biomarkers

Chapter 2. Materials and Methods

2.1 Cell culture

2.1.1 General cell culture

Cell culture work was performed using aseptic technique in a Microflow Biological Safety Cabinet (MDH, Andover, UK). All equipment, media and solutions used were sterile, either by autoclaving before use (Prior Clave, London) or as standard when purchased from the manufacturer. Additionally, the cabinet and all equipment were sanitised with 70% industrial methylated spirit prior to use.

Conditionally immortalised proximal tubular cells with a thermosensitive SV-40 construct [388] were grown in adherent culture in either T75 cm^2 (156499, Nunclon, Thermoscientific, Waltham, MA, USA) or T25 cm^2 (156367, Nunclon, Thermoscientific, Waltham, MA, USA) flasks containing 10 ml and 3 ml of modified RPMI 1640 media respectively (see appendix 1, section 10.1.3). Cells were viewed daily, and prior to passage and cryopreservation, using an inverted microcope (Nikon TMS, Japan) to assess the degree of confluence and ensure there was no bacterial or fungal contamination. Culture medium was aspirated and replaced with fresh modified RPMI medium every 3 days. Cells were incubated in a Hereus Function Line CO_2 incubator (Hereus, NJ, USA) in 5% CO_2 at either 33°C to produce cell proliferation or 37°C to stop proliferation and induce cell differentiation.

2.1.2 Passage of cells

Cell passage was performed when cells had reached 70% confluence. The medium was aspirated from the culture flask and the cell monolayer washed with sterile PBS using a volume equal to half the volume of culture medium. The PBS was aspirated, and the wash step repeated. Trypsin in EDTA (T3924, Sigma-Aldrich, St-Louis, MO, USA) was pipetted onto the cell monolayer, the flask rotated to ensure complete coverage and then placed in the 33°C incubator for 3-5 minutes. Following incubation, the flask was tapped to release any remaining attached cells and then assessed using the inverted microscope to ensure all cells were rounded and detached. The cells were resuspended in fresh modified RPMI 1640 medium and reseeded into fresh flasks at a cell density required for ongoing experiments.

Flasks were then placed in the 33°C incubator to allow cell proliferation. After each cell passage the passage number was increased by 1. The passage number of the cells used for each specific experiment will be noted alongside the results.

2.1.3 Culture on coverslips

Cell seeding onto coverslips was performed using trypsinised cells generated during cell passage. A single sterile coverslip was placed in each well of a 6-well plate (657160, Cellstar®, Greiner bio-one, Stonehouse, UK). Trypsinised cells were resuspended in fresh modified RPMI 1640 medium and 2 ml of the cell suspension added to each well of the 6-well plate. Plates were incubated at 33°C until 70% confluence was reached and then the cells thermoswitched by placing the plates in the 37°C incubator to achieve cell differentiation.

2.1.4 Cryopreservation of cells

Cell cryopreservation was performed when cells had reached 80-90% confluence. Trypsinisation to detach cells from the flask was performed in the same way as for cell passage (section 2.1.2). Cells were then resuspended in a volume of fresh modified RPMI 1640 medium at least equivalent to the volume of trypsin and then centrifuged at 1500 rpm for 5 minutes. Supernatant was aspirated, and the pellet washed with fresh medium. The cell suspension was centrifuged again at 1500 rpm for 5 minutes and the supernatant aspirated. Cells were resuspended in freeze medium (see appendix 1, section 10.1) and 1 ml aliquots of cell suspension placed in cryoprotective ampoules (10-500-25, Fisher Scientific, Loughborough, UK). Generally, cells retrieved from a single T75 flask would be split into 2-3 cryoprotective ampoules. Ampoules were placed in a passive freezer (Nalgene® Cryo 1°C, 5100-0001, Thermoscientific, Waltham, MA, USA) containing 100% isopropanol and placed in the -80°C freezer overnight allowing a gradual decline in temperature. Frozen ampoules were then transferred to liquid nitrogen storage.

2.2 Immunofluorescence of cultured cells

All incubations were carried out at room temperature unless otherwise stated. Details of primary and secondary antibody concentrations used can be found in the relevant chapters.

2.2.1 Fixation of cultured cells

Cells used for immunofluorescence were grown on coverslips in a 6 well plate (657160, Cellstar®, Greiner bio-one, Stonehouse, UK). Media was removed from cells, they were washed once with PBS, and then fixed in 4% paraformaldehyde (200 µl/well) for 15 minutes. A further ice-cold PBS wash was performed before permeabilising the cells by adding 0.2% Triton X-100 in PBS (1 ml/well) for 5 minutes. Cells were washed again with ice-cold PBS before treatment with 1 ml of sodium borohydride in PBS (1 mg/ml) for 10 minutes to quench any remaining paraformaldehyde and reduce cellular autofluorescence. Three further ice-cold PBS washes were performed.

2.2.2 Staining of cultured cells

The PBS wash was removed and primary antibody (see chapter 3 for dilutions and appendix 2, section 10.2.2 for specific antibody details) in 1% BSA/PBS was added to the surface of the coverslip (100 µl/well) and incubated performed for either 1 hour at room temperature or overnight at 4°C. Control cells not treated with primary antibody were incubated with 1% BSA/PBS only. Three further PBS washes were performed followed by addition of fluorochrome-labelled secondary antibody (see chapter 3 for dilutions and appendix 2, section 10.2.2 for specific antibody details) in sterile filtered PBS (100 µl/well) to the surface of the coverslip. Cells were incubated with secondary antibodies in the dark for 45 minutes. Three PBS washes were performed followed by a short rinse in distilled water to remove PBS associated salts. Coverslips were mounted onto glass slides using Vectashield® Hardset™ mounting medium with DAPI (H-1500, Vector Laboratories, Burlingame, CA, USA). Slides were then imaged using a fluorescent microscope.

2.3 RNA extraction from whole tissue

Whole tissue applies to all kidney samples and human renal pelvis and ureter samples

2.3.1 TRIzol® homogenisation

Whole human tissue samples were obtained with consent and appropriate ethical approval. Whole rat tissues were obtained under the regulations of an appropriate animal licence. Samples were immediately washed in ice-cold PBS five times, snap-frozen and stored at minus 80°C for later RNA extraction. Previously frozen samples were retrieved, weighed and ground to a powder under liquid nitrogen in a pre-cooled pestle and mortar (Z247464,

Z247502, Sigma-Aldrich, St-Louis, MO, USA). Tissues were homogenised with a hand glass homogeniser (11522443, Fisher Scientific, Loughborough, UK) for 10 minutes in TRIzol® reagent (15596018, Invitrogen, Paisley, Scotland, UK) using 1 ml TRIzol /100 mg tissue. This method of homogenisation was modified when processing samples obtained from the rat model (October 2016 onwards). Previously frozen samples were retrieved, weighed, transferred quickly from liquid nitrogen into TRIzol® reagent (15596018, Invitrogen, Paisley, Scotland, UK) (1 ml/100 mg tissue) and homogenised using an Ultra-Turrax homogeniser (TP18/10, Janke and Kunkel, IKA Works, Staufen, Germany). Following both homogenisation methods samples were incubated for a further 10 minutes at room temperature in TRIzol, then transferred to RNase/DNase free eppendorfs in 1 ml aliquots and either stored at -80°C or used directly for RNA isolation.

2.3.2 Phase separation

Unless proceeding directly from TRIzol homogenisation the RNA/TRIzol samples were retrieved from -80°C storage and thawed on ice. 200 µl of chloroform was added and the eppendorf shaken vigorously for 15 seconds. The sample was incubated at room temperature for 3 minutes and then centrifuged at 13500 rpm for 15 minutes at 4°C (5415R Microcentrifuge, Eppendorf, Hamburg, Germany). The clear aqueous phase was aspirated and transferred to a new 1.5 ml RNase/DNase free eppendorf.

2.3.3 RNA precipitation

500 µl of isopropanol was added to the aqueous phase, the eppendorfs inverted to mix and incubated at room temperature for 10 minutes. Following centrifugation at 13500 rpm for 10 minutes at 4°C the RNA was visible as a pellet within the eppendorf.

2.3.4 RNA wash

The supernatant was carefully removed and 1 ml of ice cold 75% ethanol added to the eppendorf. The sample was vortexed to mix and then centrifuged at 13500 rpm for 5 minutes at 4°C. This wash step was repeated ensuring that all supernatant was carefully and completely removed after the second wash.

2.3.5 Dissolving the RNA

The pellet was air dried for 5 minutes and then re-suspended in ultrapure RNase/DNase free water (Milli-Q Integral water purification system with BioPak, Merck Millipore, Billerica,

MA, USA). The RNA suspension was incubated at 55°C in the hotblock (Accublock™, Labnet International, New Jersey, USA) for 10 minutes and then immediately transferred to ice. The RNA suspension was separated in 10 µl aliquots in RNase/DNase free tubes (3412, Molecular Bioproducts, San Diego, CA, USA) which were either stored at -80°C or used for spectrophotometer analysis and reverse transcription to cDNA.

2.3.6 Spectrophotometer analysis

Estimation of the quantity and quality (A260/280 ratio) of RNA was made using the Nanodrop spectrophotometer (ND-1000, Thermoscientific, Waltham, MA, USA).

2.3.7 DNase treatment

DNase treatment was undertaken using a Primerdesign Precision DNase kit according to the manufacturers' instructions (DNASE-50, PrimerDesign, Southampton, UK). Briefly, 5 µl of Precision DNase reaction buffer and 1 µl of Precision DNase enzyme were added to 50 µl of RNA sample on ice. Samples were incubated in the thermal cycler at 30°C for 10 minutes followed by 55°C for 5 minutes. Samples then proceeded to reverse transcription.

2.4 RNA extraction from whole tissue ≤30 mg

Tissue ≤30 mg applies to all rat renal pelvis and ureter samples.

2.4.1 RNA extraction

Tissue samples were obtained under the regulations of an appropriate animal licence. Samples were immediately washed in ice-cold PBS five times, snap-frozen and stored at minus 80°C for later RNA extraction. RNA was extracted using an RNeasy Mini Kit (74104, Qiagen, Austin, Texas, USA) following the manufacturer's instructions. Briefly, previously frozen samples were retrieved, transferred quickly from liquid nitrogen into 600 µl buffer RLT (1 µl β-mercaptoethanol/100 µl buffer RLT) and homogenised using an Ultra-Turrax homogeniser (TP18/10, Janke and Kunkel, IKA Works, Staufen, Germany). The lysate was centrifuged at 16000 x g for 3 minutes and the supernatant retrieved into a fresh RNase/DNase free Eppendorf whereupon 600 µl of 70% ethanol was added and mixed by pipetting. Up to 700 µl of sample was added to an RNeasy Mini spin column placed in a 2 ml collection tube. The sample was centrifuged for 15 seconds at 14000 x g (1-14, Sigma-Aldrich, St-Louis, MO, USA) and the flow through discarded. This step was repeated using

the same spin column for any remaining sample/70% ethanol mix. Buffer RW1 (350 µl) was added to the column and the column centrifuged at 14000 x g for 15 seconds. RNase free DNase 1 (79254, Qiagen, Austin, Texas, USA) was made up as per the manufacturer's instructions and then 80 µl added directly to the column membrane and allowed to incubate at room temperature for 15 minutes. A further 350 µl of buffer RW1 was added to the column which was then centrifuged at 14000 x g and the flow-through discarded. Buffer RPE (500 µl) was then added to the column followed by centrifugation at 14000 x g for 15 seconds. The flow-through was discarded. A further 500 µl of buffer RPE was added to the spin column followed by centrifugation at 14000 x g for 2 minutes. The RNeasy column was then placed in a new 2 ml collection tube and centrifuged for 1 minute at 16000 x g to dry the membrane. The column was then placed into a new 1.5 ml collection tube and 30 µl of RNase free water added directly to the membrane. The column was centrifuged at 16000 x g to elute the RNA. The flow-through was carefully pipetted out of the collection tube and reapplied to the column membrane. A further centrifugation step at 16000 x g for 1 minute was performed to increase the RNA yield and the collection tube containing the RNA suspension was transferred to ice. The RNA suspension was separated in 10 µl aliquots in RNase/DNase free tubes (3412, Molecular Bioproducts, San Diego, CA, USA) which were either stored at -80°C or used for spectrophotometer analysis and reverse transcription to cDNA.

2.4.2 Spectrophotometer analysis

Estimation of the quantity and quality (A260/280 ratio) of RNA was made using the Nanodrop spectrophotometer (ND-1000, Thermoscientific, Waltham, MA, USA).

2.5 Reverse –transcription polymerase chain reaction (RT-PCR)

Following reverse transcription samples were either stored at -20°C for later use or used directly for end-point PCR analysis.

2.5.1 Reverse transcription

Reverse transcription was undertaken using the Applied Biosystems® high capacity RNA to cDNA™ kit (4387406, Applied Biosystems, Foster City, CA, USA) according to the manufacturer's instructions. Positive (with enzyme) and negative (without enzyme) reverse transcription reactions were mixed on ice with up to 1 µg of RNA being added to each 20 µl total reaction mix. Tubes were vortexed and underwent a brief centrifuge before being

placed in the thermal cycler (Sensoquest labcycler, Gottingen, Germany). Incubations were performed at 37°C for 60 minutes and the reaction was stopped by heating to 95°C for 5 minutes.

2.5.2 Polymerase chain reaction

Forward and reverse primers (MWG Eurofins, Germany) were dissolved in ultrapure RNase/DNase free water (Milli-Q with BioPak, Merck Millipore, Billerica, MA, USA) to a stock concentration of 100 µM and stored at -20°C. Forward and reverse primers were then mixed and diluted with ultrapure RNase/DNase free water to create a 10 µM working solution which was stored at -20°C. PCR mastermix was prepared on ice as per Table 2.1. Mastermix (23.5 µl) was added to each RNase/DNase free PCR tube (3412, Molecular Bioproducts, San Diego, CA, USA) to which 1 µl of 10 mM primers and 0.5 µl of cDNA or 0.3 µl genomic DNA (11691112001, Roche, Sussex, UK) was added to complete a single 25 µl reaction mix. Tubes were vortexed to mix and spun in the microfuge (1-14, Sigma-Aldrich, St-Louis, MO, USA) briefly to eliminate air bubbles. A negative 'no template' control which did not contain cDNA and a 'negative reverse transcription' control were included with every PCR run. PCR reactions were run on a thermal cycler (Sensoquest labcycler, Gottingen, Germany), with cycling conditions of: 95°C for 5 minutes followed by 35 cycles of 95°C for 30 seconds, annealing for 30 seconds and extension at 42°C for 40 seconds. Finally, elongation at 72°C for 10 minutes. Details of primer sequences and annealing temperatures can be found in appendix 2, section 10.2.1.

Mastermix component	**Company**	**Volume per reaction**
Ultrapure RNase/DNase free water	Milli-Q with BioPak, Merck Millipore, Billerica, MA, USA	20.25 µl (20.45 µl if using gDNA)
Deoxyribonucleotide triphosphate (dNTP)	NO447s, NEB, Ipswich, MA, USA	0.5 µl
10 x buffer	2200330, 5 Prime, Hilden, Germany	2.5 µl
Hotmaster Taq DNA polymerase	2200330, 5 Prime, Hilden, Germany	0.25 µl

Table 2.1 - Mastermix components of a single PCR reaction

2.5.3 Gel electrophoresis of PCR product

Two percent agarose gels were cast by combining agarose (BP1356-500, Fisher Scientific, Loughborough, UK) with TAE buffer. The gel mixture was heated in the microwave until boiling and then cooled before the addition of ethidium bromide (1.5-3.5 µl according to size of gel). The gel was poured into the casting tray containing a comb and allowed to set. Once set the horizontal electrophoresis tank was filled with TAE buffer to cover the surface of the gel. Two lanes were loaded with 6 µl of 100 bp DNA ladder (N3231S, NEB, Ipswich, MA, USA). Samples were mixed with 3 µl of 6 x gel loading dye (N3231S, NEB, Ipswich, MA, USA) and then loaded at a volume of 25 µl per well. The electrophoresis tank was connected to the power pack (170-3846, Bio-Rad, Richmond, CA, USA) and run at 110-120 V for 30-40 minutes until bands were adequately separated.

2.5.4 Imaging of PCR product

Gels were imaged using a Universal Hood 11, UV imager (BioRad, Richmond, CA, USA) and Quantity One® software.

2.6 Reverse-transcription real-time polymerase chain reaction (RT-qPCR)

2.6.1 Reverse transcription

Reverse transcription was undertaken using the Applied Biosystems® high capacity RNA to cDNA™ kit (4387406, Applied Biosystems, Foster City, CA, USA) according to the manufacturer's instructions. Positive (with enzyme) and negative (without enzyme) reverse transcription reactions were mixed on ice with up to 1 µg of RNA being added to each 20 µl total reaction mix. Tubes were vortexed and underwent a brief centrifuge before being placed in the thermal cycler (Sensoquest labcycler, Gottingen, Germany). Incubations were performed at 37°C for 60 minutes and the reaction was stopped by heating to 95°C for 5 minutes.

2.6.2 Spectrophotometer analysis

Estimation of the quantity and quality of DNA was made using the Nanodrop spectrophotometer (ND-1000, Thermoscientific, Waltham, MA, USA).

2.6.3 Real-time polymerase chain reaction

Forward and reverse primers (MWG Eurofins, Germany) were dissolved in ultrapure RNase/DNase free water (Milli-Q with BioPak, Merck Millipore, Billerica, MA, USA) to a stock concentration of 100 µM and stored at -20°C. Forward and reverse primers were then mixed and diluted with ultrapure RNase/DNase free water to create either a 10 µM or 5 µM (depending on primer optimisation) working solution prior to each PCR run. Within the UV PCR hood (UVP, Fisher Scientific, Loughborough, UK) PCR mastermix was prepared on ice consisting of SYBR green jumpstart TAQ readymix (S9194, Sigma-Aldrich, St-Louis, MO, USA), forward and reverse primer mix and ultrapure RNase/DNase free water (Table 2.2). Mastermix was loaded into each well of a 96 well PCR plate (72.1981.202, Sarstedt, Numbrecht, Germany) at a volume of 9 µl. Subsequently 2 µl of diluted cDNA (1/45 dilution for rat kidney and 1/29 dilution for rat renal pelvis) was added to each well, a plate sealer applied (95.1994, Sarstedt, Numbrecht, Germany) and the plate centrifuged in a plate spinner (PerfectSpin P, Peqlab, Leicestershire, UK) to eliminate air bubbles. A negative 'no template' control which did not contain cDNA and a 'negative reverse transcription' control were included with every PCR run.

Mastermix component	**Company**	**Volume per reaction**
SYBR Green TAQ Readymix	S9194, Sigma-Aldrich, St-Louis, MO, USA	5.5 µl
Forward and reverse primer mix	MWG Eurofins, Germany	2.23 µl
Ultrapure RNase/DNase free water	Milli-Q with BioPak, Merck Millipore, Billerica, MA, USA	1.35 µl

Table 2.2 - Mastermix components of a single qPCR reaction

Real time PCR reactions were run using the Step One Plus Real-time PCR system comparative CT method with cycling conditions of: 95°C for 10 minutes followed by 45 cycles of annealing and extension (95°C for 15 seconds, 60°C for 1 minute) then 95°C for 15 seconds and hold. Melt curves were generated for every reaction and the data analysed using StepOne Software v2.3. Details of primer sequences and working concentrations can be found in appendix 2, section 10.2.1.

2.7 Extraction of Protein

2.7.1 Extraction of protein from whole cells

A working solution of Triton X-100 containing protease and phosphatase inhibitors (P8340, p5726, P0044, Sigma-Aldrich, St-Louis, MO, USA) was made up immediately prior to use. Cells grown under sterile conditions within T75 cm^2 flasks were washed with ice cold PBS three times and incubated in ice-cold Triton X-100 lysis buffer (500 µl per T75 cm^2) on ice for 5 minutes. Cells were collected from the flask using a cell scraper (08-100-242, Fisherbrand™ Cell scraper, Fisher Scientific, Loughborough, UK) and transferred with the lysis buffer into a 1.5 ml eppendorf and placed on ice for 15 minutes. Eppendorfs were centrifuged at 13500 rpm (5415R Microcentrifuge, Eppendorf, Hamburg, Germany) at 4°C for 5 minutes. The supernatant was aliquoted in fresh 1.5 ml eppendorfs, snap frozen in liquid nitrogen and stored at -80°C.

2.7.2 Extraction of protein from whole tissue

Whole human tissue samples were obtained with consent and appropriate ethical approval (see section 6.2). Whole rat tissues were obtained under the regulations of an appropriate animal licence. Samples were immediately washed in ice-cold PBS five times, snap-frozen and stored at minus 80°C for later protein extraction. Previously frozen samples were retrieved, weighed and ground to a powder under liquid nitrogen in a pre-cooled pestle and mortar (Z247464, Z247502, Sigma-Aldrich, St-Louis, MO, USA). Tissues were homogenised on ice using a hand-held homogeniser (11522443, Fisher Scientific, Loughborough, UK) for 10 minutes in ice-cold radioimmunoprecipitation assay (RIPA) buffer (SC-24948, Santa Cruz, Dallas, Texas, USA) containing supplied protease inhibitor, sodium orthovanadate and PMSF at 10 µl/ml of RIPA buffer. One millilitre of RIPA buffer was used per 333 mg of tissue. This method of homogenisation was modified later in the research when processing the latter half of the samples obtained from the rat model (October 2016 onwards). Previously frozen samples were retrieved, weighed, transferred quickly from liquid nitrogen into ice-cold radioimmunoprecipitation assay (RIPA) buffer (1 ml RIPA/333 mg tissue) containing supplied protease inhibitor, sodium orthovanadate and PMSF at 10 µl/ml of RIPA buffer (SC-24948, Santa Cruz, Dallas, Texas, USA). Tissues were homogenised on ice using an Ultra-Turrax homogenizer (TP18/10, Janke and Kunkel, IKA Works, Staufen, Germany).

Following both homogenisation methods tissue lysates were transferred to 1.5 ml eppendorfs and agitated for 2 hours at 4°C and then centrifuged at 13500 rpm at 4°C for 10 minutes (5415R Microcentrifuge, Eppendorf, Hamburg, Germany). The supernatant was aliquoted into fresh 1.5 ml eppendorfs, snap frozen in liquid nitrogen and stored at -80°C.

2.7.3 Extraction of protein from whole tissue ≤30 mg

Tissue ≤30 mg applies to rat renal pelvis and ureter samples. This protein extraction was performed as an extension of the RNA extraction procedure using an RNeasy Mini Kit (74104, Qiagen, Austin, Texas, USA). Briefly, previously frozen samples were retrieved, transferred quickly from liquid nitrogen into 600 µl buffer RLT (1 µl β-mercaptoethanol/100 µl buffer RLT) and homogenised using an Ultra-Turrax homogeniser (TP18/10, Janke and Kunkel, IKA Works, Staufen, Germany). The lysate was centrifuged at 16000 x g for 3 minutes and the supernatant retrieved into a fresh RNase/DNase free Eppendorf whereupon 600 µl of 70% ethanol was added and mixed by pipetting. Up to 700 µl of sample was added to an RNeasy Mini spin column placed in a 2 ml collection tube. The sample was centrifuged for 15 seconds at 14000 x g (1-14, Sigma-Aldrich, St-Louis, MO, USA) and the flow through transferred to a fresh 1.5 ml Eppendorf. Four volumes of ice-cold acetone were added to the flow-through and the mixture incubated at on ice for 30 minutes. The sample was centrifuged at 13500 rpm at 4°C for 10 minutes (5415R Microcentrifuge, Eppendorf, Hamburg, Germany). The supernatant was discarded and the pellet air dried for 5 minutes. The pellet was washed with 100 µl of ice cold ethanol and then air dried for 3 minutes before resuspension in 100 µl of RIPA buffer (SC-24948, Santa Cruz, Dallas, Texas, USA) containing supplied protease inhibitor, sodium orthovanadate and PMSF at 10 µl/ml of RIPA buffer. The tissue lysate was agitated for 2 hours at 4°C and then centrifuged at 13500 rpm at 4°C for 5 minutes (5415R Microcentrifuge, Eppendorf, Hamburg, Germany) to pellet insoluble material. The supernatant was transferred into a fresh 1.5 ml Eppendorf on ice and used for BCA assay.

2.8 Bincinchoninic Acid (BCA) protein assay

The Bincinchoninic Acid protein assay was performed using the Pierce™ BCA protein assay kit (23227, Rockford, IL, USA). Bovine serum albumin (BSA, A9647, Sigma-Aldrich, St-Louis, MO, USA) was serially diluted in ultrapure water to create protein standards (1440 µg/ml to 11.25 µg/ml) which were added in duplicate (25 µl/well) to a 96 well flat-bottomed microplate (655180, Cellstar®, Greiner bio-one, Stonehouse, UK). Protein lysate samples

were diluted 1:25 and 1:50 with ultrapure water and loaded in duplicate to the microplate with a final volume of 25 µl/well. Working reagents A and B were mixed in a 50:1 ratio, 200 µl added to each well and then incubated at room temperature for 30 minutes. The plate was read at 570 nM using the Opsys MR™ microplate reader (Dynex Technologies, Chantilly, VA, USA). Revelation Quicklink Software Version 4.25 was used to generate a standard curve and determine the protein concentration of each sample.

2.9 Deglycosylation of proteins

N-Deglycosylation of proteins was undertaken using a PNGase F Kit according to the manufacturers' instructions (P0705, NEB, Ipswich, MA, USA). Briefly, 40 µg of protein lysate was combined, on ice, with 1 µl of 10x glycoprotein denaturing buffer and ultrapure water to make a total reaction volume of 10 µl. Samples were heated to denature the glycoprotein in the thermal cycler (Sensoquest labcycler, Gottingen, Germany) at 100°C for 10 minutes. Subsequently, 2 µl of PNGase F, 2 µl of 10% NP-40, 2 µl of 10x G7 reaction buffer and ultrapure water were added to make a 20 µl total reaction volume. The reaction was incubated in the thermal cycler at 37°C for 1 hour. Samples then proceeded to sample preparation for western blotting.

2.10 Concentration and fractionation of human urinary proteins

2.10.1 Ultrafiltration

Fresh human urine samples (15 ml) were placed on ice and 187.5 µl of protease inhibitor added (P2714, Sigma-Aldrich, St-Louis, MO, USA). Samples were centrifuged at 3000 rcf for 15 minutes at 4°C to remove cellular debris (Sorvall® Legend RT, Thermoscientific, Waltham, MA, USA). The supernatant was collected into an Amicon® Ultra-15 10K centrifugal filter device (UFC901008, Merck Millipore, Billerica, MA, USA) and centrifuged at 3000 rcf at 4°C for approximately 40 minutes until the volume of concentrate reached 400 µl. The concentrate was aspirated, placed into an eppendorf and an equal volume of 2 x sample buffer (working solution) was added. Samples were vortexed to mix, heated to 95°C for 5 minutes (unless otherwise stated) and then used for western blotting.

2.10.2 Ultrafiltration and chemical precipitation of exosomes

Fresh human urine samples (15 ml) were placed on ice and 187.5 µl of protease inhibitor added (P2714, Sigma-Aldrich, St-Louis, MO, USA). Samples were centrifuged at 3000 rcf for 15 minutes at 4°C to remove cellular debris (Sorvall® Legend RT, Thermoscientific, Waltham, MA, USA). The supernatant was collected into an Amicon® Ultra-15 10K centrifugal filter device (UFC901008, Merck Millipore, Billerica, MA, USA) and centrifuged at 3000 rcf at 4°C for approximately 40 minutes until the volume of concentrate reached 500 µl. The concentrate was aspirated, placed into an eppendorf and an equal volume of ExoQuick-TC™ exosome precipitation solution added. The samples were inverted to mix and placed at 4°C overnight. Subsequently samples were centrifuged at 1500 rcf at room temperature for 30 minutes to pellet the precipitated exosome fraction. The supernatant was aspirated and discarded, and the pellet centrifuged again at 1500 rcf for 5 minutes at room temperature. All traces of fluid were aspirated and discarded taking care not to disturb the exosome pellet. The pellet was resuspended in 200 µl of RIPA buffer (SC-24948, Santa Cruz, Dallas, Texas, USA) containing the supplied protease inhibitor, sodium orthovanadate and PMSF at 10 µl/ml of RIPA buffer. Tubes were vortexed for 15 seconds to ensure complete resuspension and then placed at room temp for 5 minutes to allow complete lysis of exosomes. 200 µl of sample buffer (working solution) was added, the sample vortexed to mix and then heated at 95°C for 5 minutes (unless otherwise stated). Samples were then used for western blotting.

2.10.3 Urine lyophilisation

Fresh human urine samples (5 ml) were centrifuged at 3000 x g for 15 minutes at 4°C to remove cellular debris (Sorvall® Legend RT, Thermoscientific, Waltham, MA, USA). The supernatant was collected into a 15 ml centrifuge tubes (188271, Cellstar®, Greiner Bio-One, Gloucestershire, UK) snap frozen and placed in -80°C freezer prior to lyophilisation. Frozen samples were retrieved, the centrifuge tube cap removed and the tube re-sealed with Parafilm® (P7793, Sigma-Aldrich, St-Louis, MO, USA). The Parafilm® seal was pierced multiple times with a 21-gauge needle and the samples transferred to the Benchtop Pro (VirTis SP Scientific, Suffolk, UK) for 16 hours to undergo lyophilisation. Following lyophilisation samples were stored at 4°C.

2.11 Western Blotting – Chemiluminescent and fluorescent

All incubations were carried out at room temperature unless otherwise stated. Details of primary and secondary antibody concentrations used can be found in the relevant chapters.

2.11.1 Apparatus

Mini PROTEAN equipment was used for gel electrophoresis (Bio-Rad, Richmond, CA, USA). Glass plates for gel preparation were washed with distilled water, cleaned with 70% ethanol and assembled on a casting stand.

2.11.2 Preparation of the acrylamide gel

Polyacrylamide gels were prepared by casting 4% stacking gels and 12.5% resolving gels to detect proteins of approximately 25-40 kDa. Gels were prepared according to the recipe detailed in appendix 1 (section 10.1.2) with ammonium persulphate and TEMED being added last to achieve gel polymerisation. The resolving gel was poured first, between the glass plates, to 1 cm below the anticipated position of the bottom of the comb. Filter paper was used to remove any air bubbles within the top of the gel. Once set, the top of the gel was washed with distilled water, the water removed with filter paper, and the stacking gel poured to reach the top of the glass plate. A 10 or 15 lane comb was then inserted, and the gel allowed to set.

2.11.3 Sample preparation and loading

Protein lysates were retrieved from -80°C storage and defrosted on ice. Protein concentration of the samples was determined by prior BCA assay (23227, Pierce Rockford, Illinois, USA).

For chemiluminescent western blotting, samples were diluted to a final concentration of 200 µg in 20 µl using ultrapure water. When performing the fluorescent technique, samples were diluted to a final concentration of 150 µg in 20 µl using ultrapure water. One microliter of Cy5 dye (diluted 1:10 with ultrapure water) was added to each sample in order to fluorescently label all protein. The sample was mixed and incubated at room temperature for 30 minutes.

Unless indicated otherwise for both chemiluminescent and fluorescent techniques, samples were then mixed 1:1 with 2 x sample buffer (working solution). Samples were then heated

at 95°C for 5 minutes (unless otherwise stated) in a hotblock (Accublock™, Labnet International, New Jersey, USA) followed by a short spin in the centrifuge (5415R Microcentrifuge, Eppendorf, Hamburg, Germany). The glass plates containing the polyacrylamide gels were loaded in the electrophoresis tank and the tank filled with 1 x running buffer. The combs were removed from the gels and sample loaded into the wells using a Gilson pipette (Pipetman®, Gilson, Wisconsin, USA) to achieve the appropriate total amount of protein concentration. Additionally, two lanes were loaded for each gel with either 3 µl BLUeye prestained protein ladder (S6-0024, Geneflow Ltd, Fradley, UK) for the chemiluminescent technique, or 3 µl of Amersham™ ECL™ Plex Fluorescent Marker (10320125, GE Healthcare, Buckinghamshire, UK) for the fluorescent technique.

2.11.4 Gel electrophoresis

Following sample loading the electrophoresis tank was connected to the power pack (170-3846, Bio-Rad, Richmond, CA, USA) and the gel run at 150 V for approximately 70 minutes until the samples had reached the bottom of the gel.

2.11.5 Protein transfer

When performing the chemiluminescent technique the gel was removed from the glass plates and the stack cut off. The PVDF membrane (88518, Perbioscience, Northumberland, UK) was pre-wet in methanol.

For fluorescent western blotting, the gel was removed from the glass plates and both the stack and the bromophenol blue front cut off. The gel was soaked in cold transfer buffer for 10 minutes. The PVDF hybond 0.2 µm low fluorescence membrane (10600060, Amersham™, GE Healthcare, Buckinghamshire, UK) was wet in methanol for 20 seconds then in ultrapure water for 20 seconds and then in cold transfer buffer for 5 minutes.

Subsequently for both techniques the transfer cassette was assembled under 1 x transfer buffer on the black side as follows: sponge, filter paper, gel, PVDF, filter paper, sponge. A roller was used to ensure no air bubbles were trapped between the layers and the cassette closed and placed in the transfer tank. The tank was filled with 1 x transfer buffer and an ice pack added. The tank was connected to the power pack (170-3846, Bio-Rad, Richmond, CA, USA) and transfer was performed at 250 mA for 1 hour.

2.11.6 Blocking of membrane

After completion of transfer, membranes were removed from the transfer cassette and placed in a square petri dish (foil covered for fluorescence) containing 10 ml of blocking solution. Blocking solutions used were either 5% skimmed milk (Tesco, Cheshunt, UK) in TBS-T or 3% BSA (A9647, Sigma-Aldrich, St-Louis, MO, USA) in TBS-T according to the primary antibody to be used. Blocking was carried out for at least 1 hour at room temperature with shaking.

2.11.7 Antibody incubation

The blocking solution was removed and 10 ml of primary antibody made up in either 3% BSA/TBS-T or 1% BSA/TBS-T was added (see individual chapters for dilutions and appendix 2, section 10.2.2 for specific antibody details). The membrane was incubated with primary antibody overnight (protected from light for fluorescence) at 4°C with shaking. Following incubation, the membrane was rinsed twice in TBS-T followed by 5 TBS-T washes, each for 5 minutes with shaking.

Subsequently, for chemiluminescent western blotting, 10 ml of horseradish peroxidase (HRP) conjugated secondary antibody made up in either 3% BSA/TBS-T or 1% BSA/TBS-T was added to the membrane. When undertaking the fluorescent technique, 10 ml of Cy3 conjugated anti-mouse secondary fluorescent antibody (PA43009V, GE Healthcare, Buckinghamshire, UK) diluted to 1:2500 in 3% BSA/TBS-T was added to the membrane (see relevant chapters for antibody dilutions and appendix 2, section 10.2.2 for specific antibody details).

The membrane was then incubated in secondary antibody specific for the primary antibody host for 1 hour at room temperature (protected from light for fluorescence) with shaking. Following incubation, the secondary antibody was removed, and the membrane rinsed twice in TBS-T followed by 5 TBS-T washes, each for 5 minutes with shaking.

2.11.8 Chemiluminescence imaging

Clarity™ Western ECL substrate (170-5061, Bio-Rad, Richmond, CA, USA) was used to detect antibody bound proteins. Luminol/enhancer reagent was mixed with an equal volume of peroxide solution and then applied to the membrane for 1-5 minutes. The membrane was then imaged using the ChemiDoc-It Imaging System (UVP Bioimaging Systems, Upland, CA, USA) and VisionWorks™ LS software. Images were obtained every 30 seconds for 10

minutes. Later western blots including all from the final male neonatal rat PUUO model were imaged using an Amersham™ Imager 600 (GE Healthcare, Buckinghamshire, UK). Analysis of western blots was conducted using ImageJ software.

2.11.9 Fluorescence imaging

The membrane was rinsed 3 times with TBS without tween and imaged using an Amersham™ Imager 600 (GE Healthcare, Buckinghamshire, UK). Analysis of western blots was conducted using ImageJ software.

2.11.10 Membrane stripping and re-probing following western blotting

Dry membranes were wet in methanol, added to stripping buffer (Appendix 1, section 10.1) ensuring the membrane was completely covered, and incubated for 20 minutes in a water bath at 55°C. Membranes were washed three times over 1 hour at 20 minute intervals in TBS-T at room temperature with shaking. Membranes were then blocked as in section 2.11.6 and immunostaining continued as previously described.

2.12 Sample processing for immunohistochemistry and histopathological staining

2.12.1 Sample fixation

Whole tissue samples were obtained with consent and appropriate ethical approval. Samples were immediately washed in ice-cold PBS five times, prepared to ensure sample thickness of 2-3mm and then fixed in 10% neutral buffered formalin (ratio of fixative volume to sample weight 20:1) for 24 hours at 4°C. Samples were transferred into 70% ethanol (for a maximum of 2 days) while awaiting dehydration and paraffin embedding. Dehydration and paraffin embedding of fixed samples was performed by University of Bristol research staff within the histology department, level 7, Bristol Royal Infirmary until June 2015. Subsequently, paraffin embedding of fixed samples was performed by University of Bristol histopathology staff within the Bristol Medical School histopathology laboratory.

2.12.2 Section cutting

Blocks were positioned face down on a cooling block for 10 minutes. Using a microtome the block was trimmed in by cutting 10 µm sections. Subsequently 4 µm sections were cut and then floated on a water bath at 37°C. Sections were then floated onto clean Superfrost®

plus slides (4951plus4, Thermoscientific, Waltham, MA, USA) and placed in a rack to allow water to drain. Slides were placed in a 37°C oven for 24 hours. From May 2016 onwards, histopathology sections were cut by University of Bristol histopathology staff within the Bristol Medical School histopathology laboratory.

2.13 Immunohistochemistry

2.13.1 Deparaffinisation/hydration

Slides were incubated in 3 washes of Histo-Clear (HS-200, National diagnostics, Hessle, UK) for 5 minutes each, then 2 washes in 100% ethanol for 10 minutes each, and finally 2 washes in 95% ethanol for 10 minutes each. Sections were then washed twice in ultrapure water for 5 minutes each.

2.13.2 Antigen unmasking

Slides were placed in 10 mM sodium citrate buffer pH6 and brought to the boil using a 700 Watt microwave. Slides were then maintained at sub-boiling temperature for 10 minutes. Slides were left to cool for 30 minutes and then washed twice in TBS-T for 5 minutes each.

2.13.3 Blocking

Sections were incubated in 80-100 µl of 1.5% blocking serum in TBS-T for 1 hour at room temperature in a humidified chamber. The blocking serum used was specific to the antibody combination being applied and derived from the same species in which the secondary antibody was raised (see chapters 3 and 5 for details of blocking serum used).

2.13.4 Antibody incubation

Blocking serum was drained from the slides and sections incubated with 80-100 µl of primary antibody made up in blocking serum overnight at 4°C in a humidified chamber (see chapters 3 and 5 for antibody dilutions and appendix 2, section 10.2.2 for specific antibody details). Following primary antibody incubation slides were washed 3 times in TBS-T for 5 minutes each. Sections were then incubated in 0.5% hydrogen peroxide in distilled water for 10 minutes at room temperature in a dark humidified chamber. Slides were washed 3 times in TBS-T for 5 minutes each. Sections were incubated in secondary HRP conjugated antibody 1-2 drops to each section for 30 minutes at room temperature in a humidified chamber. Secondary antibodies used are polymerised reporter antibody staining systems

specific for the primary antibody host, namely SignalStain® boost IHC detection reagent HRP anti-rabbit (Cell signalling, Danvers, MA, USA) and ImmPRESS HRP anti-goat polymer detection system (MP7405, Vector Laboratories, Burlingame, CA, USA)

2.13.5 Staining

Slides were washed 3 times in TBS-T for 5 minutes each. DAB chromogen 50x concentrate (SC-24982, Santa Cruz, Dallas, Texas, USA) was diluted 1:50 with 0.1 M Tris HCl/0.015 % H_2O_2. Each section was incubated with 80-100 µl of DAB chromogen/peroxidase substrate for 5 minutes.

Immunohistochemistry performed later in the research, for AQP3 only, utilised a different DAB chromogen (Signalstain® DAB chromogen kit, #8059, Cell signalling, Danvers, MA, USA) following a change of primary antibody (detailed in Chapter 5 section 5.2.2). The DAB substrate was made up as per the manufacturer's instructions and 80-100 µl added to each section for 5 minutes.

Following using either DAB substrate, sections were washed in ultrapure water for 5 minutes. Counter staining in Gill's #3 Haematoxylin solution (GHS316, Sigma-Aldrich, St-Louis, MO, USA) for 10 seconds was performed followed by washing with several changes of distilled water.

2.13.6 Dehydration and mounting

Slides were incubated in 95% ethanol for 10 seconds twice, then 100% ethanol for 10 seconds twice and finally Histo-Clear (HS-200, National diagnostics, Hessle, UK) for 10 seconds thrice. Excess Histo-Clear was wiped from slides and 1-2 drops of DPX mountant (44581, Sigma-Aldrich, St-Louis, MO, USA) immediately added to sections and covered with a glass coverslip (1233-3138, Fisher Scientific, Loughborough, UK).

2.14 Masson's Trichrome Stain

2.14.1 Deparaffinisation/hydration

Slides were incubated in 3 washes of Histo-Clear (HS-200, National diagnostics, Hessle, UK) for 5 minutes each, then 2 washes in 100% ethanol for 10 minutes each, and finally 2 washes in 95% ethanol for 10 minutes each. Sections were then washed twice in ultrapure water for 5 minutes each.

2.14.2 Staining

Slides were placed in pre-heated Bouin's solution (HT10132-1L, Sigma-Aldrich, St-Louis, MO, USA) and maintained at 56°C in a water bath for 15 minutes. The slides were subsequently cooled and washed in running in tap water to eradicate the yellow colouration from the sections. Sections were then incubated with working Weigert's Iron Haematoxylin solution (RRSP72-D and RRSP73-E, Atom Scientific, Manchetser, UK), made up of equal volumes of Solution A and B, for 10 minutes at room temperature. This was followed by a wash in running tap water for 10 mins then an ultrapure water rinse. The remainder of the staining was accomplished using a Masson's Trichrome Stain Kit used at room temperature (HT15-1KT, Sigma-Aldrich, St-Louis, MO, USA). Briefly, sections were incubated in Biebrich Scarlet-Acid Fucshin for 10 minutes followed by a rinse in ultrapure water and then immersion in working Phosphotungstic/Phosphomolybdic Acid Solution for 15 minutes. Slides were transferred into Aniline Blue Solution for 10 minutes and then 1% Acetic Acid for 2 minutes. Finally, sections were washed in ultrapure water.

2.14.3 Dehydration and mounting

Slides were incubated in 95% ethanol for 10 seconds twice, then 100% ethanol for 10 seconds twice and finally Histo-Clear (HS-200, National diagnostics, Hessle, UK) for 10 seconds thrice. Excess Histo-Clear was wiped from slides and 1-2 drops of DPX mountant (44581, Sigma-Aldrich, St-Louis, MO, USA) immediately added to sections and covered with a glass coverslip (1233-3138, Fisher Scientific, Loughborough, UK).

2.15 Periodic Acid Schiff Stain

2.15.1 Deparaffinisation/hydration

Slides were incubated in 3 washes of Histo-Clear (HS-200, National diagnostics, Hessle, UK) for 5 minutes each, then 2 washes in 100% ethanol for 10 minutes each, and finally 2 washes in 95% ethanol for 10 minutes each. Sections were then washed twice in ultrapure water for 5 minutes each.

2.15.2 Staining

Staining was performed at room temperature using a Periodic Acid Schiff Kit as per the manufacturer's instructions (395B-1KT, Sigma-Aldrich, St-Louis, MO, USA). Briefly,

sections were incubated in Periodic Acid Solution for 5 minutes then rinsed in several changes of ultrapure water. Sections were then incubated in Schiff reagent for 15 minutes followed by a rinse in running distilled water. Sections were counterstained in Gill's #3 Haematoxylin solution (GHS316, Sigma-Aldrich, St-Louis, MO, USA) and then rinsed in running distilled water for 5 minutes.

2.15.3 Dehydration and mounting

Slides were incubated in 95% ethanol for 10 seconds twice, then 100% ethanol for 10 seconds twice and finally Histo-Clear (HS-200, National diagnostics, Hessle, UK) for 10 seconds thrice. Excess Histo-Clear was wiped from slides and 1-2 drops of DPX mountant (44581, Sigma-Aldrich, St-Louis, MO, USA) immediately added to sections and covered with a glass coverslip (1233-3138, Fisher Scientific, Loughborough, UK).

2.16 Microscopy

2.16.1 Light microscopy

Imaging of immunohistochemistry sections was performed using a Leica DM IRB microscope and Leica IM50 (V1.20) software. Analysis of staining was performed using Image J software.

2.16.1.1 Counting of glomeruli

The number of glomeruli per field of view was established using axial kidney sections stained with Masson's trichrome. Glomeruli were counted from at least seven independent 20 x magnification images of an axial kidney section and the mean value calculated for each animal.

2.16.1.2 Quantification of renal fibrosis

Axial kidney sections stained with Masson's trichrome were used to undertake relative quantification of interstitial collagen deposition. Images were taken at 20 x magnification and at least 7 independent fields of view for each of the cortex and medulla were used for assessment of fibrosis. Using image J software a grid (50 μm^2 each square) was superimposed over each field of view and the number of points at which the blue stained collagenous fibrotic tissue intersected the grid were counted. The mean number from all

fields of view was then calculated for each animal and expressed as a percentage of the total number of grid points.

2.16.1.3 Grading of renal pelvis AQP3 staining

Grading of renal pelvis AQP3 staining in PUUO rats versus controls was undertaken blinded by 2 people, Professor Richard Coward and Miss Fern Barrington, Bristol Renal, University of Bristol. Multiple pictures were taken of the renal pelvis in paraffin embedded rat tissue using IHC. Then 6 images were randomly selected and scored for each condition. The relative intensity (score 0→5) and localisation were assessed. I then compared the "partially obstructed kidney" to its contralateral "non-obstructed" control and sham kidneys.

2.16.2 Fluorescent microscopy

Imaging of immunoflurescence sections was performed using a Leica DMI 6000B microscope.

2.17 Urine sample collection, processing and storage

2.17.1 Rodent urine

Urine samples were collected in accordance with the project and personal licences issued by the Home Office. Spot urine samples were collected at two weeks of age by allowing the pup to pass urine onto a sheet of clingfilm. Spot urine samples were obtained at 3 weeks of age by placing the pup into a cage containing hydrophobic sand (LABS-1, Datesand, Mancheser, UK). At 4 weeks of age rats were placed in a metabolic cage for up to 5 hours and urine was collected into ice-cold collection tubes cooled by surrounding ice-packs. Regardless of the method of collection, urine samples were transferred into 1.5 ml eppendorfs, placed on ice and transported immediately to the laboratory. Samples were centrifuged at 3000 rcf for 15 minutes at 4°C to remove cellular debris (Sorvall® Legend RT, Thermoscientific, Waltham, MA, USA) and the supernatant aliquoted into new 1.5 ml eppendorfs. Aliquots were snap-frozen in liquid nitrogen and stored at -80°C for later analysis.

2.17.2 Human urine

Urine samples were obtained with consent and appropriate ethical approval. Fresh urine samples obtained from either the bladder (voided pre-operatively and/or by urinary catheter

intra-operatively) and the renal pelvis (aspirated intra-operatively) were collected into a 50 ml centrifuge tubes (227270, Cellstar®, Greiner Bio-One, Gloucestershire, UK) and placed immediately into ice. Samples were transferred immediately to the laboratory and were centrifuged at 3000 rcf for 15 minutes at 4°C to remove cellular debris (Sorvall® Legend RT, Thermoscientific, Waltham, MA, USA). The supernatant was aliquoted into new 1.5 ml eppendorfs and 15 ml centrifuge tubes (188271, Cellstar®, Greiner Bio-One, Gloucestershire, UK) depending on the total volume obtained. Samples were snap-frozen in liquid nitrogen and stored at -80°C for later analysis.

2.18 Urinary creatinine assay

Creatinine stock solution (100 µg/ml) (C3613, Sigma-Aldrich, St-Louis, MO, USA) was serially diluted in ultrapure water to create creatinine standards (100 µg/ml to 0.78 µg/ml) which were added in duplicate (25 µl/well) to a 96 well flat-bottomed microplate (655180, Cellstar®, Greiner bio-one, Stonehouse, UK). Urine samples were diluted 1:10 and 1:20 with ultrapure water and loaded in duplicate to the microplate with a final volume of 25 µl/well. Working reagents A (37 mM picric acid) and B (0.3 M NaOH) were mixed in a 1:1 ratio, 50 µl added to each well and then incubated at room temperature for 6 minutes. The plate was read at 490 nm using the Opsys MR™ microplate reader (Dynex Technologies, Chantilly, VA, USA). Revelation Quicklink Software Version 4.25 was used to generate a standard curve and determine the creatinine concentration of each sample.

2.19 Urinary creatinine measurement

All urinary creatinines analysed from the final male neonatal rat PUUO model were processed as a single batch by Diagnostic Laboratories, Langford Veterinary Services, School of Veterinary Sciences, University of Bristol using a Konelab Prime 60i fully automated clinical chemistry analyser.

2.20 Urinary aquaporin 1 ELISA

2.20.1 Antigen coating of plate

Recombinant AQP1 protein was diluted in 0.1% SDS in PBS to achieve a stock solution of 400 ng/ml. This stock solution was then serially diluted in 0.1% SDS in PBS to create AQP1 standards (400 ng/ml to 3.125 ng/ml) which were added in duplicate or triplicate to a 96 well

flat bottomed high protein binding capacity plate (Nunc MaxiSorp®, 44-2404-21, Nalge Nunc International, NY, USA) at a volume of 50 µl per well. Frozen urine samples were defrosted, vortexed well and diluted with an equal volume of 0.2 % SDS in PBS. A further 2 to 3 2-fold serial dilutions were performed using 0.1% in PBS as diluent. All urine dilutions were then added in duplicate or triplicate to the 96 well plate at a volume of 50 µl per well. Blank wells were included on each plate in duplicate and triplicate and contained only 0.1% SDS in PBS. A plate sealer was applied, and the plate incubated at 4°C overnight (16 hours).

2.20.2 Blocking of plate

The plate was retrieved from incubation at 4°C and allowed to acclimatise to room temperature for 90 minutes. The antigen solution was removed and 3 washes of each well with 300 µl of PBS-T performed. Each well was incubated with 300 µl of 3% BSA (A9647, Sigma-Aldrich, St-Louis, MO, USA) in PBS blocking solution for 1 hour at room temperature.

2.20.3 Antibody incubation

The blocking solution was removed and 50 µl of anti-AQP1 antibody diluted to 1:60 in 3% BSA/PBS was added to each well. The plate was sealed and incubated for 2 hours at 37°C with agitation (70-80 rpm)(Orbital Incubator S150, Stuart Scientific, Staffordshire, UK). The antibody was removed, and 4 washes of each well was performed with 300 µl PBS-T. Fifty microlitres of HRP conjugated anti-rabbit antibody diluted 1:5000 in 3% BSA (A9647, Sigma-Aldrich, St-Louis, MO, USA) in PBS was added to each well. The plate was sealed and incubated for 1 hour at 37°C with agitation (70-80 rpm)(Orbital Incubator S150, Stuart Scientific, Staffordshire, UK).

2.20.4 Substrate incubation

The antibody solution was removed, and 5 washes of each well was performed with 300 µl of PBS-T. Tetramethylbenzidine (TMB) was added at a volume of 100 µl per well and the plate incubated in the dark for 15 minutes. One hundred microliters of 0.18 M H_2SO_4 was added to each well to stop the reaction.

2.20.5 Plate reading

The plate was read at 450 nm using the Bio-Rad iMark™ microplate reader (Bio-Rad, CA, USA). Microplate manager 6 software was used to generate a standard curve and determine the AQP1 concentration of each sample using 4 parameter logistic regression.

2.21 Statistical analysis

Microsoft Excel Software (Microsoft Corporation, WA, USA) was used to collate raw data from western blotting densitometry, qPCR CT values and microplate reader optical density values. GraphPad Prism 5 (GraphPad Software Inc, CA, USA) was used to produce descriptive statistics, generate graphical representations of the data and to undertake specific statistical analyses. For parametric data a two-tailed t-test was used to compare 2 groups while a one-way ANOVA was used for multiple group comparisons with a Tukey post-test correction. Repeated measures of multiple groups were analysed using a two-way ANOVA with Bonferroni post-test correction. Correlation of results was assessed using an XY scatter plot and Pearsons correlation test. $P<0.05$ was accepted as statistical significance.

Chapter 3. Establishing and optimising molecular biological techniques to analyse aquaporin expression

3.1 Introduction

In order to successfully meet the aims and objectives of this research it was necessary to establish and optimise a number of molecular biological techniques.

The first major aim was to measure the distribution and quantity of AQPs in the kidney and lower urinary tract in rodent and human models of neonatal PUJO and compare this with non-obstructed kidneys. At the mRNA level this was achieved by endpoint RT-PCR (reverse transcription-polymerase chain reaction) to determine the presence or absence of individual AQP isoforms (AQP0-12), followed up by real-time RT-PCR (qRT-PCR) to determine comparative expression between obstructed and non-obstructed systems.

At the protein level western blotting and immunohistochemistry was utilised to determine AQP isoform quantity and distribution respectively in obstructed versus non-obstructed systems.

Although a number of AQP isoforms (1-8, 11 in kidney and 1-4, 7, 9 in lower urinary tract) are expressed by the human and rodent renal tract, efforts were concentrated on optimising techniques to analyse the effect of urinary tract obstruction on the protein expression of AQPs 1-4. The rationale was twofold:

1. Within the nephron AQPs 1-4 are the major isoforms responsible for water re-absorption. AQP1 is localised to the apical and basolateral membranes of the proximal tubular cells and is responsible for near iso-osmolar water re-absorption whereby the vast majority of the filtered fluid is re-absorbed. AQP1 is also found in the thin descending limb of the loop of Henle and the vasa recta and is involved in generating medullary interstitial hypertonicity thus enabling the production of concentrated urine. AQP2 shuttles between cytoplasmic vesicles and the apical membrane of the collecting duct cells and is responsible for vasopressin regulated water re-absorption from the collecting duct. AQPs 3 and 4 are sited on the basolateral membrane of collecting duct cells with AQP3 tending to be situated in the proximal collecting duct whereas AQP4 is sited more distally in the inner

medulla. Thus AQPs 2, 3 and 4 work in concert to allow transepithelial movement of water [255]. The vital role of renal AQPs 1-4 is powerfully demonstrated by transgenic mice studies. Mice with AQP1-4 deletions all show varying degrees of polyuria. Conversely AQP5, 7, 8 and 11 knockout mice do not develop polyuria and do not show a renal phenotype other than increased urinary glycerol clearance in AQP7 null mice and polycystic kidneys in AQP11 null mice [255, 389]. Moreover, mutations in AQPs 1 and 2 are described in humans leading to an inability to concentrate urine in response to water deprivation and nephrogenic diabetes insipidus respectively [255].

2. The lower urinary tract rat bladder and ureter expresses AQPs 1-3 at the protein level with AQP1 localising to the vascular endothelium while AQPs 2 and 3 are present in the urothelium [249]. Although AQP2 has not been demonstrated in human urothelium, AQPs 3, 4, 7 and 9 are expressed by these cells [369]. Rodent and human studies suggest urothelial expression of AQPs 2, 3 and 9 can be regulated by hydration status or surrounding osmolality [249, 369].

Ultimately, AQPs 1-4 are the most studied of the renally expressed AQPs giving solid scientific groundwork on which to base this research. However analysis of the mRNA expression of the other AQPs, 0 and 5-12, in renal and lower urinary tract tissue will be undertaken to establish specifically which of the 13 isoforms are expressed by these tissues enabling later analysis of whether they are regulated by PUJO.

The second major aim of the research was to establish the urinary AQP profile in high pressure (damaging) and low pressure (non-damaging) PUJO in rodents and humans. AQPs 1 and 2 are both excreted within exosomes in the urine therefore giving the opportunity for urine AQP and tissue AQP results to be correlated in obstructed versus non-obstructed systems [365, 386]. Additionally, reduced urinary excretion of both AQP isoforms has been noted post-operatively in children undergoing pyeloplasty highlighting their relevance to this study. Efforts were therefore concentrated on establishing techniques to identify and quantify AQPs 1 and 2 in the urine.

Presented below are the techniques that were established during the research project.

3.2 Reverse transcription polymerase chain reaction (RT-PCR)

The end point RT-PCR technique was undertaken as per the methods detailed in Chapter 2. The technique was performed using primer sequences as described by Rubenwolf *et al.* [259] (see appendix 2, section 10.2.1 for primer sequences and annealing temperatures).

PCR using human genomic DNA (11691112001, Roche, Sussex, UK) (Figure 3.1) in place of cDNA was initially performed as positive control to confirm the suitability of the primers. As illustrated, a single band of the correct size was achieved for each primer pair.

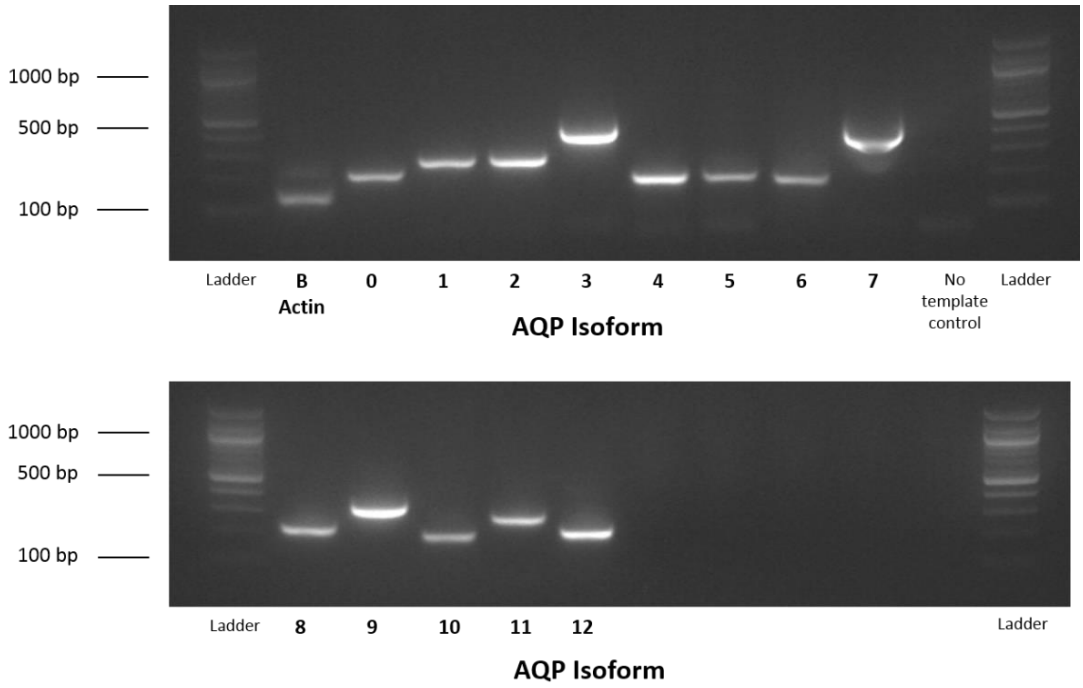

Figure 3.1 Endpoint PCR using human genomic DNA

PCR was performed using human genomic DNA and the product run on a 2% agarose gel. Bands of the appropriate size for AQP isoforms 0-12 and b-actin were demonstrated. See appendix 2, section 10.2.1 for product sizes.

Subsequently the same primers were used, under the same conditions, for cDNA obtained following reverse transcription of RNA isolated from human kidney, ureter and renal pelvis. Positive (with enzyme) and negative (without enzyme) reverse transcription (RT) reactions were performed on the RNA obtained from each tissue sample. The products from both RT positive and RT negative reactions were used when performing PCR with each set of AQP primers. The presence of bands in some of the lanes containing RT negative samples indicated genomic DNA contamination of the RNA extraction. This was seen in both kidney and ureter RNA samples used for RT-PCR. The gel shown in Figure 3.2 illustrates this, as

RT negative samples show a band the same size as the genomic DNA controls seen in Figure 3.1. Empty lanes left between loaded samples ensured contamination was not due to spill over.

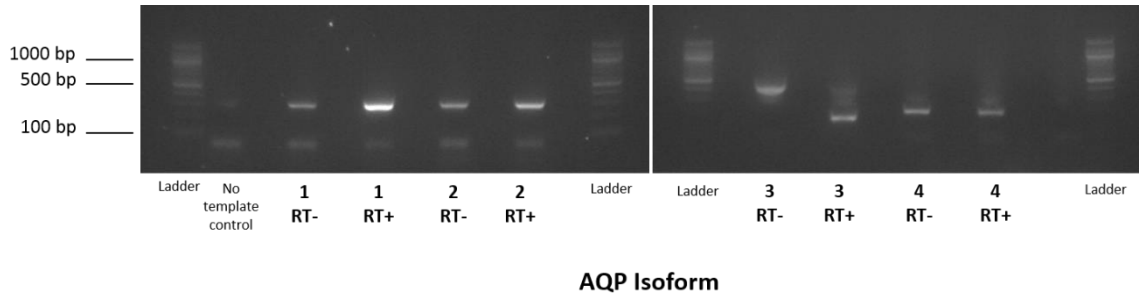

Figure 3.2 Genomic DNA contamination of human whole ureter RT-PCR

RT-PCR including positive and negative reverse transcription (RT) reactions for each AQP1-4 isoform. Bands are seen in negative RT reactions indicating genomic contamination.

All reagents were changed, and new RNA samples extracted however this issue of genomic DNA contamination was only finally resolved by treating RNA samples with a DNAase (DNASE-50, PrimerDesign, Southampton, UK) prior to reverse transcription.

A further issue that was encountered was the appearance of a hazy opacity present at about 250 bp on a number of gels. This opacity didn't have the appearance of a classic band representing PCR product (Figure 3.3). All reagents were changed sequentially, and repeat RT-PCR performed. Eventually the sample loading buffer was identified as the source of the problem (Figure 3.4).

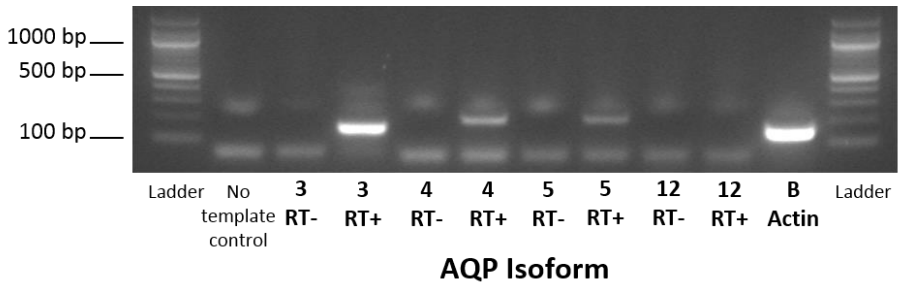

Figure 3.3 Ill-defined opacities present on all lanes of PCR gels

Hazy opacities were noted at approximately 250 bp across all lanes of numerous PCR gels. This gel demonstrates RT-PCR product from human whole kidney using AQP3, 4, 5, 12 and b-actin primers. Reverse transcription (RT) positive and negative reactions for each AQP isoform are shown.

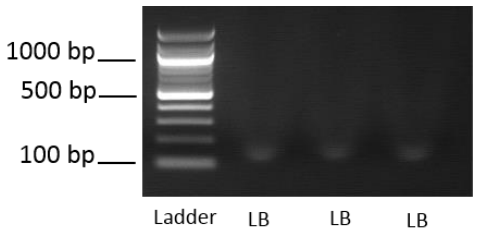

Figure 3.4 Loading buffer causes ill-defined opacities on PCR gels

Loading buffer only was loaded to 3 wells of a 2% agarose gel and run as per the method section in Chapter 2.

The sample loading buffer was substituted for the commercial gel loading dye which accompanies the DNA ladder and the hazy opacities resolved on subsequent gels.

Once optimised this technique was used to assess AQP isoform expression by human kidney, renal pelvis and ureter (see Chapter 6). The same technique using newly designed primers against rat AQPs (see Section 3.3) was utilised to evaluate AQP isoform expression by rat kidney and renal pelvis (see Chapter 5).

3.3 Reverse transcription real time polymerase chain reaction (RT-qPCR)

3.3.1 Primer design for rat aquaporin isoforms

NCBI Primer-BLAST was used to design primers to detect rat AQPs 0-12. Briefly, the National Center for Biotechnology Information (NCBI) nucleotide database was used to search for the relevant aquaporin and the NCBI reference sequence obtained (Figure 3.5 A). The reference sequence was entered into NCBI/Primer-Blast (Figure 3.5 B) (https://www.ncbi.nlm.nih.gov/tools/primer-blast) and the parameters for primer generation specified, aiming for a product size of 80-200 base pairs, a melting temperature of 60°C, a primer GC content of 40-60%, maximum self-complementarity of 4 and maximum 3' self-complementarity of 1. A report of potential primer pairs was then produced by the Primer-BLAST tool (Figure 3.6). Where possible primers were designed to cross exon boundaries thus eliminating the possibility of amplifying genomic DNA.

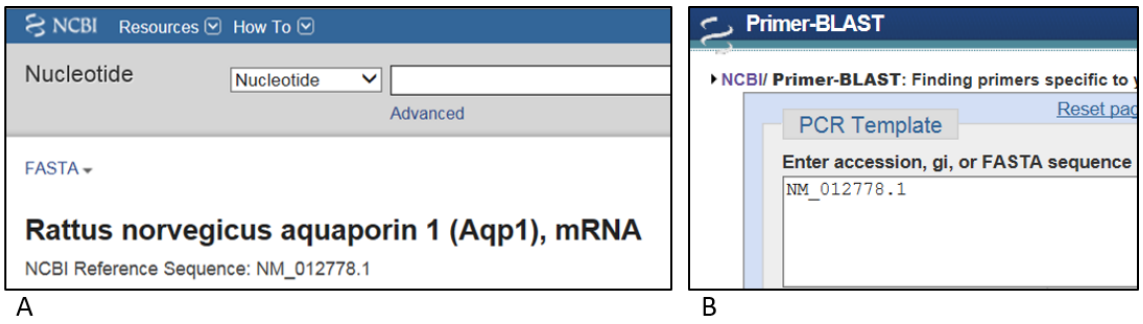

Figure 3.5 The NCBI database and Primer-BLAST are used to generate potential primer sequences for PCR

The NCBI nucleotide database is used to retrieve the reference sequence for the particular aquaporin mRNA (A). The NCBI reference sequence is entered into the Primer-BLAST website (B) and subsequently the parameters for primer generation are entered into the Primer-BLAST tool which then generates potential primer pairs.

The most suitable primer sequences generated by Primer-BLAST were then taken to the next step of primer design. CLC sequence viewer (version 6.8.2, CLC Bio, Qiagen, UK) was used to generate the cDNA product sequence for each primer pair (Figure 3.7) and the product sequence was input into mFold web server to assess likely folding of the cDNA product [390]. This software is a prediction tool which enables the user to determine whether the cDNA product is likely to form secondary structures during the PCR cycle (based on the products melting temperature), and if so their location within the PCR product (Figure 3.8). The presence of secondary structures within the region of the primer binding sites precludes the use of the primers and a new set of primers should be designed.

Forward and reverse primers designed by this method were obtained from Eurofins (MWG Eurofins, Germany) and then validated for RT-qPCR using rat kidney cDNA.

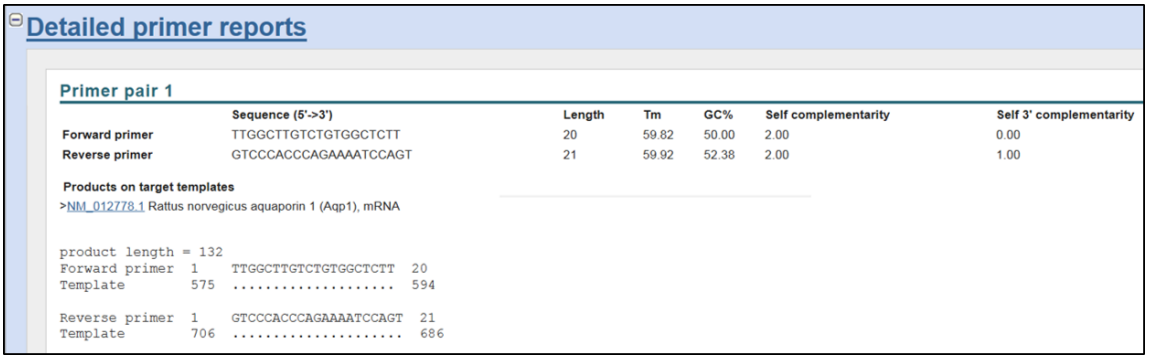

Figure 3.6 Example of a single primer pair report generated by Primer-BLAST

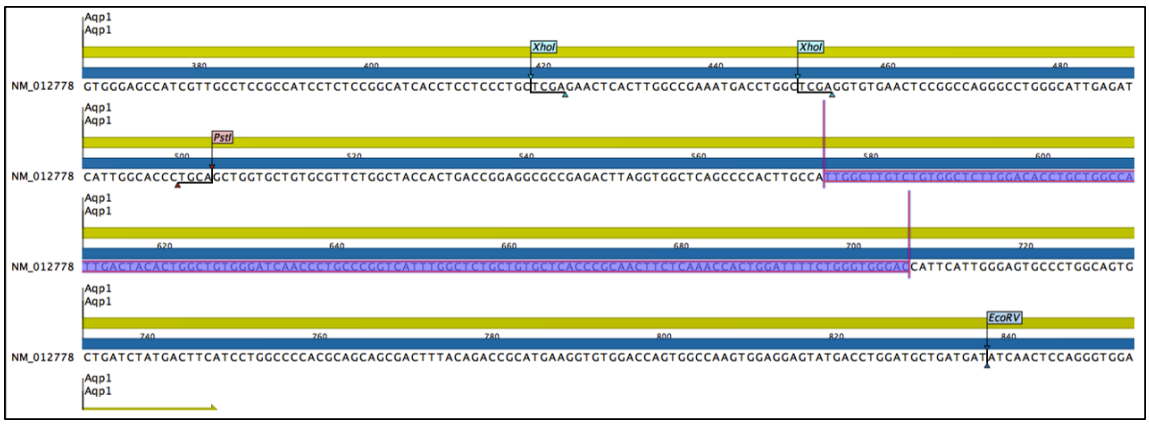

Figure 3.7 CLC sequence viewer generates the cDNA product sequence for a primer pair

CLC sequence viewer enables the nucleotide sequence of the PCR product to be identified, seen here highlighted in purple.

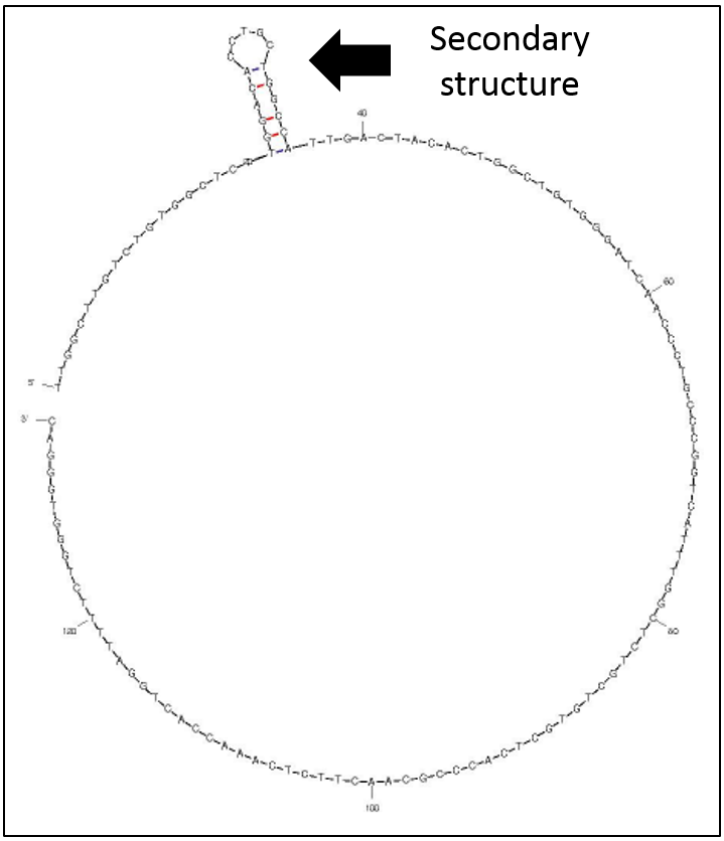

Figure 3.8 Mfold

The mfold web server generates a prediction of secondary structure formation and their potential sites within the PCR product. This PCR product demonstrates secondary structure formation (arrow) however this structure was just outside of the primer binding sites therefore not affecting primer binding

3.3.2 Primer validation

The C_t (threshold cycle) values generated during real-time PCR are inversely proportional to the DNA copy number in the original sample. In order to obtain accurate, reproducible results the reaction needs to be optimised so that the amplification process proceeds with the same efficiency regardless of the initial starting amount of template. For each set of primers this was assessed in four ways by:

- Generating a standard curve of serial dilutions of template and calculating the R^2 value. For a well optimised reaction a linear standard curve should be generated with an R_2>0.980.
- Calculating the amplification efficiency of the primers using the slope of the standard curve. Amplification efficiency should be roughly 90-105%.
- Generating a single peak on the melt curve across template dilutions.
- Demonstrating reproducibility between repeat reactions.

Failure to meet these standards led to further optimisation of the reaction parameters or redesign of the primers. Primer pairs were also tested by endpoint PCR to confirm the presence of a single product of the correct size (See Chapter 5). The final primer sequences used for RT-qPCR of rat tissue are detailed in appendix 2 (section 10.2.1.2).

3.3.2.1 Rat aquaporin 1-3 primers

Primer pairs for APQs 1-3 were tested using a 1/5 serial dilution of rat kidney cDNA. The RT-qPCR technique was undertaken as per the methods detailed in Chapter 2. The standard curves generated, and amplification efficiencies calculated were acceptable for all three primer pairs while melt curves demonstrated a single peak (Figure 3.9, Figure 3.10, Figure 3.11). These primer pairs were therefore used in sample analysis for the neonatal unilateral ureteric obstruction model.

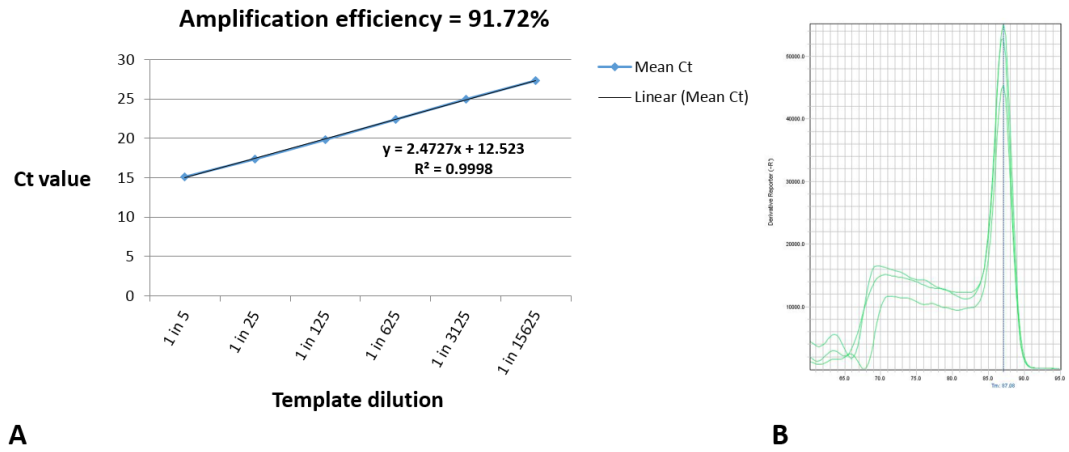

Figure 3.9 Standard curve and melt curves for real-time PCR of rat kidney cDNA using AQP1 primers

Standard curve generated for AQP1 primers using a 1/5 serial dilution of rat kidney cDNA demonstrating an R^2 = 0.9998 and amplification efficiency of 91.72% (A). Melt curves for rat kidney cDNA amplified with AQP1 primers (B).

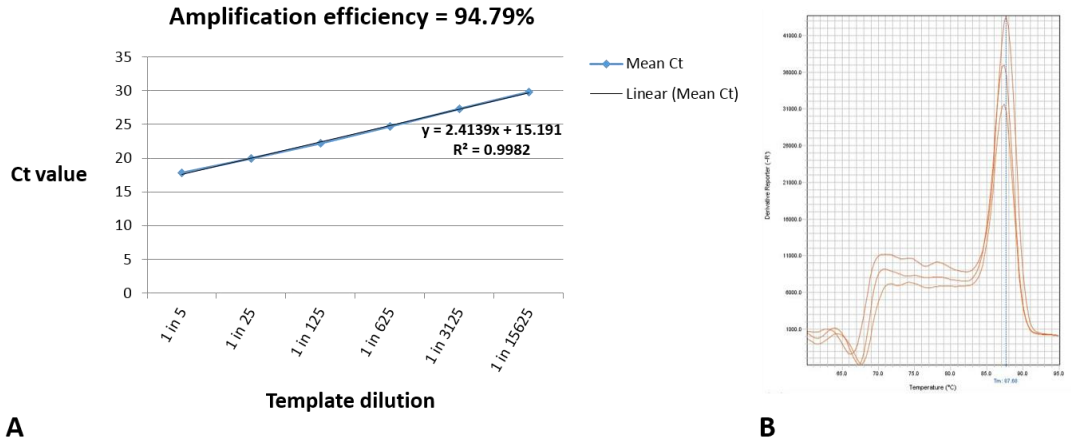

Figure 3.10 Standard curve and melt curves for real-time PCR of rat kidney cDNA using AQP2 primers

Standard curve generated for AQP2 primers using a 1/5 serial dilution of rat kidney cDNA demonstrating an R^2 = 0.9982 and amplification efficiency of 94.79% (A). Melt curves for rat kidney cDNA amplified with AQP2 primers (B).

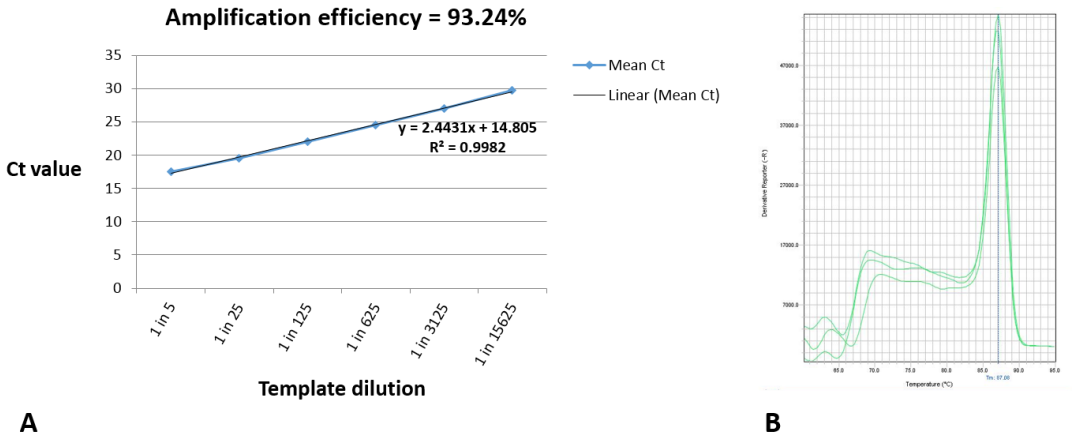

Figure 3.11 Standard curve and melt curves for real-time PCR of rat kidney cDNA using AQP3 primers

Standard curve generated for AQP3 primers using a 1/5 serial dilution of rat kidney cDNA demonstrating an R^2 = 0.9982 and amplification efficiency of 93.24% (A). Melt curves for rat kidney cDNA amplified with AQP3 primers (B).

3.3.2.2 Rat aquaporin 4 primers

The initial set of designed AQP4 primers didn't cross exon boundaries and when used for endpoint PCR demonstrated signal in the RT negative samples despite treating samples with DNase. The band in the RT negative sample was sequenced (MWG Eurofins, Germany) and confirmed to be AQP4. Two new primers pairs were therefore designed to identify the four known AQP4 transcripts. One primer pair identified transcripts 1 and 2 and the other transcripts 3 and 4. Initial optimisation for RT-qPCR using a 1/5 serial dilution of rat kidney cDNA generated melt curves with large secondary peaks corresponding to primer dimers beyond a dilution of 1 in 125 for the transcript 3/4 primers and a dilution of 1 in 625 for the transcript 1/2 primers. The amount of primers in the reaction for both primer pairs was therefore reduced by 50% and the qPCR repeated (Figure 3.12 and Figure 3.13). Although the melt curves were improved by this modification the amplification efficiencies remained unacceptably high for both sets of primers. This could be due to co-amplification of non-specific products or the presence of inhibitors. These primers were therefore discarded. Following a literature search new primer sequences identifying all 4 AQP4 transcripts were obtained from a paper published by Nicaise *et al*. [391] and these were tested using a 1/5 serial dilution of rat kidney cDNA. Initially the melt curves showed secondary peaks due to primer dimer formation at most dilutions which was improved by reducing the amount of primers in the reaction by 50% (Figure 3.14). This primer pair was thus used in sample analysis for the neonatal rat unilateral ureteric obstruction model.

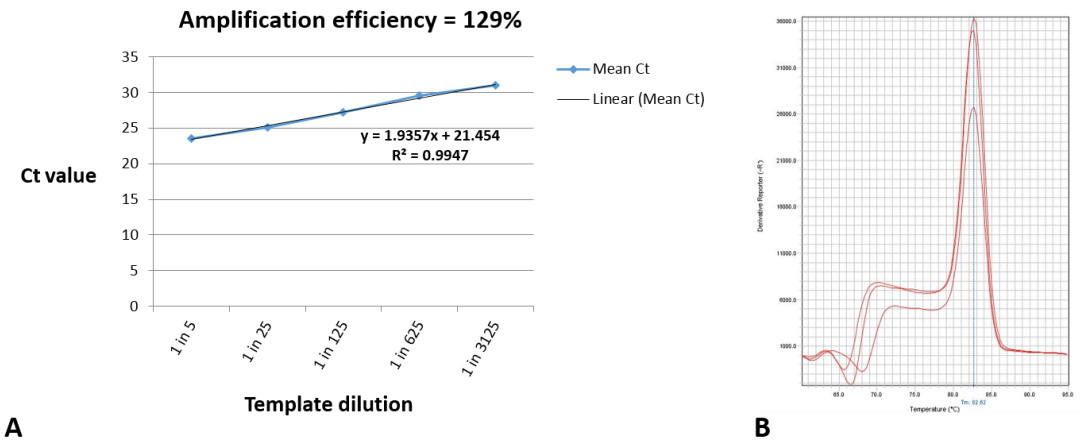

Figure 3.12 Standard curve and melt curves for real-time PCR of rat kidney cDNA using AQP4 transcript 1 and 2 primers

Standard curve generated for AQP4 transcript 1 and 2 primers using a 1/5 serial dilution of rat kidney cDNA demonstrating an R^2 = 0.9947 and amplification efficiency of 129% (A). Melt curves for rat kidney cDNA amplified with AQP4 transcript 1 and 2 primers (B).

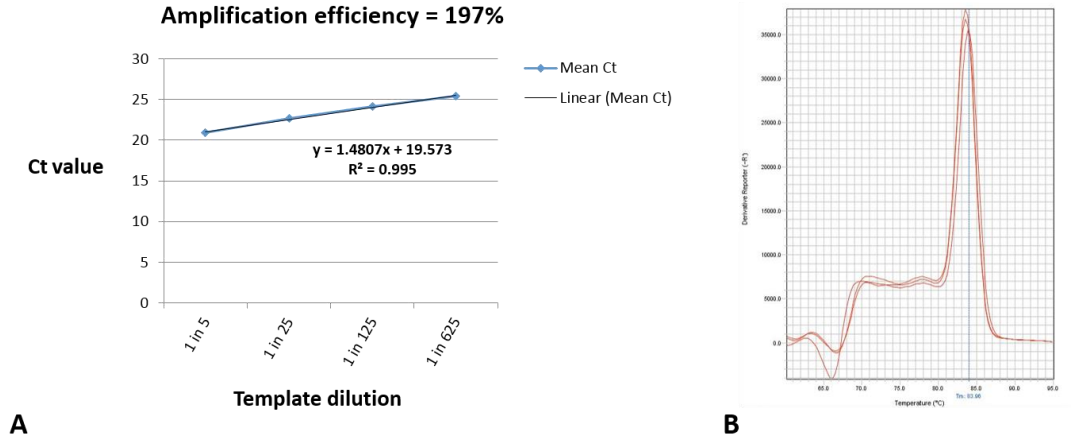

Figure 3.13 Standard curve and melt curves for real-time PCR of rat kidney cDNA using AQP4 transcript 3 and 4 primers

Standard curve generated for AQP4 transcript 3 and 4 primers using a 1/5 serial dilution of rat kidney cDNA demonstrating an R^2 = 0.9995 and amplification efficiency of 197% (A). Melt curves for rat kidney cDNA amplified with AQP4 transcript 3 and 4 primers (B).

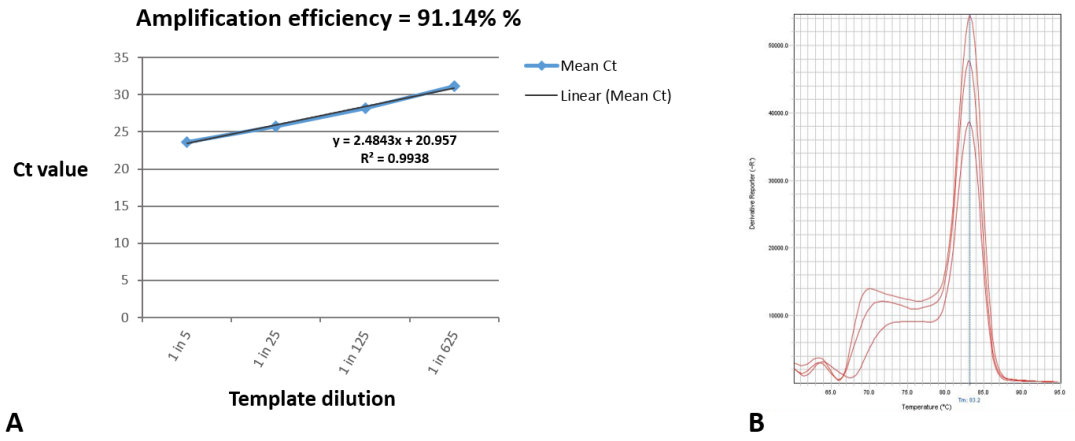

Figure 3.14 Standard curve and melt curves for real-time PCR of rat kidney cDNA using AQP4 primers

Standard curve generated for new AQP4 primers using a 1/5 serial dilution of rat kidney cDNA demonstrating an R^2 = 0.9938 and amplification efficiency of 91.14% (A). Melt curves for rat kidney cDNA amplified with new AQP4 primers (B). Primers taken from *Nicaise et al*. paper [391]

3.3.2.3 Rat aquaporin 5 primers

The first AQP5 primer pair when tested over a 1/5 serial dilution of rat kidney cDNA failed to show a rise in Ct value across the different dilutions. New AQP5 primers were therefore designed and real-time PCR repeated again using a 1/5 serial dilution of rat kidney cDNA. Unfortunately, only the first 2 cDNA dilutions had acceptable melt curves, the remainder had moderate to large secondary peaks rendering it impossible to draw a standard curve. It is likely that the amount of AQP5 cDNA is generally low in rat kidney therefore the next step will be to reduce the amount of AQP5 primers in each reaction or alternatively use cDNA from a tissue rich in AQP5 to optimise the PCR reaction. Due to time constraints further optimisation of the AQP5 primers was not performed and therefore AQP5 primers were not available when analysing tissue obtained from the neonatal rat unilateral ureteric obstruction model during this research project.

3.3.2.4 Rat aquaporin 6 and 7 primers

Initial optimisation of AQP6 and 7 primers using a 1/5 serial dilution of rat kidney cDNA for qPCR generated acceptable standard curves and amplification efficiencies, however, in both cases they were only valid up to a template dilution of 1 in 3125. Beyond this dilution the melt curves had large secondary peaks corresponding to primer dimers. The amount of primers in the reaction for both AQP6 and 7 primers was therefore reduced by 50% and the reactions performed using a 1/10 serial dilution of rat kidney cDNA. The standard curves generated, and amplification efficiencies calculated were acceptable, while the melt curves

demonstrated a single peak (Figure 3.15 and Figure 3.16). These primer pairs were therefore used in sample analysis for the neonatal rat unilateral ureteric obstruction model.

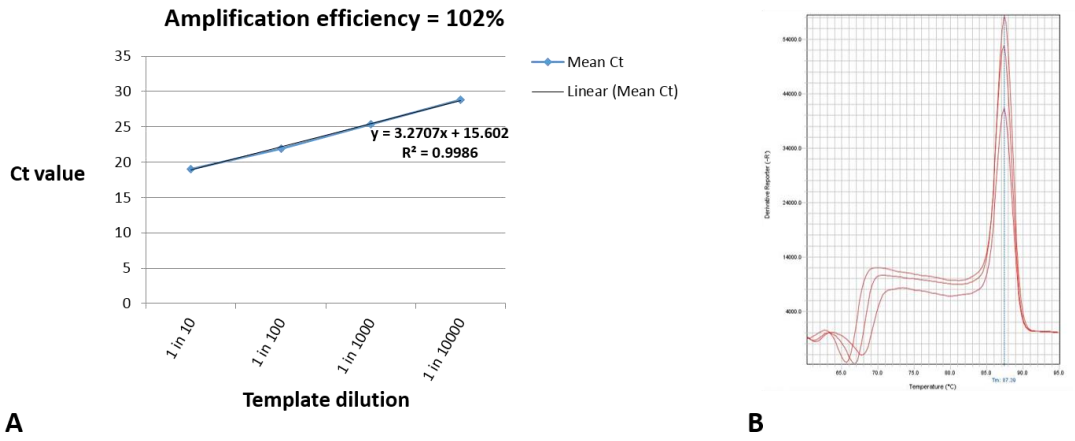

Figure 3.15 Standard curve and melt curves for real-time PCR of rat kidney cDNA using AQP6 primers

Standard curve generated for AQP6 primers using a 1/10 serial dilution of rat kidney cDNA demonstrating an $R^2 = 0.9986$ and amplification efficiency of 102% (A). Melt curves for rat kidney cDNA amplified with AQP6 primers (B).

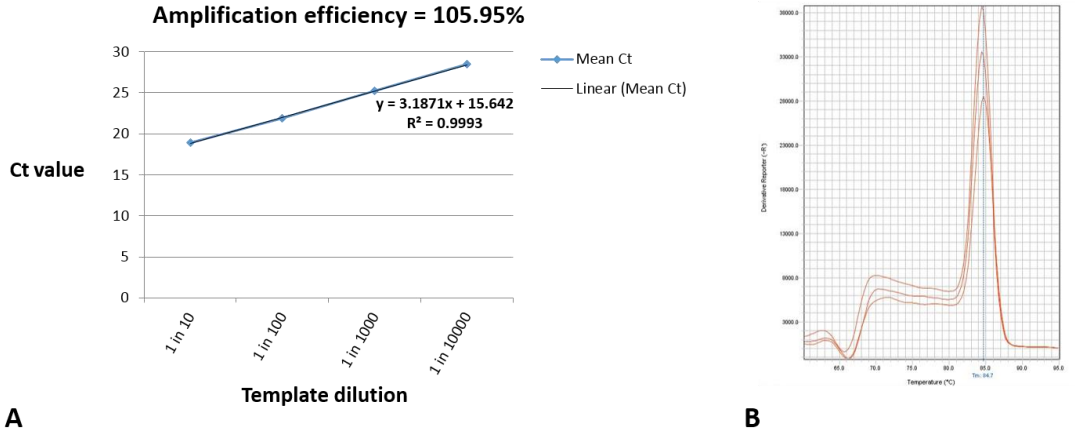

Figure 3.16 Standard curve and melt curves for real-time PCR of rat kidney cDNA using AQP7 primers

Standard curve generated for AQP7 primers using a 1/10 serial dilution of rat kidney cDNA demonstrating an $R^2 = 0.9993$ and amplification efficiency of 105.95% (A). Melt curves for rat kidney cDNA amplified with AQP7 primers (B).

3.3.2.5 Rat aquaporin 8 and 9 primers

Initial optimisation of AQP8 and 9 primers using a 1/5 serial dilution of rat kidney cDNA for qPCR demonstrated generally higher Ct values than other primer pairs alongside large secondary peaks on the melt curves at low template dilutions suggesting native expression of these AQP isoforms may be low. Reduction of the amount of primer in each reaction did

not significantly improve the situation therefore a 1/5 serial dilution of a positive control tissue (liver) was used to confirm validity of the primers. The standard curves generated, and amplification efficiencies calculated were acceptable. Additionally, the melt curves demonstrated a single peak (Figure 3.17 and Figure 3.18). These primer pairs were thus used in sample analysis for the neonatal rat unilateral ureteric obstruction model.

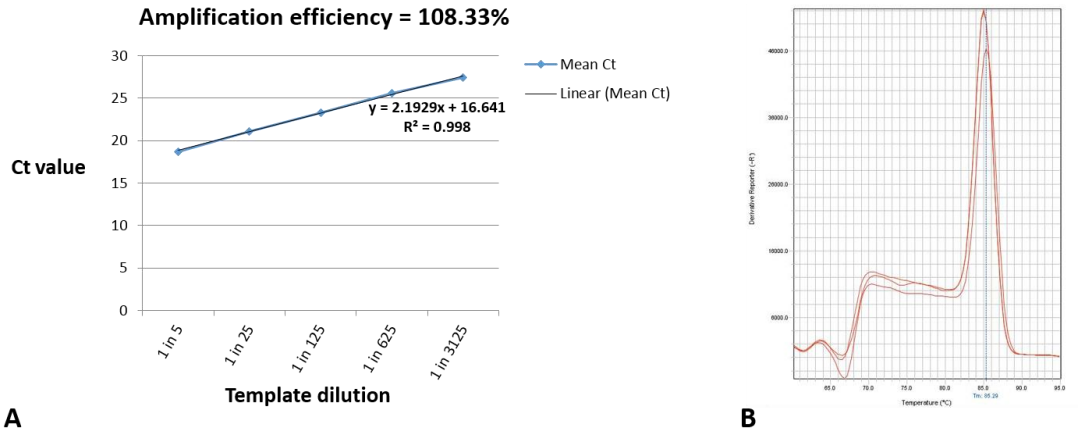

Figure 3.17 Standard curve and melt curves for real-time PCR of rat liver cDNA using AQP8 primers

Standard curve generated for AQP8 primers using a 1/5 serial dilution of rat liver cDNA demonstrating an R^2 = 0.998 and amplification efficiency of 108.33% (A). Melt curves for rat liver cDNA amplified with AQP8 primers (B).

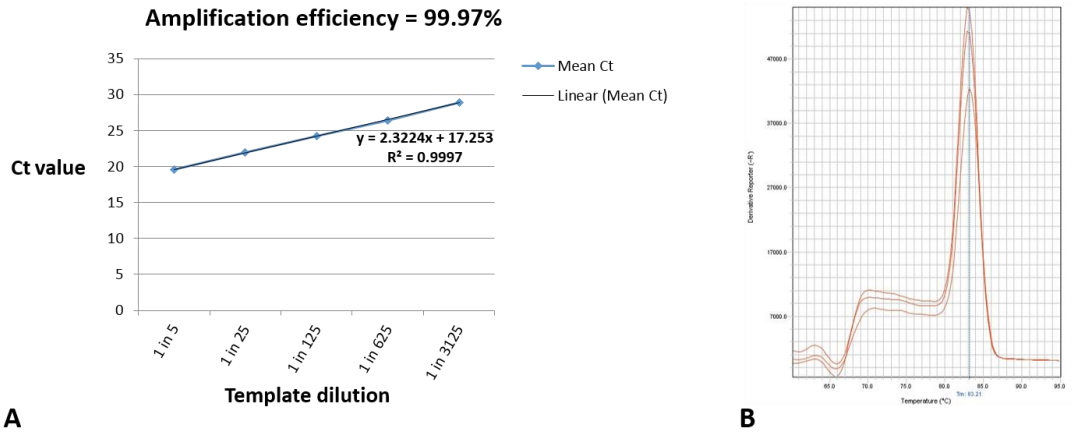

Figure 3.18 Standard curve and melt curves for real-time PCR of rat liver cDNA using AQP9 primers

Standard curve generated for AQP9 primers using a 1/5 serial dilution of rat liver cDNA demonstrating an R^2 = 0.9997 and amplification efficiency of 99.97% (A). Melt curves for rat liver cDNA amplified with AQP9 primers (B).

3.3.2.6 Aquaporin 11

AQP11 primers were tested for qPCR using a 1/10 serial dilution of rat kidney cDNA. These primers generated melt curves with a single peak, a standard curve with an R^2 = 0.9986 and

an amplification efficiency of 102%. (Figure 3.19). This primer pair was therefore used in sample analysis for the neonatal rat unilateral ureteric obstruction model.

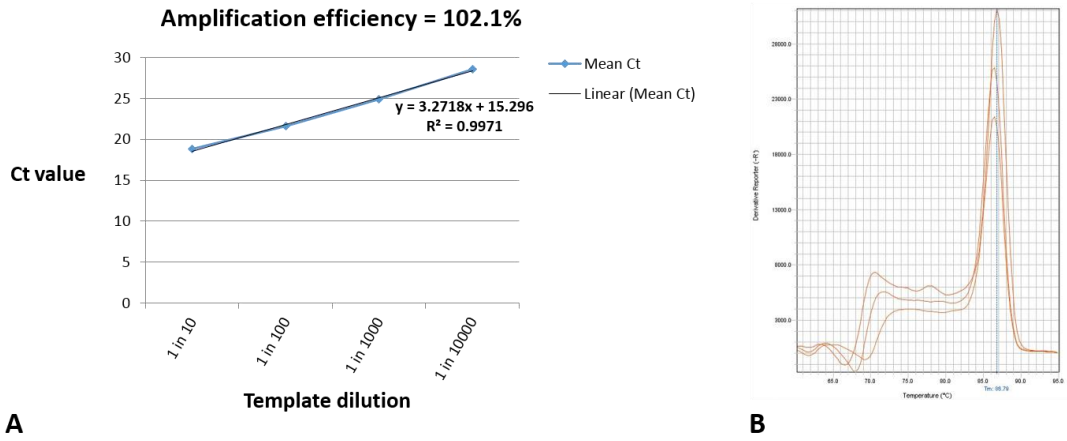

Figure 3.19 Standard curve and melt curves for real-time PCR of rat kidney cDNA using AQP11 primers

Standard curve generated for AQP11 primers using a 1/10 serial dilution of rat kidney cDNA demonstrating an R^2 = 0.9986 and amplification efficiency of 102% (A). Melt curves for rat kidney cDNA amplified with AQP11 primers (B).

3.3.2.7 Endogenous controls

Having appropriate endogenous controls (reference genes) is a commonly used method to normalise RT-qPCR data, thus controlling for experimental error. Suitable reference genes should be stably expressed across the disease conditions being investigated. However; there are many examples where classical reference genes are regulated in certain tissues/disease processes [392]. With this in mind the aim was to identify at least two suitable sets of primers for reference genes, ideally targeting different cellular processes.

Primers for rat β-actin were assessed for qPCR using a 1/5 serial dilution of rat kidney cDNA. The standard curve had an R^2 = 0.9984 and the amplification efficiency of the primers was 106%. The melt curves showed a single peak across template dilutions (Figure 3.20). This primer pair was therefore used in sample analysis for the neonatal rat unilateral ureteric obstruction model.

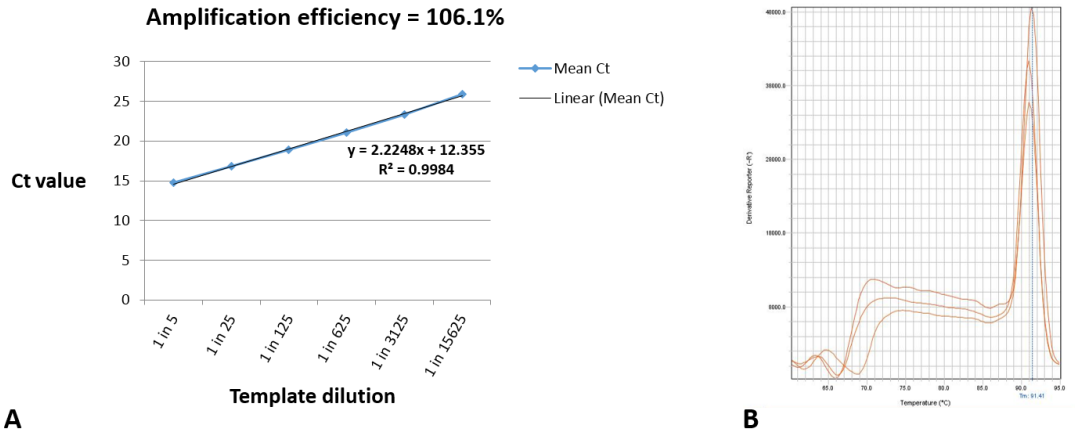

Figure 3.20 Standard curve and melt curves for real-time PCR of rat kidney cDNA using β-actin primers

Standard curve generated for β-actin primers using a 1/5 serial dilution of rat kidney cDNA demonstrating an R^2 = 0.9984 and amplification efficiency of 106.1% (A). Melt curves for rat kidney cDNA amplified with β-actin primers (B).

Ring finger protein 1 (RING 1 – binds DNA/transcriptional repressor) primers were designed and tested using rat kidney cDNA at a 1/5 dilution and a standard curve generated. Although the standard curve was generally acceptable it was only valid up to a template dilution of 1/625 as beyond that dilution there were secondary peaks on the melt curve corresponding to primer dimers. Additionally, the amplification efficiency was 116%. Reducing the amount of primers in the reaction did not improve the standard curve or amplification efficiency (Figure 3.21) and so a new set of primers was designed. Unfortunately, the new set of primers were worse and therefore not used.

Primers were also designed for mitogen activated protein kinase 14 (MAPK 14) however these suffered a similar fate to the RING 1 primers showing secondary peaks and high amplification efficiency despite modification of the amount of primers used in each reaction and were therefore discarded.

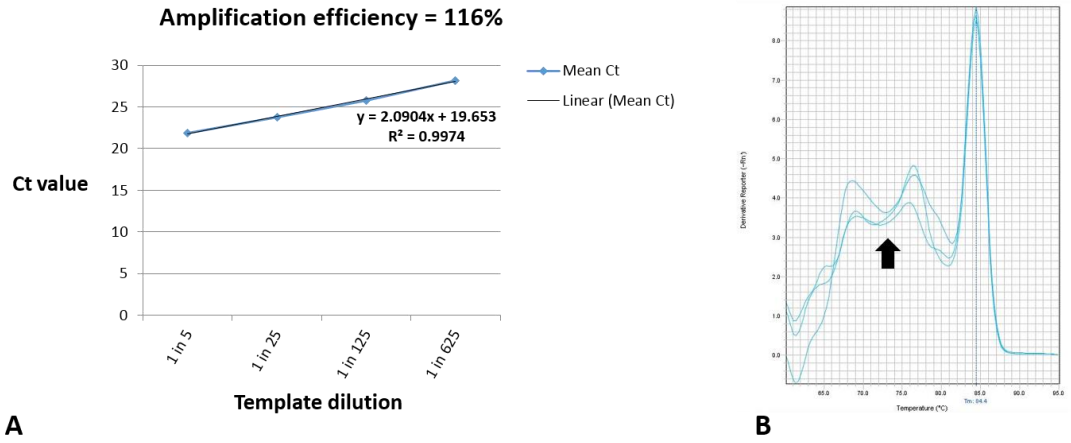

Figure 3.21 Standard curve and melt curves for real-time PCR of rat kidney cDNA using RING 1 primers

Standard curve generated for RING 1 primers using a 1/5 serial dilution of rat kidney cDNA demonstrating an R^2 = 0.9974 and amplification efficiency of 116% (A). Melt curves for rat kidney cDNA at 1/3125 dilution amplified with RING 1 primers demonstrating a secondary peak at a lower melting temperature than the intended product (B).

Cui *et al*. assessed 16 commonly used endogenous control genes in a mouse model of cystic kidney disease and identified GAPDH and PGK 1 to show low variability of expression [393]. Primers for GAPDH generated by another group within our laboratory were assessed and although a standard curve with R^2 = 0.9945 was generated the amplification efficiency was only 72% and therefore these primers were not suitable (Figure 3.22).

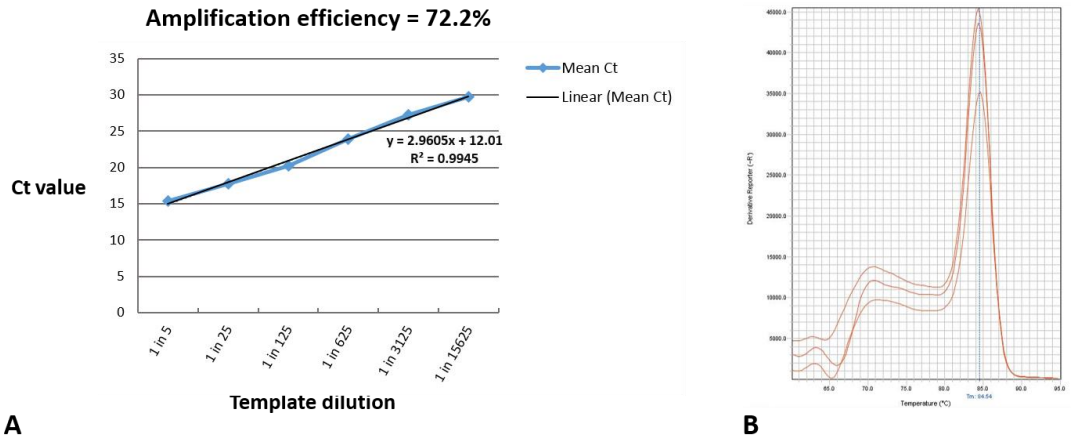

Figure 3.22 Standard curve and melt curves for real-time PCR of rat kidney cDNA using GAPDH primers

Standard curve generated for GAPDH primers using a 1/5 serial dilution of rat kidney cDNA demonstrating an R^2 = 0.9945 and amplification efficiency of 72% (A). Melt curves for rat kidney cDNA amplified with GAPDH primers (B).

Primers were therefore designed for PGK 1. These primers demonstrated nice melt curves with single peaks across the template dilutions, a standard curve with R^2 = 0.9997 and an amplification efficiency of 99% (Figure 3.23). This primer pair was therefore used in sample analysis for the neonatal rat unilateral ureteric obstruction model.

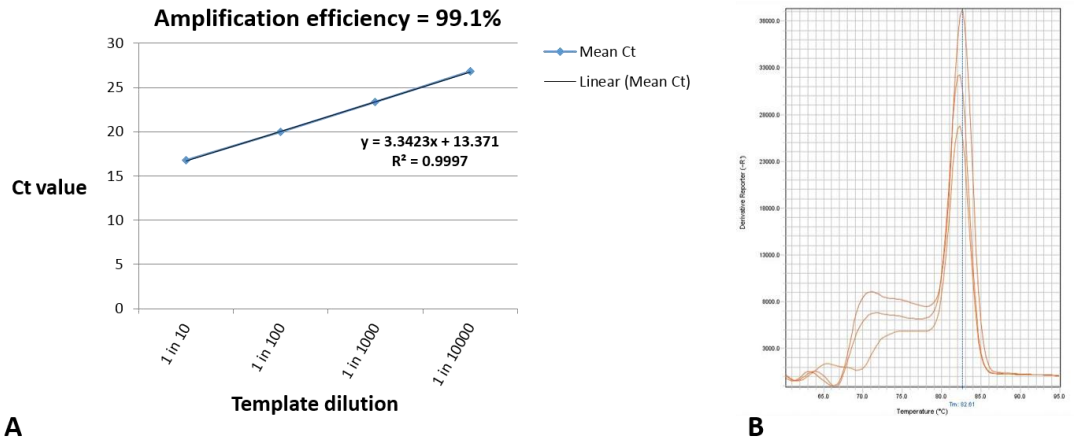

Figure 3.23 Standard curve and melt curves for real-time PCR of rat kidney cDNA using PGK 1 primers

Standard curve generated for PGK 1 primers using a 1/10 serial dilution of rat kidney cDNA demonstrating an R^2 = 0.9997 and amplification efficiency of 99.1% (A). Melt curves for rat kidney cDNA amplified with PGK 1 primers (B).

3.4 Western blotting

3.4.1 Aquaporin 1

3.4.1.1 Western blotting for aquaporin 1 in an immortalised proximal tubular cell line

Protein lysate obtained from conditionally immortalised human proximal tubular cells (ciPTEC) with SV-40 thermosensitive construct was first used to optimize the AQP1 antibody. Initial western blots performed as per the methods section in chapter 2 did not reveal a band at the predicted molecular weight (approx. 29kDa) for AQP1 (data not shown). A time course of protein extractions from ciPTEC's (clone 1) at day 0 (before thermoswitching) and days 2, 4, 6, 8 and 10 after thermoswitching to 37°C demonstrated continuing expression of SV-40 for 10 days beyond thermoswitching. This suggests that the SV-40 temperature sensitive construct was not switching off appropriately leaving the cells in a proliferative rather than differentiated state. The detection of an appropriate band at 25 kDa in human kidney lysate (positive control) and lack of this band in podocytes (negative control) supported the use of this antibody to detect AQP1 and demonstrated that this clone

of ciPTEc's does not express AQP1 at the protein level, likely due to their inability to switch to the differentiated state (Figure 3.24)

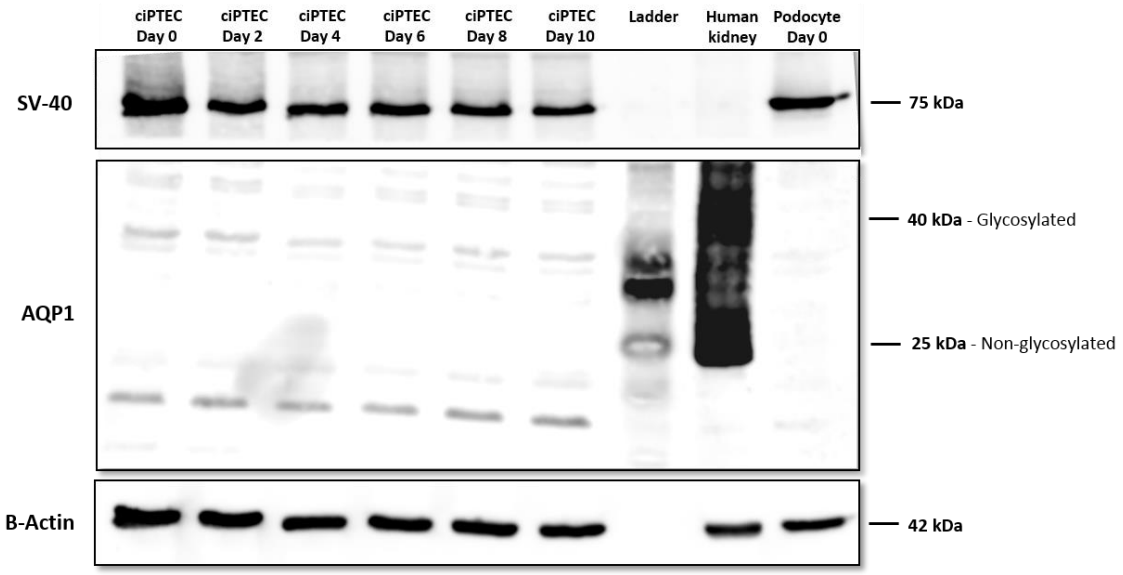

Figure 3.24 AQP1 is not expressed by conditionally immortalised proximal tubular cells

Western blot demonstrating that AQP1 is not expressed by this particular clone of conditionally immortalised human proximal tubular cells (ciPTEC). Positive and negative controls are for AQP1 expression. Lysate was extracted from cells over a range of days after thermoswitching to 37°C (day 0, 2, 4, 6, 8, 10 where day 0 = cells at 33°C). The cells continue to express SV-40 at 10 days post-thermoswitching to 37°C which may explain the lack of AQP1 expression. The non-glycosylated and glycosylated forms of AQP1 are expressed at 25 kDa and 40 kDa respectively by human kidney whole tissue lysate. As expected SV-40 is not expressed by human kidney but is expressed by ciPTEC and conditionally immortalised human podocytes. Block- 3 % BSA/TBS-T, Anti-AQP 1 1:1000 dilution, anti-SV-40 antibody 1:1000 dilution, β-actin 1:10,000 dilution.

These findings were confirmed by immunofluorescence of a time line of immortalised proximal tubular cells with SV-40 thermosensitive construct (ciPTEC clone 1) seeded on coverslips in a 6 well plate. At days 0, 6 and 11 post-thermoswitching SV-40 did not switch off in this clone of cells. Although some minor punctuate staining could be seen when day 11 cells were incubated with anti-AQP1 antibody this was achieved at the expense of high background in the images and is not conclusive of AQP1 expression by this particular clone of ciPTEC's (Figure 3.25).

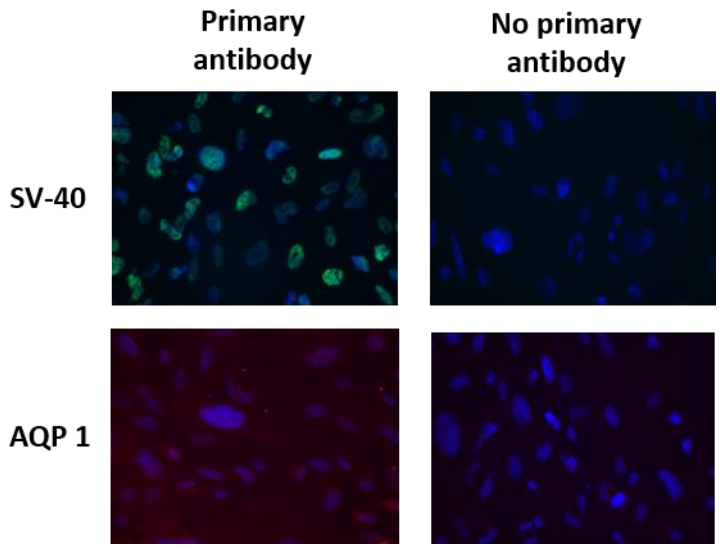

Figure 3.25 SV-40 does not switch off in conditionally immortalised proximal tubular cells

Immunofluoresence demonstrating continuing expression of SV-40 (Alexa Fluor 488 – green) by conditionally immortalised proximal tubular cells (ciPTEC) at 11 days after thermoswitching incubation to 37°C. AQP1 expression was assessed in cells 11 days after thermoswitching. Imaging shows some punctate staining of cells but is not conclusive for AQP1 expression (Alexa Fluor 568 – red). Nuclei are stained blue by DAPI. Negative controls were produced by omitting the primary antibody and incubating with the appropriate fluorescent conjugated secondary antibody. Anti-AQP1 antibody 1:250 dilution, anti-SV40 1:200 dilution.

The option of using a different clone of conditionally immortalised proximal tubular cells to ascertain whether they were thermoswitching appropriately was considered. However as this research aim was to assess AQP expression in human and rat tissue, work using cultured cells was halted and experiments progressed to characterising AQP expression in whole tissue.

3.4.1.2 Western blotting for aquaporin 1 expression in human and rat tissue

Western blots were performed to determine optimum protein loading concentration using human tissue. The protein concentrations of whole human kidney, ureter and renal pelvis lysates were determined by BCA protein assay. Western blotting was then performed loading 25, 50, 75 and 100 µg protein per lane. The membranes were subsequently stripped and re-probed with anti-B-actin. A representative blot is shown in Figure 3.26. Protein loading of 75 µg per lane was selected as optimum, striking a balance between sufficient for aquaporin detection without overloading with protein.

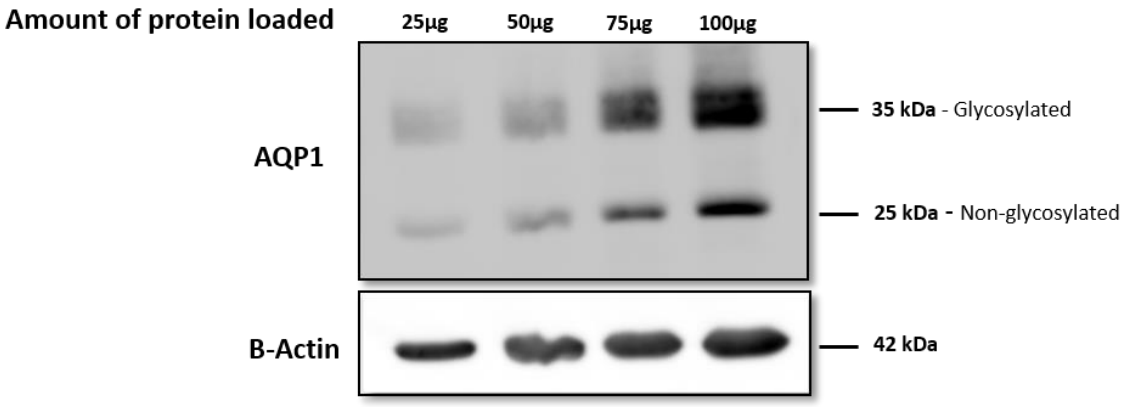

Figure 3.26 Western blot to determine optimum protein loading

Western blot showing human renal pelvis lysate loaded at different protein concentrations and probed for AQP1. The blot was stripped and re-probed for b-actin as loading control. Block- 3 % BSA/TBS-T, Anti-AQP1 1:1000 dilution, β-actin 1:10,000 dilution.

Membrane proteins such as AQPs can often be difficult to extract and the use of a urea/thiourea lysis buffer can improve their solubilisation [394]. Additionally, boiling samples following the addition of sample buffer can cause aggregation of membrane proteins. In order to optimise the results of western blotting for AQP1, different sample buffers and different incubation temperatures after addition of sample buffer were trialled. Furthermore, the use of a urea/thiourea tissue lysis buffer was compared to protein extraction using traditional RIPA buffer.

Protein was extracted from whole human kidney using urea/thiourea tissue lysis buffer in the same manner as described in methods except following homogenisation of the tissue in the urea/thiourea lysis buffer, the lysate was left to stand at room temperature for 30 minutes. A BCA protein assay was performed to determine protein concentration of the RIPA buffer lysates and samples were loaded at 75 µg per lane. It was not possible to perform a protein assay on the samples extracted in urea/thiourea buffer and so these lysates were loaded at the same volume as those extracted in RIPA buffer. Prior to loading, urea/thiourea and RIPA kidney lysates were mixed with either a 2% SDS sample buffer, a 4% SDS sample buffer or a 7 M urea/SDS sample buffer. Additionally, for each of these lysis buffer/sample buffer variables the samples were incubated at assorted temperatures, increasing the length of incubation as the temperature decreased.

The results of western blotting for AQP1 (Figure 3.27 and Figure 3.28) demonstrated there is no added benefit to using urea/thiourea tissue lysis buffer for protein extraction or using a sample buffer other than 4% SDS when preparing samples. Moreover, bands for AQP1 were

detected across the range of incubation temperatures used. Temperatures between 50-95°C produced the best resolution and there did not seem to be any benefit of a lower over a higher incubation temperature. Future experiments were therefore performed using RIPA buffer for tissue protein extraction alongside 4% SDS sample buffer with incubation at 95 °C for 5 minutes prior to sample loading.

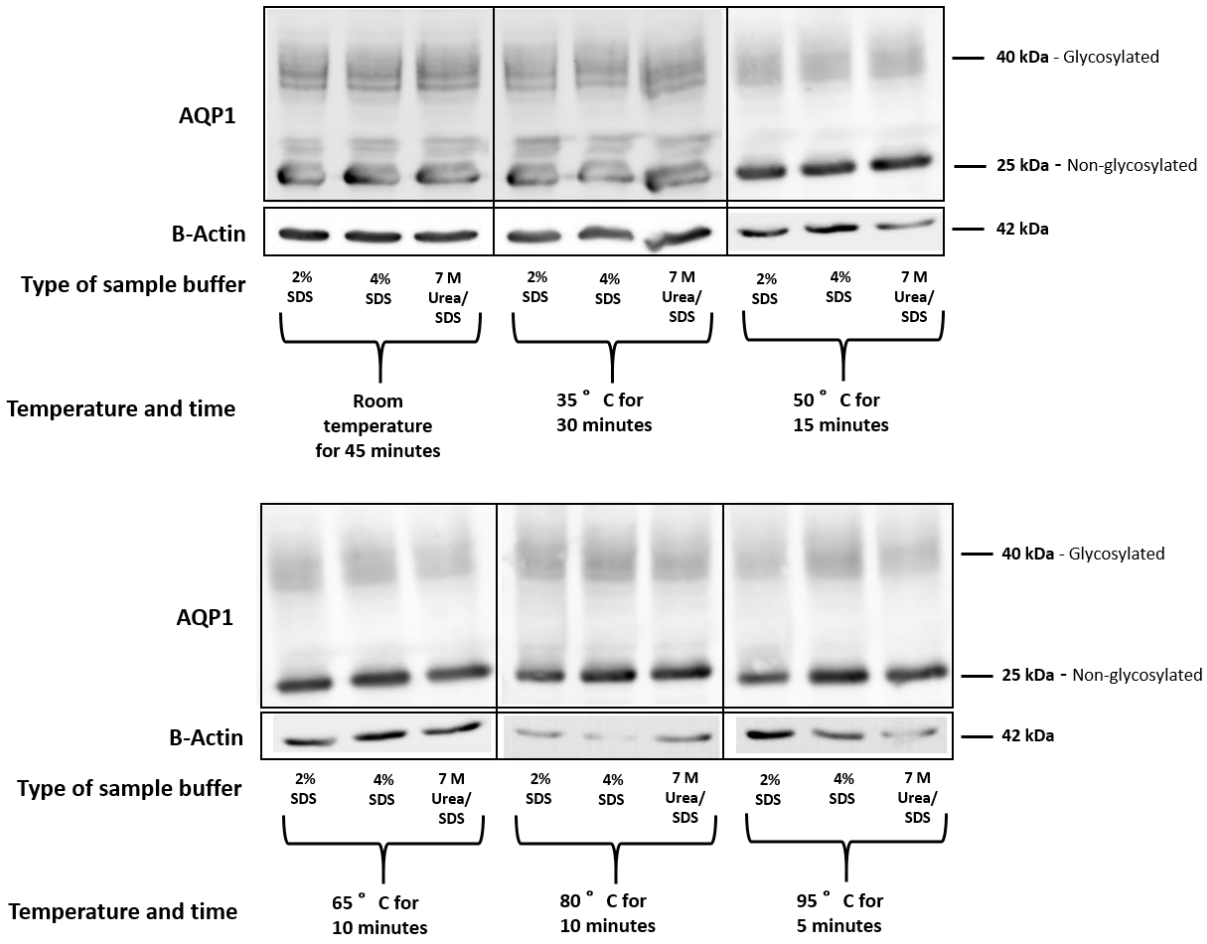

Figure 3.27 Western blots demonstrating AQP1 in human kidney lysate extracted with RIPA buffer

Human kidney protein lysate was mixed with different samples buffers (either 2% SDS, 4% SDS or 7 M urea/SDS and then incubated at different temperatures, increasing the length of incubation as the temperature decreased. Samples loaded at 75 µg protein per lane.

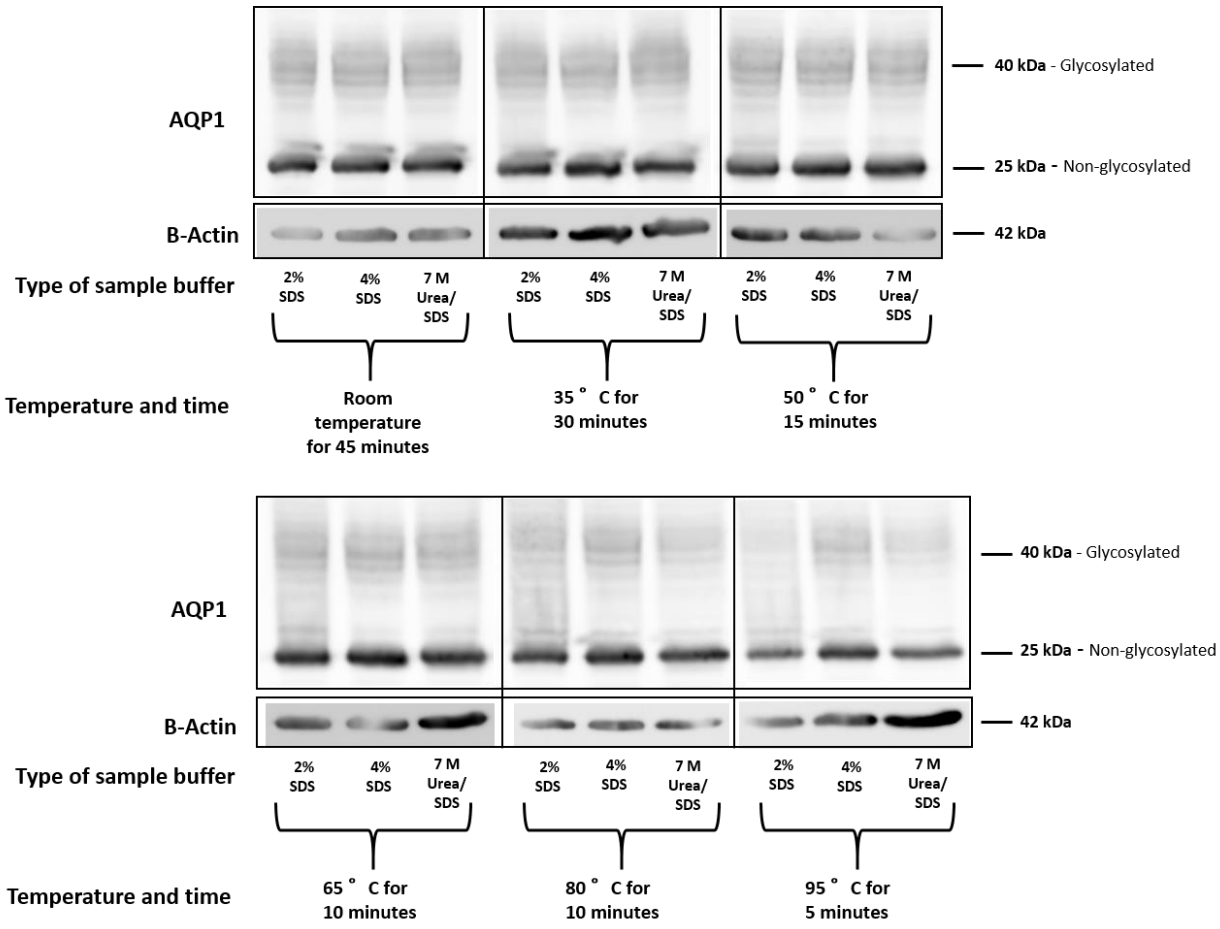

Figure 3.28 Western blot demonstrating AQP1 in human kidney lysate extracted using urea/thiourea buffer

The lysate was mixed with different samples buffers (either 2% SDS, 4% SDS or 7 M urea/SDS) and then incubated at different temperatures, increasing the length of incubation as the temperature decreased. Samples loaded at 75 µg protein per lane.

Using the optimised protocol, a western blot confirmed AQP1 expression by rat kidney, bladder and heart in addition to human urinary tract samples from two individuals. The membrane was stripped and re-probed for β-actin as loading control. Myocardium does not express β-actin, consequently, a 42kDa band for β-actin was not detected in the lane loaded with rat heart. (Figure 3.29).

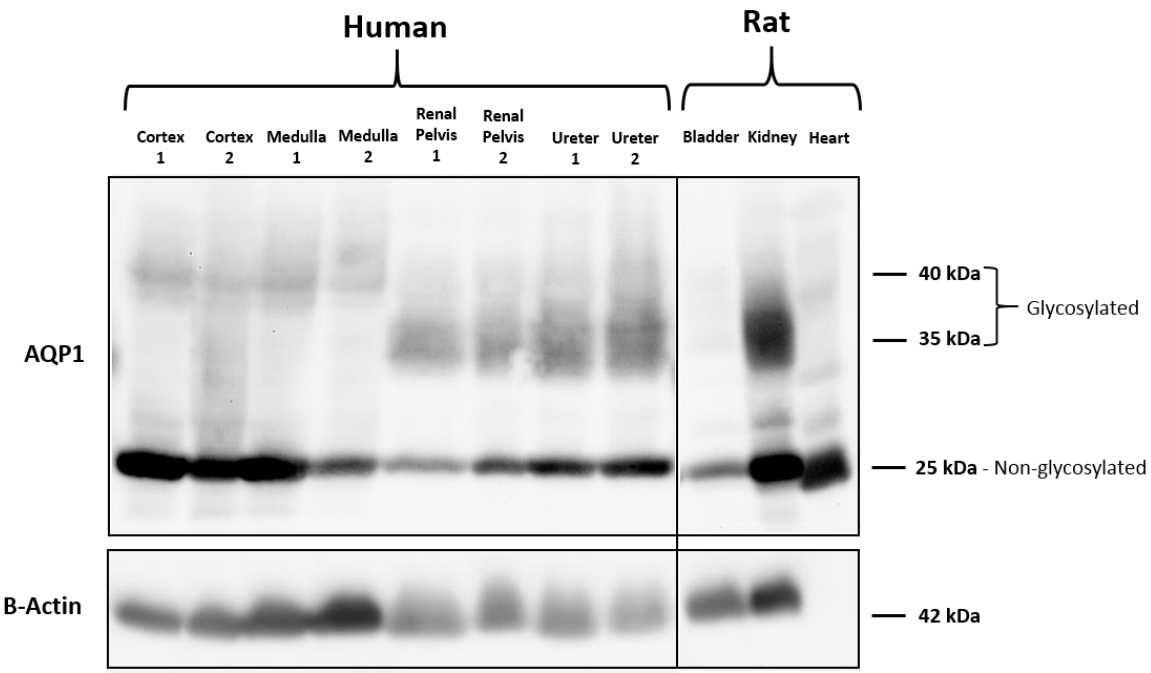

Figure 3.29 Western blot demonstrating AQP1 expression in human and rat urinary tract tissues

Western blot demonstrating the presence of AQP1 in rat kidney, bladder and heart. AQP1 is also present in 2 different human kidney cortex and medulla, renal pelvis and ureter samples. Positive control – rat heart. Rat heart did not express β-actin as expected. Block- 3 % BSA/TBS-T, Anti-AQP1 1:1000 dilution, β-actin 1:10,000 dilution.

3.4.2 Aquaporin 2

Initial western blots to detect AQP2 in human kidney cortex and medulla lysate extracted with RIPA buffer demonstrated multiple bands for each sample. AQP2 would be expected to be detected at a molecular weight of approximately 29 kDa. It was not possible from these blots to differentiate AQP2, either non-glycosylated or glycosylated, from non-specific bands. Varying the antibody dilution and the pre-loading incubation temperature did not change the outcome of the blot (Figure 3.30).

The blot was thus repeated using rabbit anti-AQP2 (Santa Cruz) at 1:500 dilution made up in 1% BSA, changing the block to 5% skimmed milk in TBS-T. Both human and rat samples were loaded to ensure detection was not species specific. Although the block reduced the non-specific binding a band at 29 kDa was still not demonstrated for any of the lysates (Figure 3.31).

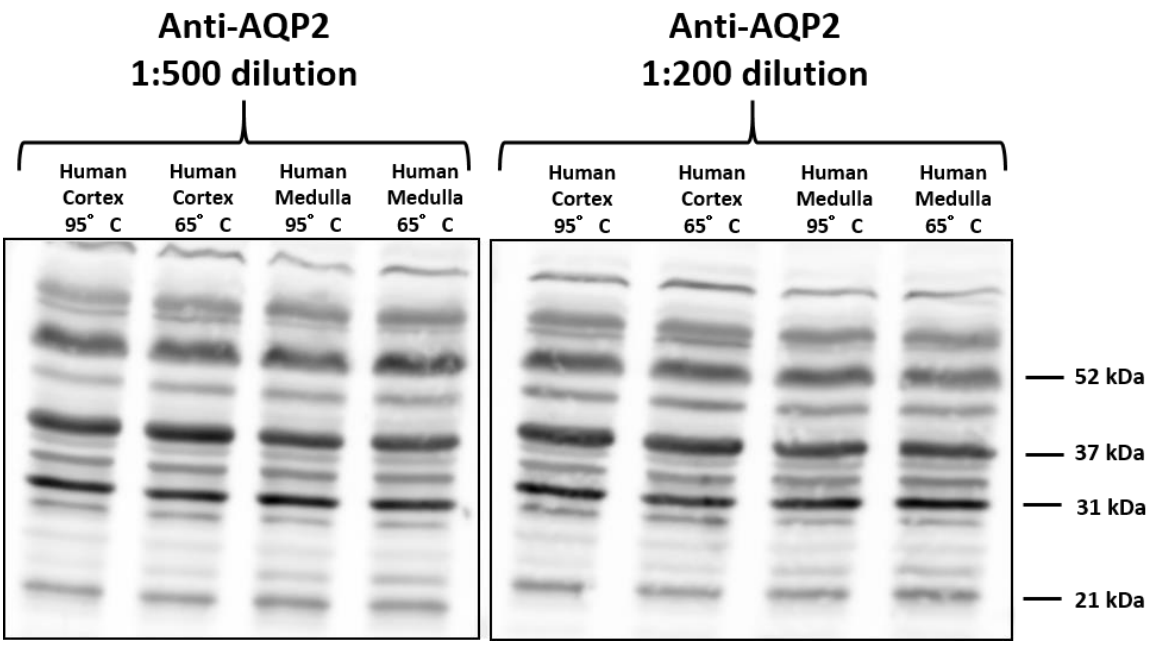

Figure 3.30 Western blot of human kidney for AQP2 generates multiple bands

Western blot demonstrating the effect of different dilutions (1:500 and 1:200) of the Santa Cruz (sc-28629) anti-AQP2 antibody and the effect of incubations at different temperatures prior to sample loading on the ability to detect AQP2 in human kidney cortex and medulla lysate. 3% BSA/TBS-T block was used. Multiple bands were demonstrated for all human kidney samples. The molecular weight of the most dominant bands has been marked.

A new antibody, kindly donated by J Bedford, New Zealand, (raised in rabbits against a synthetic peptide made from the 15C terminus of human AQP 2 [aa 257-271: VELHSPQSLPRGTKA]) was used as per instructions from the donating laboratory. Protein lysates were mixed with 4% SDS sample buffer then incubated at 95°C for 5 minutes. The blot was blocked in 5% skimmed milk in TBS-T and all antibodies were diluted in 1% BSA in TBS-T. The rabbit anti-AQP2 antibody was used at 1:2500 dilution. Human kidney, renal pelvis and ureter protein lysates were loaded and produced bands predominantly at 42 kDa (Figure 3.32). This band could represent a dimer although this is unlikely as it is not twice the size of the AQP2 monomer. To determine whether this band represented glycosylated AQP2 human samples were deglycosylated as per the protocol in the methods section and the blot repeated. This demonstrated no bands at 29 kDa in either the glycosylated or deglycosylated samples. A strong band in all samples was seen at 42 kDa (Figure 3.33). A control blot using AQP1 and rat kidney demonstrated that the deglycosylation protocol was successful therefore the 42 kDa band seen on the AQP2 blots does not represent glycosylated AQP2 (Figure 3.34).

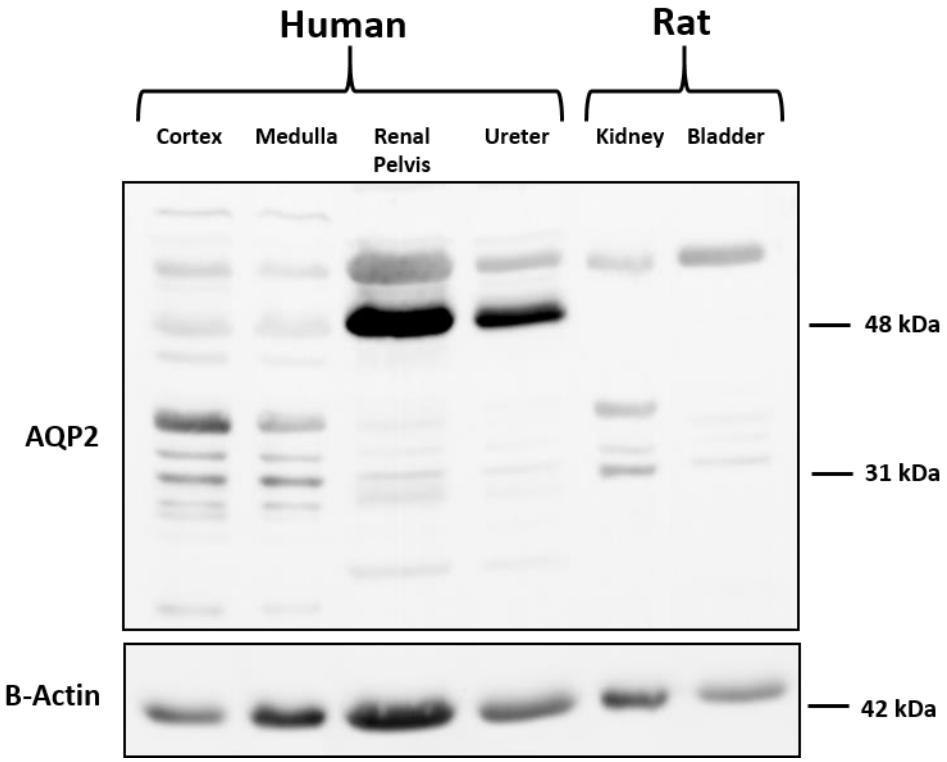

Figure 3.31 Western blotting of human kidney for AQP2 generates multiple bands with 5% milk block

Western blot performed using 5% skimmed milk block and Santa Cruz anti-AQP2 antibody (sc-28629) at 1:500 dilution. Blocking of multiple bands was improved compared to 3% BSA block however a dominant band at approximately 29 kDa was not demonstrated in either human or rat samples.

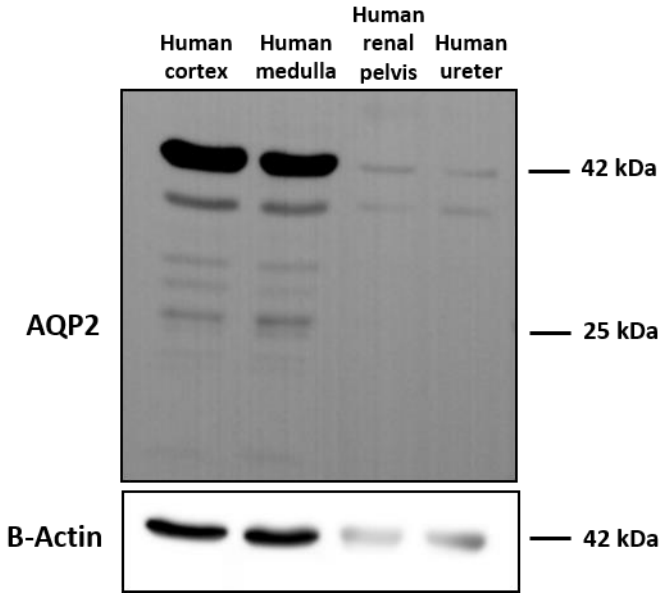

Figure 3.32 Western blot of human kidney with a new AQP2 antibody

Western blot using 5% milk block and the anti-AQP2 antibody donated by the New Zealand group at 1:2500 dilution. Human kidney cortex and medulla, renal pelvis and ureter samples showed a major band at 42 kDa but no bands at 29 kDa.

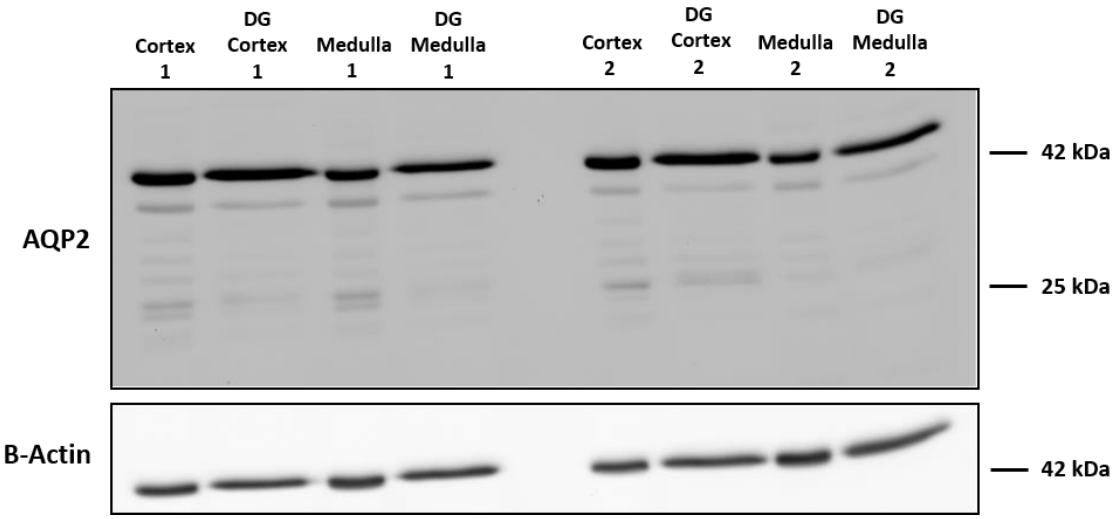

Figure 3.33 Western blot of deglycosylated and non-deglycosylated human kidney samples for AQP2

Western blot using 5% skimmed milk block and the anti-AQP2 antibody donated by the New Zealand group at 1:2500 dilution. Cortex and medulla samples from two human donors have been deglycosylated (DG) and run alongside the non-deglycosylated samples. The 42 kDa band remains at the same intensity in the deglycosylated samples. Deglycosylation of the samples does not produce a band at 29 kDa suggesting that the 42 kDa band does not represent glycosylated AQP2. DG – deglycosylated.

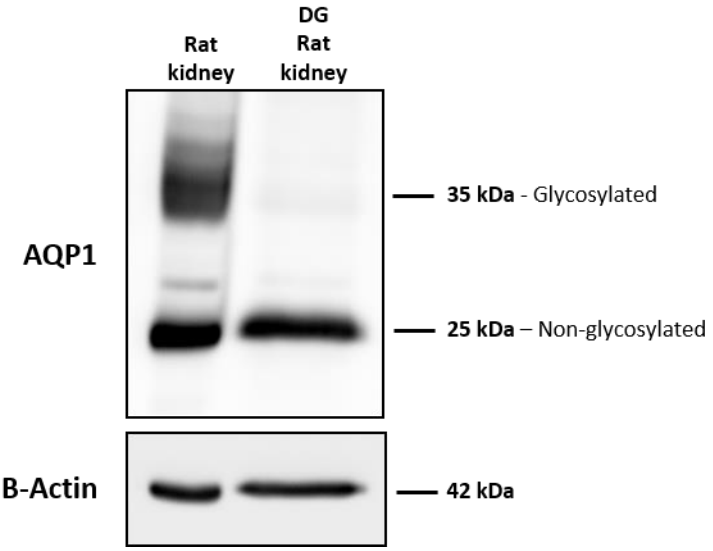

Figure 3.34 Western blot of deglycosylated and non-deglycosylated rat kidney for AQP1 expression

Deglycosylation of whole rat kidney results in loss of the 35 kDa glycosylated band on western blot compared to the non-deglycosylated (native) sample. DG – deglycosylated.

Two alternative anti-AQP2 antibodies (Merck Milllipore and Abcam) were also trialled but did not show any bands in the anticipated location for human kidney samples (data not shown).

In order to conclusively prove whether any of these antibodies could detect AQP2, a western blot using AQP2 overexpression lysate (LY424696, Origene, Rockville, MD, USA),

transiently expressed by HEK293T cells and tagged with FLAG was performed. This was incubated with all four available anti-AQP2 antibodies and demonstrated the Santa Cruz (sc-28629), and the donated antibody from New Zealand, identified AQP2 by detecting a single band at the correct molecular weight of 30 kDA. A band at the same molecular weight was identified when the same overexpression lysate was probed with anti-FLAG antibody. As expected no significant bands were identified in lanes loaded with empty vector. The remaining two anti-AQP2 antibodies (AB3066, Merck Millipore and ab15081, Abcam) did not identify a band for the AQP2 overexpression lysate (Fig 27).

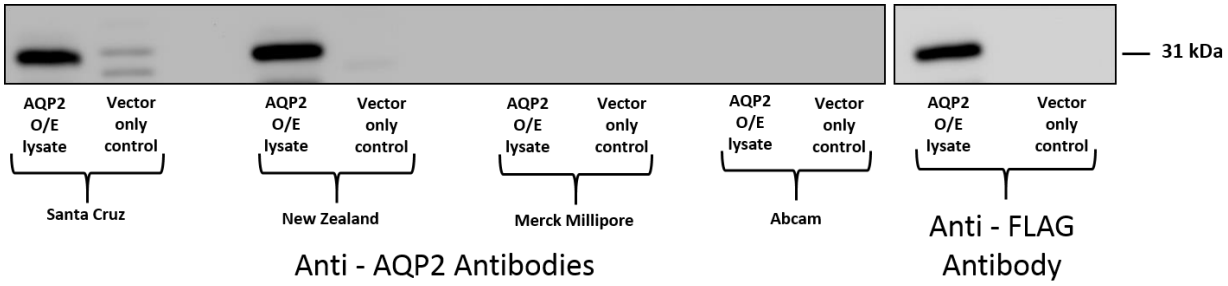

Figure 3.35 Detection of AQP2 on western blotting using AQP2 overexpression lysate

Western blot where FLAG tagged AQP2 overexpression (O/E) lysate and empty vector control lysate have been probed with 4 different anti-AQP2 antibodies. Santa Cruz 1:500, New Zealand 1:2500, Merck Millipore 1:500, Abcam 1:500). Only two of the antibodies correctly recognize AQP2. The anti-FLAG antibody confirms the correct position of the band.

As there was not sufficient of the anti-AQP2 antibody donated by the New Zealand group left for further work the Santa Cruz anti-AQP2 antibody was optimised by assessing different tissue lysis buffers and sample buffers to ensure sample extraction methods had not compromised results. During this process human and rat renal tract samples were run alongside the AQP2 overexpression lysate.

Protein lysates were extracted using either RIPA or urea/thiourea tissue lysis buffer and incubated with sample buffer containing either 2% SDS, 4% SDS or 7 M urea/SDS at varying temperatures. Human protein lysates extracted with urea/thiourea tissue lysis buffer did not exhibit a band at 31 kDa corresponding to the band detected for the overexpression lysate. Conversely AQP2 was detected in both human and rat protein lysates extracted with RIPA buffer. There was no added benefit of using a sample buffer other than 4% SDS when preparing samples (Figure 3.36). Identical blots were performed simultaneously using the Santa Cruz antibody at 1:250 and 1:500 dilutions. The results for the 2 antibody dilutions

were comparable and therefore the 1:500 antibody dilution was selected for use in future western blotting.

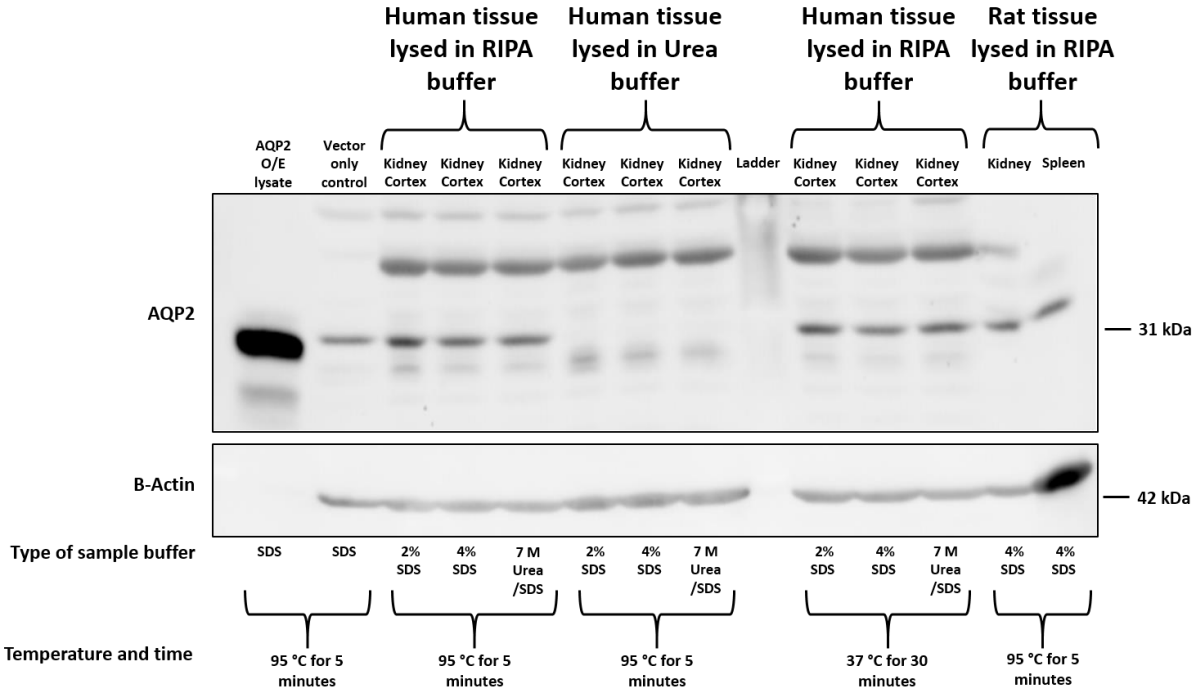

Figure 3.36 Western blot demonstrating AQP2 expression in human and rat kidney protein lysates extracted with different buffers

Human kidney cortex protein lysates were extracted using either RIPA or urea buffer and then mixed with different samples buffers (either 2% SDS, 4% SDS or 7 M urea/SDS) and then incubated at either 95°C for 5 minutes or 37°C for 30 minutes. Samples loaded at 75 µg protein per lane. Standard protein extraction and sample buffer procedures were utilized for rat kidney. The AQP 2 overexpression lysate and vector control were prepared as per the manufacturer's instructions. 5% milk block was used and an AQP2 dilution of 1:500.

Using the optimised protocol and an appropriate negative control (rat eye) AQP2 expression was confirmed in human urinary tract tissue (kidney, renal pelvis and ureter), rat kidney and spleen (Figure 3.37). AQP2 was also demonstrated in human urine concentrated and fractionated by ultrafiltration (See section 3.6.1 for western blotting of urinary AQPs). Additionally, because the manufacturer supplied vector only control in Figure 3.36 showed a weaker positive band at 31 kDa standard human embryonic kidney (HEK 293) protein lysate was run on on the blot in Figure 3.37 and was demonstrated to express AQP2.

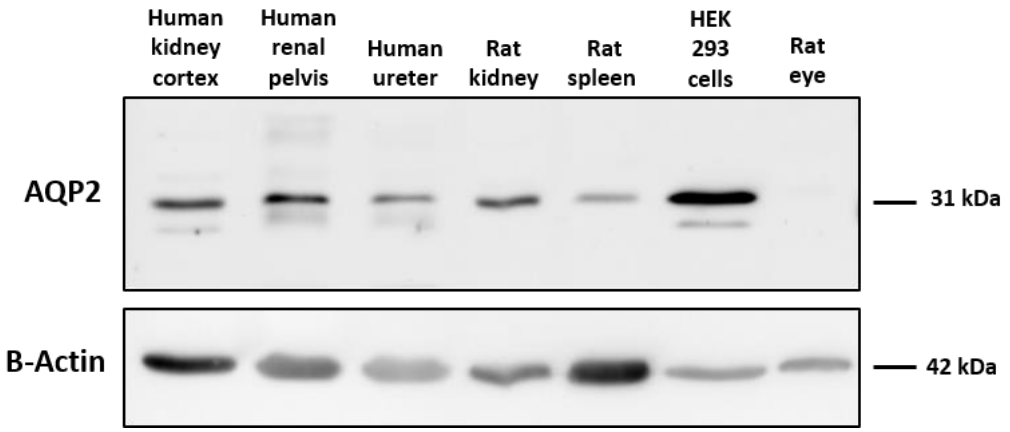

Figure 3.37 Western blot demonstrating AQP2 expression in human and rat tissues

Western blot demonstrating AQP2 expression by human kidney cortex, renal pelvis and ureter and excretion in human urine. Expression was also seen in rat kidney and spleen and HEK 293 cells. Negative control rat eye.

3.4.3 Aquaporin 3

Initial western blots to detect AQP3 in human kidney cortex and medulla lysate as per the methods section in chapter 2 demonstrated multiple bands for each sample. The block was changed from 3% BSA to 5% skimmed milk and the anti-AQP3 antibody (Santa Cruz sc-9885) was diluted in 1% BSA over a range of dilutions from 1:1000, 1:500, 1:250. 1:100. An AQP3 dilution of 1:100 was selected as giving the optimal band resolution and using rat spleen and heart as known positive and negative controls respectively the AQP3 band was documented at a molecular weight of 28 kDa (predicted 36 kDa) in human kidney, renal pelvis and ureter samples as well as rat kidney and bladder. AQP3 was not detected in human urine treated by ultrafiltration (see section 3.6.1 for western blotting of urinary AQPs). The membrane was stripped and re-probed with anti-GAPDH. AQP1 was used as loading control for the urine sample (Figure 3.38).

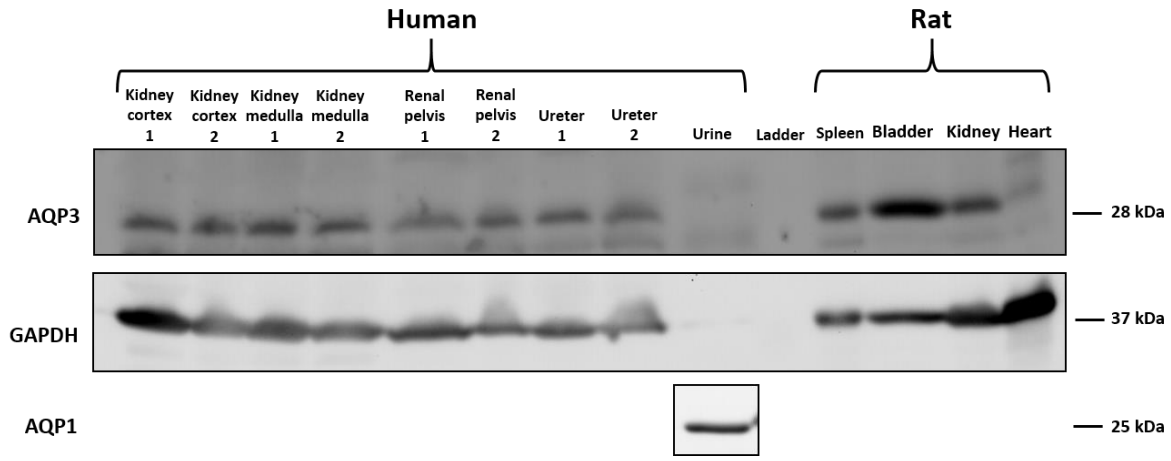

Figure 3.38 Western blot demonstrating AQP3 expression by human and rat tissues

Western blot demonstrating AQP3 expression by human kidney cortex and medulla, renal pelvis and ureter. Expression was also seen in rat kidney and bladder. AQP3 was not detected in human urine. Loading controls were GAPDH for tissue and AQP1 for urine. Positive control – rat spleen, negative control rat heart.

3.4.4 Aquaporin 4

Initial western blots to detect AQP4 in human kidney cortex and medulla lysate as per the methods section in chapter 2 demonstrated multiple bands for each sample. The block was changed from 3% BSA to 5% skimmed milk and the anti-AQP4 antibody (Santa Cruz sc-9888) was diluted in 1% BSA in dilutions of 1:1000, 1:500. An AQP4 dilution of 1:500 gave better band resolution, and using rat brain and spleen as known positive and negative controls respectively, the AQP4 band was documented at a molecular weight of 34 kDa (predicted 34kDa) in human kidney cortex and medulla samples as well as rat kidney and bladder (Figure 3.39). AQP4 was not detected in human renal pelvis and ureter, however it has been detected on RT-PCR (Chapter 6). The membrane was stripped and reprobed with anti-GAPDH.

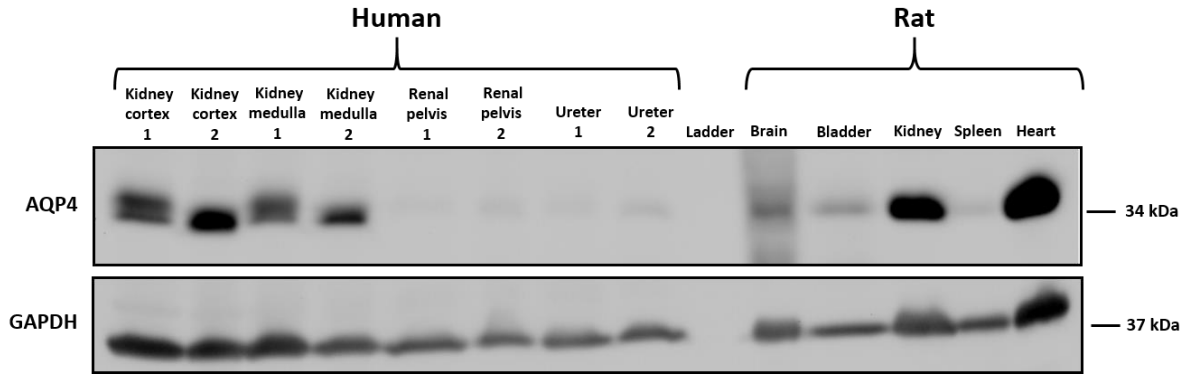

Figure 3.39 Western blot demonstrating AQP4 expression by human and rat tissues

Western blot demonstrating AQP4 expression by human kidney cortex and medulla, and rat kidney, bladder, brain and heart. AQP4 was not detected in human renal pelvis and ureter. GAPDH was used as loading control. Positive control – Rat brain and heart, negative control rat spleen.

3.5 Immunohistochemistry for aquaporins in formalin fixed paraffin embedded human tissue

3.5.1 Aquaporin 1

When first optimising human kidney immunohistochemistry for AQP1 the rabbit IgG control sections demonstrated non-specific tubular DAB staining despite blocking with increasing concentrations of normal goat serum with or without 1% BSA (Figure 3.40).

Subsequently immunohistochemistry using either no primary antibody or no primary and no secondary antibody followed by an HRP conjugated avidin biotin complex (ABC) system was performed. Again, non-specific tubular staining throughout the renal cortex and medulla was noted (Figure 3.41). This indicted either endogenous peroxidase or endogenous biotin activity.

Human kidney sections were tested for endogenous peroxidase activity by incubating in a range of concentrations of hydrogen peroxide (0.5%, 1% and 3% diluted in ultrapure water) as well as ultrapure water (control) for 10 minutes at room temperature followed by incubation with DAB substrate. Light microscopy imaging did not show DAB staining of any of the sections (Figure 3.42) indicating endogenous peroxidase activity was not the cause of the tubular staining seen on negative control slides. The lowest concentration of hydrogen peroxide (0.5%) was selected for ongoing immunohistochemistry experiments.

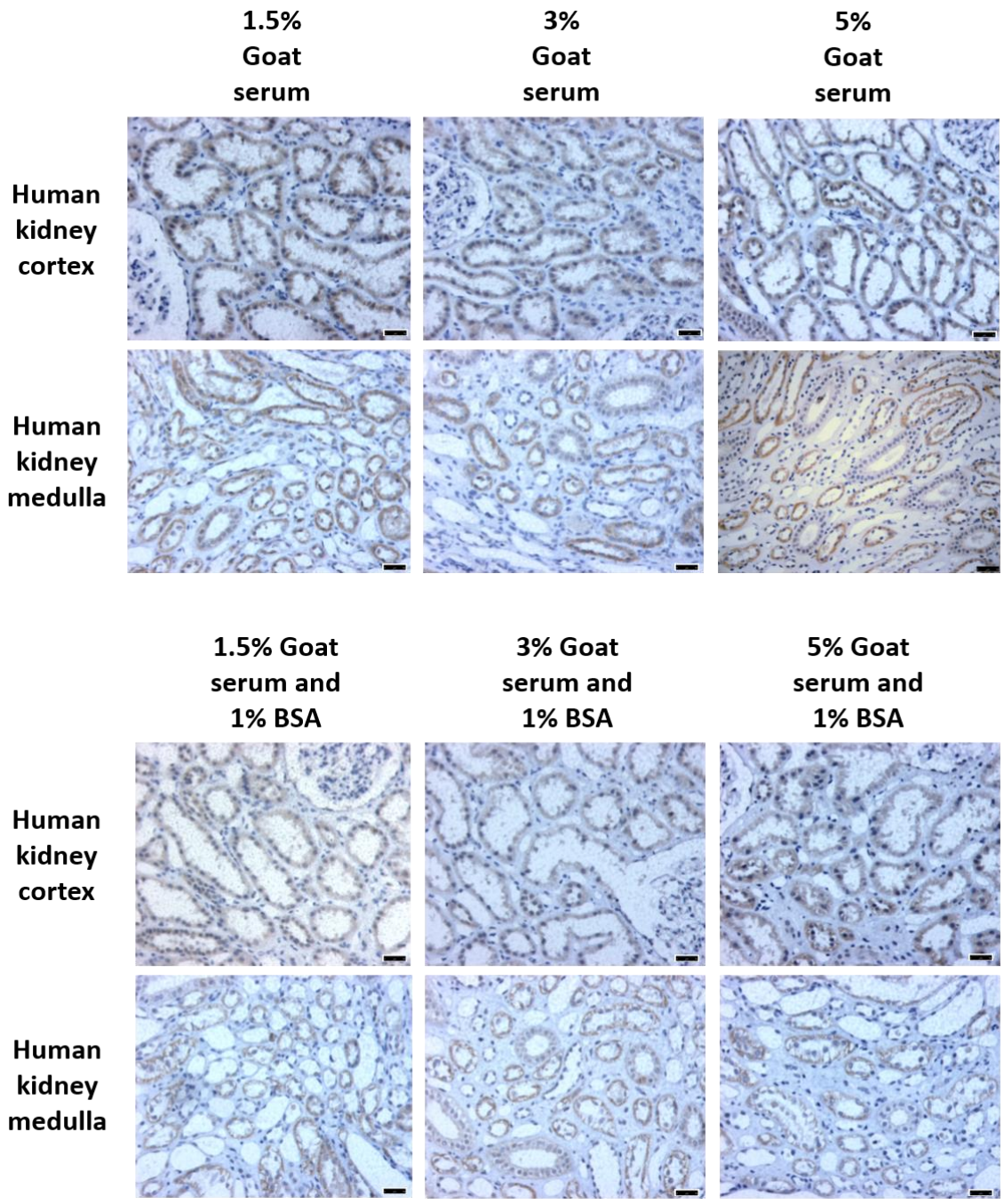

Figure 3.40 Immunohistochemistry demonstrating tubular staining of IgG control human kidney sections

Human kidney sections were incubated with rabbit IgG instead of primary antibody. Imaging demonstrated non-specific tubular DAB staining despite blocking sections with increasing concentrations of normal goat serum with or without 1% BSA. Scale bar = 50 μm.

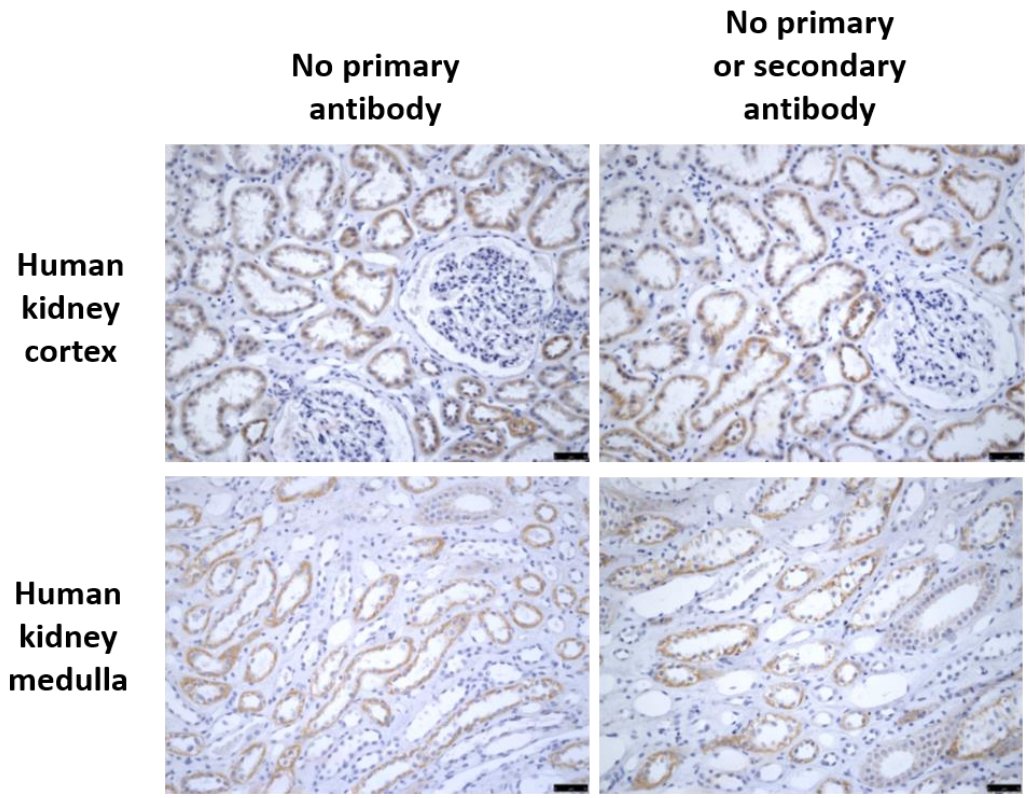

Figure 3.41 DAB staining of human kidney in the absence of primary and secondary antibodies

Immunohistochemistry of human kidney sections involving the use of either no primary antibody or no primary and no secondary antibodies was performed. Sections were incubated with antibody diluent in place of antibodies. An HRP conjugated avidin biotin complex system was used to amplify signal using DAB substrate. Non-specific tubular DAB binding in all sections suggests either endogenous biotin or peroxidase activity.

The experiments in Figure 3.40 and Figure 3.41 had used a Santa Cruz ABC (avidin biotin complex) secondary antibody system. In the absence of significant endogenous peroxidase activity, it was likely the non-specific staining was due to endogenous biotin activity as renal tissue is known to have high biotin content [395]. The potential options to resolve this issue were either to include an avidin/biotin blocking step or to use a different secondary antibody. A polymerised reporter antibody staining system (SignalStain® boost IHC detection reagent HRP anti-rabbit, Cell signalling, Danvers, MA, USA) resolved the problem and enabled the detection of AQP1 with low background. The rabbit anti-AQP1 antibody (Santa Cruz, sc-20810) was used at 1:250 dilution. Rabbit IgG (used at the same concentration as primary antibody) and no primary antibody controls were included. 1.5% goat serum in TBS-T was used to block slides and to make up the primary antibody dilution.

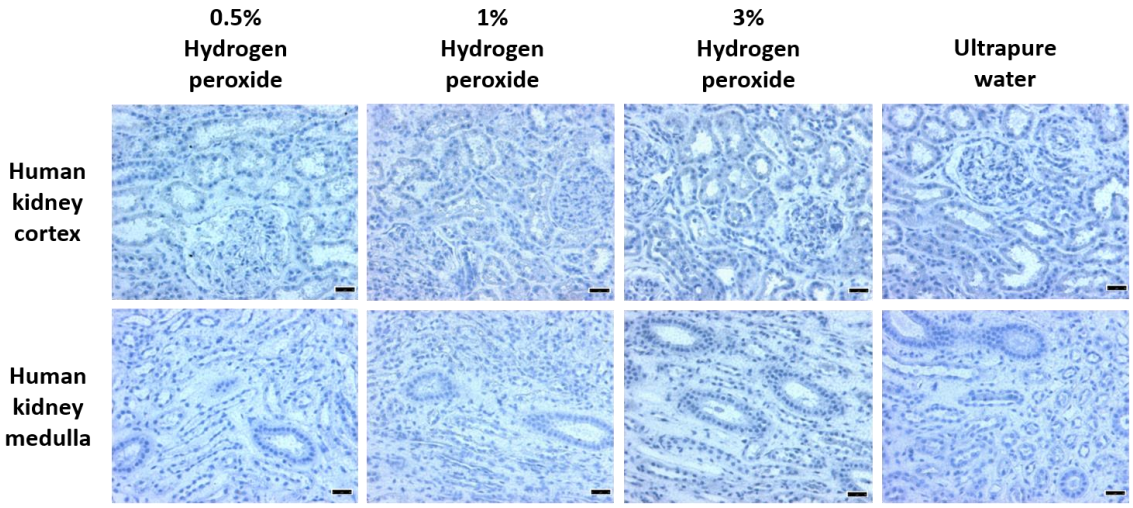

Figure 3.42 Human kidney sections do not demonstrate endogenous peroxidase activity

Human kidney sections were incubated with increasing concentrations of hydrogen peroxide diluted in ultrapure water or ultrapure water as control. Sections were then incubated in DAB substrate. None of the sections including the controls showed any DAB staining indicating minimal endogenous peroxidase activity. Scale bar = 50 μm.

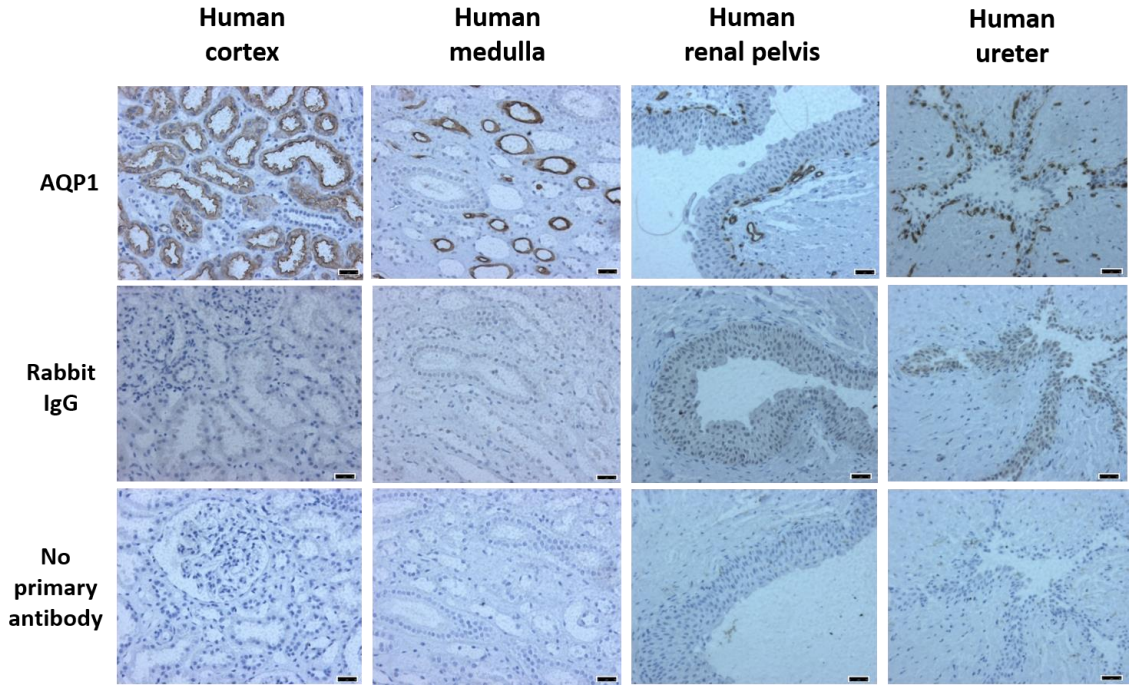

Figure 3.43 Immunohistochemistry demonstrating AQP1 expression by human kidney, renal pelvis and ureter

Immunohistochemistry using anti-AQP1 at a dilution of 1:250 and rabbit IgG at a corresponding concentration. Sections labelled no primary antibody were incubated with 1.5% goat serum. AQP1 expression is demonstrated in the apical and basolateral membranes of the proximal tubules within the kidney cortex, while AQP1 expression in the loop of Henle and vasa recta but not within collecting ducts is seen in the kidney medulla. AQP1 is also detected in the vasculature of the lamina propria of the renal pelvis and ureter. Scale bar = 50 μm.

AQP1 was detected in the apical and basolateral membranes of the proximal tubules, the loop of Henle and vasa recta of human kidney, however it was not present in the kidney collecting ducts. AQP1 was also present in the vasculature of human renal pelvis and ureter but was not detectable in urothelium. (Figure 3.43).

3.5.2 Aquaporin 2

The same protocol was employed for detection of AQP2 using rabbit anti-AQP2 (Santa Cruz, sc-28629) as was used for AQP1. Primary antibody dilutions of 1:100 and 1:250 were assessed. At 1:100 dilution the corresponding concentration of rabbit IgG control gave too much non-specific staining (data not shown) whereas the 1:250 anti-AQP2 and corresponding rabbit IgG control concentration demonstrated luminal staining of the collecting ducts without any non-specific staining. The 1:250 antibody dilution was selected for future experiments. Immunohistochemistry of human ureter and renal pelvis for AQP2 did not show any staining suggesting AQP2 is not expressed by urothelium (Figure 3.44).

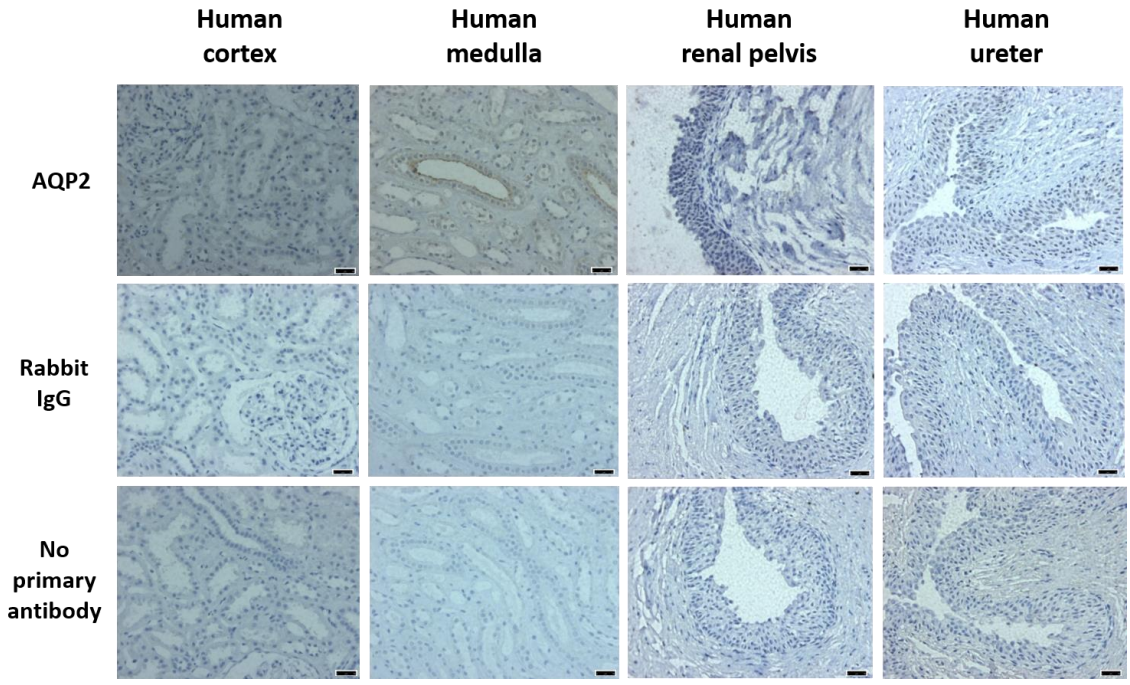

Figure 3.44 Immunohistochemistry demonstrating AQP2 expression by human kidney and not by human renal pelvis and ureter

Immunohistochemistry using anti-AQP2 at a dilution of 1:250 and rabbit IgG at a corresponding concentration. Sections labelled no primary antibody were incubated with 1.5% goat serum. Images show AQP2 is present in the luminal membranes of the collecting duct. AQP2 is not detected in human renal pelvis and ureter. Scale bar = 50 μm.

3.5.3 Aquaporin 3

AQP3 within human kidney, renal pelvis and ureter was detected using goat anti-AQP3 (Santa Cruz, sc-9885), 1.5% horse serum in TBS-T for blocking and a polymerised reporter antibody staining system ImmPRESS HRP anti-goat polymer detection system (MP7405, Vector Laboratories, Burlingame, CA, USA). Primary antibody dilutions of 1:50 and 1:200 were assessed based on reports from other groups using the same antibody [259]. At 1:50 dilution both primary antibody and the corresponding concentration of goat IgG control gave too much non-specific staining (data not shown). At a primary antibody dilution of 1:200, anti-AQP3 demonstrated appropriate staining of the basolateral membrane of the human kidney collecting ducts and also staining of the human renal pelvis and ureteric urothelium, while the IgG control did not show non-specific staining (Figure 3.45).

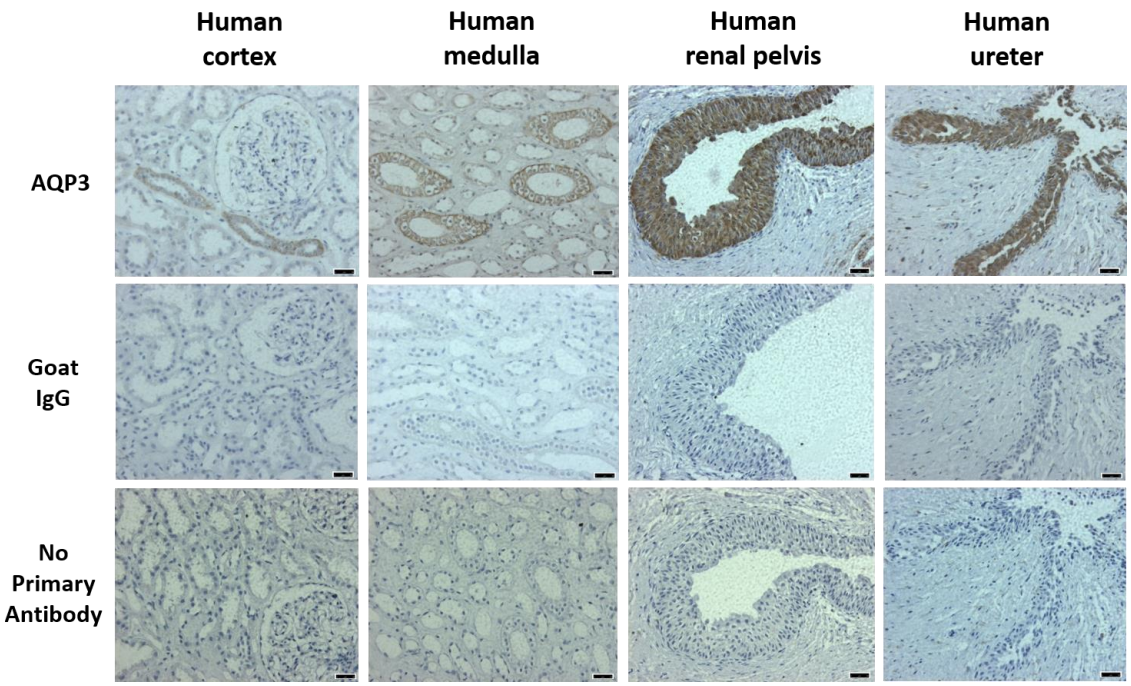

Figure 3.45 Immunohistochemistry demonstrating AQP3 expression by human kidney, renal pelvis and ureter

Immunohistochemistry using anti-AQP3 at a dilution of 1:200 and goat IgG at a corresponding concentration. Sections labelled no primary antibody were incubated with 1.5% horse serum. Images show AQP3 is expressed in the basolateral membranes of the kidney collecting ducts as well as in the urothelium of human renal pelvis and ureter. Scale bar = 50 μm.

3.5.4 Aquaporin 4

Immunohistochemistry for AQP4 was performed using a goat anti-AQP4 antibody (Santa Cruz, sc-9888) using the same protocol as when staining for AQP3. AQP4 antibody dilutions of 1:50 and 1:200 were used alongside negative controls of goat IgG at a corresponding concentration and no primary antibody. The anti- AQP4 antibody staining was non-specific, being cytoplasmic rather than predominantly basolateral membrane, and staining all tubules within the renal medulla rather than the collecting ducts (data not shown). The achieved staining pattern was not consistent with the known location of AQP4 [396] and therefore further studies were performed using different blocking steps to eliminate non-specific binding at the same, and reduced, anti-AQP4 antibody concentrations (Figure 3.46).

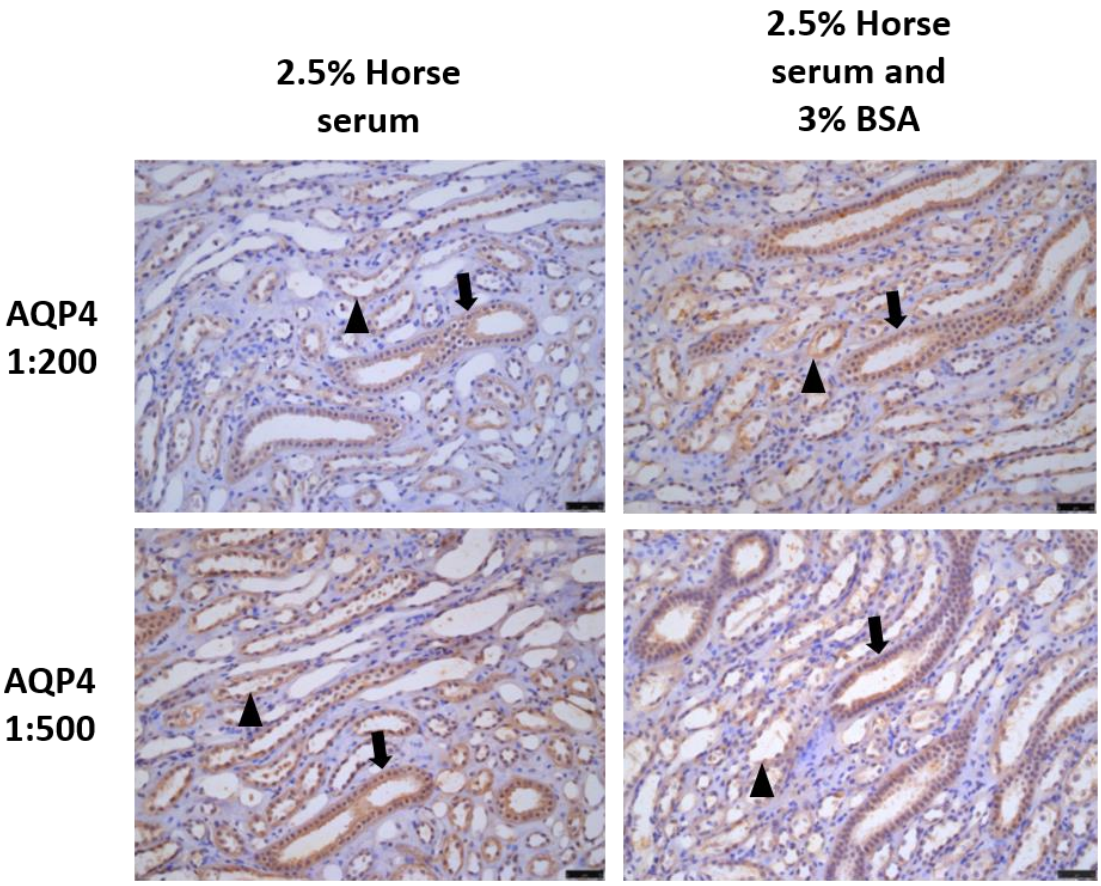

Figure 3.46 Immunohistochemistry for AQP4 in human kidney medulla using a Santa Cruz anti-AQP4 antibody

Immunohistochemistry of human kidney medulla sections using anti-AQP4 (Santa Cruz) at 1:200 and 1:500 dilutions. Sections were blocked with either 2.5% horse serum or 2.5% horse serum with 3% BSA. Non-specific tubular DAB binding in all sections questions the specificity of the antibody. Regardless of the antibody concentration or the blocking step used both the collecting ducts (arrow) and other tubular structures (arrowhead) such as the loops of Henle are stained. Additionally, the collecting duct staining is predominantly cytoplasmic rather than at the basolateral membrane as shown by others. Scale bar = 50 μm.

A new rabbit anti-AQP 4 antibody was sourced from Alomone (249-323, Jerusalem, Israel) and immunohistochemistry using human kidney sections performed using an antibody dilution of 1:500 based on the manufacturers recommendations. Sections were blocked with either 1.5% or 5% goat serum and the SignalStain® boost secondary HRP anti-rabbit antibody was used. Again, non-specific tubular binding was noted throughout the section. Although an increased concentration of blocking serum attenuated the non-specific binding the remaining DAB staining was not localized to the collecting duct basolateral membrane as previously reported [187].

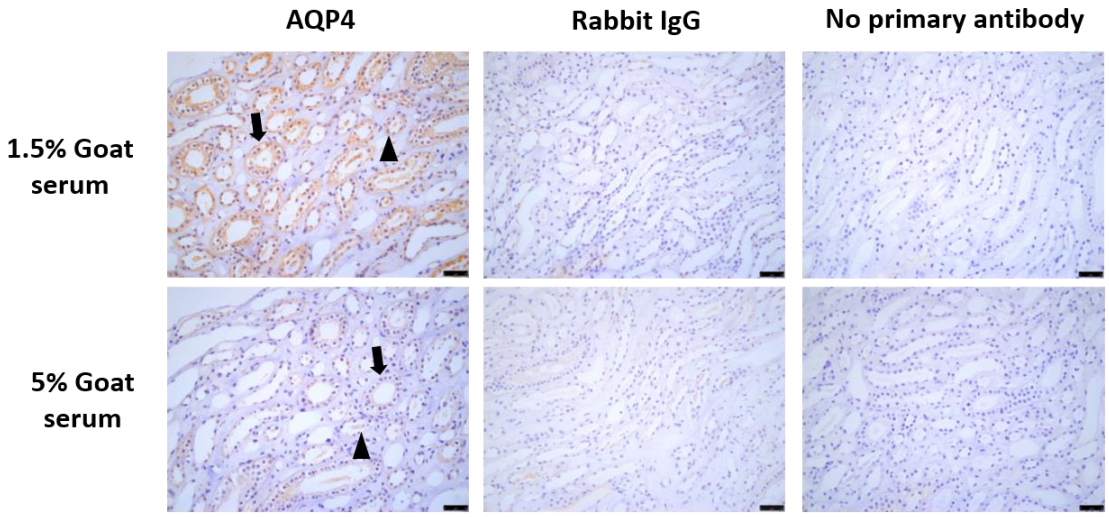

Figure 3.47 Immunohistochemistry for AQP4 in human kidney medulla using an Alomone anti-AQP4 antibody

Immunohistochemistry of human kidney medulla sections using anti-AQP4 (Alomone) at 1:500 dilution and rabbit IgG at a corresponding concentration. Sections labelled no primary antibody were incubated with antibody diluent only. Sections were blocked with either 1.5% or 5% goat serum. Sections stained with anti-AQP4 antibody demonstrated non-specific tubular binding with both the collecting ducts (arrow) and other tubular structures (arrowhead) such as the loops of Henle being stained. Although the DAB staining was attenuated by using a higher concentration of blocking serum, the remaining staining was again not localized correctly to the collecting duct. Scale bar = 50 μm.

The sequence of slides seen in Figure 3.47 was repeated using Tris–EDTA (pH 9) antigen retrieval buffer instead of citrate (pH 6) buffer however the results were unchanged (data not shown) and no further attempts were made to optimise this antibody.

Due to time constraints accurate detection of AQP4 by immunohistochemistry on human or rat, kidney, renal pelvis or ureter, was not possible during this research project. I would have liked to have performed this to confirm whether AQP4 is expressed by the urothelium of the ureter and renal pelvis and specifically by the umbrella cells of the urothelium which contact the urinary lumen. Optimising this technique to detect AQP4 by immunohistochemistry will be a priority for future work related to this thesis.

Results for the detection and localisation of AQPs 1-3 in rat kidney, renal pelvis and ureter tissue are presented in Chapter 5.

3.6 Detecting urinary aquaporins

3.6.1 Demonstrating urinary aquaporin 1 by western blotting

The initial attempt to identify AQP 1 in human urine involved ultrafiltration of the urine (Amicon® Ultra-15 10K centrifugal filter device) to generate urine concentrate followed by chemical precipitation of exosomes. This was performed as described in the methods section except the urine concentrate: ExoQuick-TC ratio was 5:1 (rather than 1:1 in the final protocol). After incubation with the ExoQuick-TC it was noted that a visible exosome pellet had not formed and on western blotting AQP1 could not be identified in the exosome fraction. Running of the aspirated supernatant which is normally discarded did however produce some murky bands suggesting there was simply not enough ExoQuick-TC to precipitate the exosomes. Subsequently, the ratio of urine concentrate:ExoQuick-TC was increased to 1:1, which enabled AQP1 detection with a major band at 25 kDa corresponding to the non-glycosylated band of the human kidney lysate positive control (Figure 3.48). As a comparison, urine concentrate generated by ultrafiltration only from the same initial urine sample, along with urine concentrate mixed with RIPA buffer in a ratio of 2.5:1, were also run on western blot and probed for AQP1. Figure 3.48 demonstrates that AQP1 can be detected in the urine using all three extraction techniques; ultrafiltration, ultrafiltration + RIPA buffer, and ultrafiltration + ExoQuick-TC. Ultrafiltration and ultrafiltration + ExoQuick- TC generated the best results. There was no benefit to adding RIPA buffer to the urine concentrate and if anything it made detection worse. Ultrafiltration alone (producing urine concentrate) gives bands that are much better defined than those with ultrafiltration + Exo-Quick-TC, and using ultrafiltration alone does not seem to reduce the detection of AQP1. Samples of the urine filtered through the Amicon membrane and the supernatant from the Exo-Quick-TC sample were run on western blot and AQP1 was not detected (results not shown). This suggests that all of these extraction techniques are isolating the majority of available urinary AQP1.

Although the method of chemical precipitation of exosomes is designed to isolate exosomes for downstream applications, the field of work on exosomes is expanding rapidly and this method is probably an oversimplification and does not produce a purely exosomal fraction.

However for the purpose of the research the aim was to find a robust, reproducible, economically viable method of isolating aquaporins from the urine for further analysis initially by western blotting. With this in mind the method of ultrafiltration was used to concentrate and fractionate urine for ongoing aquaporin analysis with the proviso that it did not reflect a truly exosomal population.

Using this method of urine ultrafiltration to isolate AQPs, western blotting has confirmed in addition to AQP1 the presence of AQP2 and the absence of AQP3 in human urine (Figure 3.37 and Figure 3.38, pages 113-114).

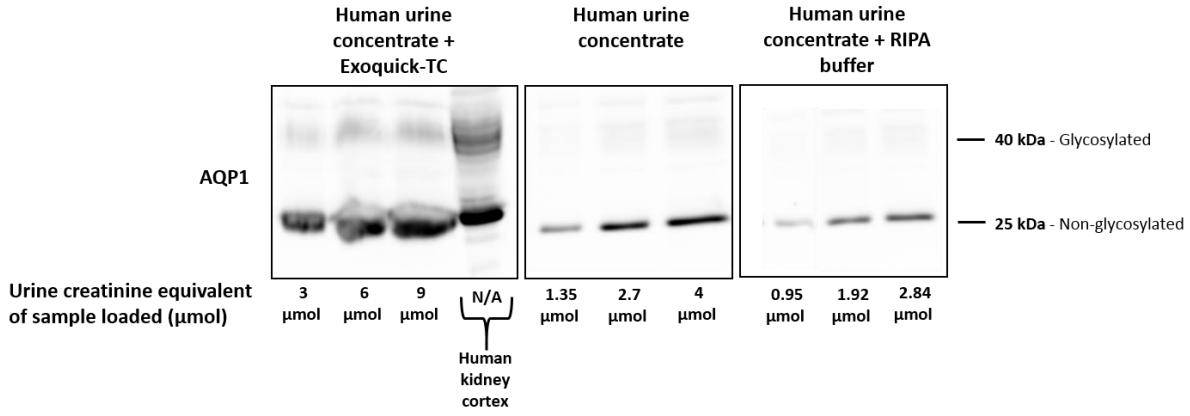

Figure 3.48 Comparison of different methods of AQP1 isolation from urine

Western blots demonstrating the presence of AQP1 in human urine using three different extraction techniques; ultrafiltration + chemical precipitation with ExoQuick-TC, ultrafiltration alone and ultrafiltration + addition of RIPA buffer. The samples were loaded at three different volumes and the urinary creatinine equivalent (µmol) of each sample has been indicated.

3.6.2 Urinary aquaporin 1 ELISA

Looking forward, the application of this research would be a clinical test which would need to be reproducible, produce quantitative results and be cost effective. A urinary AQP ELISA has the potential to meet these objectives and given the prohibitive costs of buying a commercial ELISA, an indirect ELISA using colorimetric substrate was designed in house using a method reported by Umenishi *et al*. [397]. Although both AQP1 and AQP2 are detected in the urine, for reasons which are reviewed in the discussion (section 3.7), a urinary AQP1 ELISA was developed rather than an AQP2 ELISA.

Initially the ELISA was conducted as per the methods section in chapter 2 except using anti-AQP1 antibody at a 1 in 30 dilution, 0.01% SDS/PBS as standard and sample diluent and 2, 2'-Azino-bis(3-ethylbenzothiazoline-6-sulfonic acid) (ABTS liquid substrate system,

A3219, Sigma-Aldrich, St-Louis, MO, USA) as substrate. A 2-fold serial dilution of the AQP1 standards returned a reasonable standard curve with an $R^2 = 0.987$ however the overall level of signal in the standards could be improved (Figure 3.49).

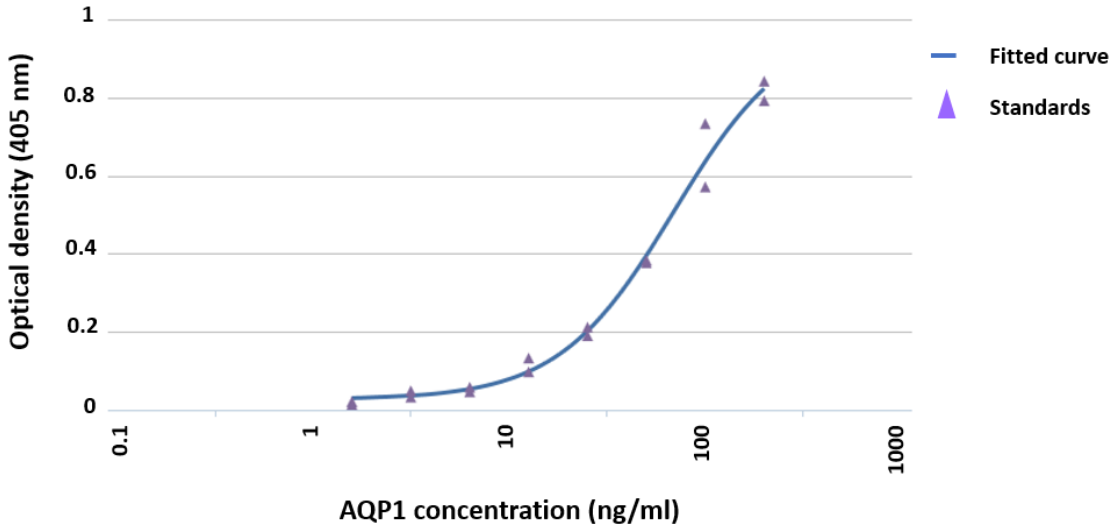

Figure 3.49 Urinary AQP1 ELISA standard curve

The standard curve demonstrates a serial dilution of AQP1 standards from 1.5625-200 ng/ml. Analysis performed by 4 parameter logistic regression. $R^2 = 0.987$. Anti- AQP1 antibody was used at 1:30 dilution and standard/sample diluent was 0.01% SDS in PBS. ABTS substrate was applied for 30 minutes in the dark followed by 1% SDS stop solution.

A 2-fold serial dilution of a single human urine sample was analysed alongside these standards and returned an optical density equivalent to the blank wells for all dilutions signifying that the assay was not detecting the AQP1 in the sample. Additionally, the mean optical density of the blank wells was too high at 0.369 indicating significant background signal.

Factors potentially responsible for the high optical density in the blank wells include:

- Bovine serum albumin (BSA) grade
- Insufficient washing of wells
- Primary or secondary antibody binding

An ELISA to establish the cause of high background was undertaken which involved:

- Blank wells – 0.01% SDS/PBS, primary antibody and secondary antibody
- Control wells – primary and secondary antibodies used but without initial addition of 0.01% SDS/PBS

- Secondary antibody only – as above except without addition of primary antibody

Additionally, each of the above was performed with 2 different types of BSA as well as trialling 5% tween 20 in PBS for block and antibody diluent instead of BSA. Special attention was paid to adequate washing of the wells. Table 3.1 demonstrates the results of this ELISA where the optical density for all wells is perfectly acceptable suggesting that the washing step could have been responsible for the increased signal in the blank wells on the first ELISA run.

Well	Block/antibody diluent	Optical density 1	Optical density 2	Mean optical density
Blank	3% BSA (A9647, Sigma)	0.093	0.093	0.093
Control	3% BSA (A9647, Sigma)	0.080	0.078	0.079
Secondary antibody	3% BSA (A9647, Sigma)	0.071	0.073	0.072
Blank	3% BSA (A7030, Sigma)	0.091	0.088	0.0895
Control	3% BSA (A7030, Sigma)	0.075	0.075	0.075
Secondary antibody	3% BSA (A7030, Sigma)	0.072	0.072	0.072
Blank	5% tween 20	0.094	0.091	0.0925
Control	5% tween 20	0.079	0.080	0.0795
Secondary antibody	5% tween 20	0.074	0.075	0.0745

Table 3.1 AQP1 ELISA investigating high background in blank wells

Anti-AQP1 antibody used at 1 in 30 dilution. ABTS substrate was applied for 30 minutes in the dark followed by 1% SDS stop solution. Blank wells – 0.01% SDS/PBS, primary antibody and secondary antibody. Control wells – primary (anti-AQP1) and secondary (anti-rabbit) antibodies used but without initial addition of 0.01% SDS/PBS. Secondary antibody only – secondary antibody used but without 0.01% SDS/PBS and primary (anti-AQP 1) antibody. For each permutation 3 different types of blocking step were used – 3% BSA (A9647) in PBS, 3% BSA (A7030) in PBS and 5% tween 20 in PBS.

The AQP1 ELISA was repeated using a 2-fold serial dilution of a single human urine sample run alongside AQP1 standards used to generate a standard curve. The blank was much improved at (0.092), however the signal obtained from the standards was significantly less than that achieved with the previous ELISA (Figure 3.50). The ELISA was able to detect AQP1 in the diluted urine sample however the optical density even in the undiluted sample was very low and at the bottom of the standard curve (Table 3.2). Attention was turned to trying to concentrate the AQP1 protein in the sample by either ultrafiltration or lyophilisation (see 3.6.2.1).

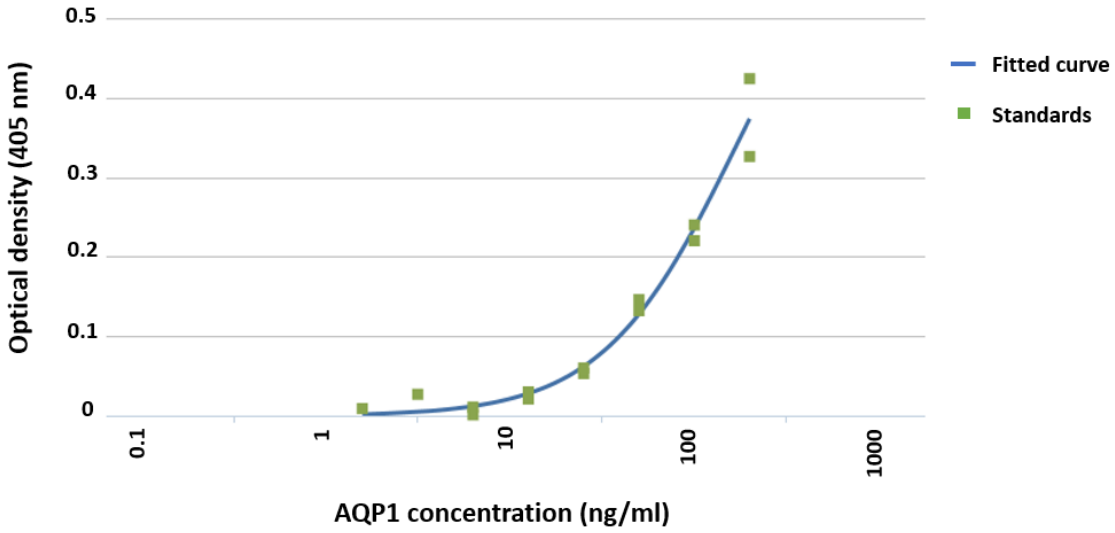

Figure 3.50 Urinary AQP1 ELISA standard curve associated with Table 3.2

The standard curve demonstrates a serial dilution of AQP1 standards from 1.5625-200 ng/ml and reveals that the optical densities obtained for the individual AQP1 concentrations are much lower than on the previous ELISA assay. Analysis performed by 4 parameter logistic regression. R^2 = 0.976. Anti- AQP1 antibody was used at 1:30 dilution and standard/sample diluent was 0.01% SDS in PBS. ABTS substrate was applied for 30 minutes in the dark followed by 1% SDS stop solution.

Urine dilution	Optical density 1	Optical density 2	Mean optical density	AQP1 concentration (ng/ml)
1	0.02	0.007	0.014	6.884
1:2	0.034	0.034	0.034	14.615
1:4	0.023	0.032	0.032	13.866
1:8	0.034	0.022	0.028	12.357
1:16	0.021	0.019	0.02	9.474
1:32	0.011	0.009	0.01	5.431
1:64	0.016	0.002	0.009	4.789
1:128	0.006	-0.004	0.001	0.959

Table 3.2 Urinary AQP1 ELISA for serial dilutions of a single human urine sample

Serial dilution of a single human urine sample was undertaken with 0.01% SDS in PBS from undiluted sample to 1 in 128 dilution. Although AQP1 was detected in the urine samples the optical density was very low placing the results at the bottom end of the standard curve.

3.6.2.1 Lyophilisation and concentration of urine samples

In order to try and improve detection of AQP1 in the urine samples a single human urine sample was split and used in three ways on the same ELISA plate:

- Concentrated urine - Urine sample (15 ml) concentrated and fractionated in an Amicon® Ultra-15 10K centrifugal filter device (UFC901008, Merck Millipore, Billerica, MA, USA) to a volume of 500 µl followed by 2-fold serial dilutions using 0.01% SDS/PBS as diluent
- Lyophilised urine - lyophilisation of the urine sample (15 ml) and reconstitution to a volume of 600 µl with 0.01% SDS/PBS
- Urine - 2-fold serial dilutions of the native urine sample using 0.01% SDS/PBS as diluent

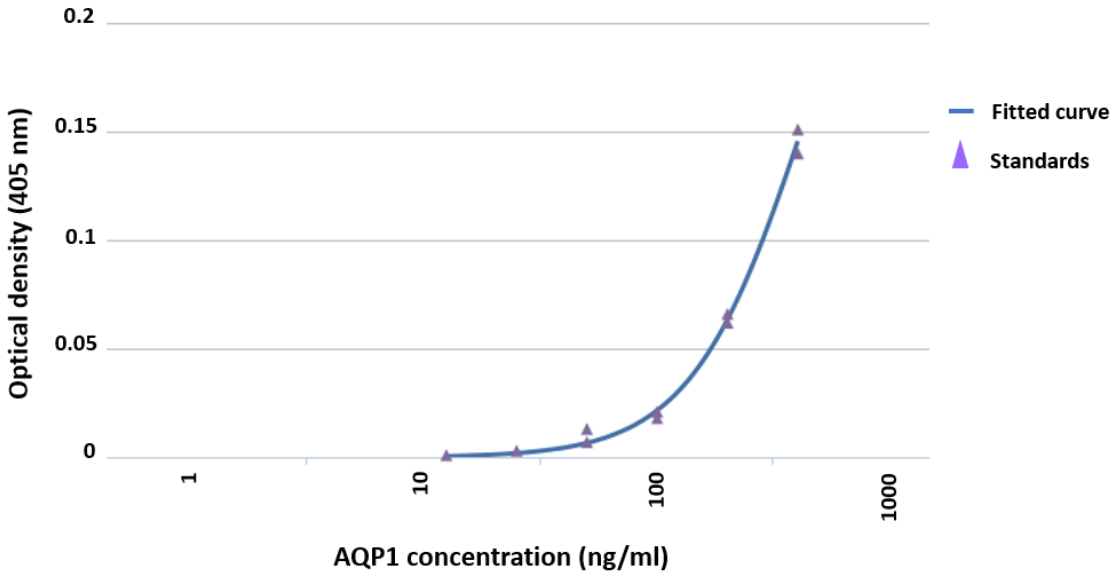

Figure 3.51 Urinary AQP1 ELISA standard curve associated with Table 3.3

The standard curve demonstrates a serial dilution of AQP1 standards from 12.5-400 ng/ml however the optical densities are very low. Analysis performed by 4 parameter logistic regression reveals an R^2 = 0.996. Anti-AQP1 antibody was used at 1:30 dilution and standard/sample diluent was 0.01% SDS in PBS. ABTS substrate was applied for 30 minutes in the dark followed by 1% SDS stop solution.

Urine sample (dilution)	Optical density 1	Optical density 2	Mean optical density
Urine (1)	0.082	0.08	0.082
Urine (1:2)	0.108	0.108	0.108
Urine (1:4)	0.114	0.114	0.114
Urine (1:8)	0.095	0.104	0.1
Urine (1:16)	0.067	0.07	0.069
Urine (1:32)	0.052	0.044	0.048
Urine (1:64)	0.028	0.023	0.026
Concentrated Urine (1)	0.178	0.136	0.158
Concentrated Urine (1:2)	0.134	0.164	0.149
Concentrated Urine (1:4)	0.11	0.101	0.106
Concentrated Urine (1:8)	0.093	0.092	0.092
Concentrated Urine (1:16)	0.082	0.07	0.076

Concentrated Urine (1:32)	0.062	0.063	0.063
Concentrated Urine (1:64)	0.055	0.036	0.045
Lyophilised Urine (1)	0.099	0.092	0.096
Lyophilised Urine (1:2)	0.155	0.182	0.168
Lyophilised Urine (1:4)	0.153	0.194	0.173
Lyophilised Urine (1:8)	0.153	0.158	0.156
Lyophilised Urine (1:16)	0.217	0.2	0.208
Lyophilised Urine (1:32)	0.161	0.176	0.168
Lyophilised Urine (1:64)	0.142	0.143	0.142

Table 3.3 AQP1 ELISA of concentrated/fractionated or lyophilised urine

A single human urine sample was split into 3 aliquots which were processed differently to produce: concentrated/fractionated urine, lyophilized urine and urine. All 3 aliquots were serially diluted by a factor of 2 with 0.01% SDS in PBS from undiluted sample to 1 in 64 dilution. Lyophilisation and concentration/fractionation of the urine did not significantly improve the detection of AQP1.

Unfortunately, the standards didn't work very well reaching a maximum optical density of 0.15 nm for the largest concentration of 400 ng/ml. This may have been due to freeze-thaw effect (see 3.6.2.2) as the aliquot of standard used had been thawed before. Moreover, concentration/fractionation and lyophilisation of the urine samples didn't considerably improve the detection of urinary AQP1 compared to control urine. The next avenue was to explore different substrates used for peroxidase-based enzyme immunoassays to try and improve assay sensitivity.

3.6.2.2 Freeze-thaw effect on recombinant aquaporin 1 protein standard and effect of different colorimetric based substrates

A further ELISA was performed comparing TMB substrate which has higher sensitivity for HRP detection than ABTS. Additionally, for both substrates, a new aliquot of AQP1 standard was compared with a freeze-thawed aliquot of AQP1 standard.

	ABTS Substrate		TMB Substrate	
AQP 1 concentration ng/ml	New standard Mean OD	Freeze-thaw standard Mean OD	New standard Mean OD	Freeze-thaw standard Mean OD
6.25	0.034	0.001	0.13	0.01
12.5	0.07	0.004	0.258	0.014
25	0.138	-0.005	0.548	0.004
50	0.287	-0.001	1.07	0.009
100	0.567	0.002	2.23	0.026
200	1.065	0.015	>4	0.071
400	1.557	0.043	>4	0.156

Table 3.4 Recombinant AQP1 protein standard is rendered unusable by freeze-thawing

A 2-fold serial dilution of AQP1 standards from 6.25-400 ng/ml was undertaken for both a new aliquot of protein standard alongside an aliquot which had undergone freeze-thaw. Anti-AQP1 antibody was used at 1:30 dilution and standard/sample diluent was 0.01% SDS in PBS. ABTS substrate was applied for 30 minutes in the dark followed by 1% SDS stop solution. TMB was applied for 15 minutes in the dark followed by 0.18 M H_2SO_4 stop solution. These readings demonstrate that TMB has a much greater sensitivity than ABTS and freeze thaw of the AQP1 standard degrades the protein. ABTS substrate mean blank optical density 0.095. TMB substrate mean blank optical density 0.189. OD = optical density.

Table 3.4 demonstrates that following a single freeze-thaw cycle the AQP1 protein standard is no longer detected by the ELISA, suggesting that freeze-thawing affects the stability of the protein quickly degrading the recombinant AQP1 protein standard. Additionally, this data confirms that TMB is a more sensitive substrate enabling lower protein concentrations to be discerned. During this experiment this was at the expense of higher background signal with the mean blank optical density for ABTS being 0.095 compared to 0.189 for TMB substrate. Furthermore, AQP1 detection in the ABTS group using new standard was clearly improved compared to previous ELISAs. This is likely due to a protocol modification made for this ELISA run whereby the ELISA plate was removed from incubation at 4°C and allowed to equilibrate to room temperature for 90 minutes before the ELISA was continued.

3.6.2.3 Effect of different colorimetric based substrates on urine AQP 1 detection

Using the newly modified protocol and comparing ABTS and TMB substrates directly on a single 96 well plate a single urine sample was split and used in four ways:

- Concentrated urine - Urine sample (15 ml) was concentrated and fractionated in an Amicon® Ultra-15 10K centrifugal filter device (UFC901008, Merck Millipore, Billerica, MA, USA) to a volume of 500 µl followed by 2-fold serial dilutions using 0.01% SDS/PBS as diluent
- Urine - 2-fold serial dilutions of the native urine sample using 0.01% SDS/PBS as diluent
- Urine RIPA – urine was diluted with an equal volume of RIPA buffer containing protease inhibitor and was not diluted any further
- Urine 0.1% SDS - urine was diluted with an equal volume of 0.2% SDS/PBS to create final concentration of 0.1% SDS.

Nice AQP1 standard curves were generated for both substrates. TMB substrate showed greater sensitivity, albeit with a greater blank well optical density reading of (0.2575 for TMB versus 0.1135 for ABTS) which would need to be rectified before application to samples from the human or rat models (Figure 3.52 and Figure 3.53). Generally speaking both substrates demonstrated roughly the same amount of AQP1 protein in the sample however the sensitivity of the assay to lower amounts of protein in more diluted samples was better with TMB. Consequently, TMB would be a better substrate to use when analysing samples from the human and rat models as it was expected AQP1 excretion would be reduced in the obstructed model. Interestingly concentration/fractionation of the urine sample with the centrifugal filter worsened the detection of AQP1 in urine as did the addition of RIPA buffer to the native urine sample. Increasing the amount of SDS in the urine sample, however, augmented AQP1 detection by over 2-fold when analysed with both TMB substrate and ABTS substrates (Table 3.5).

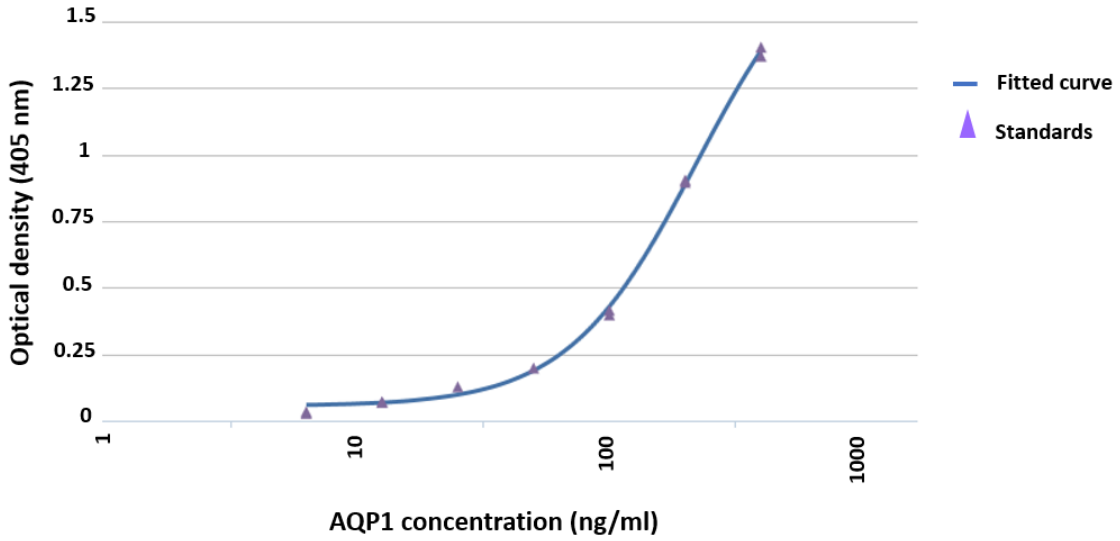

Figure 3.52 Urinary AQP1 ELISA standards using ABTS substrate associated with Table 3.5

The standard curve demonstrates a serial dilution of AQP1 standards from 6.25-400 ng/ml Analysis performed by 4 parameter logistic regression reveals an R^2 = 0.998. Anti- AQP1 antibody was used at 1:30 dilution and standard/sample diluent was 0.01% SDS in PBS. ABTS substrate mean blank optical density = 0.1135.

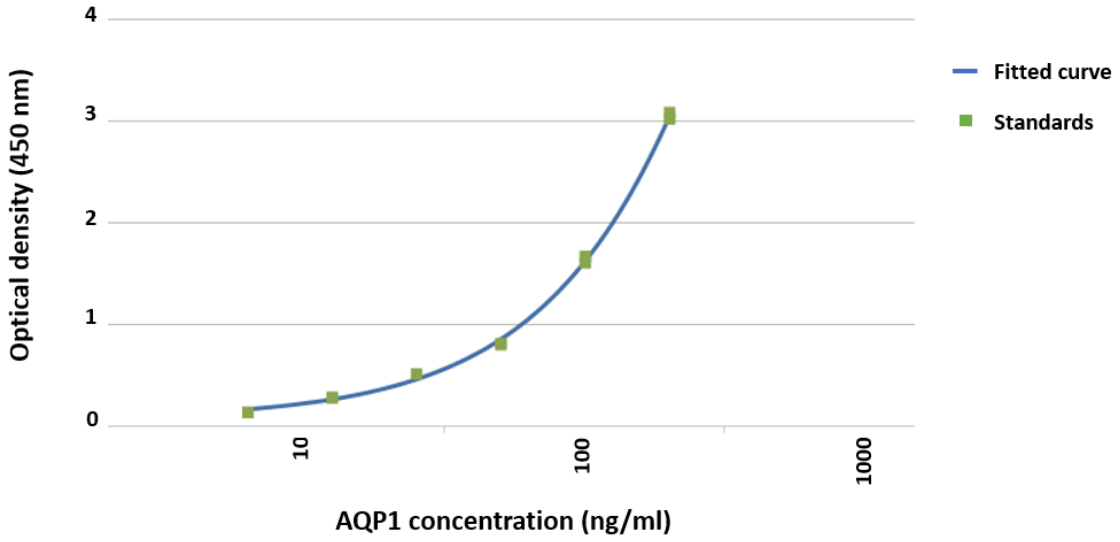

Figure 3.53 Urinary AQP1 ELISA standards using TMB substrate associated with Table 3.5

The standard curve demonstrates a serial dilution of AQP1 standards from 6.25-400 ng/ml Analysis performed by 4 parameter logistic regression reveals an R^2 = 0.999. Anti- AQP1 antibody was used at 1:30 dilution and standard/sample diluent was 0.01% SDS in PBS. TMB substrate mean blank optical density 0.2575.

	ABTS Substrate		TMB Substrate	
Urine sample (dilution)	Mean OD	AQP1 concentration (ng/ml)	Mean OD	AQP1 concentration (ng/ml)
Urine (1)	0.185	39.616	0.692	40.063
Urine (1:2)	0.138	26.316	0.57	32.282
Urine (1:4)	0.111	18.675	0.448	24.638
Urine (1:8)	0.07	6.931	0.268	13.202
Urine (1:16)	0.041	-	0.191	8.271
Urine (1:32)	0.021	-	0.102	2.422
Urine (1:64)	0.007	-	0.052	-
Concentrated urine (1)	0.055	2.687	0.222	10.197
Concentrated urine (1:2)	0.064	5.375	0.247	11.862
Concentrated urine (1:4)	0.048	0.847	0.198	8.724
Concentrated urine (1:8)	0.039	-	0.162	6.367
Concentrated urine (1:16)	0.032	-	0.14	5.032
Concentrated urine (1:32)	0.031	-	0.121	3.718
Concentrated urine (1:64)	0.029	-	0.128	4.18
Urine RIPA (1:2)	-0.037	-	-0.136	-
Urine 0.1 % SDS (1:2)	0.304	-	1.366	-

Table 3.5 Human urine AQP1 ELISA comparing ABTS and TMB substrates and concentrated versus native urine

A single human urine sample was split into 4 aliquots which were processed differently to produce: concentrated/fractionated urine, urine, urine 0.1% SDS, urine RIPA. Aliquots were serially diluted by a factor of 2 with 0.01% SDS in PBS from undiluted sample to 1 in 64 dilution except sample 'urine 0.1% SDS' which was diluted with an equal volume of 0.2% SDS/PBS and 'urine RIPA' which was diluted with an equal volume of RIPA buffer containing protease inhibitor. Anti- AQP1 antibody was used at a 1:30 dilution. 'Concentrated urine' - urine concentrated and fractionated in a centrifugal filter device. 'Urine' – native urine sample. TMB shows a higher sensitivity for HRP than ABTS for both AQP1 standards and urine samples. Concentration of the urine samples or the addition of RIPA buffer worsened APQ1 detection. Increasing the SDS concentration in the sample diluent improved AQP1 protein detection. OD = optical density.

3.6.2.4 Addition of detergent to urine samples analysed using TMB substrate

The AQP1 ELISA was repeated using TMB substrate alongside an increased SDS concentration in the sample/standard diluent of 0.1%. The enhanced concentration of SDS augmented the signal obtained from the standards significantly necessitating exclusion of the two top standards of 100 and 200 ng/ml from the standard curve as the optical densities were >4 (Figure 3.54). Fortuitously the sensitivity of AQP1 detection was increased even more so in the urine samples (Table 3.6). Consequently, urine sample optical densities were placed in the middle third of the standard curve increasing the accuracy of the calculated AQP1 concentration. It was noted that the initial urine dilutions for each sample paradoxically revealed increasing optical densities. This phenomenon has been noted by others [397] and is likely due to additional substances in the urine such as Tamm-Horsfall protein (THP) interfering with the assay. This indicates that for ongoing experiments serial dilutions would be required for each urine sample. The urine dilution at which the optical density first decreased would be used to calculate the urine AQP1 concentration.

The mean blank well optical density remained a little high at 0.1455 which was addressed by the experiments presented in section 3.6.2.5.

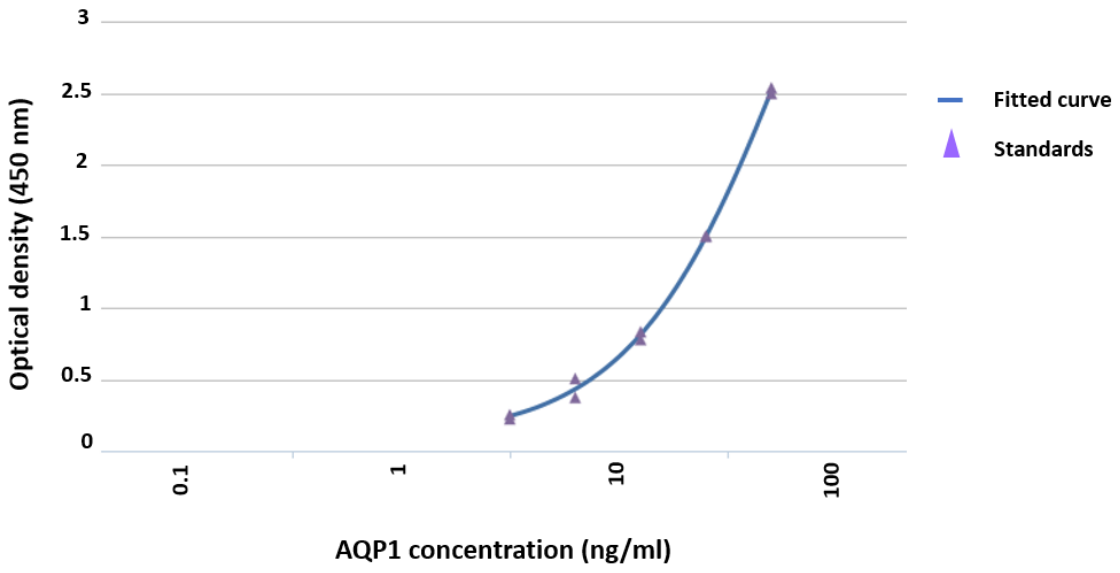

Figure 3.54 Urinary AQP1 ELISA using 0.1% SDS/PBS standard and sample diluent

The standard curve demonstrates a serial dilution of AQP1 standards from 3.125-50 ng/ml Analysis performed by 4 parameter logistic regression reveals an $R^2 = 0.998$. Anti- AQP1 antibody was used at 1:30 dilution and standard/sample diluent was 0.1% SDS in PBS. TMB substrate mean blank optical density 0.1455.

Urine dilution	OD 1	OD 2	Mean OD	AQP1 concentration (ng/ml)
1	0.67	0.69	0.68	10.305
1:2	1.114	1.152	1.132	18.068
1:4	1.314	1.3	1.308	21.275
1:8	0.828	0.836	0.832	12.835
1:16	0.684	0.714	0.699	10.618
1:32	0.472	0.478	0.476	6.956
1:64	0.28	0.274	0.277	3.698

Table 3.6 AQP1 ELISA using TMB substrate and 0.1% SDS/PBS as standard/sample diluent

Serial dilution of a single human urine sample was undertaken with 0.1% SDS in PBS from undiluted sample to 1 in 64 dilution. The addition of 0.1% SDS in PBS significantly improved the detection of AQP1 in the urine bringing the optical density values closer to the centre of the standard curve. Increasing optical density values of the initial urine dilutions likely represents inhibitors within the urine sample which are diluted down at higher urine dilutions. OD = optical density.

3.6.2.5 Optimisation of ELISA blank wells using TMB substrate

TMB is known to have high sensitivity for HRP which can lead to increased background in blank wells. Factors potentially responsible for this phenomenon include:

- Bovine serum albumin (BSA) grade
- Increased concentration of SDS
- Primary or secondary antibody binding

An ELISA to establish the cause of high background was undertaken which involved:

- Blank wells – 0.1% SDS/PBS, primary antibody and secondary antibody
- Control wells – primary and secondary antibodies used but without initial addition of 0.1% SDS/PBS
- Secondary antibody only – as above except without addition of primary antibody

Additionally, each of the above was performed with 2 different types of BSA as well as testing 5% tween 20 in PBS for block and antibody diluent instead of BSA.

Table 3.7 demonstrates that the background is worse with 5% tween while it was slightly improved with the BSA A7030 compared to BSA A9647. There was little difference between the two types of BSA. Moreover, there is little difference in optical density values between blank and control wells indicating that the 0.1% SDS/PBS sample diluent is not responsible. A significant decrease in signal from the control to the secondary antibody wells suggests the primary antibody concentration could be the culprit and therefore the ELISA was repeated using decreasing concentrations of anti-AQP1 antibody on blank wells (incubated with 0.1% SDS/PBS diluent at 4°C only before addition of primary and secondary antibodies). The mean optical density decreased with decreasing anti-AQP1 antibody concentration and a primary antibody dilution of 1:60 was selected for use in further ELISA assays as this dilution demonstrated acceptable background signal (Table 3.8).

Well	Block/antibody diluent	Optical density 1	Optical density 2	Mean optical density
Blank	3% BSA (A9647, Sigma)	0.134	0.161	0.1475
Control	3% BSA (A9647, Sigma)	0.124	0.179	0.1515
Secondary antibody	3% BSA (A9647, Sigma)	0.044	0.046	0.045
Blank	3% BSA (A7030, Sigma)	0.108	0.116	0.112
Control	3% BSA (A7030, Sigma)	0.098	0.098	0.098
Secondary antibody	3% BSA (A7030, Sigma)	0.040	0.038	0.039
Blank	5% tween 20	0.381	0.411	0.396
Control	5% tween 20	0.276	0.410	0.343
Secondary antibody	5% tween 20	0.048	0.049	0.0485

Table 3.7 AQP1 ELISA to investigate factors responsible for high background in blank wells using TMB substrate

Anti-AQP1 antibody used at 1 in 30 dilution with TMB substrate. Blank wells – 0.1% SDS/PBS, primary antibody and secondary antibody. Control wells – primary (anti-AQP1) and secondary (anti-rabbit) antibodies used but without initial addition of 0.1% SDS/PBS. Secondary antibody only – secondary antibody used but without 0.1% SDS/PBS and primary (anti-AQP1) antibody. For each permutation 3 different types of blocking

step were used – 3% BSA (A9647) in PBS, 3% BSA (A7030) in PBS and 5% tween 20 in PBS. This data demonstrates the primary antibody concentration to be the likely cause of increased background signal.

Primary antibody dilution	Optical density 1	Optical density 2	Mean optical density
1 in 30	0.110	0.119	0.1145
1 in 40	0.102	0.110	0.106
1 in 50	0.101	0.099	0.1
1 in 60	0.088	0.089	0.0885
1 in 100	0.075	0.076	0.0755
1in 200	0.058	0.060	0.059
1 in 400	0.049	0.055	0.052
1 in 1000	0.041	0.044	0.0425

Table 3.8 AQP1 ELISA to determine the optimum anti-AQP1 antibody dilution

An increasing dilution of anti-AQP1 antibody (1 in 30 – 1 in 1000) was applied to blank wells containing 0.1% SDS/PBS. Secondary antibody and TMB substrate were applied as per the usual protocol. A primary antibody dilution of 1 in 60 was selected for future use as this dilution demonstrated an acceptable level of background signal.

Using anti-AQP1 at 1 in 60 dilution, two new human urine samples and one rat urine sample, the AQP1 ELISA was repeated with each sample being performed in triplicate. Triplicate repeats of AQP1 standards show good reproducibility with low intra assay variability (percentage co-efficient variation of the optical density ranging 1.833 – 7.566) and an acceptable R2 = 0.997 (Figure 3.55 and Table 3.9).

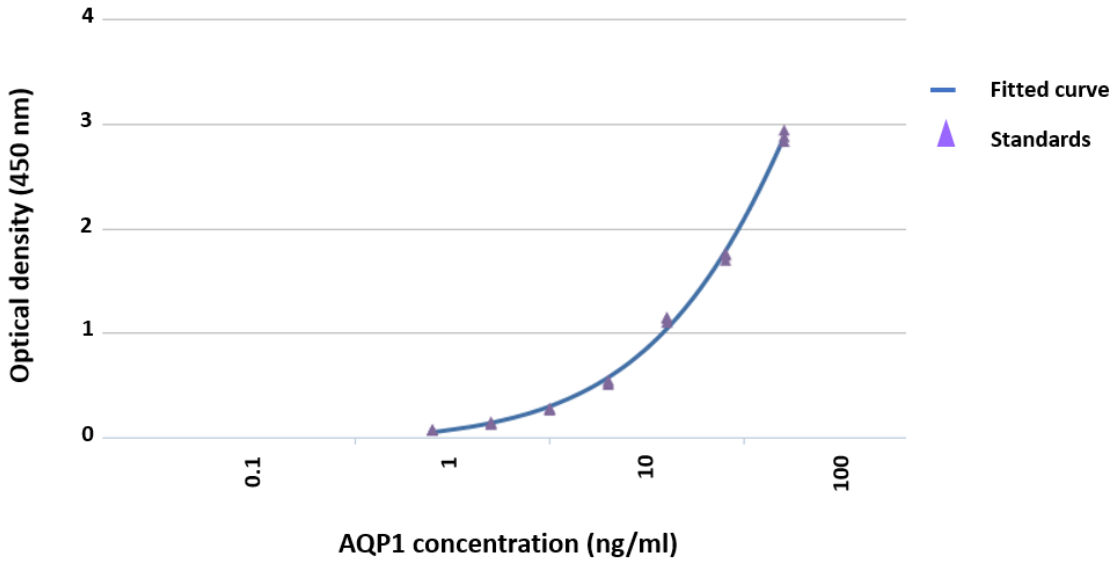

Figure 3.55 Urinary AQP1 ELISA standard curve using anti- AQP1 at 1 in 60 dilution associated with Table 3.9 and Table 3.10

The standard curve demonstrates a serial dilution of AQP1 standards from 0.39-50 ng/ml. Analysis performed by 4 parameter logistic regression reveals an $R^2 = 0.997$. Anti- AQP1 antibody was used at 1:60 dilution and standard/sample diluent was 0.1% SDS in PBS. TMB substrate mean blank optical density 0.102.

AQP1 concentration ng/ml	Optical density 1	Optical density 2	Optical density 3	Mean optical density	Standard deviation	% CV optical density
0.78	0.068	0.07	0.072	0.07	0.002	2.871
1.56	0.147	0.131	0.128	0.135	0.01	7.566
3.125	0.276	0.272	0.262	0.27	0.007	2.674
6.25	0.544	0.529	0.507	0.526	0.019	3.536
12.5	1.101	1.147	1.139	1.129	0.025	2.177
25	1.694	1.74	1.758	1.73	0.033	1.907
50	2.830	2.875	2.938	2.88	0.054	1.883

Table 3.9 Optical densities of AQP1 standards using anti-AQP1 at 1 in 60 dilution

A 2-fold serial dilution of recombinant AQP1 protein standards was performed from 50 ng/ml to 0.78 ng/ml in 0.1% SDS/PBS. Protein standards were performed in triplicate. Individual, and mean optical densities measured at 450 nm are presented for each AQP1 protein concentration alongside the standard deviation and percentage coefficient variation. Anti-AQP1 antibody was used at 1 in 60 dilution alongside TMB substrate.

This ELISA demonstrated that AQP1 can be detected in rat urine as well as human urine. Similar to the AQP1 standards, good reproducibility with low intra-assay variation was

shown between sample triplicates (percentage coefficient variation of optical densities ranging 2.55 – 7.82). Using the standard curve generated by 4 parameter logistic regression the urine AQP1 concentration was calculated. This value was then corrected by the factor of the sample dilution. The AQP1 concentration was calculated for the urine dilution that first generated a decrease in optical density in order to account for the presence of inhibitors in the more concentrated dilutions (Table 3.10).

Subsequently this modified AQP1 ELISA protocol was used for analysis of rat neonatal unilateral ureteric obstruction model samples, adjusting the AQP1 result to urine creatinine to correct for urine concentration in a random sample.

Urine (dilution)	Optical density 1	Optical density 2	Optical density 3	Mean optical density	% CV optical density	AQP1 conc-entration (ng/ml)	Corrected AQP1 conc-entration (ng/ml)
Human A (1:2)	0.871	0.833	0.793	0.832	4.69		
Human A (1:4)	0.924	0.834	0.889	0.882	5.14		
Human A (1:8)	0.482	0.453	0.462	0.465	3.19	4.994	39.952
Human B (1:2)	1.528	1.408	1.375	1.437	5.60		
Human B (1:4)	1.329	1.202	1.177	1.236	6.59	15.541	62.164
Human B (1:8)	0.549	0.47	0.504	0.507	7.82		
Rat (1:2)	0.827	0.791	0.792	0.803	2.55		
Rat (1:4)	0.344	0.356	0.333	0.344	3.34	3.64	14.56

Table 3.10 The AQP1 ELISA detects both human and rat urinary AQP1

Two-fold serial dilutions of 2 human urine samples and a single rat urine sample were performed using 0.1% SDS/PBS. Samples were analysed in triplicate. Individual, and mean optical densities measured at 450 nm are presented for each sample alongside the percentage coefficient variation, calculated AQP1 concentration and the AQP1 concentration corrected for the dilution. The urine dilution at which the optical density first decreased was used to calculate the AQP1 concentration. The anti-AQP1 antibody was used at 1 in 60 dilution alongside TMB substrate.

3.7 Discussion

Endpoint RT-PCR is a useful method to demonstrate the presence or absence of mRNA for a particular gene within cells or tissues [398]. Using this technique contamination of the human kidney samples with genomic DNA was detected and rectified by implementing a DNase step in the RNA extraction protocol. As a result of these experiments the endpoint PCR technique was optimised for future use in both the human and rat studies.

Although semi-quantitative analysis of end-point PCR has been reported in the literature [187] this technique is imprecise having low sensitivity to detect changes in yield. By definition, the amount of product is measured at the end of the reaction when the starting and final amount of template do not necessarily have a direct correlation [399]. Real time PCR provides accurate quantitation of the starting amount of cDNA in a sample as it measures the accumulation of template in real time during the exponential phase of the PCR reaction [398, 399]. Real time (quantitative) PCR would be the optimum method to compare AQP expression between obstructed and non-obstructed urinary tracts in the human and rat models. Primers suitable for real time PCR were designed and validated [400] using standard techniques to detect rat AQP isoforms 1-4, and 6-11 as well as the reference genes, β-actin and PKG 1. Primers were also designed and tested to detect rat AQP5 however they were unsuitable for real time PCR and thus not used in sample analysis. Primers to detect rat AQPs 0 and 12 were also designed but were not validated for real time PCR as endpoint PCR demonstrated these isoforms were not expressed by rat urinary tract (Chapter 5). Unfortunately, due to time constraints primers suitable for real time PCR which detect human AQPs were not developed.

The technique of western blotting has been optimised, via testing a number of well described protocol modifications, to detect and quantify AQPs 1-4 in both human and rat tissue. AQP1 was detected at the protein level in human kidney, renal pelvis and ureter, as well as rat kidney and bladder by western blotting. The protein was identified by a 25 kDa non-glycosylated band, and a 35-40 kDa glycosylated band. The glycosylated band arises due to N-glycosylation of AQP1, which was confirmed by deglycosylation studies. Interestingly western blotting of human kidney revealed a glycosylated band of higher molecular weight (40 kDa) than that of human ureter, human renal pelvis and rat kidney (35 kDa). This could be due to differential glycosylation between distinct tissue types or potentially could be related to the protein extraction technique. The glycosylated band was reported between 35-

50 kDa in human and rat kidneys by Frokiaers group [187, 189], however, samples from the two species were not assessed simultaneously.

AQP2 detection by western blotting proved much more difficult to establish and following trials of a number of antibodies ultimately required the use of FLAG tagged AQP2 overexpression lysate as a positive control to identify the correct band at 31 kDa. Subsequently AQP2 was detected in human kidney, renal pelvis and ureter, and rat kidney.

Following optimisation of the blocking agent used and the primary antibody concentration AQP3 was detected by western blotting in human kidney, renal pelvis and ureter, and rat kidney and bladder while AQP4 expression was noted in human and rat kidney and rat bladder. Failure to detect AQP4 in human renal pelvis and ureter on western blotting may reflect lack of expression at the protein level in these tissues. Alternatively, it has been reported that AQP4 is specifically expressed by the urothelium of the lower urinary tract [259]. Low expression levels within urothelium, combined with urothelium forming a relatively small percentage of the tissue lysed within a ureter or renal pelvis specimen, could also explain the absence of expression.

Following optimisation of antibody dilutions and the introduction of a polymerised secondary reporter antibody to combat issues with endogenous biotin content, immunohistochemistry of human kidney was undertaken. This revealed AQP1 expression in the apical and basolateral membranes of the proximal tubules, the loop of Henle and vasa recta. AQP2 and AQP3 were localised to the apical and basolateral cell membranes of the renal collecting duct respectively. These expression patterns were consistent with previous reports in human and rodent tissue [187, 255]. Within the renal pelvis and ureter AQP1 was localized to the vasculature of the lamina propria but was not detectable in urothelium, while AQP3 was highly expressed by the urothelial cells. Although AQP1 expression has previously been reported in the vascular endothelial cells of rat ureter and bladder, its expression pattern has not been documented before in human ureter or renal pelvis [249]. Contrary to the western blotting results, immunohistochemistry of human ureter and renal pelvis failed to demonstrate AQP2 in any area of the tissue. RT-PCR of human renal pelvis and ureter (Chapter 6), however, confirms AQP2 expression at the mRNA level thus supporting the western blotting results. Conflicting reports regarding AQP2 expression are noted in the literature with rat ureter and bladder urothelium demonstrating AQP2 expression by immunohistochemistry [249] whereas human ureter and bladder urothelium did not demonstrate AQP2 mRNA expression [259]. Given that both RT-PCR and western blotting

of whole ureter and renal pelvis demonstrated AQP2 expression it is likely that the error lies with the immunohistochemistry. Potential causes of lack of staining include:

- Sample fixation with 10% neutral buffered formalin. This crosslinking fixative is good at preserving cell structure however crosslinking, particularly if the sample is over-fixed, can interfere with antibody-epitope binding.
- Ineffective antigen retrieval. The antigen retrieval solution used needs to be tailored to the protein.
- Antibody specificity for the native protein. During western blotting proteins are reduced and denatured while during immunohistochemistry proteins remain in their native form where they may also be obscured by fixative related crosslinking.
- Protein not expressed by human renal pelvis and ureter.

Future work will involve analysis of more human samples paying attention to sample fixation and antigen retrieval techniques which should definitively resolve this issue.

Unfortunately, an antibody which reliably detected AQP4 was not found and therefore AQP4 expression by urinary tract tissues was not assessed during this research. Future studies will involve establishing a reliable AQP4 immunohistochemistry method to apply to samples from both the human and rat models.

A major aim of this research was to establish the urinary AQP profile in high pressure (damaging) and low pressure (non-damaging) PUJO in rodents and humans. The clinical application being the development of urinary AQP quantification as a novel operative biomarker. Techniques were therefore developed to firstly identify and then quantify AQPs in the urine. AQPs are excreted within exosomes into the urine, and although a number of methods reportedly isolate urinary exosomes, many of these do not provide a purely exosomal population. Ultracentrifugation particularly when followed by a double cushion sucrose/D_2O centrifugation step returns the purest exosomal protein fraction. This technique, however, is time consuming, processes few samples simultaneously, and would be inefficient for use in the clinical setting [376].

With an initial aim to simply identify urinary AQPs, western blotting of urine concentrate generated by ultrafiltration was undertaken. This confirmed the presence of AQP1 and 2 and the absence of AQP3 in human urine. These findings are consistent with previous reports [365, 372, 386].

Ultimately the aim of this research would be to develop a clinical test, which would need to be efficient, reproducible, quantitative and cost effective. Umenishi *et al*. compared 3 techniques to quantify urinary AQP2 levels; radioimmunoassay, quantitative immunoblotting and an in-house designed AQP2 ELISA, and showed significant correlation between the results from all 3 techniques [397]. Based on the method described by these authors an AQP1 ELISA was developed as this technique meets the aforementioned attributes and avoids the radiation exposure associated with radioimmunoassay.

An AQP1 in preference to an AQP2 ELISA was developed for a number of reasons. Firstly, because urinary AQP1 excretion is not known to be significantly regulated whereas urinary AQP2 excretion is mediated by vasopressin [372]. Results of an AQP1 ELISA are therefore less likely to be affected by hydration status of the individual. Secondly, adult and neonatal murine UUO models have revealed that the proximal tubule is the most severely affected portion of the nephron demonstrating apoptosis, autophagy and atubular glomeruli formation [98]. AQP1 is expressed in the proximal tubule and thus may act as an early marker of this damage. Finally results from western blotting suggest the anti-AQP1 antibody has better specificity than the anti-AQP2 antibody.

During the process of developing the ELISA a number of modifications were made to the original protocol in order to improve detection of urinary AQP1 protein and are summarised below:

- Steps to reduce background signal in blank wells.
    - Thorough washing of wells
    - Assessment of the BSA used for blocking. Some BSA grades can be problematic if certain molecules remain following purification. Both BSA grades used in these experiments were produced by heat shock fractionation, however A7030 was also protease, fatty acid and globulin free.
- Recombinant AQP1 protein should be stored in single use aliquots thus avoiding freeze-thaw effects which degrade the protein.
- Enabling the plate to equilibrate with room temperature for 90 minutes after overnight incubation at 4 °C improved the signal obtained from both the AQP1 standards and the urine samples.
- TMB colorimetric substrate augmented the signal obtained from both AQP1 standards and urine samples when compared to ABTS. The increased sensitivity of

TMB was at the expense of increased background signal which required further investigation.

- Increasing the dilution of anti-AQP1 antibody from 1 in 30 to 1 in 60 reduced the background signal to an acceptable level in blank wells when using TMB substrate.
- Increasing the amount of SDS from 0.01% to 0.1% in the standard and sample diluent improved the signal obtained from the AQP1 standards and even more so the urinary AQP1 protein. This brought the urine AQP1 results up into the middle third of the standard curve theoretically increasing accuracy.

In summary, methods have been optimised to detect and quantify AQP expression at the mRNA level by Polymerase Chain Reaction and at the protein level by Western Blotting. Furthermore, techniques have been established to determine cellular location of AQPs by immunohistochemistry and quantify urinary AQP1 excretion by ELISA. These techniques were utilised to analyse samples obtained from the neonatal rat unilateral ureteric obstruction model and will be employed in the future to assess human samples.

Chapter 4. Establishing a neonatal rat partial unilateral ureteric obstruction model

4.1 Introduction

Adult and neonatal rodent models of unilateral ureteric obstruction (UUO) are well established and have been used by many groups to investigate the pathogenesis of obstructive nephropathy. Although adult and neonatal UUO models show a broadly similar pathological progression in terms of inflammatory, apoptotic and fibrotic processes, the response of the neonatal kidney reveals clear differences such as impeded renal maturation and growth as well as early nephron loss [90, 91, 94, 96-101]. These disparities in response to UUO arise because rodent nephrogenesis continues for the first week postnatally and renal maturation for the subsequent week. Fortuitously, this signifies that at birth and 1 week of age rodent renal development is equivalent to humans at the second trimester gestation and birth respectively [87]. Thus, surgery performed in the rodent neonatal period can simulate human in utero obstruction and is more informative in the setting of congenital PUJO.

A comprehensive review comparing existing neonatal animal models with human PUJO suggests they are a legitimate approach for investigating the mechanism of obstructive nephropathy [88]. Nevertheless, the majority of children undergoing pyeloplasty have fewer renal histological abnormalities than their animal counterparts with complete UUO [86]. Models of variable partial unilateral ureteric obstruction (PUUO) show renal pelvic dilatation [91] and raised renal pelvic pressure [401] but less severe histological changes [91] than complete UUO and likely provide a better approximation to human disease.

An animal model of partial UUO was undertaken during this research to complement the clinical study of human PUJO for a number of reasons:

1. Animal models can be manipulated to produce different severities of obstruction
2. Sacrificing rat pups at variable time points allows changes in aquaporin expression/distribution to be monitored over time, particularly enabling assessment of whether aquaporin down-regulation predates histopathological changes of nephropathy
3. Control tissues are easily available
4. Renal tissue was accessible which was not available for the human PUJO study

5. Once established the model can be extended to AQP mutant mice to further develop the research. Despite their smaller size compared to rats this should be technically possible. Thornhill *et al*. have previously successfully undertaken PUUO in 2 day old neonatal mice in order to investigate the pathogenesis of obstructive nephropathy [94]

A number of methods have been utilised to create partial unilateral ureteric obstruction in different species of animal. Chevalier *et al*. described the creation of chronic partial ureteric obstruction in the guinea pig by placing a 2mm sterilized piece of polyethylene tubing around the distal third of the ureter which was left in situ for up to 8 weeks [402]. More commonly, a method first described in 1962 by Ulm and Miller as a technique to create reversible hydronephrosis in dogs, has been utilised [403]. This technique to create partial UUO has since been applied to neonatal and adult rodents and involves embedding the upper section of the ureter in a groove created in the psoas muscle [120, 364, 401]. Increasing the amount of ureter embedded in the psoas muscle increases the severity of obstruction as demonstrated in the acute setting by proportionately raised baseline renal pelvis pressure [401].

More recently Thornhill *et al.* described an alternative method to create variable partial ureteric obstruction in the neonatal rat. This method involved placing a wire template of known diameter (0.25 – 0.9mm) alongside the PUJ, tying a ligature of non-absorbable suture around both ureter and wire and then removing the wire. Histology demonstrated the suture did not lead to significant inflammatory reaction within the ureter. Decreasing wire diameter resulted in increasing severity of obstruction with an increasing renal pelvis diameter proportional to the degree of obstruction at 14 days post PUUO. This method was reported to generate reproducible, variable degrees of obstruction which could be precisely regulated, thus enabling the possibility of serial measurements [91]. On the basis of these reported results combined with the procedure being the least invasive this technique was selected for use in this research study. Due to the technical challenges of establishing a technique new to the laboratory and performing PUUO surgery on neonatal animals, rats rather than mice were chosen to develop this model due their larger neonatal size.

4.2 Methods

4.2.1 Training and licensing for animal studies

Following successful completion of the Home Office Training in Animal Scientific Procedures Course and procurement of a personal animal licence (Ref: I57BOBE74) (Figure 4.1) procedures were performed under the Project Licence of Professor Richard Coward (Licence number: 30/2787, part F, protocol number 6).

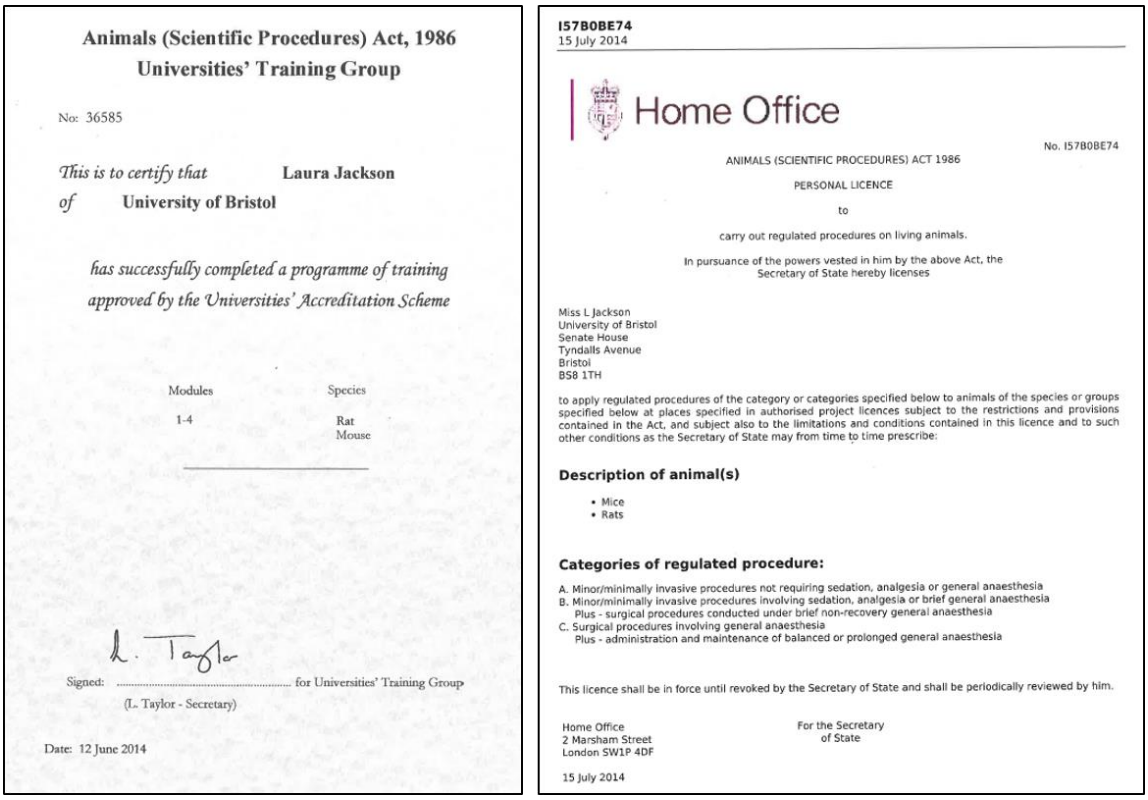

Animals (Scientific Procedures) Act, 1986
Universities' Training Group

No: 36585

This is to certify that **Laura Jackson**
of **University of Bristol**

has successfully completed a programme of training approved by the Universities' Accreditation Scheme

Modules	Species
1-4	Rat Mouse

Signed: ..... for Universities' Training Group
(L. Taylor - Secretary)

Date: 12 June 2014

I57B0BE74
15 July 2014

Home Office

No. I57B0BE74

ANIMALS (SCIENTIFIC PROCEDURES) ACT 1986

PERSONAL LICENCE

to

carry out regulated procedures on living animals.

In pursuance of the powers vested in him by the above Act, the Secretary of State hereby licenses

Miss L Jackson
University of Bristol
Senate House
Tyndalls Avenue
Bristol
BS8 1TH

to apply regulated procedures of the category or categories specified below to animals of the species or groups specified below at places specified in authorised project licences subject to the restrictions and provisions contained in the Act, and subject also to the limitations and conditions contained in this licence and to such other conditions as the Secretary of State may from time to time prescribe:

Description of animal(s)

- Mice
- Rats

Categories of regulated procedure:

A. Minor/minimally invasive procedures not requiring sedation, analgesia or general anaesthesia
B. Minor/minimally invasive procedures involving sedation, analgesia or brief general anaesthesia
Plus - surgical procedures conducted under brief non-recovery general anaesthesia
C. Surgical procedures involving general anaesthesia
Plus - administration and maintenance of balanced or prolonged general anaesthesia

This licence shall be in force until revoked by the Secretary of State and shall be periodically reviewed by him.

Home Office
2 Marsham Street
London SW1P 4DF

For the Secretary of State

15 July 2014

Figure 4.1 Certificates of training and licensing in animal procedures

4.2.2 Surgical access and feasibility studies for the PUUO procedure

The first consideration when establishing the PUUO procedure was optimal surgical access as p2 rat pups are quite small (Figure 4.2).

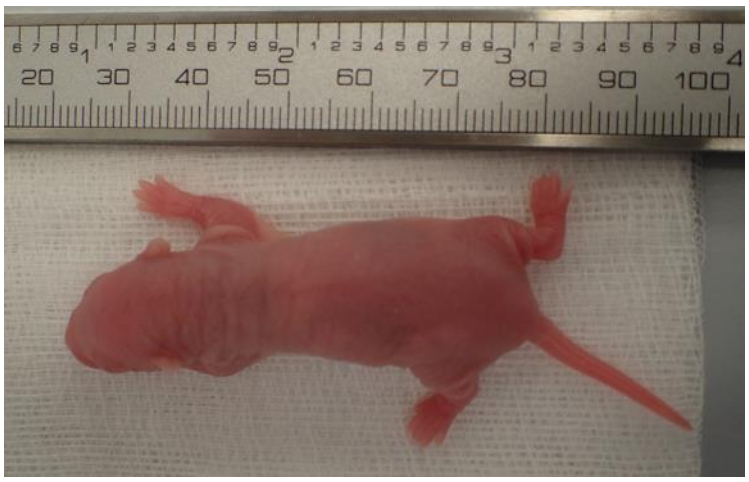

Figure 4.2 Size of a p2 rat pup

P2 Han-Wistar rat pups are approximately 5-6 cm in length from nose to base of tail, weighing on average 7g (range 5.5g – 8.9g).

Potential options were a midline laparotomy or a flank incision. A midline laparotomy would provide good access but involves opening the peritoneal cavity alongside bowel handling and mobilisation. This incision may cause a degree of post-operative ileus impairing the pups ability to feed post-operatively. Additionally, a midline incision would be larger and more painful potentially further hindering post-operative recovery. Although this incision would be required in order to perform the Ulm and Miller method of PUUO [401, 403] whereby the ureter is buried in the psoas muscle, it would not be necessary to perform Thornhill's method of PUUO using a wire template [91].

Flank incisions also provide excellent access to the kidney/ureter, while being smaller and less painful than a midline laparotomy. Additionally, they avoid the general exposure of intra-abdominal organs. This incision was selected as most appropriate, especially as the technique to be used was that described by Thornhill *et al.* involving the use of a wire template, which incidentally this group had performed via a flank incision [91].

In human neonates the liver is incredibly friable and easily damaged during surgical procedures. Extrapolating this to the neonatal rat pups it was decided to perform the procedure on the left kidney in order to avoid the liver on the right side of the abdomen.

Having determined that a flank incision would be most appropriate, the positioning of the pup, the exact placement of the incision and the steps of the procedure were established using wild-type Han-Wistar p3 and p4 pups that had already been culled by schedule 1 methods for another indication. All procedures were performed using 2.5 x standard loupes for magnification of the surgical field.

Right lateral positioning with a slight prone tilt was required for a left flank incision. A gauze roll was placed under the right flank to lift the kidney and proximal ureter towards the incision. Relevant anatomical features were marked including the costal margin, lateral border of the paraspinal muscles and the iliac crest. Following a trial of various flank incisions (longitudinal, oblique, transverse subcostal) an oblique incision commencing just inferior to the costal margin at the lateral border of the paraspinal muscles continuing anteroinferiorly across the flank was selected as optimum (Figure 4.3). Care was made not to locate the incision too far cranially in order to avoid accidental pleurotomy.

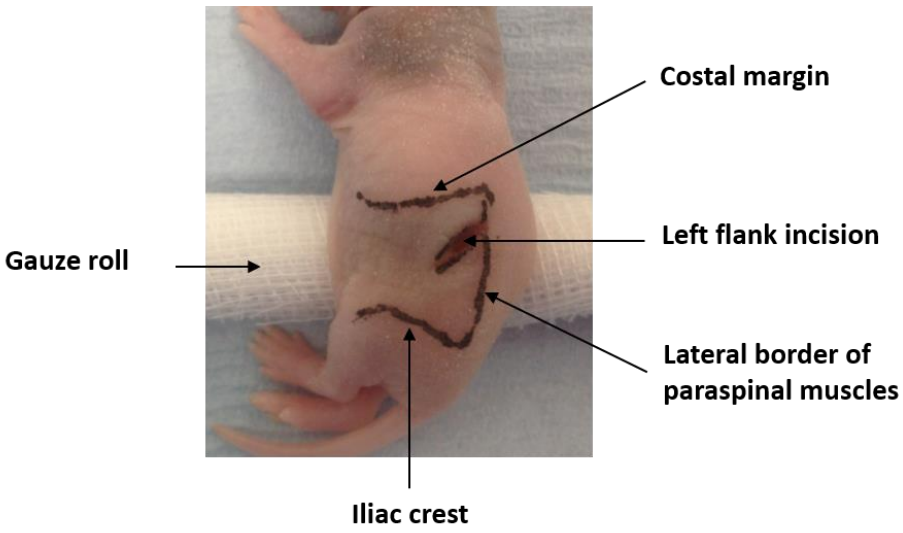

Figure 4.3 Left flank incision to access the left kidney and ureter

P3 rat pup in right lateral position with a gauze roll positioned underneath the right loin. Pen markings illustrate anatomic features defined before siting the incision, namely the costal margin, lateral border of the paraspinal muscles and the iliac crest. The incision was commenced just inferior to the costal margin at the lateral border of the paraspinal muscles, continuing obliquely, anteroinferiorly across the flank.

Subsequently the technique to mobilise the kidney, identify the proximal ureter and bluntly dissect around the PUJ/proximal ureter using 2 pairs of extra fine Graefe forceps (11152-10, Interfocus, Fine Science Tools, UK) was refined. Once mobilised an 8/0 ethilon suture (BV 130-4, Ethicon, OH, USA) was passed underneath the proximal ureter. The suture was ligated around both the ureter and a 4-5 mm long wire template, and the wire template subsequently removed. The procedure was tested using both 0.3mm and 0.5mm stainless steel wire templates (FF215130/3 and FF215140/2 Goodfellow, Huntingdon, UK). Confirmation that a partial obstruction had been created using both wire templates was obtained by injecting blue dye (PBS containing bromophenol blue) into the renal pelvis whereby it was noted to flow past the suture and into the bladder (Figure 4.4). Although Figure 4.4 demonstrates the kidney being grasped by the forceps and drawn out of the wound

this was for the purposes of illustration. It was noted during development of the technique that the kidney is very friable and easily injured. It should not be held at any time by forceps as this causes significant renal damage.

4.2.3 Recoverable neonatal rat anaesthesia

A number of methods of neonatal rodent anaesthesia have been employed in order to create ureteric obstruction models including: deep hypothermia [120], injectable intra-peritoneal agents (e.g. pentobarbital sodium) [137] and inhalant anaesthetics [91].

New born rats are poikilothermic with immature thermoregulatory capabilities. Unlike adult mammals they can tolerate prolonged periods of severe hypothermia without experiencing complications. Additionally, due to their small body size and high surface area to body weight ratio their core temperature may be cooled rapidly by surface cooling [404]. Cooling may be initiated by putting the pup in a cold room, immersing the pup in iced water or placing the pup on crushed ice [120, 404]. Measures to induce hypothermia generally result in anaesthesia lasting approximately 10 minutes although this can be extended by placing the pup on ice or a cold pack during the procedure [404]. Safe hypothermic anaesthesia has been demonstrated for 30–40 minutes [120, 405]. In addition to inducing analgesia, hypothermia also reduces intra-operative bleeding secondary to reduced circulatory flow [404].

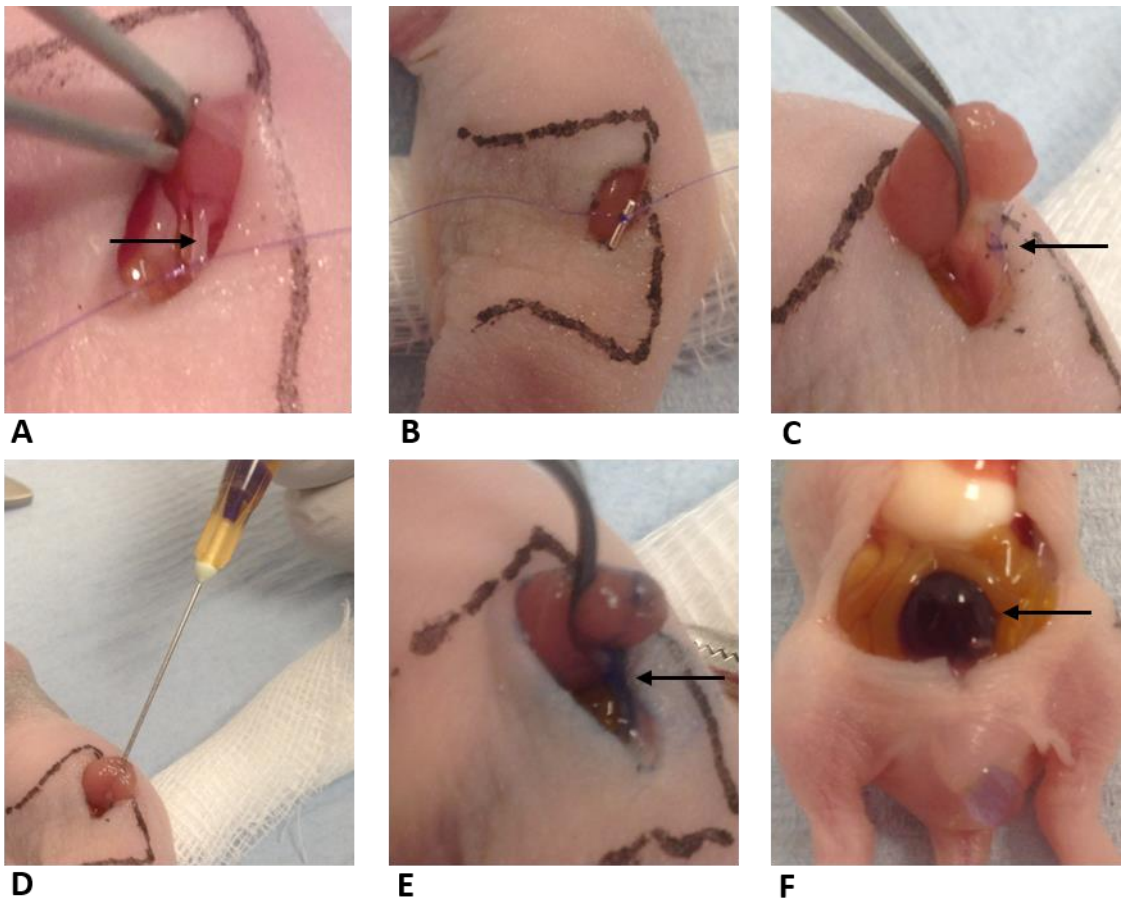

Figure 4.4 Stages of procedure to create left partial ureteric obstruction

Following mobilisation of the kidney and ureter an 8/0 ethilon suture was passed underneath the proximal ureter (arrow - ureter) (A). The suture was tied around the ureter and a wire template (0.5mm) (B). The wire template was removed leaving the suture (arrow) tied around the proximal ureter (C). A needle was inserted through the renal parenchyma into the renal pelvis. PBS containing bromophenol blue dye was injected into the renal pelvis (D). The dye flowed past the suture and down the ureter (arrow)(E). Dye reached the bladder (arrow) following injection into the renal pelvis confirming this was not a complete ureteric obstruction (F). Stages demonstrated using a p3 pup already culled by schedule 1 method for another indication.

Although previously used for surgical anaesthesia intraperitoneal injectable anaesthetics (e.g. ketamine, pentobarbital and a combination of fentanyl-droperidol) should be avoided as the level of anaesthesia is difficult to regulate, they may be ineffective for short term anaesthesia and have been associated with excessive mortality (>50%) [405].

Alongside deep hypothermia, inhalant anaesthetics are safer and more effective than injectable anaesthetics [405]. Isoflurane, a halogenated ether, is a commonly used inhalant anaesthetic agent in both veterinary and human medicine. The advantage of inhalant anaesthetics is that their delivery can be easily adjusted throughout the procedure to maintain a level plane of anaesthesia and can be terminated at the end of the procedure enabling rapid recovery of the pup.

Having more personal experience using inhalant anaesthesia alongside performing both this procedure and recovery neonatal surgery for the first time in our unit, isoflurane was selected as the anaesthetic of choice. This would give more flexibility as the operative time and thus the duration of the anaesthetic was initially uncertain. Additionally, it would be easier to maintain a sterile field using isoflurane rather than crushed ice which would potentially melt and track around the operative site.

When setting up the anaesthetic circuit it was noted that the normal rat co-axial mask (Size 1, VetTech Solutions, Congleton, UK) for anaesthetic delivery and waste extraction was much too large for a neonatal rat pup. One option was to perform the surgery in an extraction hood where the isoflurane would be piped in from the anaesthetic circuit and delivered to the rat pups nose/mouth in a suitable sized tube. Waste anesthetic gases would then be scavenged by the extraction hood. The second option was to try an extra small rodent mask usually used for mice (AN005F, VetTech Solutions, Congleton, UK). Although rat pups are about a third to half the size of an adult mouse a mouse co-axial nose cone used on the bench was tested and worked well enabling maintenance of anaesthesia without escape of waste anaesthetic gases.

4.2.4 Creation of neonatal rat PUUO

Following the establishment of the anaesthetic and surgical procedures pups underwent creation of left PUUO according to the protocol outlined below.

A Han-Wistar pregnant dam was obtained from the University of Bristol H-floor colony and transferred to the animal facility at e16. The dam was housed singly with enrichment and appropriate bedding and nesting material. The dam was fed standard rodent diet (Eurodent diet 22 %, Labdiet, PMI nutrition, MO, USA), allowed free access to water and housed at 21 °C, 50 % humidity in a 12 hour light:dark cycle. Pups underwent surgery between 24-48 hours of age during the light phase. All procedures were carried out in accordance with the Animals (Scientific Procedures) Act 1986.

4.2.4.1 Retrieval of pups from the cage for surgery

The mother was removed from the cage, the pups counted and the male pups marked. Males were identified by having a longer anogenital distance than females. A single pup was moved into a transfer cage while the remaining pups were rubbed in the bedding to reduce the smell

of them being handled. The mother was returned to the cage and the retrieved pup was transferred to the surgery room and weighed prior to anaesthesia.

4.2.4.2 General anaesthesia

General anaesthesia was induced using a small induction chamber (AN010SR, VetTech Solutions, Congleton, UK) with a mixture of 3 % isoflurane (Merial, Essex, UK) and oxygen with the flow set at 1l/min. This would usually take approximately 3-4 minutes until surgical anaesthesia was reached, assessed by loss of the pedal reflex and lack of response to painful stimulus.

When fully anaesthetised the pup was moved to the surgical area and its nose placed within the extra small rodent co-axial mask. The isoflurane/oxygen mix was delivered via the co-axial system with an oxygen flow of 0.8 l/min and isoflurane concentration of 1.5-2%.

4.2.4.3 Positioning and skin preparation

The pup was positioned on a covered warming pad that was maintained on a low setting to generate an element of hypothermia which proved anaesthetic sparing and reduced intra-operative bleeding. The pup was placed in the right lateral position, slightly tilted prone with a gauze roll under the right flank. It was ensured the pup's nose was securely in the anaesthetic mask. Tape was placed over the front and hind paws to stabilise the pup.

The costal margin, lateral border of the paraspinal muscles and the iliac crest were marked with permanent ink. The skin of the surgical area was cleaned with 70% ethanol using a sterile cotton bud and allowed to dry. Ethanol rather than chlorhexidine or iodine skin preparation was used as ethanol doesn't leave a residual smell which may be detected by the mother when the pup is returned to the litter. The pup was draped with transparent sterile drapes.

4.2.4.4 Surgical procedure to create left partial ureteric obstruction

The respiratory rate and depth, and animal colour were monitored throughout the procedure as indicators of the depth of anaesthesia. Sterile technique was used to perform the surgery and 2.5 x surgical loupes were used for magnification of the surgical field. Figure 4.5 illustrates the key steps in the creation of neonatal rat PUUO. A left flank incision was made with number 15 blade (10015-00, Interfocus, Fine Science Tools, UK) and scissors were used to split and open the muscle layer from the medial end. The fascia overlying the kidney

was opened and the inferior pole of the kidney mobilized and tilted anteriorly until the posterior surface of the kidney was visible noting the vessels at the hilum and the ureter running inferiorly. The proximal ureter was identified and two pairs of Graefe forceps used to bluntly dissect around the PUJ/proximal ureter. The tips of the forceps were then passed posterior to the PUJ, one end of the 8/0 ethilon suture (BV 130-4, Ethicon, OH, USA) was grasped with the forceps and the forceps withdrawn to bring the suture posterior to the PUJ. A stainless steel wire template (size 0.3mm – 0.6mm diameter) was applied parallel to the proximal ureter and then a double throw of the suture was placed ensuring it was closed around the wire and ureter but not tightened and stretched. A further single throw was closed around the wire and ureter but again not tightened. The final throw of the knot was tightened to prevent future slipping or loosening. A single operator performed all PUUO procedures and paid attention to maintaining equal tension in the ligatures between animals. Following completion of the ligature the wire template was carefully removed, and the ureter was returned to its anatomical position. The muscle layer was closed with interrupted 6/0 vicryl sutures (J833G, Ethicon, OH, USA) and the skin with interrupted subcuticular 6/0 vicryl sutures (J833G, Ethicon, OH, USA). Initially the skin was closed with standard interrupted skin sutures with the knot tied on the skin surface. Unfortunately, the mother managed to remove those sutures in 1 pup in the first litter within 2 hours of surgery (see section 4.2.5.4.1) therefore it was necessary to modify the closure and effectively bury the sutures. Although this results in a slightly crumpled looking wound initially (Figure 4.5F) the wound heals nicely (Figure 4.6) and there were no further episodes of wound dehiscence throughout the study.

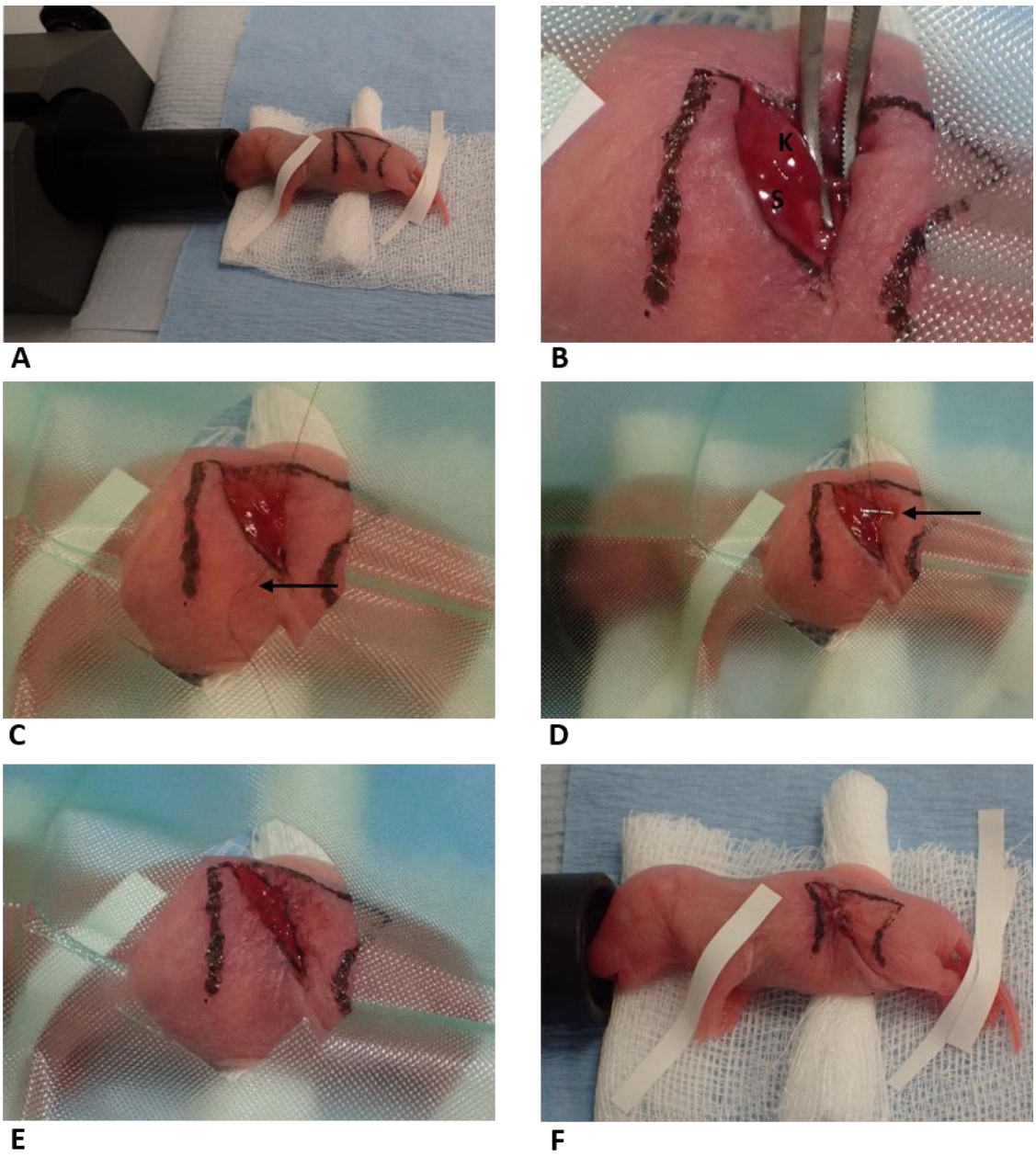

Figure 4.5 Creation of PUUO under isoflurane general anaesthetic

P2 rat pup in right lateral position with a gauze roll positioned underneath the right loin. The pup was laid on a covered warming pad with its nose within a co-axial mask delivering isoflurane anaesthetic (A). The inferior pole of the kidney was mobilised and the proximal ureter dissected out. The tips of the forceps were positioned posterior to the ureter ready to grasp the 8/0 ethilon suture (K – kidney, S – spleen) (B). An 8/0 suture (arrow) was passed posterior to the ureter (C). The suture was tied using a double throw followed by two single throws around the ureter and wire template (arrow) (D). Following removal of the wire template the ureter was returned to the abdomen and the muscle layer closed with 6/0 vicryl interrupted sutures (E). The skin was closed with interrupted subcuticular sutures using 6/0 vicryl (F).

Following closure of the wound the area was washed with 70% ethanol and the isoflurane anaesthetic discontinued.

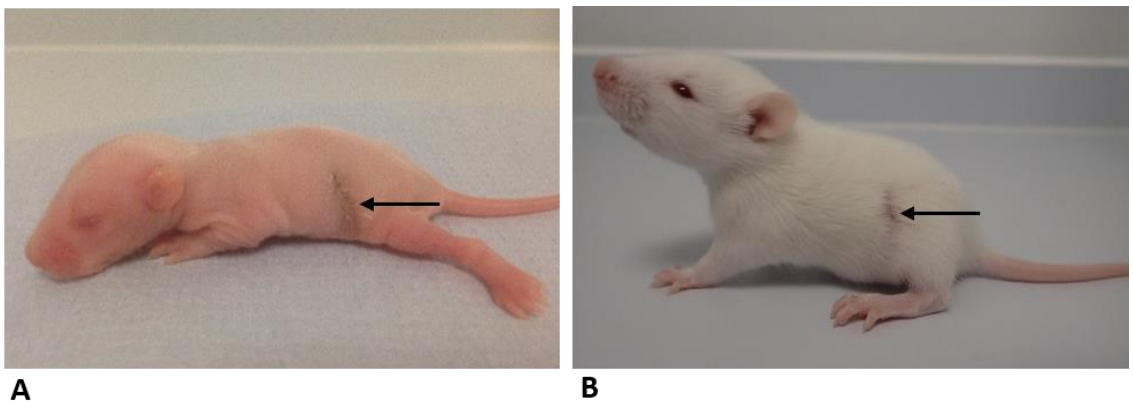

Figure 4.6 Healing left flank wound

This figure demonstrates the healing left flank wound in a p8 rat pup (A) and a p15 rat pup (B).

4.2.4.5 Sham surgery

Sham surgery was performed in an identical manner to PUUO surgery except that following mobilisation of the kidney and dissection around the proximal ureter a ligature was not placed and the ureter was simply returned to the abdomen.

4.2.5 Post-operative animal care

4.2.5.1 Post-anaesthetic recovery

Rat pups were recovered initially in 0.5 l/min of oxygen on the warming pad (at maximum temperature) for a few minutes and then transferred to incubator set at 33°C (nest temperature) [404] until they were warm, had recovered their righting reflex and were active.

4.2.5.2 Return of the neonatal rat pup to the mother and litter

When fully recovered from the anaesthetic the pup was placed in the transfer cage and taken back to the housing area of the animal facility. In order to successfully return the pup to the mother the pup must smell like their littermates and not of anything unusual. To achieve this the mother was removed from the cage. The gloved hands of the operator were rubbed in the bedding and sawdust of the cage and then the pup was rubbed in sawdust and bedding from the cage to transfer the smell. The pup was then placed amongst the other pups, leaving the operated pup underneath the others within the nest. If another pup was to be operated upon it would be removed at this point and then the mother would be returned to the cage. Post-operatively the pups were monitored hourly using the Bristol Generic Animal Welfare Scoresheet for 4 hours and then daily thereafter.

4.2.5.3 Continuing animal husbandry and monitoring

Post-operatively, the litter of pups was housed with the mother in a standard cage with enrichment in the same conditions as pre-operatively. The pups were weighed daily and assessed using the Bristol Generic Animal Welfare Scoresheet documenting their appearance, weight, clinical signs, natural behaviour and provoked behaviour for the first post-operative week and then weekly thereafter. The pups were ear-notched for identification at p8 and prior to this they were identified by permanent pen marking which was renewed on a daily basis.

Spot urines were acquired from all pups at 2 and 3 weeks post-operatively. At 2 weeks these were obtained by placing the pup on a cage lid with clingfilm underneath. At 3 weeks urine was collected by placing the pup on hydrophobic sand. Urine samples were collected into an Eppendorf on ice from either the clingfilm or hydrophobic sand and then processed as per the methods section in Chapter 2.

The pups were weaned at 3 weeks of age and the males and females separated into different cages and housed at 21°C, 50% humidity in a 12 hour light:dark cycle. Subsequently pups were fed a standard rodent diet including crushed food (Eurodent diet 22 %, Labdiet, PMI nutrition, MO, USA) and were allowed free access to water. Appropriate bedding materials and enrichment was provided.

Four weeks post-operatively metabolic cages were used to collect urine from all operated rats. Rats were placed in the metabolic cages at 1700 hours and urine collected over a roughly 4-5 hour period into the evening. This time point was chosen as, being nocturnal, the rats were more active and produced urine at a faster rate thus reducing the urine collection time. Ice packs were placed around the metabolic cage urine collection tube to keep the urine sample cooled. At the end of the collection period the urine sample was transferred to eppendorfs on ice and processed as per the methods section in Chapter 2 (section 2.17.1).

4.2.5.4 Effect of wire template diameter

It was not initially known which wire template diameter would provide the desired amount of hydronephrosis for the study and therefore this was optimised over the first three litters of rat pups that underwent the PUUO procedure.

4.2.5.4.1 PUUO using a 0.3 mm wire template

The first litter consisted of 6 pups, 5 female and 1 male. 5/6 pups underwent left PUUO with a 0.3 mm wire template (FF215130/3 Goodfellow, Huntingdon, UK). One female underwent left sham procedure. Post-operative complications included early wound dehiscence in a female pup with left PUUO requiring re-suturing of the wound and one female with PUUO was cannibalised by the mother within 1 hour of surgery. A further female pup who had undergone left PUUO died suddenly at 26 days. On inspection of the urinary tract the 8/0 ethilon suture was still in place around the proximal ureter and there was no renal pelvis or renal dilatation. No cause of death was identified. The remaining pups (4) were culled at 31 days of age by exposure to a rising concentration of CO_2 gas. All 3 with left PUUO were found to have very dilated urine filled left kidneys with little discernible renal tissue. All had normal contralateral right kidneys (Figure 4.8). The sham pup had normal kidneys and ureters bilaterally (Table 4.1). Although there were generally small numbers in this first litter there did not seem to be an obvious detrimental effect of PUUO on somatic growth compared to the single sham rat (Figure 4.7).

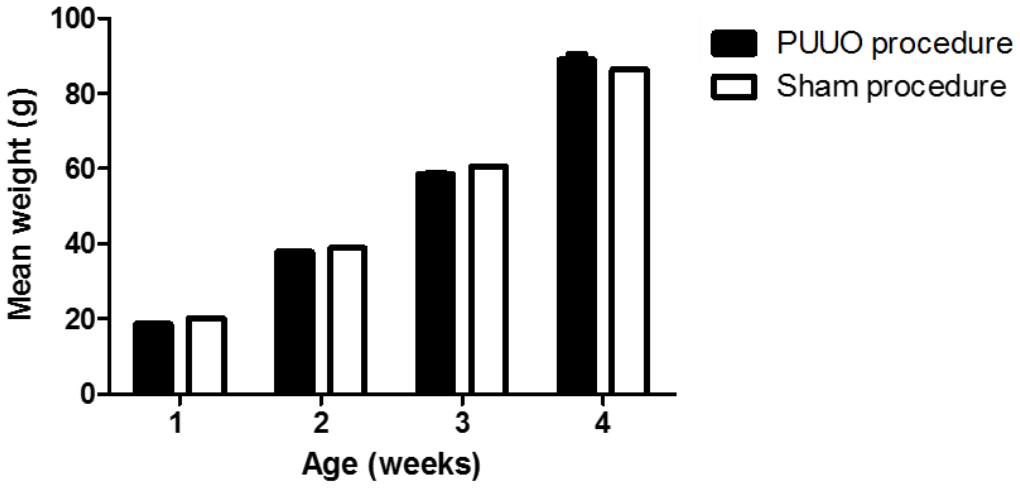

Figure 4.7 Weight of PUUO (0.3 mm wire) versus sham rats

Weekly post-operative mean weight +/- SEM presented for rat pups who underwent left PUUO with a 0.3 mm wire, n=4 except for week 4 where n=3. Weekly post-operative weights also presented for a single pup who underwent left sham procedure.

Pup	Sex	Procedure	Right kidney	Left kidney	Complications
1	F	L PUUO (0.3 mm)	-	-	Maternal cannibalism p2
2	F	L PUUO (0.3 mm)	Normal	Very dilated, little renal tissue. Decompressed before measurements obtained.	
3	F	L PUUO (0.3 mm)	Normal	Very dilated, little renal tissue L-22mm, W-16mm	Post-operative wound dehiscence re-sutured
4	M	L PUUO (0.3 mm)	Normal	Very dilated, little renal tissue L-25mm, W – 18mm	
5	F	L PUUO (0.3 mm)	-	-	Died at 26 days – normal kidneys bilaterally suture intact proximal left ureter
6	F	L sham	Normal	Normal	

Table 4.1 Outcome of PUUO created with a 0.3 mm wire template

Table of details of 6 pups who underwent either left PUUO using a 0.3 mm wire template or sham procedure. Rats were culled at day 31. L – kidney length, W – kidney width

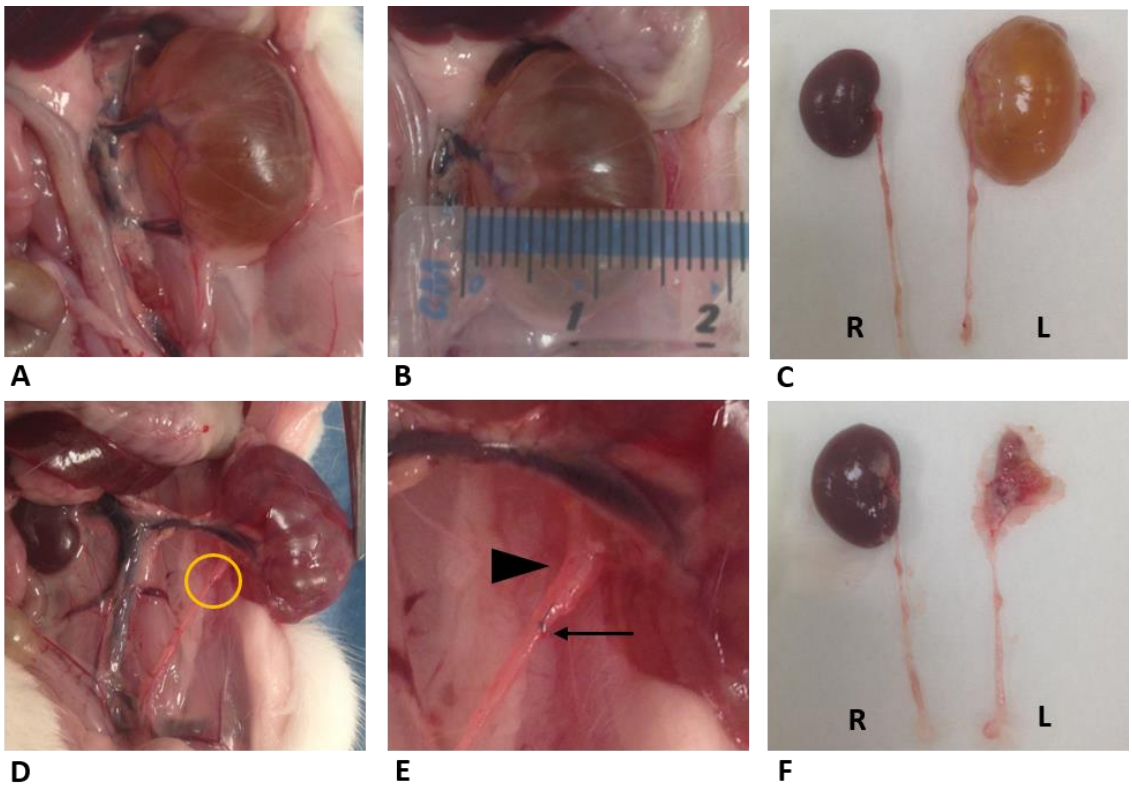

Figure 4.8 Outcome of left PUUO created using 0.3 mm wire template

Images of the findings at 31 days of 2 rat pups (one female, one male) following creation of left PUUO using a 0.3 mm wire template at p2. The female pup had a very dilated urine filled left kidney with almost no residual renal tissue noted: in situ (A), alongside a ruler to demonstrate the size (B) and following retrieval compared to the contralateral normal kidney (C). The male pup also had an extremely dilated urine filled left kidney, the yellow circle indicates the position of the suture around the upper ureter (D). The ureter and renal pelvis were dilated (arrowhead) proximal to the suture (arrow) (E). Decompression of the kidney revealed no discernable renal tissue (F). R – right kidney, L – left kidney

4.2.5.4.2 PUUO using a 0.6 mm wire template

The second litter consisted of 12 pups, 7 male and 5 female. Six pups (3 male, 3 female) underwent left PUUO using a 0.6 mm wire template (FF215145/1, Goodfellow, Huntingdon, UK). Three pups (2 male, one female) underwent left sham procedure and the three final pups (2 male, one female) did not undergo either an anaesthetic or surgical procedure. One male PUUO pup was cannibalised by the mother at p5, the cause of which is unknown. Three PUUO rats (2 female, 1 male) were culled at age 37 days by terminal isoflurane anaesthesia (See section 4.2.6). The suture was intact around the proximal left ureter in all three rats however there was no evidence of dilatation of the ureter, renal pelvis or kidney. Three sham rats (2 male, 1 female) were also culled by terminal anaesthesia at age 37 days and demonstrated normal kidneys, renal pelvices and ureters bilaterally. In view of the fact that no dilatation had been observed in the 3 PUUO rats, the remaining 2 rats (1 female, 1 male) were observed up to an age of 100 days when they were culled by terminal isoflurane

anaesthesia. Despite the prolonged length of time the sutures had been in place the male rat had a completely normal left kidney and collecting system with no discernable dilatation. The female rat had mild prominence of the proximal ureter/renal pelvis only (Table 4.2 and Figure 4.10). Both contralateral kidneys were normal. One-way ANOVA confirmed no statistical difference between the renal pelvis and ureter dimensions of PUUO, sham and control rats age 37 days. Unpaired t-tests confirmed no statistical difference between the PUUO renal pelvis and ureter dimensions compared to contralateral system dimensions in rats aged 100 days (Figure 4.11). Compared to both sham rats and non-operated rats the PUUO procedure did not affect somatic growth over the first 5 weeks of life (Figure 4.9).

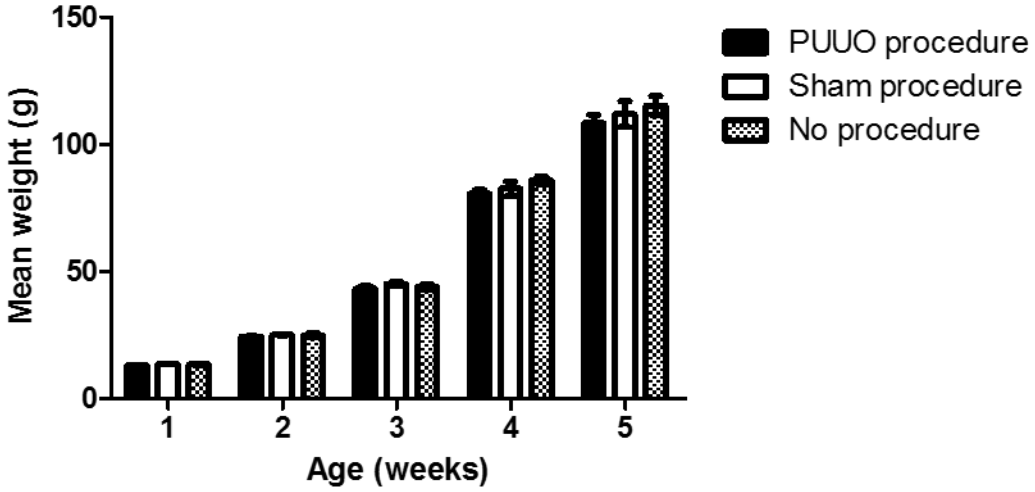

Figure 4.9 Mean weight of left PUUO (0.6 mm wire) rats versus controls

Weekly post-operative mean weights +/- SEM presented for rat pups who underwent left PUUO with a 0.6mm wire n=5, left sham procedure n=3 and non-operated rats n=3. No statistically significant difference between groups at any time point p=0.3728 (Two-way ANOVA)

Rat	Sex	Procedure	Age at cull (days)	Right renal pelvis (mm)	Left renal pelvis (mm)	Right proximal ureter (mm)	Left proximal ureter (mm)
1	M	L PUUO (0.6 mm)	37	0.9	1.05	0.6	0.9
2	F	L PUUO (0.6 mm)	37	0.98	1.14	0.72	0.71
3	F	L PUUO (0.6 mm)	37	1.15	1.27	0.71	0.65
4	M	L PUUO (0.6 mm)	100	1.97	2.14	0.99	0.95
5	F	L PUUO (0.6 mm)	100	1.51	2.35	0.95	1.68
6	F	L sham	37	1.23	1.02	0.83	0.63
7	M	L sham	37	1.02	1.18	0.86	0.82
8	M	L sham	37	1	0.9	0.7	0.6
9	M	None	37	1.19	1.1	0.95	0.84
10	M	None	37	1.27	1.53	0.65	0.71
11	F	None	37	1.07	0.91	0.74	0.62

Table 4.2 Outcome of PUUO created with a 0.6 mm wire template versus controls

Table detailing the renal pelvis and ureter dimensions of 11 rat pups who underwent either left PUUO using a 0.6 mm wire template, sham procedure or no procedure. Three PUUO rats were culled at 37 days and the remaining 2 were culled at 100 days. Using separate one-way ANOVAs for renal pelvis and ureter dimensions, no statistical difference was noted between PUUO, sham and non-operated animals. Using separate unpaired t-tests for renal pelvis and ureter measurements no significant difference was noted between PUUO and contralateral PUUO measurements.

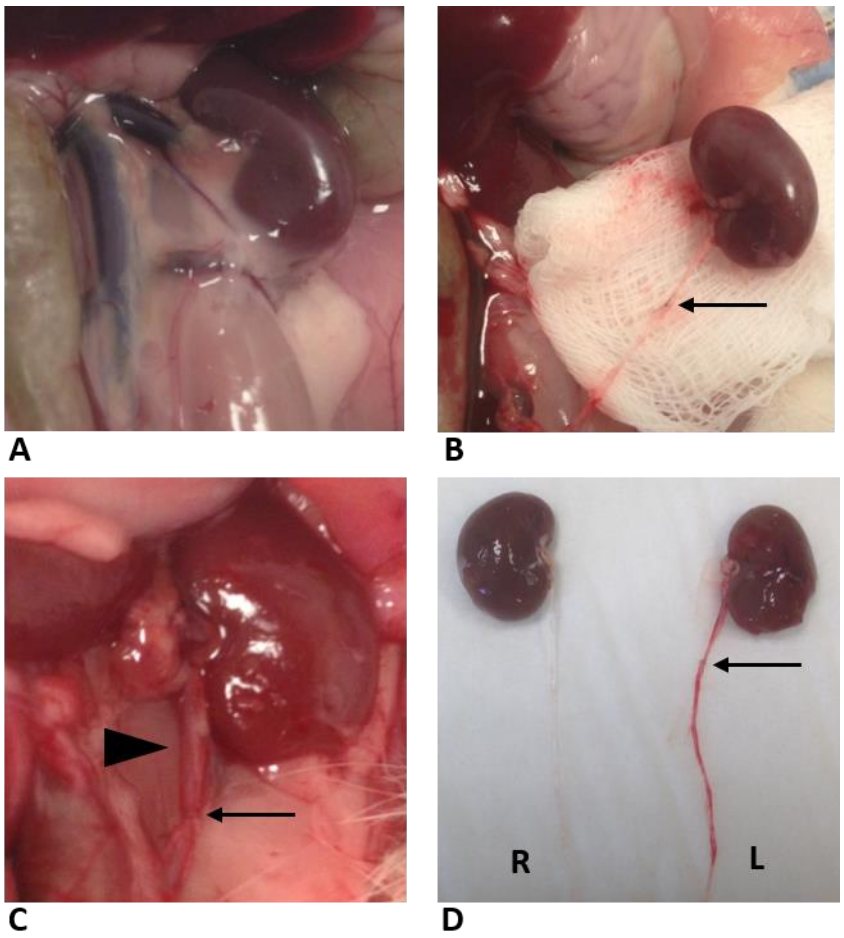

Figure 4.10 Outcome of left PUUO created with 0.6 mm wire template

Images of the findings at 37 days and 100 days of 2 female rat pups following creation of left PUUO using a 0.6 mm wire template at p2. The left kidney and collecting system was completely normal with no evidence of dilatation and the suture (arrow) in place around the proximal ureter at 37 days of age (A)(B). At 100 days following creation of PUUO one rat demonstrated prominence of the upper ureter and renal pelvis (arrowhead) proximal to the suture (arrow) (C). Left PUUO kidney with mild renal pelvis dilatation compared to the normal contralateral kidney following retrieval at 100 days (arrow – suture) (D). R – right kidney, L – left kidney

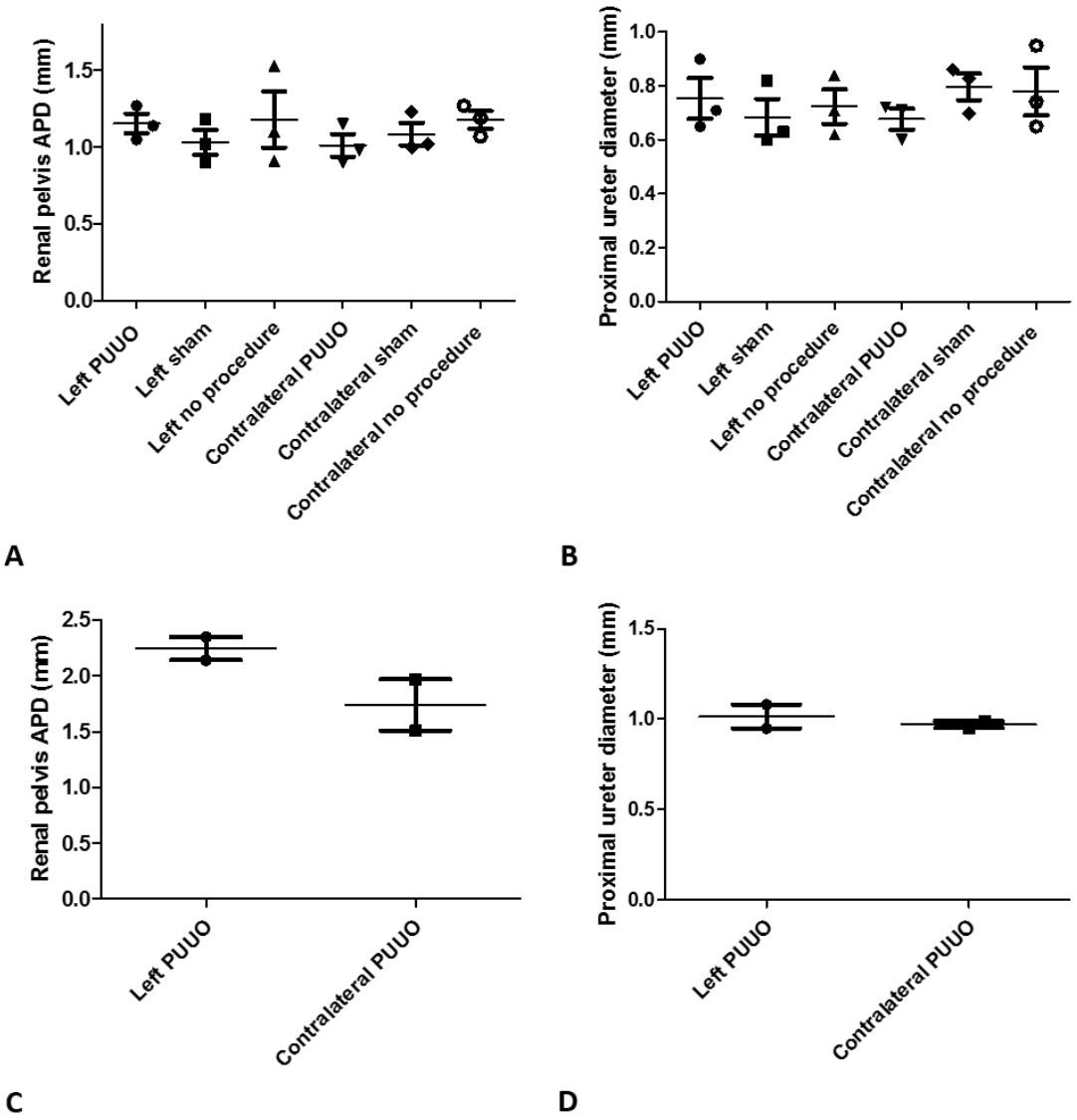

Figure 4.11 Renal pelvis and proximal ureter dimensions of PUUO (0.6 mm wire template) and control rats

Comparison of the renal pelvis anteroposterior diameter (APD) at age 37 days between the left and contralateral systems for each intervention. One-way ANOVA demonstrates no significant difference between groups p=0.723 (A). Comparison of the proximal ureter diameter at age 37 days between the left and contralateral systems for each intervention. One-way ANOVA demonstrates no significant difference between groups p=0.7257 (B). Comparison of the renal pelvis APDs after left PUUO with the contralateral renal pelvis APDs at age 100 days. Unpaired t-test demonstrated no significant difference between groups p=0.1839 (C). Comparison of the proximal ureter diameters after left PUUO with the contralateral proximal ureter diameters at age 100 days. Unpaired t-test demonstrated no significant difference p=0.5762 (D). Mean +/- SEM presented for all groups.

4.2.5.4.3 PUUO using a 0.4 mm wire template

Nine male pups from a third litter were studied, using a 0.4 mm wire template (FF215135/2, Goodfellow, Huntingdon, UK) to create PUUO in 7 of the pups. Two male pups remained non-operated. At 35 days of age all rats except one male PUUO rat (culled later at 86 days of age) were culled by terminal isoflurane anaesthesia (See section 4.2.6). There were no complications of surgery and the rats demonstrated variable amounts of hydronephrosis ranging from mild to severe. This wire diameter was selected for ongoing studies involving 3 more litters of pups (litters 4-6) and the results for these litters are discussed in Chapter 5.

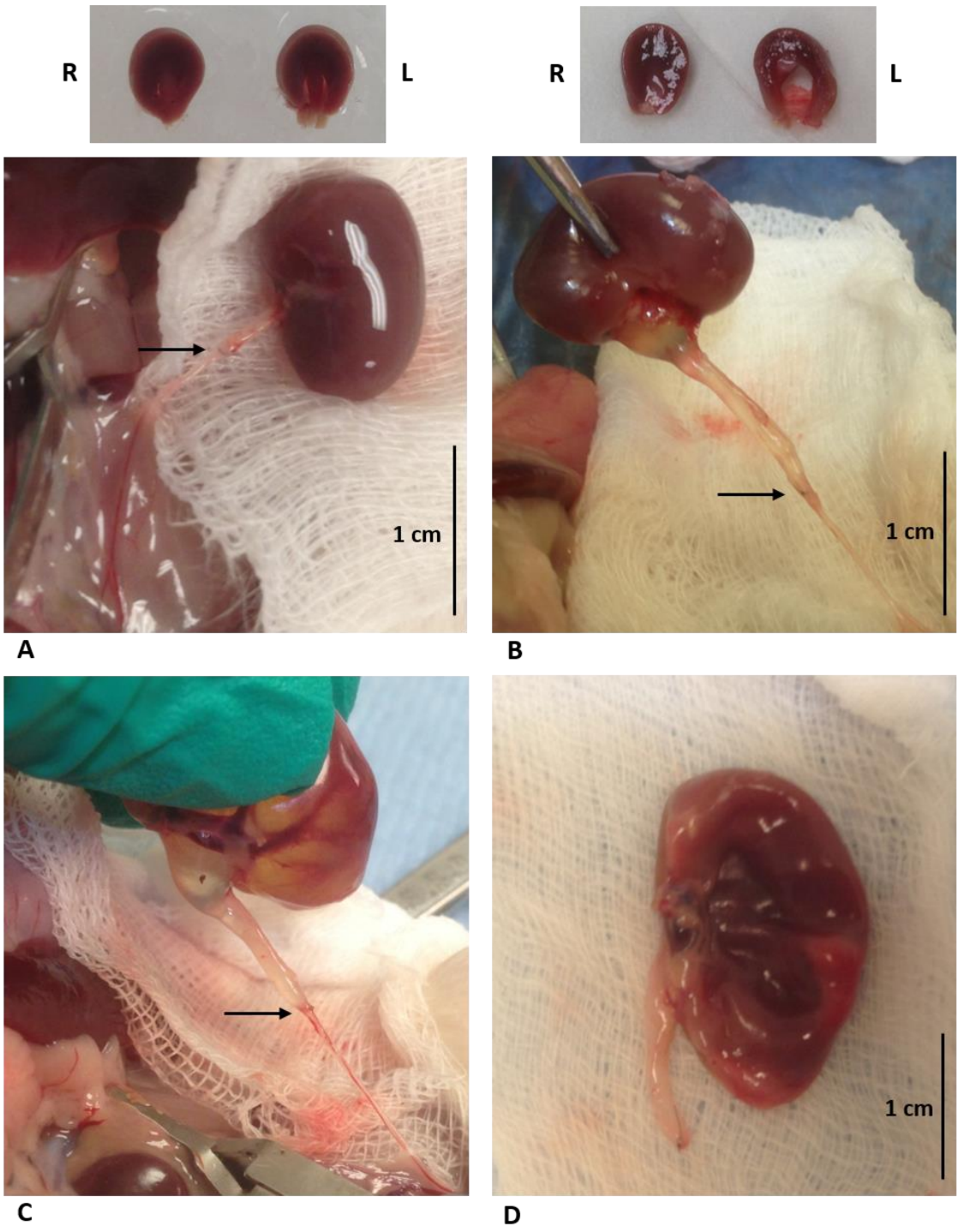

Figure 4.12 Hydronephrotic rat kidneys created using a 0.4 mm wire template

Mild hydronephrosis of the left kidney demonstrated by mild ureteric/renal pelvis dilatation above the suture (arrow). Pictured above are axial sections demonstrating preserved architecture of the left PUUO kidney in mild hydronephrosis compared to the contralateral kidney (A). Moderate hydronephrosis of the left kidney revealed by significant dilatation of the ureter/renal pelvis above the suture (arrow). Pictured above are axial sections demonstrating atrophy (medulla>cortex) of the left PUUO kidney in moderate hydronephrosis compared to the contralateral kidney (B). Severe hydronephrosis of the left kidney demonstrated by significant dilatation of the ureter/renal pelvis above the suture (arrow) and considerable dilatation of the kidney (C) Severe hydronephrosis resulted in substantial atrophy of the renal tissue as noted when the kidney was decompressed (D). All images are from rats culled at 35 days and result from PUUO performed using a 0.4 mm wire template at age p2.

4.2.6 End of study protocol

4.2.6.1 Schedule 1 methods and retrieval of tissues

The humane killing of the rats was conducted in accordance with UK Home Office legislation (Schedule 1). The first litter of rats were culled by exposure to a rising concentration of CO_2 gas at 31 days of age. All subsequent litters were culled by terminal anaesthesia using isoflurane. This method would be necessary in later experiments when establishing an intra-renal pelvis pressure measurement technique.

From litter 3 onwards all rats were culled at 35 days of age. The rats were weighed and then anaesthesia was induced using a large induction chamber (AN010ASR, VetTech Solutions Ltd, Congleton, UK) and exposure to a mixture of 3% isoflurane (Merial, Essex, UK) and oxygen with the flow set at 1 l/min. This would usually take approximately 4-5 minutes until surgical anaesthesia was reached assessed by loss of the pedal reflex and lack of response to painful stimulus.

When fully anaesthetised the rat was moved to the surgical area, laid supine with its nose placed within a co-axial mask (Size 1, Vet Tech Solutions Ltd, Essex, UK). The isoflurane/oxygen mix was delivered via the co-axial system with an oxygen flow of 0.8 l/min and isoflurane concentration of 2 - 2.5%. A midline laparotomy was performed which was extended laterally in both directions from the inferior aspect of the midline incision to enable good exposure of both kidneys and ureters. Measurements of the proximal ureter diameter, the renal pelvis anteroposterior diameter (APD) and, in cases of severe hydronephrosis, the kidney length and width were taken using digital calipers. At this point the intra-renal pelvis pressure was also measured in litters 4-6 (see 4.2.6.3). Subsequently 0.9% saline was injected into the renal pelvis to confirm the presence of partial rather than complete ureteric obstruction. This was injected through the pressure measuring equipment in litters 4-6 and via a 27-gauge needle inserted through the kidney into the renal pelvis in litter 3. A small number of additional female rats (from litters 4-6) with PUUO created using a 0.4 mm wire template, had PBS containing bromophenol blue dye injected into the renal pelvis to visually confirm patency of the proximal ureter (Figure 4.14). Dye was not used in the male rats whose tissues would be processed for AQP analysis due to concerns this may interfere with the results. Bilateral nephroureterectomy was subsequently performed and the rat was then culled by increasing the isoflurane concentration to 5%.

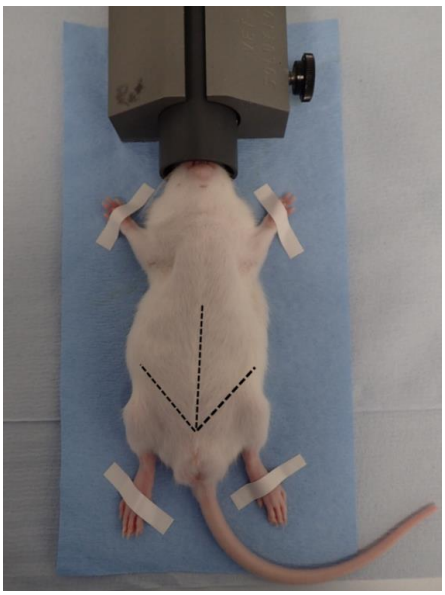

Figure 4.13 Rat positioning and incision site for intra-renal pelvis pressure measurement and tissue retrieval

The rat was laid supine on a warming pad with its nose placed within the co-axial mask. Tape was applied to all paws to secure the position. A midline laparotomy was performed and extended laterally in both directions from the inferior aspect of the midline incision (marked by dotted line).

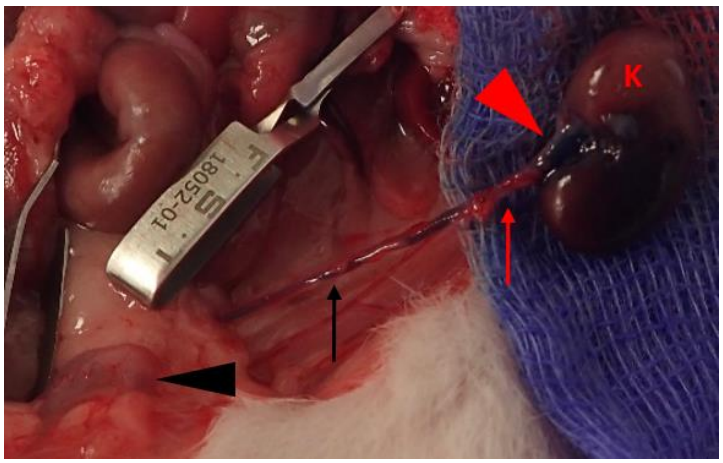

Figure 4.14 Injection of dye to confirm ureteric patency

A needle was inserted through the renal parenchyma into the renal pelvis of a 35-day old female pup with moderate hydronephrosis following PUUO using a 0.4 mm wire template at p2. PBS containing bromophenol blue dye was injected into the renal pelvis (red arrowhead). The dye flowed past the suture (red arrow) and down the ureter (black arrow). Dye reached the bladder (black arrowhead) following injection into the renal pelvis confirming this was not a complete ureteric obstruction. K – kidney.

4.2.6.2 Preparation of samples

Both kidneys, renal pelvices and ureters were dissected out and the kidneys individually weighed. The tissues were immediately washed 5 times in ice-cold PBS and then prepared as per Figure 4.15. For each kidney and its collecting system a total of 4 kidney samples were snap frozen in liquid nitrogen and stored at -80 °C for RNA and protein analysis while

1 renal pelvis sample and 1 ureter sample were snap frozen in liquid nitrogen and stored at minus 80 °C for RNA analysis. Additionally, the middle axial section of the kidney including the proximal renal pelvis as well as the middle section of ureter were placed in 10% neutral buffered formalin at 4°C for 24 hours before paraffin embedding.

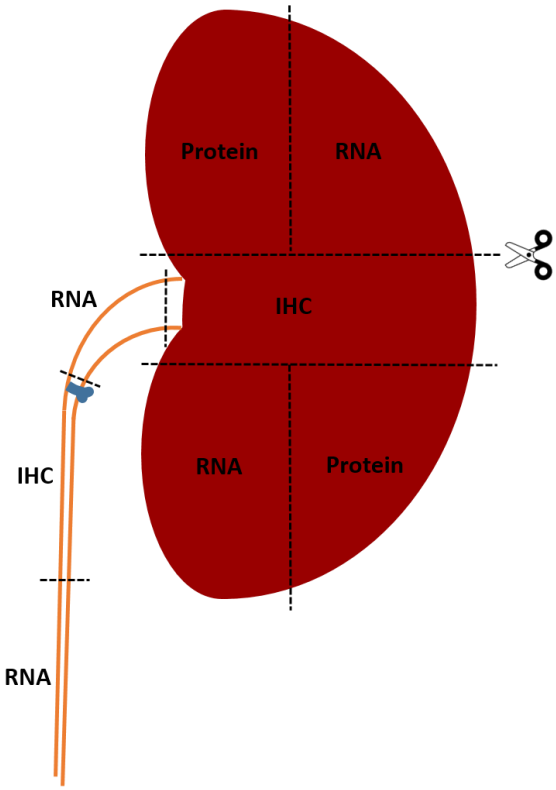

Figure 4.15 Rat model sample preparation for storage and formalin fixation

The kidney was cut into 5 sections as marked. The sample for IHC was immediately placed into 10% neutral buffered formalin at 4°C. The samples for subsequent protein and RNA extraction were snap frozen in liquid nitrogen and stored at -80 °C. The renal pelvis/ureter was cut into 3 sections as marked. The section of renal pelvis above the suture obstruction and the lower section of the ureter were snap frozen in liquid nitrogen and stored at -80°C for later RNA extraction. The middle section was placed into 10 % neutral buffered formalin at 4 °C. The site of the suture obstruction is marked in blue.

4.2.6.3 Pressure measurement within the obstructed renal pelvis

Following establishment of the surgical technique, including the specific wire diameter necessary to create the desired amount of hydronephrosis, efforts were turned to developing a method to measure the intra-renal pelvis pressure. Measurement of intra-renal pelvis pressure was conducted on all PUUO (0.4 mm wire template) and sham rats from litters 4-6 during terminal anaesthesia.

The equipment including a NeuroLog system amplifier (Digitimer, Hertfordshire, UK), a CED Micro 1401-3 data acquisition unit (Cambridge Electronic Design Limited, Cambridge,

UK) and Spike 2 software v7.10 (Cambridge Electronic Design Limited, Cambridge, UK) for data acquisition and analysis were kindly loaned for use by Dr A O'Carroll, University of Bristol. This was connected to a Digitimer fluid-filled disposable physiological pressure transducer (NL108T2, Digitimer, Hertfordshire, UK) which was placed at the level of the rats' kidney during calibration and pressure measurements (Figure 4.16). The technique developed was based on that used by Dr O'Carroll's group to measure arterial blood pressure via the femoral artery.

During initial tests of the procedure, the lumen of the pressure transducer was filled with 0.9% saline and connected via a 25G needle to Micro-Renathane® (MRE-025, Braintree Scientific, MA, USA) tubing which was then flushed through with 0.9% saline (Figure 4.16). The system was calibrated using a sphygmomanometer to pressures of 20 mmHg and 5 mmHg. These figures were chosen on the basis of previously published results and thus the expected pressures to be recorded. Wen *et al*. demonstrated baseline mean intra-renal pelvis pressures to be 4, 9 and 17 cmH2O for young rats with non-obstructed kidneys, acute mild ureteric obstruction and acute severe ureteric obstruction respectively [401]. Similar baseline pressures in non-obstructed and partially obstructed systems have been recorded in other mammals including dogs, pigs and humans [46, 112-114].

To introduce the Micro-Renathane® tubing into the renal pelvis, the needle from a 16G cannula (393209, Becton Dickinson, Swindon, UK) was inserted through the renal capsule on the anterior surface of the kidney at the intersection of the sagittal and axial planes through the centre of the kidney. The needle was then advanced through the kidney parenchyma in a postero-medial direction into the renal pelvis (Figure 4.18 and Figure 4.17). The Micro-Renathane® tubing was fed through the needle and continuous intra-renal pelvis pressure measurements recorded on the computer using Spike 2 software.

The problems noted with this set up were twofold:

1. The large size of the needle. Although this was the smallest gauge of needle that would accept the micro-renathane tubing it was huge compared to the size of the kidney. This made it difficult to guide the needle into the correct location without obliterating most of the structures.
2. Increased pressure within the kidney forced small amounts of urine up the needle around the tubing creating a small leak which inevitably affected pressure measurement.

The solution was to use a smaller needle, inserted into the renal pelvis, to measure the pressure directly without threading Micro-Renathane® tubing through it. The next issue was how to connect the needle to the pressure transducer as this would require some intermediate tubing. This was solved by using a 27G butterfly needle which has integral tubing and a screw connector (387412, Becton Dickinson, Swindon, UK) which fits perfectly onto the 3-way tap of the pressure transducer. The modified set-up is shown in Figure 4.19 and Figure 4.20 and was flushed through with 0.9% saline and calibrated in the same way using a sphygmomanometer to pressures of 20 mmHg and 5 mmHg. The transducer was placed at the level of the kidney and prior to measurement of renal pelvis pressure the bladder was emptied by aspirating urine using a 25G needle.

The 27G needle was inserted into the renal pelvis in the same manner as previously described (Figure 4.18), proving much easier to direct into the correct position (Figure 4.21) and was associated with minimal urine leakage. Continuous intra-renal pressure measurements were recorded on the laptop in mmHg using Spike 2 software. Baseline pressures were measured in both kidneys of sham and PUUO rats from litters 4-6 using this modified intra-renal pelvis pressure measuring set-up. Results were excluded from rats with leakage around the needle.

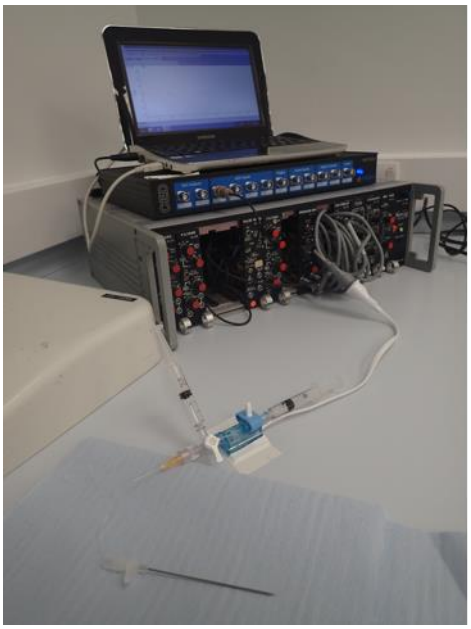

Figure 4.16 Equipment set-up to measure intra-renal pelvis pressure

The Digitimer fluid-filled physiological pressure transducer was attached to a 25G needle. One end of the Micro-Renathane tubing (0.025” OD) was applied over the 25G needle and the other end inserted through the needle from a 16G cannula. Signals from the pressure transducer were amplified, collated and analysed using a NeuroLog system amplifier, a CED micro 3 data acquisition unit and a laptop employing Spike 2 software.

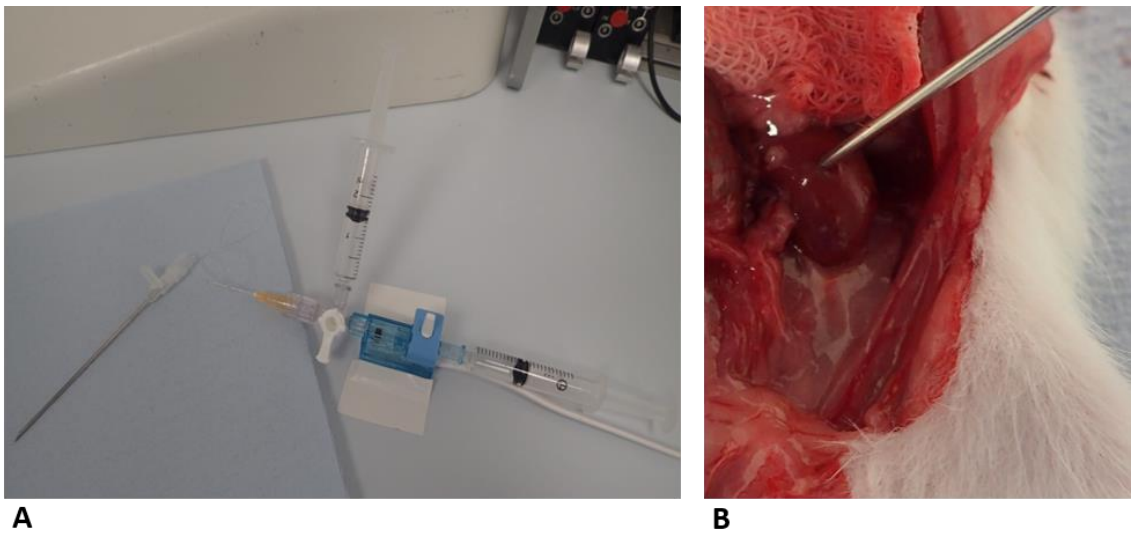

Figure 4.17 Intra-renal pelvis pressure measurement using a 16G cannula and microrenathane tubing

The Digitimer fluid-filled physiological pressure transducer was attached to a 25G needle. One end of the Micro-Renathane tubing (0.025" OD) was applied over the 25G needle and the other end inserted inside the needle from a 16G cannula. The transducer, 25G needle and Micro-Renathane tubing are all flushed through with 0.9% saline (A). The needle from a 16G cannula was inserted through the renal parenchyma as described in Figure 4.18 and the Micro-Renathane tubing advanced through the cannula enabling the tip of the tubing to lie in the renal pelvis.

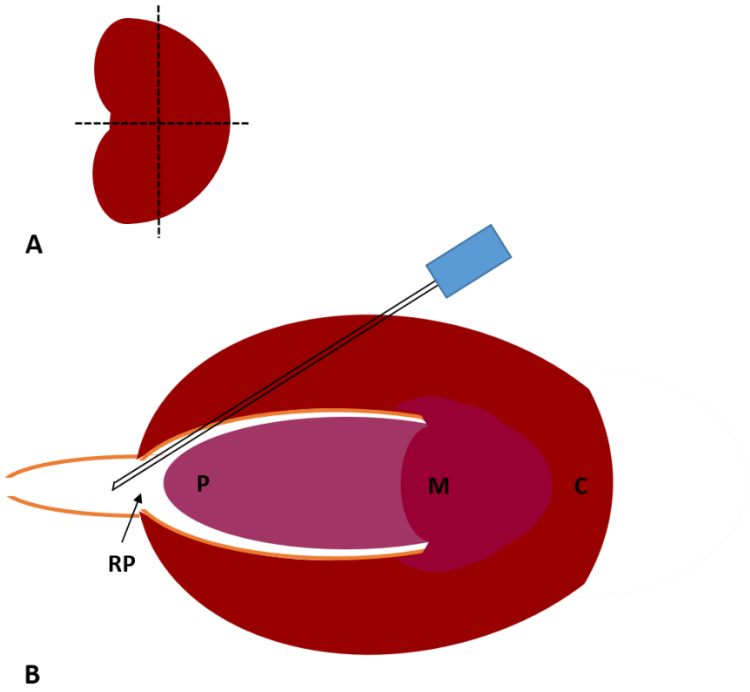

Figure 4.18 Cartoon demonstrating needle insertion technique to measure intra renal pelvis pressure

The needle was inserted through the renal capsule on the anterior surface of the kidney at the point which marks the intersection of the sagittal and axial planes through the centre of the kidney (A). The needle was directed through the kidney parenchyma in a posteromedial direction into the renal pelvis. C – renal cortex, M- renal medulla, P – renal papilla, RP – renal pelvis (B).

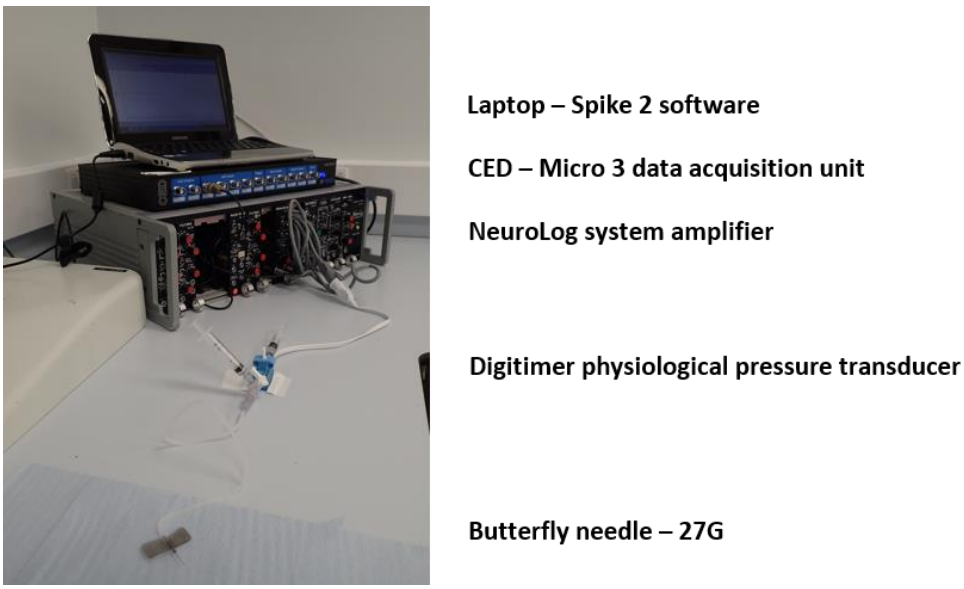

Figure 4.19 Modified equipment set-up to measure intra-renal pelvis

The digitimer fluid-filled physiological pressure transducer was attached directly to a 27G buttefly needle. Signals from the pressure transducer were amplified, collated and analysed using a NeuroLog system amplifier, a CED micro 3 data acquisition unit and a laptop employing Spike 2 software.

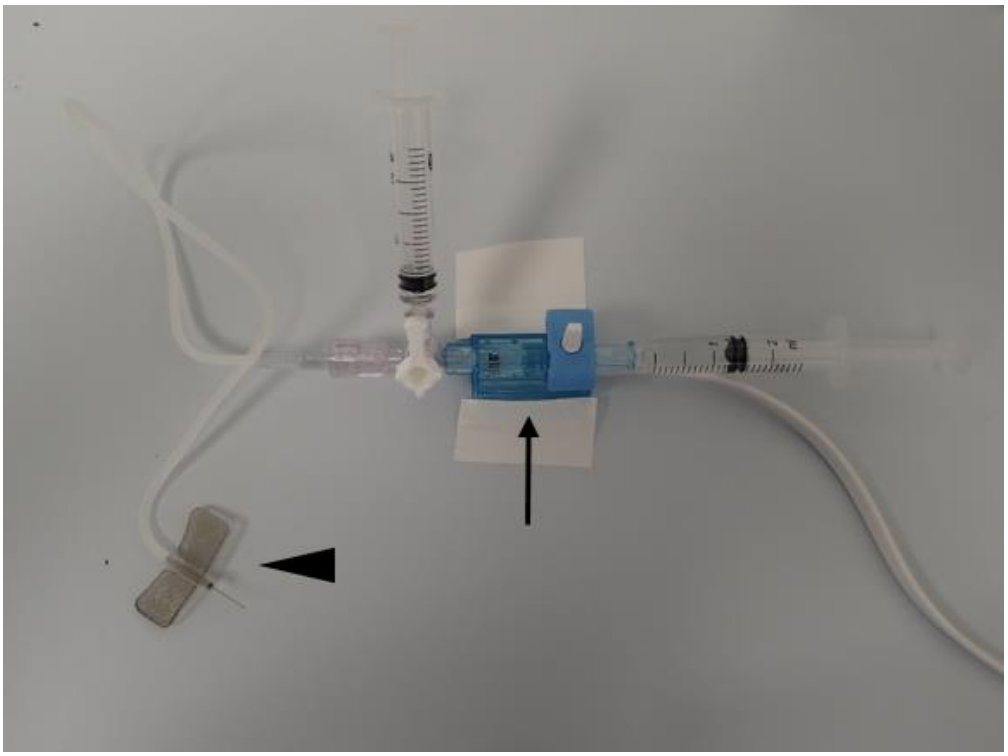

Figure 4.20 Digitimer pressure transducer with attached 27G butterfly needle

The integral tubing from the 27G butterfly needle (arrowhead) is attached directly to the digitimer fluid filled transducer (arrow) and both are flushed through with 0.9% saline.

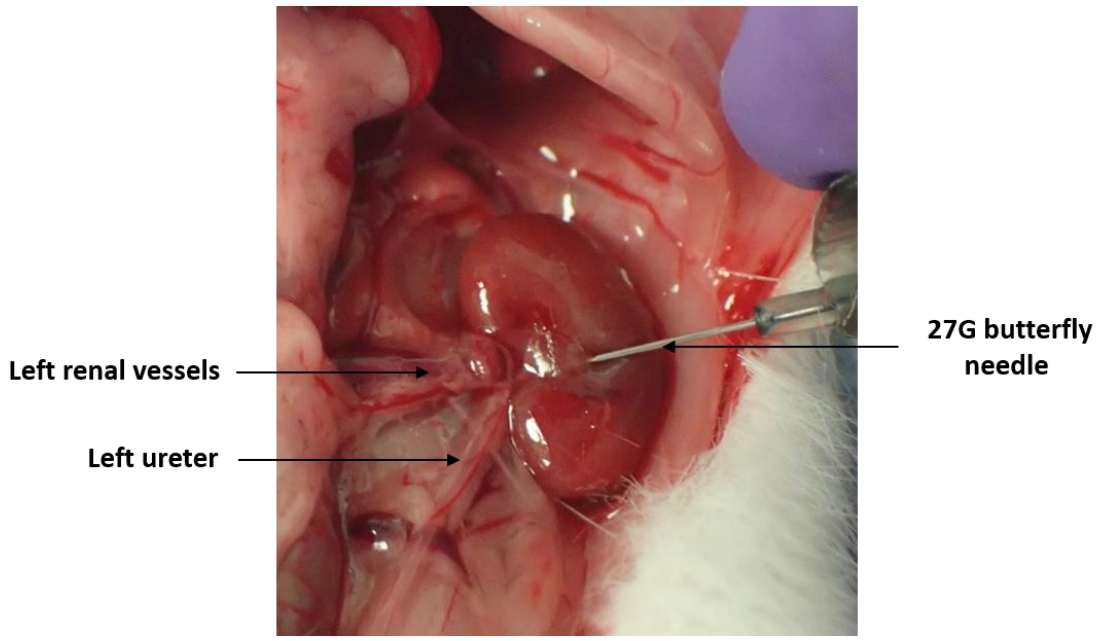

Figure 4.21 Intra renal pelvis pressure measurement with 27G butterfly needle

The 27G butterfly needle was inserted through the renal parenchyma as described in Figure 4.18 and was used to measure the pressure directly.

4.3 Discussion

This chapter has described how a neonatal rat partial unilateral ureteric obstruction model was developed based on a procedure described by Thornhill *et al.* in 2005. Initial work tested the feasibility of performing the procedure in neonatal rat pups and determined optimum surgical access for the procedure considering not only the field of vision and access to structures, but also post-operative recovery for the pup. A left oblique flank incision was determined to be optimum and procedures performed on p3/4 culled pups revealed that Thornhill's technique was achievable and did not result in complete obstruction of the ureter. This procedure was taken forward and applied to p2 pups under isoflurane anaesthesia who were subsequently recovered and returned to the litter. Thornhill's paper reported that decreasing wire diameter resulted in increasing severity of hydronephrosis and rising renal pelvis diameter proportional to the degree of obstruction at 14 days post PUUO. Wire templates of 0.35 mm were reported to create moderate PUUO, while 0.3 mm and 0.25 mm templates resulted in severe PUUO. Interestingly, this group noted that the renal pelvis became maximally dilated by 28 days post PUUO with no significant difference between the 3 sizes of wire template at this point. Wire templates of 0.6 mm were reported to create mild obstruction such that ureteric dilatation was not detected until 42 days post-operatively [91].

Based on this evidence PUUO was created in the first litter using a 0.3 mm wire template. Rats were culled at 1 month to ensure maximal dilatation of the ureter and renal pelvis was

achieved in order to test the adequacy of the template diameter chosen. At 31 days all 3 rats with left PUUO had severe hydronephrosis with extremely dilated urine filled left kidneys and severe renal atrophy such that there was little renal tissue apparent. All had normal contralateral right kidneys. This degree of hydronephrosis was too severe for the purposes of the study as some renal tissue was required for analysis. Additionally, this degree of hydronephrosis was greater than that reported by Thornhill *et al*. This could potentially be due to differences in tolerance between the wire templates used as they were sourced from different manufacturers.

A second litter therefore underwent PUUO using a 0.6 mm wire template. At 37 days of age these rats did not show any evidence of hydronephrosis with no significant difference noted between the ureteric and renal pelvis diameters of PUUO and sham rats. This remained the case at 100 days of age and therefore a further litter was operated on using a 0.4 mm wire template. This litter of 6 operated males demonstrated variable hydronephrosis at 35 days of age. Two rats demonstrated mild hydronephrosis, 1 moderate hydronephrosis and 3 severe hydronephrosis compared to normal contralateral kidneys. These results are obviously very different from those presented by Thornhill *et al*. who reported reproducible degrees of obstruction with specific wire diameters [91]. There are a number of reasons why this model may have achieved variable hydronephrosis while using a constant wire template diameter and these include:

- Natural variation in ureter size as compared to a fixed wire template size thus constricting the ureter by different proportions
- Individual renal/urothelial factors which modulate the response of the kidney and its collecting system to a fixed degree of obstruction. The degree of dilatation may be affected by the compliance of the ureter and renal pelvis as well as other potentially compensatory mechanisms to reduce pressure within the kidney such as reduced urine production and increased urine re-absorption by the venous and lymphatic systems [88, 117, 121]. Furthermore, the individual ability of a kidney to reduce pressure may predict renal insult progression and necessity for surgery in human PUJO. This research will start to investigate the role of kidney and urothelial aquaporin expression in such a renoprotective pressure reduction mechanism
- Technical issues with the procedure such as differing tension when tying the ligature around the ureter and wire template, or post-operative adhesions kinking the ureter. These problems had been anticipated and to minimise these the procedure was

performed by a single operator taking care in the method used to tie the ligature with equal tension for all operations. Attention was paid to ensuring the ureter was returned to the anatomical position within the abdomen to reduce the risk of kinking. Additionally, manoeuvres were undertaken involving injecting either bromophenol blue dye or 0.9% saline into the renal pelvis at completion of the study to ensure that a complete obstruction had not been created

Despite the fact that this method did not reproduce exactly what had been reported, the decision was made to continue the neonatal rat PUUO model using a 0.4 mm wire template as this was generating precisely what was required, differing severities of hydronephrosis which could be used to assess aquaporin expression and excretion.

Post-operative complications were noted affecting pups from the first 2 litters, however, there were no complications affecting the final 4 litters suggesting there was technical improvement as the research progressed.

One pup suffered a post-operative wound dehiscence related to the mother removing the skin sutures shortly after the procedure. This issue was rectified by amending the method of skin closure and burying the absorbable sutures. Subsequently there were no wound complications. The placement of surgical skin clips was considered as an alternative, however, these would need to be removed a few days post-operatively causing further distress to the pups. Vicryl sutures are absorbable and therefore do not require removal.

Two pups were cannibalised by the mother. A female pup who had undergone creation of PUUO using a 0.3 mm wire template was eaten by the mother shortly after surgery. It is unknown whether this pup had died as a complication of the surgery or whether it was maternal infanticide due to interference with the litter. Skin glue had been trialled for wound closure on this pup which may have rendered the pup with an unusual smell noticed by the mother. Skin glue was not used again for any future pups. A male pup from litter 2 who had undergone PUUO with a 0.6 mm wire template was also eaten by the mother at p5 for reasons which are unknown. There was no indication that this pup was unwell, and it had been gaining weight at a comparable rate to its littermates.

A female pup from litter 1 who had undergone left PUUO with a 0.3 mm wire template died suddenly at 26 days of age. A post-mortem performed by Dr J Roe, named veterinary surgeon, did not identify any evidence of chronic ill health or a cause of death.

At the end of the study protocol bilateral nephrouretectomy was performed and the rats were culled by terminal isoflurane anaesthesia. Additionally, litters 4-6 underwent basal intra-renal pelvis pressure measurement while still under surgical anaesthesia. This procedure utilized a fluid-filled pressure transducer and was based on a technique used by Dr O'Carrolls group, University of Bristol to measure arterial blood pressure via the femoral artery. This method was modified to enable simultaneous puncture of the kidney and renal pelvis pressure measurement with the same equipment, namely, a 27G butterfly needle which could be conveniently connected to the pressure transducer using the integral tubing and screw connector. The needle was inserted through the kidney parenchyma into the renal pelvis rather than into the pelvis directly to reduce the incidence of leakage around the needle which would compromise the results. This technique was utilised to measure intra-renal pelvis pressure in litters 4-6 and the results are presented in Chapter 5.

Basal intra-renal pelvis pressure measurement during the current study indicated the pressure the obstructed kidney was exposed to under physiological conditions in each rat. The relationship between intra-renal pelvis pressure and AQP expression and excretion was then analysed. It is acknowledged, however, that basal pressure measurement at a single time point within the obstructed kidney is affected by variables such as the velocity of urine flow, compliance of the system, the degree of obstruction and intra-abdominal pressure [406]. Although variation in intra-abdominal pressure was not a concern in the current study as measurements were made with abdomen open, the variable rate of urine inflow into the renal pelvis between individuals would modify intra-renal pelvis pressure. Urine production is influenced by GFR and tubular reabsorption of water and solutes, both of which are reduced in PUUO [91, 185]. To overcome this issue, fluid inflow can be standardised between individuals using a dynamic perfusion-pressure test (Whitaker technique). Using a single cannula, intra-renal pelvis pressure is measured while fluid is infused into the renal pelvis at a standard fast flow rate [406]. For future studies, further development of the intra-renal pelvis pressure measurement technique to include fluid perfusion will enable measurement of both basal and dynamic perfusion-pressure.

In summary, based on methods described by other groups, techniques were established to perform neonatal rat recoverable anaesthesia, to create neonatal rat partial UUO, and to measure intra-renal pelvis pressure in normal and hydronephrotic kidneys in young rats. These techniques were applied to further litters of rat pups in order to meet the aims and objectives of this research, the results of which are presented in Chapter 5.

Chapter 5. Aquaporin expression and urinary excretion in a neonatal rat partial unilateral ureteric obstruction model

5.1 Introduction

Various AQP isoforms are expressed by rat kidney and urothelium and are excreted into the urine within exosomes. Dysregulation of renal AQP expression has been demonstrated in both adult and neonatal models of obstructive hydronephrosis and is associated with defects of tubular solute and water handling [185]. Little is known regarding the effects of obstruction on urothelial AQP expression.

Following 24 hours of adult rat complete UUO, downregulation of AQPs 1, 2, 3, 4 and phosphorylated AQP2 expression is noted at the protein level and is associated with increased free water clearance [184, 186]. AQP2 mRNA expression is also downregulated indicating these changes may be transcriptionally regulated [186]. Concomitant downregulation of AQPs 1 and 2 in the contralateral kidney of this UUO model suggests both intrarenal and systemic factors are involved in AQP dysregulation [184, 186]. Similarly, 24 hours of complete bilateral ureteric obstruction (BUO) in adult rats is associated with reduced renal AQP1, 2 and 3 protein expression, polyuria and diminished urinary concentrating ability [188, 189]. AQP2 and 3 expression remains reduced at 14 days following release of BUO but normalises by 30 days. Conversely AQP1 expression remains downregulated at 30 days following release of BUO at which time rats continue to exhibit significant polyuria and a urinary concentrating defect in response to thirst [189].

Although informative, these models do not mimic the situation in congenital PUJO, which is better appraised by neonatal rat models involving chronic partial UUO. These models suggest the response to obstruction in PUJO may be more complicated than indicated by adult acute UUO models, being age and/or time dependent. An initial increase in AQP1, 2 and 3 protein expression in the obstructed kidney at 7 weeks post PUUO is followed by a reduction in expression of AQP1 and 2 expression and a normalisation of AQP3 expression compared to sham at 14 weeks post PUUO. The early increase in AQP expression points to possible compensatory mechanisms while the subsequent downregulation likely represents tubular dysfunction related to chronic obstruction. Interestingly, the amount of phosphorylated AQP2 (pS256-AQP 2) at both time points is reduced compared to both the

contralateral and sham kidneys implying AQP2 translocation to the apical membrane is diminished despite variations in the total expression of AQP2 protein [364]. Furthermore AQP2 protein expression remains downregulated at 24 weeks post-PUUO compared to the contralateral non-obstructed kidney which corresponds to a significant reduction in the GFR and solute free water reabsorption by the obstructed kidney at 12 and 24 weeks post PUUO [185].

AQP1, 2 and 3 proteins are also expressed by rat bladder and ureter. AQPs 2 and 3 are expressed by urothelial cells while AQP1 is located to the vascular endothelial cells of the blood vessels [249, 367, 368]. Regulation of urothelial AQPs has been noted with AQP2 and 3 expression being significantly upregulated by dehydration and downregulated by lack of oestrogen in ovariectomised female rats [249, 250]. There are very few studies that have investigated urothelial AQP expression in response to urinary tract obstruction. Partial bladder outlet obstruction in rats results in a significant upregulation of AQP1 expression in the capillaries, arterioles and venules of bladder tissue [367], while AQP2 and 3 expression is increased in the bladder urothelial cells [368]. It is postulated that this heightened AQP expression may contribute to the bladder dysfunction that characterises partial bladder outlet obstruction. There are no studies assessing AQP expression in the ureter or renal pelvis in response to urinary tract obstruction.

AQPs 1 and 2 are detected in rat urine in amounts that generally correspond to the level of renal expression [372, 381, 383]. Conversely AQP3 is not detected in urine [372]. Urinary exosomal AQP excretion likely occurs via a selective apical pathway whereby factors which change apical cell membrane AQP expression lead to altered excretion. Acetazolamide treatment of rats leads to upregulation of proximal tubular apical cell membrane AQP1 expression and is associated with increased urinary AQP1 excretion [382]. Similarly, in the basal state approximately 3-4% of total kidney AQP2 is excreted in the urine on a daily basis [372, 383], however, excretion is regulated by vasopressin and in states of significant vasopressin flux AQP2 excretion mirrors apical cell membrane expression (also vasopressin mediated) rather than total kidney abundance [371, 384, 385].

As a proxy of renal AQP expression, urinary AQP measurement has many research and potentially clinical applications, particularly given the non-invasive nature of the test. Reduced urinary excretion of AQPs 1 and 2 by the obstructed kidney has been demonstrated in the post-operative period following pyeloplasty for human PUJO [365, 386], however

there are no pre-operative studies in either humans or rodents to identify whether AQPs would be a useful biomarker of the severity of disease and the necessity of surgery for PUJO.

This chapter presents all data obtained after implementation of the neonatal PUUO model and delineates urinary tract AQP expression and urinary excretion in this model.

5.2 Methods

5.2.1 Study protocol

Male Han-Wistar p2 pups (24-48 hours of age) weighing 5.4g – 8.9g underwent creation of left PUUO (n=13) using a 0.4 mm wire template or left sham procedure (n=6) as outlined in Chapter 4. Sham and PUUO animals were derived from five litters of rats (denoted litters 2-6). Seven non-operated female rats from litter 5 underwent bilateral intra-renal pelvis pressure measurement under terminal anaesthesia at 35 days of age to establish normal intra-renal pelvis pressure. No tissue or urine samples were collected from these female animals.

A significant difference in urinary AQP1/creatinine excretion between males (mean +/- SEM 0.35 +/- 0.01 μg/mg) and females (mean +/- SEM 0.17 +/- 0.017 μg/mg) on an initial test of the urinary AQP1 ELISA necessitated the use of only male animals for the study (Figure 5.1). The urine used in this ELISA was obtained from rats who had undergone either left PUUO using a 0.6 mm wire template or sham procedure and none of the rats had hydronephrosis (discussed in Chapter 4). As expected, no significant difference was noted in urinary AQP1/creatinine excretion between PUUO compared to sham rats (data not shown).

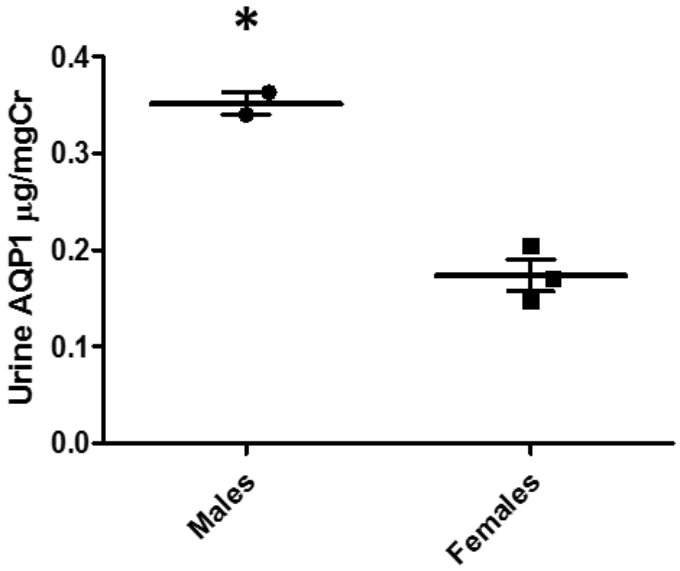

Figure 5.1 Urine AQP1 in male versus female rats

Vertical scatter plot demonstrating urine AQP1 levels normalised to creatinine for male (1 x sham, 1 x left PUUO 0.6 mm wire) compared to female (1 x sham, 2 x left PUUO 0.6mm wire) rats. *p=0.0045 compared to females. Individual data points and mean +/- SEM presented.

Following the PUUO or sham procedure pups were housed with their mother and the rest of the litter in standard conditions until three weeks of age when they were weaned and separated into male and female groups. Rats were weighed on a weekly basis and a spot urine sample was obtained at 2 and 3 weeks of age. These samples were stored at -80 °C but thus far have not been analysed due to their small volume which is unsuitable for the AQP1 ELISA. A larger urine sample was obtained at 4 weeks of age by placing the rat in a metabolic cage for up to 5 hours. These samples were used to determine AQP1/creatinine excretion during the study.

At 5 weeks (35 days) of age all rats except one underwent terminal anaesthesia, measurement of intra-renal pelvis pressure (litters 4-6 only) and retrieval of kidney, renal pelvis and ureteric tissues (PUUO n= 12, sham n=6). Kidney and renal pelvis samples were processed for later mRNA and protein analysis. Individual wet kidney weights were recorded in accordance with previous data supporting their good approximation to dry weights and renal growth in rats [93, 129]. Where possible paired left renal pelvis and bladder urine specimens were also obtained although these have not been analysed during this study due to time constraints. A timeline of the neonatal rat partial unilateral ureteric obstruction model is presented in Figure 5.2. One PUUO rat was followed up to 86 days and then underwent terminal anaesthesia, intra-renal pelvis pressure measurement and tissue collection. The

renal tissue was used for protein expression analysis by western blotting only. This was to gain a preliminary insight of how a longer period of PUUO might impact on the urinary tract and thus direct future studies.

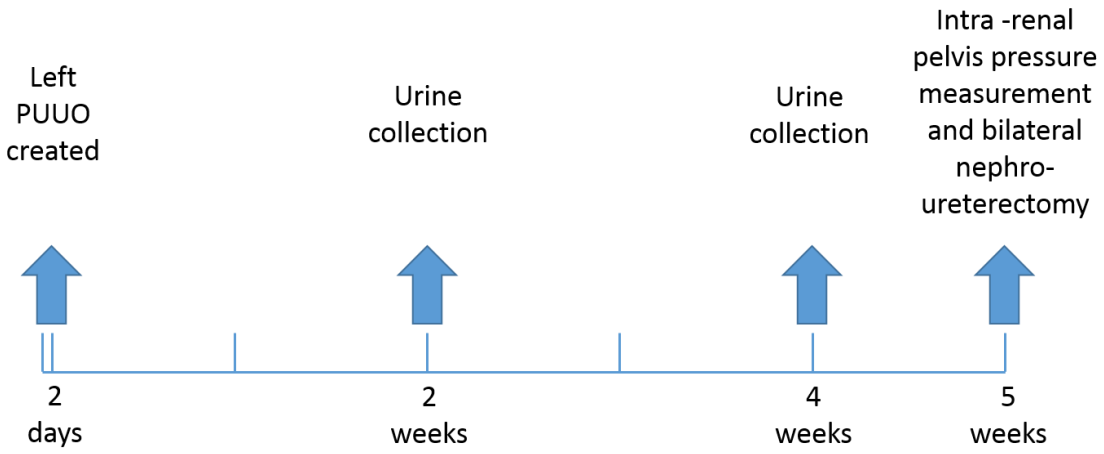

Figure 5.2 Timeline of neonatal rat partial unilateral ureteric obstruction model

5.2.2 Immunohistochemistry

Immunohistochemistry for AQP3 expression by whole renal pelvis obtained from 35-day old PUUO and sham rats was performed as a mass batch to reduce the risk of technical error between biological replicates. Unfortunately, the initial round of staining was unsuccessful as confirmed by lack of expected staining in the positive control sections. Due to time constraints, investigation into this problem was continued by a colleague within the renal group (Miss Fern Barrington). The primary antibody, which was from a new batch, was identified as being the likely cause. A new AQP3 antibody was sourced from an alternative manufacturer, the antibody dilution optimised, and the method performed as described in the methods section (Chapter 2, section 2.13). The immunohistochemistry and imaging for AQP3 using the new antibody was undertaken as a mass batch by Miss Fern Barrington. Blinded grading of AQP3 staining of all sections from PUUO and sham rats was undertaken by Professor Richard Coward and Miss Fern Barrington as detailed in the methods section (Chapter 2, section 2.16.1.3).

5.2.3 Statistics

Data is presented as mean +/- SEM. Any data group containing only one animal was not included in statistical analyses. Statistical analysis of real time RT-PCR results was

undertaken on the ΔCt values and the relative fold change calculated for graphical representation. Comparison of two groups was performed using an unpaired two tailed t-test while multiple groups (>2) comparisons were assessed using a one-way analysis of variance (ANOVA) with Tukey post-test correction. Repeated measures of multiple groups were analysed using a two-way ANOVA with Bonferroni post-test correction. Correlation of results was assessed using an XY scatter plot and Pearsons correlation test. $P<0.05$ was accepted as statistical significance.

5.3 Results

5.3.1 Body weight is reduced in PUUO rats compared to sham rats

Rat body weight was consistent between PUUO rats and sham rats from the time of surgery until 4 weeks of age. At 5 weeks of age, however, rats who had undergone left PUUO had a significantly reduced body weight compared to those treated by sham procedure (Figure 5.3).

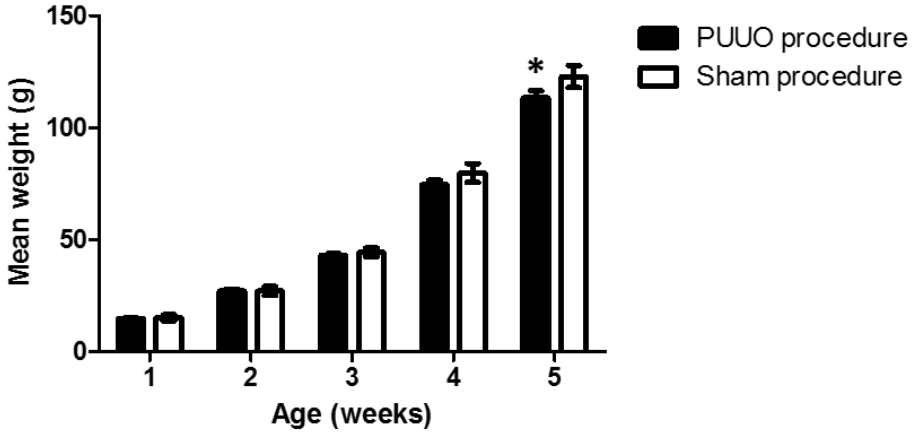

Figure 5.3 Mean weight of PUUO rats versus sham rats

Bar graph demonstrating weekly post-operative mean weights +/- SEM presented for all rats who underwent PUUO versus sham procedure. Left PUUO n=13, left sham procedure n=6. PUUO rats were significantly lighter than sham rats at 5 weeks of age. *$p<0.05$ compared to sham

5.3.2 Stratification of PUUO rats according to severity of hydronephrosis

All rats in this study had undergone PUUO using a fixed wire template size of 0.4 mm. It was known however from preliminary studies that this would generate variable degrees of hydronephrosis. Bilateral renal pelvis APD and proximal ureter diameters were therefore measured at the time of terminal anaesthesia in all animals prior to intra-renal pelvis pressure

measurement and tissue retrieval. The renal pelvis measurements alongside the degree of preservation of the renal parenchyma were then used to stratify rats arbitrarily into groups denoting the severity of hydronephrosis. Rats with a left renal pelvis APD ≥ 1.8 mm were designated to have mild hydronephrosis. Those with a left APD ≥ 3 mm, with or without mild to moderate parenchymal thinning, were assigned to the moderate hydronephrosis group. Rats with a left renal pelvis APD ≥ 3 mm and substantial parenchymal thinning were classified as severely hydronephrotic. The stratification of the PUUO rats into groups is presented in Table 5.1.

The bar graphs in Figure 5.4 show the mean renal pelvis APDs and proximal ureter diameters for sham rats and each severity of hydronephrosis alongside corresponding values for the normal contralateral kidneys. The mean renal pelvis APD and proximal ureter diameter were significantly larger in the severely hydronephrotic kidneys (renal pelvis 6.36mm +/- 0.56, ureter 2.3mm +/- 0.24) compared to sham (renal pelvis 1.2 +/- 0.09, ureter 0.76 +/- 0.04), mildly (renal pelvis 2.21 +/- 0.20, ureter 1.18 +/- 0.04) and moderately (renal pelvis 3.99 +/- 0.52, ureter 1.78 +/- 0.13) hydronephrotic kidneys. Similarly, the mean renal pelvis APD and proximal ureter diameter were significantly increased in the moderately hydronephrotic kidneys compared to sham and mild hydronephrosis but significantly smaller compared to severe hydronephrosis. Although the mean renal pelvis APD and proximal ureter diameter for the mildly hydronephrotic group were not statistically different to those of sham animals these kidneys were visibly different at the time of terminal anesthesia and the measurements show a trend towards significance which would almost certainly be achieved with larger numbers.

Rat	Severity of hydronephrosis	Left renal pelvis (mm)	Right renal pelvis (mm)	Left proximal ureter (mm)	Right proximal ureter (mm)	Parenchymal thinning
1	Mild	1.91	1.13	1.13	0.64	None
2	Mild	2.6	1.49	1.16	0.76	None
3	Mild	2.12	1.25	1.25	0.82	None
4	Moderate	5.98	1.04	1.69	0.66	Mild
5	Moderate	3.7	1.4	1.83	1.06	None
6	Moderate	3.98	1.22	1.71	0.89	None
7	Moderate	3.3	1.4	1.43	0.77	Mild
8	Moderate	3	1.39	2.22	0.82	None
9	Severe	6.55	1.01	2.14	0.61	Substantial
10	Severe	6.91	1.17	2.05	0.7	Substantial
11	Severe	7.23	1.33	2	0.86	Substantial
12	Severe	4.73	1.12	3.01	0.81	Substantial
13	Sham	1.18	1.02	0.82	0.86	None
14	Sham	0.9	1	0.6	0.7	None
15	Sham	1.4	1.46	0.81	0.82	None
16	Sham	1.03	1.31	0.73	0.82	None
17	Sham	1.33	1.44	0.84	1	None
18	Sham	1.43	1.2	0.77	0.78	None

Table 5.1 Outcome of PUUO created with a 0.4 mm wire template versus sham rats

Table detailing the renal pelvis and ureter dimensions at 35 days of age for 18 rat pups who underwent either left PUUO using a 0.4 mm wire template or sham procedure. The presence of parenchymal thinning is also noted. PUUO rats are stratified into three groups according to the severity of hydronephrosis.

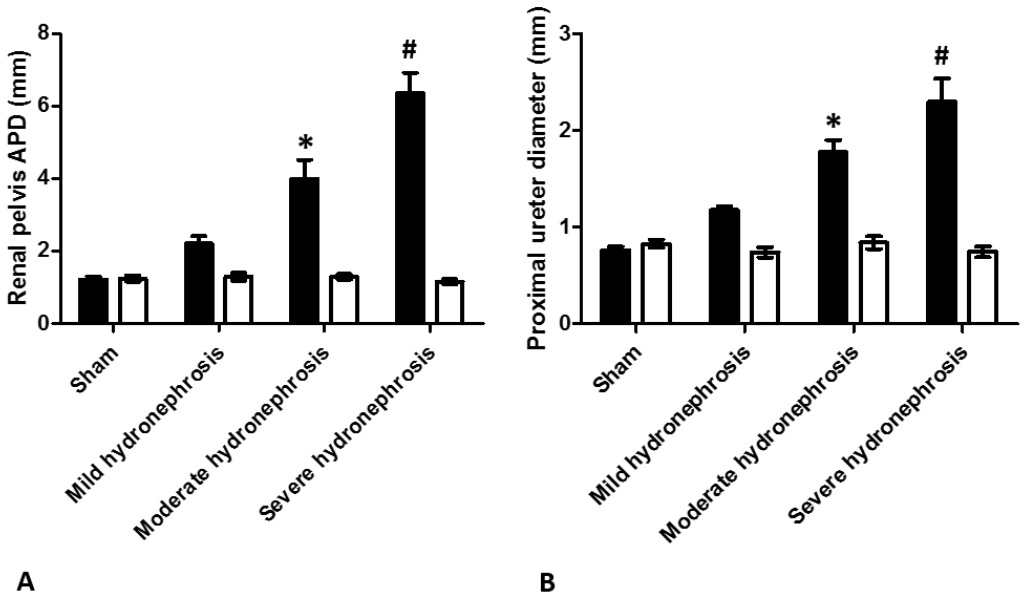

Figure 5.4 Renal pelvis and proximal ureter dimensions of PUUO and sham rats

Bar graph comparing renal pelvis APD (mean +/- SEM) between PUUO rats with varying degrees of hydronephrosis and sham rats (A). Bar graph comparing proximal ureter diameter (mean +/- SEM) between PUUO with varying degrees of hydronephrosis and sham rats. *****$p<0.05$ compared to sham, mild and severe hydronephrosis. #$p<0.05$ compared to sham, mild and moderate hydronephrosis. Sham n=6, mild hydronephrosis n=3, moderate hydronephrosis n=5, severe hydronephrosis n=4. Black bars - left obstructed/sham kidney, white bars – right contralateral kidney.

5.3.3 The individual wet weight of the obstructed kidney is unchanged compared to the sham kidney

Following retrieval of the renal tract tissues under terminal anaesthesia at 35 days of age the kidneys were dissected from the renal pelvis and ureter and separately weighed. No significant difference in mean wet kidney weight was revealed between each degree of hydronephrosis when compared to each other, sham, contralateral sham and contralateral PUUO kidneys (Table 5.2 and Figure 5.5)

Group	Mean kidney weight (g) +/- SEM
Sham	0.65 +/- 0.03
Contralateral sham	0.71 +/- 0.04
Mild hydronephrosis	0.56 +/- 0.03
Contralateral mild hydronephrosis	0.59 +/- 0.02
Moderate hydronephrosis	0.63 +/- 0.03
Contralateral moderate hydronephrosis	0.68 +/- 0.03
Severe hydronephrosis	0.64 +/- 0.08
Contralateral severe hydronephrosis	0.73 +/- 0.05

Table 5.2 Mean kidney weights of left PUUO rats

Kidney weights stratified according to severity of hydronephrosis and compared to sham and contralateral kidneys

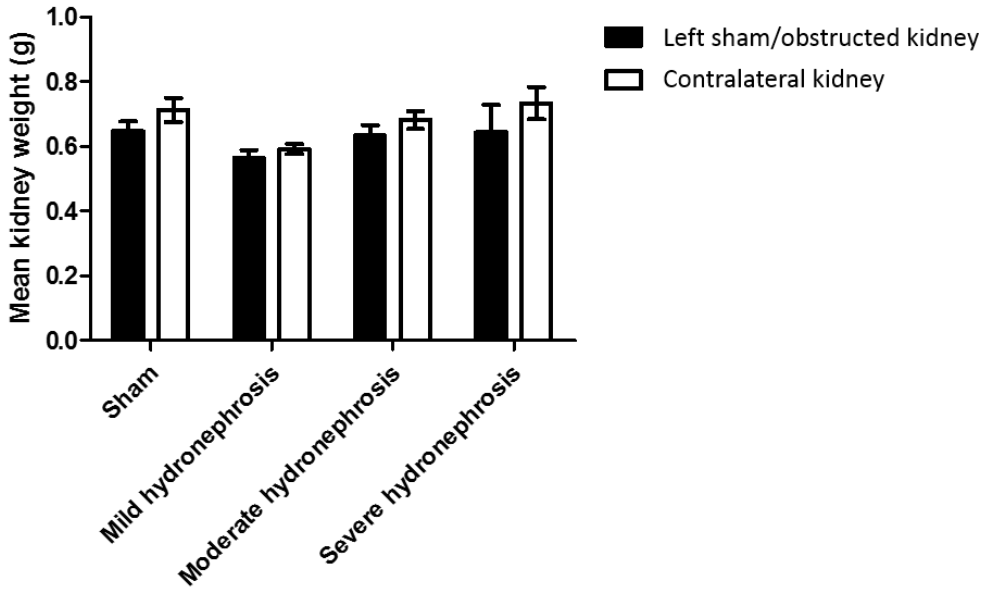

Figure 5.5 Mean kidney weights of left PUUO rats compared to controls

Bar graph demonstrating mean wet kidney weights +/- SEM at 35 days of age for all rats who underwent left PUUO versus sham procedure and are stratified according to the severity of hydronephrosis. Sham n=6, mild hydronephrosis n=3, moderate hydronephrosis n=5, severe hydronephrosis n=4. No significant difference was noted in wet kidney weight between any of the groups. p=0.1885.

5.3.4 Intra-renal pelvis pressure is increased in moderate hydronephrosis

Intra-renal pelvis pressure measurements at 35 days of age were only undertaken on PUUO and sham rats from litters 4-6 as the technique had not been fully developed when earlier litters reached the end of the protocol. Seven additional age-matched female non-operated rats from litter 5 also underwent intra-renal pelvis pressure measurement to determine normal renal pressure using this method. Eight intra-renal pelvis pressure readings were excluded from the study (2 contralateral moderate hydronephrosis, 1 contralateral severe hydronephrosis, 1 contralateral sham and 4 female non-operated kidneys) due to either failure to site the needle in the renal pelvis or because of urine leakage around the needle.

Figure 5.6 shows representative intra-renal pelvis pressure traces obtained for hydronephrotic, sham and contralateral kidneys. The traces demonstrate increased pressure, to varying degrees, following insertion of the pressure measuring needle into the renal pelvis. When results for all kidneys were analysed the intra-renal pelvis pressure was observed to be significantly elevated in moderately hydronephrotic kidneys (8.299 mmHg +/- 2.920) compared to sham (0.5011 mmHg +/- 0.1494), contralateral sham and PUUO (1.511 +/- 0.2871) and non-operated (1.518 mmHg +/- 0.1801) kidneys. The mild and severely hydronephrotic kidney groups contained only a single kidney each and therefore were excluded from statistical analysis. The pressure measured in the mildly hydronephrotic kidney (0.4 mmHg) fell within the range of sham, contralateral and non-operated kidneys whereas the severely hydronephrotic kidney pressure was slightly above their range at 2.973 mmHg. Substantial variability of the pressure measurements in the moderately hydronephrotic kidneys was noted(Figure 5.7).

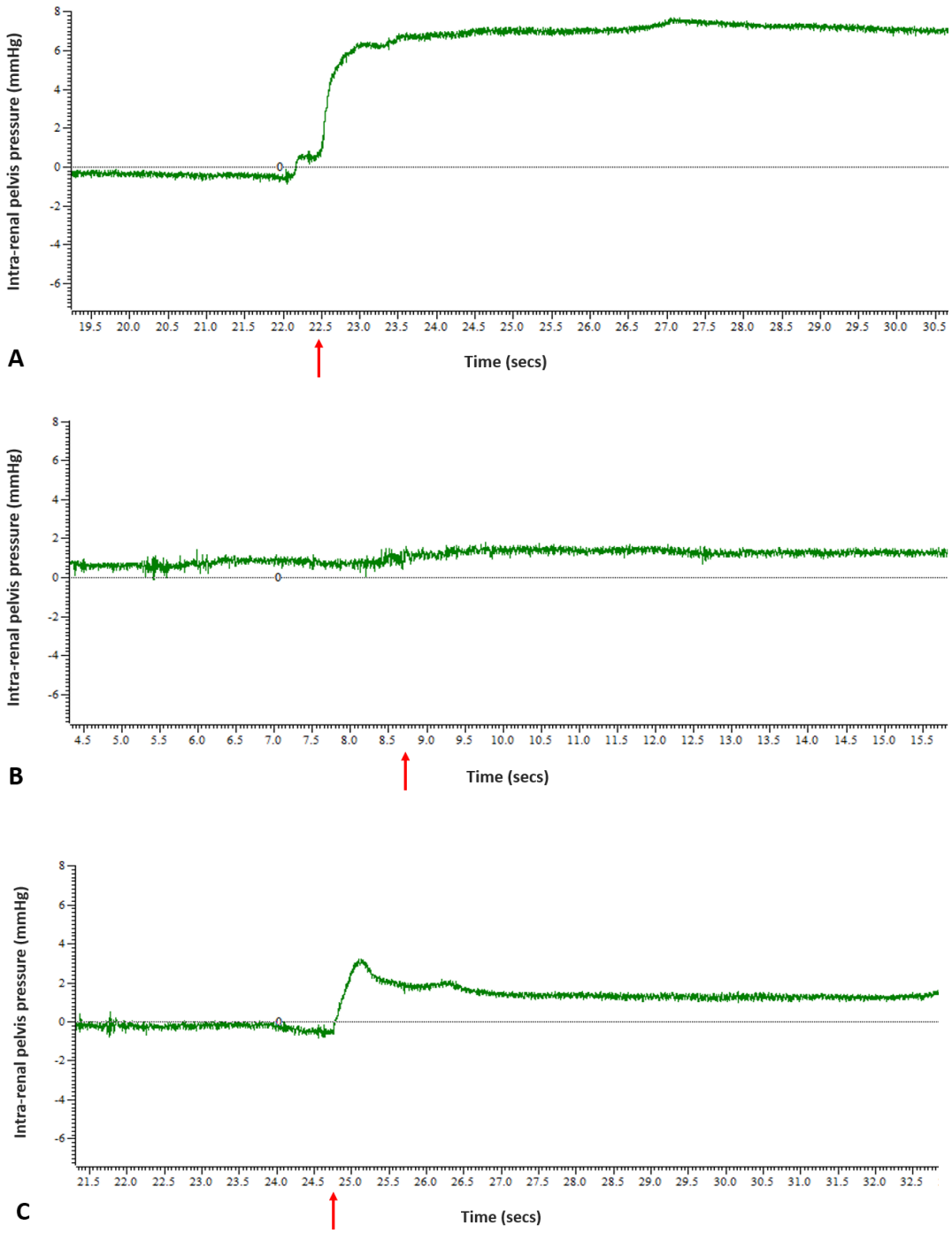

Figure 5.6 Intra-renal pelvis pressure traces for hydronephrotic, sham and contralateral kidneys

Representative pressure traces generated by Spike 2 software for a moderately hydronephrotic kidney (A), a sham kidney (B) and a contralateral sham kidney (C). Arrow indicates time at which the pressure measuring needle was inserted into the renal pelvis.

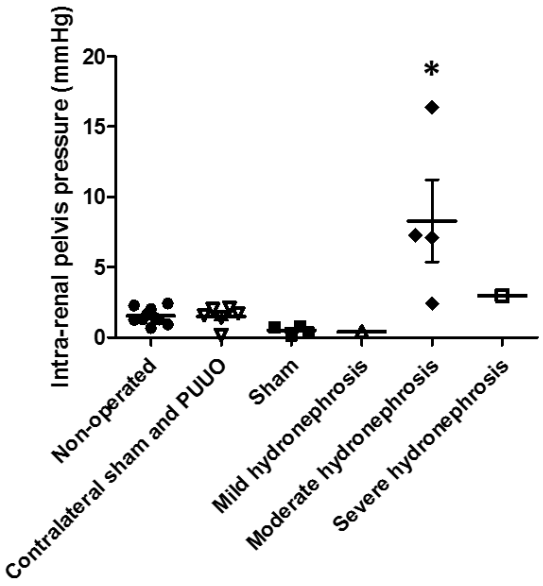

Figure 5.7 Intra-renal pelvis pressure measurements of PUUO rats compared to sham and non-operated rats

Vertical scatter plot demonstrating the intra-renal pelvis pressure measurements (mean +/- SEM) of the left PUUO kidney with mild (n=1), moderate (n=4) and severe (n=1) hydronephrosis compared to left sham (n=4) and contralateral sham /PUUO kidneys (n=6). Right and left kidney intra-renal pelvis pressure measurements from non-operated female rats (n=10) are also included. *****$p<0.05$ compared to sham, contralateral sham/PUUO and non-operated rats.

The individual intra-renal pelvis pressure measurements for each degree of hydronephrosis are presented in Table 5.3 alongside the corresponding renal pelvis APD and proximal ureter diameters. Consistent with the large variability in intra-renal pelvis pressures noted in the moderately hydronephrotic group, the scatter plot shown in Figure 5.8 using the data from Table 5.3 demonstrates that for all degrees of hydronephrosis there is no correlation between the renal pelvis APD and the intra-renal pelvis pressure ($R^2 = 0.01898$, Pearsons correlation co-efficient), however, it is acknowledged that there are few numbers for this analysis.

Rat ID	Severity of hydronephrosis	Left renal pelvis (mm)	Left proximal ureter (mm)	Parenchymal thinning	Intra-renal pelvis pressure (mmHg)
3	Mild	2.12	1.25	None	0.4
5	Moderate	3.7	1.83	None	16.38
6	Moderate	3.98	1.71	None	2.42
7	Moderate	3.3	1.43	Mild	7.12
8	Moderate	3	2.22	None	7.27
12	Severe	4.73	3.01	Substantial	2.97

Table 5.3 Renal pelvis APD and intra-renal pelvis pressure in PUUO rats

The left renal pelvis and proximal ureter dimensions are presented alongside the intra-renal pelvis pressure measurements for PUUO rats with mild, moderate and severe hydronephrosis.

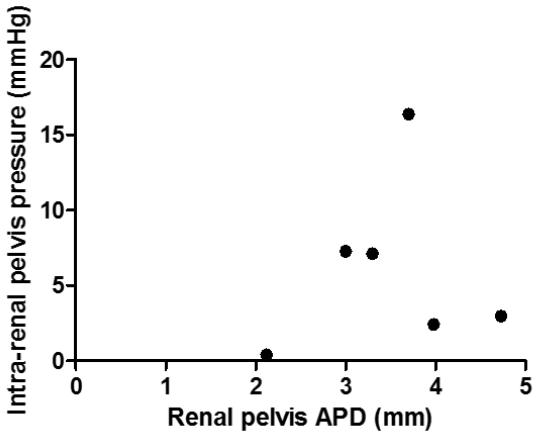

Figure 5.8 Scatter plot demonstrating renal pelvis APD and intra-renal pelvis pressure in PUUO rats

Scatter plot of renal pelvis APD versus intra-renal pelvis pressure for PUUO rats with mild, moderate and severe hydronephrosis. No correlation was noted between renal pelvis APD and intra-renal pelvis pressure $R^2 = 0.01898$.

5.3.5 Reduced numbers of glomeruli and increased renal fibrosis are noted in severe hydronephrosis

Severely hydronephrotic kidneys in PUUO rats at 35 days of age demonstrated a reduction in the number of glomeruli to 39% of sham kidneys. Mild and moderately hydronephrotic kidneys, as well as kidneys contralateral to PUUO, did not show any abnormality in glomerular number (Figure 5.9).

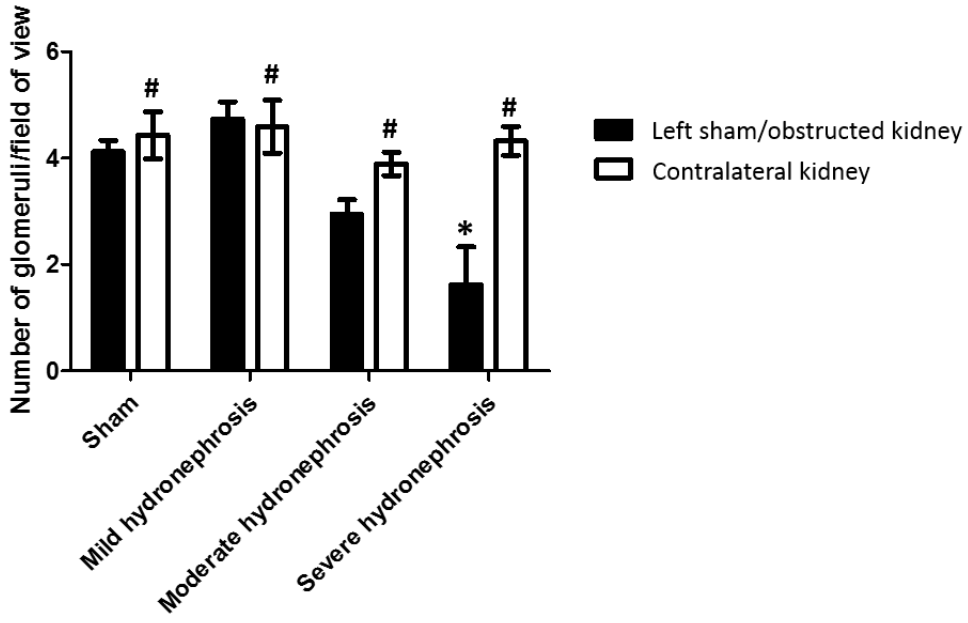

Figure 5.9 Mean number of glomeruli per field of view for PUUO and sham kidney sections

Bar graph demonstrating mean number of glomeruli +/- SEM at 35 days of age for all rats who underwent PUUO versus sham procedure. Sham n=6, mild hydronephrosis n=3, moderate hydronephrosis n=5, severe hydronephrosis n=4. *$p<0.05$ compared to left sham and left mild hydronephrosis, $^{\#}p<0.05$ compared to left severe hydronephrosis

Figure 5.10 shows representative images following Masson's trichrome staining of the renal cortex, outer medulla and inner medulla of sham and PUUO kidneys at 35 days of age. Severely hydronephrotic PUUO kidneys demonstrated a significant increase in interstitial collagen deposition compared to sham and contralateral kidneys. There was no evidence of increased fibrosis affecting the mild or moderately hydronephrotic PUUO kidneys (Figure 5.11).

Additionally, severely hydronephrotic PUUO kidneys show other parenchymal architectural abnormalities compared to mildly and moderately hydronephrotic kidneys including tubular

dilatation and abnormal glomeruli with ill-defined Bowmans capsules and shrunken capillary loops (Figure 5.12).

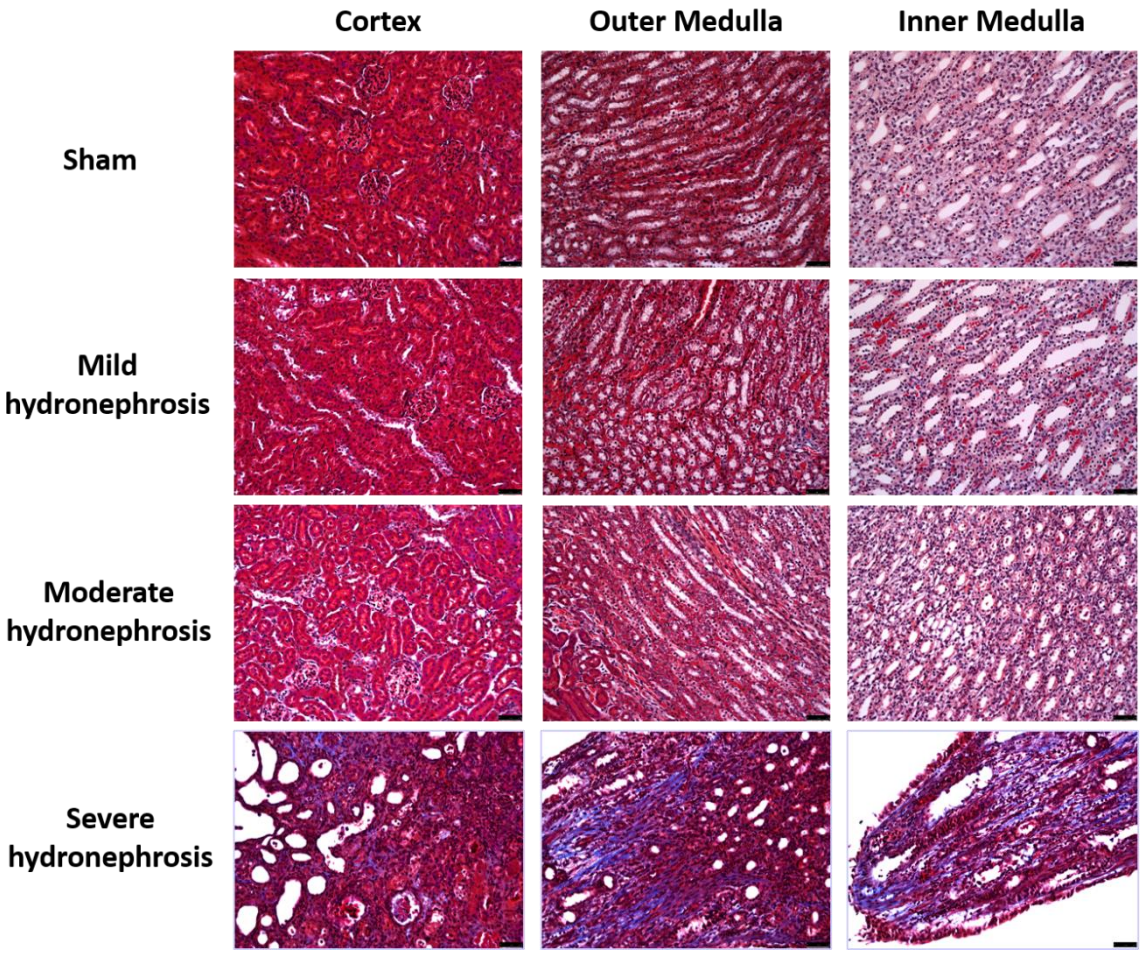

Figure 5.10 Masson's Trichrome of PUUO versus sham rat kidneys

Representative images of left kidney sections from PUUO rats with mild, moderate and severe hydronephrosis alongside left kidney sections from sham rats. Images from the renal cortex, outer and inner medulla are presented. Masson's trichrome renders the cytoplasm red and areas of collagen/fibrosis blue. Nuclei are stained black with Wiegerts haematoxylin. Scale bar = 50 μm.

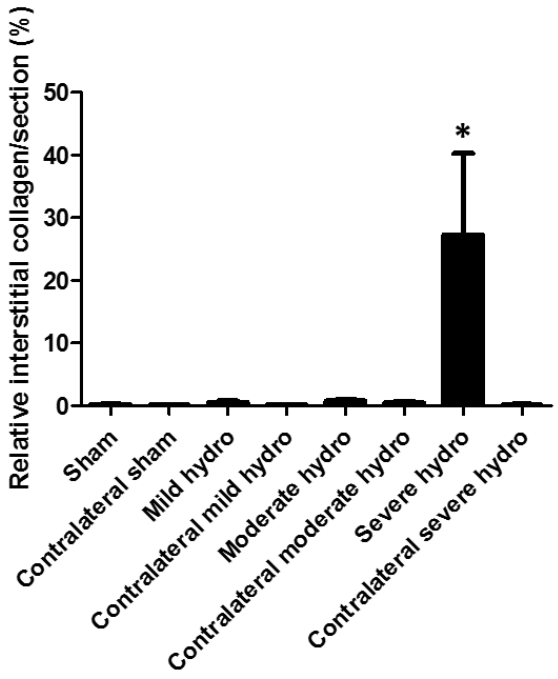

Figure 5.11 Relative interstitial fibrosis affecting PUUO compared to sham rats

Bar graph presenting mean deposition of interstitial collagen +/- SEM at age 35 days for all rats who underwent PUUO versus sham procedure. Left PUUO n=12, left sham procedure n=6. *$p<0.05$ compared to all other groups. Hydro – hydronephrosis.

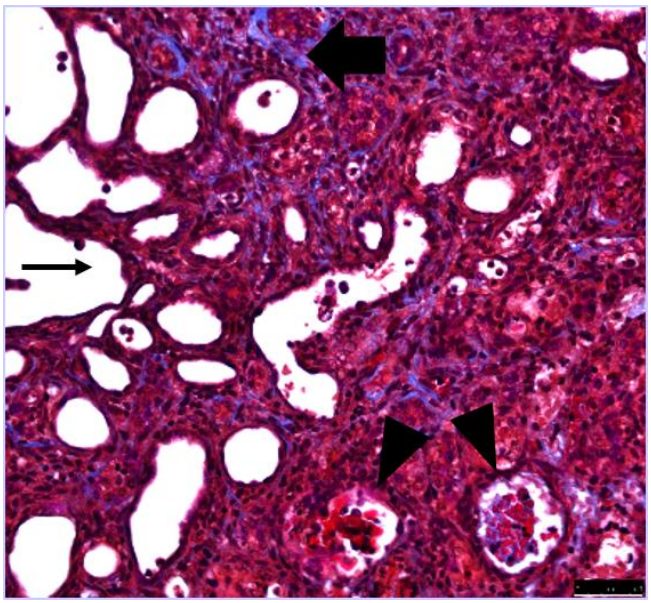

Figure 5.12 Renal histological abnormalities noted in severe hydronephrosis

An image of rat renal cortex in the presence of severe hydronephrosis following PUUO. Masson's Trichrome staining renders the cytoplasm red, collagen/fibrosis blue and the nuclei black. The glomeruli are abnormal with an ill-defined Bowmans capsule and shrunken capillary loops (arrowheads). The tubules are abnormally dilated (thin arrow) and there is interstitial fibrosis [stained blue] (thick arrow). Scale bar = 50 μm.

5.3.6 Renal aquaporin mRNA expression is reduced in severe hydronephrosis

Endpoint RT-PCR was performed to determine which AQPs are expressed at the mRNA level by normal rat kidney. Figure 5.13 shows that whole rat kidney expresses mRNA transcripts for AQPs 1, 2, 3, 4, 5, 6, 7, 8, 9 and 11. AQPs 0 and 12 are not expressed at the mRNA level. A double band for AQP8 was initially noted (Figure 5.13B) and therefore these primers were discarded. Following redesign of the primers AQP8 mRNA expression in the rat kidney was confirmed (Figure 5.13C). It was not possible to conclude whether AQP4 was expressed at the mRNA level in the rat kidney from this endpoint PCR as on two occasions a band was noted in the AQP4 RT negative sample indicating sample contamination with genomic DNA (Figure 5.13A and B). The band in the RT negative lane was confirmed as AQP4 by sequencing (as discussed in Chapter 3, section 3.3.2.2). New primers were obtained from a paper by Nicaise *et al.* [391] and subsequent real-time PCR confirmed AQP4 is expressed at the mRNA level by rat kidney (Figure 5.14).

Initial real time RT-PCR of whole kidney from PUUO rats compared to sham demonstrated that β-actin is not regulated in this PUUO model at the mRNA level and therefore was suitable to be used as a reference gene to normalize results (Figure 5.14F). Subsequent real time RT-PCR studies were conducted to assess renal mRNA expression of AQPs 1-4 and 6 at 35 days of age by rats from the PUUO model. Across all AQP isoforms assessed there was no difference in renal mRNA expression in mild or moderate hydronephrosis compared to sham or contralateral kidneys. It was established that AQP1 and 2 mRNA expression was significantly downregulated in severely hydronephrotic kidneys compared to sham (0.7 fold and 0.8 fold reduction respectively), mild and moderate hydronephrosis, and all contralateral kidney groups (Figure 5.14A and B).

No significant difference was noted in AQP3 mRNA expression between any degree of hydronephrosis and sham kidneys (Figure 5.14C).

AQP4 mRNA expression was significantly downregulated in severe hydronephrosis compared to the contralateral intact kidneys from rats with mild and moderate hydronephrosis. However AQP4 expression in severe hydronephrosis was 0.5 fold lower, but not statistically significantly different to sham kidneys. This finding could be due to the amount of variability in the results for the severe hydronephrosis group (Figure 5.14D).

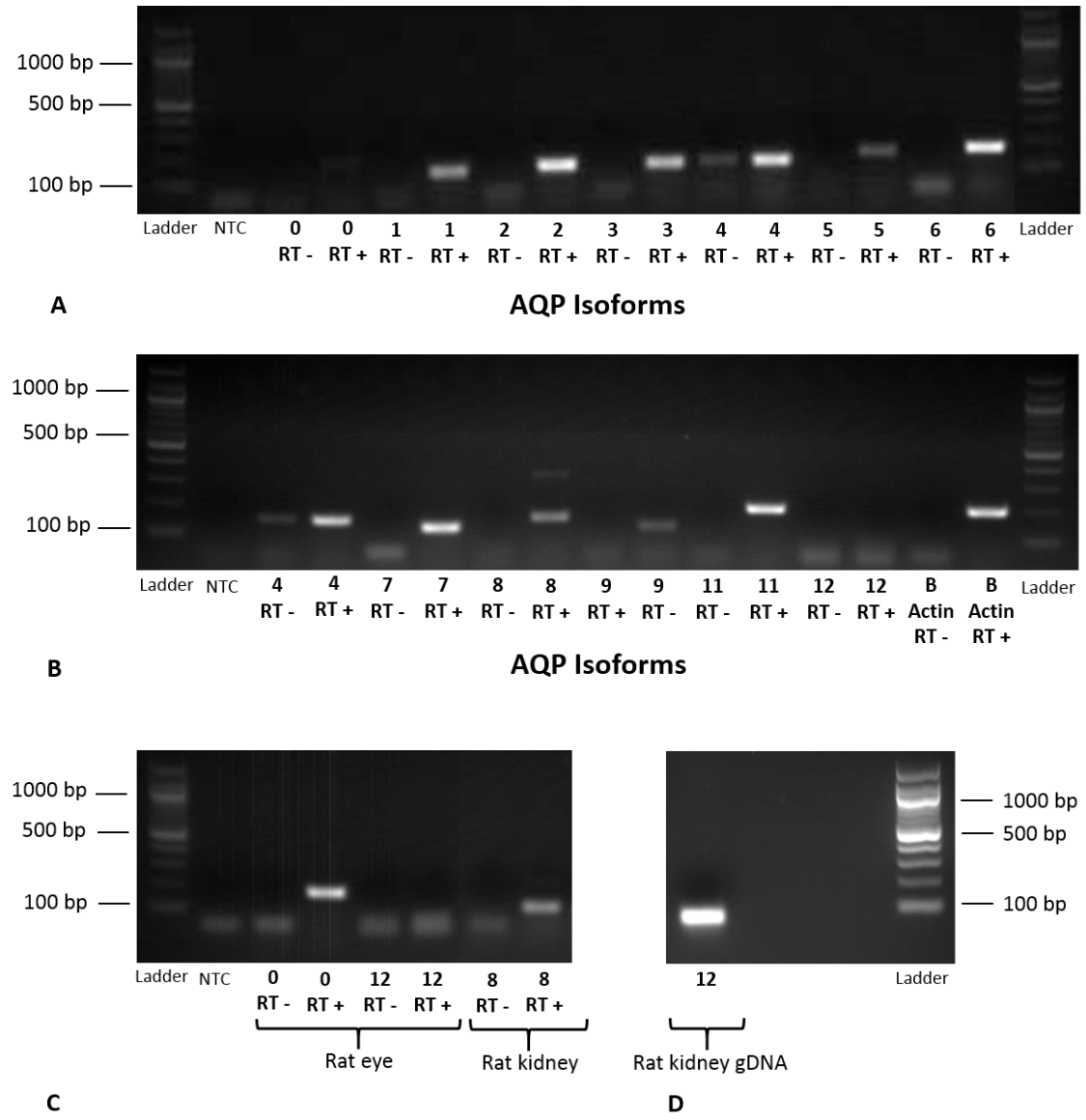

Figure 5.13 Endpoint PCR demonstrating the AQP isoforms expressed by rat whole kidney

RT-PCR was performed using mRNA extracted from whole normal rat kidney and the product run on 2% agarose gels. Bands of the appropriate size for AQP isoforms 1, 2, 3, 5, 6, 7, 9 and 11 and β-actin were noted indicating they are expressed at the mRNA level by whole rat kidney. See appendix 2 (section 10.2.1) for product sizes. A band in the AQP4 RT negative sample on 2 occasions indicated sample contamination with genomic DNA. The AQP8 primers revealed a double band and therefore were discarded (A and B). RT-PCR was performed using whole rat eye as a positive control for the AQP0 primers. RT-PCR using whole rat kidney and new AQP8 primers confirmed AQP 8 is expressed by rat kidney (C). PCR was performed using rat kidney genomic DNA as positive control for the AQP12 primers (D). NTC – no template control.

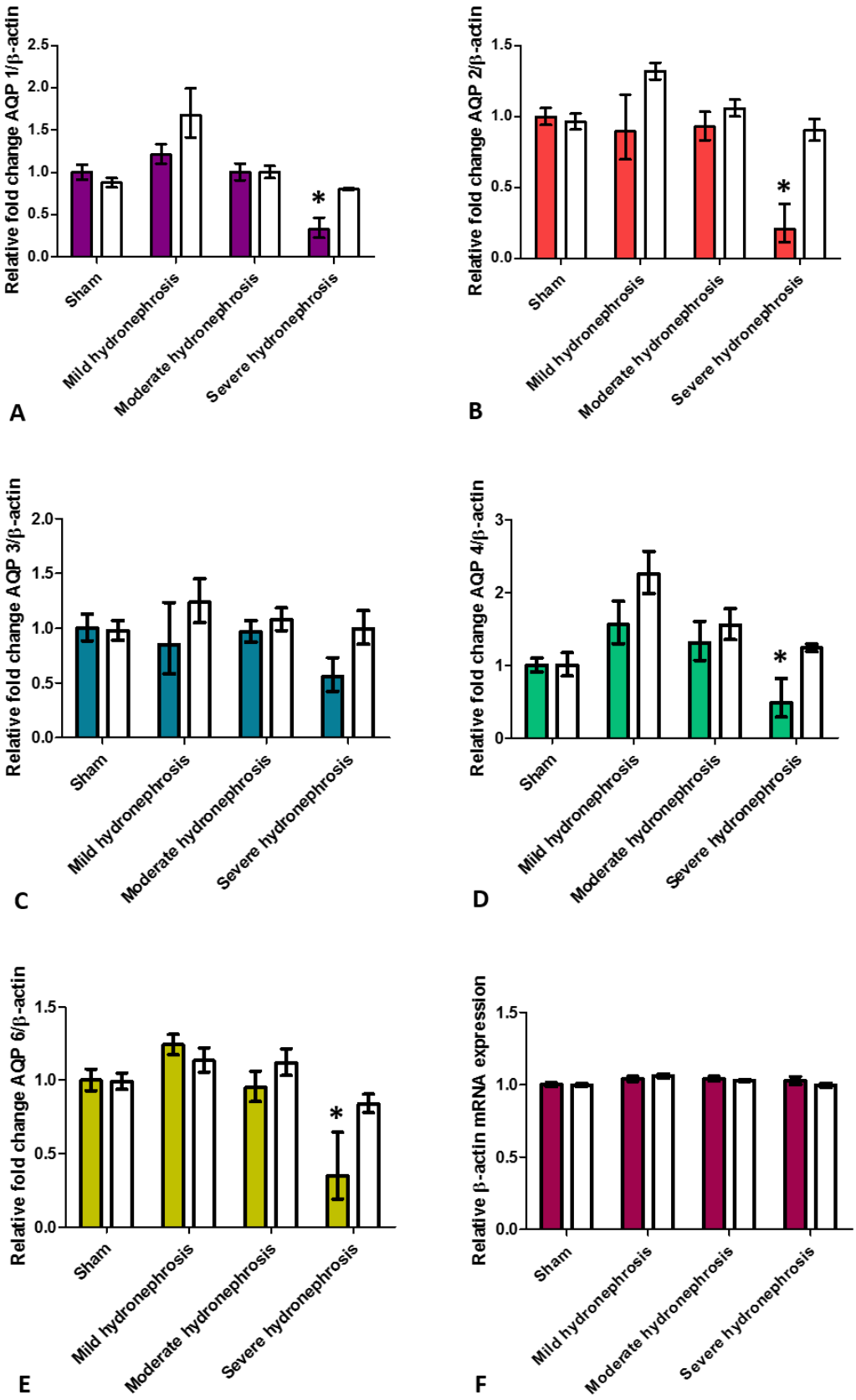

Figure 5.14 Renal AQP isoform mRNA expression by PUUO rats compared to sham rats

Relative fold change of AQP isoform expression normalized to β-actin in whole rat kidney is presented for PUUO rats compared to sham rats at 35 days of age. Coloured bars = left sham/obstructed kidney, white bars = contralateral kidney. Mean +/- SEM presented. AQP1 mRNA expression *$p<0.05$ compared to all other

groups (A). AQP2 mRNA expression *p<0.05 compared to all other groups (B). AQP3 mRNA expression demonstrated no significant differences between groups (C). AQP4 mRNA expression *p<0.05 compared to contralateral mild and contralateral moderate hydro groups (D). AQP6 mRNA expression *p<0.05 compared to all other groups except contralateral severe hydro (E). β-actin mRNA expression demonstrated no significant differences between groups (F). Sham n=6, mild hydronephrosis n=3, moderate hydronephrosis n=5, severe hydronephrosis n=4.

AQP6 mRNA expression was significantly downregulated in severe hydronephrosis compared to sham (0.6 fold reduction), mild and moderate hydronephrosis. Expression was not significantly different between the severely hydronephrotic kidney and its corresponding contralateral. However AQP6 mRNA expression was significantly reduced compared to all other contralateral kidney groups (Figure 5.14E).

In severe hydronephrosis across all AQP isoforms the intact contralateral kidney did not show any upregulation of AQP expression suggesting there was no attempt to compensate for the obstructed kidney.

5.3.7 Renal aquaporin and housekeeping gene protein expression

5.3.7.1 B-actin protein expression is regulated in PUUO rats

Initial western blotting using cy5 labelled protein lysate demonstrated that β-actin expression, when normalised to total protein loading, was significantly downregulated in the left obstructed kidney from PUUO rats (mean OD +/- SEM: 14280 +/- 1275) compared to non-operated rats (19710 +/- 1203), however expression was not significantly different to sham rats (16170 +/- 416.7) (Figure 5.15 A and C). Although a reduction in expression of GAPDH by the left obstructed kidney in PUUO (12300 +/- 1643) compared to non-operated rats (15990 +/- 52.14) was noted, this was not statistically significant. Again, there was no significant difference in expression between PUUO and sham rats (13960 +/- 72.32), which is the main comparator used in the PUUO study (Figure 5.15 B and D). GAPDH was therefore utilised in further experiments as the reference protein to normalize sample loading.

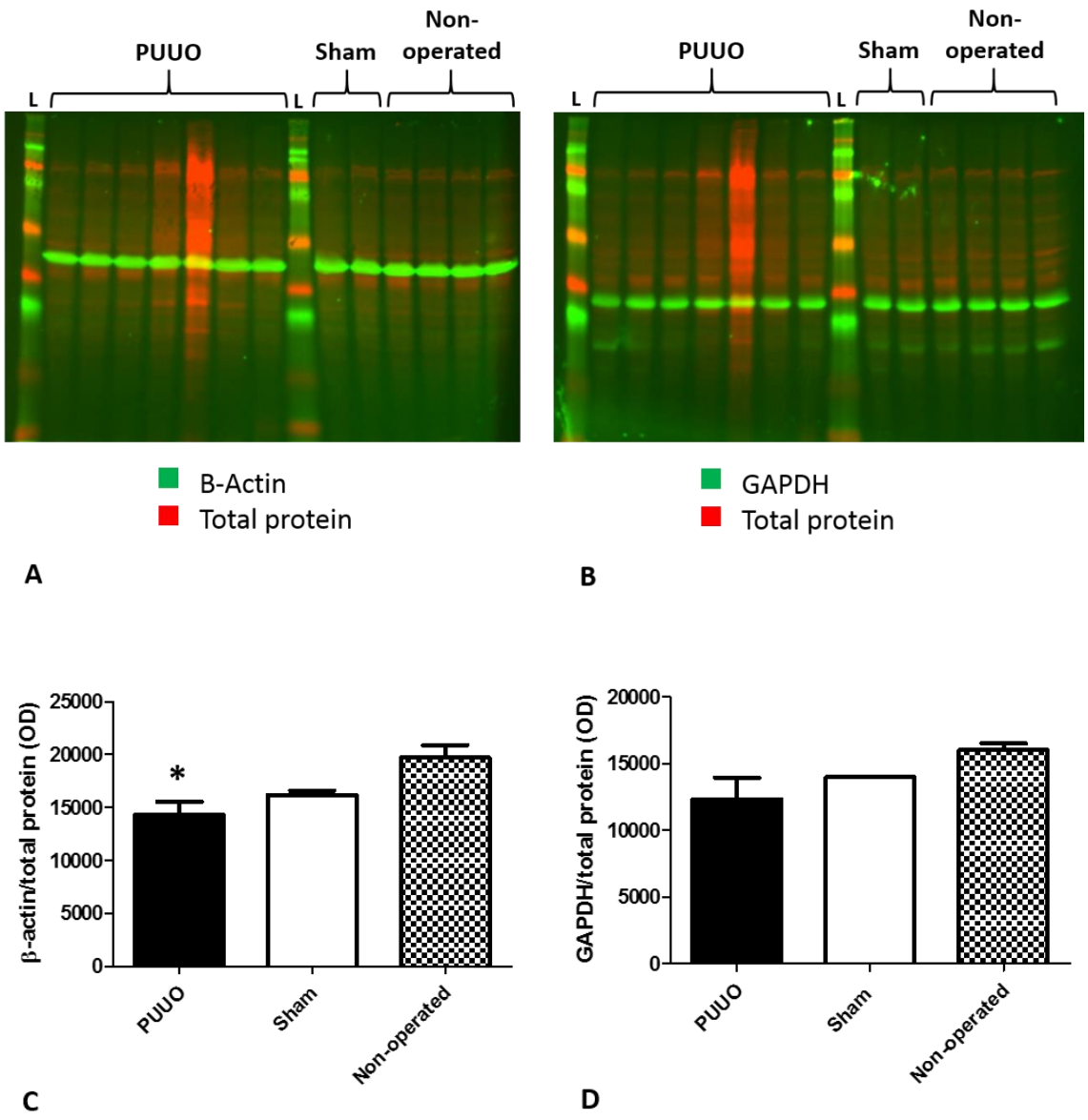

Figure 5.15 Regulation of reference proteins in PUUO

Western blots using fluorescently labelled antibodies and fluorescently labelled left total kidney protein from PUUO, sham and non-operated rats at 35 days of age. β-actin (42 kDa) and total protein (A). GAPDH (37 kDa) and total protein (B). Bar graph demonstrating β-actin (A) and GAPDH (B) expression normalised to total protein by whole rat left kidney in PUUO rats compared to sham and non-operated rats at 35 days of age. *****$p<0.05$ compared to non-operated rats. PUUO n=7 (2 x mild, 2 x moderate, 3 x severe), sham n=2 and non-operated n=4. L = ladder.

5.3.7.2 AQP1 protein is expressed by the cortex and medulla of rat kidney

Immunohistochemistry of whole rat kidney confirmed that AQP1 protein was expressed both by the renal cortex and medulla. Within the renal cortex AQP1 was expressed by the luminal and basolateral membranes of the proximal tubules (Figure 5.16A) while in the medulla it was expressed by the loop of Henle and the vasa recta (Figure 5.16B).

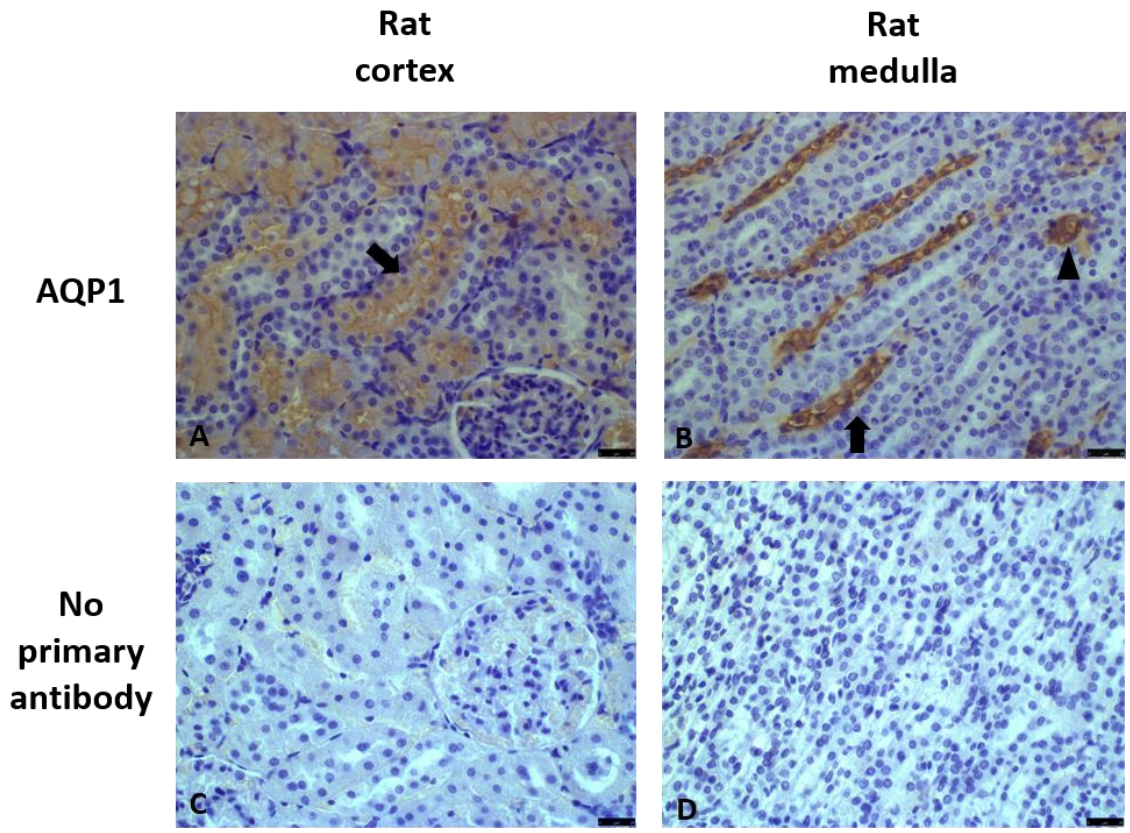

Figure 5.16 Immunohistochemistry demonstrating rat kidney AQP1 expression

AQP1 expression is demonstrated in the apical and basolateral membranes of the proximal tubules (arrow) within the kidney cortex (A), while AQP1 expression in the loop of Henle (arrow) and vasa recta (arrowhead) but not within collecting ducts is seen in the kidney medulla (B). Negative controls (no primary antibody) demonstrated an absence of staining (C, D). Scale bar = 25 μm.

5.3.7.3 Renal AQP1 protein expression is unchanged in obstructive hydronephrosis compared to sham

Western blotting and subsequent densitometry was utilised to semi-quantitatively analyse changes in AQP1 expression resulting from neonatal rat PUUO. Kidney protein lysate from litters 2-3 and 4-6 was extracted and assessed by western blot in two separate batches which unfortunately seemed to generate disparate results. This may have been due to the protein extraction methods employed which will be addressed in the discussion. Consequently, for AQP1 and all other AQP isoforms, the results for each batch processed are presented individually and then combined.

Analysis of left (obstructed) and right (contralateral) whole kidney protein lysate from PUUO and sham rats from litters 2 and 3 at 35 days of age was undertaken. Inspection of the western blots revealed very clearly that both non-glycosylated and glycosylated AQP1 were downregulated in severe hydronephrosis compared to both the contralateral kidney and

sham kidneys. This observation was borne out by subsequent semi-quantitative analysis using densitometry whereby expression of non-glycosylated and glycosylated AQP1 were statistically significantly reduced in severe hydronephrosis (non-glycosylated mean OD +/- SEM; 8132 +/- 1200, glycosylated; 9119 +/- 1971) compared to sham (non-glycosylated; 19490 +/- 773.1, glycosylated; 30020 +/- 1537). Interestingly this analysis also showed glycosylated AQP1 expression was significantly upregulated in mild hydronephrosis (42730 +/- 1206) compared to sham kidneys. Due to the small numbers involved moderate hydronephrosis could not be assessed statistically although inspection of the blot suggested a tendency toward downregulation compared to sham (Figure 5.17).

Assessment of the western blots of left (obstructed) and right (contralateral) kidney protein lysate at 35 days of age from litters 4-6 revealed a very different picture compared to litters 2 and 3. Non-glycosylated and particularly glycosylated AQP1 appeared downregulated in the contralateral kidney compared to the obstructed kidney across all degrees of hydronephrosis. Obstructed kidneys displaying moderate and severe hydronephrosis did not show any significant difference in non-glycosylated and glycosylated AQP1 expression compared to sham kidneys while in mild hydronephrosis, akin to litters 2 and 3, protein expression showed a shift towards upregulation (Figure 5.18 A). Similar trends were noted on densitometry of these blots however due to the small numbers involved statistical analysis was not possible for the majority of the groups (n=1 for both mild and severe hydronephrosis). Statistical analysis was performed to compare the obstructed and contralateral kidneys of the sham and moderate hydronephrosis groups and did not reveal a significant difference between these (Figure 5.18 B and C).

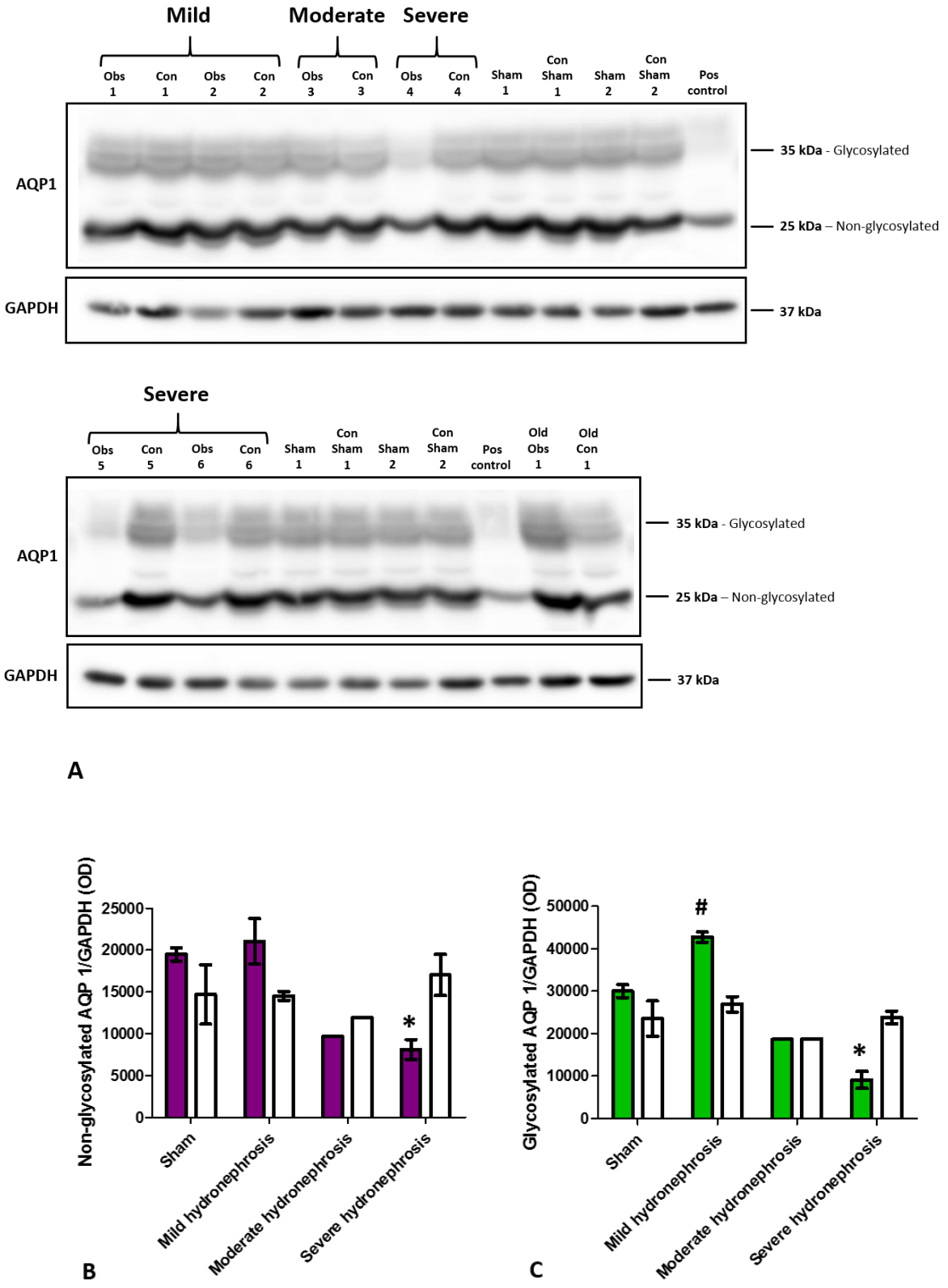

Figure 5.17 AQP1 protein expression by rat kidney in PUUO rats compared to sham rats from litters 2 and 3

Western blots demonstrating non-glycosylated and glycosylated AQP1 expression by whole kidney from PUUO and sham rats at 35 days of age from litter 2 and 3. Mild, moderate and severe indicates degree of hydronephrosis noted in PUUO rats. Obs – left/obstructed kidney, Con – contralateral kidney. GAPDH –

loading control. Old – whole kidneys, obstructed and contralateral, from PUUO rat at 86 days of age (A). Bar graphs demonstrating non-glycosylated and glycosylated AQP1 protein expression (optical density expressed as mean +/- SEM) normalised to GAPDH for PUUO compared to sham rats from litters 2 and 3. Coloured bars – left sham/obstructed kidney, white bars – contralateral kidney *$p<0.05$ compared to sham and mild hydronephrosis (B) *$p<0.05$ compared to sham, mild hydronephrosis, contralateral sham and contralateral severe hydronephrosis. #$p<0.05$ compared to sham, contralateral sham, contralateral mild hydronephrosis and contralateral severe hydronephrosis (C). Sham n=2, mild hydronephrosis n= 2, moderate hydronephrosis n=1, severe hydronephrosis n=3, old PUUO rat n=1 (not included in graph/data analysis).

A further western blot was performed using selected protein lysates from litter 2-3 and 4-6 to determine whether the obstructed and contralateral samples had been inadvertently loaded incorrectly. Additionally, a fresh aliquot of one pair of obstructed and contralateral lysates from litters 4-6 was used to determine whether samples may have been mixed up at the point of the addition of sample buffer. Lysates run on this blot demonstrated the same pattern of expression as on their original blots suggesting the differing results were not due to incorrect loading or differences between the western blotting procedure among the two batches (Figure 5.19).

When all the densitometry results were combined no significant difference was noted in non-glycosylated AQP1 expression between obstructed kidneys of any degree of hydronephrosis compared to sham kidneys or contralateral kidneys (Figure 5.20 A). Glycosylated AQP1 expression was not significantly different in severe hydronephrosis (10340 +/- 1853) compared to sham kidneys (16460 +/- 4367), but was significantly downregulated compared to mild hydronephrosis (25130 +/- 7627). Glycosylated AQP1 expression in mild hydronephrosis, in turn, was significantly upregulated compared to contralateral sham kidneys (12546 +/- 3968) and contralateral moderate hydronephrosis (8505 +/-2831) but again was not significantly different to sham (Figure 5.20 B).

As a consequence of the differences noted between the results from the two batches of protein lysates, the western blotting densitometry results from litters 2-3 and litters 4-6 for the other AQP isoforms (AQPs 2-4) were analysed as separate batches initially prior to being combined.

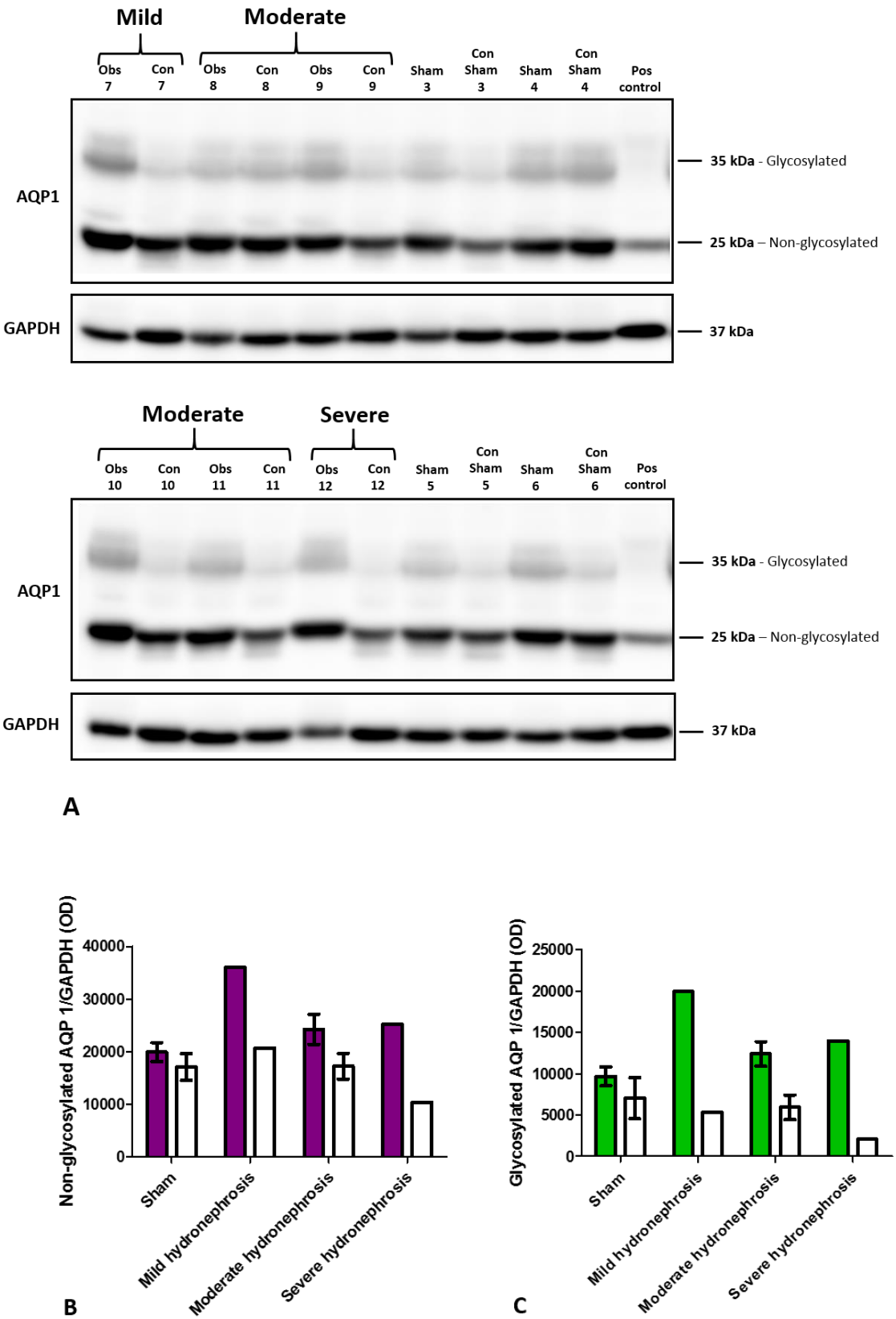

Figure 5.18 AQP1 protein expression by rat kidney in PUUO rats compared to sham rats from litters 4-6

Western blot demonstrating non-glycosylated and glycosylated AQP1 expression by whole kidney from PUUO and sham rats at 35 days of age from litters 4-6. Mild, moderate and severe indicates degree of hydronephrosis noted in PUUO rats. Obs – left/obstructed kidney, Con – contralateral kidney. GAPDH – loading control (A).

Bar graphs demonstrating non-glycosylated and glycosylated AQP1 protein expression (optical density expressed as mean +/- SEM) normalised to GAPDH for PUUO compared to sham rats from litters 4-6. Coloured bars – left sham/obstructed kidney, white bars – contralateral kidney. No significant differences were noted between groups (C and D). Sham n=4, Mild hydronephrosis n=1, moderate hydronephrosis n=4, severe hydronephrosis n=1.

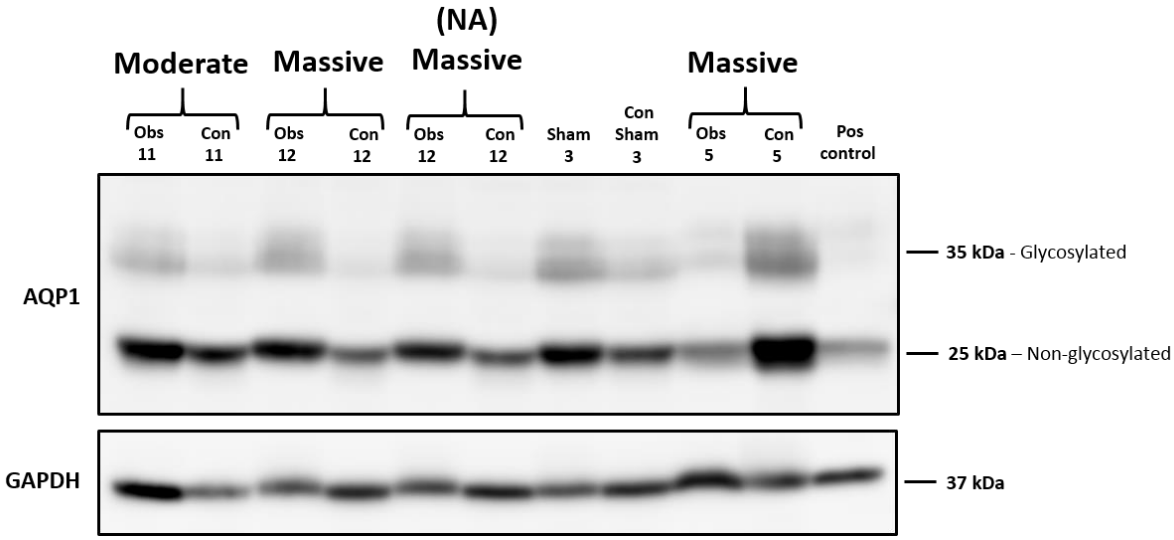

Figure 5.19 Repeat western blot of selected rat kidney lysates for AQP1 expression

Repeat western blot detecting APQ1 using selected whole kidney protein lysates from PUUO and sham rats from litters 2-6. Mild, moderate and severe indicates degree of hydronephrosis noted in PUUO rats. Obs – left/obstructed kidney, Con – contralateral kidney. GAPDH – loading control. NA – new aliquot. Rats 3, 11 and 12 were from litters 4-6 and rat 5 from litters 2-3.

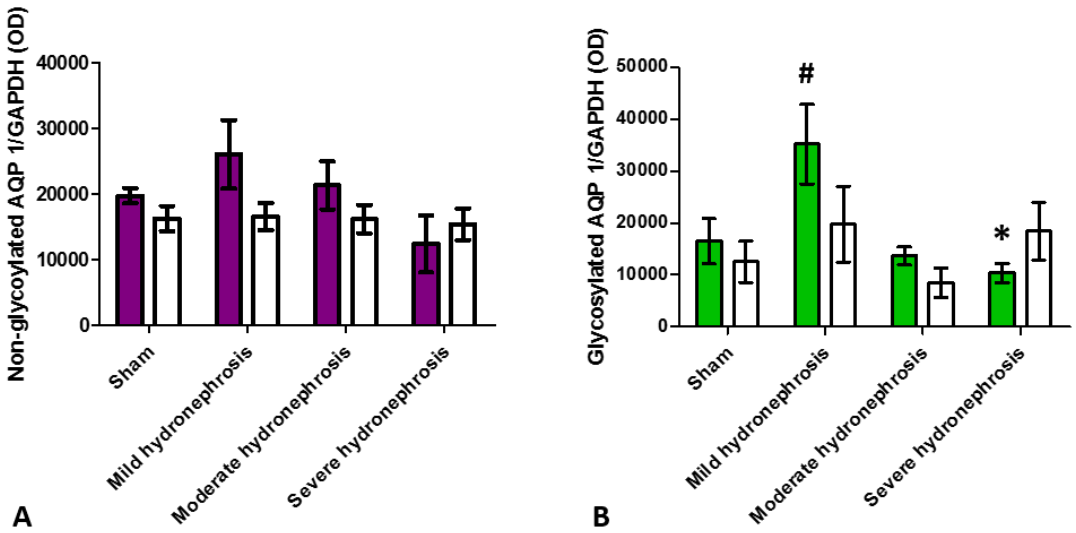

Figure 5.20 Glycosylated and non-glycosylated AQP1 expression in PUUO rats compared to sham

Bar graphs demonstrating non-glycosylated and glycosylated AQP1 protein expression (optical density expressed as mean +/- SEM) normalised to GAPDH for PUUO compared to sham rats from litters 2-6 combined at 35 days of age. Coloured bars – left sham/obstructed kidney, white bars – contralateral kidney. No significant differences were noted between groups (A). *****$p<0.05$ compared to mild hydronephrosis, $^{\#}p<0.05$ compared to contralateral sham and contralateral moderate hydronephrosis (B). Sham n=6, mild hydronephrosis n=3, moderate hydronephrosis n=5, severe hydronephrosis n=4 (A and B).

5.3.7.4 AQP2 protein is expressed by the cortex and medulla of rat kidney

Immunohistochemistry of whole rat kidney demonstrated that AQP2 is expressed at the protein level by the luminal membrane of the cortical and medullary collecting ducts, with a predominantly medullary location (Figure 5.21).

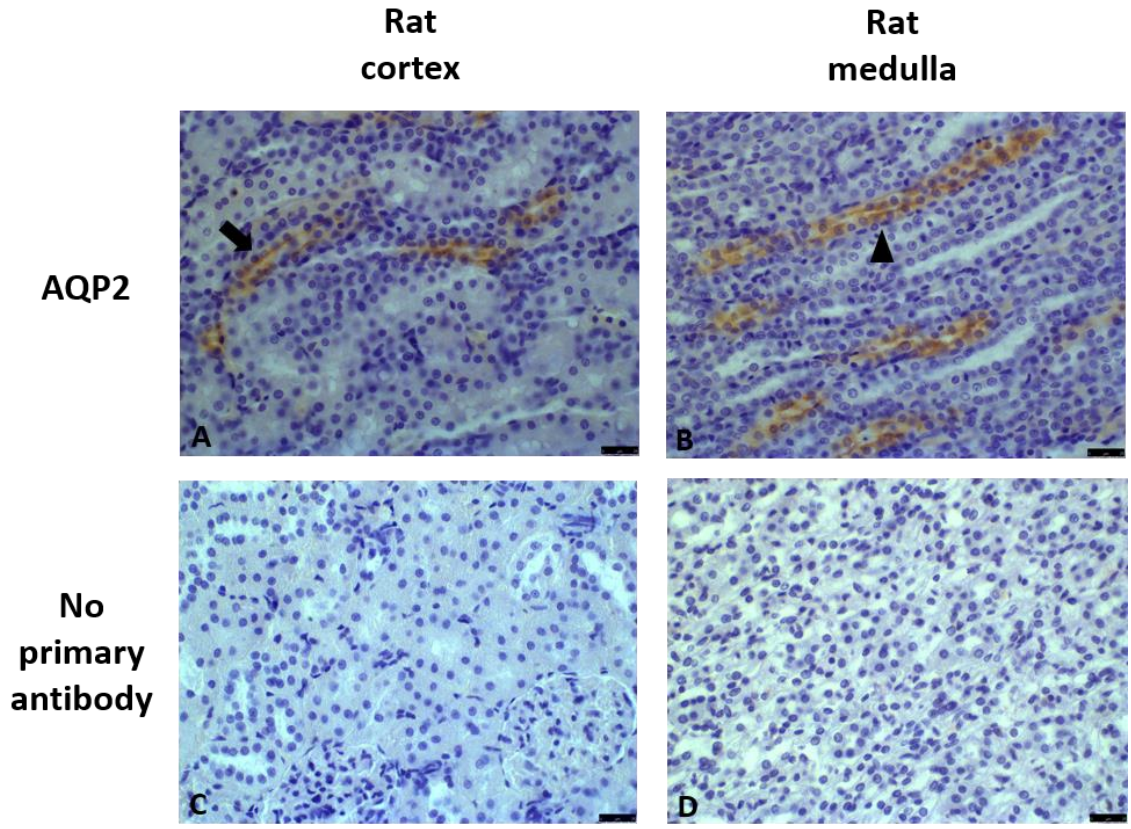

Figure 5.21 Immunohistochemistry demonstrating AQP2 expression by rat kidney

AQP2 expression is demonstrated in the luminal membranes of the cortical collecting ducts (arrow) (A) and the medullary collecting ducts (arrowhead) (B). Negative controls (no primary antibody) demonstrated an absence of staining (C, D). Scale bar = 25 μm.

5.3.7.5 Renal AQP2 protein expression is unchanged in obstructive hydronephrosis compared to sham

The effect of neonatal rat PUUO on renal AQP2 expression was assessed semi-quantitatively following western blotting for the protein. Visual review of western blots using left (obstructed) and right (contralateral) whole kidney protein lysate from PUUO and sham rats from litters 2 and 3 at 35 days of age suggested a possible downregulation of AQP2 expression in moderately hydronephrotic kidneys and an upregulation of AQP2 expression in severely hydronephrotic kidneys (Figure 5.22 A). On densitometry a marked reduction in

expression was noted in moderate hydronephrosis (OD 3667) compared to sham kidneys (Mean OD +/- SEM; 7370 +/- 110) as well as mild (8093 +/- 411.6) and severe (8231 +/- 576.3) hydronephrosis. This difference was not analysed statistically, however, due to there being only a single animal in the moderate hydronephrosis group. No statistically significant differences in AQP2 expression were demonstrated between any of the other groups (Figure 5.22 B).

Inspection of western blots using whole kidney protein lysate from PUUO and sham rats from litters 4-6 at 35 days of age revealed fairly consistent expression across the samples (Figure 5.23 A). These observations corresponded with the densitometry results which demonstrated no significant differences between the obstructed and contralateral kidneys of the sham and moderate hydronephrosis groups. Again, the mild and severe hydronephrosis groups were not included in the statistical analysis due to small number size (Figure 5.23 B).

Amalgamation of the densitometry results from litters 2-3 and litter 4-6 demonstrated no significant differences in AQP2 expression across the degrees of hydronephrosis compared to sham kidneys. A significant increase in APQ2 expression was noted in severe hydronephrosis (mean OD +/- SEM; 8068 +/- 439.6) compared to moderate hydronephrosis (4697 +/- 312), contralateral sham kidneys (5153 +/- 439.4), contralateral mild hydronephrosis (4283 +/- 572.9) and contralateral moderate hydronephrosis (4680 +/- 465.2) (Figure 5.24).

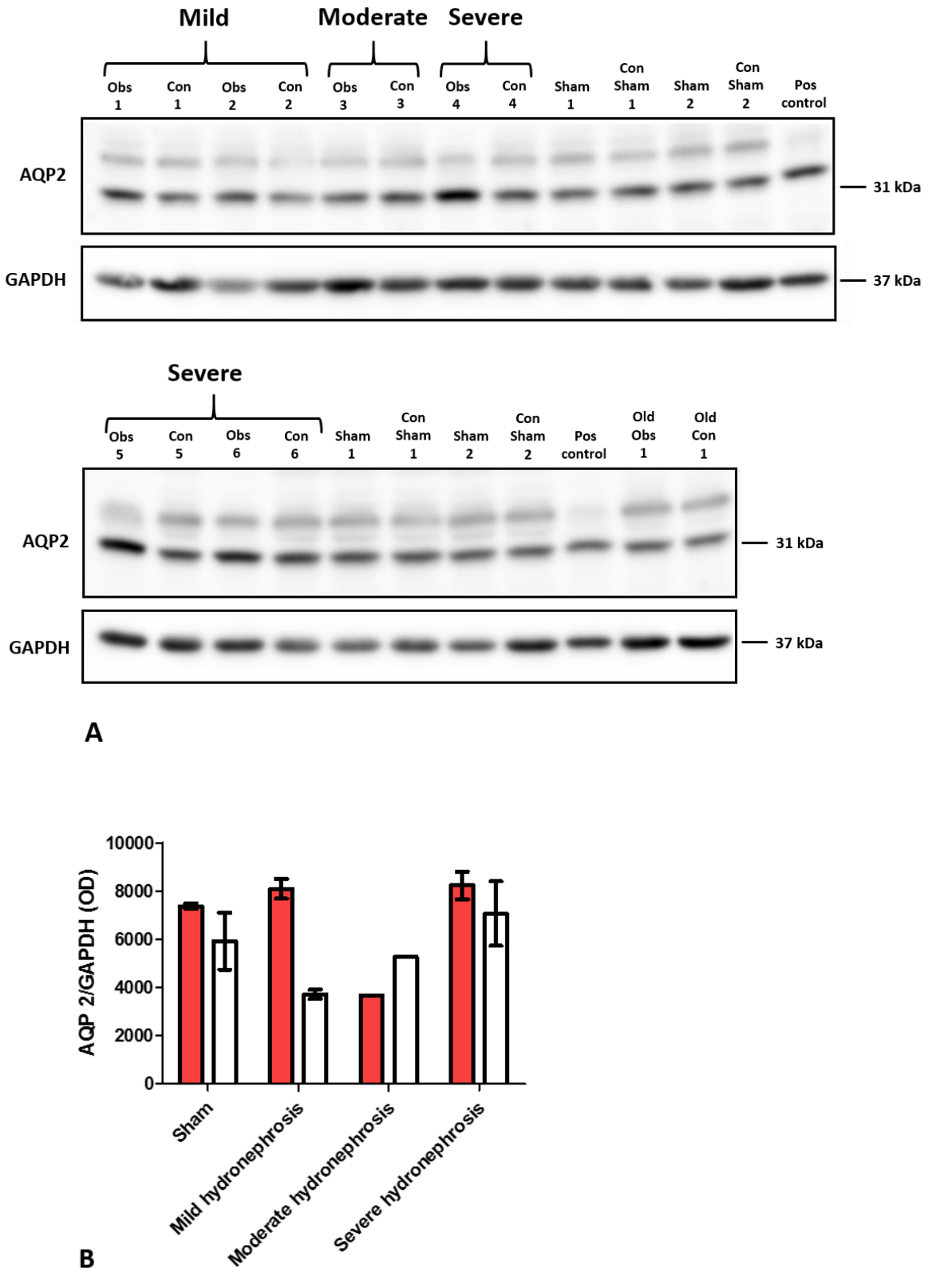

Figure 5.22 AQP2 protein expression by rat kidney in PUUO rats compared to sham rats from litters 2 and 3

Western blots demonstrating AQP2 expression by whole kidney from PUUO and sham rats at 35 days of age from litters 2 and 3. Mild, moderate and severe indicates degree of hydronephrosis noted in PUUO rats. Obs – left/obstructed kidney, Con – contralateral kidney. GAPDH – loading control. Old – whole kidneys, obstructed and contralateral, from PUUO rat at 86 days of age (A). Bar graph demonstrating AQP2 protein expression (optical density expressed as mean +/- SEM) normalised to GAPDH for PUUO compared to sham rats from

litters 2 and 3. Coloured bars – left sham/obstructed kidney, white bars – contralateral kidney. No significant differences were noted between groups (B). Sham n=2, mild hydronephrosis n= 2, moderate hydronephrosis n=1, severe hydronephrosis n=3, old PUUO rat n=1 (not included in graph/data analysis)

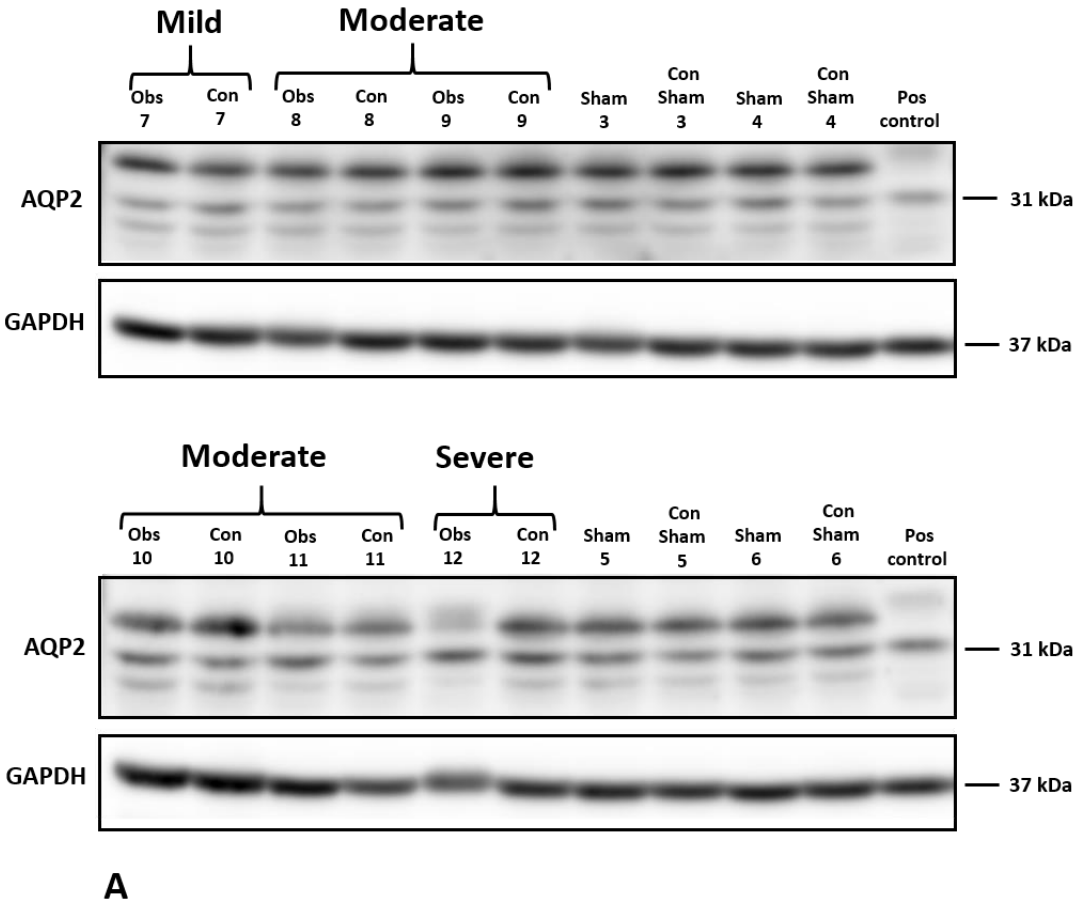

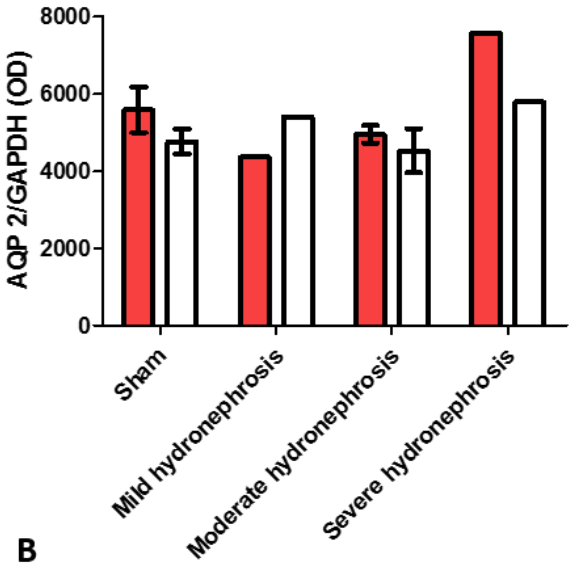

Figure 5.23 AQP2 protein expression by rat kidney in PUUO rats compared to sham rats litters 4-6

Western blot demonstrating AQP2 expression by whole kidney from PUUO and sham rats at 35 days of age from litters 4-6. Mild, moderate and severe indicates degree of hydronephrosis noted in PUUO rats. Obs – left/obstructed kidney, Con – contralateral kidney. GAPDH – loading control (A). Bar graph demonstrating AQP2 protein expression (optical density expressed as mean +/- SEM) normalised to GAPDH for PUUO compared to sham rats from litters 4-6. Coloured bars – left sham/obstructed kidney, white bars – contralateral kidney. No significant differences were noted between groups (B). Sham n=4, Mild hydronephrosis n=1, moderate hydronephrosis n=4, severe hydronephrosis n=1.

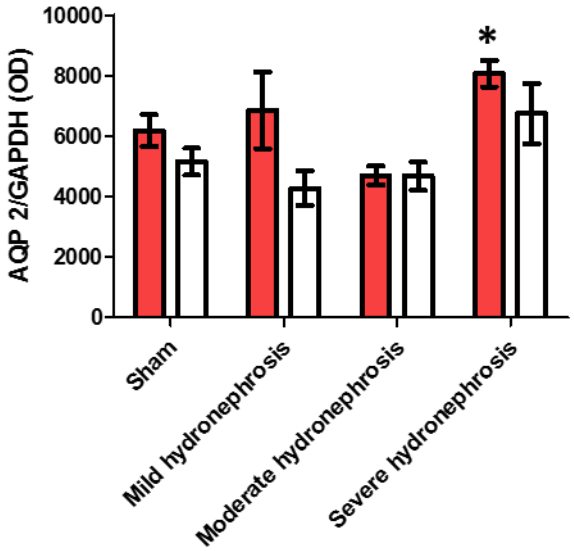

Figure 5.24 AQP2 expression in PUUO rats compared to sham rats

Bar graph demonstrating AQP2 protein expression (optical density expressed as mean +/- SEM) normalised to GAPDH for PUUO compared to sham rats from litters 2-6 combined at 35 days of age. Coloured bars – left sham/obstructed kidney, white bars – contralateral kidney. *$p<0.05$ compared to moderate hydronephrosis, contralateral sham, contralateral mild and contralateral moderate hydronephrosis. Sham n=6, mild hydronephrosis n=3, moderate hydronephrosis n=5, severe hydronephrosis n=4.

5.3.7.6 AQP3 protein is expressed by the cortex and medulla of rat kidney

Immunohistochemistry demonstrated that AQP3 is expressed by the basolateral membranes of the cortical and medullary collecting ducts of whole rat kidney (Figure 5.25).

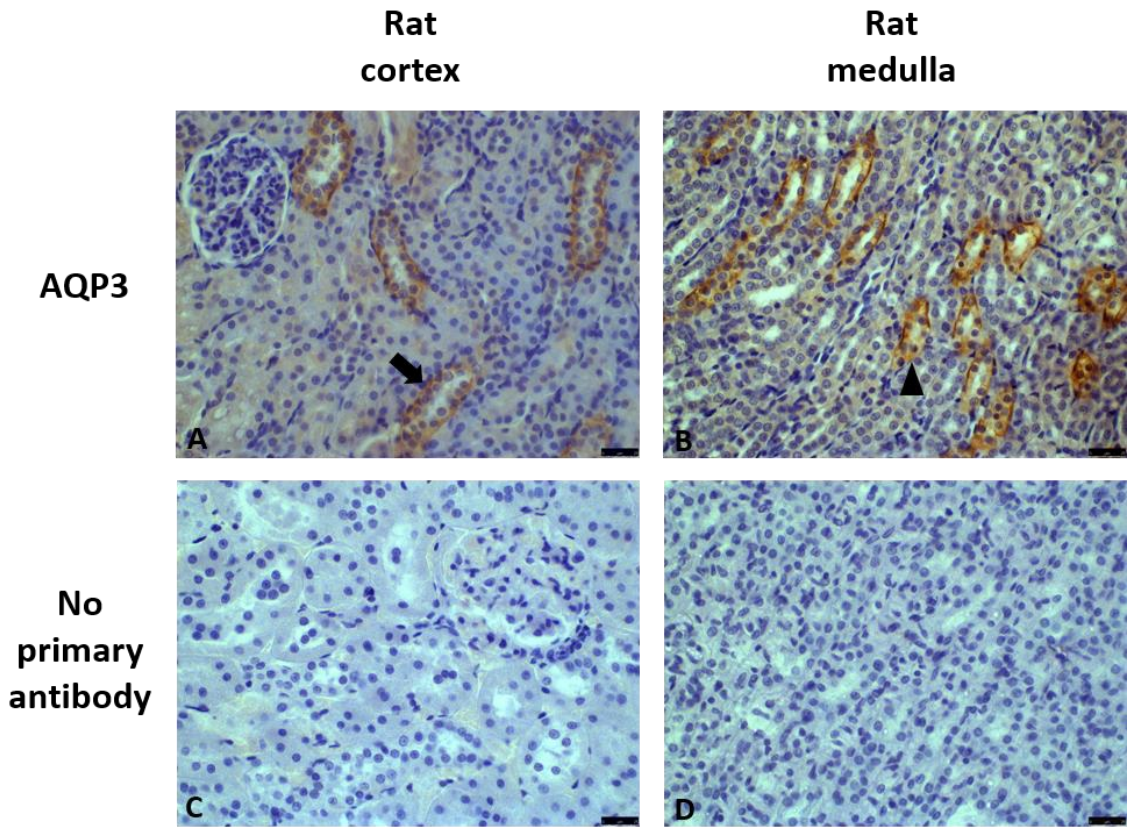

Figure 5.25 Immunohistochemistry demonstrating AQP3 expression by rat kidney

AQP3 is expressed in the basolateral membranes of the cortical collecting ducts (arrow) (A) and the medullary collecting ducts (arrowhead) (B). Negative controls (no primary antibody) demonstrated an absence of staining (C, D). Scale bar = 25 μm.

5.3.7.7 Renal AQP3 protein expression is unchanged in obstructive hydronephrosis compared to sham

Densitometry of western blots for AQP3 in whole rat kidney was used to semi-quantitatively assess the effect of neonatal PUUO on AQP3 protein expression. Evaluation of western blots using left (obstructed) and right (contralateral) whole kidney protein lysate from PUUO and sham rats from litters 2 and 3 at 35 days of age revealed a significant increase in AQP3 expression in severe hydronephrosis (mean OD +/- SEM; 10890 +/- 805.2) compared to sham kidneys (7280 +/- 90.78) as well as mild hydronephrosis (6045 +/- 581.3), contralateral sham (6923 +/- 286.9), and contralateral severe hydronephrosis (7771 +/- 773.3). No significant differences were noted in expression between other groups (Figure 5.26).

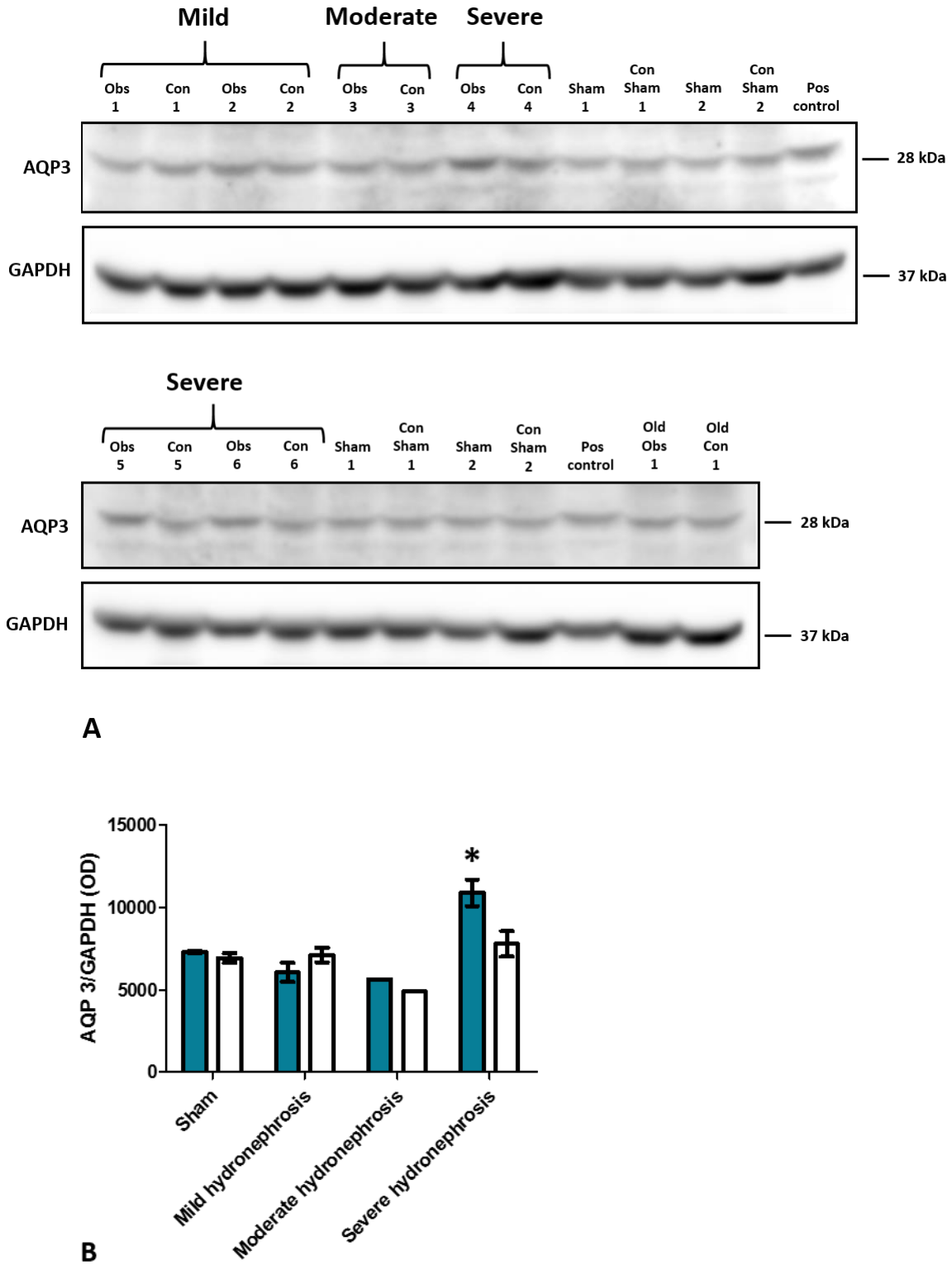

Figure 5.26 AQP3 expression by rat kidney in PUUO rats compared to sham rats litters 2 and 3

Western blots demonstrating AQP3 expression by whole kidney from PUUO and sham rats at 35 days of age from litters 2 and 3. Mild, moderate and severe indicates degree of hydronephrosis noted in PUUO rats. Obs – left/obstructed kidney, Con – contralateral kidney. GAPDH – loading control. Old – whole kidneys, obstructed and contralateral, from PUUO rat at 86 days of age (A). Bar graph demonstrating AQP3 protein expression (optical density expressed as mean +/- SEM) normalised to GAPDH for PUUO compared to sham rats from litters 2 and 3. Coloured bars – left sham/obstructed kidney, white bars – contralateral kidney. *$p<0.05$ compared to sham, contralateral sham, mild hydronephrosis and contralateral severe hydronephrosis (B). Sham

n=2, mild hydronephrosis n= 2, moderate hydronephrosis n=1, severe hydronephrosis n=3, old PUUO rat n=1 (not included in graph/data analysis).

Conversely when renal AQP3 protein expression by litter 4-6 was assessed, the visual appearance on the blots was of reduced expression in severe obstruction compared to both sham and contralateral kidney (Figure 5.27 A) which was also noted on densitometry (Figure 5.27 B). Statistical tests however could not be applied to assess this difference as there was only one animal in the severely hydronephrotic group. No statistically significant differences were noted between the moderately hydronephrotic kidneys and sham kidneys.

Combined results from litters 2-3 and litters 4-6 reveal no significant differences in renal AQP3 expression at 35 days of age between obstructed kidneys of all degrees of hydronephrosis compared to sham and contralateral kidneys (Figure 5.28).

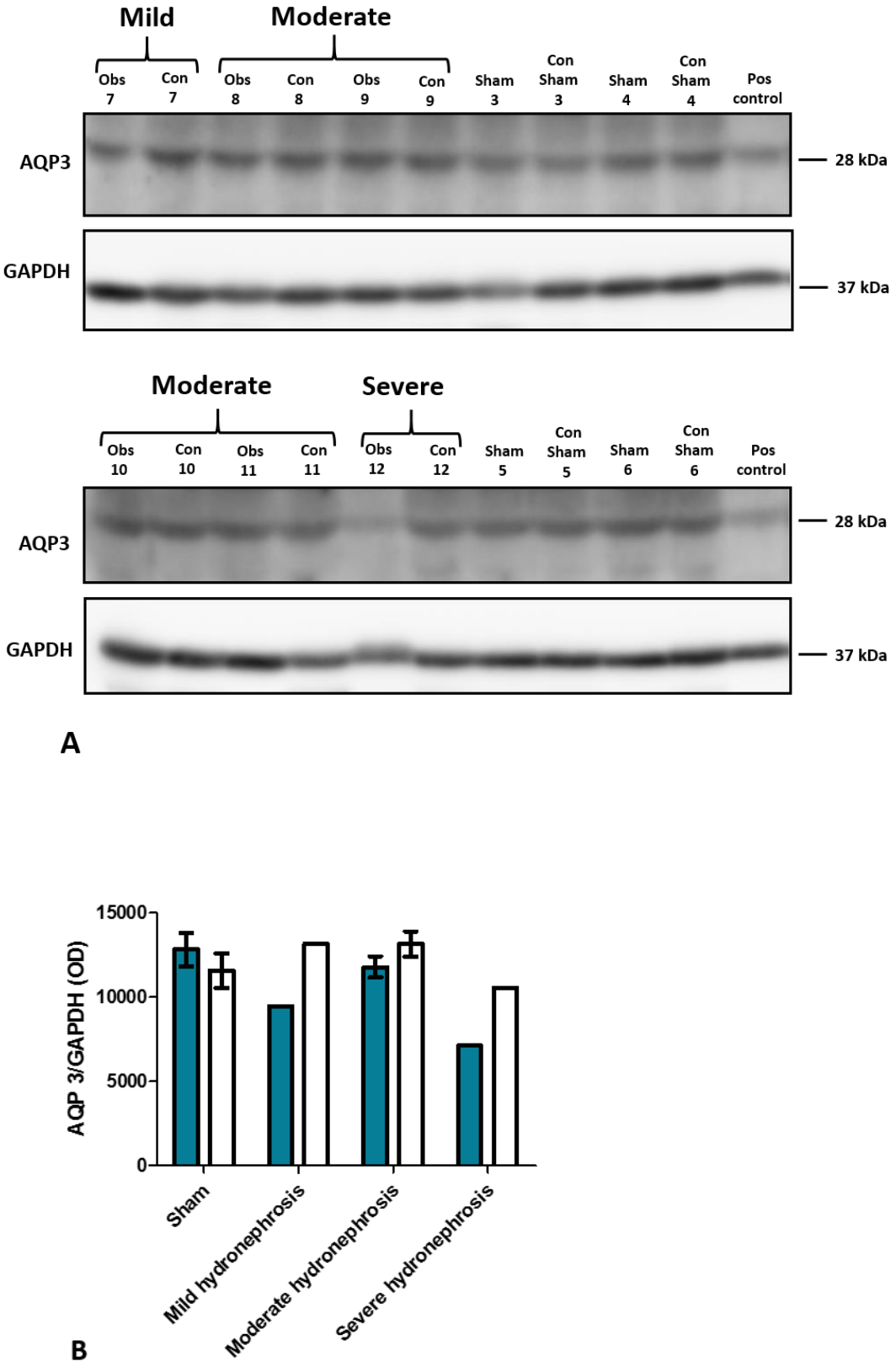

Figure 5.27 AQP3 protein expression by rat kidney in PUUO rats compared to sham rats litters 4-6

Western blot demonstrating AQP3 expression by whole kidney from PUUO and sham rats at 35 days of age from litters 4-6. Mild, moderate and severe indicates degree of hydronephrosis noted in PUUO rats. Obs – left/obstructed kidney, Con – contralateral kidney. GAPDH – loading control (A). Bar graph demonstrating AQP3 protein expression (optical density expressed as mean +/- SEM) normalised to GAPDH for PUUO

compared to sham rats from litters 4-6. Coloured bars – left sham/obstructed kidney, white bars – contralateral kidney. No significant differences were noted between groups (B). Sham n=4, Mild hydronephrosis n=1, moderate hydronephrosis n=4, severe hydronephrosis n=1.

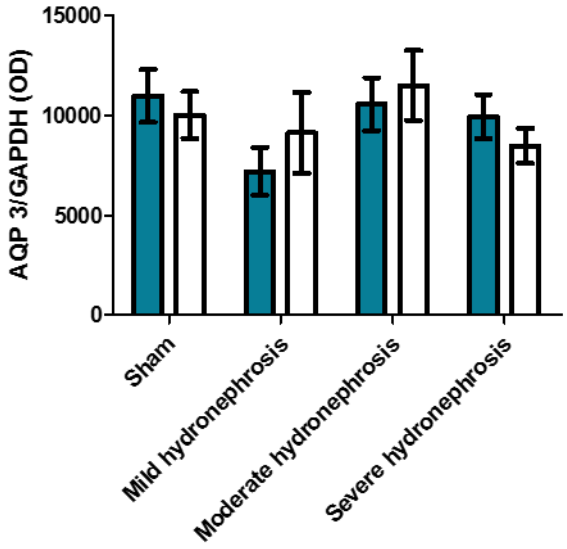

Figure 5.28 AQP3 expression in PUUO rats compared to sham rats

Bar graph demonstrating AQP3 protein expression (optical density expressed as mean +/- SEM) normalised to GAPDH for PUUO compared to sham rats from litters 2-6 combined at 35 days of age. Coloured bars – left sham/obstructed kidney, white bars – contralateral kidney. No significant differences were noted between groups. Sham n=6, mild hydronephrosis n=3, moderate hydronephrosis n=5, severe hydronephrosis n=4.

5.3.7.8 Renal AQP4 protein expression is reduced in severe hydronephrosis compared to sham

Tissue obtained from the PUUO model was not assessed by immunohistochemistry for AQP4 expression due to the lack of a suitable antibody (discussed in Chapter 3, section 3.5.4). Assessment of AQP4 protein expression and analysis of regulation in response to PUUO was therefore undertaken wholly by western blotting. Inspection of western blots using left (obstructed) and right (contralateral) whole kidney protein lysate from PUUO and sham rats from litters 2 and 3 at 35 days of age revealed substantially reduced AQP4 expression in severe hydronephrosis (Figure 5.29 A). This observation was confirmed by densitometry, which showed a significant downregulation of expression in severe hydronephrosis (mean OD +/- SEM; 4146 +/- 1696) compared to sham (15530 +/- 1167) and all other groups analysed (Figure 5.29 B).

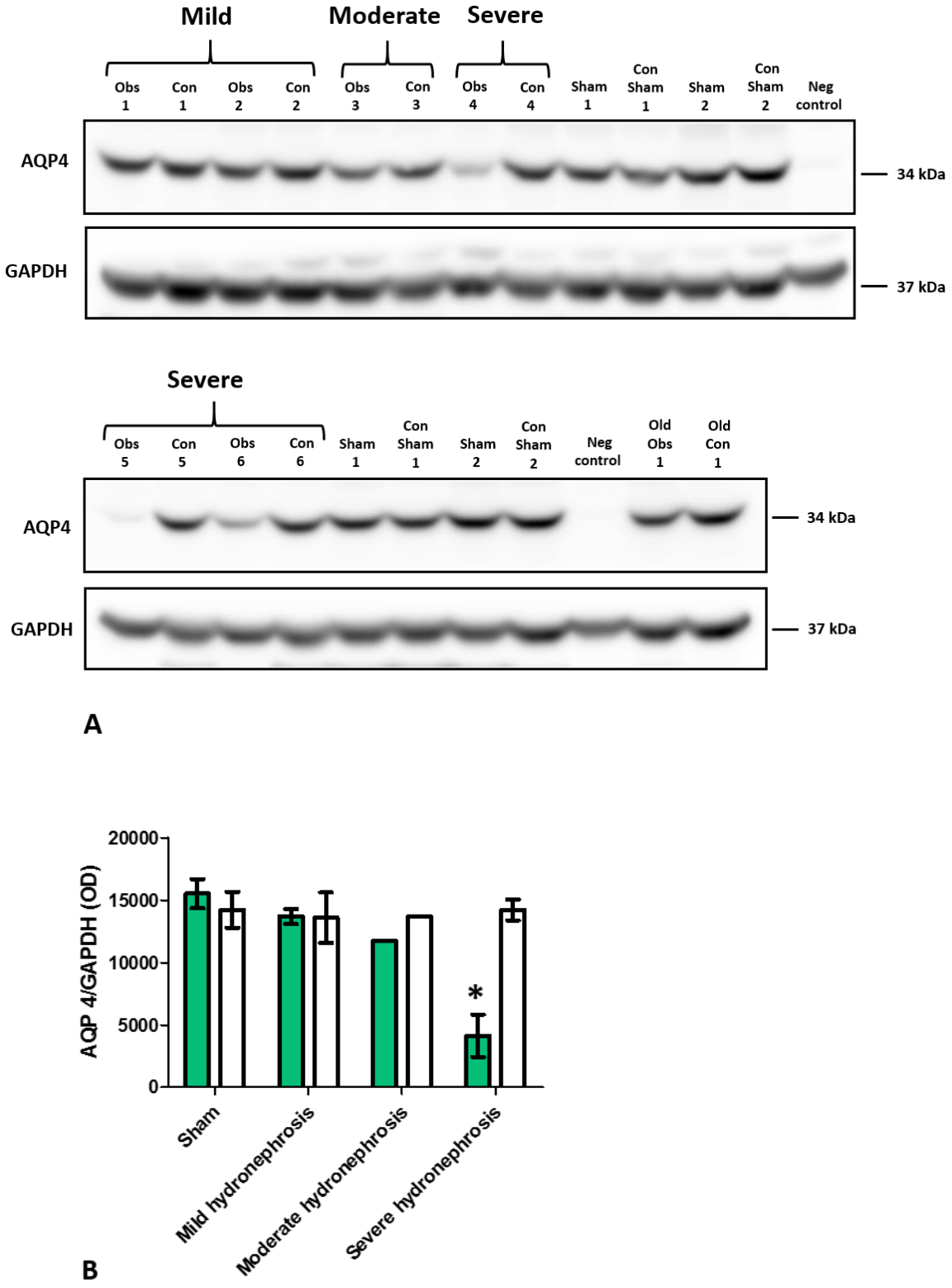

Figure 5.29 AQP4 expression by rat kidney in PUUO rats compared to sham rats litters 2 and 3

Western blots demonstrating AQP4 expression by whole kidney from PUUO and sham rats at 35 days of age from litters 2 and 3. Mild, moderate and severe indicates degree of hydronephrosis noted in PUUO rats. Obs – left/obstructed kidney, Con – contralateral kidney. GAPDH – loading control. Old – whole kidneys, obstructed and contralateral, from PUUO rat at 86 days of age (A). Bar graph demonstrating AQP4 protein expression (optical density expressed as mean +/- SEM) normalised to GAPDH for PUUO compared to sham rats from litters 2 and 3. Coloured bars – left sham/obstructed kidney, white bars – contralateral kidney. *$p<0.05$ compared to sham, contralateral sham, mild hydronephrosis, contralateral mild and contralateral severe

hydronephrosis (B). Sham n=2, mild hydronephrosis n= 2, moderate hydronephrosis n=1, severe hydronephrosis n=3, old PUUO rat n=1 (not included in graph/data analysis).

Consistent with expression patterns in litters 2-3, AQP4 expression in litters 4-6 at 35 days of age appeared reduced in the severely hydronephrotic kidney compared to sham and contralateral. Additionally, AQP4 expression in mild hydronephrosis appeared reduced although the contralateral kidney was affected to the same extent suggesting this may be due to animal related factors rather than the procedure itself (Figure 5.30A). Again, statistical analysis of the densitometry from these two groups (mild and severe hydronephrosis) was not possible due to the small numbers. No significant differences in AQP4 expression were noted in moderate hydronephrosis compared to sham (Figure 5.30).

Combined densitometry results from litter 2-3 and 4-6 confirmed a significant reduction in AQP4 expression in severe hydronephrosis (mean OD +/- SEM; 5976 +/- 2188) compared to sham (18400 +/- 3046) and contralateral sham (16740 +/- 2477) kidneys (Figure 5.31).

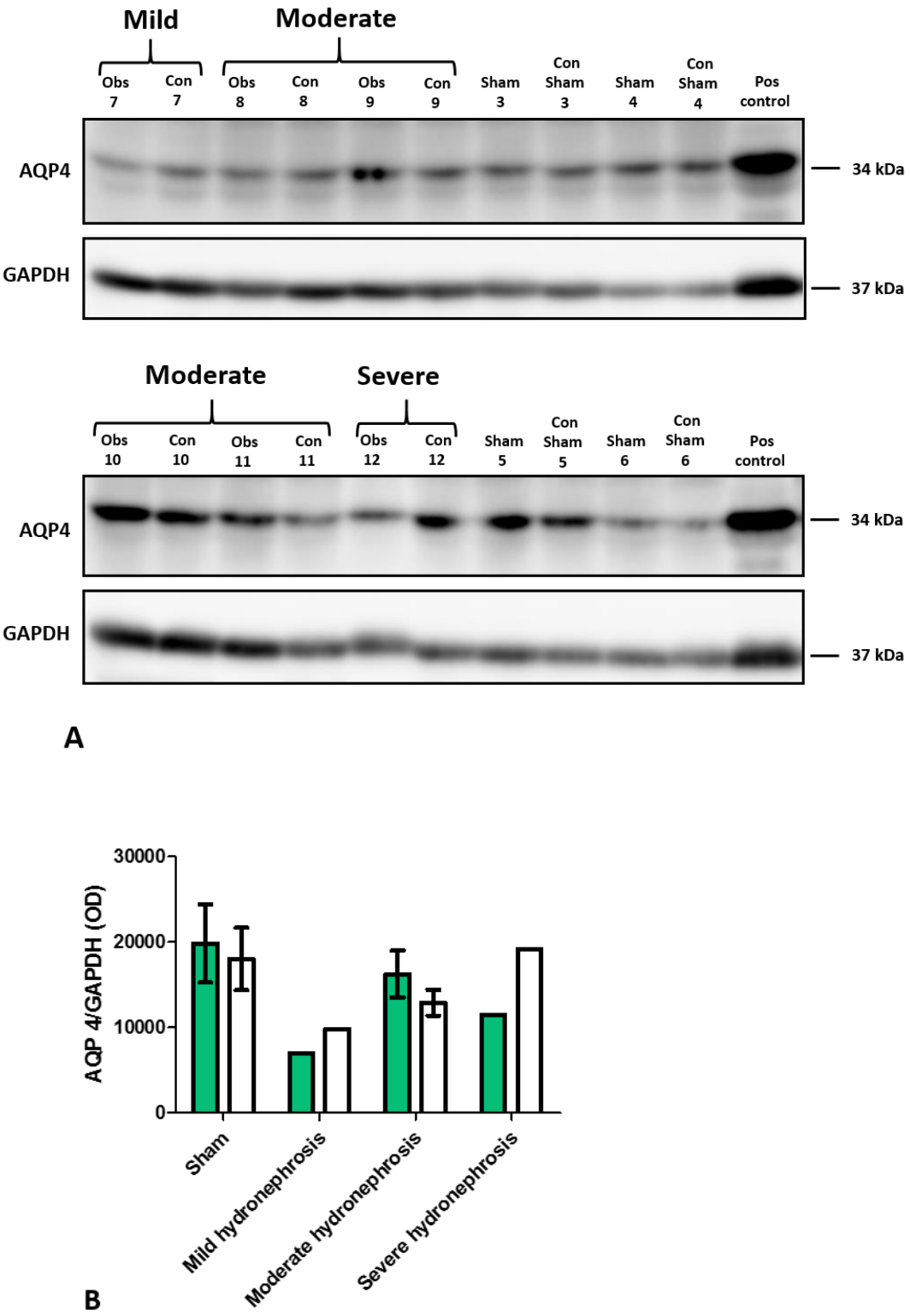

Figure 5.30 AQP4 protein expression by rat kidney in PUUO rats compared to sham rats litters 4-6

Western blot demonstrating AQP4 expression by whole kidney from PUUO and sham rats at 35 days of age from litters 4-6. Mild, moderate and severe indicates degree of hydronephrosis noted in PUUO rats. Obs – left/obstructed kidney, Con – contralateral kidney. GAPDH – loading control (A). Bar graph demonstrating AQP4 protein expression (optical density expressed as mean +/- SEM) normalised to GAPDH for PUUO compared to sham rats from litters 4-6. Coloured bars – left sham/obstructed kidney, white bars – contralateral kidney. No significant differences were noted between groups (B). Sham n=4, Mild hydronephrosis n=1, moderate hydronephrosis n=4, severe hydronephrosis n=1.

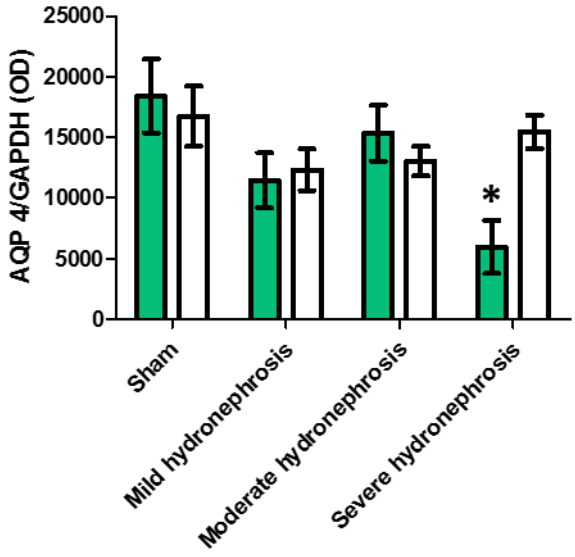

Figure 5.31 AQP4 expression in PUUO rats compared to sham rats

Bar graph demonstrating AQP4 protein expression (optical density expressed as mean +/- SEM) normalised to GAPDH for PUUO compared to sham rats from litters 2-6 combined at 35 days of age. Coloured bars – left sham/obstructed kidney, white bars – contralateral kidney. *****$p<0.05$ compared to sham and contralateral sham. Sham n=6, mild hydronephrosis n=3, moderate hydronephrosis n=5, severe hydronephrosis n=4.

5.3.8 Renal pelvis aquaporin mRNA expression is reduced in moderate and severe hydronephrosis

Endpoint PCR was performed to determine AQP isoform expression by rat renal pelvis and direct future real-time PCR. Figure 5.32 reveals that AQPs 1, 3, 4, 7, 9 and 11 are expressed at the mRNA level by normal rat renal pelvis. AQP5 mRNA expression was not tested as the primers available were not suitable for subsequent real time PCR (Figure 5.32).

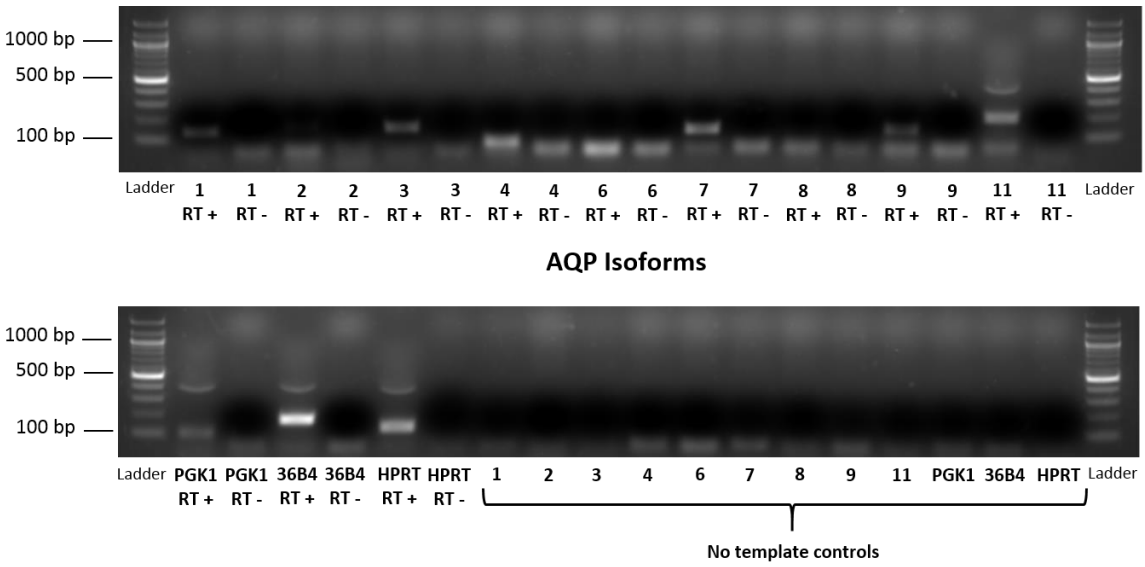

Figure 5.32 Endpoint PCR demonstrating the AQP isoforms expressed by rat renal pelvis

RT-PCR was performed using mRNA extracted from whole normal rat renal pelvis and the product run on 2% agarose gels. Bands of the appropriate size for AQP isoforms 1, 3, 4, 7, 9 and 11 and reference genes PGK-1, 36B4 and HPRT were noted indicating they are expressed at the mRNA level by whole rat renal pelvis. The 400 bp band in the lanes for AQP 11, PGK1, 36B4 and HPRT is a reference band from the sample loading buffer. See appendix 2 (section 10.2.1) for product sizes.

Initial real-time RT-PCR demonstrated a significant reduction in β-actin expression in severe hydronephrosis compared to sham kidneys. Further PCR was therefore performed to assess expression of β-actin mRNA compared to 2 other reference genes (PGK1 and 36B4). This was undertaken using the 3 samples that had shown the lowest β-actin expression from the severe hydronephrosis group and the 3 samples from the sham group with the highest levels of expression. The relative expression of β-actin in severe hydronephrosis compared to sham (0.832) was shown to be similar to that of PGK1 and 36B4 (0.867 and 0.856 respectively) confirming that the differences in reference gene expression were likely due to variations in cDNA loading rather than regulation of β-actin expression in PUUO (Figure 5.33).

Subsequently, relative quantification of the various AQP isoforms expressed by renal pelvis was undertaken in PUUO rats compared to sham rats at 35 days of age. Results were normalised to β-actin expression.

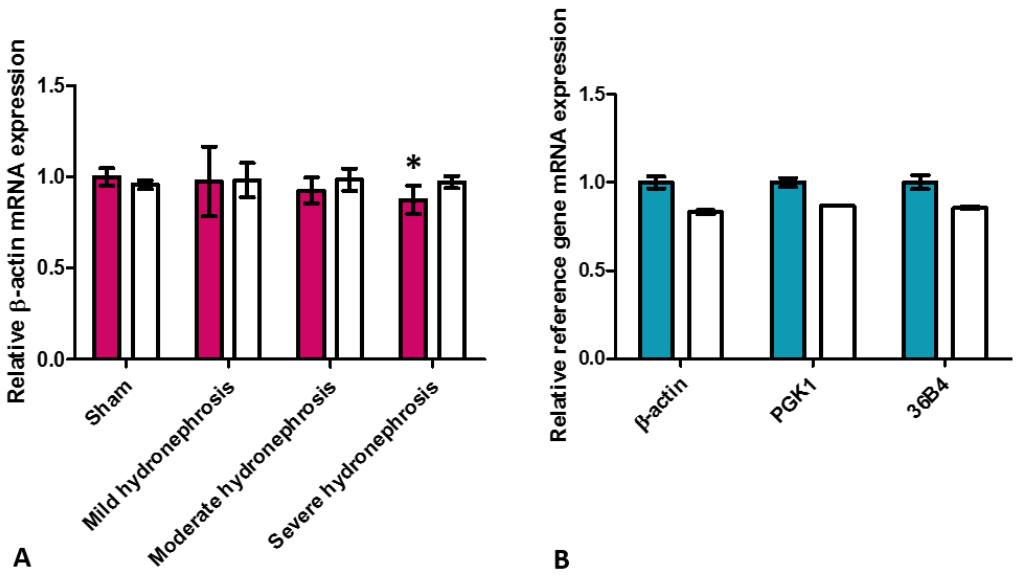

Figure 5.33 Reference genes for normalisation of rat renal pelvis mRNA expression data

Relative β-actin mRNA expression in whole rat renal pelvis for PUUO rats normalised to sham at 35 days of age. Sham n=6, mild hydronephrosis n=3, moderate hydronephrosis n=5, severe hydronephrosis n=4. Coloured bars = left sham/obstructed kidney, white bars = contralateral kidney. *$p<0.05$ compared to left sham. (A). Relative reference gene (β-actin, PGK1, 36B4) mRNA expression for left sham rat renal pelvis (coloured bars) compared to left severe hydronephrosis (white bars). The relative expression of β-actin, PGK1 and 36B4 in the severely hydronephrotic renal pelvis is 0.832, 0.867, and 0.856 respectively compared to the corresponding sham renal pelvis at 35 days of age. N=3 in each group (B). Mean +/- SEM presented for all data.

AQP1 mRNA expression in the renal pelvis was significantly reduced in moderate and severe hydronephrosis compared to sham renal pelvis (relative expression 0.63 and 0.48 respectively). AQP1 mRNA expression in severe hydronephrosis was also significantly downregulated compared to all contralateral groups (Figure 5.34 A).

Analogous to AQP1 expression, AQP3 mRNA expression was significantly decreased in moderate and severe hydronephrosis compared to sham renal pelvices (relative expression 0.48 and 0.34 respectively). Expression in severe hydronephrosis was also significantly reduced compared to the contralateral renal pelvis in rats with mild and severe hydronephrosis (Figure 5.34 B).

Analysis of AQP4 mRNA expression by rat renal pelvis demonstrated a tendency towards reduction in severe hydronephrosis versus sham (ΔCt 95% CI -0.6868 – 4.180) and moderate hydronephrosis versus sham (ΔCt 95% CI -0.8339 – 4.180) (Figure 5.34 C), however statistical significance was not achieved. This is potentially due to the number of observations not having sufficient power to detect a difference

Similar to AQP4, AQP7 mRNA expression showed a large degree of variability such that no significant differences in expression were observed between obstructive hydronephrosis, sham and contralateral renal pelvices (Figure 5.34 D). AQP9 mRNA expression within the renal pelvis was unchanged in obstructive hydronephrosis compared to sham and contralateral renal pelvices (Figure 5.34 E). It must be noted that, due to generally lower levels of expression of AQP7 and 9 mRNA in rat renal pelvis, some results were excluded due to poor melt curves or very high Ct values (Figure 5.34 legend).

AQP11 mRNA expression was significantly downregulated in severe hydronephrosis compared to sham renal pelvices (relative expression 0.27). Expression in severe hydronephrosis was also significantly reduced compared to all other groups except mild hydronephrosis and the contralateral renal pelvis from rats with moderate hydronephrosis (Figure 5.34F).

Furthermore, it was established that in moderate and severe hydronephrosis the intact contralateral renal pelvis did not show upregulation of AQP expression. This suggests there was no attempt by the contralateral renal pelvis to compensate for the downregulation in expression by the obstructed renal pelvis.

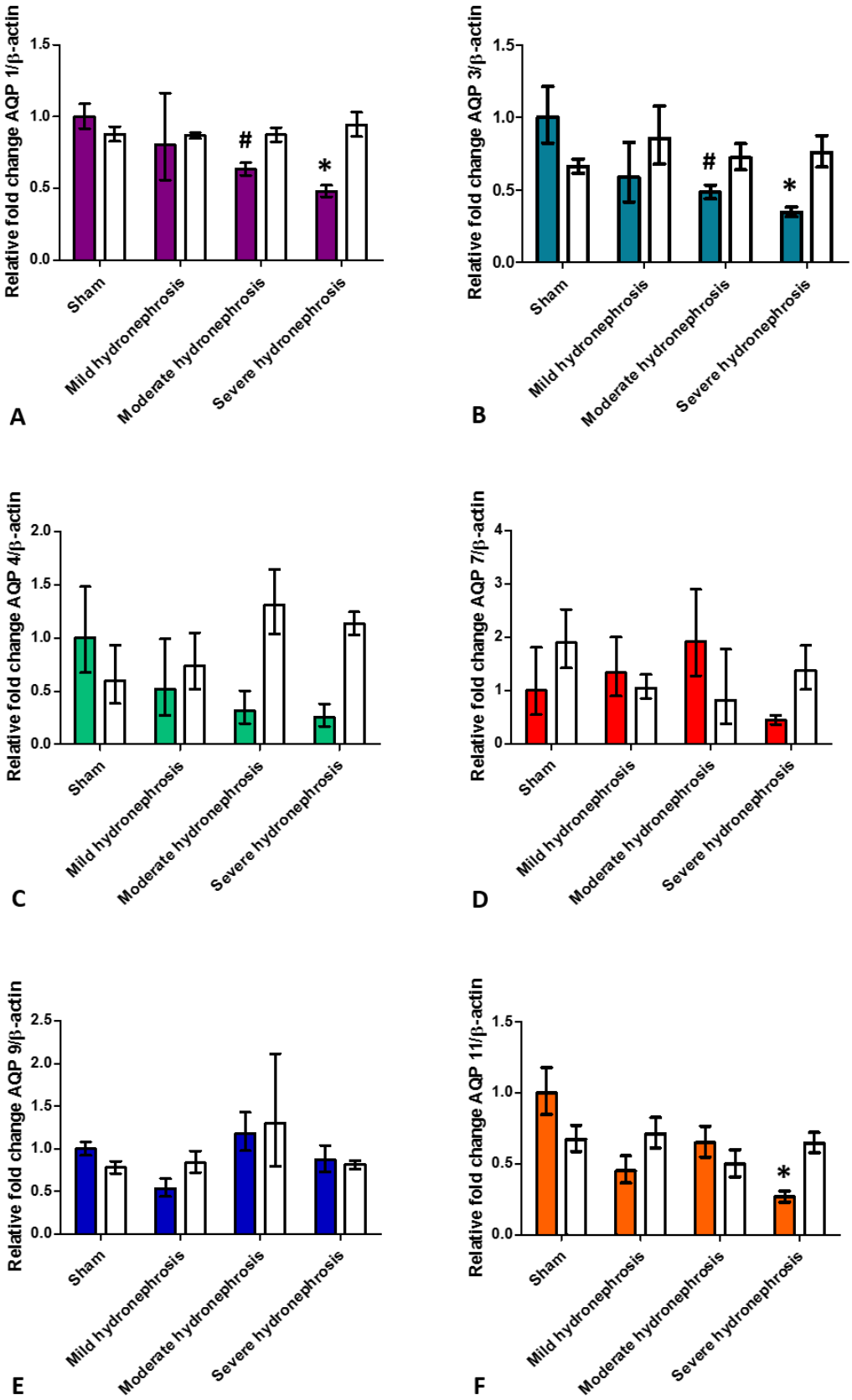

Figure 5.34 Renal pelvis AQP isoform mRNA expression by PUUO rats compared to sham rats

Relative fold change of AQP isoform expression normalised to β-actin in whole rat renal pelvis is presented for PUUO rats compared to sham rats at 35 days of age. Coloured bars = left sham/obstructed kidney, white bars = contralateral kidney. Mean +/- SEM presented. AQP1 mRNA expression *p<0.05 compared to sham

and all contralateral groups, #p<0.05 compared to sham (A). AQP3 mRNA expression *p<0.05 compared to sham, contralateral mild and contralateral severe hydronephrosis, #p<0.05 compared to sham (B). AQP isoforms 4, 7 and 9 mRNA expression demonstrated no significant differences between groups (C, D and E). AQP11 mRNA expression *p<0.05 compared to all groups except mild hydronephrosis and contralateral moderate hydronephrosis (F). Sham n=6, mild hydronephrosis n=3, moderate hydronephrosis n=5, severe hydronephrosis n=4 except for AQP7 where sham n=2 and contralateral moderate hydronephrosis n=4 and AQP9 where sham n=4, mild hydronephrosis n=2, contralateral mild n=2, contralateral moderate n=2.

5.3.9 Renal pelvis aquaporin protein expression

Confirmation of the presence and distribution of AQP isoform protein expression by rat renal pelvis was sought by two methods; western blotting and immunohistochemistry.

Immunohistochemistry of normal rat renal pelvis demonstrated that AQP1 was expressed by the vasculature within the lamina propria of the renal pelvis but was not expressed by the transitional epithelium (urothelium) of the renal pelvis. AQP2 was not expressed by any layer of the renal pelvis. AQP3 was abundantly expressed by the urothelium only of the renal pelvis (Figure 5.35).

Due to the small size of the rodent renal pelvis only a single sample was obtained from each obstructed and contralateral kidney per animal to be used for both RNA and protein work. This sample was snap frozen with the primary goal of extracting RNA, which was performed using the Qiagen RNeasy mini-kit. Using a supplementary protocol provided by Qiagen, protein extraction from the RNeasy column flow-through (which is usually discarded) was attempted on two occasions. Unfortunately, minimal protein extraction was achieved which was not sufficient to complete a western blot. No further attempts were made to extract protein from the renal pelvis samples.

Immunohistochemistry of samples was therefore utilised to assess the impact of neonatal PUUO on both the quantity and distribution of AQP 3 expression by the rat renal pelvis. This AQP was selected due to its urothelial expression pattern as demonstrated by immunohistochemistry and the proven transcriptional regulation of expression as shown by qPCR in response to PUUO. Additionally, studies in human urothelial cell culture have demonstrated AQP3 to be the major urothelial AQP demonstrating altered regulation in response to changes in osmolality. Accordingly, non-specific AQP blockade with mercurials reduces osmotic water and urea flux across these cells [369] making AQP3 a potential candidate of urine composition and volume regulation in the PUUO model.

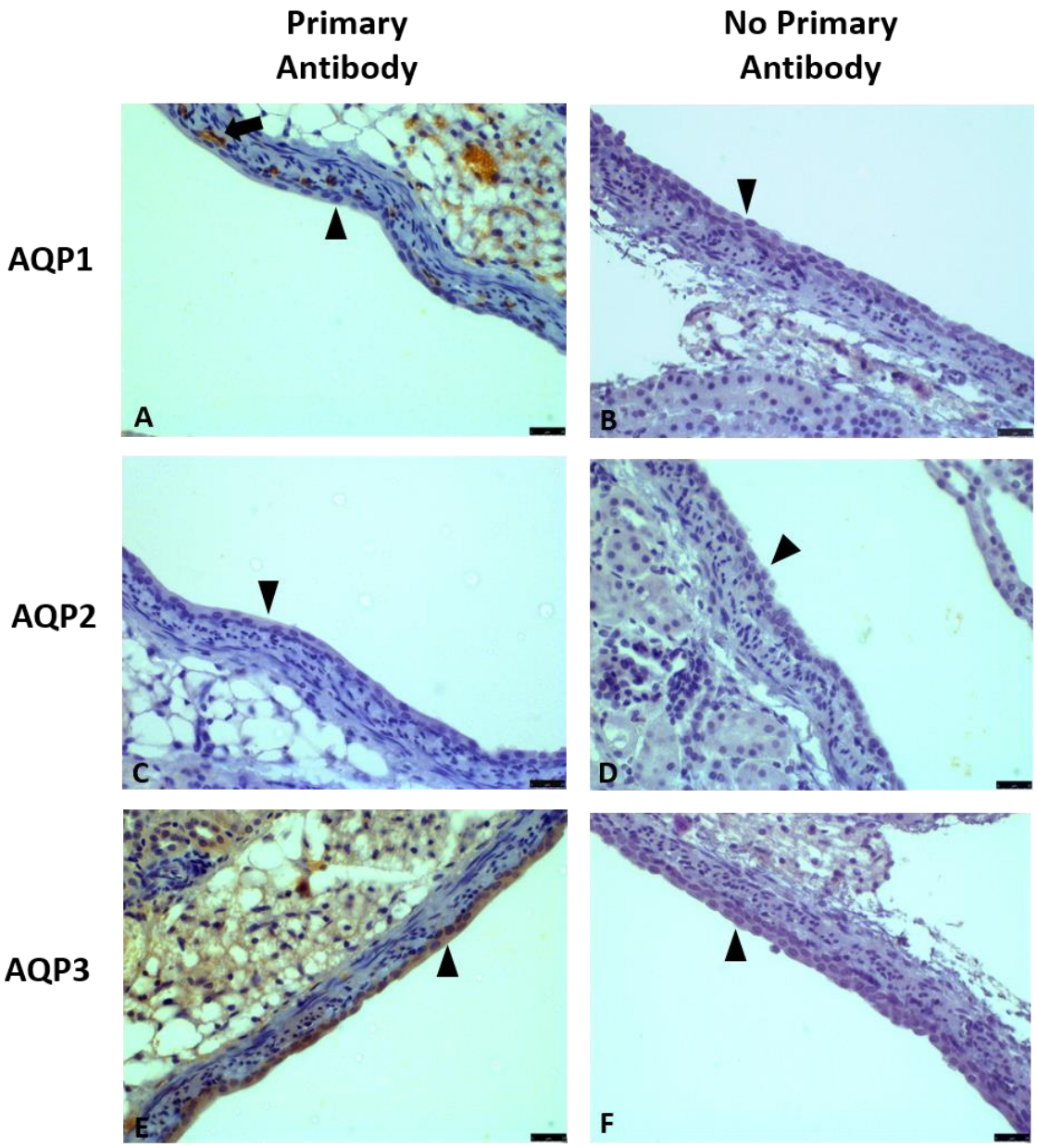

Figure 5.35 Renal pelvis aquaporin 1, 2 and 3 protein expression

Immunohistochemistry of AQP isoform protein expression by rat renal pelvis. Negative controls (no primary antibody) are included for each primary antibody presented (B, D, F). AQP1 is expressed by the renal pelvis vasculature present within the lamina propria (arrow) however it is not expressed by the renal pelvis urothelium (arrowhead (A). AQP2 is not expressed by either the urothelium (arrowhead), vasculature or muscle of the renal pelvis (B). AQP3 is expressed by the renal pelvis urothelium (arrowhead) but not the vasculature or muscle (C). Scale bar = 25 μm.

Immunohistochemistry of PUUO, sham and contralateral whole renal pelvis sections obtained from 35-day old rats was performed by Miss Fern Barrington. Blinded evaluation of staining was undertaken by both Miss Fern Barrington and Professor Richard Coward.

Evaluation of sections demonstrated no urothelial or tubular staining in negative control sections treated with rabbit IgG. Sections treated with anti-AQP3 antibody demonstrated

DAB staining of the urothelium for all sections analysed. As expected tubular staining was also noted in sections containing renal medulla/cortical tissue. In all sections, whether operated or contralateral side, and regardless of sham or PUUO procedure, staining involved the plasma membrane and the cytoplasm through all layers of the urothelium from the basal to the umbrella cells. The severity of hydronephrosis did not affect the distribution of staining through the urothelium compared to sham or contralateral kidneys (Figure 5.36). The thickness of the urothelium did vary somewhat between animals with several (6 out of 36) renal pelvis samples showing slightly thickened urothelium compared to the other samples. These samples, however, were not confined to animals which had undergone a particular procedure and included; 1 x severe hydronephrosis, 1 x mild hydronephrosis, 2 x contralateral sham, 1 x contralateral severe, 1 x sham renal pelvis.

Evaluation of the intensity of urothelial staining between samples demonstrated no significant difference between all degrees of hydronephrosis, sham and contralateral renal pelvices (Figure 5.37).

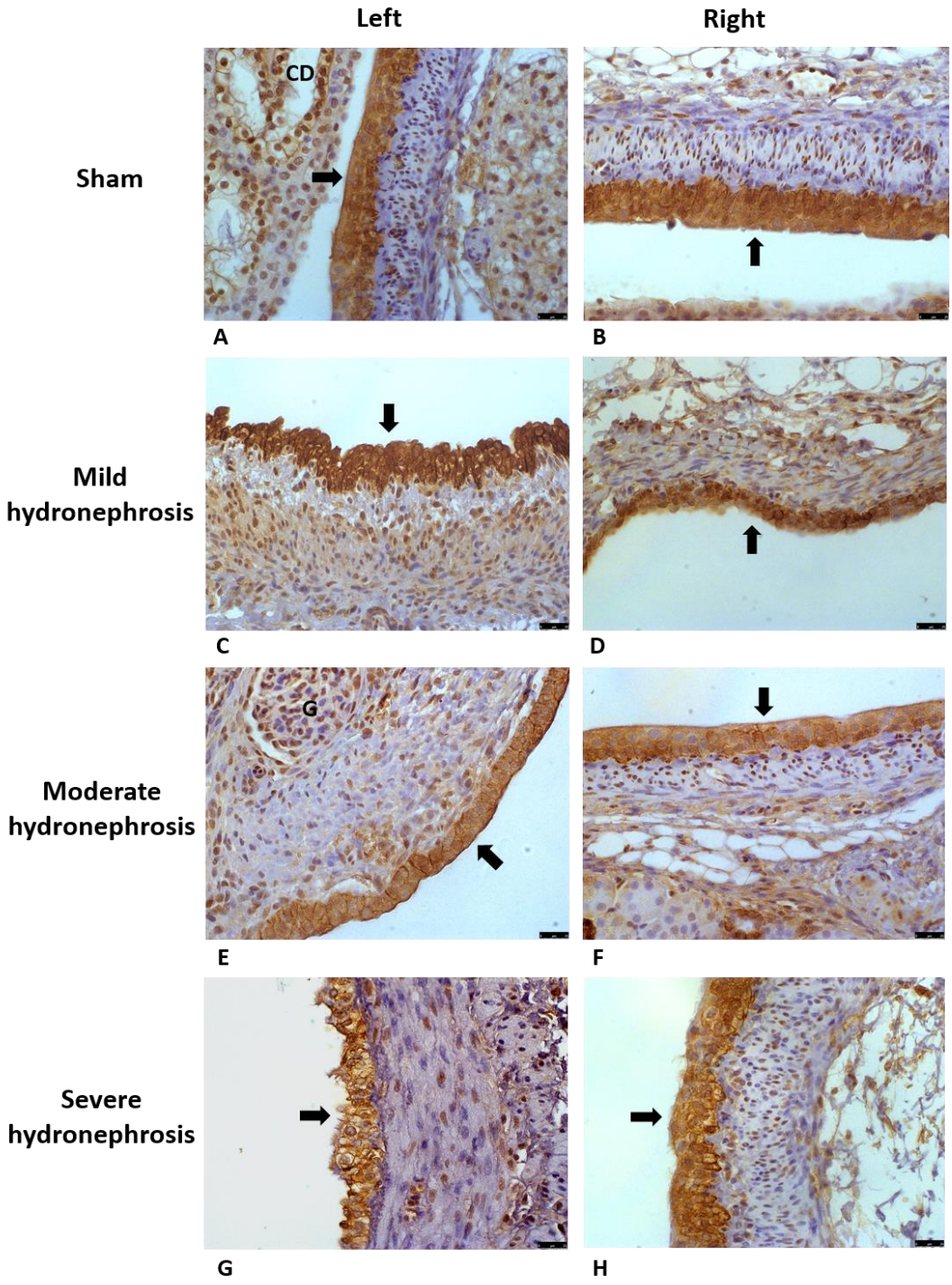

Figure 5.36 Rat renal pelvis AQP3 staining in obstructed, sham and contralateral systems

Representative immunohistochemistry of rat renal pelvis is presented for PUUO rats compared to sham rats at 35 days of age. AQP3 is expressed by all layers of the urothelium within rat renal pelvis in both the operated and contralateral kidneys regardless of the degree of hydronephrosis. The urothelial cell membrane shows predominant expression however cytoplasmic expression is also noted. No discernable differences in the amount or distribution of expression were noted between PUUO and sham rats. Sham (A, B), mild hydronephrosis (C, D) moderate hydronephrosis (E, F) and severe hydronephrosis (G, H). Left – obstructed/sham renal pelvis, Right – contralateral renal pelvis. Arrow – urothelium, CD – collecting duct, G-glomerulus. Scale bar = 25 μm. No staining was detected in rabbit IgG negative control sections (data not shown).

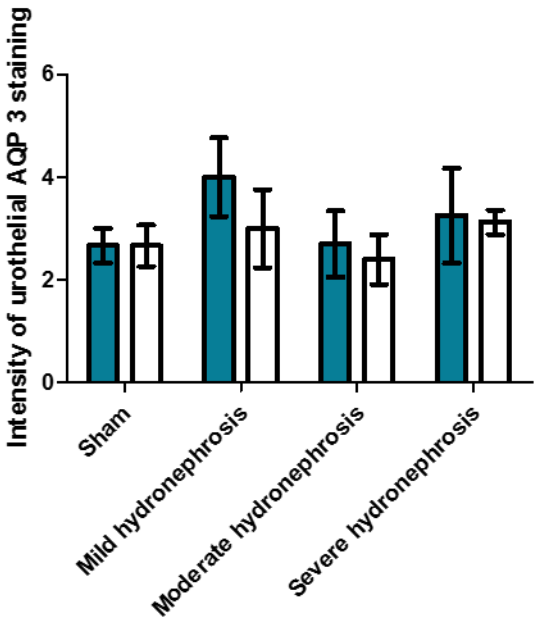

Figure 5.37 Intensity of urothelial AQP3 staining in PUUO compared to sham rats

Relative intensity of urothelial AQP3 expression on immunohistochemistry in PUUO compared to sham rats at 35 days of age. Intensity of staining was scored from 0-5 (0 = no expression, 5 = most intense expression). No significant differences were noted between obstructed, sham and contralateral renal pelvices. Coloured bars = left sham/obstructed kidney, white bars = contralateral kidney. Mean +/- SEM presented. Sham n=6, mild hydronephrosis n=3, moderate hydronephrosis n=5, severe hydronephrosis n=4.

5.3.10 Urinary AQP1 excretion is unchanged in hydronephrosis

Bladder urine obtained by placing the rats in a metabolic cage at 29 days of age was analysed by AQP1 ELISA. Initial runs of the ELISA demonstrated that the optical densities achieved for the standard curve were much lower than when the ELISA was optimised. As a new batch of AQP1 antibody was being used, a test ELISA was performed trialling this batch of antibody with a new one. Each antibody was used at the original and double concentration. This ELISA revealed that both batches of antibody achieved similar, lower optical densities for a given concentration of AQP1 standard than was achieved when optimising the ELISA previously. Increasing the concentration of the antibody did not improve the sensitivity of the assay but did increase background signal. It is likely that this reduction in sensitivity was due to diminished activity of the new batches of antibody. Despite the reduced sensitivity of the assay, the optical densities of the standards were still doubling nicely as the AQP1 concentration increased (Table 5.4). Additionally, upon using this assay to assess urine AQP1 excretion in rat samples, all results fell satisfactorily within the optical density range of the standard curve. This assay, using the AQP1 antibody at the original 1 in 60 dilution, was therefore used for ongoing analysis.

AQP1 Standard Concentration (ng/ml)	AQP1 A 1 in 60 (Mean OD)	AQP1 A 1 in 30 (Mean OD)	AQP1 B 1 in 60 (Mean OD)	AQP1 B 1 in 30 (Mean OD)
Blank	0.107	0.152	0.092	0.098
3.125	0.0285	0.013	0.0305	0.038
6.25	0.064	0.0605	0.049	0.068
12.5	0.1115	0.125	0.099	0.1285
25	0.226	0.2625	0.229	0.243
50	0.4425	0.488	0.3885	0.4365
100	0.827	0.9535	0.6745	0.799
200	1.4605	1.6175	1.299	1.4695

Table 5.4 AQP1 ELISA testing different batches of anti-AQP1 antibody and antibody dilutions

Two different batches of AQP1 antibody (A and B) were each used at 1 in 60 and 1 in 30 dilutions and applied to two-fold serial dilutions of recombinant AQP1 protein standards from 3.125 ng/ml to 200 ng/ml in 0.1% SDS/PBS. The protein standards were performed in duplicate and the mean optical densities measured at 450 nm are presented for each AQP1 protein concentration. OD – optical density.

Figure 5.38 and Table 5.5 show a representative standard curve obtained when processing urine samples from the rat PUUO model.

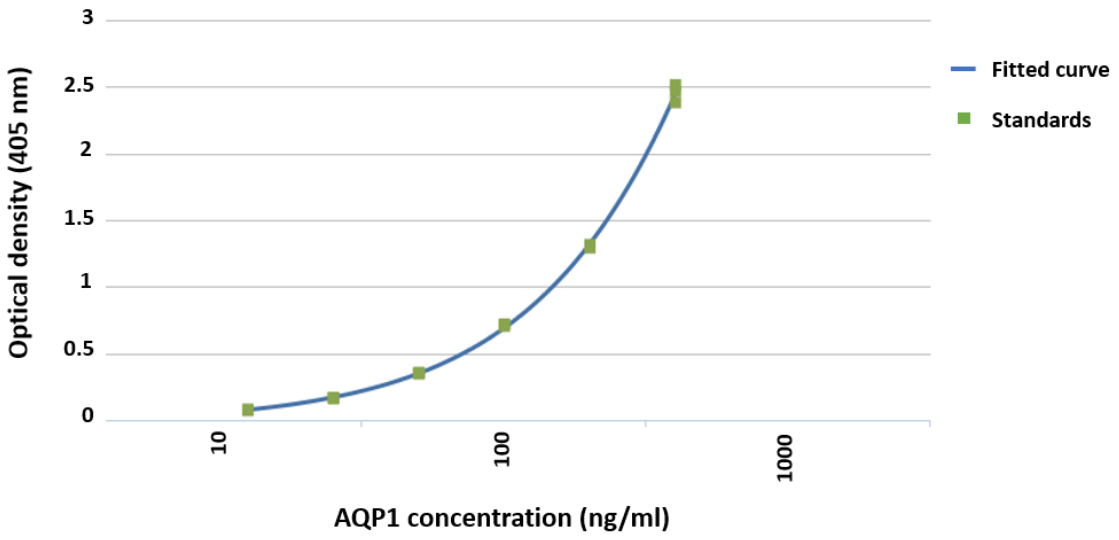

Figure 5.38 Urinary AQP1 ELISA standard curve associated with Table 5.5

A representative AQP1 standard curve generated when analyzing urine samples from the rat PUUO model. A serial dilution of AQP1 standards from 12.5-400 ng/ml is demonstrated. Analysis performed by 4 parameter

logistic regression reveals an $R^2 = 0.999$. Anti-AQP1 antibody was used at 1:60 dilution and standard/sample diluent was 0.1% SDS in PBS.

AQP1 concentration ng/ml	Optical density 1	Optical density 2	Optical density 3	Mean optical density	Standard deviation	% CV optical density
12.5	0.071	0.078	0.079	0.076	0.004	5.735
25	0.162	0.164	0.17	0.165	0.004	2.518
50	0.345	0.352	0.356	0.351	0.006	1.586
100	0.703	0.72	0.712	0.712	0.009	1.195
200	1.316	1.316	1.291	1.308	0.014	1.104
400	2.381	2.466	2.515	2.515	0.068	2.763

Table 5.5 Optical densities of AQP1 standards

Representative values obtained when performing a two-fold serial dilution of recombinant AQP1 protein standards in order to analyse samples from the rat PUUO model. Protein standards were performed in triplicate. Individual, and mean optical densities measured at 450 nm are presented for each AQP1 protein concentration alongside the standard deviation and percentage coefficient variation. Anti-AQP1 antibody was used at 1 in 60 dilution.

When analysing the urine samples from 29 day old PUUO and sham rats, the PUUO group was stratified based on the degree of hydronephrosis detected at the end of the protocol at 35 days of age. The ELISA demonstrated that regardless of whether the animal had a sham or PUUO procedure there was large individual variability in urinary AQP1 excretion. Urinary AQP1 excretion was also revealed to be not significantly different between PUUO rats across all degrees of hydronephrosis when compared to sham rats.

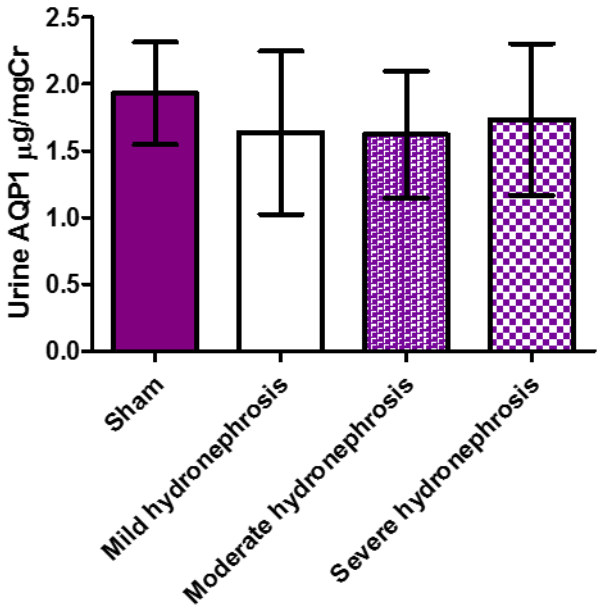

Figure 5.39 Urinary AQP1 measurements normalized to creatinine in PUUO and sham rats

Bar graph demonstrating the urinary AQP1 levels normalised to creatinine in PUUO rats with mild (n=3), moderate (n=5) or severe (n=4) hydronephrosis compared to sham (n=6) rats. No significant differences were noted between groups.

5.4 Discussion

Although no difference in growth was noted between rats up to 4 weeks of age, body weight was significantly reduced in PUUO compared to sham rats at 5 weeks of age. This finding is similar to that of Thornhill *et al.* who reported growth impairment proportional to the severity of obstruction in PUUO rats from 3-4 weeks of age whereby at 4 weeks of age, body weight in the most severely obstructed group was significantly reduced compared to sham. It is not clear why rats with unilateral PUUO show growth impairment, however, as highlighted by Thornhill *et al.*, it is unlikely this growth restriction is due to a reduction in GFR. Neonatal PUUO models show unchanged creatinine clearance (measured from bladder urine) compared to sham rats at both 7 and 14 weeks of age [364], while GFR is maintained in the normal contralateral kidney 28 days after PUUO [91]. Thornhill *et al*. suggest that reduced body weight may be related to renal acid-base disturbance which when combined with an immature compensatory response in PUUO causes renal tubular acidosis which is known to affect somatic growth [91]. Certainly, UUO for 24 hours in adult rats leads to a significant reduction in the protein expression of many major acid-base transporters along the nephron including NHE3, NBC1, NBCn1, NKCC2 and pendrin. Following an acid load, impaired renal H^+ excretion and HCO_3^- retention leads to a significant reduction in blood pH

and HCO_3^- in UUO rats compared to sham [407]. Similarly, in neonatal PUUO, altered expression of renal acid-base transporters is demonstrated and this occurs in an age/time dependent manner. NHE3, NBC1, pendrin and Na^+-K^+-ATPase are significantly upregulated in both the obstructed and contralateral kidney compared to sham at 7 weeks following obstruction. At 14 weeks following PUUO, NBC1, NBCn1 and Na^+-K^+-ATPase expression are significantly downregulated in the obstructed kidney compared to sham and are associated with impaired acid excretion and metabolic acidosis following an acid load [408]. Others have also shown NKCC2 expression to be significantly reduced 12 and 24 weeks after creation of neonatal PUUO [185]. In accordance with these observations, a study of 50 infants with either unilateral or bilateral hydronephrosis demonstrated 46% of children (39% and 61 % respectively) had evidence of renal tubular acidosis [409].

Individual kidney weight was unchanged between all degrees of partially obstructed, contralateral and sham kidneys at 5 weeks of age which is similar to observations made by Wang *et al*. at 7 weeks following neonatal PUUO. Interestingly this group reported decreased weight of the obstructed kidney compared to the contralateral but not the sham kidney at 14 weeks post PUUO [364], which may have been noted in this study had the protocol been continued for longer. Others have demonstrated reduced weight of the obstructed kidney at an earlier time point of 28 days post neonatal PUUO, the severity of which correlated non-linearly with the degree of obstruction. A key threshold of 70% luminal reduction was identified which resulted in substantial inhibition of renal growth [91], suggesting the degree of obstruction during this study may not have reached this critical point. Koff *et al*. suggested that the presence of contralateral hypertrophy in children with PUJO might aid the diagnosis of obstruction in hydronephrosis and thus the selection of patients for pyeloplasty [410]. Although contralateral renal hypertrophy has been noted at 28 days following complete neonatal UUO it was not detected at 5 weeks of age in this current study of partial obstruction and has not been reported by other groups using neonatal PUUO models until at least week 14. From this time point onwards, using MRI studies, contralateral hypertrophy was noted in the presence of severe but not mild obstruction and this persisted until the end of the study at 24 weeks [91, 364, 411]. The onset of contralateral hypertrophy, however, was significantly delayed beyond the commencement of functional deterioration in the obstructed kidney [411] thus casting doubt on the predictive value of this measurement in children.

Intra-renal pelvis pressures in mild and severe hydronephrosis were similar and slightly elevated respectively compared to sham, contralateral and non-operated kidneys.

Unfortunately, the mild and severe hydronephrosis groups contained only 1 animal each, thus precluding statistical analysis and the ability to draw meaningful conclusions. The lack of increased intra-renal pressure within the severely hydronephrotic kidney, however, suggests decompensation may have occurred with deterioration of the architecture, function and urine output of the kidney. Intra-renal pelvis pressure was significantly increased in moderate hydronephrosis compared to sham, contralateral and non-operated kidneys and is consistent with other reports of acute and chronic PUUO causing a rise in the mean basal intra-renal pelvis pressure [112, 401]. Pigs and dogs have baseline renal pelvis pressures of up to 4.12+/-0.94 cmH_2O which increases in the partially obstructed pig to 16.4+/-3.83 cmH_2O [112]. Similarly, in the supine anaesthetised human adult, mean renal pelvis pressure is 5.2+/-1.3 cmH_2O [46] which rises to 10.7 cmH_2O [113] and 8.9 mmHg (approx. 12.1 cmH_2O) in high pressure chronic urinary retention and idiopathic hydronephrosis respectively [114]. Substantial variability in the intra-renal pelvis pressure measurements for the moderate hydronephrosis group was noted.This suggests that with greater numbers assessed, this group may naturally split into kidneys with raised pressure and those with pressure equivalent to sham. Conversely, it is possible that pressure is a continuous variable in this group. Neonatal rat studies have demonstrated that functional and histological changes occur acutely after PUUO and may stabilise and not progress significantly in the longer term [412, 413]. This equilibrium may be related to compensatory mechanisms within the kidney to reduce damaging pressure rises [121] such as reduced RBF/GFR, renal pelvis dilatation, urine drainage by the venous/lymphatic systems [88, 117, 121] as well as other, as yet undefined, mechanisms. For future work this raises the question of whether, in the absence of substantial parenchymal loss, hydronephrotic animals should be stratified by intra-renal pelvis pressure rather than renal pelvis APD, thus furthering investigation of the renal mechanisms employed to relieve pressure and resist functional damage. Ultimately, more animals need to be assessed to draw firm conclusions from this aspect of the research.

In this current study significant renal parenchymal abnormalities were only noted in the severely hydronephrotic kidneys whereby the number of glomeruli per field of view was significantly reduced and the degree of interstitial fibrosis was significantly increased compared to mild and moderate hydronephrosis, sham and contralateral kidneys. The number of glomeruli per field of view was slightly reduced in the moderately hydronephrotic kidneys however this difference was not significant. PUUO did not have any effect on the number of glomeruli or interstitial fibrosis formation in the contralateral kidney. This is similar to the findings of Thornhill *et al.* who demonstrated increased interstitial fibrosis in

severely hydronephrotic kidneys at 14 days following neonatal rat PUUO alongside a reduction in the number of glomeruli in higher grade obstruction at 28 days but not 14 days post-PUUO. The loss of glomeruli after the period of nephrogenesis indicates predominantly a disappearance of previously formed but immature glomeruli. The process by which this occurs is not completely understood but involves phenotypic transformation of glomerular cells to a less differentiated state [87, 91].

In this current study, the finding of increased intra-renal pelvis pressure in moderate hydronephrosis alongside a lack of significant architectural abnormalities will be incredibly informative as any detected modifications of renal protein expression are likely due to altered regulation rather than simply structural damage and nephron loss.

Consistent with previous studies of mammalian renal AQP mRNA and protein expression [241, 296, 299], this study demonstrated that whole rat kidney expresses mRNA transcripts for AQPs 1-8 and 11. Contrary to previous studies that demonstrated an absence of AQP9 in rat kidney using northern blot analysis [286], this study demonstrated the presence of AQP9 mRNA using RT-PCR in rat kidney. At 5 weeks of age mRNA expression of AQPs 1, 2 and 6 was significantly downregulated in severe hydronephrosis. AQP3 mRNA expression was unchanged in the obstructed kidney compared to sham kidneys. Although AQP4 mRNA expression showed a tendency towards reduced expression in severe hydronephrosis compared to sham kidneys a significant difference was not detected. This was potentially due to substantial variability in the results. Increasing the number of animals assessed to increase the power of the study would be necessary toinvestigate this further. Upregulation of AQP expression in the contralateral kidney was not noted for any of the AQP isoforms suggesting there was no attempt to compensate for the reduction of AQPs in the obstructed kidney.

This is the first study to assess renal mRNA expression of a range of AQP isoforms in a neonatal PUUO model. AQP2 mRNA expression has previously been shown to be significantly downregulated 24 hours after complete UUO in adult rats [186]. Furthermore, in a study of children undergoing pyeloplasty for congenital PUJO, mRNA expression of AQPs 1-4 was shown to be significantly reduced in both grade 3 and 4 hydronephrosis (SFU grading) compared to normal kidneys [187]. Contrary to the results from the childhood PUJO research, this current study demonstrated that dysregulation of mRNA expression did not affect all AQP isoforms assessed (AQP 1-4 and 6). AQPs 1 and 2 function predominantly as water channels and are expressed on the apical and basolateral membranes of the proximal

tubular cells and the apical membrane of the collecting duct cells respectively [241]. AQPs 3 and 4 also function predominantly as water channels, however, they are located on the basolateral membrane of the collecting duct [241] where they are potentially not directly exposed to the increased intratubular pressure associated with PUJO. Further discussion of possible regulatory factors in PUJO is undertaken later in the chapter. AQP6 is an anion channel which has low permeability for water at physiological pH and is thought to be involved in acid-base balance. It is located on the membrane of intracellular vesicles within type A intercalated cells of the collecting duct [330, 332, 335]. Downregulation of this AQP within the obstructed kidney would be consistent with observations of renal tubular acidosis in neonatal PUUO models [408] and childhood PUJO [409], and additionally may contribute to the impairment of growth noted in this study.

Immunohistochemistry of whole rat kidney demonstrated that AQPs 1-3 were expressed by the cortex and medulla of rat kidney in a pattern consistent with previous reports of both rodent and human expression. AQP1 was expressed by the apical and basolateral membranes of the proximal tubules as well as the loop of Henle and vasa recta. AQPs 2 and 3 were expressed by the apical and basolateral membranes of the renal collecting ducts [187, 255].

Subsequent assessment of the effect of neonatal rat PUUO on the quantity of AQP protein expression was undertaken using semi-quantative analysis of western blotting. When assessing renal AQP protein expression by western blotting, GAPDH rather than β-actin was used as reference protein for two reasons. Firstly, in the current study GAPDH was not regulated in PUUO kidneys when compared to sham or non-operated kidneys whereas β-actin protein expression was significantly downregulated in PUUO compared to non-operated kidneys. This could be explained by their differing cellular roles; GAPDH is an enzyme involved in glycolysis amongst other functions [414] whereas β-actin is a highly-conserved cytoskeletal protein which could be affected by the histological changes detected in obstructive hydronephrosis [415]. Secondly, rat heart, which expresses GAPDH but not β-actin, was used as positive control for selected western blotting experiments.

Protein lysates for litters 2-3 and litters 4-6 were extracted and analysed for AQP expression by western blotting in 2 separate batches. This may have contributed to the significant differences noted particularly between AQP1 and 3 expression in PUUO and sham kidneys across the 2 experiments. Visual inspection of the AQP1 blots seemed to demonstrate opposite results such that in litters 2-3, downregulation of AQP expression was noted in the PUUO kidney whereas in litters 4-6 downregulation seemed to occur in the contralateral

kidneys. Inspection of AQP3 Western Blots demonstrated the reverse phenomenon with increased expression in the severely hydronephrotic kidneys of litters 2-3 and reduced expression in litters 4-6. Separate semi-quantitative densitometric analysis of the two batches was furthered hampered by the resultant small numbers in each group, precluding statistical analysis for certain degrees of hydronephrosis. The results were therefore presented separately for each batch of experiments and then combined for all experiments.

In order to ensure the differences between litters 2-3 and 4-6 were not due to inaccurate loading of samples or differences in the running of the western blot, re-runs of certain samples from both batches was undertaken in a single experiment and analysed for AQP1 expression. The results were consistent with the original experiments suggesting the variation in the results were potentially due to either:

- Different methods used to homogenise tissue between the 2 experiments. Tissue homogenisation in litters 2-3 was carried out by hand using a pestle and mortar to grind the tissue under liquid nitrogen to a powder, which was subsequently homogenised using a glass hand homogeniser on ice. In litters 4-6, due to the time-consuming nature of hand homogenisation, an electric Ultra-Turrax homogeniser was used to homogenise the samples on ice. Disparity between the results was particularly noted in severely hydronephrotic kidneys which had been demonstrated by Massons trichrome staining to have significantly increased interstitial fibrosis. Conical glass hand homogenisation, employs grinding to tear and rip tissue to release proteins and can be ineffective at disrupting fibrous/membranous tissue. Rotor-stator homogenisors such as the Ultra-Turrax work by shearing and are effective at disrupting a wide variety of sample types including those which are particularly fibrous [416]. Increased amounts of fibrosis in the severely hydronephrotic kidneys may thus have rendered the tissue more difficult to breakdown by hand homogenisation, reducing the amounts of protein of interest isolated in the first batch processed. Conversely, although roto-stators are more time efficient and disrupt fibrous tissue more easily, they produce larger particles than are achieved with a hand glass homogeniser. The glass homogeniser produces exceptionally small particle sizes thus potentially enabling them to release more protein than the roto-stators [416]. When isolating AQPs from kidney tissue some groups have used motor driven Potter-Elvehjem homogenisers [185, 364] which disrupt tissue by either grinding or shearing according to the kind of pestle employed, while others have homogenised the tissue first by an unspecified method followed by sonication [417]. Ultimately a

two-step process employing different mechanisms of tissue/cellular disruption is generally best to achieve optimum protein recovery. Cryogrinding™ followed by sonication is particularly effective at liberating proteins from tissue [416] and could be investigated for use in future experiments. To determine the effect of the method of mechanical tissue lysis on the results obtained in this study, however, both techniques of sample homogenisation need to be repeated in the future using the same samples.

- Surgery carried out at a different time. Operations on litters 2-3 and litters 4-6 were separated by a few months due to a period of leave from the laboratory. Genetic drift in the animals may have therefore affected the results.
- Changes in AQP expression related to the natural progression of the insult in PUUO. AQP expression is time/age dependent in neonatal rat PUUO [364]. Such changes in AQP expression (from increased to decreased expression) may have been occurring around the time of sacrifice of the animals although previously this had been shown to occur slightly later (>7 weeks of age) using Munich-Wistar rats. The current study used Han-Wistar rats which may account for this difference.
- Natural variation in protein expression which could be addressed by performing PUUO on a greater number of animals.

Analysis of litters 2-3 demonstrated that both glycosylated and non-glycosylated AQP1 protein expression was significantly downregulated in severe hydronephrosis compared to sham kidneys while glycosylated AQP1 was significantly upregulated in mild hydronephrosis compared to sham kidneys. No significant differences in AQP2 expression were detected between groups while AQP3 expression was significantly upregulated in severe hydronephrosis compared to sham kidneys. Conversely AQP4 was significantly downregulated in severe hydronephrosis compared to sham. Statistical tests were not applied to the moderate hydronephrosis group as this contained only one animal. Analysis of litters 4-6 demonstrated no significant differences in both glycosylated AQP1, non-glycosylated AQP1, AQP2, AQP3 and AQP4 expression compared to sham kidneys. Statistical tests were not applied to the mild and severe hydronephrosis groups as they each contained only one animal. Visual inspection of the blots alongside the densitometry results suggested both AQP3 and 4 expression was decreased in severe hydronephrosis.

Combination of the results for all 5 litters revealed that at 5 weeks of age renal protein expression of non-glycosylated AQP1 was unchanged in the obstructed kidney.

Glycosylated AQP1 was significantly upregulated in mild hydronephrosis compared to contralateral sham kidneys but not sham kidneys. This suggests a tendency towards upregulation in mild hydronephrosis, analysis of increased numbers of animals would enable a difference compared to the sham kidneys to be detected or refuted. Any upregulation of AQP1 in mild hydronephrosis would be occurring via post-transcriptional/post-translational regulation as no differences in AQP1 mRNA expression in mild hydronephrosis were detected. Increased expression in mild hydronephrosis may represent a compensatory mechanism to offset damaging intra-tubular pressure rises.

In moderate and severe hydronephrosis glycosylated AQP1 expression was unchanged compared to sham kidneys. This data conflicts with the mRNA results which demonstrated AQP1 downregulation in severe hydronephrosis. A reduction in mRNA expression potentially heralds subsequent protein downregulation which may have been detected had a later study endpoint been used.

Angiotensin II acting via the AT1 receptor has been demonstrated to upregulate AQP1 mRNA and protein expression in rat proximal tubular cells both in vitro and in vivo. Interestingly, the response is biphasic with dose dependent increases in expression at lower concentrations of angiotensin II but suppression of AQP1 mRNA expression at higher strengths. Thus, the activation of the renin angiotensin system which is known to occur in UUO, may contribute to the dysregulation of AQP1 seen following PUUO [308]. AQP1 expression is not regulated directly by vasopressin [325] but is also upregulated by hypertonicity [308].

It is not clear why glycosylated AQP1 expression seemed more affected by PUUO than non-glycosylated in this study. Glycosylation has not been identified as necessary for AQPs to be targeted to the plasma membrane and does not change the water permeability of AQP1 [242, 243]. Wang *et al.* performed neonatal PUUO in Munich-Wistar rats by embedding the upper 2/3 of the ureter into the psoas muscle, a method which they had previously described as generating severe obstruction [401]. In contrast to the current study they demonstrated AQP1 (combined glycosylated and non-glycosylated) to be upregulated at 7 weeks of age in the obstructed kidney compared to sham, however, expression subsequently fell such that it was downregulated at 14 weeks of age [364]. Conversely, in a separate study using the same neonatal PUUO model, the same group demonstrated AQP1 expression to be unchanged at 12 and 24 weeks of PUUO compared to non-obstructed kidneys [185]. These studies highlight the sometimes variable nature of AQP expression in PUUO, and indicate that

individual factors may be involved in the animal's ability to maintain AQP expression in the presence of PUUO.

Results for AQP2 expression in PUUO were more consistent between the two batches assessed, and when combined, confirmed that at 5 weeks of age AQP2 protein expression was unchanged in the obstructed kidney compared to sham kidneys. This was discordant with the mRNA results where AQP2 expression was significantly downregulated in severe hydronephrosis. Wang *et al.* demonstrated renal AQP2 protein expression in neonatal PUUO to rise at 7 weeks of age followed by downregulation at 14 weeks of age which continued until at least 24 weeks of age [185, 364]. Interestingly, the same group demonstrated phosphorylated AQP2 (pS256-AQP 2) was downregulated at both 7 and 14 weeks compared to sham suggesting that transport to the plasma membrane was impaired at both time points [364]. These studies only assessed protein expression, whereas the current study assessed both mRNA and protein expression. Again, downregulation of AQP2 mRNA in the current study likely precedes later protein downregulation, which may thus occur at an earlier time point than noted by Wang *et al*. Upregulation of AQP2 expression was not noted in the current model, however, if regulatory changes were occurring earlier than detected in other studies it is possible an initial upregulation was missed using an end point of 5 weeks of age.

Under normal circumstances short and long term regulation of AQP2 expression is predominantly controlled by vasopressin acting via the G-protein coupled V2 receptor [241]. UUO leads to upregulation of the renin angiotensin system [118], but paradoxically a significant reduction in V2 receptor and cAMP expression which consequently reduces AQP2 expression and trafficking [180]. This phenomenon is probably related to the biphasic effects exerted by angiotensin II on tubular solute and fluid transport, stimulating movement under normal physiological conditions meanwhile inhibiting fluid/solute transport when angiotensin II levels are pathologically raised [418, 419].

Adult UUO models have demonstrated that the increased COX-2 activity associated with obstructive nephropathy is vital to guard against tubular apoptosis and damage [128]. However, increased COX-2 and the resultant elevation of intra-renal prostaglandins is also involved in causing reduced mRNA and protein expression of renal AQPs 2 and 3 [127, 352]. In the case of AQP2 regulation, increased prostaglandins may reduce expression by:

- contributing to V2 receptor downregulation [420]

- inhibiting the formation of intracellular cAMP [421]
- binding the EP_3 receptor on the basolateral membrane of the collecting duct cell, activating Rho and leading to the polymerization of F-actin which obstructs APQ2 translocation [354]

Changes in environmental tonicity [356] as well as many other molecules such as ATP, dopamine [318], bradykinin [319], NO, ANP [320] and integrins [355] are also known to modulate AQP2 expression and trafficking via various mechanisms and may be involved, in ways not yet elucidated, in the context of PUUO. Nuclear factor-κB (NFκB) is a transcriptional regulator activated by angiotensin II via AT1 and AT2 receptors [101, 158, 422] which is involved in the upregulation of pro-inflammatory genes in UUO [101]. In vitro studies using immortalised collecting duct principal cells have demonstrated that NFκB activation decreases AQP2 mRNA and protein expression in a proportionate manner [423] suggesting a role for NFκB in the AQP2 downregulation noted in PUUO.

Combined results from all 5 litters confirmed that AQP3 protein expression was also unchanged in the obstructed kidney of 5 week old PUUO rats compared to sham kidneys which reflected renal AQP3 mRNA expression. This in contrast to others who described an increase in AQP3 expression in PUUO rats at 7 weeks of age which normalised by 12 weeks of age and remained comparable to non-obstructed kidneys until 24 weeks [185, 364]. It is possible, that the initial rise and return to normal levels occurred earlier in the rats in the current study and was therefore missed by the 5-week time point. Others have demonstrated that AQP3 is regulated in the long-term but not in the short term by vasopressin, likely due to the absence of intracellular stores of the protein [323, 325, 360]. The lack of long term downregulation of AQP3 in this study, which is consistent with the results of others [185, 364], suggests that the renin angiotensin system activation and V2 receptor depression known to occur in ureteric obstruction may not be the main regulators of AQP3 expression in PUUO. In vitro work in non-renal cells has demonstrated AQP3 expression to be upregulated by hypertonicity, insulin and leptin [258, 322] although a role for these factors in obstruction has not been investigated. Additionally, AQP3 is known to be regulated by gating such that at physiological pH it is permeable to both water and glycerol, but at acidic pH its water permeability is diminished [363].

Results for AQP4 protein expression were consistent between the two batches of experiments and at 5 weeks of age combined results from all 5 litters demonstrated that AQP4 protein expression was significantly downregulated in severe hydronephrosis

compared to sham kidneys. This was consistent with the tendency towards downregulation noted in renal AQP4 mRNA expression indicating that AQP4 may be transcriptionally regulated in PUUO. Renal AQP4 expression has not been studied in a neonatal PUUO model previously, however in adult rat UUO [184] as well as human congenital PUJO [187, 424], AQP4 is downregulated in the obstructed hydronephrotic kidney. There are conflicting reports regarding the regulation of AQP4 expression by vasopressin. Initially thought to be unaffected by vasopressin [325], more recent reports suggest there is differential regulation along the distal nephron in response to vasopressin. Additionally, in vitro work using non-renal cells demonstrates AQP4 is upregulated by hypertonicity [289].

All four AQP isoforms appear to be regulated by tonicity. Neonatal PUUO and adult UUO and BUO are all known to decrease renal expression of major tubular sodium transporters and increase urine fractional excretion of sodium [181, 182, 185]. Decreased tubular sodium reabsorption would be expected to reduce interstitial tonicity which in theory may lead to AQP downregulation. Certainly, extracellular hypotonicity causes AQP2 transcriptional downregulation [357, 358], as well as promoting internalisation of AQP2 from the membrane [359].

Both at the mRNA and the protein level there was no altered expression noted in the contralateral kidneys to compensate for dysregulated AQP expression in the obstructed kidney. This concurs with functional studies where a reduction in both single kidney GFR and solute free water reabsorption was noted at 12 and 24 weeks post PUUO in the obstructed kidney, while no changes in these parameters compared to control were noted in the contralateral non-obstructed kidney [185]. Interestingly, contrary to the current study, other groups have demonstrated alterations in aquaporin expression in the contralateral kidneys following UUO, indicating potential systemic in addition to intrarenal regulatory factors. Wang *et al.* demonstrated AQP2 and 3 protein expression was upregulated in the contralateral kidney at 7 weeks of age following neonatal PUUO, which corresponded with increased expression of the same AQP isoforms in the obstructed kidney. At 14 weeks of age AQP1 protein expression was downregulated in both the obstructed and contralateral kidneys compared to sham kidneys [364]. Similarly, adult rodent complete UUO models have demonstrated downregulation of AQPs 1 and 2 [184, 186] in the contralateral kidney.

Similar to recent research this study has shown that dysregulation of renal AQP expression in neonatal PUUO varies between AQP isoforms. However whereas other groups have shown a temporal change [364], this study highlights a change according to severity of

hydronephrosis. This is consistent with human studies of congenital PUJO where reduced AQP expression correlated with the severity of hydronephrosis [187] and the degree of functional impairment [424]. In the current study AQP mRNA (AQP 1-6) and protein (AQP 1-4) expression for all isoforms assessed was maintained in moderate hydronephrosis in the presence of raised intra-renal pressure. Downregulation was only noted in the severely hydronephrotic group who also demonstrated abnormalities of renal structure in the absence of raised intra-renal pelvis pressure. The presence of differential regulation of the various isoforms in this group suggests downregulation may not purely reflect kidney damage but dysregulation in response to the insult of severe obstructive hydronephrosis.

Endpoint PCR reveals that AQPs 1, 3, 4, 7, 9 and 11 are expressed at the mRNA level by normal whole rat renal pelvis. AQP5 mRNA expression was not tested as the primers available were not suitable for subsequent real time PCR. These findings are consistent with those from studies of human ureter and bladder which demonstrated AQPs 3, 4, 7, 9, 11 but not AQPs 0, 1, 2, 5, 8 and 12 to be expressed by human urothelial cells [259]. AQP1 is not expressed by either human [259] or rat urothelium but has been reported to be expressed by the blood vessel vascular endothelium of the urinary tract [249] which was confirmed by immunohistochemistry of rat renal pelvis in this study. Consistent with the results of human and rodent research, AQP3 expression was confirmed to be localised to the urothelium by immunohistochemistry in this study [249, 259]. Although previous studies have suggested AQP2 protein was expressed by rat urothelium [249] this was not confirmed in this study at either the RNA or protein level. Lack of AQP2 expression by rat urothelium is consistent however with results from human research [259]. Unfortunately, due to time constraints and the lack of suitable antibodies it was not possible to localise the expression of AQPs 4, 7, 9 and 11 in the rat renal pelvis tissue, however, the expression patterns in human urothelium would suggest that AQPs 4, 7, 9 and 11 are also likely expressed by rat urothelium [259].

Following identification of the isoforms expressed by normal rat renal pelvis, relative quantification of these AQPs in the PUUO model at 35 days of age was undertaken and results were normalised to β-actin. Although initial real-time RT-PCR suggested β-actin expression may be regulated in PUUO, further experiments using two additional reference genes involved in alternate cellular processes (PGK1 and acidic ribosomal 36B4) confirmed the discrepancy was due to cDNA loading.

AQP1 and 3 mRNA expression in the renal pelvis was significantly reduced in moderate and severe hydronephrosis compared to sham renal pelvis, while AQP11 expression was

significantly downregulated in severe hydronephrosis only. AQP4 mRNA expression demonstrated a tendency towards reduction in moderate and severe hydronephrosis, however, no significant differences between groups was detected. Assessment of greater numbers of samples to increase the power of the study would be required to gain a definitive answer. Renal pelvis AQP7 and 9 mRNA expression was unchanged in obstructive hydronephrosis compared to sham and contralateral tissue. Additionally, both AQP isoforms demonstrated generally low levels of expression compared to the other AQPs.

No changes in AQP expression by the contralateral renal pelvis were detected indicating there was no attempt to compensate for the obstructed renal pelvis. The AQP dysregulation in the obstructed renal pelvis is thus likely controlled by local rather than systemic factors.

Immunohistochemistry demonstrated that the distribution/tissue localisation of AQP3 was unchanged in obstructed compared to sham and contralateral renal pelvices at 35 days of age. All layers of the urothelium expressed AQP3 in a plasma membrane and cytoplasmic distribution across all groups assessed. Additionally, evaluation of the relative intensity of urothelial staining did not demonstrate any statistically significant differences between PUUO and sham rats. It must be remembered, however, that intensity of staining may not be a reliable indicator of the amount of antigen. DAB stain is not stoichiometric and does not follow the Beer Lambert Law, which describes the linear relationship between the concentration of an absorbing substance and absorbance [425].

These findings of renal pelvis AQP dysregulation in PUUO have significance given that urothelium is no longer considered to be an impervious membrane with a simple function of urine storage. Studies are increasingly highlighting an active role for urothelium in regulating urine composition. In a human urothelial cell culture system hyperosmolality leads to upregulation of primarily AQP3 but also AQP9 expression, associated with increased transurothelial water and urea flux along an osmotic gradient. Accordingly, in this model, non-selective blockade of AQPs with mercurials results in decreased water and urea flux [369]. Regulation of urothelial AQP2 and AQP3 expression has also been documented in rats, being significantly decreased by hypoestrogenaemia [250] and increased by dehydration [249] and partial bladder outlet obstruction [368]. Interestingly, partial bladder outlet obstruction also leads to upregulation of AQP 1 within the vasculature of bladder tissue [367].

The effect of urinary tract obstruction on the expression of AQPs by renal pelvis tissue has not before been analysed. This research demonstrated for the first time that AQPs expressed

by both the vascular endothelium (AQP1) and the urothelium (AQP3 and AQP11) are transcriptionally downregulated in the PUUO model at 35 days of age. This reduction in urothelial AQP3 and vascular endothelial AQP1 expression could seriously impair the ability of the renal pelvis to offset, by transurothelial transport and dissipation into the local capillaries, the increased fluid volume and intrarenal pressure in PUUO. Similar to renal AQP expression the reduction in renal pelvis AQP expression was related to severity of obstruction. However in the renal pelvis both AQP1 and 3 mRNA expression were downregulated in moderate hydronephrosis in the presence of raised intra-renal pelvis pressure as well as in severe hydronephrosis.

The use of a wire template in this PUUO model creates a fixed degree of obstruction. The manifestation of different severities of obstruction may indicate that, similar to human disease, factors specific to the individual determine whether the response is pathological or not. Accordingly, this data may suggest that the individual ability of the rat to maintain renal pelvis AQP expression following neonatal PUUO determines the severity of hydronephrosis developed. A failure to maintain renal pelvis AQP expression, with consequent reduced urothelial water re-absorptive capacity potentially compounds intratubular pressure rises eventually leading to severe hydronephrosis, renal damage and functional impairment. Furthermore, the degree of interstitial fibrosis is a good correlate of functional impairment [83]. Compromised function will ultimately reduce urine output and thus intra-renal pelvis pressure, as was noted in the severely hydronephrotic kidney in this study. Conversely, sustained AQP expression following PUUO may protect against continuing intra-tubular pressure rises thus manifesting in this study as mild hydronephrosis with preserved histology and normal intra-renal pelvis pressure.

Factors other than hydrostatic pressure may also influence the direction of potential transurothelial water flow across AQPs. Partial and complete ureteric obstruction causes significantly increased urine fractional excretion of sodium, reduced solute free water reabsorption [185], reduced urinary urea excretion [183] and reduced urine osmolality [185] compared to sham animals. Despite these changes in solute and water excretion, in rats with free access to water, urine from the obstructed kidney remains hyperosmotic (approximately 400 mOsmol/kgH2O) compared to plasma (approximately 295 mOsmol/kgH2O) [185] and contains substantially more urea (approximately 588 mmol/l vs 7.4 mmol/l in plasma) [183] but less sodium (approximately 78 μmol/ml vs 131 μmol/ml in plasma) [185]. When combined these factors may favour water movement across AQPs into the urine thus potentially counteracting the direction of flow due to raised hydrostatic pressure. Although

AQP 3 is regulated by gating, whereby its water permeability is reduced at acidic pH (pH ≤ 6.1) [363], this will not affect water flux in the current study as the urine pH in neonatal PUUO and sham animals is approximately 8 [407].

In order to further investigate a potential pressure reduction mechanism for AQPs, ongoing research will involve creating a neonatal mouse PUUO model using an AQP3 knockout mouse under the control of the uroplakin II promoter which is specific to urothelial cells. If, as predicted, these mice show a more severe phenotype than wild type mice, attempted rescue using an AQP3 overexpression mouse under the same promoter will be undertaken.

Table 5.6 summarises the mRNA and protein expression of the various AQP isoforms by kidney and renal pelvis in PUUO compared to sham rats. Dysregulation of expression in both kidney and renal pelvis becomes more apparent as the degree of hydronephrosis progresses.

	Mild Hydro			Moderate Hydro			Severe Hydro		
	Kidney		RP	Kidney		RP	Kidney		RP
AQP	mRNA	Protein	mRNA	mRNA	Protein	mRNA	mRNA	Protein	mRNA
1	↔	↔	↔	↔	↔	↓	↓	↔	↓
2	↔	↔	NE	↔	↔	NE	↓	↔	NE
3	↔	↔	↔	↔	↔	↓	↔	↔	↓
4	↔	↔	↔	↔	↔	↔	↔	↓	↔
6	↔		NE	↔		NE	↓		NE
7			↔			↔			↔
9			↔			↔			↔
11			↔			↔			↓

Table 5.6 Summary of AQP isoform expression following neonatal PUUO

Table summarising AQP isoform mRNA and protein expression following neonatal rat PUUO compared to sham rats, stratified according to degree of hydronephrosis. Hydro - hydronephrosis, RP - renal pelvis, G - glycosylated, NG - non-glycosylated, NE - not expressed, ↔ - unchanged expression compared to sham, ↑ - increased expression compared to sham, ↓ - decreased expression compared to sham, ▭ - AQP isoform not assessed.

The major dilemma when managing children with PUJO is deciding which require surgery and which don't. Current radiological imaging methods are not completely reliable to distinguish between these two groups [2, 26, 66]. The development of a non-invasive biomarker to aid surgical decision making would be very advantageous. Previous research has demonstrated that AQPs 1 and 2 but not AQP3 are excreted in urine [372, 381]. These

findings have been confirmed by western blotting in the current study. AQPs 1 and 2 are generally excreted in proportion with the level of renal expression [372, 381, 383], however, AQP2 excretion may be influenced by vasopressin flux [371, 384, 385]. Although urinary AQP excretion has not been measured in rat models of PUUO, human studies of PUJO have demonstrated reduced urinary excretion of both AQP1 and AQP2 by the obstructed kidney following pyeloplasty surgery [365, 386]. There have been no studies assessing the suitability of AQP1 as a pre-operative biomarker of disease severity in the obstructed kidney in either humans or rodents.

Given that the current study demonstrated reduced renal expression of AQP1 in severe hydronephrosis and reduced renal pelvis AQP1 expression in moderate and severe hydronephrosis it was anticipated that urinary AQP1 measurements would be reduced in the severely hydronephrotic PUUO rats compared to sham. Interestingly, however, urinary AQP1 excretion in this study was demonstrated by ELISA measurement to not be significantly different between PUUO rats across all degrees of hydronephrosis compared to sham rats. This contrasts with post-operative studies in humans where AQP1 excretion by the obstructed kidney was reduced compared to the normal contralateral kidney [386]. There are a number of potential reasons for the discrepancy in results:

- Large variability in the results in the current research. Significant intra and interpatient variation is a common finding with many potential biomarkers. This is because biomarkers are often excreted in health as well as disease states, and their detection may be affected by patient factors such as age, weight, and the presence of urinary tract infection [212, 213].
- Human studies used semi-quantitative methods (densitometry of western blotting) to assess urinary AQP1 excretion whereas this was a fully quantitative ELISA.
- Human studies compared urine from the obstructed kidney to urine from the normal contralateral kidney. In this study bladder urine from PUUO rats compared to sham was used for AQP1 measurement as it is a better proxy for a future non-invasive pre-operative biomarker test. Bladder urine however, is a composite of urine from both the obstructed and non-obstructed kidneys, thus any changes in excretion by the obstructed kidney will be tempered by the contralateral normal kidney. It is therefore possible that AQP1 excretion from the obstructed kidney is reduced in neonatal rat PUUO but was not detectable in this assay due to the mixing of urine in the bladder from both kidneys.

Ultimately this research demonstrated that in this rat neonatal PUUO model, urinary AQP1 measurement does not predict the severity of hydronephrosis. These results therefore cast doubt on whether urinary AQP1 measurement will be useful as a biomarker of disease in the clinical setting. Further analysis of urine samples obtained from the human study will clarify whether this is also the case in children with PUJO. Conveniently, however, valuable urine samples have been obtained and stored from this robust model of neonatal rat PUUO and will be used alongside human urine samples in future proteomics studies. These will aim to identify urinary biomarker proteins for subsequent validation which show suitability in the surgical management of children with PUJO.

Chapter 6. Childhood cross-sectional study of pelvi-ureteric junction obstruction

6.1 Introduction

Approximately 1 in 7 [5, 6, 24] neonates with antenatally detected hydronephrosis has pelvi-ureteric junction obstruction (PUJO), making PUJO one of the commonest causes of congenital urinary tract obstruction with an incidence of 1 in 1000 – 1 in 2000 live births [6, 24, 426]. Interestingly, males are affected approximately three times more frequently than females by this condition [24]. The reason for this difference is unknown. Intrinsic obstruction due to an adynamic stenotic segment at the PUJ is the most common aetiology (75% of cases) [24], where failure of peristalsis produces an incomplete, functional obstruction.

The major challenge for clinicians is deciding which of these children, who are largely asymptomatic, require a pyeloplasty to relieve obstruction. This is because two thirds of children with PUJO do not sustain renal damage or need surgery, and their hydronephrosis spontaneously stabilises or improves [26, 62, 63].

Currently, serial ultrasound and invasive isotope studies are performed to guide surgical management [24]. However their ability to accurately detect obstruction, identify children at risk of functional deterioration and predict the need for surgery is questionable. Additionally, there remains debate regarding the parameters which indicate clinically significant obstruction [2, 26, 66, 87].

Usually pyeloplasties are performed for [56]:

- differential renal function deterioration (differential function <40% or falls by >10% on serial MAG 3 renograms)
- significant hydronephrosis with a renal pelvis anteroposterior diameter >3 cm on ultrasound scan
- increasing hydronephrosis with a rising anteroposterior diameter on serial ultrasound scan
- symptomatic children

At present our understanding of the natural history of PUJO is inadequate. Available diagnostic tests cannot accurately discern whether children have PUJO that will resolve spontaneously or will persist causing functional impairment. Consequently, despite radiological monitoring, there is a risk of loss of function in the affected kidney while under observation [67].

There is significant need for greater understanding of the mechanisms underlying the clinical evolution of PUJO, and for the development of an early biomarker to distinguish between damaging hydronephrosis requiring surgery and safe hydronephrosis which might resolve spontaneously.

The underlying aetiology of PUJO is currently unknown, however, it is well-documented that there are underlying innervation [73] and myogenic abnormalities [72, 76] at the adynamic narrowed pelvi-ureteric junction. The resultant functional obstruction leads to increased pressure within the proximal urinary tract. In vivo research reveals pigs have baseline renal pelvis pressures of 4.12 +/-0.94 cmH_2O which increases in partial PUJO to 16.4 +/- 3.83 cmH2O [112]. Similarly, in humans mean renal pelvis pressure is 5.2+/- 1.3 cmH_2O [46] which rises to 10.7 cmH_2O [113] and 8.9 mmHg (approx. 12.1 cmH_2O) in high pressure chronic urinary retention and idiopathic hydronephrosis respectively [114].

Following the onset of obstruction various factors, often viewed as compensatory, may lead to a reduction in renal pelvis pressure including: tubular and renal pelvis dilatation, reduced urine production due to diminished RBF and GFR, and venous and lymphatic drainage of urine [88, 117, 121, 427, 428].

Direct transurothelial absorption of urine constituents has traditionally been thought to contribute little to the dissipation of urine volume in the obstructed kidney due to the inherent barrier function of the urothelium [427]. Urothelium lines the renal pelvis, ureters, bladder and proximal urethra and consists of an apical glycan layer plus three main cell layers [429]:

- highly differentiated single layer of apical umbrella cells connected by tight junctions which demonstrates very high transepithelial resistance
- several layers of intermediate cells
- single basal cell layer

Recently the urothelium has been recognised to have a potential role in water and solute homeostasis. Although it is well known that human urine composition changes from the

renal pelvis to the bladder [366], while bears reabsorb their daily urine output during hibernation [430], the possible underlying mechanisms are only just being described.

Aquaporins have an established role in the transmembrane movement of water [237]. Their identification in mammalian urothelium [249, 259] alongside sodium [431], potassium [432] and urea transporters [433] provides evidence of potential routes for the urothelium to achieve transport functions.

As discussed previously, AQP2 and 3 expression is upregulated in rat bladder urothelium by dehydration [249] and partial bladder outlet obstruction [368] and downregulated by hypo-oestrogenaemia [250]. AQP regulation is not confined to those detected in urothelium, vascular expression of AQP1 within rat bladder is also increased following partial bladder outlet obstruction [367]. The data presented in Chapter 5 confirms the presence of AQPs 1, 3, 4, 7, 9 and 11 in rat renal pelvis and supports the dysregulation of AQP expression in urinary tract pathology. Both AQP3 and AQP 1, which are expressed by the urothelium and suburothelial vascular-endothelial cells respectively, are significantly transcriptionally downregulated in the obstructed renal pelvis following neonatal rat PUUO.

Human urothelial cell cultures express AQPs 3, 4, 7 and 9 at the protein level [259] and demonstrate regulation of predominantly AQP3, but also AQP9, expression in response to variations in osmolality. In fact, in the presence of an osmotic gradient, the permeability of differentiated human urothelial cell constructs to water and urea significantly increases following hyperosmolar pre-conditioning compared to controls. Significantly, transurothelial permeability decreases following non-selective AQP blockade, corroborating a role for AQPs in transurothelial transport [369].

The childhood study of PUJO described in this chapter aims to build on the in vitro human urothelial cell work by Rubenwolf *et al*., and enhance the animal work reported in chapter 5. A major aim being to investigate renal pelvis urothelial AQP expression as the mechanistic link explaining why some children with PUJO have ‘safe’ hydronephrosis and others ‘damaging’ hydronephrosis. Additionally, these complementary rodent and human studies aim to investigate AQPs as a potential biomarker to aid early detection of those children with damaging hydronephrosis who require prompt surgery to protect kidney function.

A biomarker is defined as “a characteristic that is objectively measured and evaluated as an indicator of normal biological processes, pathogenic processes or pharmacological responses to a therapeutic intervention” [434]. Many potential urinary biomarkers including cytokines,

growth factors, chemokines, tubular enzymes and tubular transport proteins have been investigated in children with PUJO. Although a number have shown promise, no single biomarker or collection of markers has been identified and implemented to guide selection of patients for surgery. The urine biomarkers previously assessed in human bladder urine samples are presented in Chapter 1,Table 1.6.Those biomarkers with conservatively managed hydronephrosis as comparator are most useful in terms of discerning which children require surgery in the clinical setting, however, many studies have used healthy children only as controls. A recent systematic review of urine and serum biomarkers in 380 patients undergoing pyeloplasty for PUJO failed to draw any firm conclusions, citing a large range of occasionally opposing results and issues with study design [214].

This finding is echoed by the predictive safety testing consortium (PTSC) who in 2006 advised that good biomarkers should be: [435]

- present in peripheral body tissue and/or fluid (e.g. blood, urine, saliva, breath or cerebro-spinal fluid)
- easy to detect or quantify in assays that are both affordable and robust
- their appearance must be associated as specifically as possible with damage of a particular tissue preferably in a quantifiable manner (in terms of drug toxicity testing)

Despite meeting the above criteria many potential biomarkers from the literature have failed to achieve further development because studies are scientifically inadequate with underpowered or biased studies and/or inadequate description of methods, control groups and statistical analyses [435]. Other problems encountered in biomarker discovery are those of significant intra and inter patient variation, biomarker presence in both health and disease states with coinciding reference values, and variation with patient age and factors such as urinary tract infection and concurrent renal disorders [212, 213]. Consequently, finding a biomarker with high sensitivity, specificity and predictive value is difficult [116]. This study aims to provide robust scientific data to either confirm or refute AQP 1 as a potential biomarker of PUJO.

Four AQPs are known to be excreted in human urine. AQPs 1 and 2 are both detected on western blotting of human urine [365, 386] and in rat studies their excretion generally reflects the level of renal expression [372, 381, 383]. The excretion of AQPs 5 and 7 has been demonstrated on proteomic studies only [387]. Urinary excretion of AQPs 1 [386] and AQP 2 [365] by the obstructed kidney is significantly reduced (64% and 54% respectively)

compared to the normal contralateral kidney following pyeloplasty in childhood PUJO. This reduction in expression is noted for up to 4 days post-operatively and is associated with a marked polyuria and significant decrease in urine osmolality from the obstructed kidney which persists for at least 4 days post-operatively [365]. The potential of urinary AQPs as biomarkers to predict the need for surgery in PUJO has not previously been analysed. Consequently, there are no published studies investigating urinary AQP levels either pre-operatively in children undergoing pyeloplasty or in those under monitoring for hydronephrosis. Moreover, normal AQP levels in children are unknown.

This chapter outlines the design and implementation of a childhood study of PUJO and all preliminary results.

The aims of this study are to:

- Measure the distribution and quantity of aquaporins in the lower urinary tract in childhood PUJO
- Establish the urinary aquaporin profile in damaging (operated) and safe (non-operated) PUJO in children

Additional data is presented in a separate section of this Chapter demonstrating normal human urinary tract AQP expression and urinary excretion using samples unrelated to the childhood study.

6.2 Methods – childhood cross-sectional study of PUJ obstruction

This single-site clinical cross-sectional study recruiting children with PUJO at Bristol Children's Hospital commenced recruitment in November 2014 and is currently ongoing. Study commencement followed completion of the IRAS application (IRAS ID: 131160) and lengthy consultation with the South West - Central Bristol Research Ethics Committee (REC) and the local University Hospitals Bristol Research and Innovation department (R + D). Approval for the study to commence was given by the South West - Central Bristol Research Ethics Committee on the 2/9/14 (REC No: 14/SW/1027) and by UH Bristol Research and Innovation department on 29/9/14 (R + D number: CH/2014/4699). Permission has been given for the study to run until 31/7/20. The University of Bristol Research and Enterprise Development team has been significantly involved in the implementation of the study and the University of Bristol is the study sponsor. This study is

being conducted in accordance with the Research Governance Framework, Good Clinical Practice and NHS Trust policies and procedures.

6.2.1 Study protocol

This study involves the recruitment of three groups of children (aged 0-15 years inclusive) attending Bristol Children's Hospital as detailed below (Figure 6.2). See appendix 3 (Section 10.3) for copies of the study protocol, patient information leaflets, consent forms, and GP letters.

6.2.1.1 Group 1 – Children undergoing pyeloplasty for PUJ obstruction

Group 1 consists of children undergoing an open or laparoscopic pyeloplasty as treatment for PUJO at the Bristol Children's Hospital. Potential participants are identified by the operating consultant surgeon and given appropriate child and parent information leaflets detailing the study. Consent for the study is then obtained by the chief investigator (member of the research team) on the day of surgery after the surgeon has explained the surgical procedure. The GP is informed by letter of the child's participation in the study.

Following enrolment to the study, on the day of hospital admission, the operative data collection form documenting the child's demographic details, medical history and the results of pertinent radiological tests is completed. Prior to surgery a urine specimen is collected where possible either into a specimen pot or from the nappy in the younger child.

The pyeloplasty is performed under general anaesthetic either laparoscopically or as an open procedure in the usual manner based on the surgeon's preference and the best interests of the child.

During the pyeloplasty the following procedures are performed, and samples obtained:

- A urine sample is taken from the bladder catheter at the start of the operation for urinary aquaporin measurement.
- Intra-renal pelvis pressure is measured using a Rocket® spinal manometer (# R55990, Rocketmedical, Washington, England) connected to the needle from a 22G cannula (BD Venflon™ Pro, #393202, Becton Dickinson, Surrey, UK) (Figure 6.1) which is inserted into the renal pelvis through tissue that will be subsequently removed as part of the procedure.
- An intra-renal pelvis urine sample is obtained for urinary aquaporin measurement.

- Samples of renal pelvis and ureter obtained from the narrowed pelvi-ureteric junction (removed as part of the pyeloplasty procedure) are obtained for aquaporin analysis.
- The operative data collection form is completed by the operating surgeon at the end of the procedure detailing the procedure performed, the kidney pressure and the samples collected.

Post-operatively a urine sample is collected every 24 hours until the child is discharged from hospital (usually within 2-5 days). Initially this is taken from the bladder catheter collection bag, however once the catheter is removed voided samples are collected either into a specimen pot or from the nappy.

No changes to the routine post-operative radiological and clinic follow-up have been made for the study. The length of post-operative follow-up varies but is usually between 3 months and 2 years. When the child is discharged from clinic follow-up participation in the study concludes (Figure 6.2).

The initial requirement for the study was that at each outpatient visit the child would provide a urine specimen for aquaporin measurement and a follow-up data collection form would be completed. Unfortunately, it has proved exceptionally difficult to identify these patients when they return for follow-up, especially as many are reviewed in outreach outpatient clinics across the South-West of England. Additionally, transport of urine samples on ice from these clinics for processing in Bristol would take many hours and would likely adversely affect the results of the study. Consequently, follow-up samples have not been obtained from any of the group 1 patients recruited thus far.

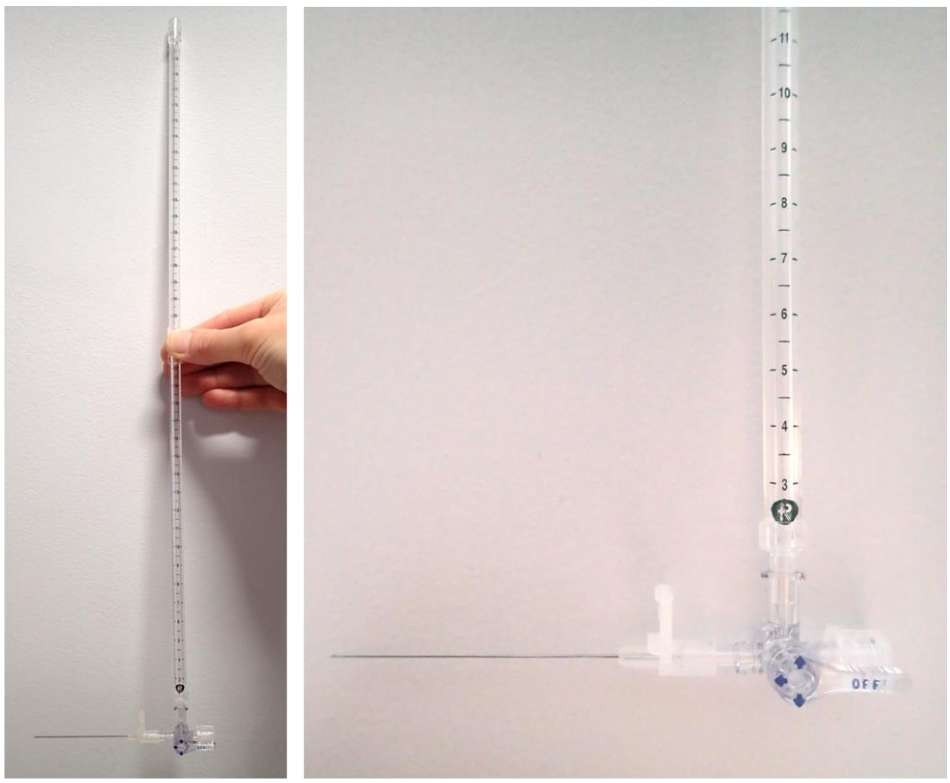

Figure 6.1 Equipment used to measure intrarenal pelvis pressure in group 1 patients

A Rocket® Spinal manometer connected to the needle from a 22G cannula (Venflon™) is inserted into the dilated renal pelvis while the child is under general anaesthetic prior to performing the pyeloplasty. When performing pressure measurement, the needle is inserted keeping both the needle and hub of the manometer at the level of the renal pelvis while the manometer is perpendicular to the renal pelvis.

6.2.1.2 Group 2 – Children with hydronephrosis not requiring surgery

Group 2 consists of children with hydronephrosis but no evidence of other causes of urinary tract obstruction. These children are identified when they attend urology outpatient clinics. The family are provided with patient information leaflets on arrival in clinic and the consulting clinician obtains consent for inclusion in the study if the family are agreeable. Following enrolment into the study a urine sample is obtained and a data collection form completed at all clinic appointments until they are discharged from follow-up. The expected length of follow-up and thus study participation for these children is up to 4 years. It is anticipated that some children from group 2 may move into group 1 if they have progression of hydronephrosis and require a pyeloplasty for PUJO (Figure 6.2).

6.2.1.3 Group 3 – Children with normal kidneys

Group 3 consists of children with no kidney tract abnormalities attending general surgical or urology outpatient clinic for consultation regarding unrelated problems. The family are

provided with patient information leaflets on arrival in clinic and the consulting clinician obtains consent for study inclusion if the family wish to take part. Following enrolment into the study a urine sample is obtained, and a data collection form completed. This concludes the involvement of this group of children in the study (Figure 6.2).

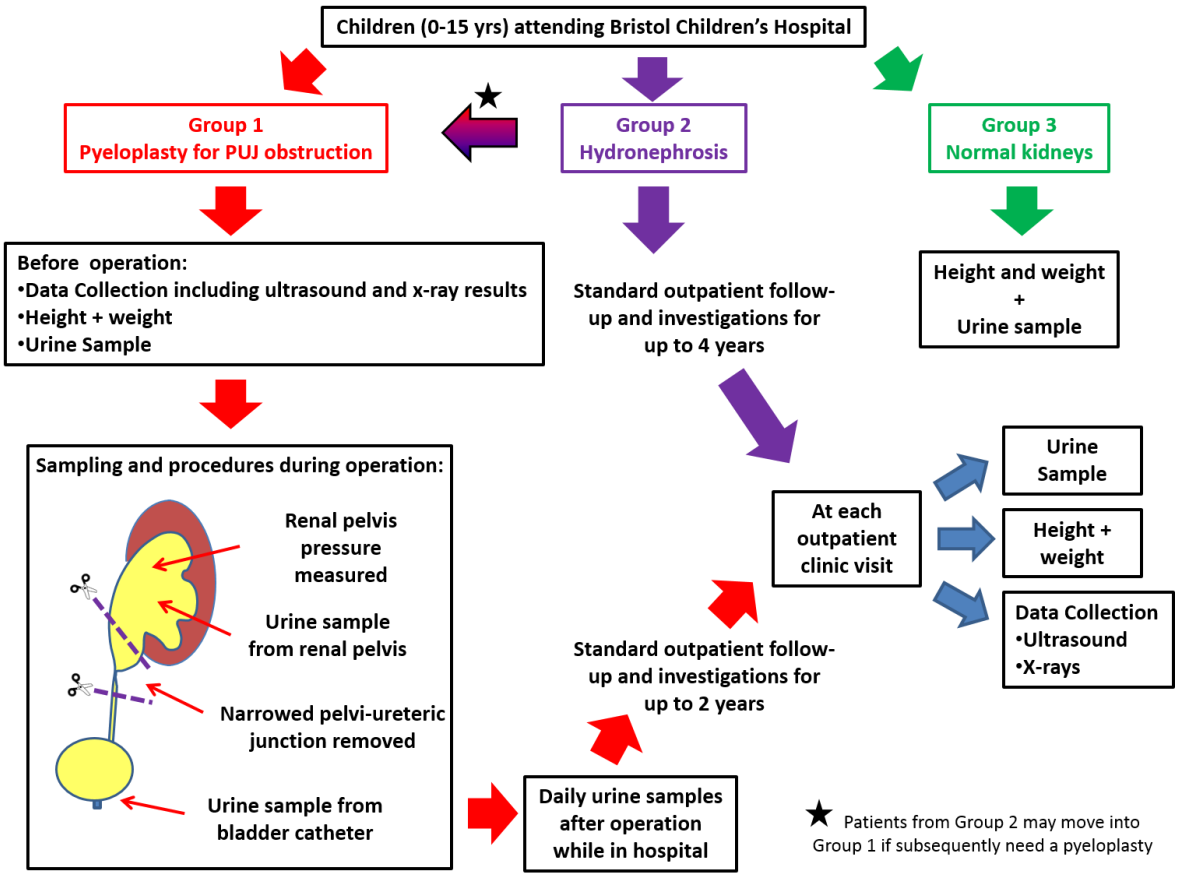

Figure 6.2 Summary of childhood cross-sectional study of pelvi-ureteric junction obstruction

6.2.1.4 Inclusion criteria

Inclusion criteria into the study include:

Group 1 - Children placed on a planned waiting list for a laparoscopic or open pyeloplasty.

Group 2 - Children with hydronephrosis but no evidence of other causes of urinary tract obstruction other than PUJO attending urology outpatient clinics

Group 3 - Children with no kidney tract problems attending general surgery/urology outpatient clinics for an unrelated issue.

6.2.1.5 Exclusion criteria

Exclusion criteria from the study include:

Group 1 - Children with other causes of urinary tract obstruction in addition to PUJO.

Group 2 - Children with differential function <40% on MAG 3 renogram of the hydronephrotic kidney**.** Children with other causes of urinary tract obstruction other than PUJO.

Groups 1-3 - Children taking medicines which affect kidney function or act on the kidney. Children who have concurrent intrinsic kidney disease.

6.2.1.6 Consent for study participation

Informed consent from at least one parent/carer with parental responsibility is required for all groups of children recruited. Consent is obtained for group 1 patients by the chief investigator. Consent for groups 2 and 3 patients is obtained by the treating NHS clinician. Older children may give assent (in addition to parental consent) to be included in the study. Due to the nature of the study, consent is obtained for the removal (consent under common law), storage (consent under Human Tissue Act), and use (consent under Human Tissue Act) of human tissue. Consent is also gained for access to medical records. Families can choose whether they will give generic consent for the tissue and urine samples to be used for ongoing/future research projects or specific consent just for this study. Thus far all families have given generic consent. See appendix 3 (section 10.3.3) for copies of the consent forms used in the study.

6.2.2 Ethical approval and study amendments

In this study the initial IRAS application was followed by a meeting with the South West - Central Bristol Research Ethics Committee in July 2014. A provisional favourable opinion was given provided that certain modifications to the study protocol were made. The major issue was the inclusion in the original study protocol of a Tru-cut® biopsy from the obstructed kidney for aquaporin analysis during the pyeloplasty. Following discussion with the Research Ethics Committee this was removed from the study protocol and after some other minor adjustments the study was approved in November 2014.

During the study any change to the protocol or study paperwork was subject to approval of an amendment which was submitted to the Research Ethics Committee and Research and

Innovation departments. Details of the requested amendments were submitted via the IRAS system and required authorisation by the study sponsor. Amended copies of the study protocol and/or study paperwork were also submitted complete with updated version numbers and dates. Depending upon the particular amendment, recruitment to the study sometimes needed to halt while approval was awaited. Table 6.1 details all amendments submitted during the study.

Date	Amendment type	Committee /Department	Reason	Outcome
6.11.14	Substantial	REC	Change of informed consent for group 1 patients to require only 1 rather than both parental signatures. Approval to use urinary tract tissues not suitable for transplant (obtained as part of another ethically approved study) to develop molecular biological techniques for this study. Correction of mistakes on patient information leaflet and study protocol.	Approved
31.5.15	Substantial	REC	Appointment of Acting Chief Investigator during a period of maternity leave for the Chief Investigator	Approved
16.9.15	Substantial	R+D	Appointment of Acting Chief Investigator during a period of maternity leave for the chief Investigator	Approved
15.6.16	Minor	REC R+D	Re-instate original Chief Investigator following maternity leave	Approved

Table 6.1 Study amendments

During the study 2 substantial and 1 minor amendments have been submitted to the Research Ethics Committee and the UH Bristol Research and Innovation Department

6.2.3 Study documentation

The implementation of a new study requires the design and production of a significant amount of study specific and supporting documentation which is included in appendix 3 (section 10.3). Documentation utilised within this study includes:

- Study protocol which details all aspects of how the study is conducted
- Specific patient information leaflets for adults, young people and children for each of the three groups
- Specific consent forms for participation in the study including assent forms for older children for each of the three groups
- Data collection forms for each of the three groups
    - Group 1 – operative case report forms and post-operative case report forms
    - Group 2 - recruitment case report forms and follow-up case report forms
    - Group 3 – case report forms
- GP letter detailing inclusion in the study which is dispatched for each child recruited to group 1

6.2.3.1 Investigator site file

In accordance with the principles of ICH-GCP (International Conference on Harmonisation – Good Clinical Practice) certain essential documents must be established prior to onset of the study, maintained throughout the study and retained following the completion of the study. This is to ensure the conduct of the study and the quality of data produced can be easily evaluated. These documents are collectively held within an investigator site file (ISF) which is maintained by the principal investigator at the study site. The principal investigator for this study is Mr Mark Woodward, Consultant Paediatric Surgeon, Bristol Royal Hospital for Children. Documentation contained within the investigator site file for this study includes:

- Details of study personnel including up to date Curriculum Vitae's and records of GCP training
- Site staff log and delegation of study tasks
- Subject screening and recruitment record enabling the calculation of recruitment rates
- Log of documentation associated with each recruit and storage of all completed consent forms

- Record of retained urine and tissue samples and their storage location
- Details of research safety reporting
- Copies of current and previous versions of study specific documentation such as patient information leaflets, consent forms, GP letters, study protocol
- Copies of the Research Ethics Committee and Research and Innovation Department approvals for commencement of the study
- Record of amendments made and dates of approval by the Research Ethics Committee and the Research and Innovation Department

Data is being collected and retained in accordance with the Data Protection Act 1998.

6.2.3.2 EDGE clinical management system

Local recruitment data is uploaded to the EDGE clinical management system to enable real time assessment of study progress.

6.2.4 Sample collection

6.2.4.1 Group 1

Tissue and urine samples are obtained with consent and appropriate ethical approval on the day of surgery. The renal pelvis and ureter samples are dissected out from the narrowed pelviureteric junction resected at the time of pyeloplasty (Figure 6.3). The samples are placed into separate collection tubes in ice cold PBS, put immediately onto ice and transferred to the laboratory. The tissues are washed 5 times in ice-cold PBS. For each renal pelvis and ureter specimen at least 2 samples are snap frozen in liquid nitrogen and stored at -80 °C for RNA and protein analysis while 1 renal pelvis sample and 1 ureter sample are placed in 10% neutral buffered formalin at 4°C for 24 hours before paraffin embedding.

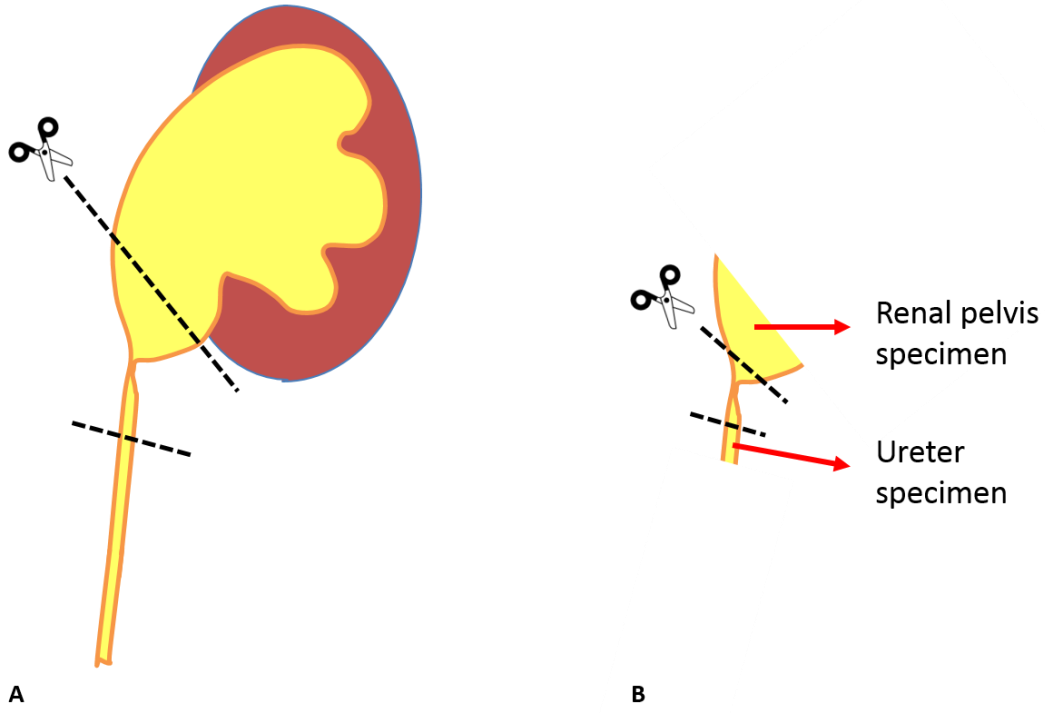

Figure 6.3 Human tissue sample preparation for storage and formalin fixation

The narrowed pelvi-ureteric junction is resected (as marked by dotted line) by standard technique during the pyeloplasty (A). The resected specimen is further cut (as marked by dotted line) to generate two separate specimens for aquaporin analysis; The renal pelvis proximal to the narrowing and the ureter distal to the narrowing (B). The renal pelvis and ureter specimens are immediately cut into at least 3 samples. Two samples are snap frozen in liquid nitrogen and stored at -80°C for later RNA and protein extraction. At least one sample from each renal pelvis and ureter specimen is placed into 10% neutral buffered formalin at 4 °C.

Fresh urine samples obtained from the bladder (voided pre-operatively and/or by urinary catheter intra-operatively) and the obstructed renal pelvis (aspirated intra-operatively) are collected into 50 ml centrifuge tubes and placed immediately onto ice and transferred to the laboratory. Chapter 2 (section 2.17.2) contains details of further processing procedures.

6.2.4.2 Group 2

A single urine sample from a patient recruited to group 2 was obtained intra-operatively by bladder catheter on the 20/9/16 and collected into a 50 ml centrifuge tube, placed immediately onto ice and transferred to the laboratory. This patient was due to have a pyeloplasty for suspected PUJO however at operation was noted to have a grossly hydronephrotic kidney with ectopic ureteric insertion and so underwent a nephrectomy. This patient had initially been recruited to group 1 but was transferred to group 2 following the operative findings. Further samples for this group however will be collected at routine outpatient clinics in the same manner as those for group 3 (see below).

6.2.4.3 Group 3

Urine samples for children recruited to group 3 were obtained with consent and appropriate ethical approval at routine outpatient clinic appointments. Fresh voided urine samples were collected into 50 ml centrifuge tubes and placed immediately onto ice and transferred to the laboratory. Chapter 2 (section 2.17.2) contains details of further processing procedures.

6.2.5 Outcome measures

6.2.5.1 Primary outcome measure

The primary outcome measure is the first bladder urine aquaporin level when recruited into the study. This may be collected intra-operatively for group 1 patients. Comparison of this first aquaporin level between children with PUJO requiring surgery (group 1) and children with non-obstructive hydronephrosis (group 2) will enable assessment of whether urine aquaporin levels are good biomarker to aid surgical decision making in PUJO.

Additionally, assessment of the urine aquaporin levels in children with no kidney abnormality will enable us to determine whether age, gender or size has any impact on normal urine aquaporin levels.

6.2.5.2 Secondary outcome measures

- Tissue (renal pelvis and ureter) aquaporin levels
- Intra-operative renal pelvis urine aquaporin levels
- Kidney pressure (measured intra-operatively)
- Pre-operative split kidney function (measured by MAG 3 renogram or DMSA)
- Post-operative urine aquaporin levels in group 1 patients
- Follow-up urine aquaporin levels in group 2 patients

6.2.6 Study sample size

The primary outcome will be analysed by comparing group 1 and group 2 urine aquaporin levels. It is known that approximately 20 children per year undergo a pyeloplasty for PUJO at the Bristol Children's Hospital. It is anticipated approximately 75% of these children will be recruited which equates to 30 children over 2 years. Recruitment to group 2 will be faster as children suitable for inclusion are seen in greater numbers throughout the year. Children will therefore be recruited in a 4:1 manner with 4 children in group 2 to every child in group

1. This method of recruitment will increase the sample size and power of the study while keeping the number needed to recruit in group 1 achievable within an appropriate timescale.

Current studies suggest a target difference of 30% between groups 1 and 2 is feasible. It is currently unclear what degree of variability there is in the data. If the target difference is hypothesized to be to 0.75 of the standard deviation of the data then with a 4:1 recruitment method, a significance of 5% and a power of 80% it is estimated the minimum number of children to be recruited is:

- Group 1: 18 children
- Group 2: 70 children

Recruitment of children in group 3 (no kidney abnormality) is necessary to determine normal urine aquaporin levels across ages 0-15 years. For simplicity the aim is to recruit similar numbers to group 2.

In view of the fact it is estimated up to 30 patients could be recruited over two years the target is to recruit 30 children to group 1 and 80 children to each of groups 2 and 3.

6.2.7 Statistical analysis

Data is presented as mean +/- SEM except for the graphical representation of renal pelvis pressure which is presented as the median value due to the non-parametric appearance of the data. Any data group containing only a single result was not included in statistical analyses. Comparison of two groups was performed using an unpaired two tailed t-test. Correlation of results was assessed using an XY scatter plot and Pearson's correlation test. $P<0.05$ was accepted as statistical significance.

6.3 Methods - Western blotting and immunohistochemistry of human urinary tract samples unrelated to the childhood study

All western blotting and immunohistochemistry results presented in this chapter were performed on tissue obtained from human kidneys with their associated renal pelvis and ureter which had been prepared for transplant but were later deemed clinically unsuitable. These kidneys were collected by our laboratory (Academic Renal Unit), with full consent for research, as part of another NHS REC approved study (Ref: 06/Q2002/101).

All urine samples used in western blotting results presented here were normal adult urine samples processed by ultrafiltration to concentrate the AQP 1 protein.

RT-PCR, western blotting, immunohistochemistry and urine ultrafiltration techniques were all undertaken as described in the methods section of Chapter 2.

6.4 Results - childhood cross-sectional study of PUJ obstruction

6.4.1 Demographic data of study population

To date, all families approached for recruitment into groups 1 and 2 have participated in the study giving a 100% recruitment rate. Study participation, of those approached, for group 3 patients is currently slightly lower at 85%, where 11 out of 13 families agreed to take part. The reasons given for non-participation in potential group 3 recruits were, lack of time following the outpatient clinic appointment and the child not being toilet-trained.

When comparing general recruitment for groups 1-3 a male predominance was noted across all groups but particularly so for group 3 children (Figure 6.4A). Group 1 contains a statistically significantly lower age group than group 3. The mean age of group 1 children at recruitment and surgery was 17.7 +/- 6.6 months compared to 7 years and 5 months +/- 16 months for group 3 children.

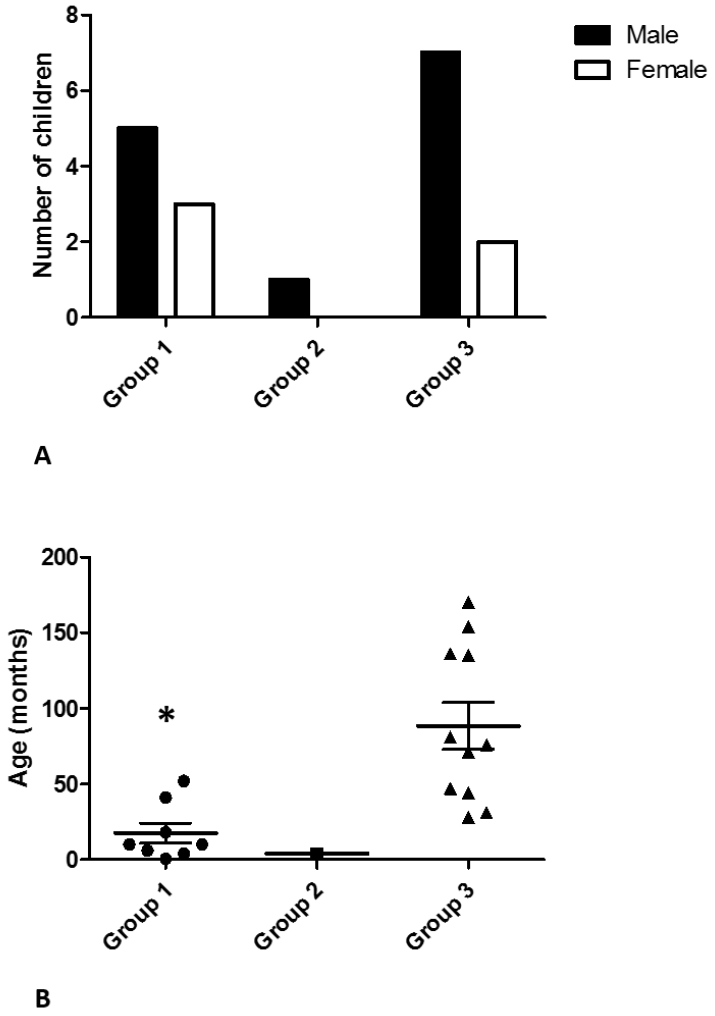

Figure 6.4 Demographic details of study population

Bar chart comparing the gender distribution of children recruited to the 3 groups in the PUJO study. A male predominance in each group was demonstrated (A). Vertical scatter plot comparing the ages of children recruited to each group of the study population. *p = 0.0018 compared to group 3. Individual data points and mean +/- SEM are presented (B).

6.4.2 Group 1 results

To date 8 children have been recruited to group 1. The male to female ratio in this group was 5:3 with a mean age at recruitment and surgery of 17.7 +/- 6.6 months (Figure 6.4). An antenatal diagnosis of hydronephrosis was made in 89% (7/8) of children, while 1 child presented at 7 months of age with pyelonephritis.

Three-quarters of children had left sided PUJO which in 2 children was associated with a solitary left kidney. One child had right sided PUJO while the remaining child presented with bilateral disease (Figure 6.5A).

Most children underwent surgery due to increasing hydronephrosis (4/8), while 3/8 children had a renal pelvis APD ≥30 mm. The remaining child underwent a pyeloplasty for reduced function on the affected side (Figure 6.5C). Overall left sided pyeloplasties were performed in three-quarters (6/8) of children and no child underwent bilateral pyeloplasty (Figure 6.5D). All children underwent an open dismembered Anderson-Hynes pyeloplasty.

Half of all children (4/8) experienced at least one urinary tract infection prior to surgery (Figure 6.5B), three-quarters of these children (3/4) were taking antibiotic prophylaxis at the time of surgery. Overall, at the time of surgery, half of children (4/8) were taking antibiotic prophylaxis.

None of the children were taking any medication other than antibiotic prophylaxis, gavison and abidec vitamin supplements.

The mean renal pelvis APD on the last pre-operative ultrasound scan was 30.2 +/- 2.9 mm (Figure 6.6A). Pre-operative calyceal dilatation of the obstructed kidney was noted in 7/8 children while cortical thinning was noted in 3/6 children. In 2 children the presence or absence of cortical thinning of the obstructed kidney was not documented (Figure 6.6B). The last pre-operative ultrasound scan was performed a mean of 3.3 months (+/- 1.1 months) prior to the surgery.

Three-quarters of children (6/8) underwent MAG 3 renogram at a mean of 7.3 months (+/- 2.1 months) prior to surgery. Five out of six children demonstrated retained split function in the obstructed kidney. In one child the split function on MAG 3 renogram was 30% in the obstructed kidney. In the remaining 2/8 children, 1 had a DMSA scan which demonstrated equal split function, and the other child underwent early pyeloplasty without pre-operative radioisotope renography due to substantial bilateral hydronephrosis. All MAG 3 renograms demonstrated delayed drainage and obstructed systems with either type 2 or type 3b curves (Table 6.2).

A pre-operative MCUG was performed in 5/8 children. This study was normal in 3 children and demonstrated concurrent VUR in 2 children (Table 6.2).

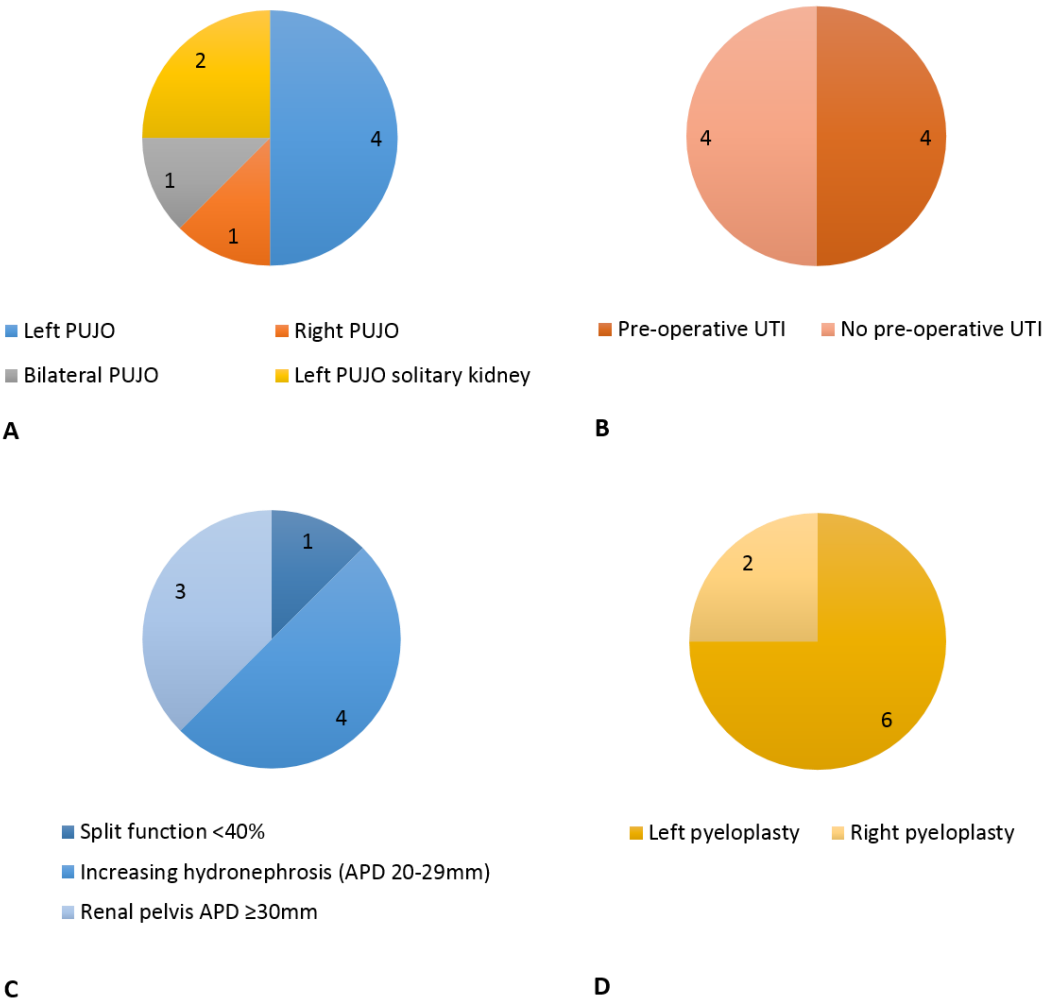

Figure 6.5 Group 1 demographic details

Pie charts demonstrating details regarding group 1 patients: The laterality of PUJO (A). The presence or absence of pre-operative urinary tract infections (B). The main radiological indication for surgery (C). The laterality of the open pyeloplasty performed (D).

Intra-operative bladder and obstructed renal pelvis urine samples along with renal pelvis and ureteric tissue specimens were collected from all children. The renal pelvis pressure of the obstructed kidney was measured in all children and had a median value of 1 cmH_2O and range 0-20 cmH_2O (Figure 6.7A).

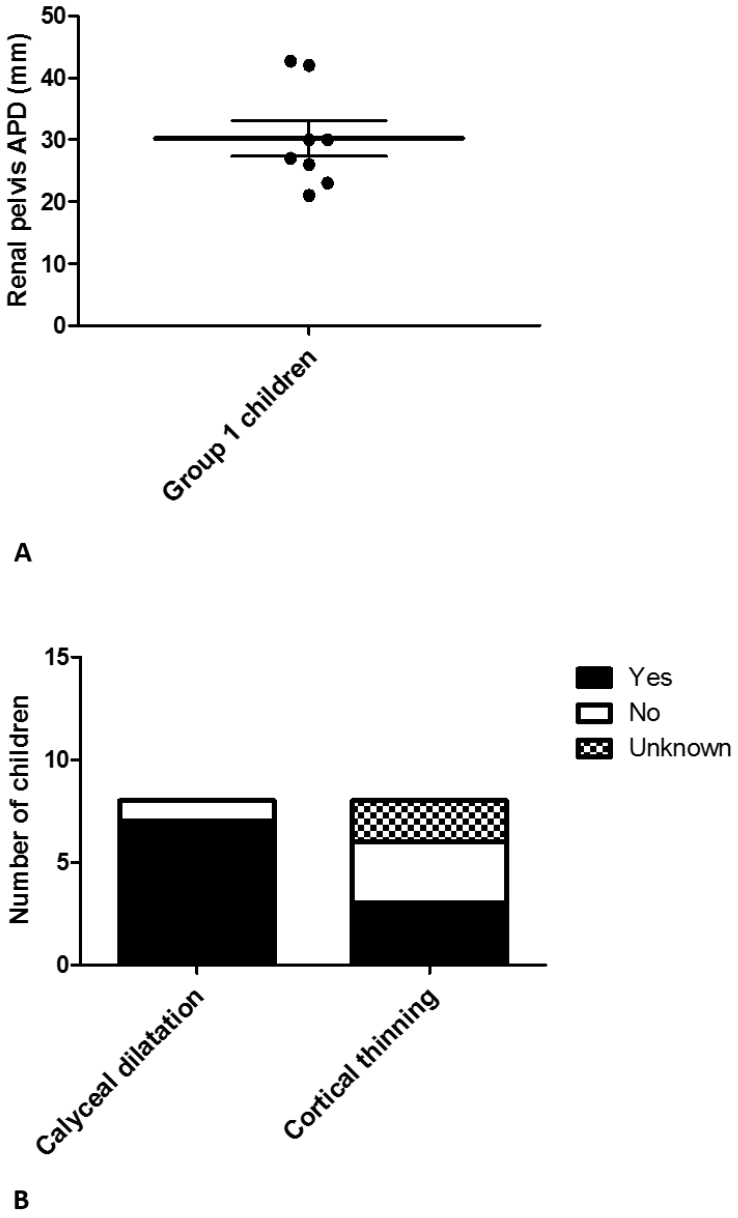

Figure 6.6 Pre-operative renal ultrasound scan features of children in group 1

Vertical scatter plot demonstrating renal pelvis APD measurements of the obstructed kidney prior to pyeloplasty in children recruited to group 1 of the PUJO study. Individual data points and the mean +/- SEM are presented (A). Stacked bar chart presenting the number of children with calyceal dilatation and/or cortical thinning of the obstructed kidney prior to pyeloplasty in children recruited to group 1 of the PUJO study. In 2 children the presence or absence of cortical thinning on the pre-operative renal ultrasound scan was unknown (B).

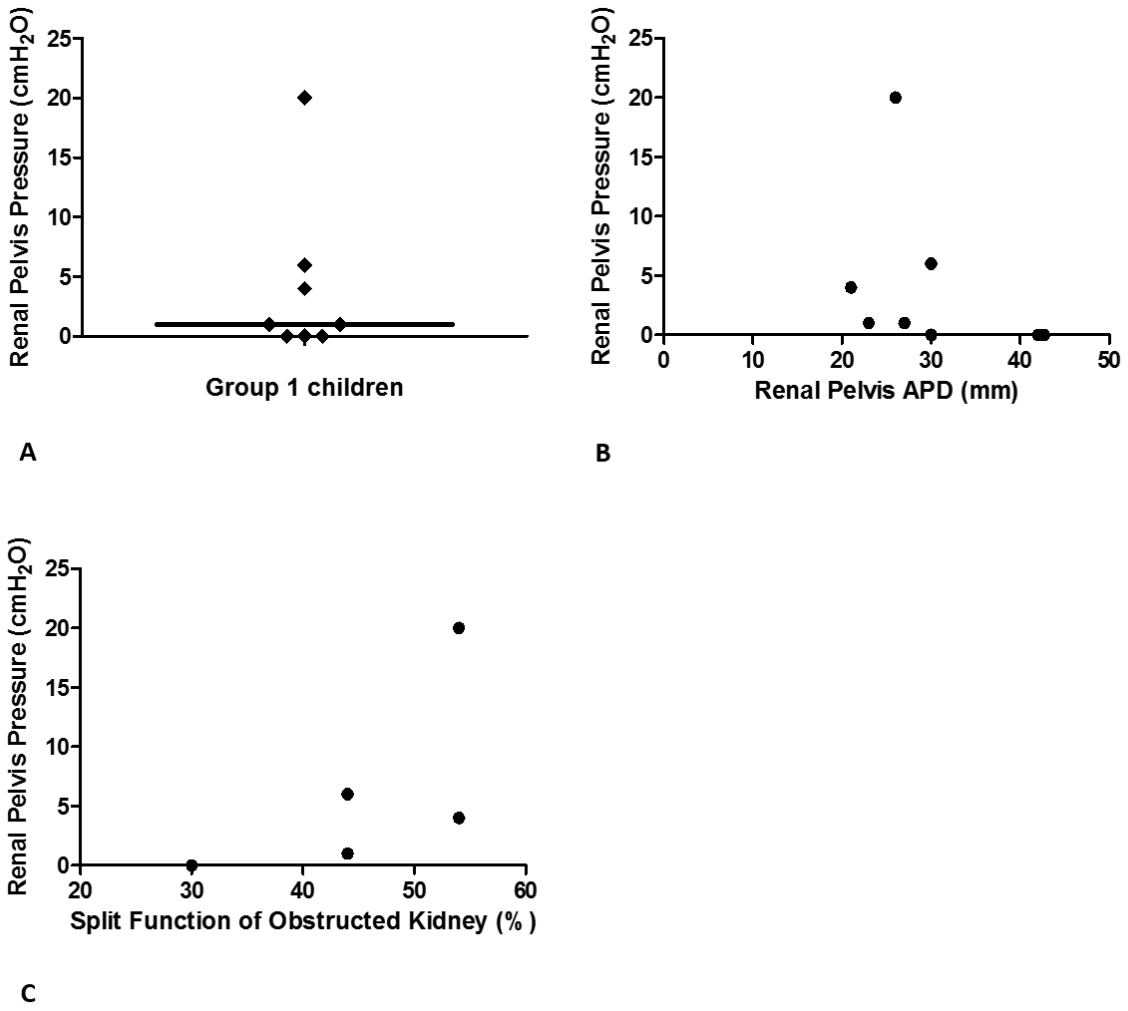

Figure 6.7 Intra-renal pelvis pressure measurements from group 1 children

Vertical scatter plot illustrating the renal pelvis pressures measured in children undergoing pyeloplasty in group 1 of the PUJO study. Individual data points and the median value are presented (A). Scatter plot of renal pelvis APD versus renal pelvis pressure of the obstructed kidney for children in group 1 with PUJO. No correlation was detected between renal pelvis APD and renal pelvis pressure $R^2 = 0.1176$ (B). Scatter plot of the split function (MAG 3 renogram or DMSA) versus renal pelvis pressure of the obstructed kidney for children in group 1 with PUJO. No correlation was detected between the parameters $R^2 = 0.4056$. Two results were omitted as the child had a solitary kidney with a split function value of 100% (C).

No correlation was detected between the intra-operative renal pelvis pressure and either the pre-operative sonographic renal pelvis APD measurements ($R^2 = 0.1176$, (Figure 6.7B) or the pre-operative split function on radioisotope renograms ($R^2 = 0.4056$, Pearson's correlation coefficient) (Figure 6.7C). Three children were excluded from the analysis of renal pelvis pressure versus split renal function: One child had not had pre-operative radionuclide imaging and 2 children had solitary kidneys rendering their split function at 100% which would confound the results. Table 6.2 summarises the demographic details and results for group 1.

ID	Sex	Age at surgery (mths)	Antenatal diagnosis	Unilateral or bilateral PUJO	Pre-operative UTI	Pre-operative APD of operated kidney by USS (mm)	Pre-operative split function of operated kidney on radioisotope renography (%)	Type of curve (O'Reilly) on MAG 3 renogram	MCUG	Pyeloplasty	Renal Pelvis Pressure (cmH_2O)
1	M	10	Y	Unilateral - SK	Y	27	100	3b	Normal	Left	1
2	F	6	Y	Unilateral	Y	23	44 (DMSA)	N/A	Left grade 2 VUR	Left	1
3	M	0.5	Y	Bilateral	Y	42.7	None	N/A	Bilateral PUJO + grade 4 VUR	Right	0
4	F	10	Y	Unilateral	N	21	54	2	Normal	Left	4
5	M	18	N	Unilateral	Y	30	44	2		Left	6
6	M	41	Y	Unilateral	N	26	54	3b		Left	20
7	F	4	Y	Unilateral - SK	N	42	100	3b		Left	0
8	M	52	Y	Unilateral	N	30	30	2	Normal	Right	0

Table 6.2 Demographic details of group 1 recruits

Demographic details of the 8 children recruited pre-operatively to group 1 of the PUJO study. APD – anteroposterior diameter of renal pelvis, DMSA – dimercaptosuccinic acid, F – female, MAG 3 – mercapto acetyl tri glycine, M – male, MCUG – micturating cystourethrogram, N – no, PUJO – pelvi-ureteric junction obstruction, SK – solitary kidney, USS – ultrasound scan, UTI – urinary tract infection, VUR – vesico-ureteric reflux, Y – yes.

6.4.3 Group 2 results

A single child was recruited to group 2. A four- month old male infant with an antenatal diagnosis of hydronephrosis. He was recruited during his admission where he underwent a left nephrectomy for a grossly dilated poorly functioning kidney with an ectopic ureter. Split function of the hydronephrotic kidney was 11% on pre-operative DMSA renography. An intra-operative bladder catheter specimen at the commencement of surgery was obtained.

6.4.4 Group 3 results

Eleven patients were recruited while attending routine general surgery/urology outpatient clinics however only 9 were able to give a urine sample at the time of clinic attendance (Table 6.3). None of the children were taking any medication. The recruited children showed a male preponderance similar to group 1. Mean age at recruitment and provision of the urine sample was 7 years and 5 months +/- 16 months (Figure 6.4).

ID	Sex	Age	Reason for clinic attendance
1	M	2y 4m	Undescended testis
2	M	11y 4m	Post-op hypospadias repair
3	M	3y 8m	Undescended testis
4	M	14y 2m	Buried penis correction and circumcision for BXO
5	M	6y 9m	Physiological phimosis
6	M	6y 4m	Post-op drainage of peri-anal abscess
7	F	12y 10m	Vaginal reflux
8	F	11y 3m	Bartholins cyst
9	M	5y 11m	Post-op meatotomy

Table 6.3 Demographic details of group 3 recruits

Demographic details of the 9 children recruited from outpatient clinic to group 3 of the PUJO study who provided a voided urine sample on the day of recruitment. M – male, F – female. y – years, m – months.

6.5 Results - aquaporin expression and excretion by the normal human urinary tract

Studies to develop laboratory techniques and ascertain general AQP isoform expression by the human urinary tract were undertaken on human kidney, renal pelvis and ureter tissue not suitable for transplant. This tissue was unrelated to samples obtained from the childhood study of PUJO which have not yet been analysed. Normal human adult urine samples were used to demonstrate typical urinary aquaporin excretion. The results are presented below.

6.5.1 Aquaporin isoform mRNA expression in normal human kidney, renal pelvis and ureter

Endpoint RT-PCR established that human kidney expresses AQPs 1-7 and 11 at the mRNA level (Figure 6.8) Sequencing of the AQP7 double bands (Eurofins MWG Operon, Germany) demonstrated that the lower 200bp band is AQP7 while the upper 400bp band represents an AQP7 pseudogene, consistent with reports from Rubenwolf *et al.* [259]. The detection of AQPs 1-6 in human kidney is consistent with the amalgamated results from other human studies (See Chapter 1, Table 1.8). Additionally, AQPs 7 and 11 are now known to be expressed by human kidney at the mRNA level.

Subsequent analysis of whole human renal pelvis and ureter samples demonstrated that the renal pelvis expresses AQPs 1-7, 9 and 11 at the mRNA level but not AQPs 0 or 12. Faint bands for AQPs 8 and 10 suggest these isoforms may also be expressed by human renal pelvis (Figure 6.9). Whole human ureter expresses AQPs 1-11 but not AQP 0 or AQP 12 (Figure 6.10).

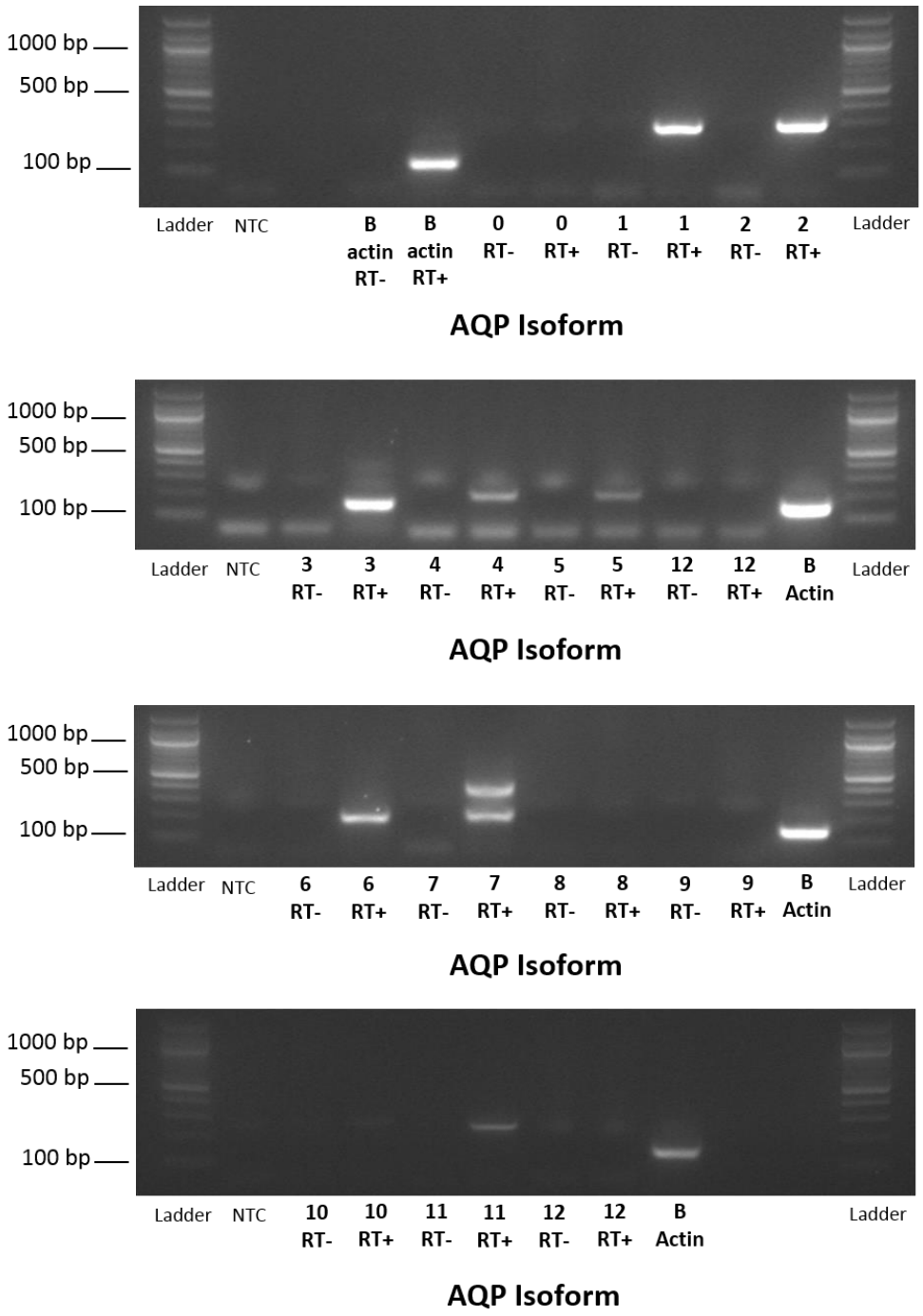

Figure 6.8 AQP isoform mRNA expression by human kidney

Endpoint RT-PCR was performed using mRNA extracted from whole normal human kidney and the product run on 2% agarose gels. Bands of the appropriate size for AQP isoforms 1, 2, 3, 4, 5, 6, 7 and 11 and β-actin were noted indicating they are expressed at the mRNA level by whole human kidney. See appendix 2 (section 10.2.1.1) for product sizes. Sequencing of the AQP7 bands confirmed that the lower band of the appropriate size is AQP7 and the upper band is a pseudogene as previously published. NTC – no template control. The hazy opacities at 250 bp on the second gel represent an artefact of loading buffer as explained in Chapter 3 (section 3.2).

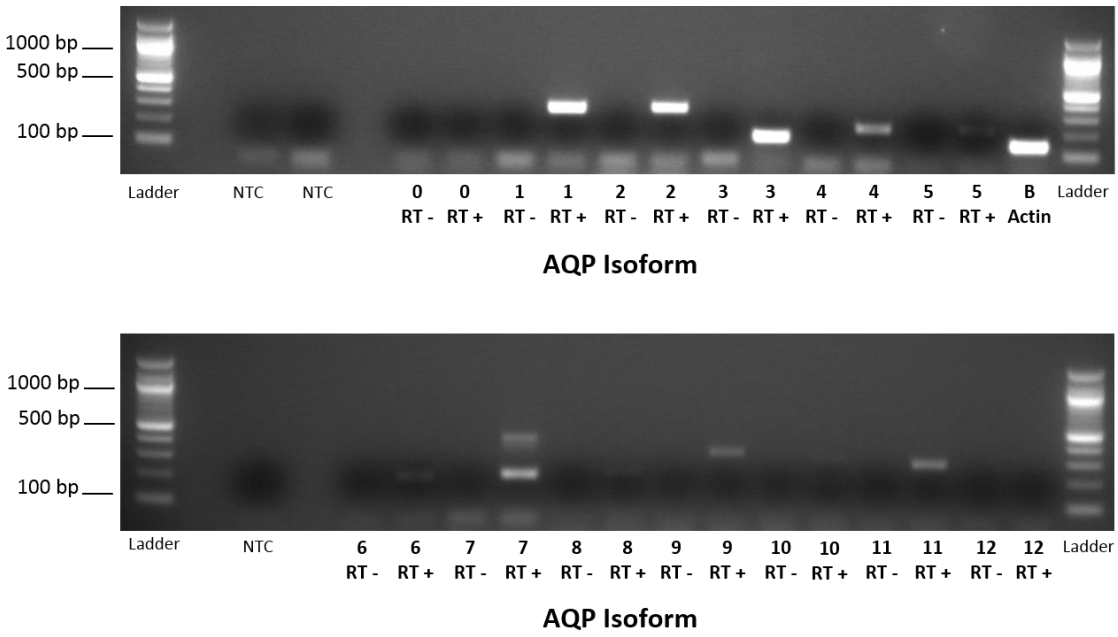

Figure 6.9 AQP isoform mRNA expression by human renal pelvis

Endpoint RT-PCR was performed using mRNA extracted from whole normal human renal pelvis and the product run on 2% agarose gels. Bands of the appropriate size for AQP isoforms 1, 2, 3, 4, 5, 6, 7, 9 and 11 and β-actin were expressed at the mRNA level by human whole renal pelvis. Faint bands for AQPs 8 and 10 suggest these isoforms may also be expressed at low level by human renal pelvis. The upper band of the AQP7 double band represents the AQP7 pseudogene while the lower band corresponds to AQP7. See appendix 2 (section 10.2.1.1) for product sizes.

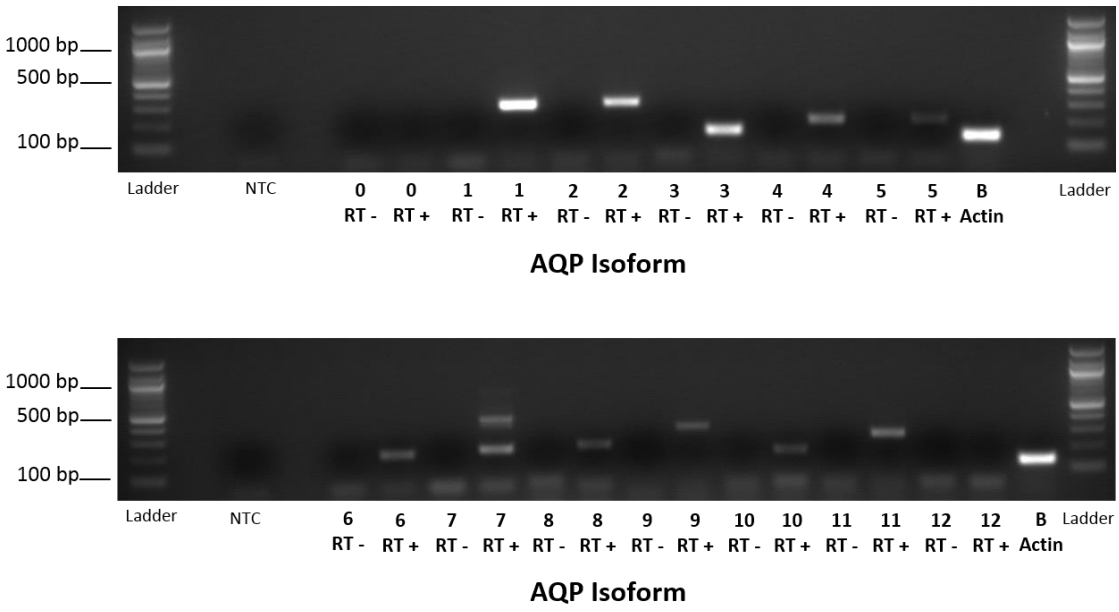

Figure 6.10 AQP isoform mRNA expression by human ureter

Endpoint RT-PCR was performed using mRNA extracted from whole normal human ureter and the product run on 2% agarose gels. Bands of the appropriate size for AQP isoforms 1, 2, 3, 4, 5, 6, 7, 8, 9, 10 and 11 and β-actin were expressed at the mRNA level by human whole renal pelvis. The upper band of the AQP7 double band represents the AQP7 pseudogene the lower band corresponds to AQP7. See appendix 2 (section 10.2.1.1) for product sizes.

6.6 Aquaporin protein expression by human kidney, renal pelvis and ureter

6.6.1 Aquaporin 1

Glycosylated (35-40 kDa) and non-glycosylated (25 kDa) AQP1 is expressed by human kidney cortex and medulla as well as whole renal pelvis and ureter (Figure 6.11). Interestingly glycosylated AQP1 in human kidney produces a band of higher molecular weight (40 kDa) than that of human ureter and renal pelvis (35kDa) which is discussed below.

Immunohistochemistry confirms AQP1 expression within the cortex and medulla of the human kidney. AQP1 is expressed by the apical and basolateral membranes of the proximal tubules and loops of Henle. It is also expressed by the endothelial cell membranes of the vasa rectae. (Figure 6.12A-D). AQP1 is also detected in the vascular endothelial cell membranes of the renal pelvis (Figure 6.12E, F) and ureter (Figure 6.12G, H) lamina propria.

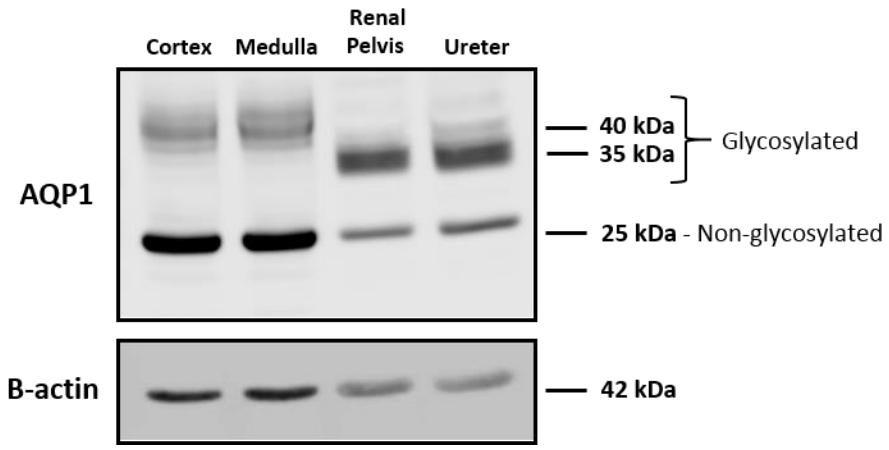

Figure 6.11 AQP1 protein expression by human urinary tract tissue

Western blot demonstrating that glycosylated and non-glycosylated AQP1 is expressed in both the kidney cortex and medulla as well as whole renal pelvis and ureter. Glycosylated AQP1 in the renal pelvis and ureter has a lower molecular weight than that of both kidney fractions.

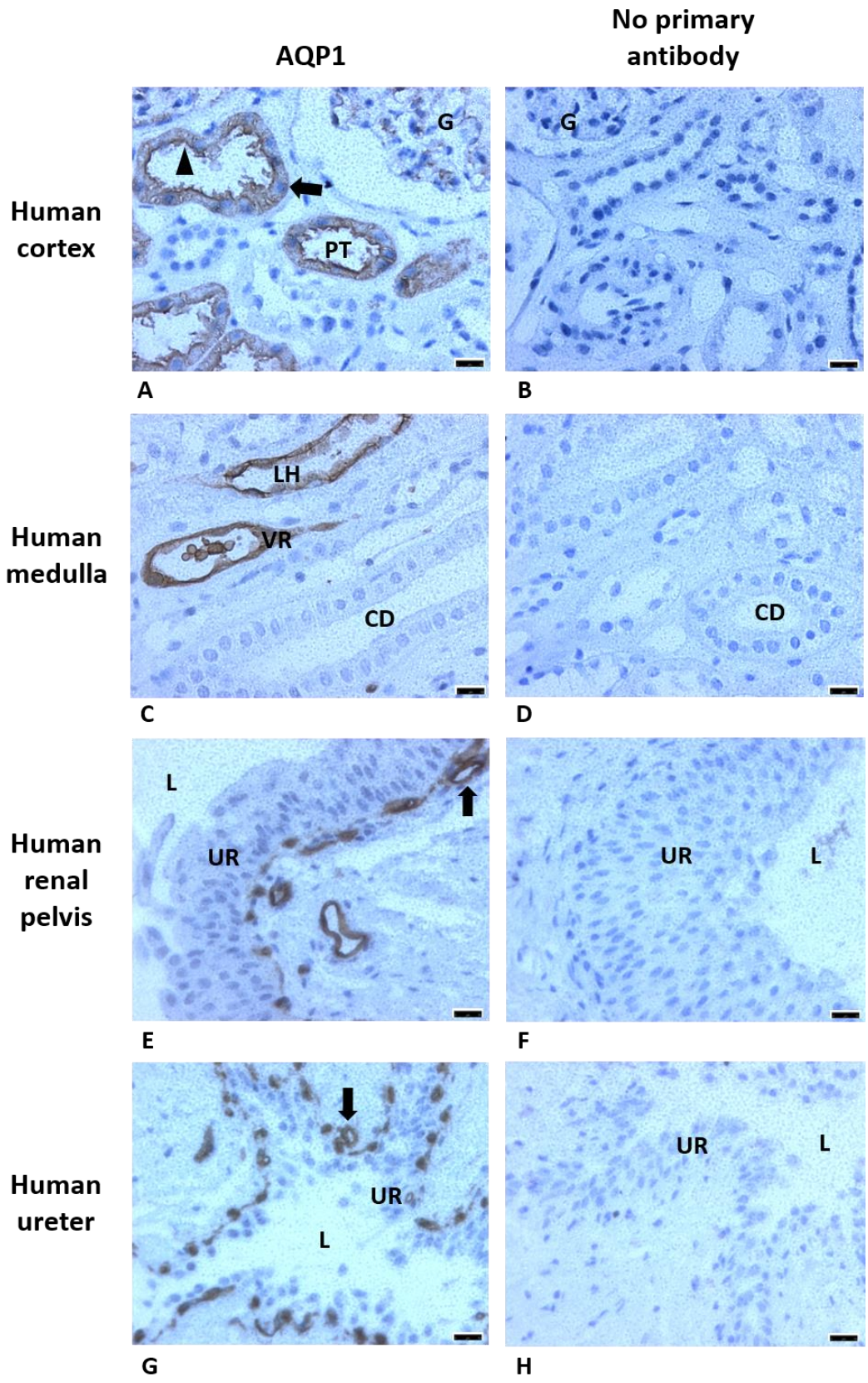

Figure 6.12 Immunohistochemistry demonstrating the distribution of AQP1 expression within human urinary tract tissue

AQP1 expression is demonstrated in the apical (arrowhead) and basolateral (arrow) membranes of the proximal tubules within the kidney cortex (A, B). AQP1 expression in the loop of Henle and vasa recta but not within collecting ducts is seen in the kidney medulla (C, D). AQP1 is also detected in the vascular endothelial cells

(arrow) in the lamina propria of the renal pelvis (E, F) and ureter (G, H). CD – collecting duct, G – glomerulus, L – lumen, LH – Loop of Henle, PT- proximal tubule, UR – Urothelium, VR – vasa recta containing red blood cells. No primary antibody negative controls are presented for each section. Scale bar = 25 μm.

6.6.2 Aquaporin 2

AQP2 is expressed by human kidney, renal pelvis and ureter as demonstrated by western blotting showing a 31 kDa band for each of these samples (Figure 6.13). Immunohistochemistry confirms that both the kidney cortex and medulla express AQP2 in the apical membranes of the collecting ducts (Figure 6.14A-D). Contrary to the western blotting results immunohistochemistry of renal pelvis and ureter samples did not show any protein expression either in the urothelium or deeper layers (Figure 6.14E-H).

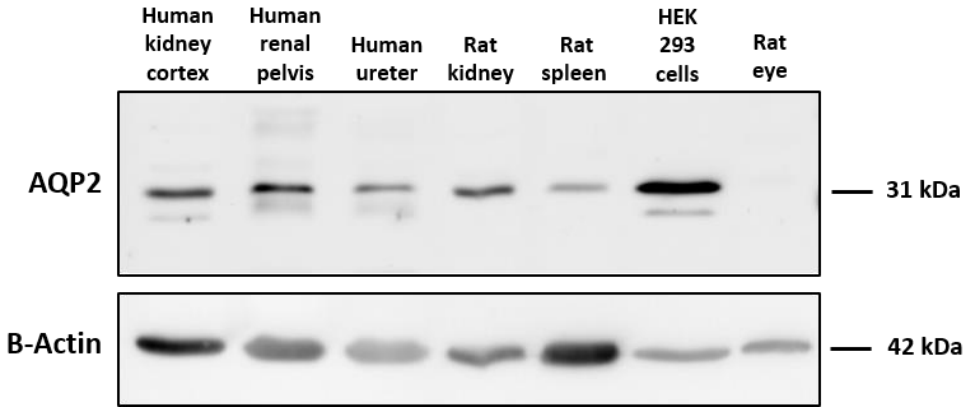

Figure 6.13 AQP2 protein expression by human urinary tract tissue

Western blot demonstrating AQP2 expression by human kidney cortex and whole renal pelvis and ureter. AQP2 expressed by HEK 293 cells is noted at the same molecular weight. Positive controls - rat spleen and rat kidney. Negative control - rat eye.

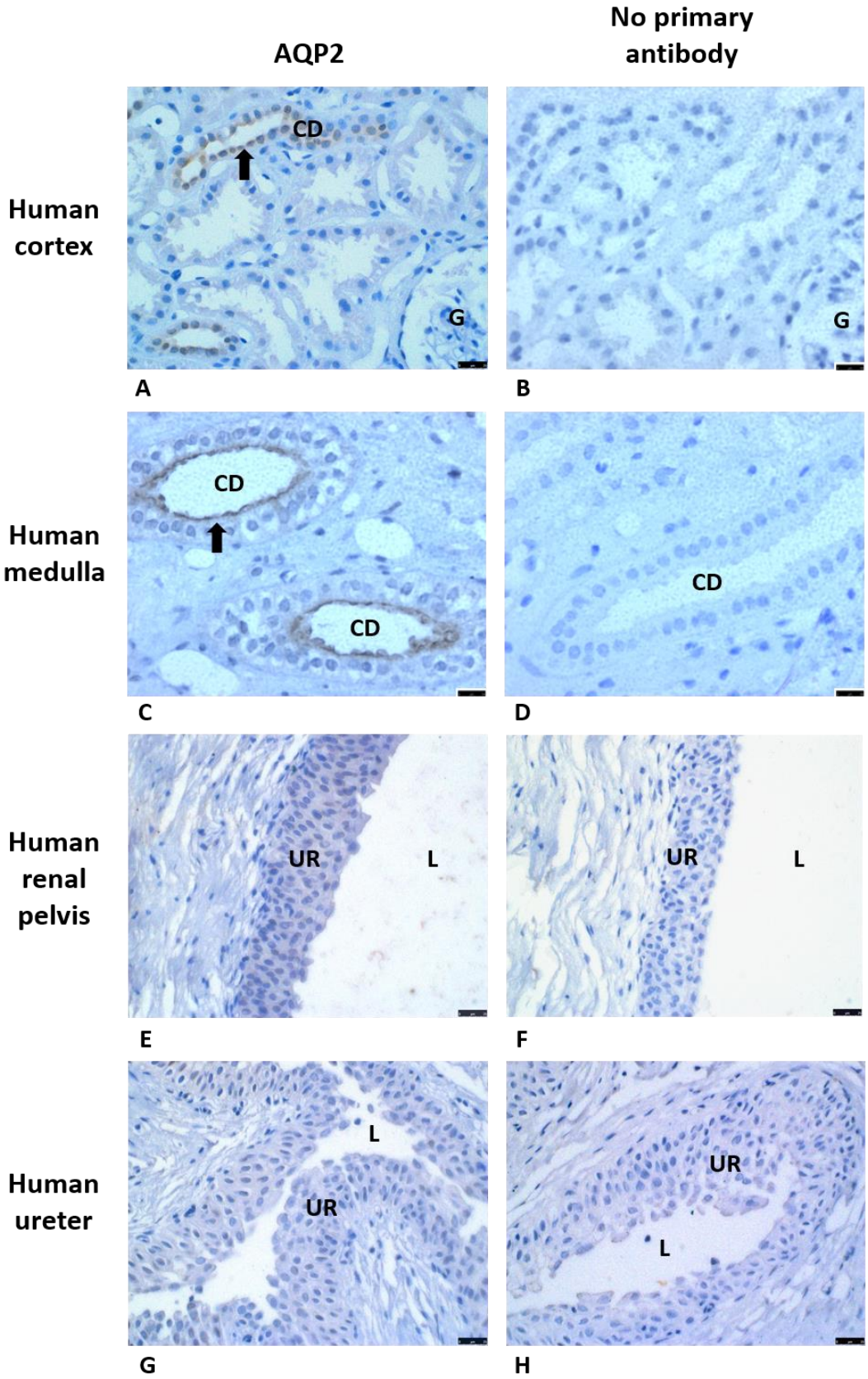

Figure 6.14 Immunohistochemistry demonstrating the distribution of AQP2 protein expression within human urinary tract tissue

AQP2 is expressed by the apical membranes (arrow) of the kidney cortical collecting ducts (A, B) and medullary collecting ducts (C, D). AQP2 was not detected in the urothelium of human renal pelvis and ureter. CD – collecting duct, G-glomerulus, L – lumen, UR – urothelium. No primary antibody negative controls are presented for each section. Scale bar = 25 μm.

6.6.3 Aquaporin 3

AQP3 protein expression (28 kDa) by human kidney cortex and medulla as well as whole renal pelvis and ureter was demonstrated by detection of the appropriate 28 kDa band on western blotting (Figure 6.15). Subsequent immunohistochemistry confirmed that AQP3 was expressed by the basolateral membranes of the cortical and medullary collecting ducts of the kidney (Figure 6.16A-D). AQP3 was abundantly expressed by the urothelium of the renal pelvis and ureter with predominantly cell membrane, but also cytoplasmic, expression thoughout all layers of the urothelium. Contrary to previous reports [249, 259] the apical membrane of the umbrella cells (best seen on the renal pelvis images) did appear to express AQP3 (Figure 6.16E-H).

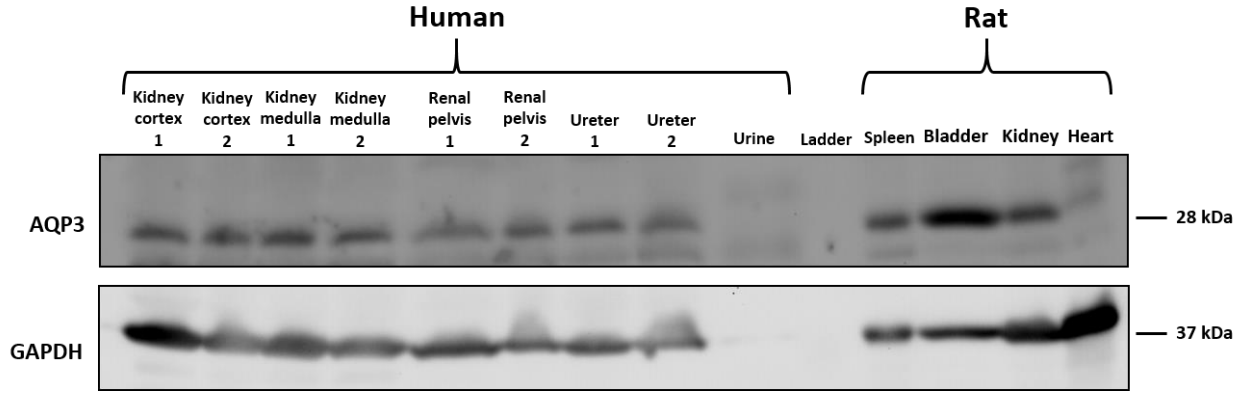

Figure 6.15 AQP3 protein expression by human urinary tract tissue

Western blot demonstrating AQP3 expression by human kidney cortex and medulla, and whole renal pelvis and ureter. AQP3 expression by rat kidney and bladder is noted at the same molecular weight. AQP3 and GAPDH were not detected in human urine. Positive control – rat spleen, negative control - rat heart.

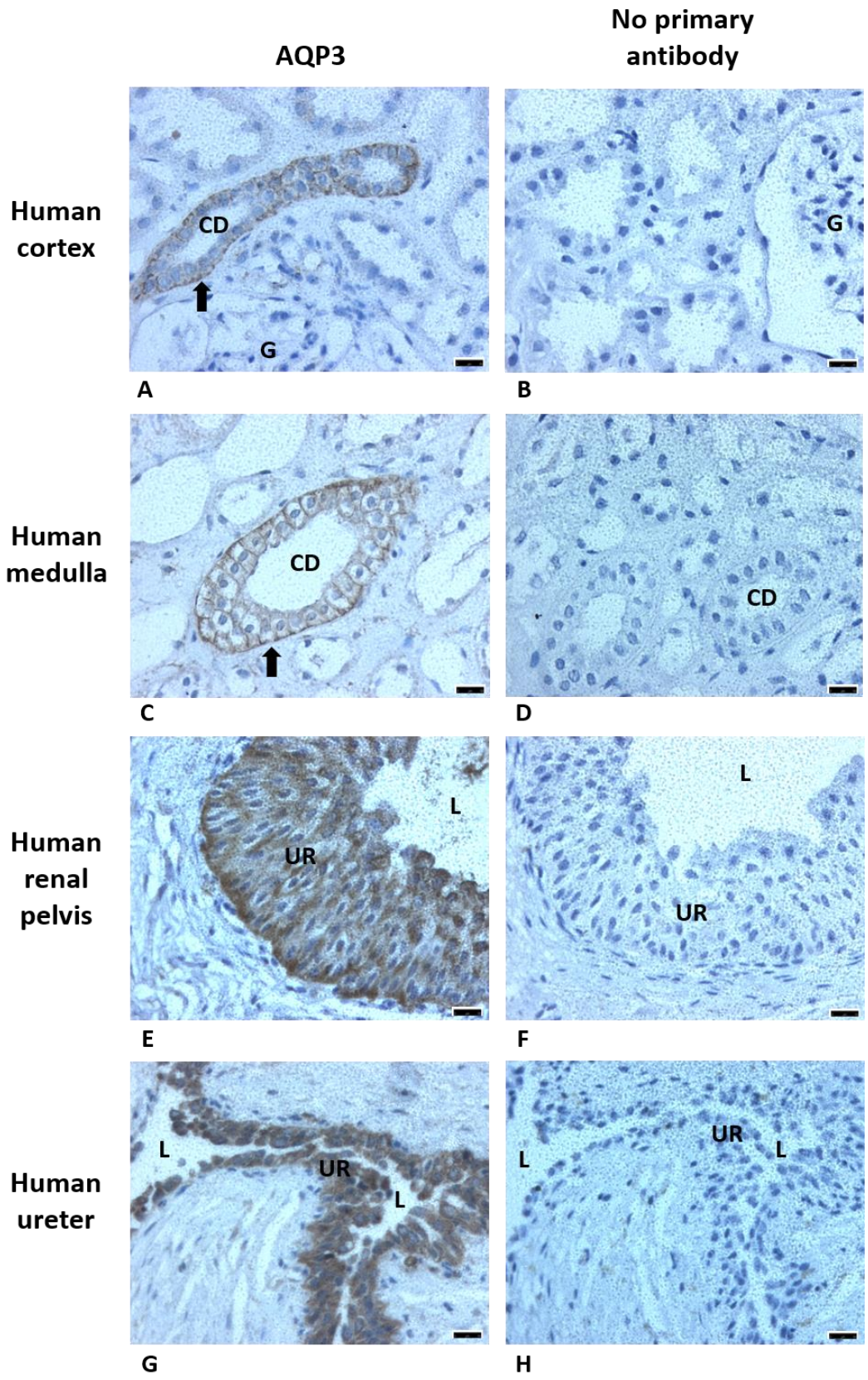

Figure 6.16 Immunohistochemistry demonstrating the distribution of AQP3 protein expression within human urinary tract tissue

AQP3 is expressed by the basolateral membranes (arrow) of the kidney cortical collecting ducts (A, B) and medullary collecting ducts (C, D). AQP3 is also abundantly expressed by all layers of the urothelium within human renal pelvis (E, F) and ureter (G, H). The urothelial cell membrane shows predominant expression

however cytoplasmic expression is also noted. CD – collecting duct, G-glomerulus, L – lumen, UR – urothelium. No primary antibody negative controls are presented for each section. Scale bar = 25 μm.

6.6.4 Aquaporin 4

Detection of an appropriate 34 kDa band on western blotting demonstrated that AQP4 was expressed at the protein level by human kidney cortex and medulla. AQP4 expression was not detected in whole human renal pelvis and ureter samples (Figure 6.17). As discussed in chapter 3, despite testing two different antibodies using different antigen retrieval techniques accurate detection of AQP4 by immunohistochemistry was not achieved within the time constraints of the project. Immunohistochemistry for AQP4 was therefore not performed on human samples.

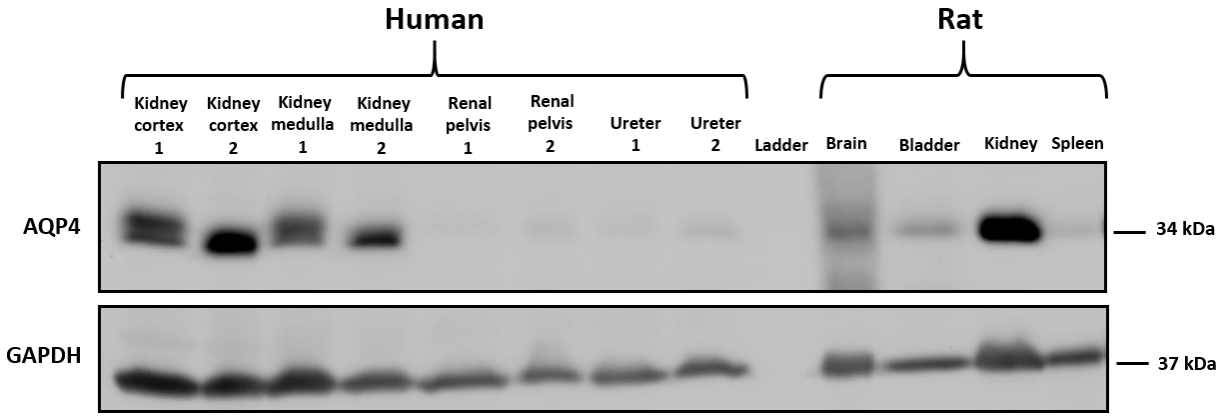

Figure 6.17 AQP4 protein expression by human urinary tract tissue

Western blot demonstrating AQP4 expression by human kidney cortex and medulla. AQP4 was not detected in human renal pelvis and ureter. AQP4 expression by rat kidney and bladder is noted at the same molecular weight. Positive control – Rat brain and heart, negative control - rat spleen.

6.7 Aquaporin protein excretion in human urine

Western blotting of adult human urine samples concentrated by ultrafiltration indicated that AQPs 1 and 2 but not AQP3 are excreted in urine (Figure 6.18, Figure 6.19, Figure 6.20).

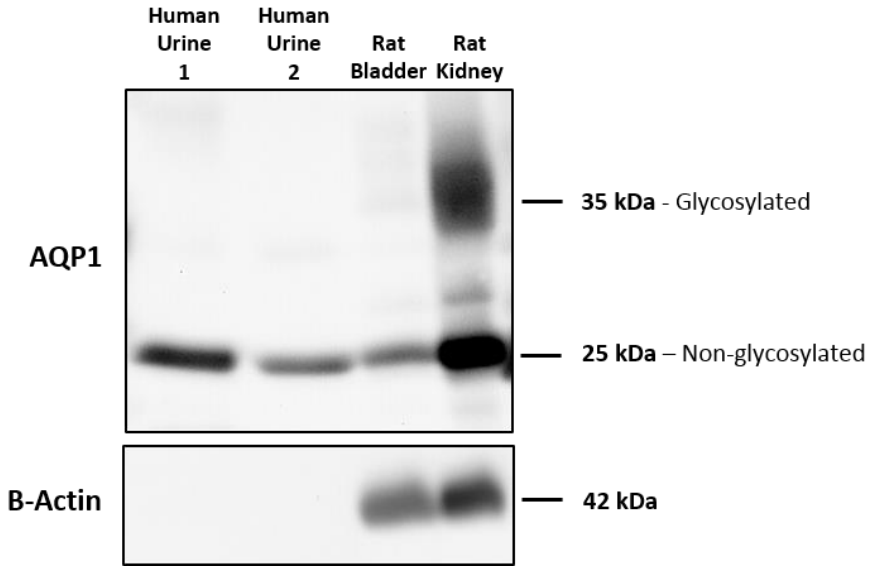

Figure 6.18 Non-glycosylated AQP1 excretion in human urine

Western blot demonstrating the excretion of non-glycosylated AQP1 in two independent samples of human urine. Positive controls – rat bladder and rat kidney. B-actin was used as loading control for the tissue samples and as expected was not excreted in urine.

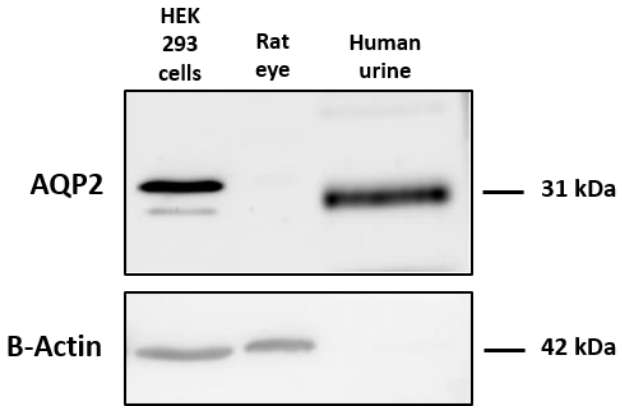

Figure 6.19 AQP2 excretion in human urine

Western blot demonstrating the excretion of AQP2 in human urine. Positive control – HEK 293 cell lysate, negative control – rat eye. B-actin was used as loading control for the control samples and as expected was not excreted in urine.

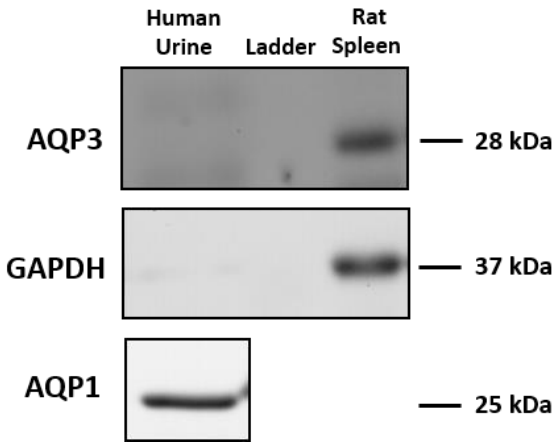

Figure 6.20 Western blot demonstrating lack of AQP3 excretion in human urine

Western blot demonstrating that AQP3 is not excreted in human urine. AQP1 was used as loading control for human urine. GAPDH was loading control for the tissue sample. Positive control – rat spleen.

6.8 Discussion

The enthusiasm of children and families to be recruited into this study has been remarkable. A 100% recruitment rate following screening for groups 1 and 2 is excellent and demonstrates that families feel this study is worthwhile. A lower recruitment rate of 85% following screening for group 3 is not unexpected yet still very good. The reasons given for non-participation in group 3 (lack of time, child not toilet trained) were anticipated given the short time interval between screening and recruitment and the time pressures associated with families visiting the outpatient department.

Generally, the study is running very well. The major difficulty identified so far has been the failure to obtain follow-up urine samples in outpatient clinic from any of the group 1 patients recruited. In part this has been due to difficulties identifying these children when they return for follow-up, particularly as many are reviewed in outreach outpatient clinics with different sets of patient notes across the South-West of England. Furthermore, transport of urine samples on ice from these distant clinics for processing in Bristol would take many hours and may adversely affect the results of the study. Although samples could be placed in liquid nitrogen for transport, ideally they need to be aliquoted first to avoid subsequent freeze-thawing. Aliquoting of samples wouldn't be possible within the time constraints and facilities of an NHS clinic. The decision has therefore been made to concentrate on obtaining follow-up samples from children attending Bristol Children's Hospital initially. In terms of children reviewed within Bristol, difficulties have been encountered due to the changeover to a computerised notes system (Evolve). Originally the method to identify study participants

was the insertion of a sticker on the patient notes to remind the clinician to undertake study follow-up. With the introduction of computerised notes this system became obsolete. Steps are now being taken alongside the Evolve administrators to add study participation to the patient alerts on the computerised system.

Thus far 8 children have been recruited to group 1, 1 child to group 2 and 11 children to group 3 (although only 9 provided urine samples). There is still a distance to go in terms of meeting the sample size target however the study is still running and there is permission for recruitment to continue until 2020.

Generally, the recruited population is as expected with a male predominance in group 1 of 1.7:1. This ratio is slightly lower than the reported M:F ratio of 3:1 and is likely due to the currently small sample size. Interestingly there is also a male predominance in group 3 which is likely because most children have been recruited from urology clinics where there is a preponderance of male referrals due to the nature of the conditions managed. This can be easily rectified by recruiting from a wide range of general surgical clinics with a more balanced male to female ratio.

Children recruited to group 3 were also noted to be significantly older than those recruited to group 1. Again, this can be easily rectified by ensuring clinics that have a younger patient base are included in patient recruitment.

Children undergoing surgery had a mean age of 17.7 months. This is consistent with observations by Ulman *et al*. who suggests the first two years of life as being the most crucial to monitor children with hydronephrosis as this is the time period over when most pyeloplasties are performed [62].

Consistent with current literature an antenatal diagnosis of hydronephrosis was made in 89% of children operated for PUJO, three-quarters of children had left sided PUJO and bilateral disease occurred in 12.5% of children [436]. Equally, the indications for surgery in group 1 were all consistent with current usual practice [56].

All children recruited to group 1 so far underwent an open dismembered Anderson-Hynes pyeloplasty. This was intentional, as currently a method to measure pressure within the kidney during a laparoscopic pyeloplasty has not been devised. The ethical approval for the study includes laparoscopic pyeloplasty therefore there is potential for children undergoing this procedure to be included, as and when possible, at a later date.

Interestingly, 1 child experienced deterioration of function (30% split function on MAG 3 renogram) in the obstructed kidney while half of all children experienced at least one urinary tract infection prior to being considered for surgery. These complications highlight the need for earlier identification of children requiring surgery for PUJO which may be achieved via the identification of new biomarkers.

The median renal pelvis pressure of the obstructed kidney was within normal limits at 1 cmH_2O (range 0-20 cmH_2O). Based on known normal [46] and pathological [113, 114] baseline renal pelvis pressures only 1 out of 8 children had a raised renal pelvis pressure (20 cmH_2O) at the time of surgery. Similar to the results of the rat model presented in Chapter 5, no correlation was detected between the pre-operative sonographic renal pelvis APD and the intra-operative renal pelvis pressure measurements. This indicates that the renal pelvis APD measurement is likely a poor predictor of the presence or absence of damaging raised intra renal pressure. However; the current sample size is small and this will need to be confirmed when all results are available at the end of the study. Additionally, the time difference between the pre-operative ultrasound scan and the intra-operative pressure measurement (mean 3.3 +/- 1.1 months), as well as the impact of factors affecting urine output and thus renal pelvis pressure (length of pre-operative fasting and intra-operative hydration) must be considered.

Likewise, no correlation was detected between the pre-operative split renal function (measured by MAG 3 or DMSA renogram) and the intra-operative renal pelvis pressure measurement. Again, these results were confounded by a small sample size particularly given that the results of three children were excluded from the analysis. Valid results will be obtained after the study when sufficient sample size has been achieved.

This childhood study has been designed to try and address some of the issues encountered when assessing previous studies in the search for non-invasive urine biomarkers to aid diagnosis, management and prognosis of PUJO.

Many previous studies have included only healthy controls as comparator for children undergoing pyeloplasty for PUJO (Chapter 1,

Table 1.6). Although these studies can highlight whether the potential biomarker is changed compared to the normal population, it is not helpful in terms of distinguishing children who require surgery from those who can be safely managed conservatively. This study has

addressed this issue by including two control groups; those with conservatively managed hydronephrosis as well as children with no urological abnormality.

Additionally, the previous studies which assessed AQP1 and 2 excretion in childhood PUJO both assessed post-operative urine from the obstructed kidney only, and used the normal kidney as comparator [386]. While this is incredibly useful data which highlights the reduction in urinary AQP excretion from the obstructed kidney following surgery, it does not indicate whether this reduction can be detected pre-operatively in bladder urine which inevitably is a mixture from both kidneys. This study assesses pre-operative bladder urine samples which are the most suitable non-invasive biomarker.

Finally, we currently do not know why the natural evolution of PUJO leads to two very different outcomes. This study aims to address the potential role of the urothelium and specifically AQPs in this conundrum.

In general, the advantages of this human study include:

- Normal childhood urinary aquaporin levels will be defined for the first time
- Comparison between groups 1 and 2 will determine whether urinary aquaporin measurement is a useful non-invasive biomarker to differentiate between those children with 'damaging' hydronephrosis who require surgery and those with 'safe' hydronephrosis which might resolve spontaneously. Inherent bias which is acknowledged with this method is that the children who need surgery have been selected by current clinical and radiological measures. It would, however, be very difficult to avoid this.
- Follow-up urine AQP levels in group 2 will provide a prospective cohort of children enabling the assessment of the early predictive value of urinary aquaporin measurement. This will be achieved by comparing those children whose hydronephrosis resolves or remains stable with those who progress to need an operation and move into group 1.
- Post-operative urinary aquaporin levels in group 1 children will determine the effect of pyeloplasty on aquaporin excretion.
- The assessment of renal pelvis (pre-obstruction) compared with ureteric (post-obstruction) tissue will enable investigation of the effect of obstruction on human urothelial AQP expression.

- The availability of corresponding radiological imaging and intra-operative pressure monitoring will enable us to correlate changes in tissue and urine aquaporin levels with currently used markers of severity, function and pressure.

Initial testing of kidney, renal pelvis and ureter samples not suitable for transplant enabled the establishment of techniques which will be used in future analysis of samples from the childhood study. Furthermore, these experiments were utilised to delineate normal urinary tract AQP isoform expression in humans as described below.

Endpoint RT-PCR demonstrated that human kidney expressed mRNA transcripts for AQPs 1-7 and 11. AQPs 0, 8, 9 and 12 were not detected. The expression of AQPs 1-6 has been documented previously by other studies, however, the detection of both AQP7 and 11 is a new finding. This is not unsurprising, however, given that these isoforms are detected in other mammals (See Chapter 1, Table 1.8). Despite AQP8 [281] and 9 (demonstrated in Chapter 5) expression being noted in rat kidney these AQP isoforms have not been detected by others in human kidney [282, 287], which is corroborated by these results. Interestingly, previous studies of AQP9 expression by various rat and human tissues concluded that the tissue distribution of this particular AQP is quite different between the two species. For example, human AQP9 is expressed in peripheral leucocytes and tissues where they accrue while rat AQP9 is not [287].

In accordance with previous studies AQPs 1-4 were all expressed by human kidney as demonstrated by both western blotting and immunohistochemistry. The cellular location of AQPs 1-3 by immunohistochemistry was as expected. AQP1 was expressed by the apical and basolateral membranes of the proximal tubular cells and the loop of Henle, as well as the endothelial cell membranes of the vasa rectae. AQP2 was expressed by the apical membrane of the cortical and medullary collecting ducts while AQP3 was expressed by the basolateral membrane of the cortical and medullary collecting ducts [187, 255]. AQP4 expression was not assessed by immunohistochemistry due to lack of a suitable antibody.

Whole human renal pelvis expressed mRNA transcripts for AQPs 1-7, 9 and 11. Faint bands on endpoint PCR were also appreciated for AQPs 8 and 10. Interestingly whole human ureter expressed AQPs 1-11. Neither renal pelvis nor ureter expressed AQPs 0 or 12 at the mRNA level. Although the bands are faint for AQPs 8 and 10 in human renal pelvis it is likely they are expressed given that there is definite expression by human ureter.

Rubenwolf *et al.* demonstrated that AQPs 3, 4, 7, 9 are expressed at the mRNA and protein level by urothelium. AQP11 was confirmed to be expressed by the urothelium at the mRNA level only, due to lack of a suitable antibody for protein work [259]. Together with the results from this study this suggests that AQPs 1, 2, 5, 6, 8 and 10 are expressed by non-urothelial elements of the renal pelvis and ureter as discussed below.

AQPs 1-3 were present at the protein level by western blotting in both whole renal pelvis and ureter while AQP4 was not detected in either tissue. AQP4 would be expected to be present given the results of the RT-PCR in this study and the finding by others of the presence of AQP4 in human urothelium at the mRNA and protein level [259]. Inability to detect it on western blotting may reflect generally low expression levels within the urothelium, which forms a relatively small percentage of the tissue lysed within a ureter or renal pelvis specimen. Further work will involve establishing a satisfactory protocol for assessing tissue AQP4 expression by immunohistochemistry to confirm cellular location of expression.

Another interesting finding on western blotting was that glycosylated AQP1 had a higher molecular weight in human kidney (40 kDa) compared to both renal pelvis and ureter (35 kDa). This likely represents differential glycosylation between distinct tissue types as a post-translational modification. Frokiaers group reported the glycosylated AQP1 band at 35-50 kDa in human kidneys [187], however, renal pelvis or ureter samples have not been assessed by this group or indeed by any other groups previously for comparison.

Cellular localisation of the AQP isoforms by immunohistochemistry demonstrated that AQP1 was present in the vascular endothelial cells of the lamina propria of both renal pelvis and ureter but was not detectable in urothelium. Although AQP1 expression has previously been reported in the capillary endothelial cells of rat ureter and bladder [249], its location within human ureter and renal pelvis has not previously been documented.

AQP3 was abundant throughout all layers of the renal pelvis and ureter urothelium. Expression was predominantly localised to the cell membrane, but cytoplasmic expression was also noted. This concurs with previous findings in human urothelium [259] but contrasts with observations by Spector *et al*. who noted that in rat urothelium AQP3 was confined to the cell membrane with no cytoplasmic expression [249]. Differing from previous findings in both human and rat tissues, however, is that AQP3 in this study appeared to be expressed equally by all layers of the urothelium and specifically was expressed by the apical cell

membrane of the umbrella cells of the urothelium. In human urothelium expression has previously been reported to be strongest in the basal layers and faint or not present in the superficial umbrella cell layer [259], while in rat tissue AQP3 was reported to be absent on the luminal surface of the umbrella cells [249]. This observation is important because it is the umbrella cells which contact the lumen of the urinary tract and thus the urine flowing through. AQP4 could facilitate transurothelial water transport across the apical membrane as it is reportedly expressed throughout all layers of human urothelium. Although, the authors describe the expression pattern as cytoplasmic [259], as noted by Khandelwal, review of the published images suggests that both AQP4 as well as AQP7 are present along the umbrella cell apical membrane [429]. It is too early to say whether AQPs such as AQP 3, 4 and 7 have a definitive role in mass water transport across the urothelium or whether their function is simply related to regulation of cell volume and tonicity in the face of fluctuating hypertonic and hypotonic urine content. The fact that AQPs 3 and 7 also transport small uncharged molecules such as urea in addition to water [238, 239, 288, 324] expands their potential role to the dissipation of urea and other solutes from the urothelium. Further studies using knockout urothelial cell lines and AQP knockout mice under control of the uroplakin II promoter will enable testing of these potential mechanisms.

Contrary to the RT-PCR and western blotting results, immunohistochemistry of human ureter and renal pelvis failed to demonstrate AQP2 in any area of the tissue. Contradictory reports regarding urothelial AQP2 expression are noted in the literature. AQP2 mRNA expression by rat whole ureter and bladder has been demonstrated by RT-PCR, which was localised by immunohistochemistry to the urothelial cytoplasm and cell membranes (excluding the apical surface of the umbrella cells) [249]. By contrast, AQP2 mRNA expression is absent in human urothelium [259]. Together, the results of this study and those of Rubenwolf suggest that AQP2 is likely not expressed by urothelium but may be expressed by another layer which was not identified on immunohistochemistry. The potential reasons for absent AQP2 staining on immunohistochemistry were discussed in Chapter 3. Continuing analysis of many samples from the childhood study paying attention to sample fixation and antigen retrieval techniques should resolve this issue. Additionally, ongoing work developing immunohistochemistry for AQPs 4 – 11 (suitable antibodies permitting) will help to clarify the tissue location of the other AQP isoforms present in human renal pelvis and ureter.

Consistent with other research, western blotting of ultrafiltered normal human urine in this study confirmed that AQPs 1 and 2, but not APQ3 are excreted into the urine. It is postulated

this differing excretion pattern occurs because AQPs are shed by an apical pathway. AQPs 1 and 2 are apically sited in the proximal tubules and collecting ducts respectively while AQP3 is located in the basolateral cell membrane of the collecting ducts [370-372].

Analysis of the human tissue and urine samples collected throughout the study has not yet commenced as the intention is to perform this in large batches to reduce inter-experimental error. As is evident from the data presented above and in Chapter 5, the major techniques are all established ready for analysis to begin. To complement this work primers suitable for real time quantitative PCR will also be developed to assess mRNA as well as protein expression by human renal pelvis and ureter in PUJO.

Although translation across species does not always occur, it is acknowledged, given the results of the neonatal rat model, that human urinary AQP1 measurement may not prove a successful biomarker. Many samples, however, will have been appropriately stored from a robust cross-sectional study which will be utilised in further analysis including proteomic studies, to identify other potential biomarkers which may facilitate the diagnosis and management of children with hydronephrosis.

Ultimately this study has the potential to improve the management of many children who are antenatally diagnosed with hydronephrosis, both nationally and globally. Development of urine aquaporin measurement as a non-invasive biomarker aims to identify children early who require a pyeloplasty for damaging hydronephrosis, while sparing those with safe hydronephrosis. Early identification of those who require surgery will reduce the risk of progressive damage to the kidney and reduce the need for repeated radiological imaging some of which is invasive and involves radiation. Furthermore, establishing the mechanism of dysregulation of tissue and urinary aquaporin expression will enable the future development of therapeutic treatment aiming to either protect renal function or reduce symptoms.

Chapter 7. Conclusions and future work

7.1 Conclusions

The main conclusions from each chapter in this thesis are summarised in Table 7.1 below.

Chapter	Findings/Outcome
3	Primers designed and validated to detect rat AQP isoforms 1-4 and 6-11 by endpoint and real-time PCR Primers designed and validated to detect AQP isoforms 0, 5 and 12 by endpoint PCR Western blotting technique optimised to detect AQP isoforms 1-4 in rat and human tissue Immunohistochemistry technique optimised to detect AQP isoforms 1-3 in rat and human tissue AQP1 ELISA developed to detect and quantify urinary excretion of AQP1 by rats and humans
4	Development of a technique to create partial unilateral ureteric obstruction in neonatal rats under recoverable general anaesthetic Development of a technique to measure intra-renal pelvis pressure under terminal anaesthesia in young rats with normal kidneys and hydronephrosis
5	**All findings are from 5-week old rats who underwent neonatal PUUO or sham procedure:** PUUO rats show reduced body weight compared to sham Individual kidney weight is unchanged between all degrees of partially obstructed, contralateral and sham kidneys Intra-renal pelvis pressure is significantly increased in moderate hydronephrosis compared to sham, contralateral and non-operated kidneys Severely hydronephrotic kidneys show a reduced number of glomeruli per field of view and increased interstitial fibrosis compared to mild and moderate hydronephrosis, sham and contralateral kidneys Whole normal rat kidney expresses mRNA transcripts for AQPs 1-9 and 11 AQP1 is expressed by the apical and basolateral membranes of the proximal tubules as well as the loop of Henle and vasa recta of normal rat kidney.

	AQPs 2 and 3 are expressed by the apical and basolateral membranes of the renal collecting ducts in normal kidney. AQP1, 2 and 6 mRNA expression is downregulated in the severely hydronephrotic kidney compared to sham. AQP3 expression is unchanged in obstruction while AQP4 shows a tendency towards downregulation in severe hydronephrosis compared to sham Non-glycosylated and glycosylated AQP1, AQP2 and AQP3 protein expression is unchanged in the obstructed kidney compared to sham kidneys. AQP4 protein expression is downregulated in severe hydronephrosis compared to sham kidneys AQP expression at the mRNA and protein level by the contralateral kidney is unchanged in PUUO rats compared to sham Normal whole rat renal pelvis expresses mRNA transcripts for AQPs 1, 3, 4, 7, 9 and 11 AQP1 and 3 mRNA expression in the renal pelvis is reduced in moderate and severe hydronephrosis compared to sham, while AQP11 expression is significantly downregulated in severe hydronephrosis only. AQP4 mRNA expression shows a tendency towards reduction in moderate and severe hydronephrosis compared to sham AQP expression by the contralateral renal pelvis is unchanged in PUUO rats compared to sham The urothelial distribution of AQP3 is unchanged in obstructed compared to sham and contralateral renal pelvices Urinary AQP1 excretion is not significantly different between PUUO rats across all degrees of hydronephrosis compared to sham rats

6	**Design and implementation of clinical cross-sectional study of childhood PUJO has been achieved with the following preliminary findings:** Children undergo open pyeloplasty for PUJO at a mean age of 17.7 months An antenatal diagnosis of hydronephrosis is made in approximately 90% of children operated for PUJO 1 out of 8 children experienced deterioration in split kidney function prior to surgery The median renal pelvis pressure of the obstructed kidney is within normal limits in children undergoing open pyeloplasty No correlation between renal pelvis pressure and pre-operative renal pelvis APD and split function is noted **Analysis of normal human tissue generated the following findings:** Whole normal human kidney expresses mRNA transcripts for AQPs 1-7 and 11 Whole normal kidney expresses AQPs 1-4 at the protein level. AQP1 is expressed by the apical and basolateral membranes of the proximal tubules as well as the loop of Henle and vasa recta. AQPs 2 and 3 are expressed by the apical and basolateral membranes of the renal collecting ducts Whole human renal pelvis expresses mRNA transcripts for AQPs 1-7, 9 and 11. Whole human ureter expresses mRNA transcripts for AQPs 1-11. AQPs 1 and 3 are expressed at the protein level by whole human renal pelvis and ureter. AQP1 is expressed by the vascular endothelial cells of the lamina propria while AQP3 is expressed by all layers of the urothelium AQPs 1 and 2, but not 3, are excreted in normal human urine

Table 7.1 Table summarising the main findings of each chapter

The over-riding aims of this research were to investigate kidney and urinary tract AQP expression in PUJO and correlate with measures of kidney function, severity of hydronephrosis, and intra-renal pelvis pressure. Furthermore, to assess urinary AQP excretion in ‘damaging’ and ‘safe’ PUJO to determine the potential of this measurement as a biomarker to aid surgical decision making in this condition. The approach employed was to develop a neonatal rat partial unilateral ureteric obstruction model and implement a

childhood cross-sectional study of PUJO. Molecular biology laboratory techniques were optimised to conduct sample analysis from each of these models.

Neonatal partial unilateral ureteric obstruction models are well described and have been used to investigate the mechanism of obstructive nephropathy [115, 120, 401, 413, 437, 438]. Additionally, these same models have been used to demonstrate renal dysregulation of AQP, sodium channel and acid base transporter expression in obstructive hydronephrosis [185, 364, 408, 439]. Several techniques have been described to create PUUO, however the model of variable PUUO described and validated most recently by Thornhill *et al.* [91] was employed in this study. This model involves tying a ligature around both the pelvi-ureteric junction and a fixed diameter wire, followed by removal of the wire to create a defined amount of obstruction. Using this neonatal rat PUUO model the current study has built on previously published work to not only assess renal AQP isoform expression but also AQP expression by urothelium, the specialised lining of the urinary tract. Additionally, these findings have been correlated with the degree of hydronephrosis, renal architecture and the intra-renal pelvis pressure.

Consistent with previous studies, the expression of selected renal AQP isoforms was dysregulated at both the mRNA and protein level in the obstructed kidney. This study also extends the known AQPs that are dysregulated to include AQP4. It is recognised that temporal variation of AQP expression occurs in the partially obstructed kidney [364]. This study, which was conducted at a single time point, highlights that changes in AQP expression are also influenced by the severity of hydronephrosis. These results are consistent with human studies of congenital PUJO where reduced AQP expression correlates with the severity of hydronephrosis and the degree of functional impairment. Furthermore, this study enabled AQP dysregulation to be related to intra-renal pelvis pressure. In moderate hydronephrosis, in the presence of raised intra-renal pressure, AQP mRNA and protein expression for all isoforms assessed was maintained. By contrast, downregulation of AQP expression was noted only in severely hydronephrotic kidneys where abnormalities of renal structure in the absence of raised intra-renal pelvis pressure was noted.

The variable degree of hydronephrosis noted in the rats in this study in response to a fixed degree of ureteric obstruction highlighted the possibility of individual renal and/or urothelial factors modulating the response of the kidney and its collecting system to obstruction. Following the identification of AQPs in human and rat urothelium, an active role for this specialised epithelium in modulating urine composition has been suggested [369].

Urothelial AQPs demonstrate regulation in response to environmental conditions [249, 369] and have been shown to facilitate transurothelial water and urea flux [369]. Until now the role of urothelial AQP expression within the obstructed renal pelvis in PUJO has not been investigated.

The chief finding in this PUUO model was that AQPs expressed by both the vascular endothelium (AQP1) and the urothelium (AQP3 and AQP11) were transcriptionally downregulated in the obstructed renal pelvis at 35 days of age. Again, reduced AQP expression was related to obstruction severity, however, in the renal pelvis both AQP1 and 3 mRNA expression were downregulated in moderate hydronephrosis in the presence of raised intra-renal pelvis pressure and normal kidney architecture as well as in severe hydronephrosis. Although AQP3 expression was downregulated in the renal pelvis, immunohistochemistry demonstrated urothelial expression of AQP3 was not completely abolished and its distribution within the renal pelvis was unaffected by obstruction.

Reduced urothelial AQP3 and vascular endothelial AQP1 expression in PUUO may critically diminish the ability of the renal pelvis to compensate for increases in intra-renal pressure by transurothelial transport and dispersion of water and solutes into the local vasculature (Figure 7.1). Thus, the individual ability of the rat to maintain renal pelvis AQP expression following neonatal PUUO may determine the severity of hydronephrosis developed. Persistent AQP expression following PUUO may protect against intra-renal pressure rises, seen in this study as rats with mild hydronephrosis with normal renal histology and intra-renal pelvis pressure. Equally, failure to maintain renal pelvis AQP expression, with resultant diminished urothelial water re-absorptive capability, theoretically augments intratubular pressure rises potentially leading to severe hydronephrosis, renal damage and functional impairment. Additionally, as discussed in chapter 5, other factors such as urine solute concentrations and gating of channels may impact on the direction of water flow across AQPs. Ultimately, it is not possible to identify from this study whether urothelial AQP expression is a significant renoprotective factor in the obstructed kidney in PUUO. This question will be addressed by further work described in section 7.2.

The other major aim of this study was to assess urinary AQP excretion in ‘safe’ and ‘damaging’ PUJO. AQPs 1 and 2 are known to be excreted in the urine of rats and humans [365, 372, 381, 386]. This was confirmed by western blotting in this study and an ELISA was subsequently developed to assess urinary AQP1 excretion. Childhood studies have previously demonstrated a significant reduction in urinary AQP1 excretion from the

obstructed compared to the normal contralateral kidney immediately following pyeloplasty. Conversely, bladder urine specimens from 29 day old rats in this study did not show any difference in urinary AQP1 excretion between PUUO rats across all degrees of hydronephrosis compared to sham rats.

Fundamentally, this result does not necessarily indicate that AQP1 excretion by the obstructed kidney is normal. It does, however, indicate that changes in excretion by the obstructed kidney may not be detectable in the bladder urine which reflects output from both kidneys. Additionally, the presence of obstruction in PUJO will physically restrict the passage of biomarkers to the bladder, further influencing AQP1 detection in voided urine. , Ultimately, this result raises scepticism on the ability of urinary AQP1 measurement to be a useful non-invasive biomarker of disease when measured pre-operatively in children using bladder urine.

In conjunction with the neonatal rat PUUO model a complementary childhood cross-sectional study of PUJO was designed and implemented with full ethical approval. Recruitment has proceeded well, and the study is predicted to run until July 2020. Laboratory testing of normal human renal tract tissue and urine unrelated to the study, has confirmed the expected expression and excretion patterns of AQP isoforms. Large batch analysis of the PUJO study samples will be undertaken in the future.

The human study will assess similar parameters to the rat model and confirm whether the animal data translates between species. Particularly, further analysis of urine samples obtained from the human study will clarify whether pre-operative bladder urine AQP1 measurement has potential as a non-invasive biomarker to aid surgical decision making in PUJO. Opportunely, even if the human study rejects urinary AQP1 measurement as a suitable biomarker, valuable urine samples have been obtained and stored from both animal and human models which will be used in future proteomics studies (See section 7.2.2.4)

In summary, despite not achieving the initial aim of identifying a novel biomarker, this research contributes significantly to current knowledge of disease mechanism in PUJO by revealing a potential role for urothelial AQPs. The following section highlights future work to be undertaken to facilitate confirmation of this function.

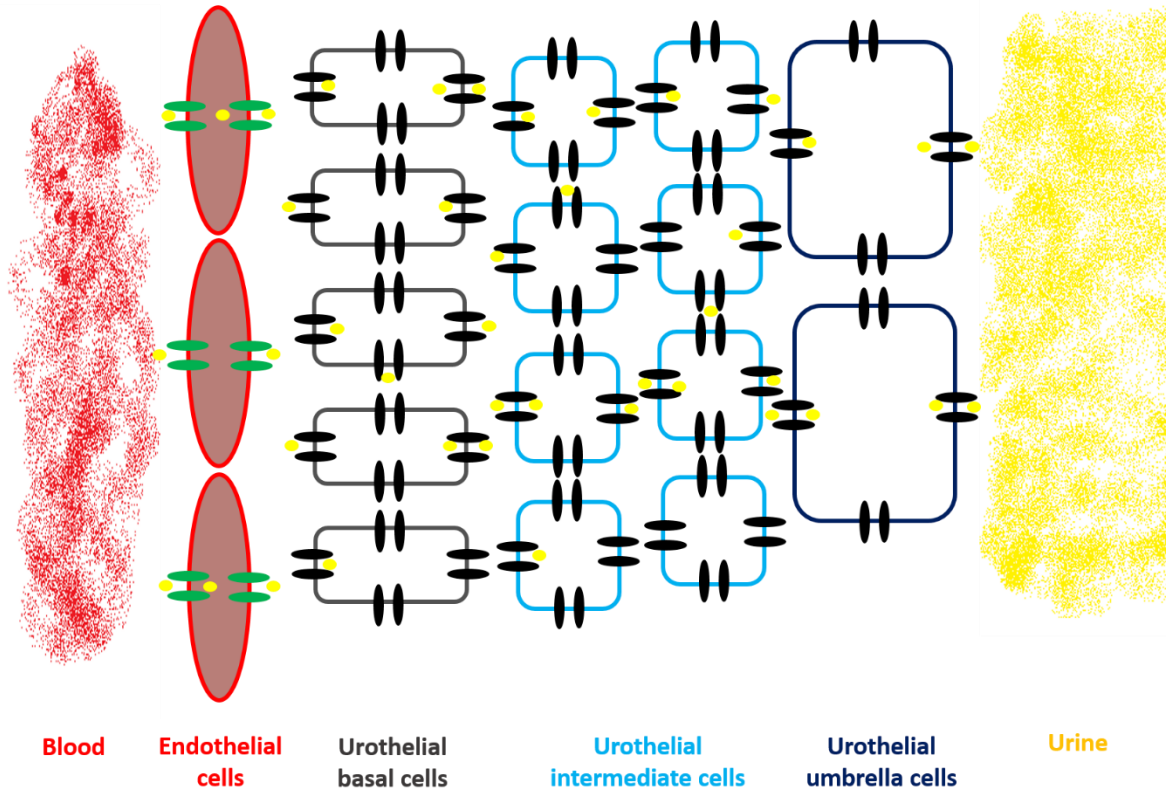

Figure 7.1 Theoretical path of transurothelial water movement

This diagram highlights the potential pathway for water from urine within the renal pelvis lumen to travel across the layers of the urothelium and into suburothelial capillaries in the lamina propria via aquaporin channels. = AQP3, = AQP1, = water derived from urine

7.2 Future work

Future work to develop this research is required in several areas:

7.2.1 Laboratory techniques

7.2.1.1 Immunohistochemistry

Unfortunately, an antibody which reliably detected AQP4 in human and rat tissues by immunohistochemistry was not discovered during this research and therefore AQP4 expression by urinary tract tissues was not assessed. Future studies will involve establishing a reliable AQP4 immunohistochemistry method to apply to samples from both the human and rat models. This will be important to localise AQP4 expression within the urothelium, particularly assessing whether it is expressed on the luminal surface of urothelial umbrella cells.

RT-PCR and western blotting of whole human ureter and renal pelvis demonstrated AQP2 expression. Immunohistochemistry, however, did not reveal expression in any layer of these tissues. Human urothelium has previously been demonstrated to not express AQP2 mRNA transcripts [259] suggesting that AQP2 expression detected from whole tissues in this study is probably from a layer other than urothelium. It is unlikely therefore that AQP2 significantly contributes to transurothelial transport. Future work to resolve this disparity between results will involve analysis of more human samples paying attention to sample fixation and antigen retrieval techniques which may affect detection of proteins by immunohistochemistry.

7.2.1.2 Western blotting

Chapter 5 discussed the differences in western blotting results achieved following protein extraction and analysis of the kidney samples for the 5 litters of rats in two separate batches. It was also noted that surgery on these litters of rats was separated in time by a few months.

Potential causes of the differences in results between litters 2-3 and 4-6 are:

- Different methods used to homogenise tissue between the 2 batches.
- Surgery carried out at a different time. Genetic drift in the animals may have therefore affected the results.
- Changes in AQP expression related to the natural progression of the insult in PUUO
- Natural variation in protein expression which could be addressed by performing PUUO on a greater number of animals

To determine the effect of the method of mechanical tissue lysis on the results obtained in this study, both techniques of sample homogenisation will be repeated using the same samples. This will be important to establish prior to analysing any further samples from either the animal model or human study.

7.2.2 Animal models

7.2.2.1 Current neonatal rat PUUO model

AQP4 mRNA expression within the renal pelvis demonstrated a tendency towards reduction in moderate and severe hydronephrosis compared to sham kidneys however significance was not achieved, potentially due to substantial variability in the results. Increasing the number of animals assessed, to increase the power of the study, will help to confirm or refute

whether a real difference exists, This could be addressed when undertaking the knockout murine model as described below.

In the later stages this study involved measuring the intra-renal pelvis pressure of PUUO and sham rats. Unfortunately, the numbers of animals involved was small and in some groups, such as those with mild and severe hydronephrosis, there was only one animal precluding meaningful analysis. Larger numbers will need to be assessed to draw firm conclusions from this aspect of the research. Additionally, the technique of intra-renal pelvis pressure measurement will be developed to enable measurement of both basal pressure and dynamic perfusion-pressure in order to control for variation in urine inflow into the renal pelvis. Again, these modifications could be achieved during completion of the knockout murine model.

In this model the sham procedure was performed the same as PUUO surgery except that following kidney mobilisation and proximal ureteric dissection a ligature was not placed and the ureter was returned to the abdomen. In the future, to ensure that appropriate sham surgery is undertaken, the sham procedure will be performed in an identical manner to PUUO surgery including placement of the metal template and ligature. The ligature will then be removed before returning the ureter to the abdomen.

7.2.2.2 Urothelium specific AQP3 knockout murine neonatal PUUO model

AQP null mouse models, including AQP3 knockouts, have been used previously to demonstrate the renal role of AQPs [255]. Future work, building on the results of this study, will aim to target AQP3 knockout to urothelium enabling investigation of the specific role of urothelial AQP3 in the outcome of PUJO. Although transgenic models targeting gene expression to the urothelium are described, using promoters for genes such as K19 [440] and fatty acid-binding protein (FABP) [441], these models are not urothelium specific.

Uroplakin II is expressed specifically by urothelial cells [442-444]. In rodents, contrary to humans, it expressed throughout all suprabasal layers of the urothelium [445, 446]. A murine uroplakin II Cre/loxP knockout system has been developed by Mo *et al.* whereby Cre expression was under the control of the uroplakin II promoter. This model demonstrated precise urothelial specificity enabling targeted gene deletion in urothelium by exclusive expression of Cre recombinase [445].

Additionally, a conditional floxed AQP3 knockout reporter mouse, strain C57BL/6NTac, is available commercially from Infrafrontier (EM:08279, Infrafrontier, Munich, Germany).

In order to further investigate this mechanism, ongoing research will involve developing urothelium specific AQP3 knockout mice using the uroplakin II Cre/loxP approach and then undertaking neonatal PUUO on these knockouts versus litter-mate and wild-type controls. If, as anticipated, the transgenic mice demonstrate a more severe phenotype than controls, attempted rescue using an AQP3 overexpression mouse under the same promoter will be undertaken.

7.2.2.3 Human study

The current major focus for the human study is ongoing recruitment of patients to all groups but particularly to group 2 (children with hydronephrosis not undergoing surgery). Furthermore, attempts will be made to recruit from clinics whereby a more balanced male:female ratio and spread of ages is obtained. Analysis of the existing demographic data for study recruits demonstrated a significant difference in the mean age between groups 1 (children undergoing pyeloplasty for PUJO) and 3 (children with normal kidneys).

A chief area to improve during ongoing running of the study is identification of follow-up patients at Bristol children's Hospital. Alongside the hospital 'Evolve' administrators, changes are being made to add study participation to the patient alerts on the computerised system. Moreover, investigative work will be needed to institute processes to gain follow-up data and urine samples from children at peripheral outreach clinics.

7.2.2.4 Urine proteomics

Identifying a non-invasive urine biomarker which enables early identification of those children requiring surgery would greatly improve the current management of children with PUJO. Currently, there is little evidence from animal studies to aid this goal. While a number of different potential biomarkers have been tested in human studies, the control groups have not always been ideal, and no biomarkers which would be cost-effective for routine implementation in the hospital setting have been identified.

Urine samples obtained from the human and rat studies will be fully interrogated using state of the art focused proteomic analysis in new facilities within the University of Bristol. Proteins in urine will be identified using an LTQ-Orbitrap Velos mass spectrometer, which combines the industry-leading Orbitrap mass analyser with the world's fastest and most

sensitive ion trap mass spectrometer. This system permits production of ultra-high resolution and precise mass data and enables the identification and quantitation of proteins, even those of low abundance, within complex mixtures in a single experiment. Firstly, this method will allow high quality assessment of urinary AQP excretion, complementing results from traditional protein analysis techniques. Secondly, proteomics will provide an unbiased screen of other excreted proteins that may be involved in the pathogenesis of 'damaging' PUJO. Identified proteins will then be further verified using a range of protein analysis techniques.

7.3 Implications of this work

During this research project an *in vivo* neonatal rat partial unilateral ureteric obstruction (PUUO) model and a complementary (fully ethically approved) human PUJO study have been implemented. This translational research project has utilised molecular biological techniques to begin investigating whether aquaporins, as key mediators of water-reabsorption, protect the kidney against high-pressure damage in PUJO.

Importantly, downregulation of urothelial and vascular endothelial AQP expression in the obstructed renal pelvis, which varies according to the severity of hydronephrosis, has been demonstrated in rat PUUO for the first time. This finding may begin to explain the mechanism behind 'safe' and 'damaging' hydronephrosis and certainly warrants further investigation which will be definitively achieved using transgenic mouse neonatal PUUO models.

AQP3 expression, and more specifically its expression in urothelium, in response to therapeutic intervention has not previously been investigated. Renal AQP2 downregulation in UUO and BUO models is attenuated by both statins [203] and COX-2 inhibitors [127] respectively, suggesting AQP expression in general is amenable to exogenous manipulation. Furthermore, AQP3 is known to show long term but not short term renal upregulation by vasopressin in rats. In non-urinary tract cells, AQP3 is upregulated by insulin and leptin acting via the PI3K/Akt/mTOR pathways [258] as well as hypertonicity [322]. These pathways provide potential targets for manipulation in order to develop new therapeutic approaches for PUJO.

Development of a non-invasive biomarker which can predict the need for pyeloplasty in PUJO would protect children from unnecessary operations, while enabling early identification of those that require timely surgery to prevent long-term kidney damage. Future analysis of human urine samples collected from the childhood PUJ study will ultimately determine whether AQP1 is a useful biomarker to guide surgical decision-making in PUJO. Additionally, further proteomic analysis of rat and human urine will enable the examination of aquaporin isoform excretion alongside performing an unbiased urine protein screen.

Our current understanding of the natural history of PUJO and our ability to distinguish which children require surgery is inadequate. Improving our understanding of the mechanism of injury in PUJO will enable earlier diagnosis and better management of this important condition through the development of novel biomarkers and new therapies.

Chapter 8. Publications and presentations

8.1 Publications

- Jackson, L., Woodward, M., Coward, R.J. The molecular biology of pelvi-ureteric junction obstruction. Pediatr Nephrol. Published online March 2017. DOI 10.1007/s00467-017-3629-0

8.2 Poster presentations

- A technical innovation in retroperitoneoscopic dismembered pyeloplasty in the presence of lower pole crossing vessels. Jackson L., Chandran, H., IPEG's 22nd Annual Congress for Endosurgery in Children. Beijing, China. June 2013
- Do aquaporins protect against renal damage in PUJ obstruction? School of clinical Sciences Academic Day, University of Bristol, UK. December 2014
- Methods utilised to demonstrate aquaporin expression and excretion in rodent and human models of PUJ obstruction. School of clinical Sciences Academic Day, University of Bristol, UK. December 2016

8.3 Oral presentations

- Do aquaporins predict and protect against renal damage in PUJ obstruction? Young Urology Meeting. Bristol, UK. September 2014
- Academic paediatric surgery. Bristol University medical students research day. April 2015
- Aquaporin expression and excretion in PUJ obstruction. School of clinical Sciences Academic Day, University of Bristol, UK. December 2016

Chapter 9. References

1. Piepsz, A., *Antenatal detection of pelviureteric junction stenosis: main controversies.* Semin Nucl Med, 2011. **41**(1): p. 11-9.

2. Ransley, P.G., et al., *The postnatal management of hydronephrosis diagnosed by prenatal ultrasound.* J Urol, 1990. **144**(2 Pt 2): p. 584-7; discussion 593-4.

3. Lee, R.S., et al., *Antenatal hydronephrosis as a predictor of postnatal outcome: a meta-analysis.* Pediatrics, 2006. **118**(2): p. 586-93.

4. Kim, H.J., et al., *Diagnostic value of anteroposterior diameter of fetal renal pelvis during second and third trimesters in predicting postnatal surgery among Korean population: useful information for antenatal counseling.* Urology, 2012. **79**(5): p. 1132-7.

5. Ismaili, K., et al., *Long-term clinical outcome of infants with mild and moderate fetal pyelectasis: validation of neonatal ultrasound as a screening tool to detect significant nephrouropathies.* J Pediatr, 2004. **144**(6): p. 759-65.

6. Jaswon, M.S., et al., *Prospective study of outcome in antenatally diagnosed renal pelvis dilatation.* Arch Dis Child Fetal Neonatal Ed, 1999. **80**(2): p. F135-8.

7. Grignon, A., et al., *Urinary tract dilatation in utero: classification and clinical applications.* Radiology, 1986. **160**(3): p. 645-7.

8. Siemens, D.R., et al., *Antenatal hydronephrosis: thresholds of renal pelvic diameter to predict insignificant postnatal pelviectasis.* Tech Urol, 1998. **4**(4): p. 198-201.

9. Scott, J.E. and M. Renwick, *Antenatal renal pelvic measurements: what do they mean?* BJU Int, 2001. **87**(4): p. 376-80.

10. Anderson, N., et al., *Detection of Obstructive Uropathy in the Fetus - Predictive Value of Sonographic Measurements of Renal Pelvic Diameter at Various Gestational Ages.* American Journal of Roentgenology, 1995. **164**(3): p. 719-723.

11. Babcook, C.J., et al., *Effect of maternal hydration on mild fetal pyelectasis.* J Ultrasound Med, 1998. **17**(9): p. 539-44; quiz 545-6.

12. Robinson, J.N., et al., *Effect of maternal hydration on fetal renal pyelectasis.* Obstet Gynecol, 1998. **92**(1): p. 137-41.

13. Mandell, J., et al., *Structural genitourinary defects detected in utero.* Radiology, 1991. **178**(1): p. 193-6.

14. Sairam, S., et al., *Natural history of fetal hydronephrosis diagnosed on mid-trimester ultrasound.* Ultrasound Obstet Gynecol, 2001. **17**(3): p. 191-6.

15. Longpre, M., et al., *Prediction of the outcome of antenatally diagnosed hydronephrosis: a multivariable analysis.* J Pediatr Urol, 2012. **8**(2): p. 135-9.

16. Dudley, J.A., et al., *Clinical relevance and implications of antenatal hydronephrosis.* Arch Dis Child Fetal Neonatal Ed, 1997. **76**(1): p. F31-4.

17. Fernbach, S.K., M. Maizels, and J.J. Conway, *Ultrasound Grading of Hydronephrosis - Introduction to the System Used by the Society-for-Fetal-Urology.* Pediatric Radiology, 1993. **23**(6): p. 478-480.

18. Nguyen, H.T., et al., *The Society for Fetal Urology consensus statement on the evaluation and management of antenatal hydronephrosis.* J Pediatr Urol, 2010. **6**(3): p. 212-31.

19. Garrett, W.J., G. Grunwald, and D.E. Robinson, *Prenatal diagnosis of fetal polycystic kidney by ultrasound.* Aust N Z J Obstet Gynaecol, 1970. **10**(1): p. 7-9.

20. Piepsz, A., *Antenatally detected hydronephrosis.* Semin Nucl Med, 2007. **37**(4): p. 249-60.

21. Grisoni, E.R., et al., *Antenatal Ultrasonography - the Experience in a High-Risk Perinatal Center.* Journal of Pediatric Surgery, 1986. **21**(4): p. 358-361.

22. D'Ottavio, G., et al., *Comparisons of first and second trimester screening for fetal anomalies.* Ann N Y Acad Sci, 1998. **847**: p. 200-9.

23. Carvalho, M.H., et al., *Detection of fetal structural abnormalities at the 11-14 week ultrasound scan.* Prenat Diagn, 2002. **22**(1): p. 1-4.

24. Woodward, M. and D. Frank, *Postnatal management of antenatal hydronephrosis.* BJU Int, 2002. **89**(2): p. 149-+.

25. Lim, D.J., et al., *Clinical characteristics and outcome of hydronephrosis detected by prenatal ultrasonography.* J Korean Med Sci, 2003. **18**(6): p. 859-62.

26. Hafez, A.T., et al., *Analysis of trends on serial ultrasound for high grade neonatal hydronephrosis.* J Urol, 2002. **168**(4 Pt 1): p. 1518-21.

27. Vemulakonda, V.M., G. Chiang, and S.T. Corbett, *Variability in use of voiding cystourethrogram during initial evaluation of infants with congenital hydronephrosis.* Urology, 2014. **83**(5): p. 1135-8.

28. Matsui, F., et al., *Late recurrence of symptomatic hydronephrosis in patients with prenatally detected hydronephrosis and spontaneous improvement.* J Urol, 2008. **180**(1): p. 322-5; discussion 325.

29. Gatti, J.M., et al., *Antenatal hydronephrosis with postnatal resolution: how long are postnatal studies warranted?* Urology, 2001. **57**(6): p. 1178.

30. Yerkes, E.B., et al., *Does every patient with prenatal hydronephrosis need voiding cystourethrography?* Journal of Urology, 1999. **162**(3): p. 1218-1220.

31. Vemulakonda, V., J. Yiee, and D.T. Wilcox, *Prenatal hydronephrosis: postnatal evaluation and management.* Curr Urol Rep, 2014. **15**(8): p. 430.

32. Takasato, M. and M.H. Little, *The origin of the mammalian kidney: implications for recreating the kidney in vitro.* Development, 2015. **142**(11): p. 1937-47.

33. Nagalakshmi, V.K. and J. Yu, *The ureteric bud epithelium: morphogenesis and roles in metanephric kidney patterning.* Mol Reprod Dev, 2015. **82**(3): p. 151-66.

34. Crelin, E.S., *Normal and abnormal development of ureter.* Urology, 1978. **12**(1): p. 2-7.

35. Matsuno, T., S. Tokunaka, and T. Koyanagi, *Muscular development in the urinary tract.* J Urol, 1984. **132**(1): p. 148-52.

36. Chang, C.P., et al., *Calcineurin is required in urinary tract mesenchyme for the development of the pyeloureteral peristaltic machinery.* J Clin Invest, 2004. **113**(7): p. 1051-8.

37. Miyazaki, Y., et al., *Angiotensin induces the urinary peristaltic machinery during the perinatal period.* J Clin Invest, 1998. **102**(8): p. 1489-97.

38. Alcaraz, A., et al., *Obstruction and recanalization of the ureter during embryonic development.* J Urol, 1991. **145**(2): p. 410-6.

39. Stringer, M.D. and S. Yassaie, *Is the pelviureteric junction an anatomical entity?* J Pediatr Urol, 2013. **9**(2): p. 123-8.

40. Woolf, A.S. and J.A. Davies, *Cell biology of ureter development.* J Am Soc Nephrol, 2013. **24**(1): p. 19-25.

41. Yu, J., T.J. Carroll, and A.P. McMahon, *Sonic hedgehog regulates proliferation and differentiation of mesenchymal cells in the mouse metanephric kidney.* Development, 2002. **129**(22): p. 5301-12.

42. Brenner-Anantharam, A., et al., *Tailbud-derived mesenchyme promotes urinary tract segmentation via BMP4 signaling.* Development, 2007. **134**(10): p. 1967-75.

43. Caubit, X., et al., *Teashirt 3 is necessary for ureteral smooth muscle differentiation downstream of SHH and BMP4.* Development, 2008. **135**(19): p. 3301-10.

44. Airik, R., et al., *Tbx18 regulates the development of the ureteral mesenchyme.* J Clin Invest, 2006. **116**(3): p. 663-74.

45. Mahoney, Z.X., et al., *Discs-large homolog 1 regulates smooth muscle orientation in the mouse ureter.* Proc Natl Acad Sci U S A, 2006. **103**(52): p. 19872-7.

46. Shafik, A. and A. Al-Sherif, *Ureteropelvic junction: A study of its anatomical structure and function. Ureteropelvic junction sphincter?* Eur Urol, 1999. **36**(2): p. 150-6; discussion 156-7.

47. Dure-Smith, P., et al., *Congenital variations in mucomuscular development of the ureter.* BJU Int, 2002. **90**(1): p. 130-4.

48. Kaneto, H., et al., *Three-D muscular arrangement at the ureteropelvic junction and its changes in congenital hydronephrosis: a stereo-morphometric study.* J Urol, 1991. **146**(3): p. 909-14.

49. Santicioli, P. and C.A. Maggi, *Myogenic and neurogenic factors in the control of pyeloureteral motility and ureteral peristalsis.* Pharmacol Rev, 1998. **50**(4): p. 683-722.

50. Nemeth, L., D.S. O'Briain, and P. Puri, *Demonstration of neuronal networks in the human upper urinary tract using confocal laser scanning microscopy.* J Urol, 2001. **166**(1): p. 255-8.

51. Lang, R.J., et al., *Pyeloureteric peristalsis: role of atypical smooth muscle cells and interstitial cells of Cajal-like cells as pacemakers.* J Physiol, 2006. **576**(Pt 3): p. 695-705.

52. Morita, T., G. Ishizuka, and S. Tsuchida, *Initiation and propagation of stimulus from the renal pelvic pacemaker in pig kidney.* Invest Urol, 1981. **19**(3): p. 157-60.

53. Tsuchida, S., et al., *Initiation and propagation of canine renal pelvic peristalsis.* Urol Int, 1981. **36**(5): p. 307-14.

54. Metzger, R., et al., *Cajal-like cells in the human upper urinary tract.* J Urol, 2004. **172**(2): p. 769-72.

55. Peters, C.A., *Urinary tract obstruction in children.* J Urol, 1995. **154**(5): p. 1874-83; discussion 1883-4.

56. Corbett H, M.L., *Hydronephrosis in children: pelviureteric junction dysfunction.* Surgery (Oxford), 2013. **31**(3): p. 135-139.

57. Hashim, H. and C.R.J. Woodhouse, *Ureteropelvic Junction Obstruction.* European Urology Supplements, 2012. **11**(2): p. 25-32.

58. Vaos, G., *Pelvi-ureteric junction obstruction*, in *Essentials in Paediatric Urology*, G. Sakellaris, Editor. 2012, Research Signpost: Kerala, India. p. 125-138.

59. Csaicsich, D., et al., *Management of congenital hydronephrosis with ureteropelvic junction obstruction: The Vienna-AKH experience 1986-2001.* Wiener Klinische Wochenschrift, 2004. **116**(21-22): p. 725-729.

60. Koff, S.A. and K. Campbell, *Nonoperative management of unilateral neonatal hydronephrosis.* J Urol, 1992. **148**(2 Pt 2): p. 525-31.

61. Koff, S.A. and K.D. Campbell, *The nonoperative management of unilateral neonatal hydronephrosis: natural history of poorly functioning kidneys.* J Urol, 1994. **152**(2 Pt 2): p. 593-5.

62. Ulman, I., V.R. Jayanthi, and S.A. Koff, *The long-term followup of newborns with severe unilateral hydronephrosis initially treated nonoperatively.* Journal of Urology, 2000. **164**(3): p. 1101-1105.

63. Chertin, B., et al., *Conservative treatment of ureteropelvic junction obstruction in children with antenatal diagnosis of hydronephrosis: lessons learned after 16 years of follow-up.* Eur Urol, 2006. **49**(4): p. 734-8.

64. Calderon-Margalit, R., et al., *History of Childhood Kidney Disease and Risk of Adult End-Stage Renal Disease.* N Engl J Med, 2018. **378**(5): p. 428-438.

65. O'Reilly, P.H., et al., *Diuresis renography in equivocal urinary tract obstruction.* Br J Urol, 1978. **50**(2): p. 76-80.

66. Gordon, I., et al., *Antenatal diagnosis of pelvic hydronephrosis: assessment of renal function and drainage as a guide to management.* J Nucl Med, 1991. **32**(9): p. 1649-54.

67. Csaicsich, D., L.A. Greenbaum, and C. Aufricht, *Upper urinary tract: when is obstruction obstruction?* Curr Opin Urol, 2004. **14**(4): p. 213-7.

68. Palmer, L.S., et al., *Surgery versus observation for managing obstructive grade 3 to 4 unilateral hydronephrosis: a report from the Society for Fetal Urology.* J Urol, 1998. **159**(1): p. 222-8.

69. Subramaniam, R., C. Kouriefs, and A.P. Dickson, *Antenatally detected pelvi-ureteric junction obstruction: concerns about conservative management.* BJU Int, 1999. **84**(3): p. 335-8.

70. Knoedler, J., et al., *Population-based comparison of laparoscopic and open pyeloplasty in paediatric pelvi-ureteric junction obstruction.* BJU Int, 2013. **111**(7): p. 1141-7.

71. Silay, M.S., et al., *Global minimally invasive pyeloplasty study in children: Results from the Pediatric Urology Expert Group of the European Association of Urology Young Academic Urologists working party*. J Pediatr Urol, 2016. **12**(4): p. 229 e1-7.

72. Zhang, P.L., C.A. Peters, and S. Rosen, *Ureteropelvic junction obstruction: morphological and clinical studies.* Pediatr Nephrol, 2000. **14**(8-9): p. 820-6.

73. Murakumo, M., et al., *Structural changes of collagen components and diminution of nerves in congenital ureteropelvic junction obstruction.* J Urol, 1997. **157**(5): p. 1963-8.

74. Demirbilek, S., et al., *Glial cell line-derived neurotrophic factor and synaptophysin expression in pelviureteral junction obstruction.* Urology, 2006. **67**(2): p. 400-5.

75. Ozel, S.K., et al., *The roles of extracellular matrix proteins, apoptosis and c-kit positive cells in the pathogenesis of ureteropelvic junction obstruction.* J Pediatr Urol, 2010. **6**(2): p. 125-9.

76. Hosgor, M., et al., *Structural changes of smooth muscle in congenital ureteropelvic junction obstruction.* J Pediatr Surg, 2005. **40**(10): p. 1632-6.

77. Solari, V., A.P. Piotrowska, and P. Puri, *Altered expression of interstitial cells of Cajal in congenital ureteropelvic junction obstruction.* J Urol, 2003. **170**(6 Pt 1): p. 2420-2.

78. Yang, X., Y. Zhang, and J. Hu, *The expression of Cajal cells at the obstruction site of congenital pelviureteric junction obstruction and quantitative image analysis.* J Pediatr Surg, 2009. **44**(12): p. 2339-42.

79. Koleda, P., et al., *Changes in interstitial cell of Cajal-like cells density in congenital ureteropelvic junction obstruction.* Int Urol Nephrol, 2012. **44**(1): p. 7-12.

80. Aoki, Y., et al., *Id2 haploinsufficiency in mice leads to congenital hydronephrosis resembling that in humans.* Genes Cells, 2004. **9**(12): p. 1287-96.

81. Valles, P.G., et al., *Role of endogenous nitric oxide in unilateral ureteropelvic junction obstruction in children.* Kidney Int, 2003. **63**(3): p. 1104-15.

82. Huang, W.Y., et al., *Renal biopsy in congenital ureteropelvic junction obstruction: evidence for parenchymal maldevelopment.* Kidney Int, 2006. **69**(1): p. 137-43.

83. Murer, L., et al., *Clinical and molecular markers of chronic interstitial nephropathy in congenital unilateral ureteropelvic junction obstruction.* Journal of Urology, 2006. **176**(6): p. 2668-2673.

84. Han, S.W., et al., *Does delayed operation for pediatric ureteropelvic junction obstruction cause histopathological changes?* Journal of Urology, 1998. **160**(3): p. 984-988.

85. Lama, G., et al., *Pelviureteral junction obstruction: correlation of renal cell apoptosis and differential renal function.* J Urol, 2003. **169**(6): p. 2335-8.

86. Rosen, S., et al., *The kidney in congenital ureteropelvic junction obstruction: a spectrum from normal to nephrectomy.* J Urol, 2008. **179**(4): p. 1257-63.

87. Chevalier, R.L., et al., *Mechanisms of renal injury and progression of renal disease in congenital obstructive nephropathy.* Pediatr Nephrol, 2010. **25**(4): p. 687-97.

88. Klein, J., et al., *Congenital ureteropelvic junction obstruction: human disease and animal models.* Int J Exp Pathol, 2011. **92**(3): p. 168-92.

89. Josephson, S., *Experimental obstructive hydronephrosis in newborn rats. III. Long-term effects on renal function.* J Urol, 1983. **129**(2): p. 396-400.

90. Chevalier, R.L., et al., *Recovery following relief of unilateral ureteral obstruction in the neonatal rat.* Kidney Int, 1999. **55**(3): p. 793-807.

91. Thornhill, B.A., et al., *Variable chronic partial ureteral obstruction in the neonatal rat: A new model of ureteropelvic junction obstruction.* Kidney International, 2005. **67**(1): p. 42-52.

92. Cachat, F., et al., *Ureteral obstruction in neonatal mice elicits segment-specific tubular cell responses leading to nephron loss.* Kidney Int, 2003. **63**(2): p. 564-75.

93. Chevalier, R.L., et al., *Recovery from release of ureteral obstruction in the rat: relationship to nephrogenesis.* Kidney Int, 2002. **61**(6): p. 2033-43.

94. Thornhill, B.A., et al., *Glomerulotubular disconnection in neonatal mice after relief of partial ureteral obstruction.* Kidney Int, 2007. **72**(9): p. 1103-12.

95. Chevalier, R.L., B.A. Thornhill, and A.Y. Chang, *Unilateral ureteral obstruction in neonatal rats leads to renal insufficiency in adulthood.* Kidney Int, 2000. **58**(5): p. 1987-95.

96. Chevalier, R.L., B.A. Thornhill, and J.T. Wolstenholme, *Renal cellular response to ureteral obstruction: role of maturation and angiotensin II.* Am J Physiol, 1999. **277**(1 Pt 2): p. F41-7.

97. Forbes, M.S., B.A. Thornhill, and R.L. Chevalier, *Proximal tubular injury and rapid formation of atubular glomeruli in mice with unilateral ureteral obstruction: a new look at an old model.* Am J Physiol Renal Physiol, 2011. **301**(1): p. F110-7.

98. Forbes, M.S., et al., *Chronic unilateral ureteral obstruction in the neonatal mouse delays maturation of both kidneys and leads to late formation of atubular glomeruli.* Am J Physiol Renal Physiol, 2013. **305**(12): p. F1736-46.

99. Lange-Sperandio, B., et al., *Selectins mediate macrophage infiltration in obstructive nephropathy in newborn mice.* Kidney Int, 2002. **61**(2): p. 516-24.

100. Lange-Sperandio, B., et al., *Distinct roles of Mac-1 and its counter-receptors in neonatal obstructive nephropathy.* Kidney Int, 2006. **69**(1): p. 81-8.

101. Esteban, V., et al., *Angiotensin II, via AT1 and AT2 receptors and NF-kappaB pathway, regulates the inflammatory response in unilateral ureteral obstruction.* J Am Soc Nephrol, 2004. **15**(6): p. 1514-29.

102. Wang, Y., et al., *Abnormal innervation and altered nerve growth factor messenger ribonucleic acid expression in ureteropelvic junction obstruction.* J Urol, 1995. **154**(2 Pt 2): p. 679-83.

103. Cutroneo, G., et al., *Altered cytoskeletal structure of smooth muscle cells in ureteropelvic junction obstruction.* J Urol, 2011. **185**(6): p. 2314-9.

104. Esther, C.R., Jr., et al., *Mice lacking angiotensin-converting enzyme have low blood pressure, renal pathology, and reduced male fertility.* Lab Invest, 1996. **74**(5): p. 953-65.

105. Shindo, T., et al., *ADAMTS-1: a metalloproteinase-disintegrin essential for normal growth, fertility, and organ morphology and function.* J Clin Invest, 2000. **105**(10): p. 1345-52.

106. Nagata, M., et al., *Nephrogenesis and renovascular development in angiotensinogen-deficient mice.* Lab Invest, 1996. **75**(5): p. 745-53.

107. McDill, B.W., et al., *Congenital progressive hydronephrosis (cph) is caused by an S256L mutation in aquaporin-2 that affects its phosphorylation and apical membrane accumulation.* Proc Natl Acad Sci U S A, 2006. **103**(18): p. 6952-7.

108. Lu, W., et al., *NFIA haploinsufficiency is associated with a CNS malformation syndrome and urinary tract defects.* PLoS Genet, 2007. **3**(5): p. e80.

109. Vivante, A., et al., *Mutations in TBX18 Cause Dominant Urinary Tract Malformations via Transcriptional Dysregulation of Ureter Development.* Am J Hum Genet, 2015. **97**(2): p. 291-301.

110. Jenkins, D., et al., *Analysis of TSHZ2 and TSHZ3 genes in congenital pelvi-ureteric junction obstruction.* Nephrol Dial Transplant, 2010. **25**(1): p. 54-60.

111. Lye, C.M., L. Fasano, and A.S. Woolf, *Ureter myogenesis: putting Teashirt into context.* J Am Soc Nephrol, 2010. **21**(1): p. 24-30.

112. Pope, J.C., et al., *Intrapelvic Pressure Monitoring in the Partially Obstructed Porcine Kidney.* Urology, 1994. **44**(4): p. 565-571.

113. Holden, D., et al., *Renal pelvic pressures in human chronic obstructive uropathy.* Br J Urol, 1984. **56**(6): p. 565-70.

114. Kinn, A.C., *Pressure flow studies in hydronephrosis.* Scand J Urol Nephrol, 1981. **15**(3): p. 249-55.

115. Chevalier, R.L., *Chronic Partial Ureteral Obstruction in the Neonatal Guinea-Pig .2. Pressure-Gradients Affecting Glomerular-Filtration Rate.* Pediatric Research, 1984. **18**(12): p. 1271-1277.

116. Madsen, M.G., *Urinary biomarkers in hydronephrosis.* Danish Medical Journal, 2013. **60**(2).

117. Moody, T.E., E.D. Vaughn, Jr., and J.Y. Gillenwater, *Relationship between renal blood flow and ureteral pressure during 18 hours of total unilateral uretheral occlusion. Implications for changing sites of increased renal resistance.* Invest Urol, 1975. **13**(3): p. 246-51.

118. el-Dahr, S.S., et al., *Upregulation of renin-angiotensin system and downregulation of kallikrein in obstructive nephropathy.* Am J Physiol, 1993. **264**(5 Pt 2): p. F874-81.

119. el-Dahr, S.S., et al., *In situ localization of renin and its mRNA in neonatal ureteral obstruction.* Am J Physiol, 1990. **258**(4 Pt 2): p. F854-62.

120. Topcu, S.O., et al., *Candesartan prevents long-term impairment of renal function in response to neonatal partial unilateral ureteral obstruction.* Am J Physiol Renal Physiol, 2007. **292**(2): p. F736-48.

121. Koff, S.A., *Pressure volume relationships in human hydronephrosis.* Urology, 1985. **25**(3): p. 256-8.

122. Yoo, K.H., et al., *Regulation of angiotensin II AT1 and AT2 receptors in neonatal ureteral obstruction.* Am J Physiol, 1997. **273**(2 Pt 2): p. R503-9.

123. Durvasula, R.V., et al., *Activation of a local tissue angiotensin system in podocytes by mechanical strain.* Kidney Int, 2004. **65**(1): p. 30-9.

124. Taneda, S., et al., *Obstructive uropathy in mice and humans: potential role for PDGF-D in the progression of tubulointerstitial injury.* J Am Soc Nephrol, 2003. **14**(10): p. 2544-55.

125. Manucha, W., et al., *eNOS/Hsp70 interaction on rosuvastatin cytoprotective effect in neonatal obstructive nephropathy.* Eur J Pharmacol, 2011. **650**(2-3): p. 487-95.

126. Misseri, R., et al., *TNF-alpha mediates obstruction-induced renal tubular cell apoptosis and proapoptotic signaling.* Am J Physiol Renal Physiol, 2005. **288**(2): p. F406-11.

127. Norregaard, R., et al., *COX-2 inhibition prevents downregulation of key renal water and sodium transport proteins in response to bilateral ureteral obstruction.* Am J Physiol Renal Physiol, 2005. **289**(2): p. F322-33.

128. Nilsson, L., et al., *Disruption of cyclooxygenase type 2 exacerbates apoptosis and renal damage during obstructive nephropathy.* Am J Physiol Renal Physiol, 2015. **309**(12): p. F1035-48.

129. Chung, K.H. and R.L. Chevalier, *Arrested development of the neonatal kidney following chronic ureteral obstruction.* J Urol, 1996. **155**(3): p. 1139-44.

130. Bartoli, F., et al., *Renal expression of monocyte chemotactic protein-1 and epidermal growth factor in children with obstructive hydronephrosis.* J Pediatr Surg, 2000. **35**(4): p. 569-72.

131. Yang, Y., et al., *Renal expression of epidermal growth factor and transforming growth factor-beta1 in children with congenital hydronephrosis.* Urology, 2006. **67**(4): p. 817-21; discussion 821-2.

132. Cai, G., et al., *Tissue inhibitor of metalloproteinase-1 exacerbated renal interstitial fibrosis through enhancing inflammation.* Nephrol Dial Transplant, 2008. **23**(6): p. 1861-75.

133. Yeh, Y.C., et al., *Transforming growth factor-{beta}1 induces Smad3-dependent {beta}1 integrin gene expression in epithelial-to-mesenchymal transition during chronic tubulointerstitial fibrosis.* Am J Pathol, 2010. **177**(4): p. 1743-54.

134. Hamzeh, M.T., R. Sridhara, and L.D. Alexander, *Cyclic stretch-induced TGF-beta1 and fibronectin expression is mediated by beta1-integrin through c-Src- and STAT3-dependent pathways in renal epithelial cells.* Am J Physiol Renal Physiol, 2015. **308**(5): p. F425-36.

135. Silverstein, D.M., et al., *Altered expression of immune modulator and structural genes in neonatal unilateral ureteral obstruction.* Kidney Int, 2003. **64**(1): p. 25-35.

136. Samarakoon, R., et al., *TGF-beta1 --> SMAD/p53/USF2 --> PAI-1 transcriptional axis in ureteral obstruction-induced renal fibrosis.* Cell Tissue Res, 2012. **347**(1): p. 117-28.

137. Garcia, I.M., et al., *Caveolin-1-eNOS/Hsp70 interactions mediate rosuvastatin antifibrotic effects in neonatal obstructive nephropathy.* Nitric Oxide, 2012. **27**(2): p. 95-105.

138. Pimentel, J.L., Jr., et al., *Regulation of renin-angiotensin system in unilateral ureteral obstruction.* Kidney Int, 1993. **44**(2): p. 390-400.

139. Ricardo, S.D., et al., *Angiotensinogen and AT(1) antisense inhibition of osteopontin translation in rat proximal tubular cells.* Am J Physiol Renal Physiol, 2000. **278**(5): p. F708-16.

140. Kaneto, H., J. Morrissey, and S. Klahr, *Increased expression of TGF-beta 1 mRNA in the obstructed kidney of rats with unilateral ureteral ligation.* Kidney Int, 1993. **44**(2): p. 313-21.

141. Morrissey, J.J., et al., *Nitric oxide generation ameliorates the tubulointerstitial fibrosis of obstructive nephropathy.* J Am Soc Nephrol, 1996. **7**(10): p. 2202-12.

142. Mazzei, L.J., et al., *Rosuvastatin preserves renal structure following unilateral ureteric obstruction in the neonatal rat.* Am J Nephrol, 2012. **35**(2): p. 103-13.

143. Han, H., et al., *Renal recruitment of B lymphocytes exacerbates tubulointerstitial fibrosis by promoting monocyte mobilization and infiltration after unilateral ureteral obstruction.* J Pathol, 2017. **241**(1): p. 80-90.

144. Burt, L.E., et al., *Renal vascular endothelial growth factor in neonatal obstructive nephropathy. I. Endogenous VEGF.* Am J Physiol Renal Physiol, 2007. **292**(1): p. F158-67.

145. Yang, Y., et al., *The expression of epidermal growth factor and transforming growth factor-beta1 in the stenotic tissue of congenital pelvi-ureteric junction obstruction in children.* J Pediatr Surg, 2003. **38**(11): p. 1656-60.

146. Knerr, I., et al., *Increased endothelin-1 and decreased adrenomedullin gene expression in the stenotic tissue of congenital pelvi-ureteric junction obstruction in children.* BJU Int, 2001. **87**(7): p. 667-71.

147. Seremetis, G.M. and M. Maizels, *TGF-beta mRNA expression in the renal pelvis after experimental and clinical ureteropelvic junction obstruction.* J Urol, 1996. **156**(1): p. 261-6.

148. Klahr, S., S. Ishidoya, and J. Morrissey, *Role of angiotensin II in the tubulointerstitial fibrosis of obstructive nephropathy.* Am J Kidney Dis, 1995. **26**(1): p. 141-6.

149. Picard, N., et al., *Origin of renal myofibroblasts in the model of unilateral ureter obstruction in the rat.* Histochem Cell Biol, 2008. **130**(1): p. 141-55.

150. Hinz, B., et al., *Alpha-smooth muscle actin expression upregulates fibroblast contractile activity.* Mol Biol Cell, 2001. **12**(9): p. 2730-41.

151. Strutz, F. and M. Zeisberg, *Renal fibroblasts and myofibroblasts in chronic kidney disease.* J Am Soc Nephrol, 2006. **17**(11): p. 2992-8.

152. Zeisberg, M., F. Strutz, and G.A. Muller, *Renal fibrosis: an update.* Curr Opin Nephrol Hypertens, 2001. **10**(3): p. 315-20.

153. Border, W.A. and N.A. Noble, *Interactions of transforming growth factor-beta and angiotensin II in renal fibrosis.* Hypertension, 1998. **31**(1 Pt 2): p. 181-8.

154. Fern, R.J., et al., *Reduced angiotensinogen expression attenuates renal interstitial fibrosis in obstructive nephropathy in mice.* J Clin Invest, 1999. **103**(1): p. 39-46.

155. Ishidoya, S., et al., *Angiotensin II receptor antagonist ameliorates renal tubulointerstitial fibrosis caused by unilateral ureteral obstruction.* Kidney Int, 1995. **47**(5): p. 1285-94.

156. Guo, G., et al., *Contributions of angiotensin II and tumor necrosis factor-alpha to the development of renal fibrosis.* Am J Physiol Renal Physiol, 2001. **280**(5): p. F777-85.

157. Fukuda, K., et al., *Quantification of TGF-beta1 mRNA along rat nephron in obstructive nephropathy.* Am J Physiol Renal Physiol, 2001. **281**(3): p. F513-21.

158. Klahr, S. and J. Morrissey, *Angiotensin II and gene expression in the kidney.* Am J Kidney Dis, 1998. **31**(1): p. 171-6.

159. Chevalier, R.L., et al., *Responses of proximal tubular cells to injury in congenital renal disease: fight or flight.* Pediatr Nephrol, 2014. **29**(4): p. 537-41.

160. Miyajima, A., et al., *Antibody to transforming growth factor-beta ameliorates tubular apoptosis in unilateral ureteral obstruction.* Kidney Int, 2000. **58**(6): p. 2301-13.

161. Manucha, W., et al., *Losartan modulation on NOS isoforms and COX-2 expression in early renal fibrogenesis in unilateral obstruction.* Kidney Int, 2004. **65**(6): p. 2091-107.

162. Jensen, A.M., et al., *Angiotensin II mediates downregulation of aquaporin water channels and key renal sodium transporters in response to urinary tract obstruction.* Am J Physiol Renal Physiol, 2006. **291**(5): p. F1021-32.

163. Kellner, D., et al., *Angiotensin receptor blockade decreases fibrosis and fibroblast expression in a rat model of unilateral ureteral obstruction.* J Urol, 2006. **176**(2): p. 806-12.

164. Derynck, R. and Y.E. Zhang, *Smad-dependent and Smad-independent pathways in TGF-beta family signalling.* Nature, 2003. **425**(6958): p. 577-84.

165. Lan, H.Y., et al., *Inhibition of renal fibrosis by gene transfer of inducible Smad7 using ultrasound-microbubble system in rat UUO model.* J Am Soc Nephrol, 2003. **14**(6): p. 1535-48.

166. Meng, X.M., et al., *Diverse roles of TGF-beta receptor II in renal fibrosis and inflammation in vivo and in vitro.* J Pathol, 2012. **227**(2): p. 175-88.

167. Galarreta, C.I., et al., *Transforming growth factor-beta1 receptor inhibition preserves glomerulotubular integrity during ureteral obstruction in adults but worsens injury in neonatal mice.* Am J Physiol Renal Physiol, 2013. **304**(5): p. F481-90.

168. Sato, M., et al., *Targeted disruption of TGF-beta1/Smad3 signaling protects against renal tubulointerstitial fibrosis induced by unilateral ureteral obstruction.* J Clin Invest, 2003. **112**(10): p. 1486-94.

169. Yang, S.P., et al., *Deregulation of renal transforming growth factor-beta1 after experimental short-term ureteric obstruction in fetal sheep.* Am J Pathol, 2001. **159**(1): p. 109-17.

170. Chung, K.H., R.A. Gomez, and R.L. Chevalier, *Regulation of renal growth factors and clusterin by AT1 receptors during neonatal ureteral obstruction.* Am J Physiol, 1995. **268**(6 Pt 2): p. F1117-23.

171. Pimentel, J.L., et al., *Role of Angiotensin-Ii in the Expression and Regulation of Transforming Growth-Factor-Beta in Obstructive Nephropathy.* Kidney International, 1995. **48**(4): p. 1233-1246.

172. Forbes, M.S., et al., *Lack of endothelial nitric-oxide synthase leads to progressive focal renal injury.* Am J Pathol, 2007. **170**(1): p. 87-99.

173. Sun, D., et al., *Effects of nitric oxide on renal interstitial fibrosis in rats with unilateral ureteral obstruction.* Life Sci, 2012. **90**(23-24): p. 900-9.

174. Chang, B., et al., *Nitric oxide in obstructive uropathy: role of endothelial nitric oxide synthase.* J Urol, 2002. **168**(4 Pt 2): p. 1801-4.

175. Valles, P.G., et al., *Renal caveolin-1 expression in children with unilateral ureteropelvic junction obstruction.* Pediatr Nephrol, 2007. **22**(2): p. 237-48.

176. Nasu, T., et al., *Sustained-release prostacyclin analog ONO-1301 ameliorates tubulointerstitial alterations in a mouse obstructive nephropathy model.* Am J Physiol Renal Physiol, 2012. **302**(12): p. F1616-29.

177. Miyajima, A., et al., *Role of nitric oxide in renal tubular apoptosis of unilateral ureteral obstruction.* Kidney Int, 2001. **59**(4): p. 1290-303.

178. Mazzei, L., et al., *WT-1 mRNA expression is modulated by nitric oxide availability and Hsp70 interaction after neonatal unilateral ureteral obstruction.* Biocell, 2010. **34**(3): p. 121-32.

179. Becknell, B., et al., *Urine Stasis Predisposes to Urinary Tract Infection by an Opportunistic Uropathogen in the Megabladder (Mgb) Mouse.* PLoS One, 2015. **10**(9): p. e0139077.

180. Jensen, A.M., et al., *Angiotensin II regulates V2 receptor and pAQP2 during ureteral obstruction.* Am J Physiol Renal Physiol, 2009. **296**(1): p. F127-34.

181. Li, C., et al., *Altered expression of major renal Na transporters in rats with unilateral ureteral obstruction.* Am J Physiol Renal Physiol, 2003. **284**(1): p. F155-66.

182. Li, C., et al., *Altered expression of major renal Na transporters in rats with bilateral ureteral obstruction and release of obstruction.* Am J Physiol Renal Physiol, 2003. **285**(5): p. F889-901.

183. Li, C., et al., *Altered expression of urea transporters in response to ureteral obstruction.* Am J Physiol Renal Physiol, 2004. **286**(6): p. F1154-62.

184. Li, C., et al., *Downregulation of renal aquaporins in response to unilateral ureteral obstruction.* Am J Physiol Renal Physiol, 2003. **284**(5): p. F1066-79.

185. Shi, Y., et al., *Neonatal ureteral obstruction alters expression of renal sodium transporters and aquaporin water channels.* Kidney Int, 2004. **66**(1): p. 203-15.

186. Frokiaer, J., et al., *Downregulation of aquaporin-2 parallels changes in renal water excretion in unilateral ureteral obstruction.* Am J Physiol, 1997. **273**(2 Pt 2): p. F213-23.

187. Wen, J.G., et al., *Expression of renal aquaporins is down-regulated in children with congenital hydronephrosis.* Scand J Urol Nephrol, 2009. **43**(6): p. 486-93.

188. Frokiaer, J., et al., *Bilateral ureteral obstruction downregulates expression of vasopressin-sensitive AQP-2 water channel in rat kidney.* Am J Physiol, 1996. **270**(4 Pt 2): p. F657-68.

189. Li, C., et al., *Downregulation of AQP1, -2, and -3 after ureteral obstruction is associated with a long-term urine-concentrating defect.* Am J Physiol Renal Physiol, 2001. **281**(1): p. F163-71.

190. Ishidoya, S., et al., *Delayed treatment with enalapril halts tubulointerstitial fibrosis in rats with obstructive nephropathy.* Kidney Int, 1996. **49**(4): p. 1110-9.

191. Kaneto, H., et al., *Enalapril reduces collagen type IV synthesis and expansion of the interstitium in the obstructed rat kidney.* Kidney Int, 1994. **45**(6): p. 1637-47.

192. Klahr, S. and J. Morrissey, *Comparative effects of ACE inhibition and angiotensin II receptor blockade in the prevention of renal damage.* Kidney Int Suppl, 2002(82): p. S23-6.

193. Chen, C.O., et al., *Angiotensin-converting enzyme inhibition aggravates renal interstitial injury resulting from partial unilateral ureteral obstruction in the neonatal rat.* Am J Physiol Renal Physiol, 2007. **292**(3): p. F946-55.

194. Coleman, C.M., et al., *Angiotensin AT1-receptor inhibition exacerbates renal injury resulting from partial unilateral ureteral obstruction in the neonatal rat.* Am J Physiol Renal Physiol, 2007. **293**(1): p. F262-8.

195. Webb, N.J., et al., *Losartan and enalapril are comparable in reducing proteinuria in children.* Kidney Int, 2012. **82**(7): p. 819-26.

196. Ardissino, G., et al., *No clear evidence of ACEi efficacy on the progression of chronic kidney disease in children with hypodysplastic nephropathy--report from the ItalKid Project database.* Nephrol Dial Transplant, 2007. **22**(9): p. 2525-30.

197. Hari, P., et al., *Effect of enalapril on glomerular filtration rate and proteinuria in children with chronic kidney disease: a randomized controlled trial.* Indian Pediatr, 2013. **50**(10): p. 923-8.

198. Moriyama, T., et al., *Fluvastatin suppresses oxidative stress and fibrosis in the interstitium of mouse kidneys with unilateral ureteral obstruction.* Kidney Int, 2001. **59**(6): p. 2095-103.

199. Mizuguchi, Y., et al., *Atorvastatin ameliorates renal tissue damage in unilateral ureteral obstruction.* J Urol, 2004. **172**(6 Pt 1): p. 2456-9.

200. Rodriguez-Pena, A.B., et al., *Effect of angiotensin II and small GTPase Ras signaling pathway inhibition on early renal changes in a murine model of obstructive nephropathy.* Biomed Res Int, 2014. **2014**: p. 124902.

201. Jasinska, M., J. Owczarek, and D. Orszulak-Michalak, *Statins: a new insight into their mechanisms of action and consequent pleiotropic effects.* Pharmacol Rep, 2007. **59**(5): p. 483-99.

202. Kamdar, C., et al., *Atorvastatin protects renal function in the rat with acute unilateral ureteral obstruction.* Urology, 2010. **75**(4): p. 853-7.

203. Danilovic, A., et al., *Atorvastatin prevents the downregulation of aquaporin-2 receptor after bilateral ureteral obstruction and protects renal function in a rat model.* Urology, 2012. **80**(2): p. 485 e15-20.

204. Ramkumar, S., A. Raghunath, and S. Raghunath, *Statin Therapy: Review of Safety and Potential Side Effects.* Acta Cardiol Sin, 2016. **32**(6): p. 631-639.

205. Kusters, D.M., et al., *Ten-year follow-up after initiation of statin therapy in children with familial hypercholesterolemia.* JAMA, 2014. **312**(10): p. 1055-7.

206. Moon, J.A., et al., *IN-1130, a novel transforming growth factor-beta type I receptor kinase (ALK5) inhibitor, suppresses renal fibrosis in obstructive nephropathy.* Kidney Int, 2006. **70**(7): p. 1234-43.

207. Morris, J.C., et al., *Phase I/II study of GC1008: A human anti-transforming growth factor-beta (TGF beta) monoclonal antibody (MAb) in patients with advanced malignant melanoma (MM) or renal cell carcinoma (RCC).* Journal of Clinical Oncology, 2008. **26**(15).

208. Cheng, X., et al., *Cyclooxygenase-2 inhibitor preserves medullary aquaporin-2 expression and prevents polyuria after ureteral obstruction.* J Urol, 2004. **172**(6 Pt 1): p. 2387-90.

209. Kamata, M., et al., *Role of cyclooxygenase-2 in the development of interstitial fibrosis in kidneys following unilateral ureteral obstruction in mice.* Biomed Pharmacother, 2015. **70**: p. 174-80.

210. Sobel, R.E., et al., *Safety of celecoxib and nonselective nonsteroidal anti-inflammatory drugs in juvenile idiopathic arthritis: results of the Phase 4 registry.* Pediatr Rheumatol Online J, 2014. **12**: p. 29.

211. Yuan, Y., et al., *Urinary candidate biomarker discovery in a rat unilateral ureteral obstruction model.* Sci Rep, 2015. **5**: p. 9314.

212. Madsen, M.G., et al., *Urinary biomarkers in prenatally diagnosed unilateral hydronephrosis.* J Pediatr Urol, 2011. **7**(2): p. 105-12.

213. Grandaliano, G., et al., *MCP-1 and EGF renal expression and urine excretion in human congenital obstructive nephropathy.* Kidney Int, 2000. **58**(1): p. 182-92.

214. Papachristou, F., A. Pavlaki, and N. Printza, *Urinary and serum biomarkers in ureteropelvic junction obstruction: a systematic review.* Biomarkers, 2014. **19**(7): p. 531-40.

215. Decramer, S., et al., *Predicting the clinical outcome of congenital unilateral ureteropelvic junction obstruction in newborn by urinary proteome analysis.* Nat Med, 2006. **12**(4): p. 398-400.

216. Drube, J., et al., *Urinary proteome analysis identifies infants but not older children requiring pyeloplasty.* Pediatr Nephrol, 2010. **25**(9): p. 1673-8.

217. Taha, M.A., et al., *Obstructed versus dilated nonobstructed kidneys in children with congenital ureteropelvic junction narrowing: role of urinary tubular enzymes.* J Urol, 2007. **178**(2): p. 640-6.

218. Taranta-Janusz, K., et al., *Urinary angiotensinogen as a novel marker of obstructive nephropathy in children.* Acta Paediatr, 2013. **102**(9): p. e429-33.

219. Bartoli, F., et al., *Urinary epidermal growth factor, monocyte chemotactic protein-1, and beta2-microglobulin in children with ureteropelvic junction obstruction.* J Pediatr Surg, 2011. **46**(3): p. 530-6.

220. Madsen, M.G., et al., *Urinary NGAL, cystatin C, beta2-microglobulin, and osteopontin significance in hydronephrotic children.* Pediatr Nephrol, 2012. **27**(11): p. 2099-106.

221. Atar, A., et al., *The roles of serum and urinary carbohydrate antigen 19-9 in the management of patients with antenatal hydronephrosis.* J Pediatr Urol, 2015. **11**(3): p. 133 e1-5.

222. Kajbafzadeh, A.M., et al., *Urinary and serum carbohydrate antigen 19-9 as a biomarker in ureteropelvic junction obstruction in children.* J Urol, 2010. **183**(6): p. 2353-60.

223. Madsen, M.G., et al., *Epidermal growth factor and monocyte chemotactic peptide-1: potential biomarkers of urinary tract obstruction in children with hydronephrosis.* J Pediatr Urol, 2013. **9**(6 Pt A): p. 838-45.

224. Taha, M.A., et al., *Pelvi-ureteric junction obstruction in children: the role of urinary transforming growth factor-beta and epidermal growth factor.* BJU Int, 2007. **99**(4): p. 899-903.

225. Taha, M.A., et al., *Diagnosis of ureteropelvic junction obstruction in children: role of endothelin-1 in voided urine.* Urology, 2007. **69**(3): p. 560-4; discussion 564-5.

226. Li, Z., et al., *Urinary heme oxygenase-1 in children with congenital hydronephrosis due to ureteropelvic junction obstruction.* Biomarkers, 2012. **17**(5): p. 471-6.

227. Wasilewska, A., et al., *KIM-1 and NGAL: new markers of obstructive nephropathy.* Pediatr Nephrol, 2011. **26**(4): p. 579-86.

228. Taranta-Janusz, K., et al., *Urinary cytokine profiles in unilateral congenital hydronephrosis.* Pediatr Nephrol, 2012. **27**(11): p. 2107-13.

229. Cost, N.G., et al., *Urinary NGAL levels correlate with differential renal function in patients with ureteropelvic junction obstruction undergoing pyeloplasty.* J Urol, 2013. **190**(4 Suppl): p. 1462-7.

230. Almodhen, F., et al., *The role of bladder urine transforming growth factor-beta1 concentrations in diagnosis and management of unilateral prenatal hydronephrosis.* J Urol, 2009. **182**(1): p. 292-8; discussion 298.

231. Kruse, E., N. Uehlein, and R. Kaldenhoff, *The aquaporins.* Genome Biol, 2006. **7**(2): p. 206.

232. Denker, B.M., et al., *Identification, purification, and partial characterization of a novel Mr 28,000 integral membrane protein from erythrocytes and renal tubules.* J Biol Chem, 1988. **263**(30): p. 15634-42.

233. Agre, P., et al., *Aquaporin water channels--from atomic structure to clinical medicine.* J Physiol, 2002. **542**(Pt 1): p. 3-16.

234. Chen, Y.C., M.A. Cadnapaphornchai, and R.W. Schrier, *Clinical update on renal aquaporins.* Biol Cell, 2005. **97**(6): p. 357-71.

235. Day, R.E., et al., *Human aquaporins: Regulators of transcellular water flow.* Biochimica Et Biophysica Acta-General Subjects, 2014. **1840**(5): p. 1492-1506.

236. Tamma, G., et al., *Cell culture models and animal models for studying the patho-physiological role of renal aquaporins.* Cell Mol Life Sci, 2012. **69**(12): p. 1931-46.

237. Verkman, A.S. and A.K. Mitra, *Structure and function of aquaporin water channels.* American Journal of Physiology-Renal Physiology, 2000. **278**(1): p. F13-F28.

238. Michalek, K., *Aquaglyceroporins in the kidney: present state of knowledge and prospects.* J Physiol Pharmacol, 2016. **67**(2): p. 185-93.

239. Geyer, R.R., et al., *Relative CO(2)/NH(3) selectivities of mammalian aquaporins 0-9.* Am J Physiol Cell Physiol, 2013. **304**(10): p. C985-94.

240. Watanabe, S., et al., *Aquaporin-9 facilitates membrane transport of hydrogen peroxide in mammalian cells.* Biochem Biophys Res Commun, 2016. **471**(1): p. 191-7.

241. Nielsen, S., et al., *Aquaporins in the kidney: from molecules to medicine.* Physiol Rev, 2002. **82**(1): p. 205-44.

242. Baumgarten, R., et al., *Glycosylation is not essential for vasopressin-dependent routing of aquaporin-2 in transfected Madin-Darby canine kidney cells.* J Am Soc Nephrol, 1998. **9**(9): p. 1553-9.

243. van Hoek, A.N., et al., *Purification and structure-function analysis of native, PNGase F-treated, and endo-beta-galactosidase-treated CHIP28 water channels.* Biochemistry, 1995. **34**(7): p. 2212-9.

244. Berry, V., et al., *Missense mutations in MIP underlie autosomal dominant 'polymorphic' and lamellar cataracts linked to 12q.* Nat Genet, 2000. **25**(1): p. 15-7.

245. King, L.S., et al., *Decreased pulmonary vascular permeability in aquaporin-1-null humans.* Proc Natl Acad Sci U S A, 2002. **99**(2): p. 1059-63.

246. Nielsen, S., et al., *Distribution of the aquaporin CHIP in secretory and resorptive epithelia and capillary endothelia.* Proc Natl Acad Sci U S A, 1993. **90**(15): p. 7275-9.

247. Richardson, S.M., et al., *Aquaporin expression in the human intervertebral disc.* J Mol Histol, 2008. **39**(3): p. 303-9.

248. Lopez, I.A., et al., *Immunohistochemical localization of aquaporins in the human inner ear.* Cell Tissue Res, 2007. **328**(3): p. 453-60.

249. Spector, D.A., et al., *Expression, localization, and regulation of aquaporin-1 to -3 in rat urothelia.* Am J Physiol Renal Physiol, 2002. **282**(6): p. F1034-42.

250. Kim, S.O., et al., *Changes in aquaporin (AQP)2 and AQP3 expression in ovariectomized rat urinary bladder: potential implication of water permeability in urinary bladder.* World J Urol, 2012. **30**(2): p. 207-12.

251. Jablonski, E.M., et al., *Estrogen regulation of aquaporins in the mouse uterus: potential roles in uterine water movement.* Biol Reprod, 2003. **69**(5): p. 1481-7.

252. Shahzad, H., et al., *Quercetin alters uterine fluid volume and aquaporin (AQP) subunits (AQP-1, 2, 5 & 7) expression in the uterus in the presence of sex-steroids in rats.* Reprod Toxicol, 2017. **69**: p. 276-285.

253. He, R.H., et al., *Aquaporin-2 expression in human endometrium correlates with serum ovarian steroid hormones.* Life Sci, 2006. **79**(5): p. 423-9.

254. Borsani, E., et al., *Alterations of AQP2 expression in trigeminal ganglia in a murine inflammation model.* Neurosci Lett, 2009. **449**(3): p. 183-8.

255. Verkman, A.S., *Roles of aquaporins in kidney revealed by transgenic mice.* Semin Nephrol, 2006. **26**(3): p. 200-8.

256. Koyama, Y., et al., *Expression and localization of aquaporins in rat gastrointestinal tract.* Am J Physiol, 1999. **276**(3 Pt 1): p. C621-7.

257. Sougrat, R., et al., *Functional expression of AQP3 in human skin epidermis and reconstructed epidermis.* J Invest Dermatol, 2002. **118**(4): p. 678-85.

258. Rodriguez, A., et al., *Insulin- and leptin-mediated control of aquaglyceroporins in human adipocytes and hepatocytes is mediated via the PI3K/Akt/mTOR signaling cascade.* J Clin Endocrinol Metab, 2011. **96**(4): p. E586-97.

259. Rubenwolf, P.C., et al., *Expression and localisation of aquaporin water channels in human urothelium in situ and in vitro.* Eur Urol, 2009. **56**(6): p. 1013-23.

260. Mobasheri, A., M. Shakibaei, and D. Marples, *Immunohistochemical localization of aquaporin 10 in the apical membranes of the human ileum: a potential pathway for luminal water and small solute absorption.* Histochem Cell Biol, 2004. **121**(6): p. 463-71.

261. Frigeri, A., et al., *Aquaporins in skeletal muscle: reassessment of the functional role of aquaporin-4.* FASEB J, 2004. **18**(7): p. 905-7.

262. Manley, G.T., et al., *Aquaporin-4 deletion in mice reduces brain edema after acute water intoxication and ischemic stroke.* Nat Med, 2000. **6**(2): p. 159-63.

263. Li, J., R.V. Patil, and A.S. Verkman, *Mildly abnormal retinal function in transgenic mice without Muller cell aquaporin-4 water channels.* Invest Ophthalmol Vis Sci, 2002. **43**(2): p. 573-9.

264. Lu, D.C., et al., *Impaired olfaction in mice lacking aquaporin-4 water channels.* FASEB J, 2008. **22**(9): p. 3216-23.

265. Butler, T.L., et al., *Cardiac aquaporin expression in humans, rats, and mice.* Am J Physiol Heart Circ Physiol, 2006. **291**(2): p. H705-13.

266. Cheng, C., et al., *The role of anti-aquaporin 4 antibody in the conversion of acute brainstem syndrome to neuromyelitis optica.* BMC Neurol, 2016. **16**(1): p. 203.

267. Zeppenfeld, D.M., et al., *Association of Perivascular Localization of Aquaporin-4 With Cognition and Alzheimer Disease in Aging Brains.* JAMA Neurol, 2017. **74**(1): p. 91-99.

268. Nielsen, S., et al., *Specialized membrane domains for water transport in glial cells: high-resolution immunogold cytochemistry of aquaporin-4 in rat brain.* J Neurosci, 1997. **17**(1): p. 171-80.

269. Tsubota, K., et al., *Defective cellular trafficking of lacrimal gland aquaporin-5 in Sjogren's syndrome.* Lancet, 2001. **357**(9257): p. 688-9.

270. Liu, X., et al., *A role for AQP5 in activation of TRPV4 by hypotonicity: concerted involvement of AQP5 and TRPV4 in regulation of cell volume recovery.* J Biol Chem, 2006. **281**(22): p. 15485-95.

271. Nielsen, S., et al., *Aquaporins in complex tissues. II. Subcellular distribution in respiratory and glandular tissues of rat.* Am J Physiol, 1997. **273**(5 Pt 1): p. C1549-61.

272. Mhatre, A.N., et al., *Identification of aquaporin 5 (AQP5) within the cochlea: cDNA cloning and in situ localization.* Biochem Biophys Res Commun, 1999. **264**(1): p. 157-62.

273. Ma, T., et al., *Defective secretion of saliva in transgenic mice lacking aquaporin-5 water channels.* J Biol Chem, 1999. **274**(29): p. 20071-4.

274. Matsuki-Fukushima, M., et al., *Presence and localization of aquaporin-6 in rat parotid acinar cells.* Cell Tissue Res, 2008. **332**(1): p. 73-80.

275. Iandiev, I., et al., *Immunolocalization of aquaporin-6 in the rat retina.* Neurosci Lett, 2011. **490**(2): p. 130-4.

276. Gregoire, F., et al., *Analysis of aquaporin expression in liver with a focus on hepatocytes.* Histochem Cell Biol, 2015. **144**(4): p. 347-63.

277. Suzuki-Toyota, F., K. Ishibashi, and S. Yuasa, *Immunohistochemical localization of a water channel, aquaporin 7 (AQP7), in the rat testis.* Cell and Tissue Research, 1999. **295**(2): p. 279-285.

278. McConnell, N.A., et al., *Water permeability of an ovarian antral follicle is predominantly transcellular and mediated by aquaporins.* Endocrinology, 2002. **143**(8): p. 2905-12.

279. Hibuse, T., et al., *Aquaporin 7 deficiency is associated with development of obesity through activation of adipose glycerol kinase.* Proc Natl Acad Sci U S A, 2005. **102**(31): p. 10993-8.

280. Hurley, P.T., et al., *Expression and immunolocalization of aquaporin water channels in rat exocrine pancreas.* Am J Physiol Gastrointest Liver Physiol, 2001. **280**(4): p. G701-9.

281. Elkjaer, M.L., et al., *Immunolocalization of aquaporin-8 in rat kidney, gastrointestinal tract, testis, and airways.* Am J Physiol Renal Physiol, 2001. **281**(6): p. F1047-57.

282. Koyama, N., et al., *Cloning and functional expression of human aquaporin8 cDNA and analysis of its gene.* Genomics, 1998. **54**(1): p. 169-72.

283. Yang, B., et al., *Phenotype analysis of aquaporin-8 null mice.* Am J Physiol Cell Physiol, 2005. **288**(5): p. C1161-70.

284. Su, W., et al., *Occurrence of multi-oocyte follicles in aquaporin 8-deficient mice.* Reprod Biol Endocrinol, 2013. **11**: p. 88.

285. Grande, M.T., et al., *Deletion of H-Ras decreases renal fibrosis and myofibroblast activation following ureteral obstruction in mice.* Kidney Int, 2010. **77**(6): p. 509-18.

286. Tsukaguchi, H., et al., *Molecular characterization of a broad selectivity neutral solute channel.* J Biol Chem, 1998. **273**(38): p. 24737-43.

287. Tsukaguchi, H., et al., *Functional and molecular characterization of the human neutral solute channel aquaporin-9.* Am J Physiol, 1999. **277**(5 Pt 2): p. F685-96.

288. Litman, T., R. Sogaard, and T. Zeuthen, *Ammonia and urea permeability of mammalian aquaporins.* Handb Exp Pharmacol, 2009(190): p. 327-58.

289. Yang, M., et al., *Hyperosmotic induction of aquaporin expression in rat astrocytes through a different MAPK pathway.* J Cell Biochem, 2013. **114**(1): p. 111-9.

290. Rojek, A.M., et al., *Defective glycerol metabolism in aquaporin 9 (AQP9) knockout mice.* Proc Natl Acad Sci U S A, 2007. **104**(9): p. 3609-14.

291. Laforenza, U., M.F. Scaffino, and G. Gastaldi, *Aquaporin-10 represents an alternative pathway for glycerol efflux from human adipocytes.* PLoS One, 2013. **8**(1): p. e54474.

292. Ishibashi, K., et al., *Cloning and identification of a new member of water channel (AQP10) as an aquaglyceroporin.* Biochim Biophys Acta, 2002. **1576**(3): p. 335-40.

293. Morinaga, T., et al., *Mouse aquaporin 10 gene (AQP10) is a pseudogene.* Biochem Biophys Res Commun, 2002. **294**(3): p. 630-4.

294. Morishita, Y., et al., *Disruption of aquaporin-11 produces polycystic kidneys following vacuolization of the proximal tubule.* Mol Cell Biol, 2005. **25**(17): p. 7770-9.

295. Yakata, K., et al., *Aquaporin-11 containing a divergent NPA motif has normal water channel activity.* Biochim Biophys Acta, 2007. **1768**(3): p. 688-93.

296. Ishibashi, K., Y. Tanaka, and Y. Morishita, *The role of mammalian superaquaporins inside the cell.* Biochim Biophys Acta, 2014. **1840**(5): p. 1507-12.

297. Itoh, T., et al., *Identification of a novel aquaporin, AQP12, expressed in pancreatic acinar cells.* Biochem Biophys Res Commun, 2005. **330**(3): p. 832-8.

298. Ohta, E., et al., *Pancreas-specific aquaporin 12 null mice showed increased susceptibility to caerulein-induced acute pancreatitis.* Am J Physiol Cell Physiol, 2009. **297**(6): p. C1368-78.

299. Procino, G., et al., *AQP5 Is Expressed In Type-B Intercalated Cells in the Collecting Duct System of the Rat, Mouse and Human Kidney.* Cellular Physiology and Biochemistry, 2011. **28**(4): p. 683-692.

300. Curthoys, N.P. and O.W. Moe, *Proximal tubule function and response to acidosis.* Clin J Am Soc Nephrol, 2014. **9**(9): p. 1627-38.

301. Nielsen, S., et al., *CHIP28 water channels are localized in constitutively water-permeable segments of the nephron.* J Cell Biol, 1993. **120**(2): p. 371-83.

302. Maunsbach, A.B., et al., *Aquaporin-1 water channel expression in human kidney.* J Am Soc Nephrol, 1997. **8**(1): p. 1-14.

303. Bedford, J.J., J.P. Leader, and R.J. Walker, *Aquaporin expression in normal human kidney and in renal disease.* Journal of the American Society of Nephrology, 2003. **14**(10): p. 2581-2587.

304. Nielsen, S., et al., *Aquaporin-1 water channels in short and long loop descending thin limbs and in descending vasa recta in rat kidney.* Am J Physiol, 1995. **268**(6 Pt 2): p. F1023-37.

305. Pallone, T.L., et al., *Requirement of aquaporin-1 for NaCl-driven water transport across descending vasa recta.* J Clin Invest, 2000. **105**(2): p. 215-22.

306. Preston, G.M., et al., *Mutations in aquaporin-1 in phenotypically normal humans without functional CHIP water channels.* Science, 1994. **265**(5178): p. 1585-7.

307. King, L.S., et al., *Defective urinary-concentrating ability due to a complete deficiency of aquaporin-1.* N Engl J Med, 2001. **345**(3): p. 175-9.

308. Bouley, R., et al., *Angiotensin II and hypertonicity modulate proximal tubular aquaporin 1 expression.* Am J Physiol Renal Physiol, 2009. **297**(6): p. F1575-86.

309. Jenq, W., et al., *Aquaporin-1 expression in proximal tubule epithelial cells of human kidney is regulated by hyperosmolarity and contrast agents.* Biochem Biophys Res Commun, 1999. **256**(1): p. 240-8.

310. Jenq, W., et al., *Aquaporin-1: an osmoinducible water channel in cultured mIMCD-3 cells.* Biochem Biophys Res Commun, 1998. **245**(3): p. 804-9.

311. Umenishi, F. and R.W. Schrier, *Hypertonicity-induced aquaporin-1 (AQP1) expression is mediated by the activation of MAPK pathways and hypertonicity-responsive element in the AQP1 gene.* J Biol Chem, 2003. **278**(18): p. 15765-70.

312. Nielsen, S., et al., *Cellular and subcellular immunolocalization of vasopressin-regulated water channel in rat kidney.* Proc Natl Acad Sci U S A, 1993. **90**(24): p. 11663-7.

313. Nielsen, S., et al., *Vasopressin increases water permeability of kidney collecting duct by inducing translocation of aquaporin-CD water channels to plasma membrane.* Proc Natl Acad Sci U S A, 1995. **92**(4): p. 1013-7.

314. Kishore, B.K., et al., *Rat renal arcade segment expresses vasopressin-regulated water channel and vasopressin V2 receptor.* J Clin Invest, 1996. **97**(12): p. 2763-71.

315. Christensen, B.M., et al., *Localization and regulation of PKA-phosphorylated AQP2 in response to V(2)-receptor agonist/antagonist treatment.* Am J Physiol Renal Physiol, 2000. **278**(1): p. F29-42.

316. Biner, H.L., et al., *Human cortical distal nephron: distribution of electrolyte and water transport pathways.* J Am Soc Nephrol, 2002. **13**(4): p. 836-47.

317. Deen, P.M., et al., *Requirement of human renal water channel aquaporin-2 for vasopressin-dependent concentration of urine.* Science, 1994. **264**(5155): p. 92-5.

318. Boone, M., et al., *Counteracting vasopressin-mediated water reabsorption by ATP, dopamine, and phorbol esters: mechanisms of action.* Am J Physiol Renal Physiol, 2011. **300**(3): p. F761-71.

319. Tamma, G., et al., *Bradykinin signaling counteracts cAMP-elicited aquaporin 2 translocation in renal cells.* J Am Soc Nephrol, 2005. **16**(10): p. 2881-9.

320. Klokkers, J., et al., *Atrial natriuretic peptide and nitric oxide signaling antagonizes vasopressin-mediated water permeability in inner medullary collecting duct cells.* Am J Physiol Renal Physiol, 2009. **297**(3): p. F693-703.

321. Kortenoeven, M.L., et al., *Hypotonicity-induced reduction of aquaporin-2 transcription in mpkCCD cells is independent of the tonicity responsive element, vasopressin, and cAMP.* J Biol Chem, 2011. **286**(15): p. 13002-10.

322. Sugiyama, Y., et al., *Osmotic stress up-regulates aquaporin-3 gene expression in cultured human keratinocytes.* Biochim Biophys Acta, 2001. **1522**(2): p. 82-8.

323. Ecelbarger, C.A., et al., *Aquaporin-3 water channel localization and regulation in rat kidney.* Am J Physiol, 1995. **269**(5 Pt 2): p. F663-72.

324. Ishibashi, K., et al., *Molecular cloning and expression of a member of the aquaporin family with permeability to glycerol and urea in addition to water expressed at the basolateral membrane of kidney collecting duct cells.* Proc Natl Acad Sci U S A, 1994. **91**(14): p. 6269-73.

325. Terris, J., et al., *Long-term regulation of four renal aquaporins in rats.* Am J Physiol, 1996. **271**(2 Pt 2): p. F414-22.

326. Terris, J., et al., *Distribution of aquaporin-4 water channel expression within rat kidney.* Am J Physiol, 1995. **269**(6 Pt 2): p. F775-85.

327. Poulsen, S.B., et al., *Long-term vasopressin-V2-receptor stimulation induces regulation of aquaporin 4 protein in renal inner medulla and cortex of Brattleboro rats.* Nephrol Dial Transplant, 2013. **28**(8): p. 2058-65.

328. Procino, G., et al., *Co-regulated pendrin and aquaporin 5 expression and trafficking in Type-B intercalated cells under potassium depletion.* Cell Physiol Biochem, 2013. **32**(7): p. 184-99.

329. Yamamura, Y., et al., *TNF-alpha inhibits aquaporin 5 expression in human salivary gland acinar cells via suppression of histone H4 acetylation.* J Cell Mol Med, 2012. **16**(8): p. 1766-75.

330. Yasui, M., et al., *Aquaporin-6: An intracellular vesicle water channel protein in renal epithelia.* Proc Natl Acad Sci U S A, 1999. **96**(10): p. 5808-13.

331. Ma, T., et al., *cDNA cloning and gene structure of a novel water channel expressed exclusively in human kidney: evidence for a gene cluster of aquaporins at chromosome locus 12q13.* Genomics, 1996. **35**(3): p. 543-50.

332. Promeneur, D., et al., *Regulation of AQP6 mRNA and protein expression in rats in response to altered acid-base or water balance.* Am J Physiol Renal Physiol, 2000. **279**(6): p. F1014-26.

333. Holm, L.M., D.A. Klaerke, and T. Zeuthen, *Aquaporin 6 is permeable to glycerol and urea.* Pflugers Arch, 2004. **448**(2): p. 181-6.

334. Ikeda, M., et al., *Characterization of aquaporin-6 as a nitrate channel in mammalian cells. Requirement of pore-lining residue threonine 63.* J Biol Chem, 2002. **277**(42): p. 39873-9.

335. Yasui, M., et al., *Rapid gating and anion permeability of an intracellular aquaporin.* Nature, 1999. **402**(6758): p. 184-7.

336. Ishibashi, K., M. Imai, and S. Sasaki, *Cellular localization of aquaporin 7 in the rat kidney.* Exp Nephrol, 2000. **8**(4-5): p. 252-7.

337. Sohara, E., S. Uchida, and S. Sasaki, *Function of aquaporin-7 in the kidney and the male reproductive system.* Handb Exp Pharmacol, 2009(190): p. 219-31.

338. Calamita, G., et al., *The inner mitochondrial membrane has aquaporin-8 water channels and is highly permeable to water.* J Biol Chem, 2005. **280**(17): p. 17149-53.

339. Saparov, S.M., et al., *Fast and selective ammonia transport by aquaporin-8.* J Biol Chem, 2007. **282**(8): p. 5296-301.

340. Bienert, G.P., et al., *Specific aquaporins facilitate the diffusion of hydrogen peroxide across membranes.* J Biol Chem, 2007. **282**(2): p. 1183-92.

341. Soria, L.R., et al., *Aquaporin-8-facilitated mitochondrial ammonia transport.* Biochem Biophys Res Commun, 2010. **393**(2): p. 217-21.

342. Molinas, S.M., L. Trumper, and R.A. Marinelli, *Mitochondrial aquaporin-8 in renal proximal tubule cells: evidence for a role in the response to metabolic acidosis.* Am J Physiol Renal Physiol, 2012. **303**(3): p. F458-66.

343. Yang, M.H., A. Dibas, and Y.C. Tyan, *Changes in retinal aquaporin-9 (AQP9) expression in glaucoma.* Biosci Rep, 2013.

344. Lindskog, C., et al., *A Systematic Characterization of Aquaporin-9 Expression in Human Normal and Pathological Tissues.* J Histochem Cytochem, 2016. **64**(5): p. 287-300.

345. Wei, X., et al., *Phosphorylation of p38 MAPK mediates aquaporin 9 expression in rat brains during permanent focal cerebral ischaemia.* J Mol Histol, 2015. **46**(3): p. 273-81.

346. Mulders, S.M., et al., *An aquaporin-2 water channel mutant which causes autosomal dominant nephrogenic diabetes insipidus is retained in the Golgi complex.* J Clin Invest, 1998. **102**(1): p. 57-66.

347. Bichet, D.G., *Nephrogenic diabetes insipidus.* Am J Med, 1998. **105**(5): p. 431-42.

348. Ala, Y., et al., *Functional studies of twelve mutant V2 vasopressin receptors related to nephrogenic diabetes insipidus: molecular basis of a mild clinical phenotype.* J Am Soc Nephrol, 1998. **9**(10): p. 1861-72.

349. Walker, R.J., et al., *Lithium-induced reduction in urinary concentrating ability and urinary aquaporin 2 (AQP2) excretion in healthy volunteers.* Kidney Int, 2005. **67**(1): p. 291-4.

350. Kwon, T.H., et al., *Angiotensin II AT1 receptor blockade decreases vasopressin-induced water reabsorption and AQP2 levels in NaCl-restricted rats.* Am J Physiol Renal Physiol, 2005. **288**(4): p. F673-84.

351. Yasui, M., et al., *Adenylate cyclase-coupled vasopressin receptor activates AQP2 promoter via a dual effect on CRE and AP1 elements.* Am J Physiol, 1997. **272**(4 Pt 2): p. F443-50.

352. Nilsson, L., et al., *Disruption of cyclooxygenase-2 prevents downregulation of cortical AQP2 and AQP3 in response to bilateral ureteral obstruction in the mouse.* Am J Physiol Renal Physiol, 2012. **302**(11): p. F1430-9.

353. Zelenina, M., et al., *Prostaglandin E(2) interaction with AVP: effects on AQP2 phosphorylation and distribution.* Am J Physiol Renal Physiol, 2000. **278**(3): p. F388-94.

354. Tamma, G., et al., *The prostaglandin E2 analogue sulprostone antagonizes vasopressin-induced antidiuresis through activation of Rho.* J Cell Sci, 2003. **116**(Pt 16): p. 3285-94.

355. Tamma, G., et al., *Integrin signaling modulates AQP2 trafficking via Arg-Gly-Asp (RGD) motif.* Cell Physiol Biochem, 2011. **27**(6): p. 739-48.

356. Storm, R., et al., *Osmolality and solute composition are strong regulators of AQP2 expression in renal principal cells.* Am J Physiol Renal Physiol, 2003. **284**(1): p. F189-98.

357. Hasler, U., *Controlled aquaporin-2 expression in the hypertonic environment.* Am J Physiol Cell Physiol, 2009. **296**(4): p. C641-53.

358. Saito, T., et al., *Hypotonicity reduces the activity of murine aquaporin-2 promoter induced by dibutyryl cAMP.* Exp Physiol, 2008. **93**(10): p. 1147-56.

359. Tamma, G., et al., *Hypotonicity induces aquaporin-2 internalization and cytosol-to-membrane translocation of ICln in renal cells.* Endocrinology, 2007. **148**(3): p. 1118-30.

360. Yamamoto, T., et al., *Vasopressin increases AQP-CD water channel in apical membrane of collecting duct cells in Brattleboro rats.* Am J Physiol, 1995. **268**(6 Pt 1): p. C1546-51.

361. Van Hoek, A.N., et al., *Vasopressin-induced differential stimulation of AQP4 splice variants regulates the in-membrane assembly of orthogonal arrays.* Am J Physiol Renal Physiol, 2009. **296**(6): p. F1396-404.

362. Hasegawa, H., et al., *Molecular cloning of a mercurial-insensitive water channel expressed in selected water-transporting tissues.* J Biol Chem, 1994. **269**(8): p. 5497-500.

363. Zeuthen, T. and D.A. Klaerke, *Transport of water and glycerol in aquaporin 3 is gated by H(+).* J Biol Chem, 1999. **274**(31): p. 21631-6.

364. Wang, G., et al., *Age-related changes in expression in renal AQPs in response to congenital, partial, unilateral ureteral obstruction in rats.* Pediatr Nephrol, 2012. **27**(1): p. 83-94.

365. Murer, L., et al., *Selective decrease in urinary aquaporin 2 and increase in prostaglandin E2 excretion is associated with postobstructive polyuria in human congenital hydronephrosis.* J Am Soc Nephrol, 2004. **15**(10): p. 2705-12.

366. Cahill, D.J., C.H. Fry, and P.J. Foxall, *Variation in urine composition in the human urinary tract: evidence of urothelial function in situ?* J Urol, 2003. **169**(3): p. 871-4.

367. Kim, S.O., et al., *Changes in aquaporin 1 expression in rat urinary bladder after partial bladder outlet obstruction: preliminary report.* Korean J Urol, 2010. **51**(4): p. 281-6.

368. Kim, S.O., et al., *Effect of detrusor overactivity on the expression of aquaporins and nitric oxide synthase in rat urinary bladder following bladder outlet obstruction.* Can Urol Assoc J, 2013. **7**(5-6): p. E268-74.

369. Rubenwolf, P.C., et al., *Aquaporin expression contributes to human transurothelial permeability in vitro and is modulated by NaCl.* PLoS One, 2012. **7**(9): p. e45339.

370. Deen, P.M., et al., *Urinary content of aquaporin 1 and 2 in nephrogenic diabetes insipidus.* J Am Soc Nephrol, 1996. **7**(6): p. 836-41.

371. Kanno, K., et al., *Urinary excretion of aquaporin-2 in patients with diabetes insipidus.* N Engl J Med, 1995. **332**(23): p. 1540-5.

372. Wen, H.J., et al., *Urinary excretion of aquaporin-2 in rat is mediated by a vasopressin-dependent apical pathway.* Journal of the American Society of Nephrology, 1999. **10**(7): p. 1416-1429.

373. Oshikawa, S., H. Sonoda, and M. Ikeda, *Aquaporins in Urinary Extracellular Vesicles (Exosomes).* Int J Mol Sci, 2016. **17**(6).

374. Pisitkun, T., R.F. Shen, and M.A. Knepper, *Identification and proteomic profiling of exosomes in human urine.* Proc Natl Acad Sci U S A, 2004. **101**(36): p. 13368-73.

375. Dimov, I., L. Jankovic Velickovic, and V. Stefanovic, *Urinary exosomes.* ScientificWorldJournal, 2009. **9**: p. 1107-18.

376. Alvarez, M.L., et al., *Comparison of protein, microRNA, and mRNA yields using different methods of urinary exosome isolation for the discovery of kidney disease biomarkers.* Kidney Int, 2012. **82**(9): p. 1024-32.

377. Hiemstra, T.F., et al., *Human urinary exosomes as innate immune effectors.* J Am Soc Nephrol, 2014. **25**(9): p. 2017-27.

378. Franzen, C.A., et al., *Urothelial cells undergo epithelial-to-mesenchymal transition after exposure to muscle invasive bladder cancer exosomes.* Oncogenesis, 2015. **4**: p. e163.

379. Street, J.M., et al., *Exosomal transmission of functional aquaporin 2 in kidney cortical collecting duct cells.* J Physiol, 2011. **589**(Pt 24): p. 6119-27.

380. Oosthuyzen, W., et al., *Vasopressin Regulates Extracellular Vesicle Uptake by Kidney Collecting Duct Cells.* J Am Soc Nephrol, 2016. **27**(11): p. 3345-3355.

381. Sonoda, H., et al., *Decreased abundance of urinary exosomal aquaporin-1 in renal ischemia-reperfusion injury.* Am J Physiol Renal Physiol, 2009. **297**(4): p. F1006-16.

382. Abdeen, A., et al., *Acetazolamide enhances the release of urinary exosomal aquaporin-1.* Nephrol Dial Transplant, 2016. **31**(10): p. 1623-32.

383. Rai, T., et al., *Urinary excretion of aquaporin-2 water channel protein in human and rat.* J Am Soc Nephrol, 1997. **8**(9): p. 1357-62.

384. Elliot, S., et al., *Urinary excretion of aquaporin-2 in humans: a potential marker of collecting duct responsiveness to vasopressin.* J Am Soc Nephrol, 1996. **7**(3): p. 403-9.

385. Al-Dameh, A., et al., *Urinary aquaporin-2 levels in healthy volunteers.* Nephrology (Carlton), 2003. **8**(3): p. 139-41.

386. Li, Z.Z., et al., *Early alteration of urinary exosomal aquaporin 1 and transforming growth factor beta1 after release of unilateral pelviureteral junction obstruction.* J Pediatr Surg, 2012. **47**(8): p. 1581-6.

387. Wang, Z., et al., *Proteomic analysis of urine exosomes by multidimensional protein identification technology (MudPIT).* Proteomics, 2012. **12**(2): p. 329-38.

388. Wilmer, M.J., et al., *Novel conditionally immortalized human proximal tubule cell line expressing functional influx and efflux transporters.* Cell Tissue Res, 2010. **339**(2): p. 449-57.

389. Verkman, A.S., *Dissecting the roles of aquaporins in renal pathophysiology using transgenic mice.* Semin Nephrol, 2008. **28**(3): p. 217-26.

390. Zuker, M., *Mfold web server for nucleic acid folding and hybridization prediction.* Nucleic Acids Res, 2003. **31**(13): p. 3406-15.

391. Nicaise, C., et al., *Aquaporin-4 overexpression in rat ALS model.* Anat Rec (Hoboken), 2009. **292**(2): p. 207-13.

392. Huggett, J., et al., *Real-time RT-PCR normalisation; strategies and considerations.* Genes Immun, 2005. **6**(4): p. 279-84.

393. Cui, X., et al., *Validation of endogenous internal real-time PCR controls in renal tissues.* Am J Nephrol, 2009. **30**(5): p. 413-7.

394. Ngoka, L.C., *Sample prep for proteomics of breast cancer: proteomics and gene ontology reveal dramatic differences in protein solubilization preferences of radioimmunoprecipitation assay and urea lysis buffers.* Proteome Sci, 2008. **6**: p. 30.

395. West, P.M. and W.H. Woglom, *The Biotin Content of Tumors and Other Tissues.* Science, 1941. **93**(2422): p. 525-7.

396. Verkman, A.S., *Lessons on renal physiology from transgenic mice lacking aquaporin water channels.* J Am Soc Nephrol, 1999. **10**(5): p. 1126-35.

397. Umenishi, F., et al., *Comparison of three methods to quantify urinary aquaporin-2 protein.* Kidney Int, 2002. **62**(6): p. 2288-93.

398. Garibyan, L. and N. Avashia, *Polymerase chain reaction.* J Invest Dermatol, 2013. **133**(3): p. e6.

399. Valasek, M.A. and J.J. Repa, *The power of real-time PCR.* Adv Physiol Educ, 2005. **29**(3): p. 151-9.

400. Bustin, S.A., et al., *The MIQE guidelines: minimum information for publication of quantitative real-time PCR experiments.* Clin Chem, 2009. **55**(4): p. 611-22.

401. Wen, J.G., et al., *Experimental partial unilateral ureter obstruction. I. Pressure flow relationship in a rat model with mild and severe acute ureter obstruction.* J Urol, 1998. **160**(4): p. 1567-71.

402. Chevalier, R.L., et al., *Morphologic correlates of renal growth arrest in neonatal partial ureteral obstruction.* Pediatr Res, 1987. **21**(4): p. 338-46.

403. Ulm, A.H. and F. Miller, *An operation to produce experimental reversible hydronephrosis in dogs.* J Urol, 1962. **88**: p. 337-41.

404. Phifer, C.B. and L.M. Terry, *Use of hypothermia for general anesthesia in preweanling rodents.* Physiol Behav, 1986. **38**(6): p. 887-90.

405. Danneman, P.J. and T.D. Mandrell, *Evaluation of five agents/methods for anesthesia of neonatal rats.* Lab Anim Sci, 1997. **47**(4): p. 386-95.

406. Johnston, R.B. and C. Porter, *The Whitaker test.* Urol J, 2014. **11**(3): p. 1727-30.

407. Wang, G., et al., *Unilateral ureteral obstruction alters expression of acid-base transporters in rat kidney.* J Urol, 2009. **182**(6): p. 2964-73.

408. Wang, G., et al., *Age-dependent renal expression of acid-base transporters in neonatal ureter obstruction.* Pediatr Nephrol, 2009. **24**(8): p. 1487-500.

409. Chandar, J., et al., *Renal tubular abnormalities in infants with hydronephrosis.* J Urol, 1996. **155**(2): p. 660-3.

410. Koff, S.A., et al., *The assessment of obstruction in the newborn with unilateral hydronephrosis by measuring the size of the opposite kidney.* J Urol, 1994. **152**(2 Pt 2): p. 596-9.

411. Wen, J.G., et al., *Contralateral compensatory kidney growth in rats with partial unilateral ureteral obstruction monitored by magnetic resonance imaging.* Journal of Urology, 1999. **162**(3): p. 1084-1089.

412. Claesson, G., S. Josephson, and B. Robertson, *Experimental partial ureteric obstruction in newborn rats. VII. Are the long term effects on renal morphology avoided by release of the obstruction?* J Urol, 1986. **136**(6): p. 1330-4.

413. Claesson, G., et al., *Experimental obstructive hydronephrosis in newborn rats. XI. A one-year follow-up study of renal function and morphology.* J Urol, 1989. **142**(6): p. 1602-7.

414. Nicholls, C., H. Li, and J.P. Liu, *GAPDH: a common enzyme with uncommon functions.* Clin Exp Pharmacol Physiol, 2012. **39**(8): p. 674-9.

415. Bunnell, T.M., et al., *beta-Actin specifically controls cell growth, migration, and the G-actin pool.* Mol Biol Cell, 2011. **22**(21): p. 4047-58.

416. Burden, D.W., *Guide to the homogenization of biological samples.* Random Primers, 2008(7): p. 1-14.

417. Procino, G., et al., *Altered expression of renal aquaporins and alpha-adducin polymorphisms may contribute to the establishment of salt-sensitive hypertension.* Am J Hypertens, 2011. **24**(7): p. 822-8.

418. Schuster, V.L., J.P. Kokko, and H.R. Jacobson, *Angiotensin II directly stimulates sodium transport in rabbit proximal convoluted tubules.* J Clin Invest, 1984. **73**(2): p. 507-15.

419. Reilly, A.M., P.J. Harris, and D.A. Williams, *Biphasic effect of angiotensin II on intracellular sodium concentration in rat proximal tubules.* Am J Physiol, 1995. **269**(3 Pt 2): p. F374-80.

420. Machida, K., et al., *Downregulation of the V2 vasopressin receptor in dehydration: mechanisms and role of renal prostaglandin synthesis.* Am J Physiol Renal Physiol, 2007. **292**(4): p. F1274-82.

421. Sonnenburg, W.K. and W.L. Smith, *Regulation of cyclic AMP metabolism in rabbit cortical collecting tubule cells by prostaglandins.* J Biol Chem, 1988. **263**(13): p. 6155-60.

422. Ruiz-Ortega, M., et al., *Systemic infusion of angiotensin II into normal rats activates nuclear factor-kappaB and AP-1 in the kidney: role of AT(1) and AT(2) receptors.* Am J Pathol, 2001. **158**(5): p. 1743-56.

423. Hasler, U., et al., *NF-kappaB modulates aquaporin-2 transcription in renal collecting duct principal cells.* J Biol Chem, 2008. **283**(42): p. 28095-105.

424. Li, Z.Z., et al., *Decrease of renal aquaporins 1-4 is associated with renal function impairment in pediatric congenital hydronephrosis.* World J Pediatr, 2012. **8**(4): p. 335-41.

425. van der Loos, C.M., *Multiple immunoenzyme staining: methods and visualizations for the observation with spectral imaging.* J Histochem Cytochem, 2008. **56**(4): p. 313-28.

426. Morris, R.K. and M.D. Kilby, *Congenital urinary tract obstruction.* Best Pract Res Clin Obstet Gynaecol, 2008. **22**(1): p. 97-122.

427. Hinman, F. and R.K.L. Brown, *Pyelovenous back flow - Its relation to pelvic reabsorption to hydronephrosis and to accidents of pyelography.* Journal of the American Medical Association, 1924. **82**: p. 607-613.

428. Naber, K.G. and P.O. Madsen, *Renal function in chronic hydronephrosis with and without infection and the role of the lymphatics. An experimental study in dogs.* Urol Res, 1974. **2**(1): p. 1-9.

429. Khandelwal, P., S.N. Abraham, and G. Apodaca, *Cell biology and physiology of the uroepithelium.* Am J Physiol Renal Physiol, 2009. **297**(6): p. F1477-501.

430. Nelson, R.A., et al., *Nitrogen metabolism in bears: urea metabolism in summer starvation and in winter sleep and role of urinary bladder in water and nitrogen conservation.* Mayo Clin Proc, 1975. **50**(3): p. 141-6.

431. Smith, P.R., et al., *Expression and localization of epithelial sodium channel in mammalian urinary bladder.* American Journal of Physiology-Renal Physiology, 1998. **274**(1): p. F91-F96.

432. Spector, D.A., et al., *The ROMK potassium channel is present in mammalian urinary tract epithelia and muscle.* American Journal of Physiology-Renal Physiology, 2008. **295**(6): p. F1658-F1665.

433. Lucien, N., et al., *UT-B1 urea transporter is expressed along the urinary and gastrointestinal tracts of the mouse.* Am J Physiol Regul Integr Comp Physiol, 2005. **288**(4): p. R1046-56.

434. Naylor, S., *Biomarkers: current perspectives and future prospects.* Expert Rev Mol Diagn, 2003. **3**(5): p. 525-9.

435. *Biomarkers on a roll.* Nat Biotechnol, 2010. **28**(5): p. 431.

436. Al-Salem, A.H., *Pelviureteric Junction Obstruction*, in *An Illustrated Guide to Pediatric Surgery*. 2014, Springer International Publishing: Cham. p. 559-567.

437. Wen, J.G., et al., *Severe partial ureteric obstruction in newborn rats can produce renal dysplasia.* Bju International, 2002. **89**(7): p. 740-745.

438. Eskild-Jensen, A., et al., *Glomerular and tubular function during AT1 receptor blockade in pigs with neonatal induced partial ureteropelvic obstruction.* Am J Physiol Renal Physiol, 2007. **292**(3): p. F921-9.

439. Topcu, S.O., et al., *Regulation of aquaporins and sodium transporter proteins in the solitary kidney in response to partial ureteral obstruction in neonatal rats.* Urol Int, 2011. **87**(1): p. 94-104.

440. Grippo, P.J. and E.P. Sandgren, *Highly invasive transitional cell carcinoma of the bladder in a simian virus 40 T-antigen transgenic mouse model.* Am J Pathol, 2000. **157**(3): p. 805-13.

441. Saam, J.R. and J.I. Gordon, *Inducible gene knockouts in the small intestinal and colonic epithelium.* J Biol Chem, 1999. **274**(53): p. 38071-82.

442. Yue, F., et al., *A comparative encyclopedia of DNA elements in the mouse genome.* Nature, 2014. **515**(7527): p. 355-64.

443. Lin, J.H., H. Zhao, and T.T. Sun, *A tissue-specific promoter that can drive a foreign gene to express in the suprabasal urothelial cells of transgenic mice.* Proc Natl Acad Sci U S A, 1995. **92**(3): p. 679-83.

444. Hall, G.D., et al., *Transcriptional control of the human urothelial-specific gene, uroplakin Ia.* Biochim Biophys Acta, 2005. **1729**(2): p. 126-34.

445. Mo, L., et al., *Gene deletion in urothelium by specific expression of Cre recombinase.* Am J Physiol Renal Physiol, 2005. **289**(3): p. F562-8.

446. Lobban, E.D., et al., *Uroplakin gene expression by normal and neoplastic human urothelium.* Am J Pathol, 1998. **153**(6): p. 1957-67.

Chapter 10. Appendices

10.1 Appendix 1 Solution and gel recipes, cell culture media

10.1.1 Solution recipes

Solution	Constituents	pH
Phosphate buffered saline (PBS)	8g Sodium chloride, 1.16g Sodium phosphate dibasic, 0.2g Potassium chloride, 0.2g Potassium phosphate monobasic, made up to 1 litre with ultrapure water	7.4
Phosphate buffered saline with 0.1% tween 20 (PBS-T)	1000 ml of PBS, 1ml Tween 20	7.4
10 x Tris buffered saline (TBS)	24.23g Tris base, 80.06g Sodium chloride, made up to 1 litre with ultrapure water	7.5
1 x Tris buffered saline with 0.1% tween 20 (TBS-T)	100ml of 10 x TBS, 899ml ultrapure water, 1ml Tween 20	7.5
3M Tris-HCl	36.342g Tris base made up to 100ml final volume with ultrapure water. Adjust pH with concentrated HCl	8.8
0.5M Tris-HCl	6.057g Tris base made up to 100ml final volume with ultrapure water. Adjust pH with concentrated HCl	6.8
0.1M Tris-HCl	1.211g Tris base made up to 100ml final volume with ultrapure water. Adjust pH with concentrated HCl	7.6
30mM Tris-HCl	0.363g Tris base made up to 100ml final volume with ultrapure water. Adjust pH with concentrated HCl	8.5
10 x Running buffer	30.3g Tris base, 144g Glycine, 10g Sodium dodecyl sulfate, made up to 1 litre with ultrapure water	N/A
1 x Running buffer	100ml of 10 x Running buffer, 900ml ultrapure water	N/A

10 x Transfer buffer	30g Tris base, 144g Glycine, made up to 1 litre with ultrapure water	N/A
1 x Transfer buffer	100ml Methanol, 100ml 10 x Transfer buffer, 800ml ultrapure water	N/A
2 x Sample buffer (Stock solution)	3.4ml ultrapure water, 1ml 0.5M Tris-HCl pH6.8, 2ml Glycerol, 1.6ml 20% sodium dodecyl sulfate, sprinkle bromophenol blue.	N/A
2 x Sample buffer (Working solution)	950µl 2 x Sample buffer stock solution, 50µl β-mercaptoethanol	N/A
2 x Sample buffer + 7M urea	2ml 20% Sodium dodecyl sulfate, 2ml Glycerol, 2.5ml 0.5M Tris-HCl pH 6.8, 4.2g Urea, 0.5ml β-mercaptoethanol, make up to 10ml with ultrapure water	N/A
Stripping buffer	4ml 0.5Mtris-HCl pH6.8, 2g Sodium dodecyl sulfate, 700µl β-mercaptoethanol, make up to 100ml with ultrapure water	N/A
Urea/thiourea tissue lysis buffer (Stock solution)	4.2g Urea, 1.52g Thiourea, 0.4g CHAPS, 10ml 30mM Tris-HCl (pH8.5)	N/A
Urea/thiourea tissue lysis buffer (Working Solution)	Add 10µl protease inhibitor (#p8340, Sigma-Aldrich, St-Louis, MO, USA), 10µl phosphatase inhibitor cocktail 2 (#p5726, Sigma-Aldrich) and 10µl phosphatase inhibitor cocktail 3 (#p0044, Sigma-Aldrich) to 1ml of Urea/thiourea tissue lysis buffer stock solution	N/A
Triton X-100 cell lysis buffer (Stock solution)	3.03g Tris base, 0.186g EDTA, 0.19g EGTA, 46.2g Sucrose, 1.05g Sodium fluoride, 1.12g Sodium pyrophosphate, 0.078g Benzamidine, make up to 495ml with ultrapure water, pH to 7.5 then add 5ml Triton X-100	7.5
Triton X-100 cell lysis buffer (Working solution)	Add 10µl protease inhibitor (#p8340, Sigma-Aldrich, St-Louis, MO, USA), 10µl phosphatase inhibitor cocktail 2 (#p5726,	7.5

	Sigma-Aldrich) and 10µl phosphatase inhibitor cocktail 3 (#p0044, Sigma-Aldrich) to 1ml of Triton X-100 cell lysis buffer stock solution	
4% Paraformaldehyde	Add 40g Paraformaldehyde powder to 800ml of PBS heated to 60°C. Add 1N Sodium hydroxide until solution clears. Make up to 1 litre with ultrapure water, cool and filter. Adjust pH to 6.9 with HCl. Aliquot and store at -20°C.	6.9
10% Neutral buffered formalin	100ml of 37% formaldehyde, 4g Sodium phosphate monobasic, 6.5g Sodium phosphate dibasic (anhydrous), make up to 1 litre with ultrapure water	N/A
10mM Sodium citrate buffer	2.94g Sodium citrate trisodium salt dihydrate, make up to 1 litre with ultrapure water	6
50 x TAE	242g Tris base, 100ml of 0.5M EDTA pH8, 57.1ml of acetic acid, make up to 1 litre with ultrapure water	N/A
37mM Picric acid	32ml of 1.3% picric acid, 28ml ultrapure water	N/A
0.3M NAOH	30ml of 1M NaOH, 70ml of ultrapure water	N/A
0.5M EDTA	18.61g EDTA disodium salt dihydrate, make up to 100ml with ultrapure water, filter through a 0,5 micron filter	8

10.1.2 Western blotting gel recipe

Constituent (per 2 gels)	**Stacking 4% Gel**	**Resolving 12.5% Gel**
Ultrapure Water	5.65ml	7.9ml
30% bis acrylamide	1.25ml	8.4ml
0.5MTris-HCl pH6.8	2.5ml	N/A
3M Tris-HCl pH8.8	N/A	2.5ml
10% Sodium dodecyl sulfate	100µl	200µl

Ammonium Persulphate (100mg/ml)	0.5ml	1ml
TEMED	5µl	10µl

10.1.3 Cell culture media

Medium	**Constituents**
Modified RPMI 1640 culture media	500ml of RPMI 1640 with L-glutamine (#R8758, Sigma-Aldrich, St-Louis, MO, USA), 5ml Insulin-transferrin-selenium (41400-045, Gibco, Invitrogen, Paisley, Scotland, UK) 50ml Fetal bovine serum (10500-064, Gibco, Invitrogen, Paisley, Scotland, UK)
Freeze media	10ml of Fetal bovine serum (10500-064, Gibco, Invitrogen, Paisley, Scotland, UK), 8ml of modified RPMI 1540 culture medium, 2ml DMSO (#D8418, Sigma-Aldrich, St-Louis, MO, USA).

10.2 Appendix 2 Primer sequences and antibodies

10.2.1 Primer sequences

10.2.1.1 Human primer sequences

Gene	**Direction**	**Primer Sequence (5'-3')**	**Annealing Temperature (°C)**	**Product size (bp) cDNA (gDNA)**
AQP0	Forward	TGTTCTGCAGGTGGCTATG	59.9	232 (232)
	Reverse	TGCTAGGTTTCCTCGGACAG		

AQP1	Forward	TCATCAGCATCGGTTCTGC	58.4	297 (297)
	Reverse	CAAGCGAGTTCCCAGTCAG		
AQP2	Forward	TAGCCTTCTCCAGGGCTGT	58.8	305 (305)
	Reverse	CGTGATCTCATGGAGCAGAG		
AQP3	Forward	GTCACTCTGGGCATCCTCAT	59.8	157 (464)
	Reverse	CTATTCCAGCACCCAAGAAGG		
AQP4	Forward	GCCCATCATAGGAGCTGTC	58.4	209 (209)
	Reverse	GGTCAACGTCAATCACATGC		
AQP5	Forward	CCACCCTCATCTTCGTCTTC	59.9	212 (212)
	Reverse	GTAGAAGAAAGCCCGGAGC		
AQP6	Forward	AGTCTTGGGGGAGAAAGGAA	58.4	196 (196)
	Reverse	AACCACACCCAAGGTCAGAG		
AQP7	Forward	TGCCACCTACCTTCCTGATC	59.9	210 (420)
	Reverse	GACGGGTTGATGGCATATCC		
AQP8	Forward	TGAGCCTGAATTTGGCAATG	60	226 (226)
	Reverse	CAGCGTGGCAATCACGAGC		
AQP9	Forward	CTCAGTGTCATCATGTAGTG	59.7	336 (336)
	Reverse	GACTATCGTCAAGATGCCG		
AQP10	Forward	GCACTGGGATGCTGATTGT	60	190 (190)
	Reverse	CCAGCCACGTAGGTGAAGAG		
AQP11	Forward	GACGCTGACGCTCGTCTACT	59.7	279 (279)
	Reverse	TCTGTGATGACCGCTTTGAG		
AQP12	Forward	GAACCTGTTCTACGGCCAGA	59.3	204 (204)
	Reverse	GTTCCAGGGTCCAGCTACAA		
B-Actin	Forward	GACAGGATGCAGAAGGAGATTACT	60	142
	Reverse	TGATCCACATCTGCTGGAAGGT		

10.2.1.2 Rat primer sequences

Gene	Direction	Primer Sequence (5'-3')	Annealing Temp °C	Product size (bp) cDNA	Primer Conc for qPCR (µM)
AQP0	Forward	GGGCACCTCTTTGGGATGTATT	60	177	-
	Reverse	ACTCTTGAGCCGTGGGAAGA			
AQP1	Forward	TTGGCTTGTCTGTGGCTCTT	60	132	10
	Reverse	GTCCCACCCAGAAAATCCAGT			
AQP2	Forward	GTGGGTTGCCATGTCTCCTT	60	145	10
	Reverse	CGTTGTTGTGGAGAGCATTGAC			
AQP3	Forward	TTGAACCCTGCTGTGACCTT	60	145	10
	Reverse	AGGCCCAGATTGCATCATAGTAG			
AQP4	Forward	CCACTGGATATATTGGGTTGGA	60	83	5
	Reverse	CCACGTCAGGACAGAAGACATA			
AQP5	Forward	TGCGCTGAACAACAACACAA	60	182	-
	Reverse	CGGTGAAGTAGATCCCCACAA			
AQP6	Forward	AGTTGGTTCTCTGTGTCTTTGCT	60	200	5
	Reverse	CGGTCCTACCCAGAAGATCCA			
AQP7	Forward	GCTTCGTGGATGAGGTATTTGTG	60	134	5
	Reverse	CACCCCAAGAACGCAAACAA			
AQP8	Forward	GCTGTGATGGCTGGCTACT	60	163	10
	Reverse	AAGTGTCCACCGCTGATGTTC			
AQP9	Forward	CTGCAACGGTCTTTGGCATT	60	130	10
	Reverse	CCTGGCGTGGATATGAATGGA			
AQP11	Forward	GGCGTGATGATGCAGATGATT	60	195	10
	Reverse	CGCTTTGGATATGTCGGTGTTG			
AQP12	Forward	TACCGGCAGAAAAGCAAATACC	60	81	-
	Reverse	CTCCCCTTTGAGCATCTTGGT			
B-Actin	Forward	ACAACCTTCTTGCAGCTCCTC	60	200	10

	Reverse	CTGACCCATACCCACCATCAC			
Pgk1	Forward	TTTGGACAAGCTGGACGTGA	60	107	10
	Reverse	CAGCAGCCTTGATCCTTTGG			
36b4	Forward	TGCCCAGGGAAGACAGGGCGA	60	185	10
	Reverse	GCGCATCATGGTGTTCTTG			

10.2.2 Antibodies

10.2.2.1 Primary antibodies

Antibody	**Host**	**Catalogue number and supplier**
Anti-AQP1	Rabbit	sc-20810, Santa Cruz, Dallas, Texas, USA
Anti-AQP2	Rabbit	sc-28629 Santa Cruz, Dallas, Texas, USA
Anti-AQP2	Rabbit	Gift from J Bedford, New Zealand
Anti-AQP2	Rabbit	AB3066, Merck Millipore, Billerica, MA, USA
Anti-AQP2	Rabbit	ab15081, Abcam, Cambridge, UK
Anti-AQP3	Goat	sc-9885, Santa Cruz, Dallas, Texas, USA
Anti-AQP3	Rabbit	ab125045, Abcam, Cambridge, UK
Anti-AQP4	Goat	sc-9888, Santa Cruz, Dallas, Texas, USA
Anti-FLAG®	Mouse	F1804, Sigma-Aldrich, St-Louis, MO, USA
Anti-SV-40	Mouse	GTX16879, Genetex, Irvine, CA, USA
Anti-β-actin	Mouse	A5441, Sigma-Aldrich, St-Louis, MO, USA
Anti-GAPDH	Mouse	MAB374, Merck Millipore, Billerica, MA, USA

10.2.2.2 Secondary antibodies

Antibody	**Host**	**Conjugation**	**Supplier**
Anti-Goat	Donkey	HRP	sc-2020Santa Cruz, Dallas, Texas, USA
Anti-Rabbit	Goat	HRP	A6667, Sigma-Aldrich, St-Louis, MO, USA
Anti-Mouse	Rabbit	HRP	A9044, Sigma-Aldrich, St-Louis, MO, USA

Anti-Mouse	Goat	Alexa Fluor® 488	A-11001, Invitrogen, Paisley, Scotland, UK
Anti-Rabbit	Donkey	Alexa Fluor® 568	A-10042, Invitrogen, Paisley, Scotland, UK
Anti-Mouse	Goat	Cy3	PA43009V, GE Healthcare, Buckinghamshire, UK

10.3 Appendix 3 Study specific documentation

10.3.1 Study protocol

Do aquaporins protect against renal damage in PUJ obstruction

Title

An investigation of whether renal and lower urinary tract aquaporin expression protects kidney function from the pressure effects of pelvi-ureteric junction (PUJ) obstruction in children. Furthermore, this study aims to develop urine aquaporin measurement as a novel, non-invasive, biomarker of childhood pelvi-ureteric junction obstruction.

General Information

Sponsor

Birgit Whitman

University of Bristol

Research and Enterprise Development

3rd Floor, Senate House

Tyndall Avenue

Bristol

BS8 1TH

Tel: 0117 3317130

Chief Investigator

Miss Laura Jackson

MD Student (University of Bristol) and Paediatric Surgery Registrar (Bristol Royal Hospital for Children)

Academic Renal Unit

Dorothy Hodgkin Building

Whitson Street

Bristol

BS1 3NY

Tel: 0117 3313171

Mob: 07930 868195

E mail: laura.jackson@bristol.ac.uk

Acting Chief Investigator (Period 15/06/2015 - 03/04/2016)

Miss Rebecca Cooksey

Paediatric Surgery /Urology Registrar

Bristol Royal Hospital for Children

Paul O'Gorman Building

Upper Maudlin Street

Bristol

BS2 8BJ

Tel: 0117 923 0000 Bleep 5171

E mail: rebecca.cooksey@uhbristol.nhs.uk

Co-investigators/Supervisors

Mr Mark Woodward

Consultant Paediatric Urologist

Bristol Royal Hospital for Children

Paul O'Gorman Building

Upper Maudlin Street

Bristol

BS2 8BJ

Tel: 0117 3428840

E mail: mark.woodward@uhbristol.nhs.uk

Prof Richard Coward

Consultant Paediatric Nephrologist and MRC Clinician Scientist

Academic Renal Unit

Dorothy Hodgkin Building

Whitson Street

Bristol

BS1 3NY

Tel: 01173313181

E mail: richard.coward@bristol.ac.uk

Dr Gavin Welsh

Senior Lecturer

Academic Renal Unit

Dorothy Hodgkin Building

Whitson Street

Bristol

BS1 3NY

Tel: 0117 3387848

E mail: g.i.welsh@bristol.ac.uk

Study Sites

Bristol Royal Hospital for Children

Paul O'Gorman Building

Upper Maudlin Street

Bristol

BS2 8BJ

Tel: 0117 3428460

Academic Renal Unit

Dorothy Hodgkin Building

Whitson Street

Bristol

BS1 3NY

Tel:

Abbreviations

AQP – Aquaporin

GP – General Practitioner

IHC - Immunohistochemistry

MCUG – Micturating cystourethrogram

mRNA – Messenger Ribonucleic Acid

NHS – National Health Service

PACS – Picture Archiving and Communications System

PUJ Obstruction – Pelvi-ureteric junction obstruction

R & D – Research and Development Department

REC – Research Ethics Committee

RT-PCR – Reverse Transcription Polymerase Chain Reaction

Definitions

Antenatal – Before Birth

Biomarker - A naturally occurring substance by which a particular pathological process or disease can be identified.

Biopsy - An examination of tissue removed from a living body to discover the presence, cause, or extent of a disease.

Hydronephrosis – Dilatation and distension of the collecting system (renal pelvis and calyces) of the kidney.

Isoforms – Protein isoforms are slightly different forms of the same protein.

MAG 3 Renogram – A test which involves injecting a radioisotope dye into a vein which is subsequently excreted by the kidneys. The kidneys are then scanned with a gamma camera to work out their function compared to each other and to estimate how well the kidneys drain.

MCUG – A test where dye is inserted into the bladder via a catheter and x-ray images are taken as the bladder fills and then as the patient voids the dye.

Nephron – Each of the functional units in the kidney, consisting of a glomerulus and its associated tubule, through which the glomerular filtrate passes before emerging as urine.

Paediatric Urologist – A children's surgeon who is concerned with the function and disorders of the urinary system.

PUJ Obstruction – Obstruction to the flow of urine from the renal pelvis into the proximal ureter most commonly caused by narrowing of the junction between the renal pelvis and the proximal ureter.

Pyeloplasty – Surgical reconstruction of the junction between the renal pelvis and the ureter to decompress the kidney and allow it to drain urine properly.

Renal Pelvis – A funnel-like structure that connects the kidney to the ureter.

Ultrasound Scan - A type of medical imaging that uses echoes of ultrasound pulses to delineate objects or areas of different density in the body.

Ureter – A tube that carries urine from the kidney to the bladder.

Urinary tract – The organs of the body that produce, drain, store and discharge urine. These are the kidneys, renal pelvis, ureters, bladder and urethra.

Urothelium – The urothelium is the epithelium that lines much of the urinary tract. It is a layer of tissue that lines the renal pelvis, the ureters, the bladder, and parts of the urethra.

Vesico-ureteric reflux – Condition where there is flow of urine from the bladder back into the ureters

Background

Antenatal hydronephrosis is a major clinical issue for paediatric urologists (incidence of 1 in 200)[1], which has become more problematic since antenatal scanning became routine. Of these children approximately 1 in 7 will have pelviureteric junction (PUJ) obstruction[2], which causes a blockage to urine drainage from the kidney. The major surgical issue is deciding which children require urgent surgery to relieve obstruction and limit kidney damage, and which do not. This is because some children with PUJ obstruction do not damage their kidneys, do not require surgery and ultimately grow out of the problem. We currently do not know how to distinguish effectively between those children with high pressure damaging obstruction and those with safe non-renal damaging PUJ obstruction[3].

Ultrasound scans and MAG 3 renograms are currently used to diagnose PUJ obstruction, however there is limited consensus on diagnostic thresholds, and ultimately these tests are unable to adequately predict which children will need surgery and which won't. Children are therefore 'observed' and undergo repeated radiological investigations over the first few years of life in order to finally determine the need for intervention. Kidney function becomes adversely affected during this period of observation in up to a quarter of children[3]. Moreover, there are no good biomarkers currently available to aid diagnosis, assess severity of obstruction and direct treatment.

Once diagnosed however, treatment of PUJ obstruction involves a well described operation called a pyeloplasty to remove the narrowed junction between the renal pelvis and ureter. This procedure is successful in 95% -97% of cases.[4]

It is known that urinary tract obstruction at any level causes raised intratubular hydrostatic pressure throughout the nephron. A resultant cascade of signaling pathways leads to interstitial fibrosis, tubular atrophy and nephron loss.[5] We propose that water channels called aquaporins are key mediators of water resorption from the renal tract in this situation, relieving kidney pressure and explaining the mechanism behind "safe" and "damaging" PUJ obstruction. Furthermore we propose that urinary levels of aquaporins are good biomarkers for determining high and low pressure systems and could be useful in our surgical practice.

Aquaporins are transmembrane proteins, normally expressed by the kidney and urothelium, which regulate urine volume by reabsorbing water. There are 13 mammalian aquaporin isoforms, which have diverse expression patterns among different tissues.[6] Certain aquaporin isoforms are also excreted within exosomes in urine. Animal and human data suggests ureteric obstruction causes downregulation of renal aquaporin expression and urinary exosomal aquaporin excretion[7,8,9]. There is very limited evidence that severity of renal down-regulation correlates with the degree of hydronephrosis[8] and renal impairment[10]. The effect of urinary tract obstruction on urothelial aquaporin expression is currently unknown.

The central hypothesis is thus:

Aquaporins in the renal tract protect the kidney against high-pressure damage in PUJ obstruction. Detecting them in the urine and manipulating them in the kidney and lower urinary tract will result in the development of novel operative biomarkers and new therapeutic approaches for this condition.

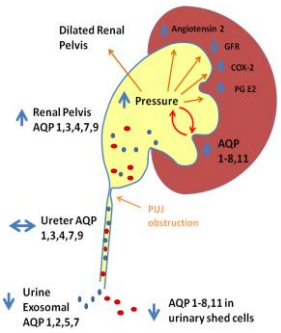

Through preliminary work (Fig.1) in the Academic Renal Unit all the necessary protein and molecular biology techniques for the identification of aquaporin isoforms at the mRNA and protein level within renal tract tissue have been established. (Fig.1a-d,f) Exosomes have also been successfully extracted from urine and it has been demonstrated that exosomal aquaporin levels can be measured.(Fig.1e)

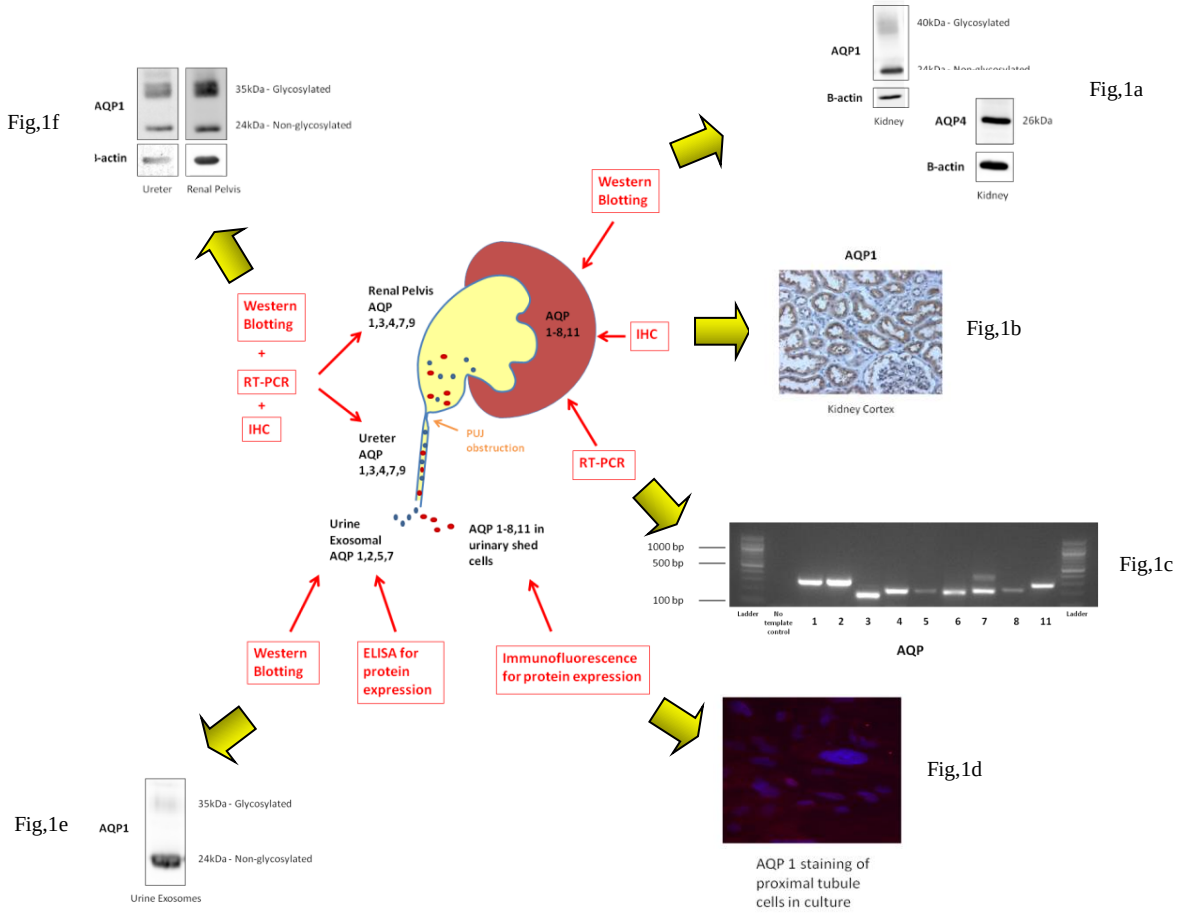

Figure 1. Selection of Initial Results.**(1a)** Western blots of human kidney demonstrating AQP 1 and 4 protein expression. **(1b)** Immunohistochemistry of human kidney cortex demonstrating AQP 1 staining of proximal tubules. **(1c)** RT-PCR of human kidney demonstrating AQP 1-8 and 11 expression at mRNA level. AQP 0,9,10,12 not expressed (data not shown) **(1d)** Immunofluorescence of proximal tubule cells in culture demonstrating the presence of AQP 1**(1e)** Western blot demonstrating AQP 1 protein detected in urine exosomes **(1f)** Western blots of human ureter and renal pelvis demonstrating AQP 1 protein expression

This study will build on the above preliminary work in order to:

- Measure the distribution and quantity of aquaporins in the lower urinary tract and kidney in childhood PUJ obstruction
    - Comparing renal pelvis (pre-obstruction) with ureteric (post-obstruction) aquaporin expression will enable assessment of the effect of obstruction on human urothelium.
- Establish the urinary aquaporin profile in high pressure (damaging) and low pressure (non-damaging) PUJ obstruction in children
    - Normal childhood urinary exosomal aquaporin levels will also be defined for the first time
- Determine whether urinary aquaporin measurement is a useful non-invasive biomarker directing the timing and necessity of corrective surgery for children with hydronephrosis and potential PUJ obstruction.
    - The availability of corresponding radiological imaging and intra-operative pressure monitoring will enable us to correlate changes in tissue and urine aquaporin levels with currently used markers of severity, function and pressure to determine the predictive value of urinary exosomal aquaporin measurement.
- Establish the mechanism behind changes in tissue and urinary aquaporin expression, enabling the future development of therapeutic treatment aiming to either protect renal function or reduce symptoms.
- Continuing work will involve further analysis of urine samples, including proteomic studies, to identify other potential biomarkers which may facilitate the diagnosis and management of children with hydronephrosis.

Potential Study Benefits

This project has the potential to improve the management of many children who are antenatally diagnosed with hydronephrosis, both nationally and globally.

- Development of urine aquaporin measurement as a non-invasive biomarker aims to identify children early who require a pyeloplasty for 'harmful' hydronephrosis, while sparing those with harmless hydronephrosis.
- Early identification of those with harmful hydronephrosis requiring a pyeloplasty will:
    - Reduce the risk of progressive damage to the kidney
    - Reduce the need for repeated radiological imaging some of which is invasive and involves radiation
- Shedding light on the mechanism of aquaporin downregulation will help achieve new therapies to:
    - Reduce progression of the renal injury after surgical release of obstruction
    - Reduce symptoms, particularly in patients with significant dieresis
- Other potential urine biomarkers for the diagnosis of PUJ obstruction may be revealed through further analysis including proteomic screening of urine samples.

Study Feasibility

There are many causes of urinary tract obstruction in childhood, however we have chosen to study PUJ obstruction for a number of reasons:

1. These are an easily identified group of children who attend outpatient clinic and are monitored regularly as part of their normal management. By comparison with other causes of urinary tract obstruction PUJ obstruction is relatively common, therefore recruitment of enough children to make a meaningful study over a reasonable time frame will be possible. All radiological investigations required for correlation of study results will already have been performed as per usual management for this group. Additional radiological investigations will therefore not be required as part of the study. Radiological reports will be easily accessible on the NHS PACS system enabling efficient data collection for the study.

2. On the basis of radiological imaging results and/or the presence of symptoms such as pain or urine infections a proportion of children with hydronephrosis will require a pyeloplasty to correct PUJ obstruction. This provides an opportunity to collect tissue and urine samples while the child is under general anaesthetic, when informed consent has been given. The integral part of a pyeloplasty for correction of PUJ obstruction involves removing the narrowed section of renal pelvis/ureter causing the obstruction and then joining the remaining tube back together. This section of removed renal pelvis/ureter is normally discarded. Laboratory analysis of this tissue will not change the way the operation is performed or the outcome from surgery in any way. Analysis of this tissue will, however, allow us to assess for the first time the effect of urinary tract obstruction on urothelial aquaporin expression.

3. Finally, a major reason for investigating this group is the potential to improve current evaluation and management of children with hydronephrosis and improve our understanding of the mechanism of disease.

Summary

Our current understanding of the natural history of PUJ obstruction and our ability to distinguish which children require surgery is inadequate. Improving our understanding of the mechanism of renal injury will enable earlier diagnosis and better management of this important condition through the development of novel biomarkers and new therapies.

Aims and Objectives

This study is non-commercial and will form part of an MD thesis.

Research Objectives

To determine whether urine aquaporin measurement can improve our ability to distinguish between children with 'damaging' PUJ obstruction who require urgent surgery to protect their kidney function, and those with 'safe' non-kidney damaging PUJ obstruction in whom surgery should be avoided.

To investigate the mechanism by which kidneys are damaged in PUJ obstruction, and to define the role of aquaporins in protecting kidney function in this situation. This will involve assessing urine and tissue aquaporin levels and determining whether changes in kidney function and /or pressure are associated with a significant change in aquaporin levels. Knowledge in this area will pave the way

for new therapies to manipulate aquaporin levels and protect kidney function in children with urinary tract obstruction.

Study Design

This is a cross-sectional study involving the laboratory analysis of urine and tissue samples. It will involve the recruitment of three groups of children attending Bristol Children's Hospital:

Group 1 will consist of children undergoing an open or laparoscopic (keyhole) pyeloplasty at the Bristol Children's Hospital. Potential participants will be identified in outpatient clinic and given information leaflets detailing the study. Consent for the study will then be obtained by the chief investigator (member of the research team) on the day of surgery after the surgeon has explained the surgical procedure.

Following enrolment to the study, on the day of hospital admission, the doctors will complete the initial data collection form documenting the child's demographic details, information about their medical history and the results of radiological tests.

Prior to surgery the child will be asked to provide a urine specimen; this may be into a pot if the child is old enough or collected from the nappy in younger children.

The pyeloplasty will be performed under general anaesthetic either laparoscopically (keyhole) or as an open (traditional) procedure. This decision will be based on the surgeons' preference and the best interests of the child. Participation in the study will not influence the way the procedure is performed.

During the child's operation samples will be obtained and procedures performed while they are under general anaesthetic. These are:

- All children undergoing a pyeloplasty normally have a bladder catheter inserted at the beginning of the procedure. A urine sample will be taken from the bladder catheter for laboratory analysis for the levels of water channels.
- A pressure reading will be taken from the obstructed kidney before the obstruction is relieved. This involves inserting a small pressure probe through the piece of drainage tube tissue that will subsequently be removed as part of the operation. Measuring the pressure in the kidney is an extra procedure for the child.
- During pyeloplasty surgery urine is usually removed from the obstructed kidney to reduce the size of the renal pelvis and make surgery easier. This urine is normally discarded however we will take a sample of this urine for laboratory analysis for the levels of water channels.
- The narrow section of tube at the junction of the renal pelvis and ureter will be removed and then the tube will be joined back together. Removing this narrowed piece of drainage tube is a normal part of the operation to correct PUJ obstruction and this piece of tissue is normally disposed of at the end of the operation. The narrowed piece of renal pelvis/ureter will be sent to the research laboratory in Bristol where the levels of water channels will be measured.

- An operative data collection form will be completed by the operating surgeon at the end of the procedure detailing the procedure performed, the kidney pressure and the samples collected.

Post-operatively a urine sample will be collected every 24 hours until the child is discharged from hospital (usually within 2-5 days). Initially this can be taken from the bladder catheter collection bag, however once the catheter is removed the child will be asked to pass urine into a pot or the sample will be collected from the nappy in younger children.

Children will attend outpatient clinic post-operatively as part of their routine surgical follow-up. No changes to the usual regime of radiological and clinic follow-up will be made for the study. The only requirement of the study will be that at each visit the child provides a urine specimen for laboratory analysis. The consulting doctor will be asked to complete a copy of the follow-up data collection form at each clinic visit. The length of post-operative follow-up varies depending on the age of the child and their post-operative progress and usually is between 3 months and 2 years. Participation in the study will terminate when the child is discharged from clinic follow-up.

Group 2 will consist of children with hydronephrosis but no evidence of other causes of urinary tract obstruction. These children will be identified when they attend general surgical or urology outpatient clinics. This group is necessary in order to find out if it is possible to differentiate between those children with 'safe' hydronephrosis and those with 'damaging' hydronephrosis. The child will be weighed and measured (if not already performed) and asked to provide a urine sample for analysis (either into a pot or collected from the nappy). This group of children will be asked to provide a urine sample at every clinic attendance. A data collection form will be completed at each clinic attendance. The expected length of follow-up and thus study participation in these children will be up to 4 years. Participation in the study will terminate when they are discharged from clinic follow-up.

Group 3 will consist of children with no kidney tract abnormalities attending general surgical or urology outpatient clinic for consultation regarding unrelated problems. This group is necessary in order to generate a table/graph of normal aquaporin excretion across varying ages and weights against which to compare group 1 patients. The child will then be weighed and measured (if not already performed) and asked to provide a urine sample for analysis (either into a pot or collected from the nappy). The consulting doctor will complete a data collection form. This will conclude the involvement of this group of children in the study.

Obtaining Kidneys Prepared for Transplantation

Kidneys which have been prepared for transplant but are later deemed clinically unsuitable are collected by our laboratory (Academic Renal Unit), with full consent for research, as part of another NHS REC approved study (Ref: 06/Q2002/101). In order to make full use of these organs which have been donated for research, the ureter and renal pelvis (which is often discarded as surplus tissue) will be used to develop and refine the laboratory techniques that will subsequently be employed for sample analysis during this childhood PUJ obstruction study.

Criteria for Discontinuation of Part of the Study

None

Subject Selection

Children with PUJ obstruction are an easily identified group who attend outpatient clinic and are monitored regularly as part of their normal management. By comparison with other causes of urinary tract obstruction PUJ obstruction is relatively common, therefore recruitment of enough children to make a meaningful study over a reasonable time frame will be possible. All children within the South West region have their pyeloplasty surgery at the Bristol Children's Hospital so this study will capture children from a large geographical area. All children will be identified as potential participants in the outpatient clinic setting and will be invited to take part in the study.

This is a single-centre study involving the Bristol Royal Hospital for Children where it is estimated there will be 20 pyeloplasties performed per year in children eligible for the study. It is hoped that 75% will agree to participate in the study.

Inclusion Criteria

Group 1 - Children (aged 0-15 years) placed on a planned waiting list for a laparoscopic or open pyeloplasty.

Group 2 - Children (aged 0-15 years) with hydronephrosis but no evidence of other causes of urinary tract obstruction attending general surgery/urology outpatient clinics

Group 3 - Children (aged 0-15 years) with no kidney tract problems attending general surgery/urology outpatient clinics for an unrelated issue.

Exclusion Criteria

Group 1

Children with other causes of urinary tract obstruction in addition to PUJ obstruction.

Group 2

Children with differential function <40% on MAG 3 renogram of the hydronephrotic kidney

Children with other causes of urinary tract obstruction other than PUJ obstruction.

Groups 1-3

Children taking medicines which affect kidney function or act on the kidney.

Children who have other intrinsic kidney disease.

Subject Recruitment

All patients will be identified when they attend the Bristol Children's Hospital outpatient clinics. There will not be any financial remuneration for participants.

Group 1 (undergoing pyeloplasty) participants will be identified by their paediatric urologist during the same clinic visit as the decision is made to place them on the planned waiting list for a pyeloplasty operation. The decision to perform an operation will be made by the operating surgeon, based solely on the usual diagnostic methods/criteria. Consideration of recruitment into the study will only possible once the decision to proceed with surgery has been made. The paediatric urologist will then review their notes and radiology reports to ensure suitability for inclusion in the study.

At the end of the consultation, following a discussion of the details of surgery, the urologist will give the family patient information leaflets (adult and child/young adult) detailing the study to take home and read. Contact details for the chief investigator will be provided on the leaflet should the families have any questions. The child's details will be added to a patient database as a potential participant. The family will have the time from their outpatient clinic appointment until the child's admission for surgery to decide whether they wish to consent to be included in the study. This period of time will be variable but in the order of a few weeks.

The family will next be met on the day of the child's operation when they are admitted for surgical pre-assessment. After the surgeon (paediatric urologist) has explained the surgical procedure the chief investigator (member of the research team) will go through all aspects of the study with the parents and child. This is to ensure the study is explained correctly, and also that there is no undue pressure for the family to consent. If the family wish to be included in the study they will be able to provide written consent in the presence of the lead researcher at this point.

Enrolment onto the patient database will be completed and the child will be assigned a numeric code. This numeric code will be used throughout the study to enable the child's clinical data to be linked to their tissue and urine sample analyses.

A coloured sticker will be applied to the front of the child's notes to identify participation in the study.

Group 2 and 3 participants will be identified during general surgery or urology outpatient clinics by their treating clinician. All patients attending outpatient clinic will be considered a potential participant and the clinician will review their notes and radiology reports to ensure suitability for inclusion in the study.

The families will be given adult and child patient information leaflets by the outpatient clinic nurse on arrival at the hospital. At the end of the clinic appointment the clinician will explain the details of the study and go through a written consent form with them if they wish to take part. This means families in these groups will have had about 30 minutes – 1 hour to decide whether they wish to be included in the study if they wish to be recruited and participate on the day. Ultimately, however, families with children in groups 2 and 3 have an unlimited amount of time to make a decision and we would be happy to accommodate them at later date should they wish to take part.

The patient database will then be completed by the clinician and the child assigned a numeric code. A coloured sticker will be applied to the front of the child's notes to identify participation in the study, and the consulting doctor will complete a data collection form.

For all groups of children a standard letter will be sent to their GP indicating they have been enrolled into a study. In addition a copy of the signed consent form and patient information leaflets will be filed in the child's notes and in the investigator site file. A copy will also be given to the parents.

Gaining Patient Consent

Children in all groups will require consent from at least one parent/carer with parental responsibility. Consent will be obtained for group 1 patients by the chief investigator. Consent for groups 2 and 3 patients will be obtained by the treating NHS clinician. A witness will not be required. Due to the nature of the study, consent will be obtained for the removal (consent under common law), storage (consent under Human Tissue Act), and use (consent under Human Tissue Act) of human tissue. Consent will also be gained for access to medical records.

We aim to gain generic consent for the tissue and urine samples which means they can be used for ongoing/future research projects and this will be explained to the families.

This study will involve recruiting children who are under the age of 16 years. Valid informed written consent will therefore be obtained from one adult (parent or carer) with parental responsibility in addition to obtaining assent from the child if they have sufficient understanding.

If the child and family do not have adequate understanding of English due to linguistic or hearing issues then a qualified medical interpreter will be engaged to enable effective communication with the family. Due to financial and logistical constraints it will not be possible to provide patient information leaflets and consent forms in languages other than English however an interpreter will be requested to read through these with the family to enable them to be included if they wish.

Subject Compliance

All families who are identified as potential participants will be recorded on a patient database and their decision whether to participate in the study or not will also be recorded. In this way we will be able to calculate the uptake rate for the study.

Inability to obtain tissue or urine samples during the inpatient stay of group 1 will be documented on the appropriate data collection form.

Failure to attend routine outpatient clinic follow-up will be documented on a data collection form and in the patient's clinical notes (usual procedure). On the data collection form it will be indicated whether a further appointment is planned and the form will be returned as usual for analysis.

If two outpatient appointments are missed a telephone call will be made to the family to assess whether they wish to continue in the study or whether they would like to leave the study. If the family cannot be contacted with a minimum of three telephone calls a letter will be sent to enquire of their well-being and their intentions regarding the study. This will be in addition to the usual NHS procedures followed when a child does not attend successive appointments.

Withdrawal of Subjects

A patient may be withdrawn from the study by the investigators if:

- Continued participation in the study could be harmful to the patients' health
- After enrollment it is discovered that the patient does not meet the eligibility criteria
- The patient needs a medicine or other medical treatment that is not allowed in the study
- The patient was enrolled by error, e.g., due to misinterpretation of the eligibility criteria

Additionally, the family/child may request to withdraw from the study if they no longer want to participate. In this case it would be documented in the patient notes and on a data collection form the reason why the family wanted to withdraw from the study (if they wish to disclose this) and the date of withdrawal. In this scenario all results gained so far would be used in the analysis but no further samples/data would be processed. The child would not be replaced in the study. Following withdrawal from the study the child will continue their usual outpatient follow-up with their treating clinician. A letter will be sent to the child's GP to inform them they are no longer participating in the study.

Sample Size Calculation

Study sample size:

Group 1: 30 patients

Group 2: 80 patients

Group 3: 80 patients

Total: 190 patients

Power of the study: 80%

Level of significance: $p<0.05$

The primary outcome will be analysed by comparing group 1 and group 2 urine aquaporin levels. It is known that approximately 20 children per year undergo a pyeloplasty for PUJ obstruction at the Bristol Children's Hospital. It is anticipated approximately 75% of these children will be recruited which equates to 30 children over 2 years. Recruitment to group 2 will be much faster as children suitable for inclusion are seen in greater numbers throughout the year. Children will therefore be recruited in a 4:1 manner with 4 children in group 2 to every child in group 1. This method of recruitment will increase the sample size and power of the study while keeping the number needed to recruit in group 1 achievable within an appropriate timescale.

Current studies suggest a target difference of 30% between groups 1 and 2 is feasible. It is currently unclear what degree of variability there is in the data. If the target difference is hypothesized to be to 0.75 of the standard deviation of the data then with a 4:1 recruitment method, a significance of 5% and a power of 80% it is estimated the minimum number of children to be recruited is:

Group 1: 18 children

Group 2: 70 children

Recruitment is therefore planned over two years, predicting recruitment of approximately 30 patients to group 1 and 80 patients to group 2 will be achieved.

Recruitment of children in group 3 (no kidney abnormality) is necessary to determine normal urine aquaporin levels across ages 0-15 years. For simplicity the aim is to recruit similar numbers to group 2.

There are no statistical criteria for termination of the study however a descriptive analysis of the data will be performed at 1 year. It is understood that descriptive analysis of the resultant data may demonstrate the variability to be different to that hypothesized. In this scenario the results obtained will form a pilot study from which the true variability can be ascertained and used to appropriately predict sample size for a subsequent full-scale study.

Data Collection

Primary Outcome Measure

- First urine aquaporin level when recruited into the study

In order to determine whether urine aquaporin levels are a good biomarker to aid surgical decision making the first urine aquaporin level will be of prime importance. This will enable us to compare aquaporin levels between children with PUJ obstruction requiring surgery and children with hydronephrosis but no evidence of other causes of kidney obstruction. In this way we will be able to demonstrate whether urine aquaporin levels can differentiate between those children with 'damaging' PUJ obstruction and those with 'safe' non-kidney damaging PUJ obstruction.

Additionally, assessment of the urine aquaporin levels in children with no kidney abnormality will enable us to determine whether age, gender or size has any impact on normal urine aquaporin levels.

Secondary Outcome Measures

- Tissue (renal pelvis and ureter) aquaporin levels
- Intra-operative urine aquaporin levels
- Kidney pressure (measured intra-operatively)
- Pre-operative kidney function (measured by MAG 3 renogram)
- Post-operative urine aquaporin levels in group 1 patients
- Follow-up urine aquaporin levels in group 2 patients

Tissue (renal pelvis and ureter) aquaporin levels and intra-operative urine aquaporin levels when combined with intra-operative kidney pressure measurement and results from tests of kidney function will enable us to determine whether significant changes in aquaporin levels are seen with increased pressure and reduced kidney function in PUJ obstruction.

Post-operative urine aquaporin levels will enable us to determine whether pyeloplasty restores aquaporin levels to normal.

Follow-up urine aquaporin levels in group 2 will provide a prospective cohort of children enabling the assessment of the predictive value of urinary aquaporin measurement. This will be achieved by

comparing those children whose hydronephrosis resolves with those who progress to need an operation and move into group 1.

Data Collection

Source of data	Time point for collection	Who will collect data	Reason for data collection	Type of data
Group 1-3 Gender	Baseline	Treating Clinician	Baseline	Binary
Group 1-3 Age	Baseline and every follow-up	Treating Clinician	Baseline comparison data	Continuous
Group 1 Weight	Baseline and every follow-up	Treating Clinician/Nurse	Baseline comparison data	Continuous
Group 1 Height	Baseline and every follow-up	Treating Clinician/Nurse	Baseline comparison data	Continuous
Group 2 Weight	Baseline and every follow-up	Treating Clinician/Nurse	Baseline comparison data	Continuous
Group 2 Height	Baseline and every follow-up	Treating Clinician/Nurse	Baseline comparison data	Continuous
Group 3 Weight	Baseline	Treating Clinician/Nurse	Baseline comparison data	Continuous
Group 3 Height	Baseline	Treating Clinician/Nurse	Baseline comparison data	Continuous
Group 1-3 Current medications	Baseline and every follow-up	Treating Clinician	Baseline comparison data	Descriptive
Group 1-3 Diagnosis	Baseline	Treating Clinician	Baseline comparison data	Categorical
Group 1 Urine sample for biomarker estimation	Baseline	Sample collection - Treating Clinician/Nurse Lab analysis – Laura Jackson	Main outcome	Continuous
Group 2	Baseline	Sample collection - Treating Clinician/Nurse	Main outcome	Continuous

Urine sample for biomarker measurement		Lab analysis – Laura Jackson		
Group 3 Urine sample for biomarker measurement	Baseline	Sample collection - Treating Clinician/Nurse Lab analysis – Laura Jackson	Main outcome	Continuous
Group 1 Catheter urine sample for biomarker measurement	During surgery	Sample collection - Treating Clinician Lab analysis – Laura Jackson	Secondary outcome	Continuous
Group 1 Kidney urine specimen for biomarker measurement	During surgery	Sample collection - Treating Clinician Lab analysis – Laura Jackson	Secondary outcome	Continuous
Group 1 Kidney pressure measurement	During surgery	Sample collection - Treating Clinician Lab analysis – Laura Jackson	Secondary outcome	Continuous
Group 1 Renal pelvis and ureter tissue for aquaporin measurement	During surgery	Sample collection - Treating Clinician Lab analysis – Laura Jackson	Secondary outcome	Continuous
Group 1 Urine samples for biomarker measurement	Post-operative	Sample collection - Treating Clinician/Nurse Lab analysis – Laura Jackson	Secondary outcome	Continuous
Group 1 Urine samples for biomarker measurement	Follow-up	Sample collection - Treating Clinician/Nurse Lab analysis – Laura Jackson	Secondary outcome and prognostic variable	Continuous
Group 2 Urine samples for biomarker measurement	Follow-up	Sample collection - Treating Clinician/Nurse	Explanatory and prognostic variable	Continuous

		Lab analysis – Laura Jackson		
Group 1 and 2 Ultrasound measurement of hydronephrosis as reported by radiologist (APD measurement)	Baseline	Treating Clinician	Explanatory variable	Continuous
Group 1 and 2 Ultrasound measurement of hydronephrosis as reported by radiologist (APD measurement)	Follow-up	Treating Clinician	Explanatory variable	Continuous
Group 1 and 2 Presence of kidney calyceal dilation and cortical thinning on ultrasound scan	Baseline	Treating Clinician	Explanatory variable	Descriptive
Group 1 and 2 Presence of kidney calyceal dilation and cortical thinning on ultrasound scan	Follow-up	Treating Clinician	Explanatory variable	Descriptive
Group 1 and 2 MAG 3 measurement of function of hydronephrotic kidney as reported by radiologist	Baseline	Treating Clinician	Explanatory variable	Continuous
Group 1 and 2 MAG 3 measurement of function of hydronephrotic kidney as reported by radiologist	Follow-up	Treating Clinician	Explanatory variable	Continuous

Group 1 and 2 MAG 3 type of curve as reported by radiologist	Baseline	Treating Clinician	Explanatory variable	Categorical
Group 1 and 2 MAG 3 type of curve as reported by radiologist	Follow-up	Treating Clinician	Explanatory variable	Categorical
Group 1 and 2 Additional radiological imaging performed	Baseline	Treating Clinician	Baseline comparison data	Descriptive
Group 1 and 2 Additional radiological imaging performed	Follow-up	Treating Clinician	Explanatory variable	Descriptive
Group 1 and 2 Prenatal diagnosis of hydronephrosis	Baseline	Treating Clinician	Baseline comparison data	Binary
Group 1 and 2 Symptoms associated with hydronephrosis	Baseline	Treating Clinician	Baseline comparison data	Binary
Group 1 and 2 Symptoms associated with hydronephrosis	Follow-up	Treating Clinician	Explanatory variable	Descriptive

The chief investigator will perform all urine and tissue analysis within the laboratories at the Dorothy Hodgkin Building, Bristol. All samples will be labelled with the individual patients' numeric code and sample type and will be transferred to the laboratory on ice. Samples will be processed in batches but analysis will run in parallel with recruitment.

Data Handling and Record Keeping

The chief investigator will be responsible for monitoring the accuracy and quality of data collection. Routine monitoring of trial progress will be made every 4 months, checking protocol compliance, accurate data collection form completion and monitoring of adverse events. Telephone contact will be made with clinicians if incomplete data collection is noted.

In order to ensure the study is run in accordance with ICH-GCP (ICH Harmonised Tripartite Guideline for Good Clinical Practice) certain essential documents will be compiled and retained at the study site within an investigator site file (ISF).
Data will be collected and retained in accordance with the Data Protection Act 1998.

Methods to Ensure Data Quality

Data extracted by the treating clinician from the patient medical records will be recorded on specific paper data collection forms according to the group the patient is recruited to and which point of the study they are at. These forms will contain clear instructions to minimize errors in data recording. In terms of measurements of kidney pressure, the instrument will first be calibrated and then the measurement will be recorded 3 times. Tissue and urine samples will each be analysed twice in order to check the accuracy of the data.

Medical and laboratory data will be entered by the chief investigator into a specially designed database created using Microsoft Access. Data entry will be performed via a standardized and consistent procedure. Data checking will be performed by verifying random samples of the digital data against the original data, double entry of data and statistical analyses such as frequencies, means and ranges to detect errors and anomalous values.

Data Security/Storage

For the duration of the study patient identifiable data including only the patient name, date of birth and Bristol Children's Hospital Identification Number will be stored on a database on the secure Bristol Children's Hospital NHS Trust server. Each child will be assigned a unique numeric code on this database. This network is only accessible to approved members of the NHS clinical workforce.

Data extracted from the child's records (demographic data, results of ultrasound scans and x-ray tests) will be recorded on a paper data collection form as described above and the child's unique numeric code placed on the record. No personal details of the child will be recorded on the data collection form and completed forms will be stored in a locked drawer in the Dorothy Hodgkin Building, University of Bristol. Only the chief investigator will have access to this drawer. The building itself is very secure with swipe card and biometric authorisation necessary for access.

Data from the data collection form and laboratory sample analysis results will be stored on the secure password protected University of Bristol Local Research Data Storage System. This data will only be accessible by the chief investigator.

The University of Bristol provides a dedicated Research Data Service as part of the Library (http://data.bris.ac.uk/research/). The Service offers advice, support and training in all areas of research data management and is responsible for Bristol's data.bris, Research Data Repository. The Service has it's own Steering Group and is responsible for the University's Research Data Principles (http://data.bris.ac.uk/research/support/).

Long-term Data Storage/Archiving

Following completion of the study, the data from the Bristol Children's Hospital NHS system and the University of Bristol Local Research Data Storage System will be encrypted and stored within the secure University of Bristol Research Data Storage Facility (RDSF) for 20 years. Dr Richard Coward will be the Data Steward and the chief investigator (Laura Jackson) and Mr Mark Woodward will also have access to the data.

The University of Bristol Research Data Storage Facility (RDSF) provides secure, long-term storage for research data. This two million pound investment provides nightly backup of all data, with further resilience provided by three geographically distinct storage locations. A tape library is used for backup purposes and also for long-term, offline data storage. Only authorised users can access data stored within the RDSF.

The RDSF is managed by Bristol's Advanced Computing Research Centre (ACRC) which has a dedicated steering group and a rigorous data storage policy (https://www.acrc.bris.ac.uk/acrc/RDSF_policy.pdf). The RDSF upholds and reinforces Bristol's wider Information Security Policy (www.bris.ac.uk/infosec/policies/docs/isp-01.pdf).

Public Sharing of Non-Confidential Research Data

Anonymous data will be stored on the University of Bristol long term Research Data Repository in order to publicly share research results.

The data.bris Research Data Repository offers a means for Bristol's researchers to openly share non-confidential research data, without the need for external data users to undergo any form of authentication. Each deposit is accompanied by appropriate metadata and is assigned a unique Digital Object Identifier (DOI) via the DataCite scheme. All data published by the Repository is available under a permissive re-use license.

Statistical Analysis

The statistical requirements of this study have been discussed with Professor Tim Peters, Professor of Primary Care Health Services Research and Head of The School of Clinical Sciences

All recruited patients will be included in the analysis. Descriptive statistical analysis will be applied to the study in order to quantitatively evaluate the basic features of the data. This will include measures of central tendancy (mean, median, mode), measures of dispersion (range and quartiles) and measures of variability (standard deviation).

The distribution of the data will be assessed to determine normality of distribution which will impact on further choices of statistical test. Anticipated statistical tests are listed below:

Primary outcome measure will be analysed using:

- Unpaired T-test/Mann-Whitney Test
- Logistic regression model to generate receiver operating characteristic curve (ROC curve) which will allow the threshold to be determined for the urine biomarker test.

Secondary outcomes measures will be analysed using:

- Unpaired T-test/Mann-Whitney Test
- One way ANOVA/Kruskal Wallis Test

Safety Assessments

All adverse events will be recorded in the investigator site file, documenting when the event occurred, details of the adverse event, any potential relation to the study, action taken and resolution / closure of the adverse event. An assessment of seriousness will be made and serious adverse events will be recorded and reported in accordance with UH Bristol's Research Related Adverse Event Reporting Policy in line with University of Bristol guidance. All serious adverse events will also be reported to the NHS Research Ethics Committee in the Annual Progress Report.

The type and duration of follow-up will be specific to the adverse event and will be determined by the study investigators. However; all adverse events will be followed through to resolution or until the adverse event is either attributed to a cause other than the study or assessed as chronic or stable.

Stopping/Discontinuation Rules

Definitions of Study Completion and Premature Discontinuation of the Study:

- Completion of the study will be achieved when all data collection and analysis has been completed for all patients enrolled in the study.
- Premature discontinuation of the study will occur if patient recruitment is terminated before full recruitment is achieved. The chief investigator, Research and Innovation Team and Research and Enterprise Development Team will discuss whether premature discontinuation is required following completion of the interim analysis.

Routine monitoring of trial progress will be made every 4 months, checking protocol compliance, accurate proforma completion and monitoring of adverse events. An interim descriptive statistical analysis of the data will be performed at 1 year

At study completion or if the study is prematurely discontinued, the Research and Innovation Department (NHS) and the Research and Enterprise Development Department (University) will be notified in writing. A 'Declaration of the End of a Study' form will be completed and sent to the Research Ethics Committee (REC). A copy will also be sent to the sponsor. The funding body will be notified in writing.

Research Governance, Monitoring and Ethics and R and D Approval

The study will be monitored and audited in accordance with University of Bristol policies. All trial related documents will be made available on request for monitoring and audit by UH Bristol, University of Bristol and the relevant Research Ethics Committee.

The study will be performed subject to Research Ethics Committee (REC) approval and local Research and Development (R&D) approval.

This study will be conducted in accordance with the Research Governance Framework for Health and Social Care and Good Clinical Practice.

If any changes to the study are required, necessary amendments will be made in agreement with the sponsors following approval from the REC and R&D. An annual report will be submitted to the REC and the sponsor.

Ethical Issues Related to the Study

Consent

Children in all groups will require consent from at least one parent/carer with parental responsibility. Due to the nature of the study consent will be obtained for the removal (consent under common law), storage (consent under Human Tissue Act), and use (consent under Human Tissue Act) of human tissue. Consent will also be gained for access to medical records. We aim to gain generic consent for the samples which means they can be used for ongoing/future research projects and this will be explained to the families.

This study will involve recruiting children who are under the age of 16 years. Valid informed written consent will therefore be obtained from one adult (parent or carer) with parental responsibility in addition to obtaining assent from the child if they have sufficient understanding.

It will be emphasized to all families involved that they may withdraw their consent at any time during the process and this will not affect their ongoing treatment.

If the child and family do not have adequate understanding of English due to linguistic or hearing issues then a qualified medical interpreter will be engaged to enable effective communication with the family. Due to financial and logistical constraints it will not be possible to provide patient information leaflets and consent forms in languages other than English however an interpreter would be requested to read through these with the family to enable them to be included if they wish.

Risks, Burdens and Benefits

Benefits of the Study to the Child

The benefits of collecting and analyzing urine samples are far reaching if it leads to the generation of a new urine test to help diagnose PUJ obstruction earlier thus reducing the risk to the kidney. If the urine aquaporin test can then be implemented into clinical practice, children with hydronephrosis may benefit from using the test to help decide their ongoing managment.

Although the study will not influence the frequency of outpatient clinic follow-up appointments it is reasonable to assume that those children in the study will benefit from slightly more attentive follow-up than their counterparts.

There are no other direct benefits of the study to the children's health however they may take personal pleasure from being able to participate in a study that will help future generations of children with the same condition as them.

Risks/Burdens of the Study to the Child

For children in Groups 2 and 3 the risks/burden relate to the inconvenience of spending time in the outpatient clinic providing a urine sample and discussing with the clinician whether to take part in the study. As we are recruiting children their ability to provide a specimen on demand is very variable. In order to minimise inconvenience families will be provided with patient information leaflets on arrival to outpatient clinic by the clinic nurse. This will give them time to read and digest

the information before meeting the clinician for their appointment. Water will be made available in the clinic to encourage the timely production of a urine sample.

Children in group 3 will only be asked to provide a urine sample on one occasion. Children in group 2 will be asked to provide a urine sample at each outpatient clinic appointment over a period of up to 4 years. This will cause some inconvenience at each visit while obtaining a urine sample however the time spent should be shorter than the first visit. This is because we hope to gain consent at the first visit for ongoing samples which means they will not need to go through the consent process each time.

Children in group 1 undergoing a pyeloplasty will have the same burden of inconvenience as group 2 in terms of providing urine samples for analysis and additionally they will be required to give urine samples while an inpatient in hospital.

Confidentiality

During this study the "Caldicott Principles" will be utilized as a framework when dealing with patient confidentiality issues. In order to correlate the findings from laboratory tissue/urine analysis with knowledge of severity of hydronephrosis, kidney function and patient demographics, it will be necessary to access patient NHS records and use patient identifiable data. Without this data it will be impossible to know whether there is any difference between those children with hydronephrosis who maintain their kidney function and those who don't.

With this in mind we propose to use linked-anonymised data. In this way the data will be anonymous to the chief investigator (the researcher who will receive and hold the data) but it will contain a code that will allow the supplier of the data (NHS healthcare team) to identify people from it. In this way it will also allow us to link data from before and after surgery for patients, and also provide an avenue for the healthcare team to contact participants at the end of the study with a copy of the study results.

Patient identifiable data including only the patient name, date of birth and Bristol Children's Hospital Identification Number will be stored on a database on the secure Bristol Children's Hospital Network. Each child will be assigned a unique numeric code on this database. This network is only accessible to approved members of the NHS clinical workforce.

Data extracted from the child's records (demographic data, results of ultrasound scans and x-ray tests) will be recorded on a paper data collection form and the child's unique numeric code placed on the record. No personal details of the child will be recorded on the data collection form. The data collection form will be stored in a locked drawer in the Dorothy Hodgkin Building, University of Bristol. Only the chief investigator will have access to this drawer. The building itself is very secure with swipe card and biometric authorisation necessary for access. Information from the data collection forms and laboratory sample analysis results will be stored on the secure password protected University of Bristol Local Research Data Storage. Only the chief investigator will have access to this data.

Families will be informed during the consent process that access to medical records will be required to complete the study. Medical records will only be accessed by the healthcare team involved in the direct care of the patient and data extraction will be kept to the absolute minimum necessary. Families will also be informed that information gleaned from the study will ultimately be published in journal articles and presented to other health professionals and researchers at national and international meetings. All data will by anonymised at the time of publication and it will not be possible to identify individual patients from the data.

Finance

This study is financially supported by the David Telling Charitable Trust. No payments will be made to participants.

Indemnity

The University of Bristol has arranged Public Liability insurance to cover the legal liability of the University as Research Sponsor in the eventuality of harm to a research participant arising from management of the research by the University.

This does not in any way affect an NHS Trust's responsibility for any clinical negligence on the part of its staff (including the Trust's responsibility for University of Bristol employees acting in connection with their NHS honorary appointments).

The University of Bristol holds Professional Negligence insurance to cover the legal liability of the University, for harm to participants arising from the design of the research, where the research protocol was designed by the University.

The University of Bristol's Public Liability insurance policy provides an indemnity to our employees for their potential liability for harm to participants during the conduct of the research.

This does not in any way affect an NHS Trust's responsibility for any clinical negligence on the part of its staff (including a Trust's responsibility for University of Bristol employees acting in connection with their NHS honorary appointments).

Miss Laura Jackson, Mr Mark Woodward and Dr Richard Coward all hold substantive appointments with University Hospitals Bristol NHS Foundation Trust giving them the protection of the NHS indemnity scheme.

Reporting and Dissemination

Regular reports will be submitted to the NHS REC, to the funding body (The David Telling Charitable Trust) and to the sponsor during the running of the study. Study results will be published in peer-reviewed scientific journals and presented at conferences, nationally and internationally. Anonymous data will be stored on the University of Bristol long term Research Data Repository in order to publicly share research results. Additionally, a summary sheet of the study results will be compiled following completion of the study and will be distributed to the participants by their NHS clinician.

References

1. Dudley, J.A.,et al.Clinical relevance and implications of antenatal hydronephrosis.Arch Dis Child Fetal Neonatal Ed,1997.**76**(1):p.F31-4.
2. Woodward,M.,et al.Postnatal management of antenatal hydronephrosis.BJU Int, 2002.**89**(2):p.149-156.
3. Csaicsich,D.,et al.Upper urinary tract:when is obstruction obstruction? Curr Opin Urol, 2004.**14**(4):p.213-7.
4. Knoedler, J., et al. Population-based comparison of laparoscopic and open pyeloplasty in paediatric pelvi-ureteric junction obstruction. BJU Int, 2013. **111**(7):p.1141-7
5. Chevalier, RL., et al. Mechanisms of renal injury and progression of renal disease in congenital obstructive nephropathy. Pediatr Nephrol, 2010. **25**(4):p.687-9
6. Procino, G., et al., AQP5 Is Expressed In Type-B Intercalated Cells in the Collecting Duct System of the Rat, Mouse and Human Kidney. Cell Physiol and Biochem, 2011. **28**(4): p. 683-692.
7. Wang,G.,et al.Age-related changes in expression in renal AQPs in response to congenital, partial, unilateral ureteral obstruction in rats. Pediatr Nephrol, 2012. **27**(1): p. 83-94.
8. Wen, J.G.,et al.Expression of renal aquaporins is down-regulated in children with congenital hydronephrosis. Scand J Urol Nephrol,2009.**43**(6):p.486-93.
9. Li, Z.Z.,et al.Early alteration of urinary exosomal aquaporin 1 and transforming growth factor beta-1 after release of unilateral pelviureteral junction obstruction.J Pediatr Surg,2012.**47**(8):p.1581-6.
10. Li, Z.Z.,et al.Decrease of renal aquaporins 1-4 is associated with renal function impairment in pediatric congenital hydronephrosis.World J Pediatr,2012.**8**(4):p.335-41.

10.3.2 Patient information leaflets

Patient information leaflets provided to parents, young adults and children recruited to groups 1-3 are presented in the following section.

Do aquaporins protect against renal damage in PUJ obstruction?

Information Sheet for Parents/Guardians of Children having a Pyeloplasty for PUJ Obstruction (Group 1)

Your child is being invited to participate in a research study. Before you decide, it is important for you to understand why the research is being done and what it will involve for you and your child.

Please take time to read the following information carefully and discuss it with others if you wish. If appropriate, please encourage your child to read their information sheet and discuss the study with them.

Your child's specialist doctor will explain if there is anything that is not clear or if you would like more information. Thank you for taking the time to read this.

The purpose of this study

Your child has been diagnosed with pelvi-ureteric junction (PUJ) obstruction which is the most common cause of obstruction (blockage) in the urinary tract. Your doctor has recommended that your child has an operation called a pyeloplasty to treat this condition.

The kidneys produce urine by filtering the blood and removing waste products and water. The urine must then drain out of the kidney through a funnel shaped structure called the renal pelvis and into a tube called the ureter which transports urine to the bladder where it is stored.

PUJ obstruction is caused by a narrowing at the point where the ureter joins the renal pelvis. This obstruction, which forms before the baby is born, means that urine can't drain out of the kidney as fast as it is produced. Urine therefore accumulates inside the kidney causing the kidney to swell. This swelling (dilatation) is seen on ultrasound scan and is called hydronephrosis. Accumulating urine may increase the pressure inside the kidney and in some children this can damage the kidney.

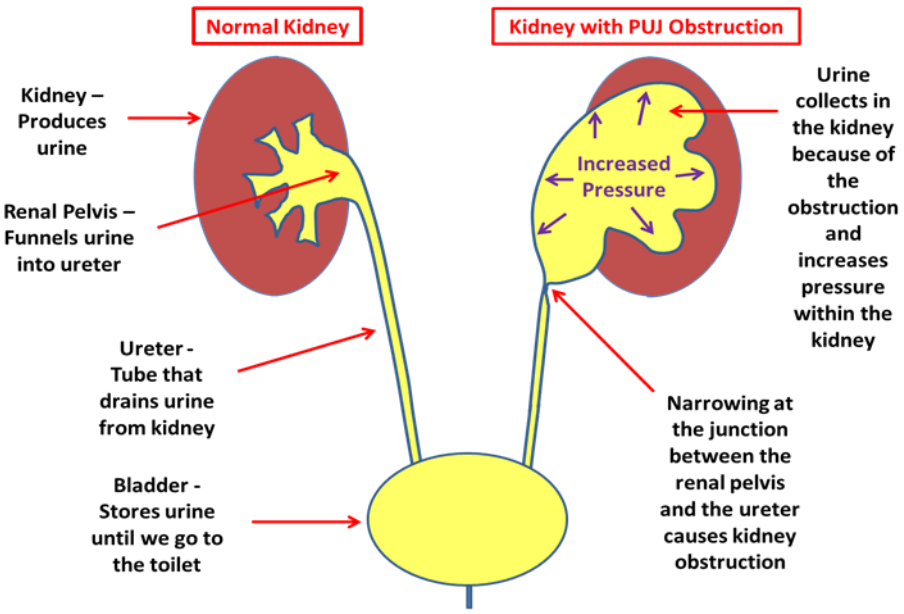

The major issue for doctors is deciding which children require surgery to relieve PUJ obstruction and limit kidney damage, and which do not. This is because some children with PUJ obstruction do not damage their kidneys, do not require surgery and ultimately grow out of the problem.

Our current ability to distinguish between those children with high pressure "damaging" obstruction and those with low pressure "safe" non-kidney damaging PUJ obstruction is limited.

Current research suggests that special water channels (proteins called aquaporins) in the kidney and its drainage tubes may help to protect the kidney from damage. By reabsorbing water from the urinary tract, these channels may reduce the pressure in the system, and explain the mechanism behind "safe" and "damaging" PUJ obstruction. We want to learn more about these channels so in the future we can develop new treatments to help protect the kidneys of all children and young adults with PUJ obstruction.

In addition, everybody sheds some of these water channels in their urine. We want to collect these special proteins from the urine, measure their amount and show whether they are a good marker of high pressure and low pressure kidneys. This will enable us to work out if a new type of urine test could help doctors decide which children with PUJ obstruction need an operation and which don't.

We hope that by improving our understanding of how the kidneys become damaged in PUJ obstruction we will be able to develop new tests and new treatments. These will enable us to diagnose damaging obstruction earlier and provide better treatment for affected children.

Why has my child been chosen?

Every patient with pelvi-ureteric junction (PUJ) obstruction who attends the Bristol Children's Hospital will be invited to participate.

Does my child have to take part?

It is up to you to decide whether your child takes part. If you decide they can take part you will be asked to sign a consent form. You are still free to change your mind and withdraw your child from the study at any time without giving a reason, and this will not affect the treatment your child receives.

What will happen if my child agrees to take part?

There are three parts to this study:

Firstly, when your child is admitted to hospital on the day of their operation they will be weighed and measured. With your permission we would also like them to provide a urine sample into a pot, or in younger children this may be collected from their nappy. The urine sample will be sent to the research laboratory in Bristol where the levels of water channels will be measured.

Secondly, during your child's operation (pyeloplasty), with your consent, samples will be obtained and procedures performed while your child is under general anaesthetic. These are:

- All children undergoing a pyeloplasty normally have a bladder catheter inserted at the beginning of the procedure. We would like to take a urine sample from the bladder catheter for laboratory analysis for the levels of water channels.
- We would also like to take a pressure reading from the obstructed kidney before the obstruction is relieved. This involves inserting a small pressure probe through the piece of drainage tube tissue that will subsequently be removed as part of the operation. Measuring the pressure in the kidney is an extra procedure for your child.
- During pyeloplasty surgery urine is usually removed from the obstructed kidney to reduce the size of the renal pelvis and make surgery easier. This urine is normally discarded however we would like to take a sample of this urine for laboratory analysis for the levels of water channels.
- The narrow section of tube at the junction of the renal pelvis and ureter will be removed and then the tube will be joined back together. Removing this narrowed piece of drainage tube is a normal part of the operation to correct PUJ obstruction and this piece of tissue is normally disposed of at the end of the operation. We would like the doctor to send the narrowed piece of renal

pelvis/ureter to the research laboratory in Bristol where the levels of water channels will be measured.

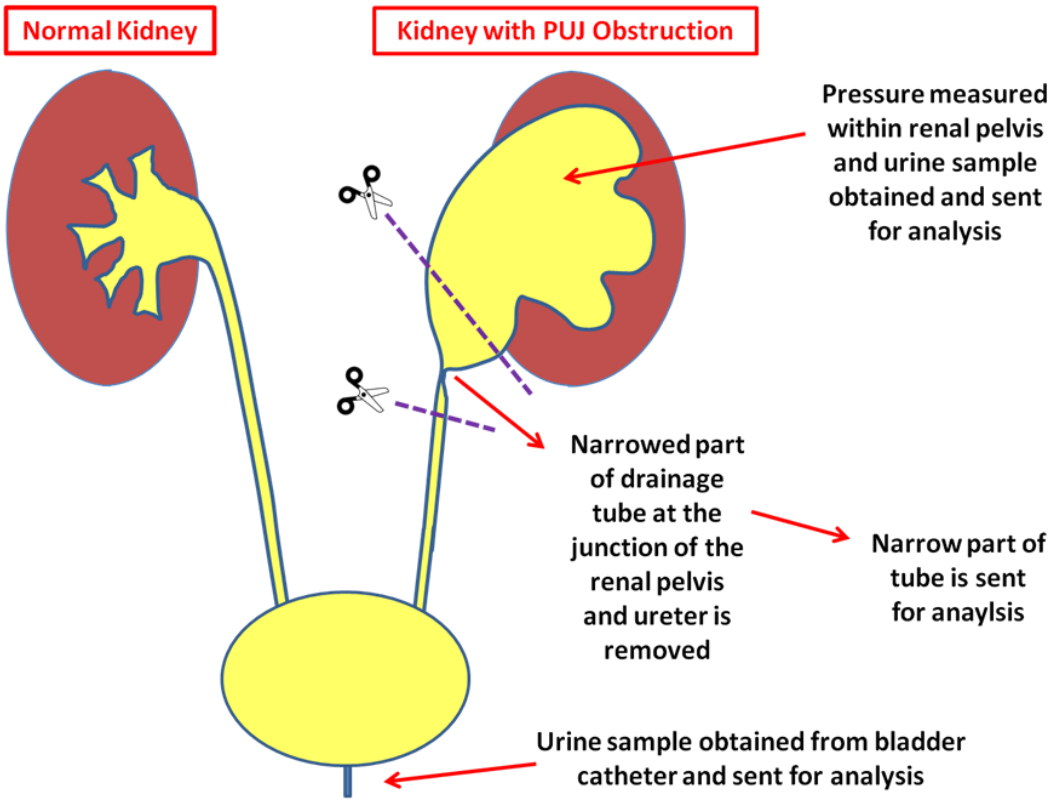

After the operation the tube from the kidney will be joined together and urine will drain out of the kidney properly. It will look like this:

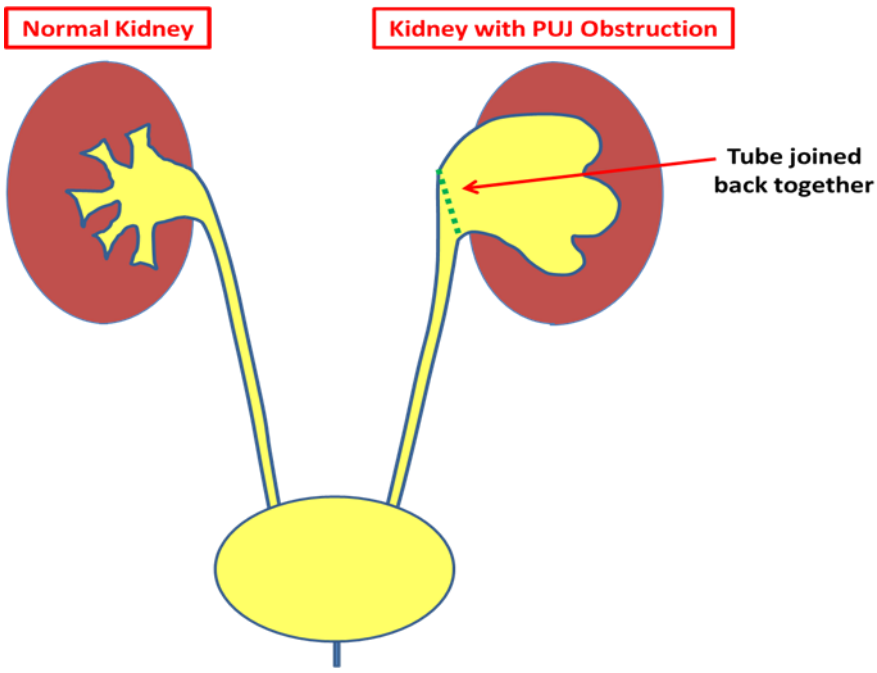

After your child's operation we would like to collect a urine sample on a daily basis until they are discharged from hospital. Initially this will be taken from the bladder catheter but once this is removed your child will be asked to provide a specimen into a pot. In younger children the sample can be collected from the nappy.

Thirdly, at each outpatient clinic visit your child will be weighed and measured and we would like them to provide a fresh urine sample into a pot, or in younger children it may be collected from their nappy. This will be sent to the research laboratory in Bristol where the levels of water channels will be measured. These results will help us to know whether treating the blockage in PUJ obstruction changes the amount of water channels shed in the urine.

During each stage, with your permission, the doctor will record some information about your child which will be taken from their medical notes/results file. These will include; their age, height and weight, any symptoms relating to PUJ obstruction, the results of their kidney scans and current medications.

With your permission we would like to store the samples after this research is complete for use in future ethically approved kidney disease research.

What will happen to any information about my child?

Any medical information about your child will be kept private. Limited personal details identifying your child as participating in the study will remain on the NHS computer system at the Bristol Children's Hospital. All children will be assigned a study number so that any samples and information collected about them is labelled with this number and no personal details when it is transferred to the research laboratory. The information your doctor sends to the researchers and the results we have from sample analysis will be stored securely at the laboratory. At the end of the study the

information will be encrypted and transferred to a secure storage facility within the University of Bristol called the Research Data Repository where it will remain for 20 years. At the end of this period of time the information will be destroyed.

What will happen to my child's samples?

Once the narrowed drainage tube and urine samples have been analysed, they will be stored securely at the research laboratory in Bristol. The samples will be labelled with your child's unique study number so that their sample results can be linked with their medical information. At the end of the study, with your permission, the samples will continue to be stored at the research laboratory pending further study. Access to this building is limited to the laboratory staff and an identification card and biometric authorisation is required for access.

What if new discoveries are made about PUJ obstruction?

The research-group want to test for water channels (aquaporins) and their role in protecting the kidney in PUJ obstruction. They also want to determine whether a urine test for these water channels will help doctors decide which children and young adults need an operation for PUJ obstruction.

In the future other proteins and substances may be found to be involved in PUJ obstruction. The group would like to be able to test for new proteins and substances, if they are found, using the original stored samples. If you don't want your child's samples to be stored and used for future research that's ok, just inform your specialist doctor and we will dispose of them at the end of this study.

How will I know the outcome of the research?

At the end of the study your doctor will send you a summary of the study results. If you don't want to receive a copy of the results please inform your specialist doctor.

Will the results be published?

All data collected will be collated and published in peer-reviewed scientific journals. The findings will also be presented at national and international scientific conferences. All this information will be anonymous and it will not be possible to identify your child from the data.

Will my GP know about this research?

If you agree we will inform your child's General Practitioner of their participation in this study.

How long will I have to decide?

We would like to give you as much time as possible to discuss the study and decide whether you wish your child to take part. However; your child's ongoing medical treatment is our greatest priority and we wouldn't want to delay their operation in order to accommodate the study. Because of the type of samples and information we would like to collect, it is not possible to join the study after your child has had surgery. Considering all these factors we would need to know by the day of your child's operation whether you would like to take part. We will be extremely happy to answer any questions you may have in the meantime and we would ask that you please contact either your specialist doctor or email the researcher listed at the bottom of the leaflet.

What if I wish to withdraw my child from the study?

A participant may withdraw at any stage without having to give an explanation. You can do this via telephone, email, or in writing to your specialist doctor or directly to the research team if you wish. The results of any tests on samples already collected will be used but no further tests will be done on these samples and no further samples will be collected. Any samples already held by the research team will be destroyed in an appropriate manner.

What are the risks/benefits in participating in this study?

This study does not require you to attend hospital more frequently however there is an extra procedure that would be undertaken during your child's operation. This is to measure the pressure in the kidney. There are no risks associated with measuring the kidney pressure as the pressure probe is inserted through the piece of drainage tube tissue that is subsequently removed as a normal part of the operation. Measuring the pressure takes about 5 minutes to perform.

The pyeloplasty operation will be performed in exactly the same manner as normal and the outcome of the surgery will not be changed by involvement in the study.

At each outpatient clinic visit and during your child's hospital stay your child will be asked to provide urine samples (or in younger children these would be taken from the nappy) for analysis. Your child will also be weighed and measured at each outpatient clinic visit. Some of these urine samples will be extra to normal requirements.

The benefits of participating in the study are that it will increase medical knowledge about PUJ obstruction potentially leading to new treatments and the development of a new urine test. We hope this urine test will allow earlier and improved detection of those children requiring surgery for PUJ obstruction.

What do I do if I have concerns about the study?

If you have any concerns or further questions about this study or the way it is carried out, you should contact the research team. You can also contact the Patient Support and Complaints Team within the Bristol Children's Hospital.

Will this study have an educational role?

This study is being undertaken as part of a higher degree educational project.

Has this research study been approved by an ethics committee?

All research in the NHS is looked at by an independent group of people, called a Research Ethics Committee, to protect your interests. This study has been reviewed and approved by South West - Central Bristol Research Ethics Committee.

Researchers	***Patient Support and Complaints Team***
Miss Laura Jackson, Mr Mark Woodward and Prof Richard Coward	*Patient Support and Complaints Team*
Academic Renal Unit	*Trust Headquarters*
University of Bristol	*University Hospitals Bristol*
Dorothy Hodgkin Building, Level 1	*Marlborough Street*
Whitson Street	*Bristol*
Bristol	*BS1 3NU*
BS1 3NY	
Contact email: laura.jackson@bristol.ac.uk	*Tel: 0117 342 3604*

Do aquaporins protect against renal damage in PUJ obstruction?

Information Sheet for Young Adults having a Pyeloplasty for PUJ Obstruction (Group 1)

You are being invited to take part in a project. Before you decide, it is important for you to understand why we want to do it and what it means for you.

Please take time to read this and chat about it with others if you want.

Your specialist doctor will explain anything that is confusing, or give you more information. Thank you for taking the time to read this.

The purpose of this study

You have a blockage of your kidney called pelvi-ureteric junction (PUJ) obstruction which needs an operation known as a pyeloplasty to make it better. PUJ obstruction is caused by a narrowing in the upper part of the tube that drains urine out of the kidney. Urine therefore builds up and can increase the pressure inside the kidney. In some children and young adults this can cause the kidney to not work properly.

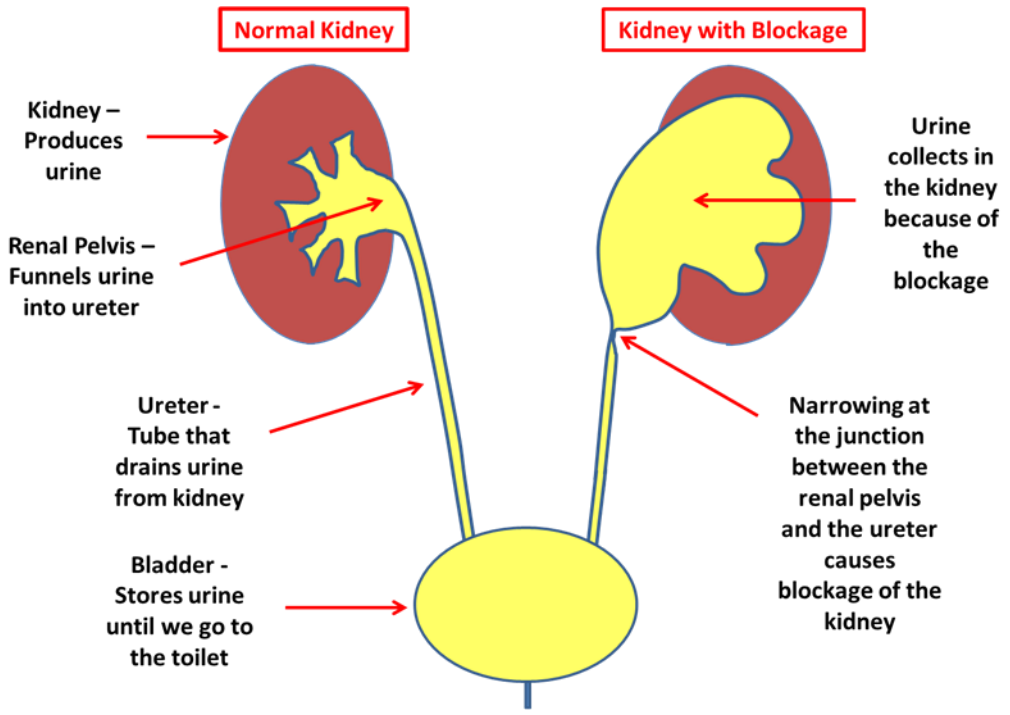

Not all people with PUJ obstruction are at risk of kidney damage if they don't have an operation. Some children grow out of the problem and their kidneys continue to work normally.

Sometimes it can be difficult for doctors to figure out which children and young adults need an operation to protect their kidney and which will simply grow out of the problem.

Current research suggests that special water channels (proteins called aquaporins) in the kidney and its drainage tubes may help to protect the kidney from damage. We want to learn more about these channels to see if we can develop new treatments to help protect the kidneys of all children and young adults with PUJ obstruction.

In addition, everybody sheds some of these water channels in their urine. We want to collect these special proteins from the urine and measure their amount. This will enable us to work out if a new type of urine test could help doctors decide which children with PUJ obstruction need an operation and which don't.

Why have I been chosen?

Every patient with pelvi-ureteric junction (PUJ) obstruction who attends the Bristol Children's Hospital will be invited to participate.

Do I have to take part?

It is up to you to decide whether you take part. You are still free to change your mind and leave the study at any time without giving a reason. If you decide not to take part or to come out of the study this will not affect the treatment you receive.

What will happen if I agree to take part?

There are three parts to this study if you decide you want to take part:

Firstly, when you come in to hospital on the day of your operation we would like you to be weighed and measured and we would like you to provide a urine sample into a pot. This will be sent to the research laboratory in Bristol where the levels of water channels will be measured.

Secondly, during your operation (pyeloplasty), your doctor would like to take some samples and perform some procedures while you are asleep under general anaesthetic. These include:

At the beginning of the operation your doctor would like to use a special machine to record the pressure in your blocked kidney. They would also like to take a urine sample directly from the blocked kidney which will be sent to the research laboratory to measure the levels of water channels.

The main part of the operation is when your doctor takes out the narrow piece of tube and joins the tube back together in order fix your kidney blockage. Normally the removed section of narrow tube is discarded, but your doctor would like to send the narrow piece of tube to the research laboratory where the levels of water channels will

be measured. All of this will happen while you are under general anaesthetic, so you will be fast asleep.

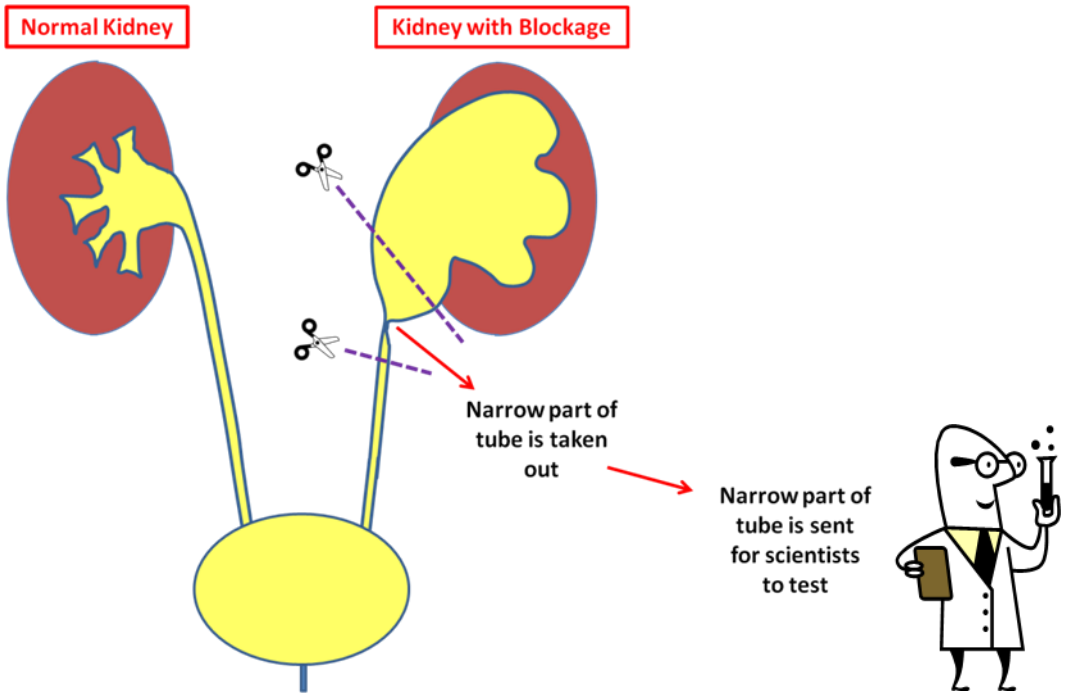

After the operation the tube from the kidney will be joined back together and urine will drain out of the kidney properly. It will look like this:

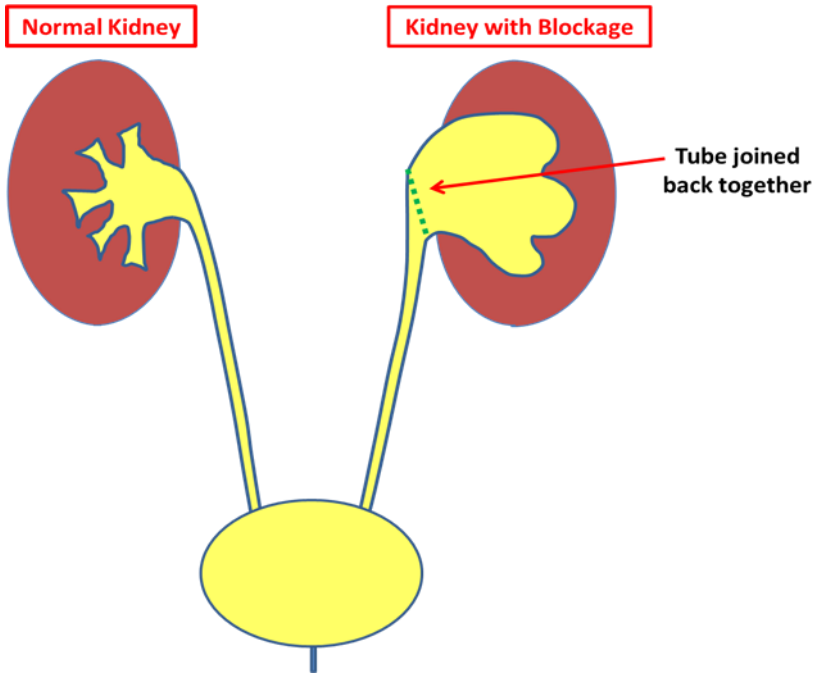

After the operation your doctor would like to collect a urine sample from you every day while you are in hospital.

Thirdly, at each outpatient clinic visit we would like you to be weighed and measured and to provide a urine sample into a pot. This will be sent to the research laboratory in Bristol where the levels of water channels will be measured.

These results will help us to know whether treating the blockage in PUJ obstruction changes the amount of water channels shed in the urine.

During each stage your doctor would like to record some information about you including; your age, your height and weight, the results of your most recent kidney scans, and if you are taking any medicines.

With your agreement and your parents' permission we would like to store your samples after this research is complete for use in future ethically approved kidney disease research.

What will happen to any information about me?

Any information about you will be kept private. The information your doctor sends us will be stored securely at the laboratory. At the end of the study the information will be encrypted and transferred to a secure storage facility within the University of Bristol called the Research Data Repository where it will remain for 20 years. At the end of this period of time the information will be destroyed.

What will happen to my drainage tube and urine samples?

Once the drainage tube and urine samples have been analysed, they will be stored securely at the research laboratory in Bristol. At the end of the study, with your agreement, the samples will continue to be stored at the research laboratory in Bristol. Only people in the research group with special passes can get in. The samples are kept in a freezer until they are used.

What if new discoveries are made about PUJ obstruction?

The research-group want to test for water channels (aquaporins) and their role in protecting the kidney in PUJ obstruction. They also want to determine whether a urine test for these water channels will help doctors decide which children and young adults need an operation for PUJ obstruction.

In the future other proteins and substances may be found to be involved in PUJ obstruction. The group would like to be able to test for new proteins and substances, if they are found, using the original stored samples. If you don't want your samples to be stored and used for future research that's ok, just tell us and we will dispose of them at the end of this study.

How will I know the results of the study?

At the end of the study your doctor will send you a summary of the study results. If you don't want to receive a copy of the results that's fine just let us know.

Will my GP know about this research?

If you and your parents agree we will inform your General Practitioner of your participation in this project.

How long do I have to decide?

We would like to give you as much time as possible to discuss the study and decide whether you want to take part. However; your medical treatment is our greatest priority and we wouldn't want to delay your operation because of the study. Since the samples and information we would like to collect are mostly obtained during your operation, it is not possible to join the study after you have had your operation. Considering all these factors we would need to know by the day of your operation whether you would like to take part. We will be extremely happy to answer any questions you may have in the meantime. Please contact either your specialist doctor or email the researcher listed at the bottom of the leaflet with any questions you have.

What if I wish to leave the study?

You can leave the study at any stage without having to give a reason. You can do this via telephone, email, or in writing to your specialist doctor or directly to the research team if you wish. The results of any tests on samples already collected will be used but no further tests will be done on these samples and no further samples will be collected. Any samples already held by the research team will be destroyed in an appropriate manner.

What do I do if I have concerns about the study?

If you have any concerns or further questions about this study or the way it is carried out, you should contact the research team. You can also contact the Patient Support and Complaints Team within the Bristol Children's Hospital.

Will this study have an educational role?

This study is being undertaken as part of a higher degree educational project.

Has this research study been approved by an ethics committee?

All research in the NHS is looked at by an independent group of people, called a Research Ethics Committee, to protect your interests. This study has been reviewed and approved by South West – Central Bristol Research Ethics Committee.

Researchers	***Patient Support and Complaints Team***
Miss Laura Jackson, Mr Mark Woodward and Prof Richard Coward	*Patient Support and Complaints Team*
Academic Renal Unit	*Trust Headquarters*
University of Bristol	*University Hospitals Bristol*
Dorothy Hodgkin Building, Level 1	*Marlborough Street*
Whitson Street	*Bristol*
Bristol	*BS1 3NU*
BS1 3NY	
Contact email: laura.jackson@bristol.ac.uk	*Tel: 0117 342 3604*

Studying Kidney Blockage

Information Sheet for Children having an Operation for a Kidney Blockage (Group 1)

Hello!

Thank you for reading this. You can ask someone to help you read it if you want.

Please ask if you don't understand.

Your doctor thinks you have a blockage of your kidney which needs an operation to make it better. We call this blockage pelvi-ureteric junction (PUJ) obstruction. It happens because part of the tube that drains wee out of the kidney is too narrow. There are other children, just like you, in Bristol and the rest of the country who also have this problem.

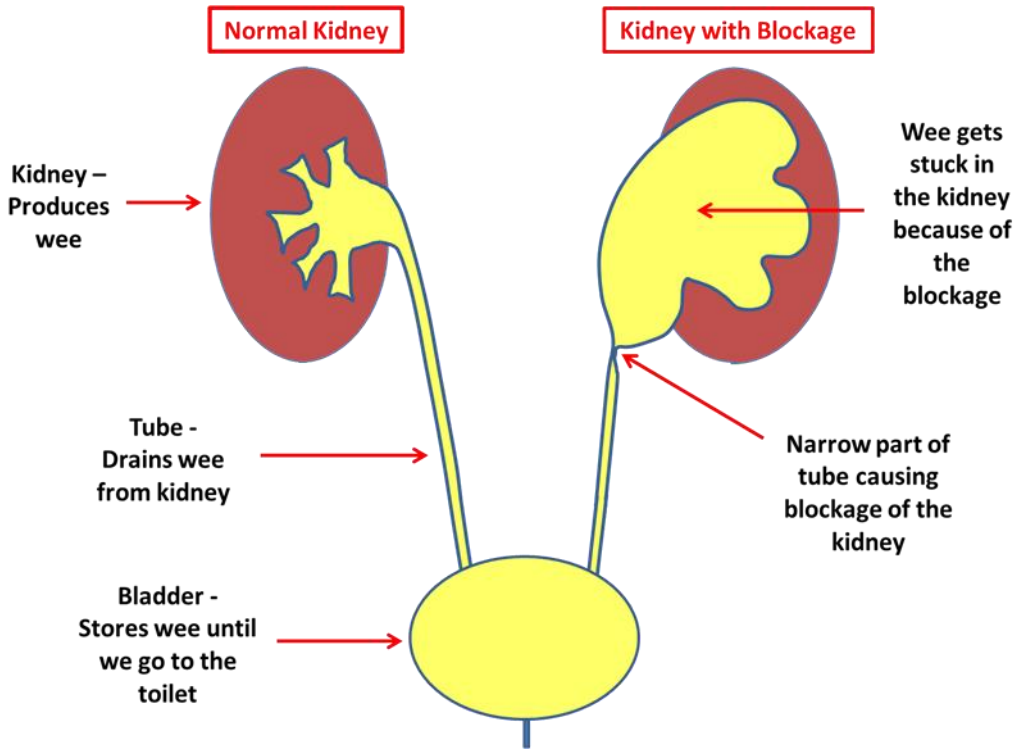

There is a group of doctors and scientists in Bristol who want to find out more about it. They want to try and find out why the blockage sometimes makes the kidney not work properly. They also want to find out if a new test using a sample of wee can help doctors decide which children need an operation to fix this problem.

They will do this by asking all the children who come to Bristol Children's Hospital with a kidney blockage to join in this project. They would like to collect information about how old you are, how heavy you are and what tests and scans you've already had.

The doctors would also like you to give them a sample of your wee each time you come to the hospital. The sample will be tested to see how much of a special type of protein is in your wee.

When you have your operation to fix the kidney blockage your doctor will take out the narrow bit of tube and join the tube back together. Your doctor would like to send the narrow bit of tube to the scientists to be tested just like the wee sample. All this would happen while you are fast asleep.

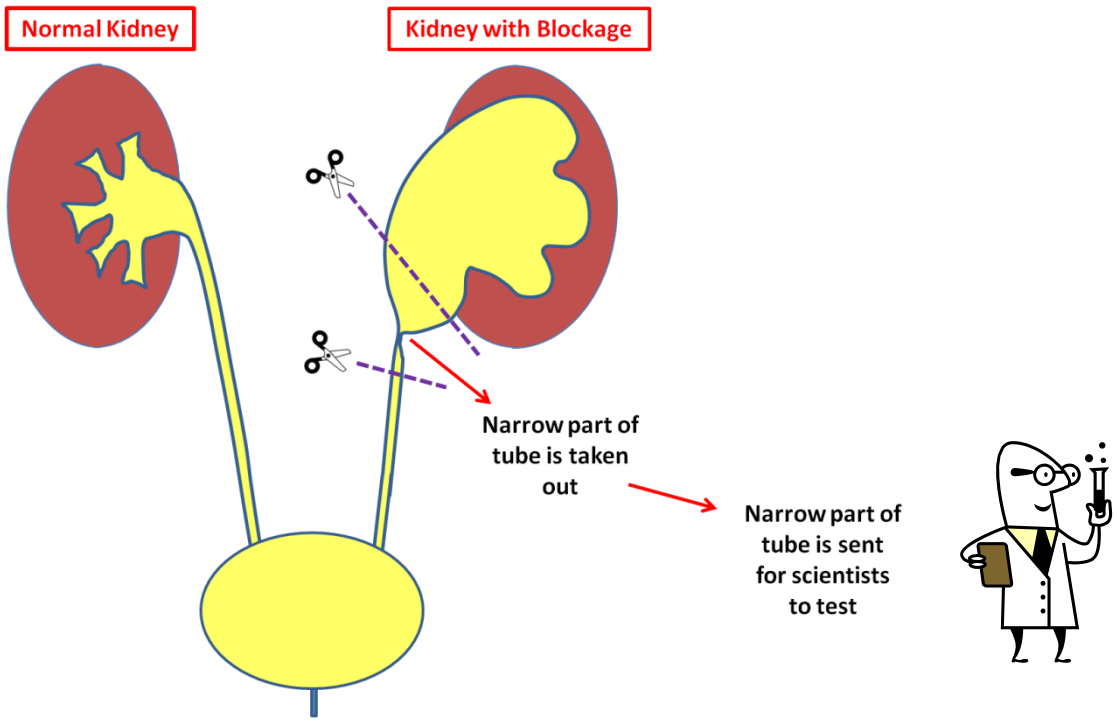

After the operation the tube from the kidney will be joined back together and the kidney won't be blocked anymore. It will look like this:

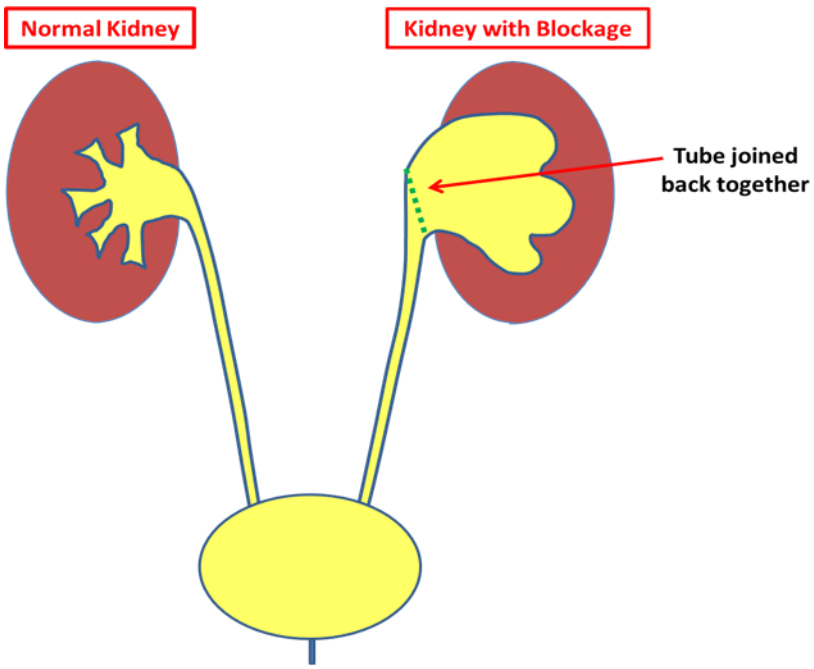

If you don't want to take part that's ok and it won't affect your treatment.

So that's it!

Do you want to ask any questions?

Researchers

Miss Laura Jackson, Mr Mark Woodward and Prof Richard Coward

Academic Renal Unit

University of Bristol

Dorothy Hodgkin Building, Level 1

Whitson Street

Bristol, BS1 3NY

Contact email: laura.jackson@bristol.ac.uk

This study has been reviewed and approved by South West – Central Bristol Research Ethics Committee and is being undertaken as part fulfilment of an educational project.

Do aquaporins protect against renal damage in PUJ obstruction?

Information Sheet for Parents/Guardians of Children with Hydronephrosis (Group 2)

Your child is being invited to participate in a research study. Before you decide, it is important for you to understand why the research is being done and what it will involve for you and your child.

Please take time to read the following information carefully and discuss it with others if you wish. If appropriate, please encourage your child to read their information sheet and discuss the study with them.

Your child's specialist doctor will explain if there is anything that is not clear or if you would like more information. Thank you for taking the time to read this.

The purpose of this study

There a number of children and young adults who come to the Bristol Children's Hospital because they have pelvi-ureteric junction (PUJ) obstruction which is the most common cause of obstruction (blockage) in the urinary tract. Some need an operation known as a pyeloplasty to treat this condition.

The kidneys produce urine by filtering the blood and removing waste products and water. The urine must then drain out of the kidney through a funnel shaped structure called the renal pelvis and into a tube called the ureter which transports urine to the bladder where it is stored.

PUJ obstruction is caused by a narrowing at the point where the ureter joins the renal pelvis. This obstruction, which forms before the baby is born, means that urine can't drain out of the kidney as fast as it is produced. Urine therefore accumulates inside the kidney causing the kidney to swell. This swelling (dilatation) is seen on ultrasound scan and is called hydronephrosis. Accumulating urine may increase the pressure inside the kidney and in some children this can damage the kidney.

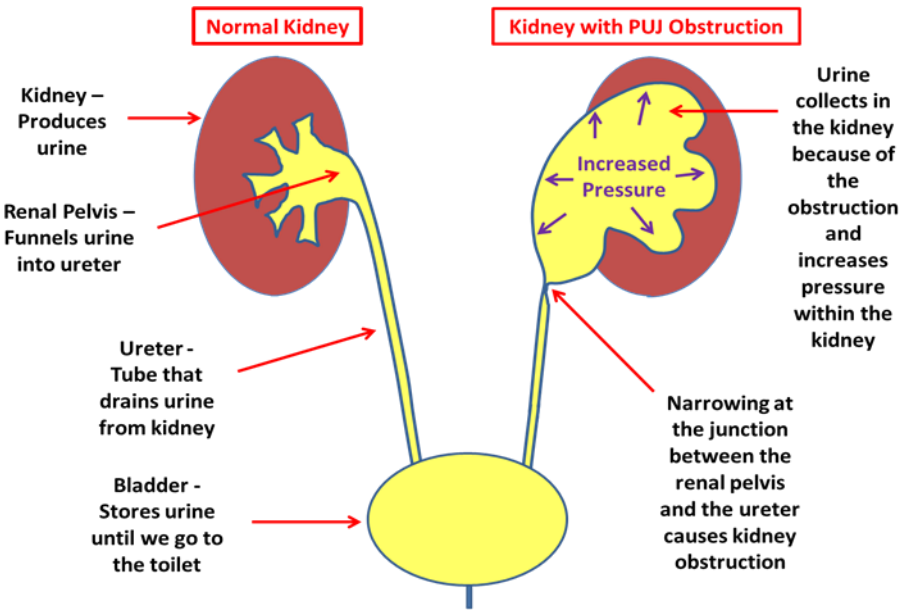

The major issue for doctors is deciding which children require surgery to relieve PUJ obstruction and limit kidney damage, and which do not. This is because some children with PUJ obstruction do not damage their kidneys, do not require surgery and ultimately grow out of the problem.

Our current ability to distinguish between those children with high pressure "damaging" obstruction and those with low pressure "safe" non-kidney damaging PUJ obstruction is limited.

Current research suggests that special water channels (proteins called aquaporins) in the kidney and its drainage tubes may help to protect the kidney from damage. By reabsorbing water from the urinary tract, these channels may reduce the pressure in the system, and explain the mechanism behind "safe" and "damaging" PUJ obstruction.

Everybody sheds some of these water channels in their urine. We want to collect these special proteins from the urine, measure their amount and show whether they are a good marker of high pressure and low pressure kidneys. This will enable us to work out if a new type of urine test could help doctors decide which children with PUJ obstruction need an operation and which don't.

In order to know whether the test correctly identifies which children need an operation we need to know what the levels of these water channels are in children who have a swollen kidney but no evidence of a kidney obstruction.

For this reason the kidney research unit in Bristol is asking children who have a swollen kidney (but not a kidney obstruction) if they'd like to take part in the study.

Why has my child been chosen?

Every child/young adult with a swollen kidney (but not a kidney obstruction) who attends the Bristol Children's Hospital surgery/urology clinics on specified recruitment days will be invited to participate.

Does my child have to take part?

It is up to you to decide whether your child takes part. If you decide they can take part you will be asked to sign a consent form. You are still free to change your mind and withdraw your child from the study at any time without giving a reason, and this will not affect the treatment your child receives.

What will happen if my child agrees to take part?

Your child's scheduled appointment with the doctor will go ahead today as planned. With your consent at the end of the appointment your child will be weighed and measured and we would like them to provide a urine sample into a pot. In younger children the sample can be collected from the nappy. The urine sample will be sent to the research laboratory in Bristol where the levels of water channels will be measured.

Subsequently each time you attend a urology appointment your child will be weighed and measured and we would like them to provide a fresh urine sample into a pot, or in younger children it may be collected from their nappy. Again, this will be sent to the research laboratory where the levels of water channels will be measured.

At each visit, with your permission, the doctor will record some information about your child which will be taken from their medical notes/results file. This will include; their age, their height and weight, the cause of their swollen kidney, results of any kidney scans and current medications.

With your permission we would like to store the samples after this research is complete for use in future ethically approved kidney disease research.

What will happen to any information about my child?

Any medical information about your child will be kept private. Limited personal details identifying your child as participating in the study will remain on the NHS computer system at the Bristol Children's Hospital. All children will be assigned a study number so that their urine sample and information collected about them is labelled with this number and no personal details when it is transferred to the research laboratory. The information your doctor sends to the researchers and the results we have from sample analysis will be stored securely at the laboratory. At the end of the study the information will be encrypted and transferred to a secure storage facility within the University of Bristol called the Research Data Repository where it will remain for 20 years. At the end of this period of time the information will be destroyed.

What will happen to my child's samples?

Once the urine samples have been analysed, they will be stored securely at the research laboratory in Bristol. The samples will be labelled with your child's unique study number so that their sample results can be linked with their medical information. At the end of the study, with your permission, the samples will continue to be stored at the research laboratory pending further study. Access to this building is limited to the laboratory staff and an identification card and biometric authorisation is required for access.

What if new discoveries are made about PUJ obstruction?

The research-group is interested in water channels (aquaporins) and their role in protecting the kidney in PUJ obstruction. They want to determine whether a urine test for these water channels will help doctors decide which children and young adults need an operation for PUJ obstruction.

In the future other proteins and substances may be found to be involved in PUJ obstruction. The group would like to be able to test for new proteins and substances, if they are found, using the original stored samples. If you don't want your child's samples to be stored and used for future research that's ok, just inform your specialist doctor and we will dispose of them at the end of this study.

How will I know the outcome of the research?

At the end of the study your doctor will send you a summary of the study results. If you don't want to receive a copy of the results please inform your specialist doctor.

Will the results be published?

All data collected will be collated and published in peer-reviewed scientific journals. The findings will also be presented at national and international scientific conferences. All this information will be anonymous and it will not be possible to identify your child from the data.

Can I have more time to decide?

Yes. There is no time limit.

What if I wish to withdraw my child from the study?

A participant may withdraw at any stage without having to give an explanation. You can do this via telephone, email, or in writing to your specialist doctor or directly to the research team if you wish. The results of any tests on samples already collected will be used but no further tests will be done on these samples and no further samples will be collected. Any samples already held by the research team will be destroyed in an appropriate manner.

What are the risks/benefits in participating in this study?

This study does not require you to make an extra visit to the hospital however it does require your child to be weighed and measured and provide a urine samples at the end of each urology clinic appointment you attend.

The benefits of participating in the study are that it will increase medical knowledge about PUJ obstruction potentially leading to the development of a new urine test. We hope this urine test will allow earlier and improved detection of those children requiring surgery for PUJ obstruction.

W*hat do I do if I have concerns about the study?*

If you have any concerns or further questions about this study or the way it is carried out, you should contact the research team. You can also contact the Patient Support and Complaints Team within the Bristol Children's Hospital.

Will this study have an educational role?

This study is being undertaken as part of a higher degree educational project.

Has this research study been approved by an ethics committee?

All research in the NHS is looked at by an independent group of people, called a Research Ethics Committee, to protect your interests. This study has been reviewed and approved by South West - Central Bristol Research Ethics Committee.

Researchers	***Patient Support and Complaints Team***
Miss Laura Jackson, Mr Mark Woodward and Prof Richard Coward	*Patient Support and Complaints Team*
Academic Renal Unit	*Trust Headquarters*
University of Bristol	*University Hospitals Bristol*
Dorothy Hodgkin Building, Level 1	*Marlborough Street*
Whitson Street	*Bristol*
Bristol	*BS1 3NU*
BS1 3NY	
Contact email: laura.jackson@bristol.ac.uk	*Tel: 0117 342 3604*

Do aquaporins protect against renal damage in PUJ obstruction?

Information Sheet for Young Adults with a Swollen Kidney (Group 2)

You are being invited to take part in a project. Before you decide, it is important for you to understand why we want to do it and what it means for you.

Please take time to read this and chat about it with others if you want.

Your specialist doctor will explain anything that is confusing, or give you more information. Thank you for taking the time to read this.

The purpose of this study

There a number of children and young adults who come to the Bristol Children's Hospital because they have a blockage of their kidney called pelvi-ureteric junction (PUJ) obstruction. Some need an operation known as a pyeloplasty to make it better.

PUJ obstruction is caused by a narrowing in the upper part of the tube that drains urine out of the kidney. Urine therefore builds up and the kidney becomes swollen. In some children and young adults this can cause the kidney to not work properly.

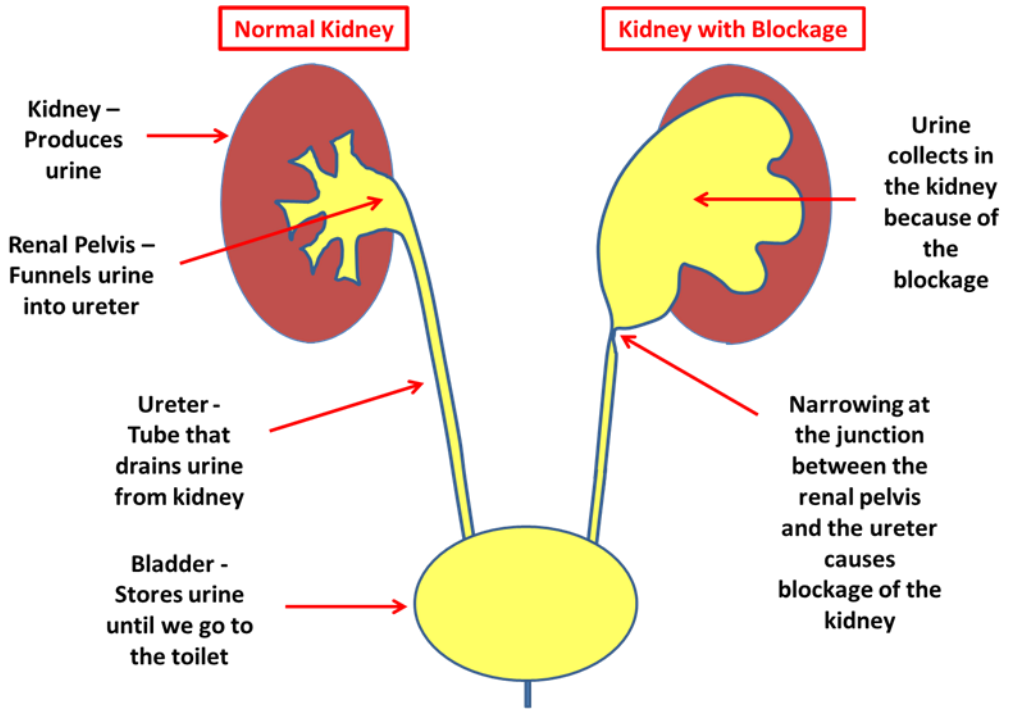

Not all people with PUJ obstruction are at risk of kidney damage if they don't have an operation. Some children grow out of the problem and their kidneys continue to work normally.

Sometimes it can be difficult for doctors to figure out which children and young adults need an operation to protect their kidney and which will simply grow out of the problem.

Current research suggests that special water channels (proteins called aquaporins) in the kidney and its drainage tubes may help to protect the kidney from damage. Everybody sheds some of these water channels in their urine. We are currently measuring the amount of these special proteins in the urine of children who have had an operation for PUJ obstruction. The aim is to work out if a new type of urine test could help doctors decide which children with PUJ obstruction need an operation and which don't.

In order to know whether the test works properly we need to know what the levels of these water channels are in children/young adults who have a swollen kidney but not a kidney blockage.

For this reason the kidney research unit in Bristol is asking children and young adults like you who have a swollen kidney if they'd like to take part in the study.

Why have I been chosen?

All children/young adults who have a swollen kidney (but not a kidney blockage) will be invited to participate if their clinic appointment at the Bristol Children's Hospital falls on a specified recruitment day.

Do I have to take part?

It is up to you to decide whether you take part. You are still free to change your mind and leave the study at any time without giving a reason. If you decide not to take part or to come out of the study this will not affect the treatment you receive.

What will happen if I agree to take part?

Your scheduled appointment with your doctor will go ahead today as planned. At the end of the appointment we would like you to be weighed and measured and we would like you to provide a urine sample into a pot. This will be sent to the research laboratory in Bristol where the levels of water channels will be measured.

Subsequently each time you attend an appointment we would like you to be weighed and measured and to provide a fresh urine sample into a pot.

At each clinic appointment your doctor would also like to record some information about you including; your age, your height and weight, the reason for your swollen kidney and if you are taking any medicines.

With your agreement and your parents' permission we would like to store your samples after this research is complete for use in future ethically approved kidney disease research.

What will happen to any information about me?

Any information about you will be kept private. The information your doctor sends us will be stored securely at the laboratory. At the end of the study the information will be encrypted and transferred to a secure storage facility within the University of Bristol called the Research Data Repository where it will remain for 20 years. At the end of this period of time the information will be destroyed.

What will happen to my urine samples?

Once the urine samples have been analysed, they will be stored securely at the research laboratory in Bristol. At the end of the study, with your agreement, the samples will continue to be stored at the research laboratory in Bristol. Only people in the research group with special passes can get in. The samples are kept in a freezer until they are used.

What if new discoveries are made about PUJ obstruction?

The research-group is interested in water channels (aquaporins) and their role in protecting the kidney in PUJ obstruction. They want to determine whether a urine test for these water channels will help doctors decide which children and young adults need an operation for PUJ obstruction.

In the future other proteins and substances may be found to be involved in PUJ obstruction. The group would like to be able to test for new proteins and substances, if they are found, using the original stored samples. If you don't want your samples to be stored and used for future research that's ok, just tell us and we will dispose of them at the end of this study.

How will I know the results of the study?

At the end of the study your doctor will send you a summary of the study results. If you don't want to receive a copy of the results that's fine just let us know.

Can I have more time to decide?

Yes. There is no time limit.

What if I wish to leave the study?

You can leave the study at any stage without having to give a reason. You can do this via telephone, email, or in writing to your specialist doctor or directly to the research team if you wish. The results of any tests on samples already collected will be used but no further tests will be done on these samples and no further samples will be collected.

Any samples already held by the research team will be destroyed in an appropriate manner.

What do I do if I have concerns about the study?

If you have any concerns or further questions about this study or the way it is carried out, you should contact the research team. You can also contact the Patient Support and Complaints Team at the Bristol Children's Hospital.

Will this study have an educational role?

This study is being undertaken as part of a higher degree educational project.

Has this research study been approved by an ethics committee?

All research in the NHS is looked at by an independent group of people, called a Research Ethics Committee, to protect your interests. This study has been reviewed and approved by South West – Central Bristol Research Ethics Committee.

Researchers	***Patient Support and Complaints Team***
Miss Laura Jackson, Mr Mark Woodward and Prof Richard Coward	*Patient Support and Complaints Team*
Academic Renal Unit	*Trust Headquarters*
University of Bristol	*University Hospitals Bristol*
Dorothy Hodgkin Building, Level 1	*Marlborough Street*
Whitson Street	*Bristol*
Bristol	*BS1 3NU*
BS1 3NY	
Contact email: laura.jackson@bristol.ac.uk	*Tel: 0117 342 3604*

Studying Kidney Blockage

Information Sheet for Children with a Swollen Kidney (Group 2)

Hello!

Thank you for reading this. You can ask someone to help you read it if you want.

Please ask if you don't understand.

There is a group of doctors and scientists in Bristol who are trying to help children who have a blockage of their kidney. We call this blockage pelvi-ureteric junction (PUJ) obstruction. It happens because part of the tube that drains wee out of the kidney is too narrow. Sometimes the blockage makes the kidney not work properly.

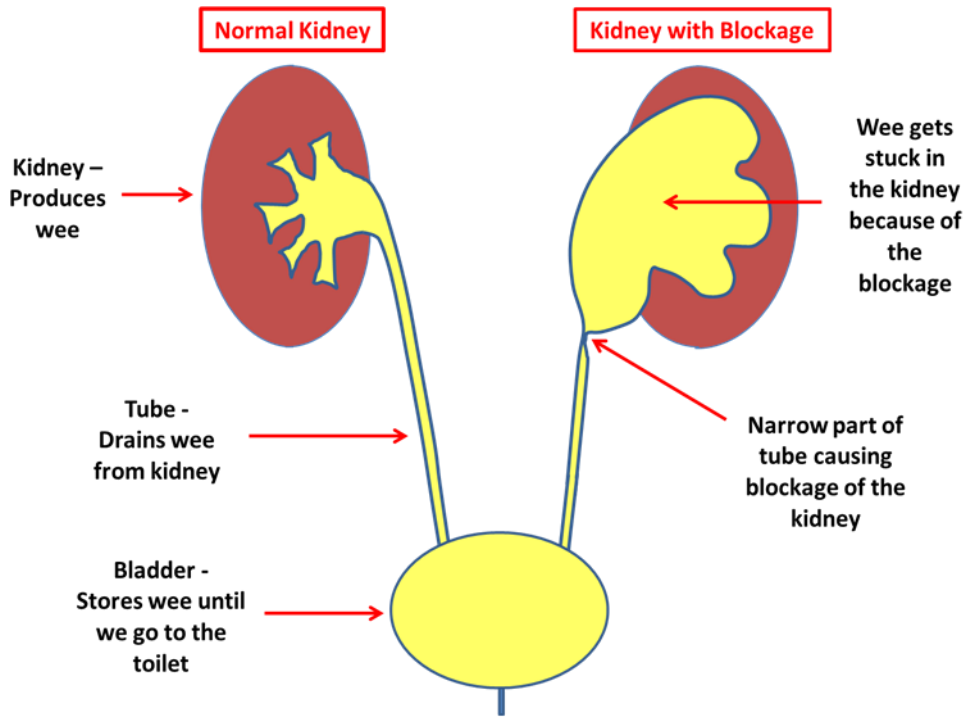

The doctors and scientists want to find out if a new test using a sample of wee can help them decide which children need an operation to fix this problem. The test will show how much of a special protein there is in the wee.

To find out how good the new test is we need to know what the levels of this special protein are in wee from children like you who have a swollen kidney. That's why we're asking you if you'd like to take part.

Taking part will mean that every time you come to see the doctor at the Children's Hospital we would like you to give us a sample of your wee. Each time the sample will be tested to see how much of the special protein it contains.

Also, each time you come to the hospital the doctor would like to measure how heavy and tall you are and collect some information about how old you are, and if you take any medicines.

If you don't want to take part that's ok and it won't affect your treatment.

So that's it!

Do you want to ask any questions?

Researchers

Miss Laura Jackson, Mr Mark Woodward and Prof Richard Coward

Academic Renal Unit

University of Bristol

Dorothy Hodgkin Building, Level 1

Whitson Street

Bristol, BS1 3NY

Contact email: laura.jackson@bristol.ac.uk

This study has been reviewed and approved by South West – Central Bristol Research Ethics Committee and is being undertaken as part fulfilment of an educational project.

Do aquaporins protect against renal damage in PUJ obstruction?

Information Sheet for Parents/Guardians of Children with Normal Kidneys (Group 3)

Your child is being invited to participate in a research study. Before you decide, it is important for you to understand why the research is being done and what it will involve for you and your child.

Please take time to read the following information carefully and discuss it with others if you wish. If appropriate, please encourage your child to read their information sheet and discuss the study with them.

Your child's specialist doctor will explain if there is anything that is not clear or if you would like more information. Thank you for taking the time to read this.

The purpose of this study

There a number of children and young adults who come to the Bristol Children's Hospital because they have pelvi-ureteric junction (PUJ) obstruction which is the most common cause of obstruction (blockage) in the urinary tract. Some need an operation known as a pyeloplasty to treat this condition.

The kidneys produce urine by filtering the blood and removing waste products and water. The urine must then drain out of the kidney through a funnel shaped structure called the renal pelvis and into a tube called the ureter which transports urine to the bladder where it is stored.

PUJ obstruction is caused by a narrowing at the point where the ureter joins the renal pelvis. This obstruction, which forms before the baby is born, means that urine can't drain out of the kidney as fast as it is produced. Urine therefore accumulates inside the kidney causing the kidney to swell. This swelling (dilatation) is seen on ultrasound scan and is called hydronephrosis. Accumulating urine may increase the pressure inside the kidney and in some children this can damage the kidney.

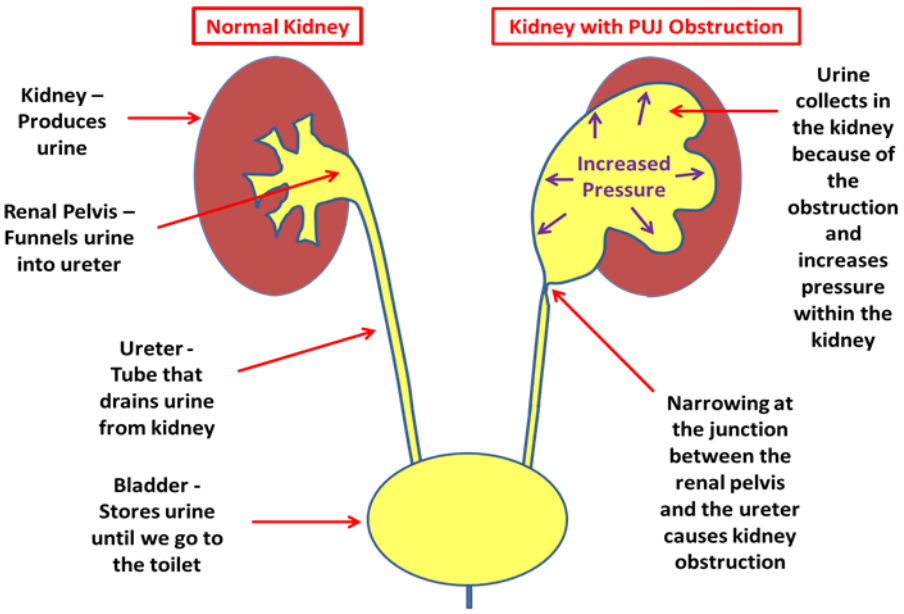

The major issue for doctors is deciding which children require surgery to relieve PUJ obstruction and limit kidney damage, and which do not. This is because some children with PUJ obstruction do not damage their kidneys, do not require surgery and ultimately grow out of the problem.

Our current ability to distinguish between those children with high pressure "damaging" obstruction and those with low pressure "safe" non-kidney damaging PUJ obstruction is limited.

Current research suggests that special water channels (proteins called aquaporins) in the kidney and its drainage tubes may help to protect the kidney from damage. By reabsorbing water from the urinary tract, these channels may reduce the pressure in the system, and explain the mechanism behind "safe" and "damaging" PUJ obstruction.

Everybody sheds some of these water channels in their urine. We want to collect these special proteins from the urine, measure their amount and show whether they are a good marker of high pressure and low pressure kidneys. This will enable us to work out if a new type of urine test could help doctors decide which children with PUJ obstruction need an operation and which don't.

In order to know whether the test correctly identifies which children need an operation we need to know what the normal levels of these water channels are as a comparison.

For this reason the kidney research unit in Bristol is asking children who have normal kidneys if they'd like to take part in the study.

Why has my child been chosen?

Every child/young adult with normal kidneys who attends the Bristol Children's Hospital surgery/urology clinics on specified recruitment days will be invited to participate.

Does my child have to take part?

It is up to you to decide whether your child takes part. If you decide they can take part you will be asked to sign a consent form. You are still free to change your mind and withdraw your child from the study at any time without giving a reason, and this will not affect the treatment your child receives.

What will happen if my child agrees to take part?

Your child's scheduled appointment with the doctor will go ahead today as planned. With your consent at the end of the appointment your child will be weighed and measured and we would like them to provide a urine sample into a pot. In younger children the sample can be collected from the nappy. The urine sample will be sent to the research laboratory in Bristol where the levels of water channels will be measured.

The doctor will record some information about your child which, with your permission, will be taken from their medical notes/results file. This will include; their age, their height and weight, the reason for their hospital appointment and current medications.

With your permission we would like to store the urine sample after this research is complete for use in future ethically approved kidney disease research.

What will happen to any information about my child?

Any medical information about your child will be kept private. Limited personal details identifying your child as participating in the study will remain on the NHS computer system at the Bristol Children's Hospital. All children will be assigned a study number so that their urine sample and information collected about them is labelled with this number and no personal details when it is transferred to the research laboratory. The information your doctor sends to the researchers and the results we have from sample analysis will be stored securely at the laboratory. At the end of the study the information will be encrypted and transferred to a secure storage facility within the University of Bristol called the Research Data Repository where it will remain for 20 years. At the end of this period of time the information will be destroyed.

What will happen to my child's samples?

Once the urine sample has been analysed, it will be stored securely at the research laboratory in Bristol. The sample will be labelled with your child's unique study number so that their sample results can be linked with their medical information. At the end of the study, with your permission, the sample will continue to be stored at the

research laboratory pending further study. Access to this building is limited to the laboratory staff and an identification card and biometric authorisation is required for access.

What if new discoveries are made about PUJ obstruction?

The research-group is interested in water channels (aquaporins) and their role in protecting the kidney in PUJ obstruction. They want to determine whether a urine test for these water channels will help doctors decide which children and young adults need an operation for PUJ obstruction.

In the future other proteins and substances may be found to be involved in PUJ obstruction. The group would like to be able to test for new proteins and substances, if they are found, using the original stored samples. If you don't want your child's sample to be stored and used for future research that's ok, just inform your specialist doctor and we will dispose of it at the end of this study.

How will I know the outcome of the research?

At the end of the study your doctor will send you a summary of the study results. If you don't want to receive a copy of the results please inform your specialist doctor.

Will the results be published?

All data collected will be collated and published in peer-reviewed scientific journals. The findings will also be presented at national and international scientific conferences. All this information will be anonymous and it will not be possible to identify your child from the data.

Can I have more time to decide?

Yes. There is no time limit.

What if I wish to withdraw my child from the study?

A participant may withdraw at any stage without having to give an explanation. You can do this via telephone, email, or in writing to your specialist doctor or directly to the research team if you wish. The results of any tests on samples already collected will be used but no further tests will be done on these samples and no further samples will be collected. Any samples already held by the research team will be destroyed in an appropriate manner.

What are the risks/benefits in participating in this study?

This study does not require you to make an extra visit to the hospital however it does require your child to be weighed and measured and provide a urine sample at the end of today's clinic appointment.

The benefits of participating in the study are that it will increase medical knowledge about PUJ obstruction potentially leading to the development of a new urine test. We hope this urine test will allow earlier and improved detection of those children requiring surgery for PUJ obstruction.

What do I do if I have concerns about the study?

If you have any concerns or further questions about this study or the way it is carried out, you should contact the research team. You can also contact the Patient Support and Complaints Team at the Bristol Children's Hospital.

Will this study have an educational role?

This study is being undertaken as part of a higher degree educational project.

Has this research study been approved by an ethics committee?

All research in the NHS is looked at by an independent group of people, called a Research Ethics Committee, to protect your interests. This study has been reviewed and approved by South West – Central Bristol Research Ethics Committee.

Researchers	***Patient Support and Complaints Team***
Miss Laura Jackson, Mr Mark Woodward and Prof Richard Coward	*Patient Support and Complaints Team*
Academic Renal Unit	*Trust Headquarters*
University of Bristol	*University Hospitals Bristol*
Dorothy Hodgkin Building, Level 1	*Marlborough Street*
Whitson Street	*Bristol*
Bristol	*BS1 3NU*
BS1 3NY	
Contact email: laura.jackson@bristol.ac.uk	*Tel: 0117 342 3604*

Do aquaporins protect against renal damage in PUJ obstruction?

Information Sheet for Young Adults with Normal Kidneys (Group 3)

You are being invited to take part in a project. Before you decide, it is important for you to understand why we want to do it and what it means for you.

Please take time to read this and chat about it with others if you want.

Your specialist doctor will explain anything that is confusing, or give you more information. Thank you for taking the time to read this.

The purpose of this study

There a number of children and young adults who come to the Bristol Children's Hospital because they have a blockage of their kidney called pelvi-ureteric junction (PUJ) obstruction. Some need an operation known as a pyeloplasty to make it better.

PUJ obstruction is caused by a narrowing in the upper part of the tube that drains urine out of the kidney. Urine therefore builds up and can increase the pressure inside the kidney. In some children and young adults this can cause the kidney to not work properly.

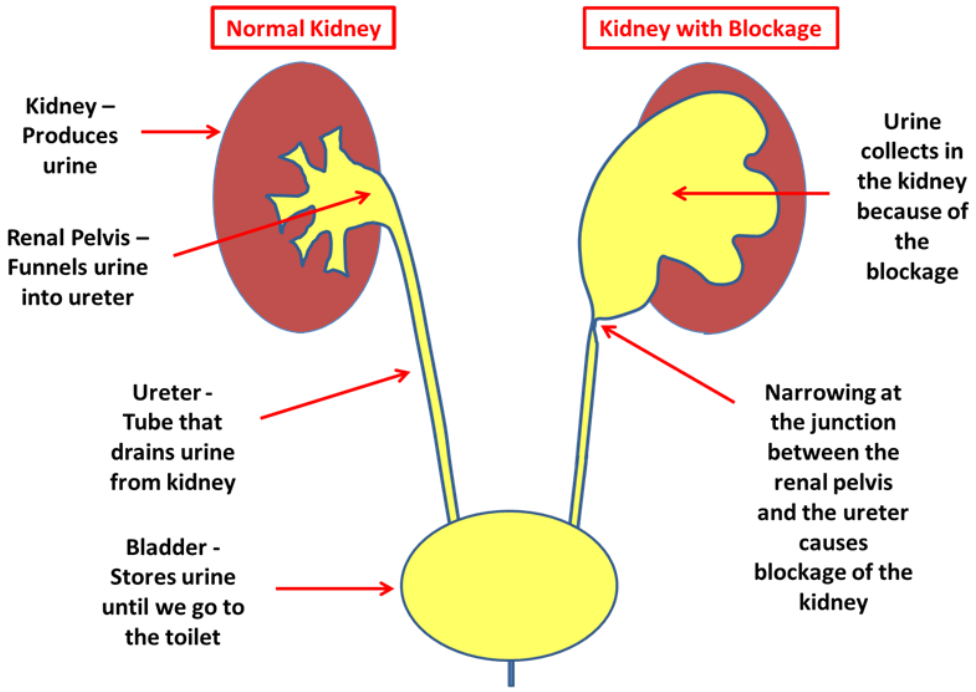

Sometimes it can be difficult for doctors to figure out which children and young adults need an operation to protect their kidney and which will simply grow out of the problem.

Current research suggests that special water channels (proteins called aquaporins) in the kidney and its drainage tubes may help to protect the kidney from damage. Everybody sheds some of these water channels in their urine. We are currently collecting these special proteins from the urine of children with PUJ obstruction and measuring their amount. The aim is to work out if a new type of urine test could help doctors decide which children with PUJ obstruction need an operation and which don't.

In order to know whether the test works properly we need to know what the normal levels of these water channels are as a comparison.

For this reason the kidney research unit in Bristol is asking children and young adults like you who have normal kidneys if they'd like to take part in the study.

Why have I been chosen?

Every child/young adult with normal kidneys who attends the Bristol Children's Hospital surgery/urology clinics on specified recruitment days will be invited to participate.

Do I have to take part?

It is up to you to decide whether you take part. You are still free to change your mind and leave the study at any time without giving a reason. If you decide not to take part or to come out of the study this will not affect the treatment you receive.

What will happen if I agree to take part?

Your scheduled appointment with your doctor will go ahead today as planned. At the end of the appointment we would like you to be weighed and measured and we would like you to provide a urine sample into a pot. This will be sent to the research laboratory in Bristol where the levels of water channels will be measured.

Your doctor would also like to record some information about you including; your age, your height and weight, the reason for your clinic appointment and if you are taking any medicines.

With your agreement and your parents' permission we would like to store your sample after this research is complete for use in future ethically approved kidney disease research.

What will happen to any information about me?

Any information about you will be kept private. The information your doctor sends us will be stored securely at the laboratory. At the end of the study the information will

be encrypted and transferred to a secure storage facility within the University of Bristol called the Research Data Repository where it will remain for 20 years. At the end of this period of time the information will be destroyed.

What will happen to my urine sample?

Once the urine sample has been analysed, it will be stored securely at the research laboratory in Bristol. At the end of the study, with your agreement, the sample will continue to be stored at the research laboratory in Bristol. Only people in the research group with special passes can get in. The samples are kept in a freezer until they are used.

What if new discoveries are made about PUJ obstruction?

The research-group is interested in water channels (aquaporins) and their role in protecting the kidney in PUJ obstruction. They want to determine whether a urine test for these water channels will help doctors decide which children and young adults need an operation for PUJ obstruction.

In the future other proteins and substances may be found to be involved in PUJ obstruction. The group would like to be able to test for new proteins and substances, if they are found, using the original stored samples. If you don't want your sample to be stored and used for future research that's ok, just tell us and we will dispose of it at the end of this study.

How will I know the results of the study?

At the end of the study your doctor will send you a summary of the study results. If you don't want to receive a copy of the results that's fine just let us know.

Can I have more time to decide?

Yes. There is no time limit.

What if I wish to leave the study?

You can leave the study at any stage without having to give a reason. You can do this via telephone, email, or in writing to your specialist doctor or directly to the research team if you wish. The results of any tests on the sample already collected will be used but no further tests will be done on this sample. The sample held by the research team will be destroyed in an appropriate manner.

What do I do if I have concerns about the study?

If you have any concerns or further questions about this study or the way it is carried out, you should contact the research team. You can also contact the Patient Support and Complaints Team at the Bristol Children's Hospital.

Will this study have an educational role?

This study is being undertaken as part of a higher degree educational project.

Has this research study been approved by an ethics committee?

All research in the NHS is looked at by an independent group of people, called a Research Ethics Committee, to protect your interests. This study has been reviewed and approved by South West – Central Bristol Research Ethics Committee.

Researchers	***Patient Support and Complaints Team***
Miss Laura Jackson, Mr Mark Woodward and Prof Richard Coward	*Patient Support and Complaints Team*
Academic Renal Unit	*Trust Headquarters*
University of Bristol	*University Hospitals Bristol*
Dorothy Hodgkin Building, Level 1	*Marlborough Street*
Whitson Street	*Bristol*
Bristol	*BS1 3NU*
BS1 3NY	
Contact email: laura.jackson@bristol.ac.uk	*Tel: 0117 342 3604*

Studying Kidney Blockage

Information Sheet for Children with Normal Kidneys (Group 3)

Hello!

Thank you for reading this. You can ask someone to help you read it if you want.

Please ask if you don't understand.

There is a group of doctors and scientists in Bristol who are trying to help children who have a blockage of their kidney. We call this blockage pelvi-ureteric junction (PUJ) obstruction. It happens because part of the tube that drains wee out of the kidney is too narrow. Sometimes the blockage makes the kidney not work properly.

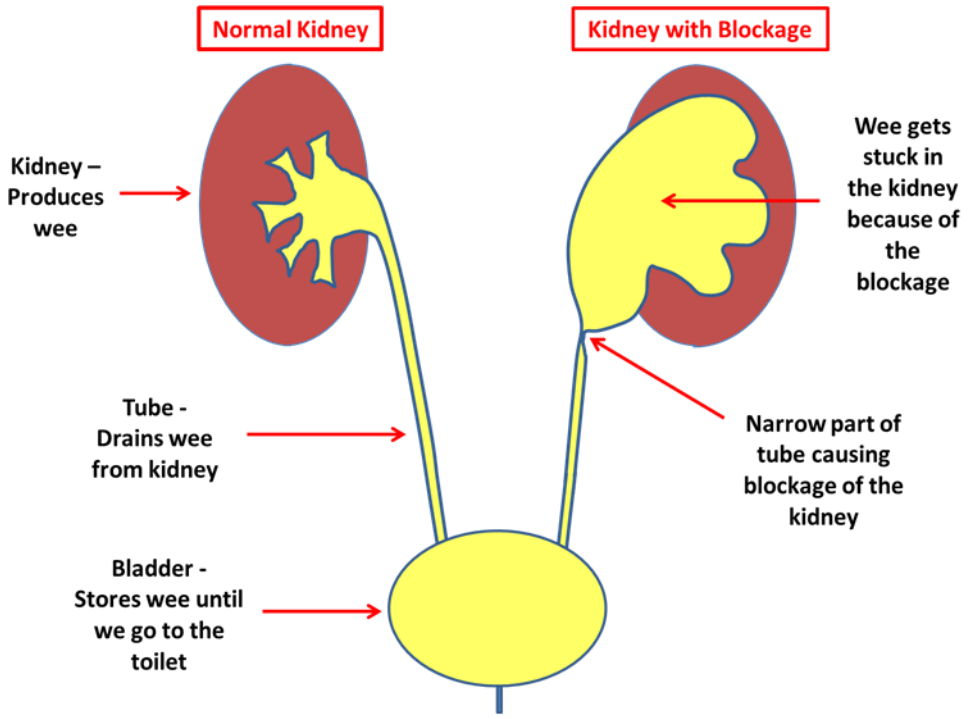

The doctors and scientists want to find out if a new test using a sample of wee can help them decide which children need an operation to fix this problem. The test will show how much of a special protein there is in the wee.

To find out how good the new test is we need to know what the normal levels of this special protein are in wee from children like you who don't have blocked kidneys. That's why we're asking you if you'd like to take part.

Taking part means we would like you to give us a sample of your wee. The wee sample will be tested to see how much of the special protein it contains.

Your doctor would also like to measure how heavy and tall you are and collect some information about how old you are and if you take any medicines.

If you don't want to take part that's ok and it won't affect your treatment.

So that's it!

Do you want to ask any questions?

Researchers

Miss Laura Jackson, Mr Mark Woodward and Prof Richard Coward

Academic Renal Unit

University of Bristol

Dorothy Hodgkin Building, Level 1

Whitson Street

Bristol, BS1 3NY

Contact email: laura.jackson@bristol.ac.uk

This study has been reviewed and approved by South West – Central Bristol Research Ethics Committee and is being undertaken as part fulfilment of an educational project.

10.3.3 Study consent forms

Consent forms completed when recruiting children to groups 1-3 are presented in the following section.

University of BRISTOL

Do aquaporins protect against renal damage in PUJ obstruction?

Consent Form for Parents/Guardians — Group 1

(Name of Patient)

(DOB)

(Study Assigned ID Number)

Please initial each box

I confirm that I have read and understood the information sheet (PUJO Group 1 Version 5) for the above study and I have had the opportunity to ask questions.	☐
I agree for my child to take part in the study.	☐
I understand my child's participation is voluntary and that my child is free to withdraw at any time without giving any reason, and without my child's medical care or legal rights being affected.	☐
I understand that sections of my child's medical notes may be looked at by responsible individuals from the NHS Trust, Sponsor or from regulatory authorities where it is relevant to my child's participation in research. I give permission for these individuals to have access to my child's records.	☐
I agree that my child's medical notes and test results can be looked at by Bristol Children's Hospital NHS doctors. I give permission for information relevant to the study to be collected for analysis.	☐
I agree for my child to be weighed and measured at each hospital attendance.	☐
I agree for my child to provide urine samples before, during and after their operation.	☐
I agree for my child to have the pressure within their obstructed kidney measured during their operation.	☐
I agree that the narrowed piece of drainage tube tissue (renal pelvis/ureter junction) removed during the operation can be tested in the laboratory.	☐
I agree that my child's General Practitioner will be informed of their participation in this study.	☐
I agree that if new proteins and substances associated with PUJ obstruction were to be found that my child's samples could be tested for these.	☐
I agree that the samples may be stored and used by researchers in future ethically approved research into kidney conditions.	☐

Name of parent/guardian..... Date .....
Signature.....

Name of person taking consent..... Date.....
Signature.....

Assent Form for Children/Young People

For children/young people who would like to co-sign this form to confirm you want to take part, you can write your name here:

Child (or if unable, parent on their behalf) /young person to circle all they agree with:

Have you read (or had read to you) about this project?	Yes/No
Has somebody else explained this project to you?	Yes/No
Do you understand what this project is about?	Yes/No
Have you asked all the questions you want to ask?	Yes/No
Have you had your questions answered in a way you understand?	Yes/No
Do you understand it's OK to stop taking part at any time?	Yes/No
Are you happy to take part?	Yes/No

If <u>any</u> answers are 'no' or you don't want to take part, don't sign your name!

If you <u>do</u> want to take part, you can write your name below

Your name..... Date .....

Name of person taking consent..... Date.....

Signature.....

Thank you

Copies 1 for patient, 1 for hospital notes, 1 for Investigator site file

University of BRISTOL

Do aquaporins protect against renal damage in PUJ obstruction?

Consent Form for Parents/Guardians Group 2

(Name of Patient)

(DOB)

(Study Assigned ID Number)

Please initial each box

I confirm that I have read and understood the information sheet (PUJO Group 2 Version 1) for the above study and I have had the opportunity to ask questions.	☐
I agree for my child to take part in the study.	☐
I understand my child's participation is voluntary and that my child is free to withdraw at any time without giving any reason, and without my child's medical care or legal rights being affected.	☐
I understand that sections of my child's medical notes may be looked at by responsible individuals from the NHS Trust, Sponsor or from regulatory authorities where it is relevant to my child's participation in research. I give permission for these individuals to have access to my child's records.	☐
I agree that my child's medical notes and test results can be looked at by Bristol Children's Hospital NHS doctors. I give permission for information relevant to the study to be collected for analysis.	☐
I agree for my child to be weighed and measured at every urology outpatient clinic attendance.	☐
I agree for my child to provide a urine sample at every urology outpatient clinic attendance.	☐
I agree that my child's General Practitioner will be informed of their participation in this study.	☐
I agree that if new proteins and substances associated with PUJ obstruction were to be found that my child's urine samples could be tested for these.	☐
I agree that the urine samples may be stored and used by researchers in future ethically approved research into kidney conditions.	☐

Name of parent/guardian..... Date .....

Signature.....

Name of person taking consent..... Date.....

Signature.....

Assent Form for Children/Young People

For children/young people who would like to co-sign this form to confirm you want to take part, you can write your name here:

Child (or if unable, parent on their behalf) /young person to circle all they agree with:

Have you read (or had read to you) about this project?	Yes/No
Has somebody else explained this project to you?	Yes/No
Do you understand what this project is about?	Yes/No
Have you asked all the questions you want to ask?	Yes/No
Have you had your questions answered in a way you understand?	Yes/No
Do you understand it's OK to stop taking part at any time?	Yes/No
Are you happy to take part?	Yes/No

If <u>any</u> answers are 'no' or you don't want to take part, don't sign your name!

If you <u>do</u> want to take part, you can write your name below

Your name..... Date .....

Name of person taking consent..... Date.....
Signature.....

Thank you

Copies 1 for patient, 1 for hospital notes, 1 for Investigator site file

Do aquaporins protect against renal damage in PUJ obstruction?

Consent Form for Parents/Guardians Group 3

(Name of Patient)

(DOB)

(Study Assigned ID Number)

Please initial each box

I confirm that I have read and understood the information sheet (PUJO Group 3 Version 1) for the above study and I have had the opportunity to ask questions.	☐
I agree for my child to take part in the study.	☐
I understand my child's participation is voluntary and that my child is free to withdraw at any time without giving any reason, and without my child's medical care or legal rights being affected.	☐
I understand that sections of my child's medical notes may be looked at by responsible individuals from the NHS Trust, Sponsor or from regulatory authorities where it is relevant to my child's participation in research. I give permission for these individuals to have access to my child's records.	☐
I agree that my child's medical notes and test results can be looked at by Bristol Children's Hospital NHS doctors. I give permission for information relevant to the study to be collected for analysis.	☐
I agree for my child to be weighed and measured.	☐
I agree for my child to provide a urine sample.	☐
I agree that my child's General Practitioner will be informed of their participation in this study.	☐
I agree that if new proteins and substances associated with PUJ obstruction were to be found that my child's urine sample could be tested for these.	☐
I agree that the urine sample may be stored and used by researchers in future ethically approved research into kidney conditions.	☐

Name of parent/guardian..... Date .....
Signature.....

Name of person taking consent..... Date.....
Signature.....

Assent Form for Children/Young People

For children/young people who would like to co-sign this form to confirm you want to take part, you can write your name here:

Child (or if unable, parent on their behalf) /young person to circle all they agree with:

Have you read (or had read to you) about this project?	Yes/No
Has somebody else explained this project to you?	Yes/No
Do you understand what this project is about?	Yes/No
Have you asked all the questions you want?	Yes/No
Have you had your questions answered in a way you understand?	Yes/No
Do you understand it's OK to stop taking part at any time?	Yes/No
Are you happy to take part?	Yes/No

If <u>any</u> answers are 'no' or you don't want to take part, don't sign your name!

If you <u>do</u> want to take part, you can write your name below

Your name..... Date .....

Name of person taking consent..... Date.....
Signature.....

Thank you

Copies 1 for patient, 1 for hospital notes, 1 for Investigator site file

10.3.4 GP letter for group 1 patients

A copy of the covering letter overleaf was attached to a copy of the Group 1 parent patient information leaflet and sent to the GP for all children recruited to Group 1.

Academic Renal Unit
University of Bristol
Dorothy Hodgkin Building, Level 1
Whitson Street
Bristol, BS1 3NY
Tel: 07930 868195

Date.....

Do aquaporins protect against renal damage in pelvi-ureteric junction (PUJ) obstruction?

RE: Name:.....

Date of Birth:.....

Dear Dr.....,

I am writing to inform you that the above-named patient has been recruited to a study being undertaken at the Bristol Royal Hospital for Children in conjunction with the University of Bristol. This study is designed to investigate the mechanism of renal injury in PUJ obstruction, and to determine whether urine aquaporin measurement is a useful biomarker to direct the timing and necessity of surgical intervention. I have enclosed a copy of the patient information leaflet detailing the study received by the child and their family.

Please do not hesitate to contact me should you have any questions or require a copy of the scientific protocol.

Yours Sincerely,

Miss Laura Jackson

Research Fellow in Paediatric Surgery

Researchers: Miss Laura Jackson, Mr Mark Woodward and Prof Richard Coward

Contact email: laura.jackson@bristol.ac.uk

This study has been reviewed and approved by South West – Central Bristol Research Ethics Committee and is being undertaken as part fulfilment of an educational project. This study is sponsored by the University of Bristol.